University of Minho
Departament of Civil Engineering

ICPIC
INTERNATIONAL CONGRESS ON POLYMERS IN CONCRETE

# International Symposium Polymers in Concrete

José Barroso de Aguiar  Saíd Jalali  Aires Camões  Rui Miguel Ferreira



## Proceedings of ISPIC 2006

## 2-4 April 2006 - University of Minho - Guimarães, Portugal

**International Symposium Polymers in Concrete**
**2 - 4 April 2006**
**Guimarães, Portugal**

ISBN 972-99179-1-4
© Department of Civil Engineering – University of Minho

All rights, including translation, reserved. Except as permitted by the Copyright, Designs and Patents Act 1988, no part of this publication may be reproduced, stored in a retrieval system or transmitted in any form or by any means, electronic, mechanical, photocopying or otherwise, without the prior written permission of the editors; University of Minho, Department of Civil Engineering , Campus de Azurém, 4800-058, Guimarães, Portugal.

This book is published on the understanding that the authors are solely responsible for the statements made and opinions expressed in it and that its publication does not necessarily imply that such statements and/or opinions are or reflect the views or opinions of the editors. While every effort has been made to ensure that the statements made and the opinions expressed in this publication provide a safe and accurate guide, no liability or responsibility can be accepted in this respect by the authors or editors.

Printed and bound in Portugal by Oficinas Gráficas de Barbosa & Xavier, Lda, Braga.

**International Symposium Polymers in Concrete**
**2 - 4 April 2006**
**Guimarães, Portugal**

**Editors**

**José Barroso de Aguiar**
**Saíd Jalali**
**Aires Camões**
**Rui Miguel Ferreira**

# Contents

**Preface** **IX**

**International Scientific Committee** **X**

**Cooperating Organizations** **XI**

**Sponsors** **XII**

**Keynote Papers** **XIII**

*Cement concrete and concrete-polymer composites: two merging worlds* 1
Van Gemert, D., Catholic University of Leuven, Belgium

*Essential concrete-polymer composite* 13
Czarnecki, L., Warsaw Technical University, Poland

*Behaviour of RC structures strengthened with CFRP under load test and thermal effects* 33
Juvandes, L.F., Silva, P.C., Figueiras, J.A., University of Porto, Portugal

**Session 1** **47**

*Properties of polymer-modefied mortars using hardener-free resin with nitrite-type hydrocalumite* 49
Ota, M., Ohama, Y., Tatematsu, H.

*Particulate composite materials with modulated mechanical properties* 61
Sandrolini, F., Manzi, S.

*Influence of the viscoelastic nature of the polymer concrete in its structural behaviour* 69
Tomás San-José, J., Aguado, A.

*Water-soluble polymers for modification of cement mortars* 85
Knapen, E., Van Gemert, D.

**Session 2** **97**

*Concrete substrate evaluation and adhesion of repair materials* 99
Courard, L., Schwall, D., Garbacz, A., Piotrowski, T.

*Application of percolation theory for explaining of microstructure forming in polymer-cement concretes* 111
Lukowski, P.

*Effect of plastic reject and natural sand additions on the microstructure and mechanical behaviour of cellular concrete* 119
de Freitas, I.M., Allende, K.A., Darwish, F.A.
*Experimental analysis of cork as a concrete aggregate* 131
Branco, F.G., Tadeu, A., Reis, M.L.

*Study of the resistance to impact of light panels made with residue of expanded polystyrene* 139
Trindade, G.
*Different gradation influence of tire rubber scraps in the behavior of the high performance concrete* 149
Martins, I.R, Akasaki, J.L.

**Session 3** **159**

*Core reinforced braided composite armour as a substitute to steel in concrete reinforcement* 161
Fangueiro, R., Sousa, G., de Araújo, M., Pereira, C.G., Jalali, S.
*Bond behaviour of polymer impregnated AR-Glass textile reinforcement in concrete* 173
Butler, M., Hempel, R., Schorn, H.
*Composite Improvement of Textile Reinforced Concrete by Polymeric Impregnation of the Textiles* 185
Dilthey, U., Schleser, M.
*Comparative study with alternative materials for manufacture of machine tool structures* 193
Ducatti, V.A., Santos, J.M., Lintz, R.C.
*Carbonation resistance of different concrete mixtures. Effect of the presence of coatings* 205
Rodrigues, P., Bettencourt, A.
*Mechanisms of blistering of coatings on concrete* 213
Wolff, L., Hailu, K., Raupach, M.

*Systems for superficial protection of concretes* 225
Moreira, P.M., Aguiar, J.B., Camões, A.

*UV Curing behaviour of a vinylester resin for concrete restoration* 237
Serrano, R., Maffezzoli, A., Tarzia, A., Stifani, C.

**Session 4** **247**

*FRP Reinforcement for Damaged R/C Bridge Decks* 249
Aprile, A., Capuani, D.

*CFRP-Based Confinement Strategies for Rc Columns-Experimental and Analytical Research* 261
Ferreira, D., Barros, J.

*Analysis of the design models suggested on Fib bulletin 14 related to the flexural strengthening of reinforced concrete elements by CFRP systems* 273
Bogas, J.A., Gomes, A.
*Prediction of durability of cold-curing epoxy resins: comparison between natural and artificial weathering* 285
Lettieri, M., Frigione, M., Stefanelli, M.
*Influence of moisture and moderate temperatures on the properties of polymer composite materials for concrete repair* 297
Frigione, M., Sciolti, M.S.
*An application of impact-echo and ultrasonic methods for repair efficiency assessment* 305
Garbacz, A.

**Session 5** 317

*Modelling the behaviour of the bonding of fibre reinforced concrete at the plate end* 319
Neto, P., Vinagre, J., Alfaiate, J.
*The study of the performance of present models for the concrete reinforced by CFRP sheets* 331
Nourivand, A., Majolan A.S., Sadeghi, C.A.
*Development of a ultrasonic system to monitor the mechanical properties of CFRP on concrete* 341
Luprano, V., Caretto, F., Tatì, A.
*Development of new casted-in-place water sealant materials* 355
Pereira, P.S., Bordado, J. C., Paula, R.F.
*Concrete workability and water resistance improvement using polymeric admixtures polymers* 367
Pires, P., Machado, A.V., Azevedo, I., Aguiar, J.L., Ferreira, R.M.
*Strength and Chemical Resistance of Fiber Reinforced Concrete Based on Polybutadiene Matrix* 383
Borisov, Y., Potapov, Y., Panfilov, D., Figovsky, O., Beilin, D.
*Effect of the addition of synthetic fibers to concrete thin slabs on plastic shrinkage cracking* 393
Neto, A.B., Pelisser, F., da Silva, D., La Rovere, H.L., Pinto, R.C.
*Flexural strength of reinforced concrete beams repaired with Polymer-modified cementitious mortars* 405
Nsambu. R., Gomes. A.
*Impact resistance of single-span concrete frames reinforced by polypropylene fibers* 417
Nourivand A , Majolan A. S. , Abbasi S.
*Technical advances within maintenance and repair of concrete structures* 425
Azamirad, H., Beheshti zadeh, D., Taghizadeh, M.

**Author Index** **435**

# Preface

The use of polymers and concrete can be considered a good combination. In some cases polymers are the best solution to increase some specific property of concrete and to guarantee a secure and durable repair of this material. The use of small quantities of polymers enhances the durability of concrete. This aspect is especially relevant to the development of the world and to contribute to the sustainability of construction materials.

Polymers in Concrete cover a vast field of knowledge and technology so it was decided to limit the scope of the Conference and to on a few aspects such as innovations in concrete polymer composites (CPC), the applications of FRP for reinforcements and CPC as coatings. Also considered were topics that covered: testing methods, industrial applications, ecological aspects, durability of repair works, repair of repair, polymer based industrial floor systems, research and case studies. It is hoped that the papers included in the Proceedings will in some way contribute to objectives of this Symposium.

All the papers included in the Proceedings have been reviewed by two specialists of the field of the paper concerned. I am very much grateful to all members of the International Scientific Committee who gave much of their time and effort in reviewing the papers. In some cases external experts were also included in the peer review of papers and I want to express my thanks to all of them. I would also to acknowledge the support given by all the sponsors of the Symposium. Organization of an International Symposium requires support from many people. I thank all those who have helped us, but my particular thanks go to Daniel Pinheiro, Lídia Gonçalves and Daniela Silva whose enthusiasm and help was a key element in the success of the Symposium. I would also like to than all the authors for their relevant contributions. Important contribution was also received from the students of the Civil Engineering Course.

If the work and ideas expressed in these papers have contributed in some way to further development of polymers in concrete, and consequently to sustainable construction, then our efforts have not been in vain.

José Barroso de Aguiar
Guimarães, April 2006

# International Scientific Committee

J. Barroso de Aguiar - Chairman - University of Minho (POR)

Said Jalali - Co-chairman - University of Minho (POR)

António Aguado - Technical University of Catalonia (SPA)

Ivan Ramalho de Almeida - Fluminense Federal University (BRA)

Carlos Bernardo - University of Minho (POR)

Fernando Branco - Technical University of Lisbon (POR)

Lech Czarnecki - Warsaw Technical University (POL)

Mariaenrica Frigione - University of Lecce (ITA)

Dionys van Gemert - Catholic University of Leuven (BEL)

Arlindo Gonçalves - LNEC (POR)

Paulo Helene - University of São Paulo (BRA)

Torres Marques - University of Porto (POR)

António Pouzada - University of Minho (POR)

Moshe Putterman - Technion - Israel Institute of Technology (ISR)

Tomas San-José - LABEIN (SPA)

Harald Shorn - Dresden University of Technology (GER)

Narayan Swamy - University of Sheffield (UK)

António Tadeu - University of Coimbra (POR)

# Cooperating Organizations

University of Minho

ICPIC – International Congress on Polymers in Concrete

RILEM – International Union of Laboratories and Experts in Construction Materials, Systems and Structures

American Concrete Institute

FCT – Fundação para a Ciência e a Tecnologia

IBRACON – Brazilian Concrete Institute

Ordem dos Engenheiros

APEB – Associação Portuguesa das Empresas de Betão Pronto

# Sponsors




MOTAENGIL Engenharia




DST - Domingos da Silva Teixeira, S.A.




MAPEI




CONTRAVEN

# Keynote Papers

International Symposium Polymers in Concrete
2 - 4 April 2006
Guimarães, Portugal

# Cement concrete and concrete-polymer composites: two merging worlds A report from 11th ICPIC Congress in Berlin, 2004

D. Van Gemert[1], E. Knapen[2]

*Katholieke Universiteit Leuven, Leuven, Belgium*

L. Czarnecki[1], P. Łukowski[1]

*Warsaw University of Technology, Warsaw, Poland*

## ABSTRACT

The International Congresses on Polymers in Concrete (ICPIC) organises practitioners and scientists, dealing with concrete-polymer composites in all industrial fields, but with emphasis on construction industry. The 11th ICPIC took place in Berlin, 2-4th June 2004. New trends and evolutions have been presented and discussed. The highlights of the Congress, and the synergies that emerge from the congress for the construction world in combination with cement concrete, will be discussed in this paper. One of the research topics of the 11th ICPIC is the modelling of the microstructure building of concrete-polymer composites. The integrated Beeldens-Ohama-Van Gemert model for microstructure building in polymer cement concrete is presented. Other promising research topics are the study of mortars modified with water-soluble polymers and hardener-free epoxy-modified mortars. At the 11th ICPIC, a lot of new applications of concrete-polymer composites are proposed, e.g., the use of preplaced aggregate epoxy concrete for the structural enhancement of deteriorated beams, the use of polymer-modified porous cement mortars as sound absorbing materials, the reuse of glass waste in polymer mortars and the polymeric impregnation of textile rovings in textile reinforced concrete to improve the tensile strength and strain at failure.

## 1. INTRODUCTION

The International Congresses on Polymers in Concrete (ICPIC) aim to create a synergy between researchers and practitioners all over the world, dealing with the spectacular possibilities of concrete-polymer composites. During the 3 decades from the first congress in London in 1975 to the eleventh congress in Berlin in 2004 (Maultzsch 2004), there have been dramatic changes in the way of thinking about industrial processes and the approach and evaluation of new and innovative materials.

[1] Professor
[2] Research Assistant

In the industrialised world, the sixties and seventies of last century were characterised by an unlimited belief in new and modern materials and techniques. The use of polymers was considered to be a sign of progress and modern attitude in construction and in industry. Glass fibre reinforced polyester panels, polyester resin and polyester mortar were known as inexpensive plastics. Epoxy glues were used as highly performing adhesives in concrete prefabricated applications, epoxy resins were used as binders in chemically resistant coatings and flooring systems as well as in electrical insulation applications, acrylic resins were used in machine frame construction. Research aimed at developing new, improved polymers was continuously done, and new applications for polymers and concrete-polymer composites (CPC) were constantly developed. In building industry the use of polymers gradually extended from concrete crack injection to repair mortars for concrete and stone, consolidation of masonry, repair of timber structures, not to forget all finishing, piping and waterproofing materials. At that time, building materials science was an underdeveloped field of construction industry and science. Therefore, the extended use of pure polymers led to inherent chemical and physical incompatibility problems, mechanical malfunctioning and durability problems.

In the early seventies the oil crises learned that mineral oil as a cheap basis for polymer production was not longer available. It was also found that oil reserves were limited. As a consequence all uses of fossil resources were questioned. First of all the waste of fossil oil for energy production, and secondly the massive use of polymers as alternative for classical building materials such as concrete, masonry, timber and metals. The use of polymers became part of a search for durable and sustainable construction materials. Polymers should only be used in these areas were their specific properties are needed. The synergetic action between polymers and classical construction materials offers great opportunities for improvement and a wide range of new and innovative properties and applications of e.g. polymer modified repair mortars for concrete, stone and masonry. Pure polymer concrete building components can be partly replaced by CPC, as in flag-stones and building panels. A better knowledge of materials behaviour, especially in the field of admixtures, and a better understanding of curing processes allowed the development of highly performing mineral or modified mineral concretes, mortars and grouts. CPC-science is now an invaluable element in the development of sustainable construction materials.

The topics of the 11th ICPIC Congress reflect new approaches and findings in CPC-research. The micro-structural models are subject to changes, polymers in solution are subject of research and might become valuable alternatives for polymer emulsions and polymer dispersions, biological effects are taken into account in degradation processes but might also be turned into positive performance contributions. Sustainability, and reversibility and recycling as subtopics of it, dominate the developers' minds. The scientific program of the congress was managed by BAM, the Federal Institute for Materials Research and Testing (Germany), in collaboration with Warsaw University of Technology (Poland) and Katholieke Universiteit Leuven (Belgium).

## 2. IMPORTANCE OF POLYMERS IN EUROPEAN CONSTRUCTION INDUSTRY

During the European Colloquium Orgagec '02 organised by Laboratoire Central des Ponts et Chaussées in Poitiers, France, in March 2003, M. de Longcamp presented figures of consumption of polymers in the European Union (15 members; 330 million inhabitants) in 2000 (de Longcamp 2002). Some data for the largest components in polymer consumption are listed in Table 1.

Table 1 - European consumption of polymers in construction

| Application field | Type | Consumption |
|---|---|---|
| Textiles in architecture | Polyester/glass<br>PVC/polyester<br>Carbon/Kevlar | 28 000 tons<br>100 000 tons<br>Not significant |
| Highway noise barriers | System concrete-timber<br>Recycled plastic<br>Transparent plastics<br>Concrete<br>Timber<br>Metal<br>Vegetation screens | ± 30 %<br>± 2 %<br>± 5 %<br>± 10 %<br>± 15 %<br>± 10 %<br>± 10 %<br>Total 1.970.000 m², 15 % increase/year |
| Impermeable membranes | PVC<br>PE (HD + LD)<br>EP, PU, UP resins<br>SBS, APP bitumen modif. | 200 000 tons<br>250 000 tons<br>50 000 tons<br>88 000 tons |
| Road paintings | Liquid, hot melt, strips | 280 000 tons |
| Tubing for optical fibres | PEHD | 200 000 tons (2001)<br>600 000 tons (exp. 2010) |
| Tubes for sewers, gas, water… | PVC, PE, PP, UP | 2 761 000 tons |
| Concrete modification | | 486 000 tons |

On average about 8 % of polymer consumption concerns thermosets, the rest being thermoplasts (Commission of European Community 1999). In 2003, 7 350 000 tons or 18.5 % of the total market of polymers in Western Europe (European Union, Norway and Switzerland) were used in building and construction industry (Plastics Europe 2004). The relation to other industries is shown in Table 2.

Table 2 - Polymer consumption by industry in Western Europe (2003) (Plastics Europe 2004)

| Industry | Polymer consumption (%) |
|---|---|
| Packaging | 37.2 |
| Construction | 18.5 |
| Large Industry | 5.8 |
| Electrical/Electronic | 8.5 |
| Other Household/Domestic | 20.1 |
| Automotive | 8 |
| Agriculture | 1.9 |

However, if the consumption of polymers is compared to the consumption of other construction materials, its relative share is only about 1 % (Table 3). The share in weight is only about 1 %, but in financial turnover polymers represent more than 10 % of construction industry. It is expected that in about 10 to 15 years polymers in construction will be the prime part of the polymer market. The amount of polymers used in concrete-polymer composites, is only a minor part in polymers for modification of concrete, which also include water reducing agents (121500 tons of superplasticizer in EU in 1998). However, due to the synergetic action

between polymers and the cementitious matrices, the impact on performance of building materials largely overpasses the weight ratio.

Table 3 - Relative share of building materials in EU-construction industry (year 2000)

| Construction material | Consumption (tons) | Ratio (%) |
|---|---|---|
| Concrete and cement based | 503 000 000 | 71 |
| Tiles and bricks | 73 000 000 | 10 |
| Timber | 54 000 000 | 7 |
| Iron and steel | 24 000 000 | 3 |
| Stone, quarry | 16 000 000 | 2 |
| Asphalt and bitumen | 16 000 000 | 2 |
| Polymers | 6 850 000 | 0,97 |
| Flat glass | 5 200 000 | 0,73 |
| Mineral wool | 2 000 000 | 0,3 |
| Copper | 1 300 000 | 0,2 |
| Aluminium | 900 000 | 0,1 |

The Construction Products Directive 89/106/EEC (CPD) defines the essential requirements for construction products as follows:

1. Mechanical resistance and stability
2. Safety in case of fire
3. Hygiene, health and the environment
   - dangerous substances
   - global environment impact
4. Safety in use
5. Protection against noise
6. Energy economy and heat retention

The European Legislation assumes that a producer is responsible for knowing and complying with all applicable legislation. This is a difficult area, because up to now only national regulations exist, and chemicals and dangerous substances are also dealt with by several DGs (Directorate General), e.g., DG Enterprise, DG Environment, DG Agriculture, DG Health, DG Consumer Protection, etc. The European Commission for Standardisation CEN is now harmonising the regulations and a database on dangerous substances regulations is available (Argüelles 2002).

With respect to global environment impact, the European Union is striving at an integrated product policy, to reduce the environmental impact of the whole life cycle of products. The Union will use market forces efficiently to reach environmental policy objectives, in a way that prices should reflect also the environmental costs, demand should be more oriented towards ecological products, and supply should adapt and even promote ecological products.

All developments in using concrete-polymer composites should take into account this policy of the European Union. As engineers, we tend to stress on most of the 6 essential requirements of the construction products directive, but we have to admit that our interest in the 3rd one for hygiene and health is rather limited, presumably because of lack of knowledge in the field. Producers and construction engineers will have to collaborate with the medical world, to meet also those essential requirements.

## 3. CONCRETE-POLYMER COMPOSITES

Polymer modified concrete or mortar is a composite material consisting of two solid phases: the aggregates which are discontinuously dispersed through the material and the binder which itself consists of a cementitious phase and a polymer phase. According to the volume fraction of the polymer in the binder phase the material shifts from PCC, i.e., polymer cement concrete, to PC, i.e., polymer concrete.

In the case of PCC, the binder consists of a polymer-cement co-matrix. The polymer is added to the fresh mixture as dispersion or as redispersible polymer powders. During hardening and curing cement hydration and polymer film formation take place resulting in a co-matrix in which polymer film is intermingled with cement hydrates.

A special group of materials in which polymers are used in combination with concrete is PIC, polymer impregnated concrete. Here, low-viscosity monomers are injected in the pores of the hardened concrete and subsequently polymerized. The resultant polymers form a second matrix if the pores are interconnected throughout the material. The hardened concrete may be a cement concrete, a PCC or a PC. The properties of the composite material derive not only from its constituents, but there is also a synergetic effect.

Applications of concrete-polymer composites cover a wide range of applications in different industries: concrete and stone repair materials; polymer modified cement adhesives; prefabricated building components like flag stones, tubes, panels; porous and eco-concrete; machine base elements; insulators for electrical and chemical industry; fibre reinforced materials; chemically resistant materials; industrial floors; recycling of polymer wastes; liquid applied waterproofing materials …

## 4. INTEGRATED MODEL FOR MICROSTRUCTURE BUILDING IN POLYMER CEMENT CONCRETE (Beeldens 2004)

Cement hydration in polymer modified material is influenced by the presence of polymer particles and polymer film in the fresh state, during hydration as well as in the hardened state. The properties of the fresh mixture are influenced to a large extent by the surfactants, present at the surface of the polymer particles. The cement particles are better dispersed in the mixture and a more homogeneous material is formed. The hydration of the cement is reflected in the strength evolution of the material.

The influence of the polymer modification is twofold. Due to the presence of the polymers and the surfactants, a retardation of the cement hydration can be noticed. This is especially visible in the compressive strength of the mortar beams. On the other hand, due to the film formation or due to the interaction between the cement hydrates and the polymer particles, the tensile strength of the binder matrix as well as the adhesion strength between the aggregate and the binder increase. This is especially seen in the flexural strength of the mortar beams. The results are presented in (Beeldens 2002, Beeldens 2003, Beeldens 2005).

From the results of the compressive strength and flexural strength tests, conclusions towards film formation mechanism and especially towards the time at which film formation takes place may be drawn. After 7-day dry curing, the flexural strength is increased in relation to the strength of the unmodified mortar. Nevertheless, the cement hydration is retarded when the polymer-cement ratio is increased, illustrated by a decrease of compressive strength. This points at the existence, already at an early stage of curing, of a polymer film or at least at the interaction between polymer particles and cement particles. However, the incapacity of modified “porous” mortar specimens to overcome the large shrinkage stresses after 7-day or 28-day moist curing indicates that the continuous polymer film is not yet formed in the case of water saturated conditions. This was found from adhesion tests of the mortar phase on the

aggregates after 7, 28 and 56 days (Beeldens 1999). No influence of the polymer modification on the flexural strength is noticed in the case of standard cured and water cured samples as long as no dry curing period is applied.

Accordingly, one may conclude that at high relative humidity, the influence of polymer modification on the flexural strength at short term is limited. From the moment a dry curing period is introduced, a polymer film starts to build up through the binder phase and an increase in flexural strength is observed with increasing polymer-cement ratio. The influence on the flexural strength of the retardation of the cement hydration is compensated by the presence of the polymer film. When long-term behaviour is considered, a maximum of flexural strength is established around a polymer-cement ratio of 15 %.

The mutual influences between the cement hydrates and the polymer particles and film are incorporated in an integrated model of structure formation. The model is based on the three-step model as proposed by Ohama (Ohama 1995), but stresses the positioning of the mechanisms on the time scale and the interaction between the different components. The findings are supported by images taken with an environmental scanning electron microscope at the University of Dresden (Schorn 2001).

The formation of the polymer film can take place from the moment two polymer droplets have sufficient energy to overcome the repulsion forces originating from the surfactants. In other words, if the temperature is high enough to cause sufficient Brownian motion, or if additional forces are working on the liquid layer around the polymer droplets, such as capillary forces or water withdrawal by further cement hydration, two droplets can come close to each other and can coalesce into each other and a polymer film is formed. This process simultaneously can take place with the cement hydration mechanism, especially in the case of dry curing conditions. Therefore, partial or full encapsulation of the cement hydrates is possible, which retards the hydration process. The different steps of the conclusive model are presented in Figures 1 to 4.

Immediately after mixing, the cement particles and polymer particles are dispersed in the water. The first hydration of the cement takes place, which results in an alkaline pore solution. This is indicated as Step 1, Figure 1.

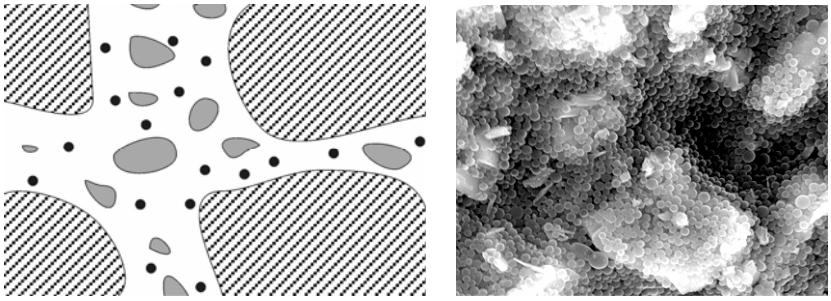


Figure 1 - Step 1, immediately after mixing, aggregates, cement particles, polymer particles and mixing water – small ettringite needles are formed

The second step is presented in Figure 2. A portion of the polymer particles is deposed on the surface of the cement grain and the aggregate. The polymer-cement ratio determines the amount of polymers present in the pore solution and present at the aggregate surface. Part of the polymer particles may coalesce into a continuous film. This preferably takes place at the surface of the cement hydrates where extra forces are exerted on the polymer particles due to the extraction of water for cement hydration. The polymer film can partly or completely envelop a cement grain, which results in a retardation or even a complete stop of the hydration of the cement grain.

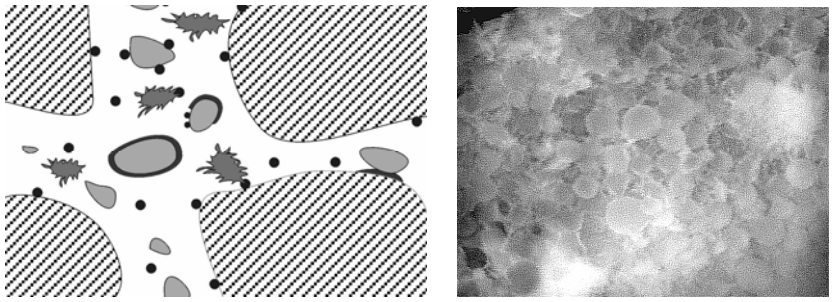


Figure 2 - Step 2, after mixing, the polymer particles interact with the cement particles and the aggregates. In the case a dry curing period is introduced, a continuous film may be formed – polymer particles flocculate together, on restricted places, no coalescence has taken place at this stage

The following step, Figure 3 consists of cement hydration, polymer flocculation and possibly polymer coalescence into a film. The processes that take place depend on the curing conditions. If no dry curing period, i.e., curing at a lower relative humidity, is included, the overall film formation is retarded and the influence on the properties of the fresh mixture is limited at this stage. If a dry curing period is included, polymer film formation takes place during this step, which influences the cement hydration process as well as the strength development at early ages. In the bulk liquid phase, hydrates are present, which form a combined inorganic and organic product. The fractions of the different types of product formed depend on the polymer/cement ratio used. The polymer fractions included in these hydration products do not contribute to the strength development of the specimen (Tabor 1997).

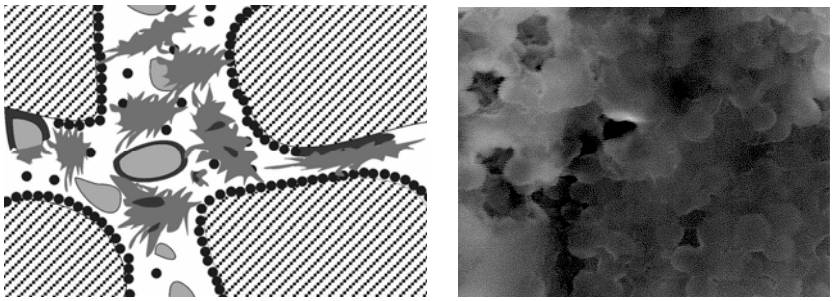


Figure 3 - Step 3, cement hydration proceeds, polymer film formation starts on specific spots – polymer particles coalesce together into a continuous film

The final step (Figure 4) includes further hydration and final film formation. Through the cement hydrates, a continuous polymer film forms as water is further removed from the pore solution. The part of the polymer particles, that is still present in the dispersion, is restricted to the capillary pores and at the interface of the aggregates and the bulk polymer-cement phase. It is this part which contributes the most to the elastic and final strength properties. The continuity of the polymer phase through the binder matrix is more pronounced in the case of a higher polymer-cement ratio. In the case the MFT of the polymer dispersion is much more elevated than the curing temperature, the polymer particles may not coalesce into a continuous film, but remain as closely packed polymer particles.

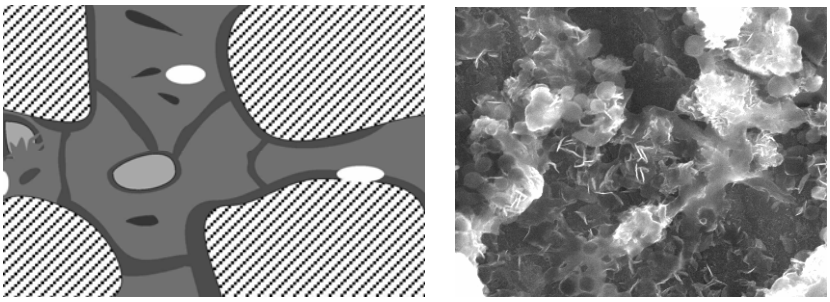


Figure 4 - Final step, cement hydration continuous, the polymer particles coalesce into a continuous film – cement particles are hydrated

The use of the integrated Beeldens-Ohama-Van Gemert model can be illustrated with the different curing conditions. From the results, it is concluded that optimal conditions towards the strength development are a wet curing period followed by a dry curing period. The longer the moist and water curing period is, the higher the final flexural strength will be if shrinkage is prevented and if a curing period at lower relative humidity is introduced. This means that first cement hydration takes place and only limited film formation. Therefore, the polymer particles remain in the pore solution and a larger amount of polymer particles will be incorporated into the continuous film, which is formed in the final stage. If the drying period is introduced earlier in the process, the film formation will start sooner, i.e., before and simultaneously with the cement hydration, resulting in enlarged encapsulation of the cement hydrates as well as incorporation of the polymer phase in the hydration product precipitated from the pore solution.

The relative humidity of the surrounding atmosphere has a large influence on the film formation and especially on the drying rate. The higher the relative humidity of the surrounding atmosphere, the lower the drying rate becomes. This influences to a large extent the film-forming temperature of the dispersion. The lower the drying rate, the lower the amount of energy needed for the polymer particles to coalesce into a continuous film. Therefore, the minimum film-forming temperature (MFT) is reduced with a reduced drying rate. Tests indicated that even at laboratory circumstances, i.e., 20°C, a poly(styrene-acrylic ester) (SAE) dispersion with a MFT of 32°C, could form a continuous film, as long as the drying rate was low enough.

The cement hydration is also influenced by the fact that water is longer retained due to the presence of the surfactants at the surface of the polymer particles. This results in a better dispersion of the polymer particles and the cement hydrates, but also retards the cement hydration. The influence increases with increasing polymer-cement ratio.

This model accentuates two important changes towards the original model of Ohama. First of all, a relation to the time scale of the different processes is made. When a dry curing period is included, cement hydration and polymer film formation coincide and encapsulation of cement particles is possible. Further, the formation of an interstitial phase, consisting of inorganic and organic precipitates in the bulk phase is pointed out. This is important towards an optimal benefit of polymer modification since the polymers present in this phase are contributing less to the final properties of the material. The optimum conditions come forward from these findings, i.e., a long period of water or moist curing (up to 28 days) during which the cement hydrates develop followed by a period of curing at lower relative humidity during which the polymer film formation is promoted.

## 5. POLYMERS AS MICROCRACK STOPPER IN CEMENT CONCRETE (Schorn 2004)

At the Building Materials Institute of Technical University of Dresden, the new technology of environmental scanning electron microscopy is being used in combination with a specially developed loading device, that allows to apply tensile load on small specimen inside the microscope chamber. They are now able to show the effects of microcrack propagation in the loaded specimen. Opening increase of microcracks can be followed and investigated from a width of about 300 nm up to about 20 µm, allowing to study the behaviour of all the particles, which are broken by the crack. Especially the polymer action as microcrack stopper can be observed by visualization of the stretching of the polymer particles over the microcrack.

The power of this innovative investigation technique can be illustrated with some pictures of a microcrack in a polymer cement concrete, with a polymer-cement ratio of 30 %, at consecutive crack widths during tensile loading. Not only the crack bridging effect can be seen, but also the moment of rupture of the polymer bridges can be observed (Figure 5). This investigation technique provides spectacular features for the study of hydration and hardening reactions, and for the study of polymer-cement hydrate interactions.

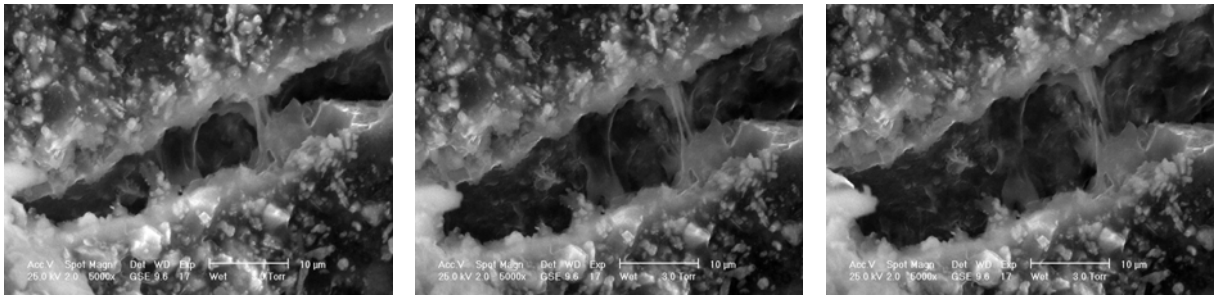


Figure 5 - Crack bridging behaviour of polymers in concrete, maximum crack width ~ 9 µm (left), 11 µm (middle) and 13 µm (right)

## 6. RESULTS AND EXPECTATIONS OF 11th ICPIC

The novelties and significant progress, reported at the 11th ICPIC Congress in Berlin, are summarized in Table 4. The paper number refers to the reference number of the paper in the proceedings (Maultzsch 2004). For each topic, we gave our appreciation of the relevance field, or the state of progress of the matter.

Two fundamental research topics of the 11th ICPIC are the study of mortars modified with water-soluble polymers and that of hardener-free epoxy-modified mortars. Knapen et al. discuss in paper 11 (Knapen 2004a) the problems that are generated by the presence of surfactants at the surface of polymer particles in polymer dispersions. The cement hydration is retarded and the polymer film formation is disturbed. Furthermore, the surfactants cause an excessive air entrapment during mixing. One of the major advantages of water-soluble polymers is the absence of surfactants. The polymer molecules are supplied on a molecular scale, improving the approximation of the relatively large cement grains by the polymers. Film formation on the hydrate crystals may proceed more easily and a lower amount of polymers may be needed to modify mortars. The second topic is studied by Ohama et al. in paper 30 (Ohama 2004), i.e. epoxy-modified mortars without hardener. The authors found that, even without any hardener, epoxy resins are able to harden in the presence of hydroxide ions, produced by the hydration of cement. At ambient temperature, the hardening rate of the

hardener-free epoxy resin is low. It is shown that accelerated curing conditions, e.g. autoclaving or steam curing followed by heat curing, result in a high-strength development.

Table 4 - Novelties and significant progress, reported at 11th ICPIC, Berlin 2004

| Description | Reference | Paper No. | Test method | Research | Applica-tion |
|---|---|---|---|---|---|
| 1. Integrated model | Beeldens et al. | 1 | | + | |
| 2. Nanomonitoring | Schorn et al. | 2 | | + | |
| interfaces | Benzarti et al. | 67 | | + | |
| 3. Soluble polymer modifiers | Knapen et al. | 11 | | + | |
| 4. Slag PCC | Joo, Ohama et | 13 | | | + |
| Fly ash PCC | al. | 60 | | | + |
| | Jolley, Kruger | | | | |
| 5. Ultrasonic evaluation methods | Garbacz | 15 | + | | |
| 6. Profilometry and surfometry analysis | Courard et al. | 16 | | + | |
| 7. CPC standardization | Ohama | 18 | | | + |
| 8. Sound absorbing materials | Knapen et al. | 24 | | | + |
| 9. Quantification of synergy | Czarnecki et al. | 25 | | + | |
| 10. High strength ECC without hardener | Ohama et al. | 30 | | + | |
| 11. Ultra-lightweight polymer concrete | Sung et al. | 35,36 | | | + |
| 12. GFRP-PC | San-José et al. | 37 | | | + |
| 13. Electrical insulators | Gunasekaran | 40,41 | | | + |
| 14. Preplaced aggregate epoxy concrete | Murray | 43 | | | + |
| 15. Ecological coatings | Erkens et al. | 44 | | | + |
| 16. Optimization thin overlays | Šušteršic | 54 | | | + |
| 17. Textile reinforced PCC | Dilthey et al. | 58 | | | + |
| 18. Waste reuse | Bignozzi et al. | 72 | | | + |
| 19. Intelligent PC | Blair et al. | 31 | | + | |
| 20. FRP strengthening | Frigione et al. | 61 | | | + |
| | Ignoul et al. | 63 | | + | + |
| | Byun et al. | 64 | | + | + |
| 21. Admixtures | Pourchez et al. | 69 | | + | |
| | Grübl et al. | 75 | | + | |

At the 11th ICPIC, a lot of new applications of concrete-polymer composites are proposed. Knapen *et al.* (paper 24 (Knapen 2004b)) studied the sound absorption by polymer-modified porous cement mortars. Having a high sound absorption coefficient and a high structural strength, these materials can be an alternative for the more conventional sound absorbing materials and contribute to a sustainable construction development and to an

improvement of acoustic conditions. Murray discusses the use of preplaced aggregate epoxy concrete for the structural enhancement of deteriorated beams in paper 43 (Murray 2004). After removal of the deteriorated concrete and cleaning of the reinforcing steel, the cement concrete is replaced with epoxy concrete with preplaced aggregates. Not only the original load carrying capacity is re-established, also any further corrosion activity is stopped in the repaired section. Dilthey *et al.* (paper 58 (Dilthey 2004)) deal with the possibility to improve the technical characteristics of textile reinforced concrete by polymeric impregnation of the rovings and by addition of polymers to the fresh concrete. The impregnation of the rovings improves the tensile strength and strain at failure due to the improved load transmission between the single filaments. This impregnation is combined with polymer modification of the cement concrete itself, increasing the strength of the concrete components even further. Bignozzi *et al.* consider the reuse of glass waste in polymer mortars in paper 72 (Bignozzi 2004). Fine glass fillers are obtained by vitrification of bottom ashes collected from incineration of urban solid wastes or derived from glassy and ceramic fractions obtained by the treatment of separated waste collection. Glass fibres, prepared by drawing waste made glasses, act as reinforcement of the materials. In terms of performance, these new composite materials appear to be promising and competitive with those usually used in the building industry. Further investigations are necessary to verify the environmental sustainability and feasibility of the entire process.

## 7. CONCLUSIONS

The use of polymers in construction industry is steadily growing. The synergetic action of polymers and cement mortar and concrete offers great opportunities for improvement and a wide range of new and innovative applications. Society and environment require corrective actions to be taken continuously. The use of polymers should be well-considered to guarantee better performance and improved sustainability.

Polymers are no longer special construction materials that replace classical mineral or organic building materials. They are now one vital component in the production of composite and sustainable building materials. They will further allow the development of new and durable constructions, as well as new and durable restoration and retrofitting techniques.

## 8. REFERENCES

Argüelles, V., Environmental and health aspects in the European Construction Products Directive, in: *Proceedings European Colloquium Orgagec '02*, 13-15 March 2002, Poitiers, Paris: LCPC (2002).

Beeldens, A. and Van Gemert, D., Paste-Aggregate Adhesion in Polymer-Cement Porous Concrete, in: *Proceedings 2nd International RILEM Symposium ISAP'99*, Dresden, Ed. by Y. Ohama and M. Puterman, vol PRO9, 93-102 (1999).

Beeldens, A., *Influence of polymer modification on the behaviour of concrete under severe conditions*, PhD dissertation, Faculty of Engineering, Katholieke Universiteit Leuven (2002).

Beeldens, A., Van Gemert, D., Ohama, Y. and Czarnecki, L., Integrated model of structure formation in polymer modified concrete, in: *Proceedings of the 11th International Congress on the Chemistry of Cement*, 11-16 May 2003, Durban (2003).

Beeldens, A., Van Gemert, D., Schorn, H. and Ohama, Y., Integrated model for microstructure building in polymer cement concrete, in: *Proceedings of the 11th Congress on Polymers in Concrete*, Ed. by M. Maultzsch, BAM, Berlin, 1-10 (2004).

Beeldens, A., Van Gemert, D., Schorn, H., Ohama, Y. and Czarnecki, L., From microstructure to macrostructure: an integrated model of structure formation in polymer modified concrete, in: *RILEM International Journal, Materials and Structures*, **38 (280)**, 601-607 (2005).

Bignozzi, M.C., Saccani, A. and Sandrolini, F., Glass waste valorization in advanced composite materials, in: *Proceedings of 11th Congress on Polymers in Concrete*, Ed. by M. Maultzsch, BAM, Berlin, 587-596 (2004).

Commission of European Community DG XI. Financial costs of plastics marking. Final report, Website: http://europa.eu.int/comm/enterprise/construction/index.htm (1999).

de Longcamp, M., Réalités économiques des polymères dans la construction, in: *Proceedings European Colloquium Orgagec '02*, 13-15 March 2002, Poitiers, Paris: LCPC (2002).

Dilthey, U., Mund, F., Raupach, M., Schleser, M. and Walk-Lauffer, B., Improvement of textile reinforced concrete by polymer additives, in: *Proceedings of 11th Congress on Polymers in Concrete*, Ed. by M. Maultzsch, BAM, Berlin, 469-476 (2004).

Knapen, E., Beeldens, A., Van Gemert, D. and Van Rickstal, F., Modification of cement concrete by means of polymers in solution, in: *Proceedings of 11th Congress on Polymers in Concrete*, Ed. by M. Maultzsch, BAM, Berlin, 83-90 (2004a).

Knapen, E., Lanoye, R., Vermeir, G., Lauriks, W. and Van Gemert, D., Sound absorption by polymer-modified porous cement mortars, in: *Proceedings of 11th Congress on Polymers in Concrete*, Ed. by M. Maultzsch, BAM, Berlin, 191-200 (2004b).

Maultzsch, M., *Proceedings of the 11th Congress on Polymers in Concrete*, Ed. by M. Maultzsch, BAM, Berlin (2004).

Murray, M., Beam repair with preplaced aggregate epoxy concrete, in: *Proceedings of 11th Congress on Polymers in Concrete*, Ed. by M. Maultzsch, BAM, Berlin, 345-348 (2004).

Ohama, Y., *Handbook of polymer-modified concrete and mortars, properties and process technology*, Park Ridge, New Jersey: Noyes Publications (1995).

Ohama, Y., Kumagai, S. and Miyamoto, Y., High strength development through accelerated curings of epoxy-modified mortars without hardener, in: *Proceedings of 11th Congress on Polymers in Concrete*, Ed. by M. Maultzsch, BAM, Berlin, 239-246 (2004).

Plastics Europe, An analysis of plastics consumption and recovery in Europe 2002&2003 (2004).

Schorn, H. and Schiekel, M., Shape and distribution of polymer particles in PMC – Investigated by Environmental Scanning Electron Microscope (ESEM), in: *Proceedings of the 10th International Congress on Polymers in Concrete*, Hawaii (2001).

Schorn, H., Butler, M. and Hempel, S., Polymers as microcrack stopper in concrete observed in ESEM, in: *Proceedings of the 11th Congress on Polymers in Concrete*, Ed. by M. Maultzsch, BAM, Berlin, 11-18 (2004).

Tabor, L.J., Dispersed polymers, revision of concrete society technical report no.9 - polymer concrete, chapter 7. *Contribution to the Fifth International Congress on Polymers in Concrete*, Brighton, 83-94 (1987).

International Symposium Polymers in Concrete
2 - 4 April 2006
Guimarães, Portugal

# Essential Concrete-Polymer Composites

Lech Czarnecki[1]

*Warsaw University of Technology, Faculty of Civil Engineering, Warsaw, Poland*

ABSTRACT

Several questions: "what we already know and what we need to know on C-PC and how could we define the C-PC trends" have been put on the beginning of the paper. They were the inspiration for a brief overview of the history, technical characteristics and possibilities of C-PC. The object of the study in short definitions has been described and classified. The C-PC profile in the framework of internet and in the light of the European White Book on Fundamental Research in Material Science has been presented. The meaning of "polymer better concrete" as well as "how polymer improves the concrete" has been explained. The lesson from the C-PC history, particularly from the output of the eleven International Congresses has been analysed. The novelties and significant progress have been presented. The development trends have been defined on the C-PC research map as well as the ways and means how to try to do that. The main research categories for future development have been established.

## 1. INTRODUCTION

International Symposium on Polymers in Concrete offers:
- a forum for discussion and transfer of technology,
- exchange of experiences and opportunity for training for newcomers, as well as opportunity to encourage research and development,
- learn and meet regional needs.

The expectations involved with the ISPIC are creation a climate for spontaneous scientific progress and innovation and development of application in the Concrete-Polymer Composites area. This means that such an event should bring to us sum up of the present status of C-PC – what we already know and what we need to know and first of all: how we could define the future trends?

What does it mean essential towards Concrete-Polymer Composites (C-PC) and what is essential in Polymers in Concrete? How could we present C-PC in essence?

[1] Ph.D., D.Sc., professor

C-PC are the result of implementation the modern polymers into the traditional concrete technology. In less than one century, concrete has become the most widely used construction material over the world (Fig. 1). According to some expectations, domination of concrete and growth of use of polymers shall be the main factors of building materials development in the near future (Fowler, 2001). "Essential" means also something basic, something necessary or even inevitable and those terms precise the C-PC among construction materials. However, "essential" means not only "of the utmost importance, basic" but also "consisting the intrinsic fundamental nature of something". This approach gives us further questions:

- for what polymers in concrete?
- what are Concrete-Polymer Composites? Polymers alone or together with portland cement:
  - as admixture,
  - as co-matrix?
- how to evaluate the efficiency of the polymer application?
- how to create/use synergy between polymer and other ingredients of concrete?
- how does polymer improve concrete – how it works?
- what could we learn from the C-PC history; how C-PC make progress?
- how could we go from better understanding of the material nature to more rational application/eco-application?

Of course, it is difficult or even impossible to answer to all questions in the brief overview, however even the recognition what are we searching for could be the source of an inspiration.

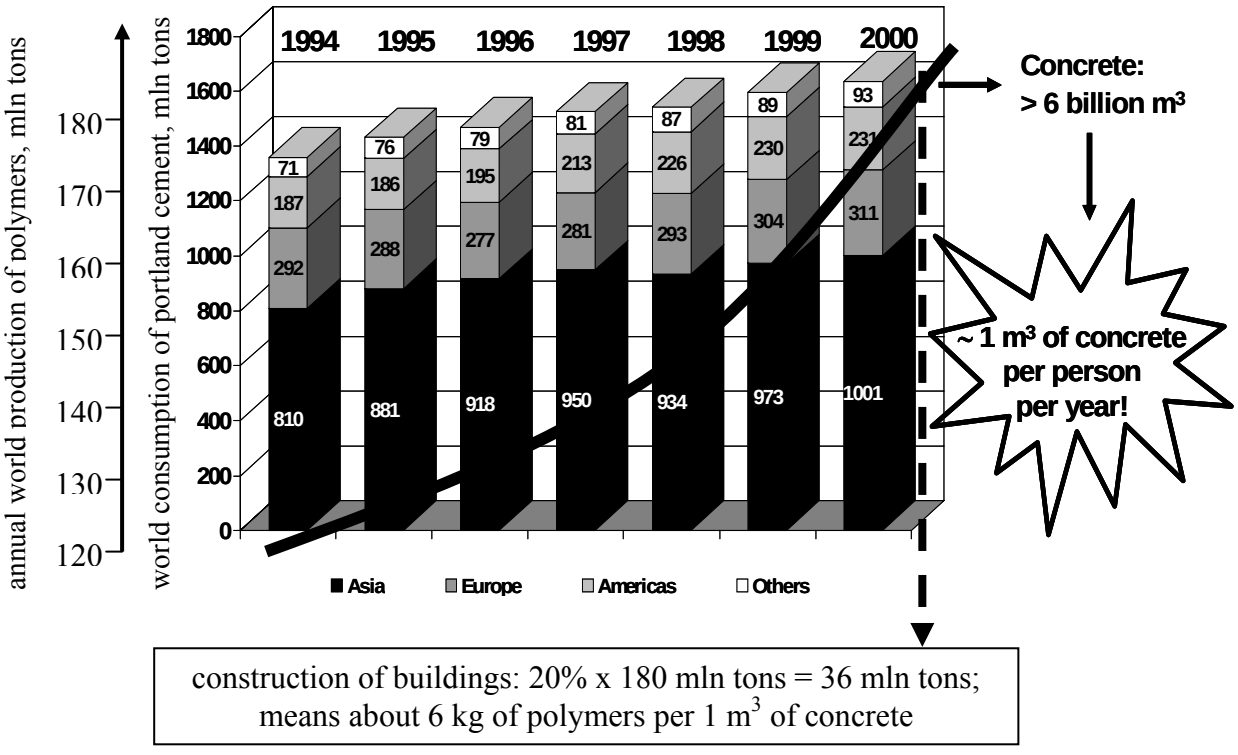



Fig. 1 – World consumption of portland cement, concrete and polymers in building industry

## 2. BASIC DEFINITIONS

There are two superior terms (Czarnecki, 2005):

- **Composite** is any solid, polyphase material with: 1) phases that cannot be mutually transformed into each other by any treatment, 2) properties that are not attainable by any one of its constitutive phases alone, and 3) properties that are not attainable by the simple sum of its constitutive phases, and
- **Concrete** is a composite material that consists essentially of a binding medium within which are embedded particles or fragments of aggregate, usually a combination of fine aggregate and coarse aggregate; in portland cement concrete, the binder is a mixture of portland cement and water, with or without admixtures.

In the broadest meaning C-PC are the concretes containing polymers. Polymers could be implemented into fresh concrete mix or into hardened portland cement concrete in the form of complete polymer (**pre-mix** polymerised latexes – elastomers or thermoplastics) or chemically reactive synthetic resins – prepolymers or monomers that may be subjected to polymerisation or polycondensation (**post-mix** polymerised) by thermocatalytic or other systems. Depending on the chemical nature of the polymers and other components, their contents and manufacturing process, an infinite number of different products can be manufactured (Fig. 2). There is great number of polymers used as concrete admixtures and additives (Table 1). High-range water-reducing admixtures are sulfonated melamine-formaldehyde resins and naphtalene-formaldehyde resins, co-polymers of formic acid with sulfonated naphtalene acid or co-polymers of metacrylic acid with polyethylene glycol. New generation of superplasticizers are polycarboxysilanes and co-polymers of acrylic acid with acrylates. The most often used pre-mix polymer additives are polyacrylic esters (PAE), styrene-butadiene rubber (SBR), polyvinyl alcohol (PVA) as well as co-polymers of styrene with butadiene (SB), styrene with acrylic esters (SAE) and ethylene with vinyl acetate (EVA). The basic – and almost only used – post-mix polymer modifier for concrete is epoxy resin (EP).

For making the polymer concretes the epoxy, acrylic and polyester (vinylester) resins, rarely furane or phenol resins, are used. There are few materials used for producing of the polymer impregnated concretes; they are usually acrylic or styrene-acrylic monomers, seldom epoxy resins of low viscosity.

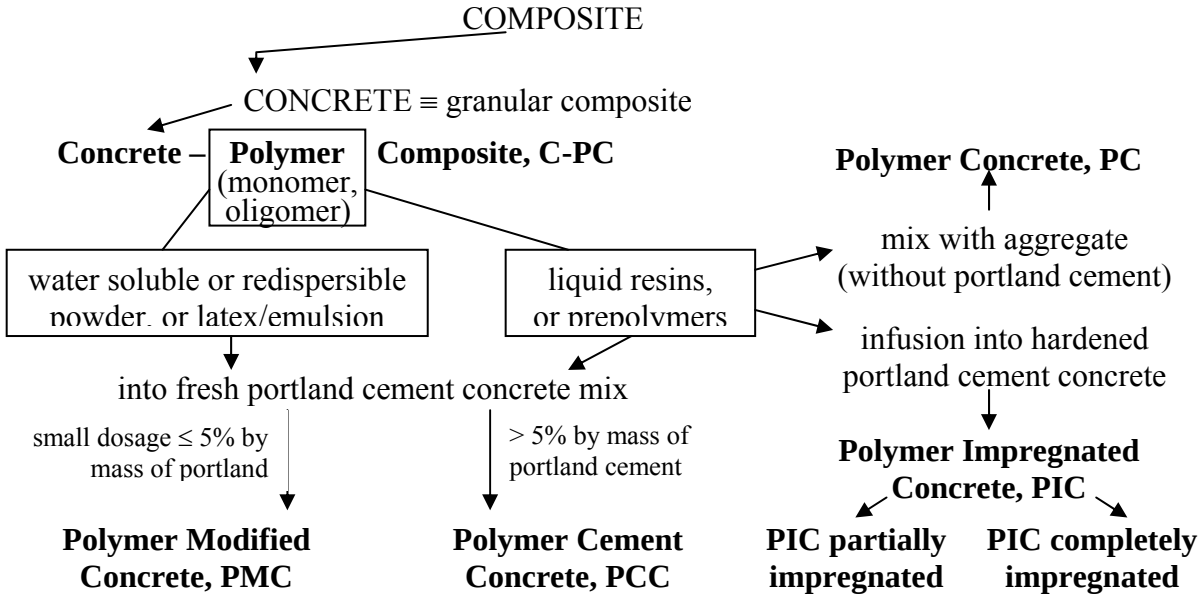
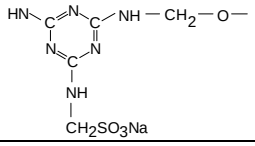
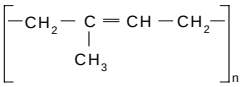
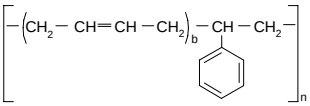
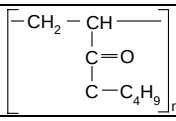
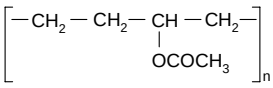
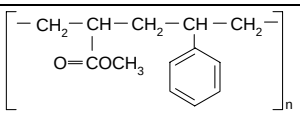
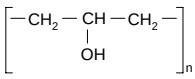
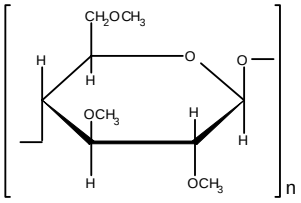
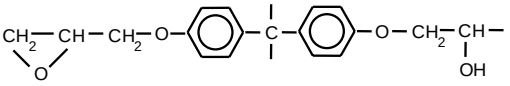
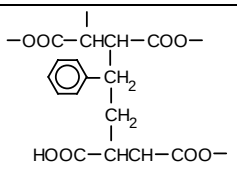
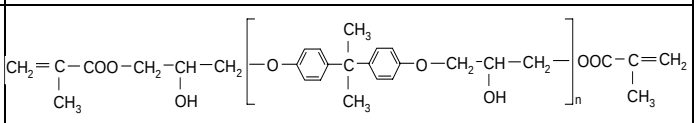
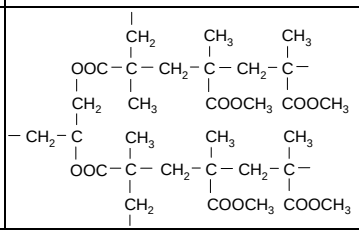



Fig. 2 – System of Concrete-Polymer Composites

Table 1 – Polymers often used in concrete-polymer composites (Czarnecki, Łukowski, 2005)

| Polymer / C-PC type | Chemical formula |
|---|---|
| Sulfonated melamine-formaldehyde resin / PMC |  |
| Natural rubber / PCC |  |
| Butadiene-styrene rubber / PCC |  |
| Buthyl polyacrylate / PCC |  |
| Co-polymer of ethylene with vinyl acetate / PCC |  |
| Styrene-acrylic co-polymer/ PCC |  |
| Polyvinyl alcohol / PCC |  |
| Methylcellulose / PCC |  |
| Epoxy resin / PCC, PC |  |
| Polyester resin / PC |  |
| Vinylester resin / PC |  |
| Acrylic resin / PC |  |

The products could be categorised as follows:

- **Concrete-Polymer Composites (C-PC)** are concrete-like polymer composites, that may contain portland cement.
- **Polymer Modified Concrete (PMC)** is concrete produced using a low dosage of polymer (≤ 5% by weight) incorporated into portland cement concrete to affect mainly, if not only, the rheological properties of the mixture. This type of composite is also called Latex Modified Concrete (LMC).
- **Polymer-Cement Concrete (PCC)** is a composite wherein either a non-reactive polymer (latex) or a reactive monomer (resin) is added to a fresh portland cement concrete mixture. More precisely, PCCs can be described as follows:
  - premix PCC, in which the modifying additive is added to the fresh concrete in the form of complete polymer (latexes, elastomers, or thermoplastics). That is, the polymerization of the modifying additive has taken place before addition to the concrete,
  - postmix PCC, in which polymerization components (chemically reactive synthetic resins or prepolymers and monomers) are mixed with fresh concrete, and the polymerization is obtained by chemical means, inside the concrete, along with hydration of the cement.

  It should be noted that in recent ACI documents such as "Polymer Modified Concrete (ACI 548.3R-03) PMC and PCC are placed in the same category, polymer modified concrete.
- Polymer Impregnated Concrete (PIC) is a composite formed by infusion of polymers into the pores in portland cement concrete (after it has hardened).
- Polymer Concrete (PC) is a composite formed using aggregate and a polymer binder (no portland cement is used).

## 3. OUTLOOK BEYOND "OWN BAILIWICK"

### 3.1. View from the White Book

The European White Book on Fundamental Research in Materials Science (European White Book, 2001) is recommended as a milestone for Materials Science in Europe. The first impression from the book is that the milestone is not built from the concrete. The category of "concrete" is mentioned in the book only one time. It is of significance that concrete is mentioned relevant to polymers: "functional polymers in the processing of concrete" (Wegner, 2001). Even so the White Book brings to us a lot of sentences which are orienting also this study. The aims are:

1. to assess the state of the art and pinpoint future challenges, needs and research priorities,
2. to highlight the fundamental scientific opportunities,
3. to consider the impact of materials science,
4. to find the way to attract more students,
5. to provide guidelines for science policy makers and to offer a basis for fundamental materials science programme,

Some principles could be addressed directly to the C-PC (Rühle, 2001):

- greater emphsis should be placed on the fundamental understanding of materials,
- application of materials is the ultimate goal, but this needs to be built on a firm theoretical basis,
- "the firm theoretical basis" will make the improvements more efficiently and reliable,
- particular attention should be given to understanding a material's behaviour from the atomic/nano level via microstructure to the macrostructure level using analytical techniques and computer modeling.

The fact that a concrete has been practically omitted in the European White Book on Fundamental Research in Materials Science makes the question about the reason. In layman's language it could be that the concrete is so traditional and conservative that the idea about "progress in concrete is hopeless". If so, it is many times wrong. The C-PC by itself is the good (but not only one) evidence of the progress in the concrete technology. Moreover, it could be reckless movement to leave a concrete to its fate. In that context, it is worth to stress that concrete with its tremendous world consumption – above twelve billion tons annually – belongs to energy- and mass- very sensitive material industry.

"Paradoxically, despite its contribution to society's prosperity, Materials Science has a low profile in the public arena" – this sentence is mentioned as message from the European Commission for Research (Busquin, 2001). Paradoxically, the omission of concrete technology problems in the White Book makes this profile even lower.

### 3.2. In the framework of internet

How does look the C-PC profile in the internet? Using the Farlex Dictionary:

- phrase *Concrete Polymer Composite* not found in the Dictionary and Encyclopedia. For *C-PC* the Encyclopedia offers the definition: "cost-per-click",
- among 122 *PCC* initialisms no one is redirected from *Polymer Cement Concrete*,
- *PC* redirected from *Polymer Concrete* and *PIC* redirected from *Polymer Impregnated Concrete* are mentioned among others 238 and 92 definitions, adequately.

The picture of C-PC in the virtual arena created by the Google Search is of interest (Table 2). The entry *Concrete-Polymer Composite* as the general category for *polymers in concrete* is not extremely popular (634 results). However, search for *Polymer in concrete* (by itself) brings more than million results; for *Polymer Concrete* – almost two millions results; for *Polymer Cement Concrete* – around 700 thousand and for *Polymer Impregnated Concrete* – about 100 thousand. Above fifty percent of the results are involved with application: in case of PCC and PIC practically all of them. It is the world of big number existing in adequate proportion to *polymer* (43 million results) and *portland cement concrete* (one and half million results).

Table 2 – Google search on C-PC

| No. | Item | Search results, thous. | | A/T |
|---|---|---|---|---|
| | | Total | Application | |
| 1 | Concrete-Polymer Composite (C-PC) | 0.634 | | |
| 2 | Polymers in concrete; in application | 1.150 | 637 | 0.55 |
| 3 | Polymer Concrete (PC); in application | 1.920 | 1.090 | 0.57 |
| 4 | Polymer Cement Concrete (PCC); in application | 696 | 624 | 0.90 |
| 5 | Polymer Impregnated Concrete (PIC); in application | 96.8 | 131 | 1.35 (?) |
| 6 | Polymers; in application | 43.200 | 12.200 | 0.28 |
| 7 | Portland Cement Concrete; in application | 1.650 | 0.839 | 0.51 |

Among top first hundred Google results, no C-PC, PCC, PC and PIC initialisms are involved with concrete. The Organisation short name ICPIC is placed first time on 25 position of the list of 27200 items. However, "ISPIC" is proudly located (and properly addressed to University of Minho) on the position 6 of the list of more than 54000 items. It demonstrates the power of event and ***gives the good opportunity to congratulate to Symposium organisers***.

Trying to make the review writer job easier, somebody could click on *polymer concrete* ***keynote*** – more than 56 thousand results. Even search for *L.Czarnecki polymer concrete state of the art* brings more than 40 results. In such situation it is difficult to prepare the general report in novel fashion.

## 4. FOR BETTER CONCRETE

Polymer added to concrete! For what? For better concrete, always. "Better concrete" means appropriately modified properties – high usability and durability (Tables 3 & 4). The addition of polymers to a given mixture of portland cement concrete could provide increased tensile strength, better adhesion, better abrasion resistance, higher resistance to water and vapour transition, or better resistance to frost and chemical attack. In case of polymer-cement concretes the barrier properties (e.g. tightness, gas diffusion coefficients, etc.) are particularly improved as compared to non-modified concrete. Therefore, improvement of durability can be expected (Swamy, Nagao, 1995). This has been confirmed by the test results (Ohama, 1984); many practical applications of PCC (particularly overlays) is in service – in good shape – for more than 40 years (Swamy, 1995), what is also of significance. Properties of PCC depend not only upon polymer type and content, but curing conditions affect the technical features in significant way as well (Fig. 3).

Table 3 – Directions of changes in PCC and PIC properties compared to Portland cement concrete (↑↑ as a rule, > 90% cases; ↑ majority, > 50% cases) (Czarnecki, Łukowski, 2005)

| Property | Composite | | |
|---|---|---|---|
| | PIC | pre-mix PCC | post-mix PCC |
| compressive strength | ↑↑ | ↓↓ | ↓↓ |
| tensile strength | ↑↑ | ↑↑ | ↑↑ |
| modulus of elasticity | ↑↑ | ↓↓ | ↓↓ |
| impact resistance | ↑↑ | ↑ | ↑↑ |
| creep resistance | ↑↑ | ↓↓ | ↑ |
| abrasion resistance | ↑↑ | ↑↑ | ↑ |
| total porosity | ↓↓ | ↑↑ | ↑ |
| absorbability | ↓↓ | ↓↓ | ↓↓ |
| thermal resistance | ↓↓ | ↓↓ | ↓↓ |
| freeze-thaw resistance | ↑↑ | ↑↑ | ↑ |
| chemical resistance | ↑↑ | ↑ | ↑ |
| ageing resistance | ↑ | ↑ | ↑ |

Table 4 – Properties of concrete-polymer composites compared to Portland cement concrete (Beeldens, 2003, Ohama, 1984)

| Property | Cement concrete | PCC | PIC | PC |
|---|---|---|---|---|
| Compressive strength, MPa | 10–60 (> 60*) | 10–75 | 100–200 | 40–150 |
| Flexural strength, MPa | 1.5–7 (> 7*) | 3–12 | 7–35 | 4–50 |
| Tensile strength, MPa | 0.6–3.0 (> 3*) | 4–9 | 4–17 | 4–20 |
| Modulus of elasticity, GPa | 15–30 | 10–25 | 30–50 | 7–45 |
| Poisson's coefficient | 0.11–0.21 | 0.23–0.33 | 0.20–0.25 | 0.16–0.33 |
| Coefficient of linear thermal expansion, $10^{-6}\cdot K^{-1}$ | 10–12 | 11–15 | 10–17 | 10–35 |
| Water absorbability, % | 4–10 | 1–3 | 0.5–1,5 | 0.5–3 |
| Chemical resistance | poor / average | average / good | good / very good | very good / excellent |
| * For High Performance Concrete (HPC) | | | | |

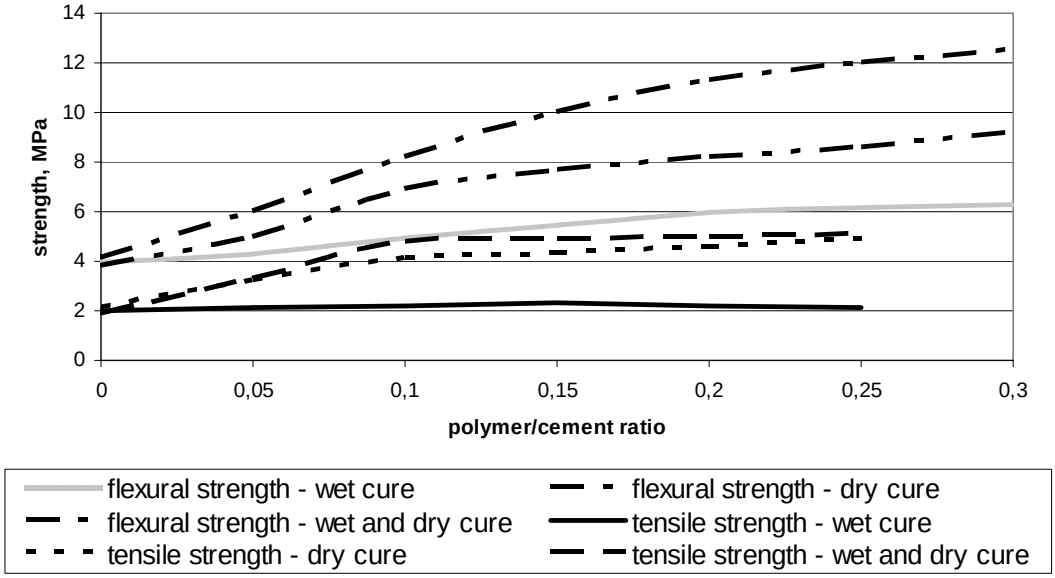



Figure 3 – Effect of curing conditions on strength of acrylic-cement composite (Lavelle, 1988)

Polymer concretes are characterised by good mechanical properties and very high chemical resistance. These factors are in favour for durability. The negative factors are low heat resistance as well as compliance in to creeping and aging, involved with the high content of the polymer.

Polymer impregnated concrete gives unique characterisation of very high compressive strength combined with relatively high flexural and tensile strength and very high modulus of elasticity plus quite good chemical resistance. It allows to expect the significant improvement of durability (pores are closed with polymer). However, due to the fact that high pressure impregnation process is complicated in technological way and expensive, PICs are not very popular. More often the concrete surface impregnation is used (partially impregnated concrete).

Using of polymers can significantly improve a number of concrete features. Material cost of polymers, however, is 10 to 100 times (depending on the type) higher than that of portland cement according to mass unit and 5 to 25 times higher according to volume unit. This is significant limitation, despite the fact that the share of polymers in building composite is usually not higher than 10% by volume. It should be also mentioned, that the concretes including polymers are not completely disadvantage-free. For example, polymer affects negatively fire resistance of concrete and its behavior under fire conditions (Yeon, 2001).

## 5. HOW POLYMER IMPROVES CONCRETE? BETWEEN COMPATIBILITY AND SYNERGY

The ability to control the properties of the concrete-polymer composites can be obtained by using the “composition – structure – properties” relationship. This relationship, called a “material model” till now has been reduced to the “composition – properties” relationship for the given composite microstructure (Clifton, 1995).

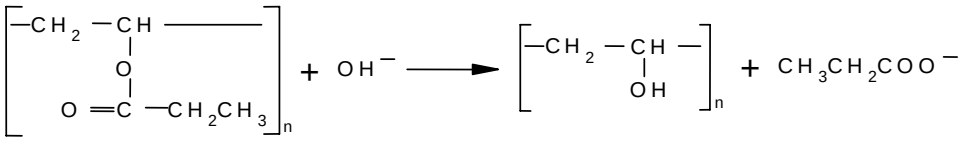
Synergy is the simultaneous action of components which together give greater total effect than the sum of their individual effects. The interactions between components of the

concrete-polymer composite should be considered as the integral part of the material model and the basis for material designing and optimisation (Ohama, 1984, Czarnecki, 1985).

Presence of polymer in the concrete affected its properties in various ways:

- properties of the polymer take part in forming of the properties of the material as a whole, according to the additive mechanism,
- polymer causes modification of the concrete microstructure, leading to the changes in its properties (synergic effects),
- the polymer particles show the orientation – the polar groups are oriented toward the surface of aggregate (microfiller) grains (synergic effects).

The requirement of necessity is intrinsic compatibility among polymer and others concrete components. Polymer affected the portland cement hydration; slowdown of the process is observed. In some cases chemical reactions of polymers with components of the cement paste take place, sometimes unfavourable for the composite end-properties (Fig. 4).




**hydrolysis of PVAc in alkaline environment of cement paste with formation of calcium acetate crystals**

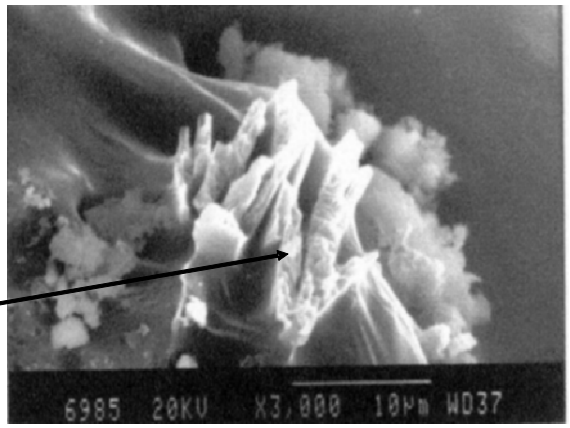
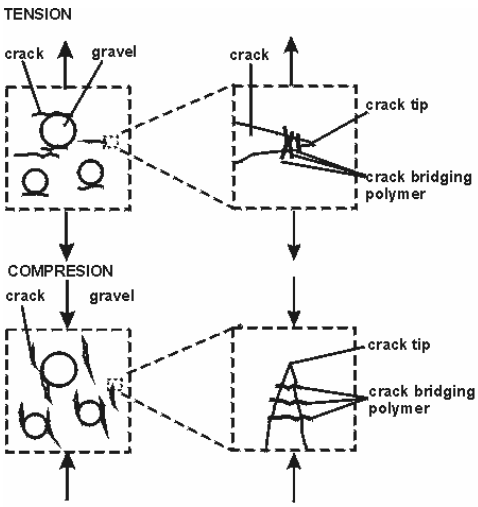



Fig. 4 – Lack of intrinsic compatibility: interaction C-S-H – polymer (Czarnecki, 2004)

Polymer influences also the transition zone between the portland cement paste and aggregate. The continuous film of the polymer can “bridge” the microcracks in the cement matrix and in the transition zone (Fig. 5).



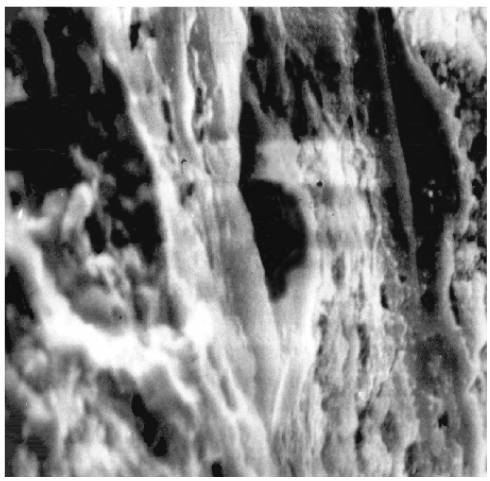



Fig. 5 – Polymer crack-bridging; SEM 2000x

About twenty years ago the statement of the author was published (Czarnecki, 1985): "After more than 50 years of searching, the least success has been attained with polymer-cement concretes. However, PCC still could have the greatest potential for field applications. For this reasons attempts to improve our understanding of PCC must be continued". Recently, new research and scientific tools became available, like environmental scanning electron microscopy (ESEM) (Czarnecki, 2002), fractal theory (Czarnecki, 2001), etc. This created new possibilities for developing the extended (Beeldens, 2005) model of concrete-polymer composites microstructure formation (Fig. 6). The integrated model is based on the three-step model as proposed by Ohama (Ohama, 1984), but stresses the positioning of the mechanisms on the time scale and the interaction between different components.

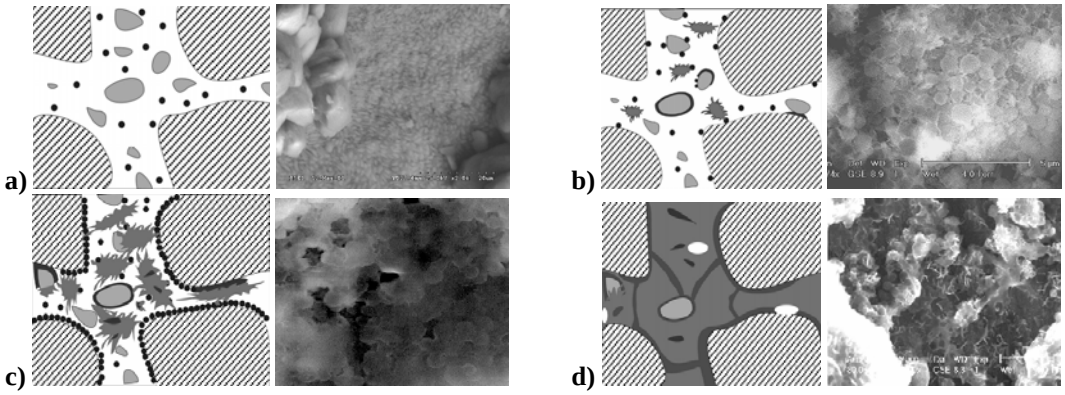



Figure 6 – Integrated model of polymer-cement concrete microstructure formation (Beeldens, 2003); a, b, c, d – the consecutive stages of forming of interpenetrating polymer-cement network

The polymer film-formation process in the post-mix PCC (e.g. epoxy-cement concrete) is based on chemical reaction. A model of that process has been recently proposed (Łukowski, 2006). The cross-linking of the polymer proceeds in the beginning only inside the micro-droplets of the resin. Moreover, the process is complicated because of the influence of two opposite factors: presence of the water hinders the hardening of the resin, but the alkaline environment of the cement paste catalytically supports the reaction. As a result, the continuous layer of epoxy resin (Fig. 7) is to some extent more irregular and porous as compared to the layers of thermoplastic polymers. However, this phenomenon seems to not affect negatively the properties of the composite, mainly due to the fact that also the fragments of the cross-linked polymer not built-in into the continuous matrix structure act as dispersed micro-reinforcement strengthening the composite; those fragments of the resin can have the diameters up to 100 μm.

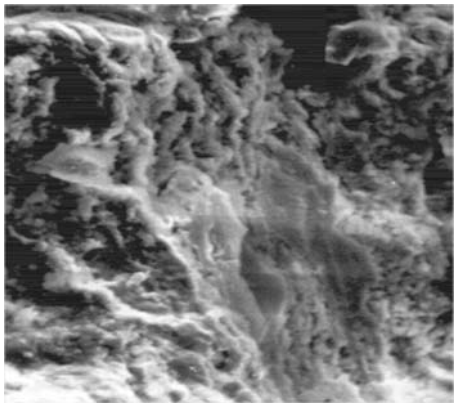


Fig. 7 – Microstructure of epoxy-cement composite; SEM 800x

Now the achievements of PCC, particularly with "epoxy-cement" and "acrylic-cement", are well-known; developing of more sophisticated material models has been one of the reasons for those successes.

In the case of polymer impregnated concretes, there is no really specific model developed. The assumption is that the polymer is introduced into the concrete pores system and is hardening there, thus reducing the pores volume. This leads to improving of the concrete strength, since the property is strongly dependent on the porosity:

$$f = f_0 (1 - p)^6 \quad (1)$$

where f is concrete strength, $f_0$ is strength of concrete with no pores, and p is concrete porosity.

Introducing the polymer into the hardened concrete also increases stiffness, as the elastic modulus E is dependent on porosity in the similar way:

$$E = E_0 (1 - p)^3. \quad (2)$$

Synergy is the simultaneous action of the components which, together, give greater total effect than the sum of their individual effects (Czarnecki, 2004):

$$Y(A, B) = Y(A) + Y(B) + Y(A) \cdot Y(B) \quad (3)$$

where: Y (A, B) is the property of the composite obtained from the components A and B,
Y (A) + Y (B) is the additive effect, Y (A) · Y (B) is the synergetic effect.

The interactions between the components of the concrete-polymer composite should be considered as the integral part of the material model and the basis for material designing and optimization.

## 6. C-PC HISTORY; WHAT COULD WE LEARN FROM THAT?

The C-PCs have their own prehistory – since thousand years before Christ (Chandra, 1995), and contemporary history that has started with the British patent 191474 (1923) on the "Latex-Hydraulic Cement System", patented by L. Cresson. Since 1975 the International Congresses on Polymers in Concrete (ICPIC) have pointed out the milestones on the way of C-PC development (Fig. 8, Table 5).

The analysis of ICPIC output (Fig. 9) gives us an impression of very quick development in the seventies and the eighties, and rather stagnation in the early nineties; some optimistic signs of change could be seen in the Congress in Oostende '95. The Congress brought the positive turning point on the C-PC development curve. The output of the recent three Congresses confirmed the optimism.

If we will untangle the C-PC life curve ("snake charmer process") it would be obvious that roughly speaking "application get ahead of science". As the reflection of that, there are the permanent demands and attempts for better material understanding, for material model, material designing and optimisation.

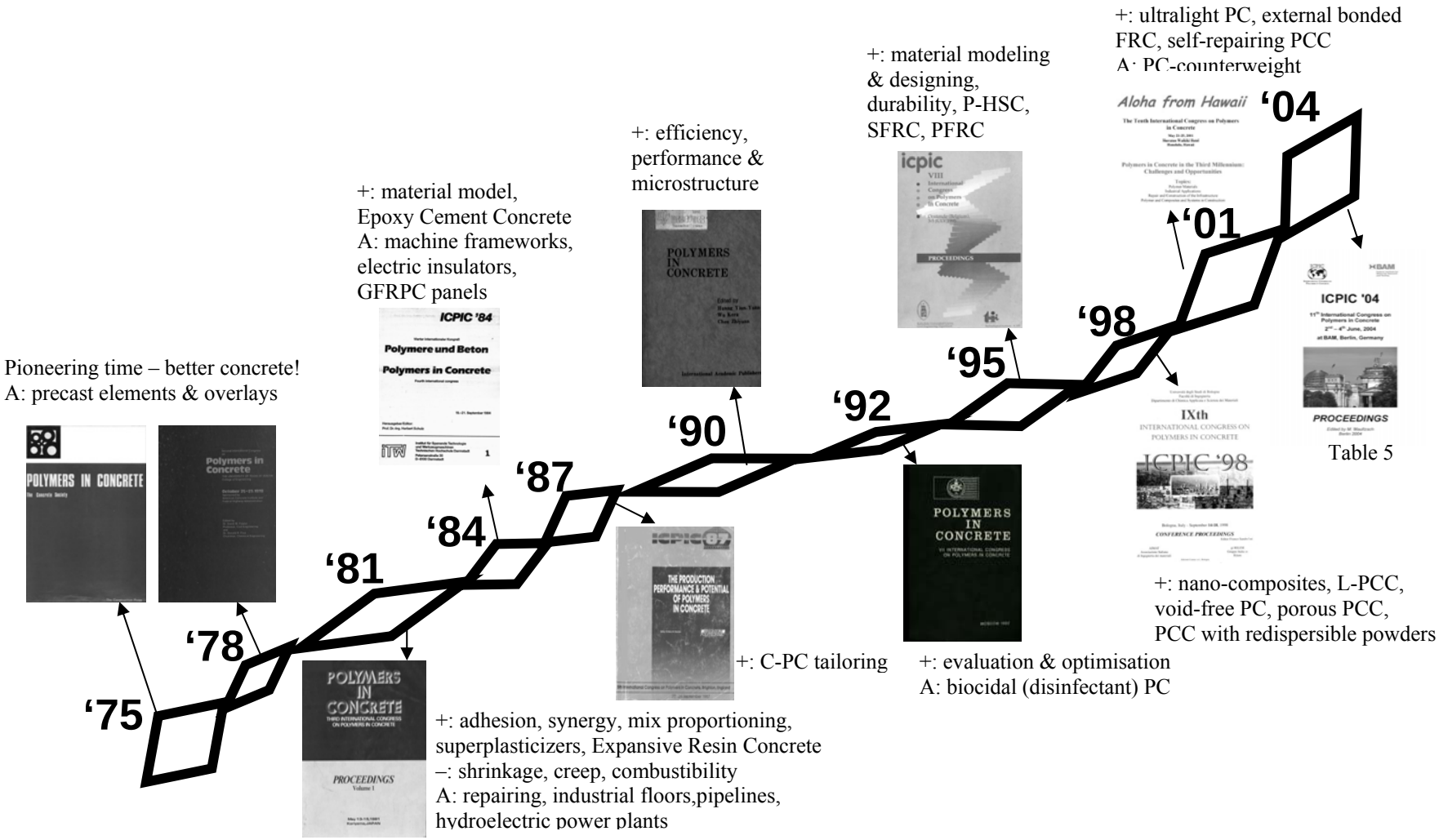



Fig.8 – C-PC development curve in the light of ICPICs results: area ◇ - number of papers, angle ∠ - degree of novelty, axis x → - number of papers "on practice", axis y ↑- number of papers on "theory"; Congresses output in keywords: + advantages, – disadvantages, A - application; GRPC - Glass Reinforced Polymer Concrete, P-HSC - Polymer High Strength Concrete, SFRC - Steel Fibre Reinforced Concrete, PFRC - Polymer Fibre Reinforced Concrete, L-PCC – Lightweight Polymer Cement Concrete

Table 5 – Novelties and significant progress reported at 11th ICPIC, Berlin 2004 (Van Gemert, 2005)

| Description | Reference | Test methods | Research | Application |
|---|---|---|---|---|
| 1. Integrated model | Beeldens e.a. | | + | |
| 2. Nanomonitoring | Schorn e.a. | | + | |
| interfaces | Benzarti e.a. | | + | |
| 3. Soluble polymer modifiers | Knapen e.a. | | + | |
| 4. Slag PCC | Joo, Ohama e.a. | | | + |
| Fly ash PCC | Jolley, Kruger | | | + |
| 5. Ultrasonic C-PC evaluation methods | Garbacz | + | | |
| 6. Profilometry and surfometry analysis | Courard e.a. | | + | |
| 7. CPC Standardization | Ohama | + | | |
| 8. Sound absorbing materials | Knapen e.a. | | | + |
| 9. Quantification of synergy | Czarnecki e.a. | | + | |
| 10. High strength ECC without hardener | Ohama e.a. | | + | |
| 11. Ultra-lightweight polymer concrete | Sung e.a. | | | + |
| 12. GFRP-PC | San-José e.a. | | | + |
| 13. Electrical insulators | Gunasekaran | | | + |
| 14. Preplaced aggregate epoxy concrete | Murray | | | + |
| 15. Ecological coatings | Erkens e.a. | | | + |
| 16. Optimization of thin overlays | Sušteršič | | | + |
| 17. Textile reinforced PCC | Dilthey e.a. | | | + |
| 18. Waste reuse | Bignozzi e.a. | | | + |
| 19. Intelligent PC | Blair e.a. | | + | |
| 20. FRP strengthening | Frigione e.a. | | | + |
| | Ignoul e.a. | | + | + |
| | Byun e.a. | | + | + |
| 21. Admixtures | Pourchez e.a. | | + | |

The tendency of ICPIC presentations has changed through the years. At the 1975 Congress, the basis for intellectual and technical stimulation could be described as “here is a concept for a very new material – like concrete, but much better. What do we do with it?” At the more recent Congresses, the emphasis has shifted to “a material with a unique set of technical properties is required. How do we formulate a suitable Concrete-Polymer Composite that meets these needs?” In this regard, many successful families of C-PC have already been created.

# PROGRESS IN C-PC IN THE LIGHT OF ICPICS RESULTS

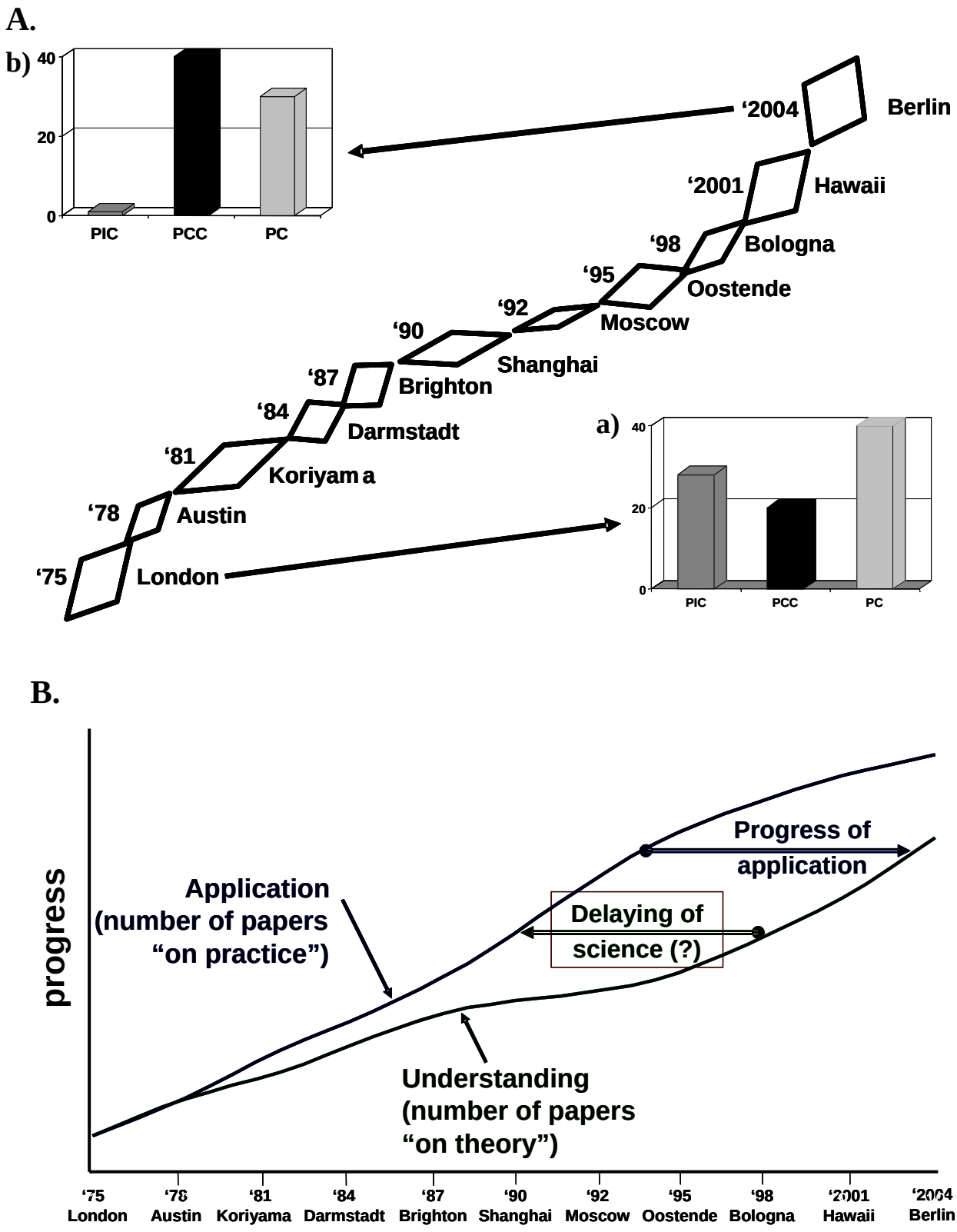



Fig. 9 – Progress of C-PC: A. C-PC life curve – "snake curve" (meaning of icons – see Fig. 8); the number of papers involving with PIC, PCC and PC on the Congresses in 1975 (a) and in 2004 (b). B. Untangled snake curve

It is also worth of note that some polymer containing concrete composites have changed names and shifted to the other families of building composites, including admixtured concrete (V.S.Ramachandran), high performance and high strength concretes (K.Buyen).

One of the significant changes in the development of C-PC is the shift in material type most often discussed at each of the ICPIC congresses. Until 1995, PC was unquestionably the dominant material, with nearly half of the papers focused on PC. Recently, however, the picture has changed dramatically. In the last four congresses, over 50% of the papers have focused on PCC, about 40% have focused on PC, and less than 10% have focused on PIC (Czarnecki, 2005).

## 7. TRENDS; WAYS AND MEANS

Since production and engineering of materials and components are increasingly knowledge based, the technology itself reveals a gap in the basic understanding of materials. The continued pursuit of additional knowledge will always be necessary. The most significant trends of basic and applied research are categorised as follows (Aldinger, 2001):

- theoretical treatment and modeling of materials and component development,
- exploitation of nanosize effects,
- increasing materials complexity because of increased functionality,
- integration of different materials into multifunctional composites.

To understand and control the C-PC bulk properties it is necessary to focus on lower levels of microstructure of composite materials (Fig. 10 & Fig. 11). The relationship between properties and microstructure, so-called "***material model***" emerged as the most important.

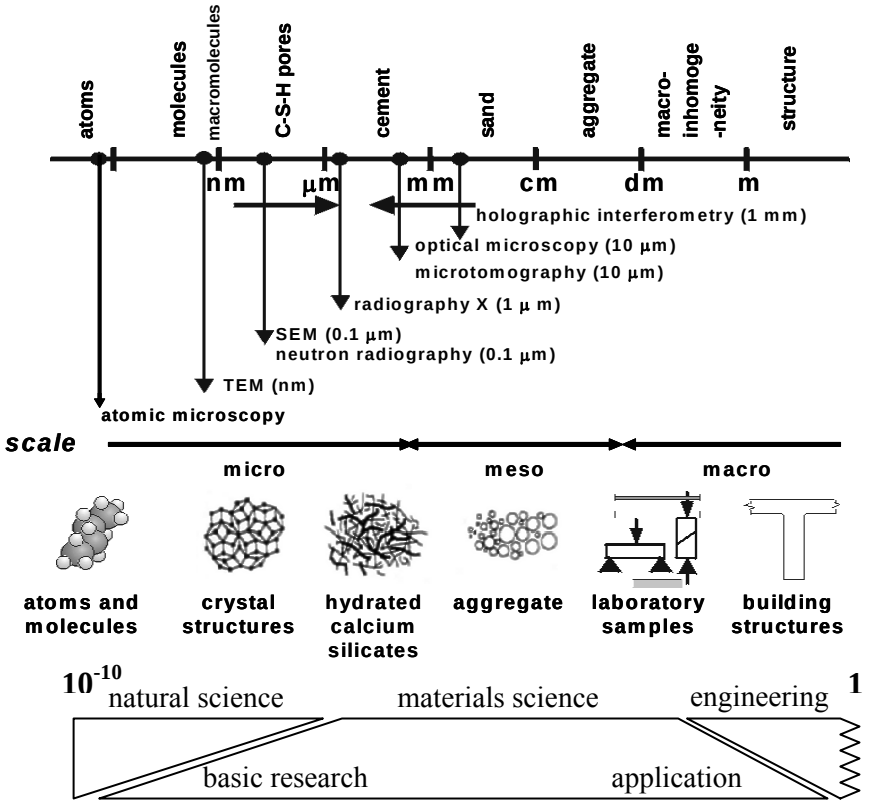
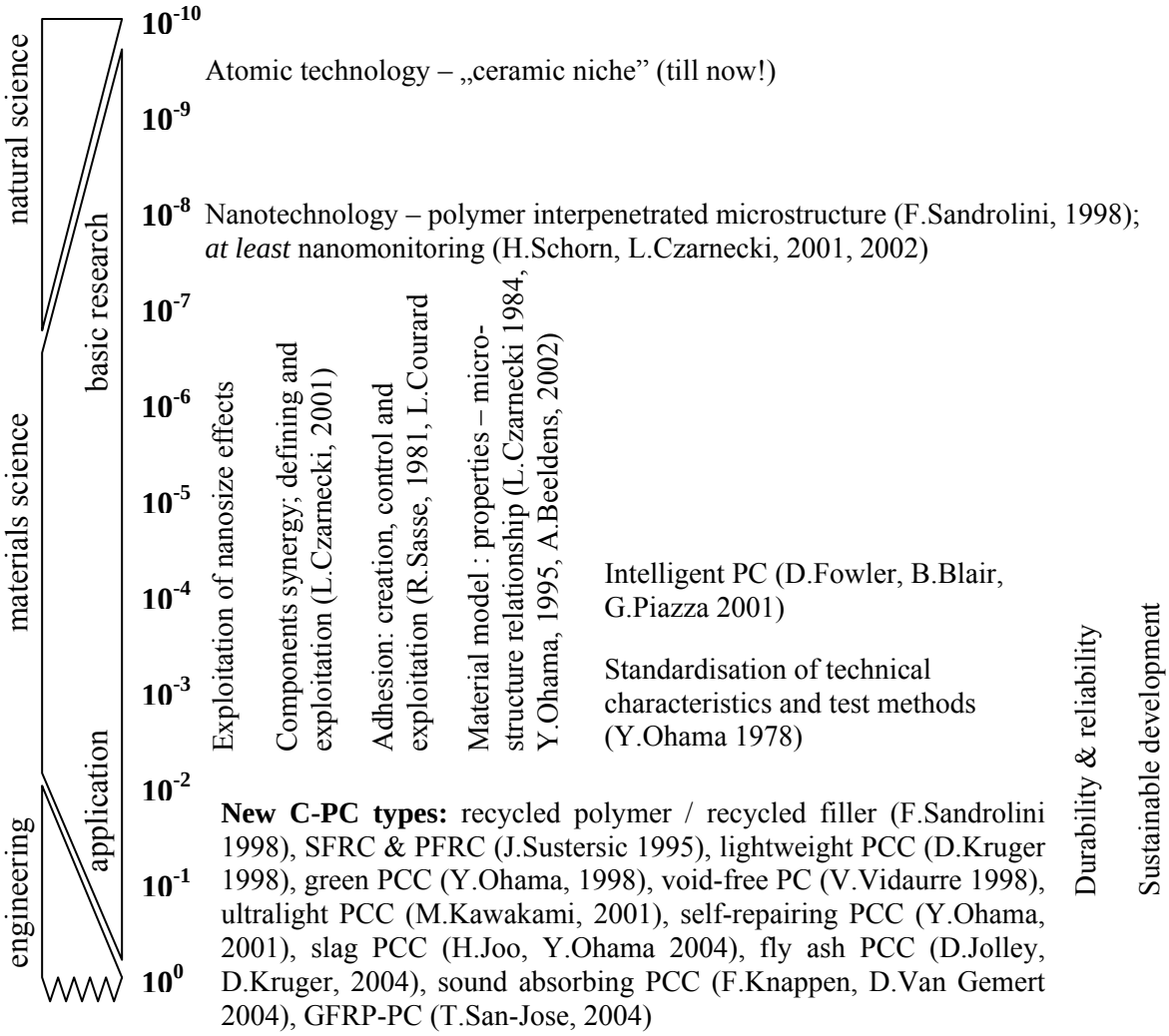



Fig. 10 – Fundamental approach to research for building materials (Beeldens, 2005, Van Mier, 1997, Aldinger, 2001, Czarnecki, 2001); from macrostructure (application) to micro- and nanostructure in hierarchic way




Processing: user friendly, self-compacting C-PC

- improvement in well established fields

* on site
- repairing
- industrial floors
- overlays
- shotcreting systems

* precast elements
- pipes
- tanks
- containers
- manholes
- machine tool structures
- artificial marble: tiles, panels, sanitary wares,
- insulators
- drains

- new generation (idea acc. to D.Fowler 2005)

- monomer vapour impregnated concrete
- PC-PCC multilayer composites
- containment vessels for toxic / hazardous wastes (PC, PIC)
- PC panels – steel or aluminium framing members

Explanations: SFRC – Steel Fibre Reinforced Concrete,
PFRC – Polymer Fibre Reinforced Concrete,
GFRP-PC – Glass Fibre Reinforced Polymer – Polymer Concrete

Fig. 11 – C-PC research trends

Influence of polymers of the composite performance is result of polymer properties as well as of modification of the composite microstructure by polymer. The influence is dependent on the type and amount of the polymer and on the method of its introduction to the concrete (Fig. 12). Searching for ***synergy effects***, particularly between polymer and other ingredients of concrete composite seems to be one of the most promising research area of practical meaning. The science and ability of making and manipulating long chain molecules is highly interesting field. There are major challenges to exploit possibilities of long chain molecules ranging from the focus on ultimate performance of 1-D, 2-D or 3-D(imensions) (Lemstra, 2001).

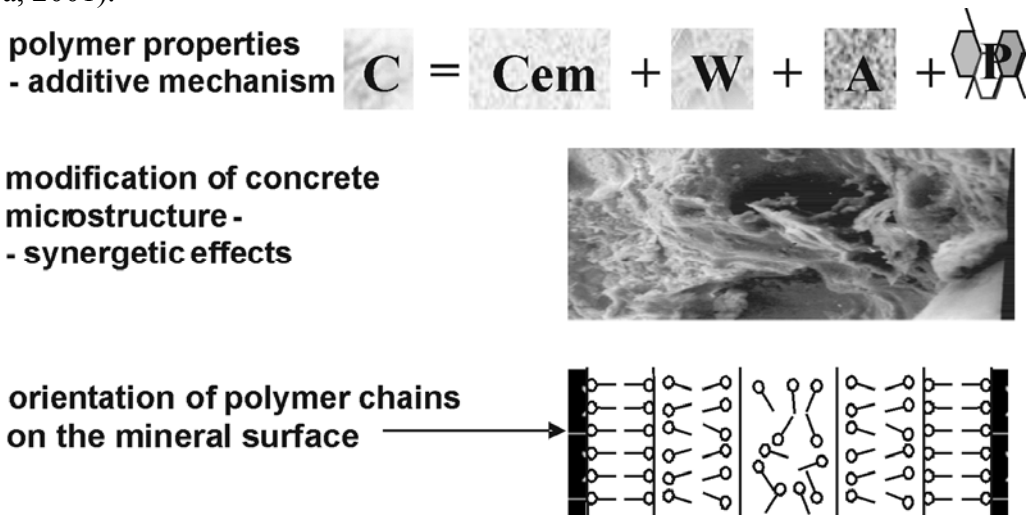



Fig. 12 – Influence of polymer on concrete properties (Czarnecki, Łukowski, 2005)

Key-word that needs attention in research is ***adhesion***; understanding and improvement of the mechanism of adhesion and failure of adhesives, prevention of adhesion by surface modification, "tacky" polymer (matrix and primer), time / temperature / pressure–dependent adhesive process, wetting and de-wetting process (Wegner, 2001, Czarnecki, Chmielewska, 2005, Aguiar, Pimenta 1999).

There are new scientific tools (Table 6) already available and sophisticated test instruments like: ESEM – Environmental Scanning Electron Microscopy or micro/nano indentation instrument. It also means that the research cost will increase significantly. In consequence, it means the need of better co-operation and synergy effect between researchers community.

The superior headlines in C-PC application at present time and for future are: ***durability*** (Aguiar, 1999), ***reliability*** and ***sustainable development***. In the near future, it is rather unlikely we'll see a completely new material concept in the C-PC domain. The focus of new developments will be on better uses of polymers, in more economical and synergistic ways with the aim to achieve the level of requirements suitable in the given application, e.g. transform from "brittle" to "ductile" – high strength concrete. More sophisticated formulation and preparation methods will be developed, special modifiers will be formulated, and cooperative systems (for example, microfillers, microfibres, and polymers) will be employed. More attention will not only be paid to the product's final properties and usability, but also to its processibility (for example, self-compacting polymer cement concretes).

Table 6 – New scientific tools

| Item | C-PC | |
|---|---|---|
| | date | pioneers |
| Theory of percolation | 2001<br>2005 | D.Whitney & D.Fowler<br>P.Łukowski |
| Fracture mechanics – fractal analyses | 2001 | J.Aguiar, K.Kim<br>K.Fukuzawa<br>J.Pretorius, D.Kruger<br>A.Garbacz |
| Nanotechnology<br>Nanomonitoring | 1998<br>2001 | F.Sandrolini<br>H.Schorn & L.Czarnecki |
| Technical homeostasis<br>Self-regulating systems | 2001<br>2001 | Y.Ohama<br>V.Ramakrishnan |
| Synergy effects analysis –quantification of synergy | 2004 | L.Czarnecki |
| Image analysis | | |
| Thermodynamics at unbalanced states & irreversible processes | | |
| Chaos theory | | |
| Theory of catastrophes | | |
| Artificial intelligent systems (artificial neural networks) | | |
| Fuzzy sets | | |

## 8. CONCLUSIONS

The age of concrete, in the singular, has definitely passed. In the present era of concrete the polymers are vital component in many concrete composites. The Concrete-Polymer Composites have made in the past decades great progress. The family of C-PC came of age but still they are very promising materials for new applications and stimulating new researches. Like other advanced materials they need a firm theoretical basis to make the improvements more efficiently and reliable; development through better material understanding. Exploitation of nanosize effects, synergy, material model and adhesion have been selected as the main key-words on the C-PC research area. The superior headlines in C-PC application are: durability, reliability and sustainable development. It is important that stimulation and inspirations will come from two sources: from the research centres and from application fields (industry). The realm of **polymers in concrete** seems to be over hermetic; it needs to be "oriented more for public". Increasing the C-PC profile on the public arena is also necessary to provide guideline for science policy makers. C-PC should present their potentiality in broad sense. The successful achievements of C-PC in the past make the good basis for further development.

## 9. ACKNOWLEDGEMENT

The paper has been partially granted by Committee for Scientific Research, Project No. 4 T07E 007 26.

## 10. REFERENCES

Aguiar B., Pimenta T.J., Influence of high temperatures on the adhesion of epoxy to hardened mortar, fresh mortar or steel plate. *International Conference on Infrastructure Regeneration and Rehabilitation*, ed. R.N. Swamy, Sheffield Academic Press, Sheffield, 995-1004 (1999).

Aguiar B., Durability of polymeric pipes in contact with domestic products. Construction and Building Materials, **13**, 155-157 (1999).

Aldinger F., Baumard J.F., Advance ceramic materials: basic research viewpoint. In *European White Book on Fundamental Research in Materials Science*, Max-Planck-Institut für Metallforschung Stuttgart, Max-Planck-Gesellschaft, 26-31 (2001).

Beeldens A., Van Gemert D., Ohama Y., Czarnecki L., From microstructure to macrostructure: an integrated model of structure formation in polymer modified concrete, *Proc. of 4th Asia Symposium on Polymers in Concrete*, Chuncheon, Korea, 211-219 (2003).

Beeldens A., Van Gemert D., Schorn H., Ohama Y., Czarnecki L., From microstructure to macrostructure: an integrated model of structure formation in polymer-modified concrete. *RILEM Materials & Structures*, **280,** 601 – 607 (2005).

Busquin P., A message from the European Commissioner for Research. In *European White Book on Fundamental Research in Materials Science*, Max-Planck-Institut für Metallforschung Stuttgart, Max-Planck-Gesellschaft (2001).

Chandra S., Historical background of polymers used in concrete. *Proc. of 8th International Congress on Polymers in Concrete*, Oostende, Belgium, 3-11 (1995).

Clifton J.R., Czarnecki L., Łukowski P., Application of material model in optimization of polymer concretes. *Proc. of 8th International Congress on Polymers in Concrete*, Oostende, Belgium, 293-298 (1995).

Czarnecki L., Status of polymer concrete. *Concrete International*, **7**, 47-53 (1985).

Czarnecki L., Schorn H., Nanomonitoring of polymer-cement concrete microstructure. *Proc. of International Conference "Concrete Days",* Szczyrk, Poland, 409-426 (2002).

Czarnecki L., Garbacz A., Kurach J., On the characterization of polymer concrete fracture surface. *Cement & Concrete Composites*, **23,** 399-409 (2001).

Czarnecki L., Challenges for building materials engineering. XLVII Scientific Conference of Polish Academy of Sciences, Krynica, Poland, 213-231 (2001) [in Polish].

Czarnecki L., Chmielewska B., Factors affecting adhesion in building joints. *Cement Wapno Beton*, **2**, 74-85 (2005).

Czarnecki L., Łukowski P., Chmielewska B., Statistical analysis of the synergetic effects in epoxy concretes. *Proc. of 11th International Congress on Polymers in Concrete*, Berlin, Germany, 201-208 (2004).

Czarnecki L., Polymers in Concrete - personal reflections on the edge of the new century. *Concrete International*, **8**, 1-7 (2005).

Czarnecki L., Łukowski P., Concrete-polymer composites: status and trends. *Proc. of 3rd International Conference on Construction Materials ConMat'05*, Vancouver, Canada (2005).

Czarnecki L., Łukowski P., Influence of polymer admixtures and additives on durability of concrete. *Cement Wapno Beton*, **1,** 38-47 (2004).

*European White Book on Fundamental Research in Materials Science*, Max-Planck-Institut für Metallforschung Stuttgart, Max-Planck-Gesellschaft (2001).

Fowler D.W., Polymers in concrete: where have we been and where are we going? *Proc. of 10th Int. Congress on Polymers in Concrete*, Hawaii, USA, 10-27 (2001).

Lavelle J.A., Acrylic latex modified portland cement. *ACI Materials Journal,* **1**, 41-48 (1988).

Lemstra P.J., Soft materials and polymers: the rise and decline of polymer science & technology in Europe. In *European White Book on Fundamental Research in Materials Science*, Max-Planck-Institut für Metallforschung Stuttgart, Max-Planck-Gesellschaft, 48-51 (2001).

Łukowski P., *Polymer-cement binders*. Warsaw University of Technology, Warsaw, Poland (2006) [in printing].

Ohama T., Moriwaki T., Shiroishida K., Weatherability of polymer-modified mortars through ten-years outdoor exposure. *Proc. of 4th International Congress on Polymers in Concrete,* Darmstadt, Germany, 67-71 (1984).

Rühle M., Dosch H., Mittemeijer E.J., Van de Voorde M.H., The importance of materials for modern technology. In *European White Book on Fundamental Research in Materials Science*, Max-Planck-Institut für Metallforschung Stuttgart, Max-Planck-Gesellschaft, 11 (2001).

Swamy R., Nagao H., Some durability properties of polymer-modified mortars. *Proc. of 8th International Congress on Polymers in Concrete*, Oostende, Belgium 257-262 (1995).

Swamy R., Durability of concrete composites with polymers. *Proc. of 8th International Congress on Polymers in Concrete*, Oostende, Belgium, 21-26 (1995).

Van Gemert D., Czarnecki L., Maultzsch M., Schorn H., Beeldens A., Łukowski P., Knapen E., Cement concrete and concrete–polymer composites: Two merging worlds. *Cement & Concrete Composites*, **9-10**, 926-933 (2005).

Van Mier J.G.M., *Fracture process of Concrete: Assessment of material parameters for fracture model*. CRC Press, Florida, USA (1997).

Wegner G., Soft materials and polymers: strategies for future areas of basic materials science. In *European White Book on Fundamental Research in Materials Science*, Max-Planck-Institut für Metallforschung Stuttgart, Max-Planck-Gesellschaft, 51-54 (2001).

Yeon K., Youn-su L., Lee B., Kim C., Fundamental study on improving the incombustibility of polymer mortar. *Proc. of 10th International Congress on Polymers in Concrete,* Hawaii, USA (2001).

International Symposium Polymers in Concrete
2 - 4 April 2006
Guimarães, Portugal

# Behaviour of RC Structures strengthened with CFRP under Load Test and Thermal Effects

L. Juvandes[1], P. Costeira Silva[2], J. Figueiras[1]

*Faculdade de Engenharia da Universidade do Porto, Depart. de Engenharia Civil, LABEST*
*Rua Dr. Roberto Frias, Porto, P - 4200-465 Porto, Portugal*

## ABSTRACT

To appraise the efficiency of the new strengthening technique by external bond of unidirectional CFRP systems, an experimental strengthening of a limited region of the top slab of N. S. da Guia bridge deck was proposed and performed. Four different CFRP systems were applied and instrumented with several strain gauges. The influence of temperature was analysed through a structural health monitoring program and several field load tests were carried out using five discrete point loads to simulate the vehicle live load specified by Portuguese Code. The load tests were previously simulated in laboratory. With the present work, the authors expect to contribute to clarify the knowledge of serviceability behaviour of this new strengthening technique, namely, when applied in the rehabilitation of reinforced or prestressed concrete bridges.

## 1. INTRODUCTION

The last few years revealed a substantial increasing of the use of Carbon Fibre Reinforced Polymer (CFRP) for rehabilitation and strengthening of concrete structures. Several researchers and institutions have helped to that acceptance, due to the experimental tests performed over concrete elements strengthened by externally bonded CFRP systems and to the development of numerical models for predicting the behaviour of a strengthened structure. However, it is convenient to increase the confidence in the strengthening of RC structures with composite materials, what can be achieved through the assessment of the material properties, the definition of applicable technical procedures and the understanding of the ultimate and serviceability behaviour of the strengthened structure.

Several applications of this new strengthened technique have been already executed in buildings and bridges, although the knowledge of the long term behaviour of the strengthened element is insufficient yet. Field load tests and long-term monitoring have been performed either in buildings (Nanni et al. (1998); Mettemeyer et al. (1999)) or in bridges (Mayo et al. (1999); Hag-Elsafi (2003); Reay et al. (2004)) in order to evaluate the efficiency of this technique.

[1] Professor
[2] PhD Student

It is generally accepted that CFRP composites have a very high level of durability. In spite of the intensive research efforts, the long-term performance of composites still needs to be demonstrated, because it depends on the processing technique used, loading history and environmental exposure.

The aim of the study performed in N. S. da Guia bridge has been: to appraise the long term behaviour of CFRP systems subjected to an action corresponding to the vehicle live load, to measure the activity of cracks, to assess the level of tensile deformation in the steel reinforcement and to quantify the effects of daily temperature on the deck slab.

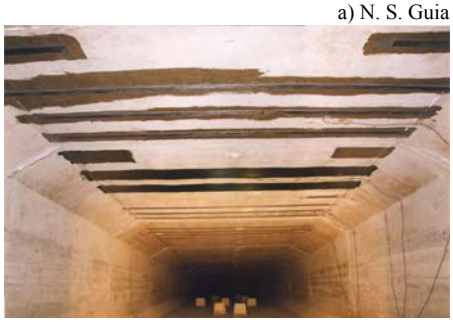
In this paper the authors present the response of the CFRP systems and the crack activity due to temperature changes and compare the results of previous laboratorial tests and the field load tests carried out in the bridge deck slab. It's also clear the contribution that, nowadays, the health monitoring gives to a major understanding of the short and long term behaviour of this strengthened technique

## 2. BRIDGE DESCRIPTION

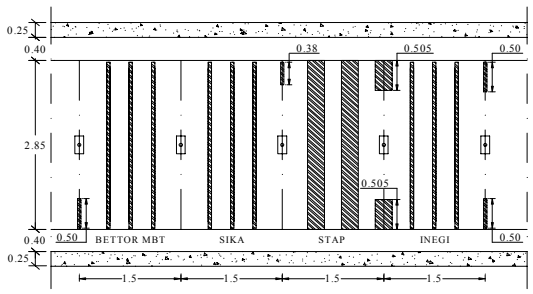
The N. S. da Guia bridge is a prestressed concrete bridge built 20 years ago at the town of Ponte de Lima, north region of Portugal. The bridge deck has a total length of 250 meters with five continuous supported spans of 38, 58, 58, 58 and 38 meters, Figure 1. The 12m width girder consists in a bicelular box of variable height. An extensive longitudinal cracking can be observed on the inner face of the top slab deck, which is reported to have been detected a few years after the bridge is opened to service. The crack spacing is about 35cm and the crack width varies between 0.25mm and 1.0mm.



a) N. S. Guia Bridge – Ponte de Lima



b) Cross-section - upstream cell




c) plan of the experimental strengthening region

Figure 1 – Experimental strengthening of the deck slab.

The bridge was analyzed in order to detect the main causes of the longitudinal cracking observed (Oliveira (1999); Silva (2002)). The different type of actions was considered, but the efforts corresponding to the vehicle live load were studied with more detail.

In 1999 an experimental strengthening program of a limited region of the top slab (0.20 m of thickness) of the box girder by external bond of CFRP systems was proposed and performed (Silva (2003a); Figueiras (1999)). Four Portuguese firms (Bettor MBT, INEGI, SIKA and STAP) took part in this pilot project by carrying out the 'in situ' strengthening of a

slab strip one meter width by using their own CFRP products, Figure 1. The proposed and performed solutions for each of the associated firms were:

*STAP*: 2 strips of Replark 20 sheet, each one with 2 layers, 25 cm width, 2.7 m length and 0.222 mm thickness. The type of impregnation resin is L700W.

*SIKA*: 3 Sika CarboDur S512 laminates with 5 cm width, 2.7 m length, 1.2 mm thickness and approximately 0.283 m spacing. The type of resin is SikaDur 30.

*BETTOR MBT*: 3 MBrace LM laminates with 5 cm width, 2.7 m length, 1.4 mm thickness and approximately 0.283 m spacing. The type of resin is MBrace Laminate Resin.

*INEGI*: 3 Carbon/Epoxy laminates manufactured by INEGI with 5 cm width, 2.7 m length, 1.4 mm thickness and approximately 0.283 m spacing. The type of resin is Fermapoxy (weber & broutin).

## 3. INSTRUMENTATION

The limited region of the slab and the four CFRP systems were instrumented in a way that it was possible to obtain: i) CFRP systems and steel reinforcement strains; ii) vertical displacement at different points of the strengthened region of the slab; iii) crack widths; and iv) temperatures.

The monitoring system used was able to automatically and simultaneously measure all this quantities, with the minimum human interference. The plan with all the sensors location used in this study is illustrated in Figure 2.

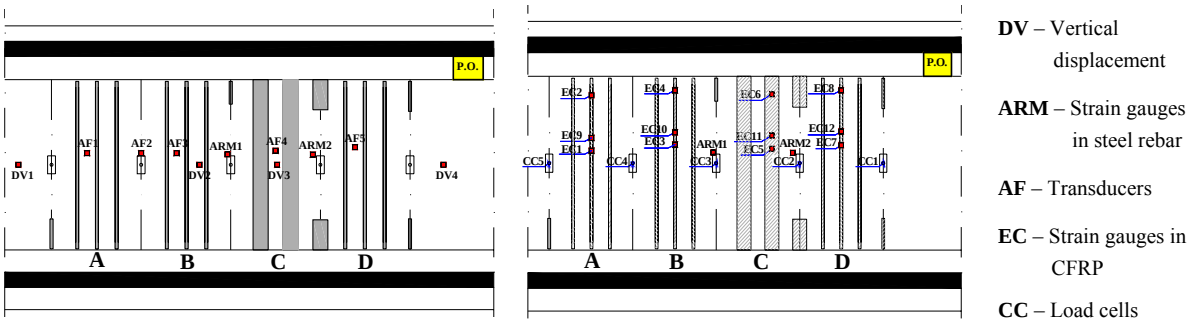



Figure 2 – Plan showing sensors location.

In the first stage were installed eight strain gauges (EC1 to EC8) on the four CFRP systems, half near the end and another half near the slab middle span, in a cracked section, and two temperature sensors (TI and TE). This stage ends with the setting of the observation post (P.O.). Afterwards, to perform the load tests it was installed displacement transducers for measuring either the central deflection (DV1 to DV4) or the crack widths (AF1 to AF5). To control the applied load it were used five load cells (CC1 to CC5). The first results advised the installation of more four strain gauges (EC9 to EC12) in the CFRP systems, but now in an uncracked section near the previous ones. Finally, the last stage included another temperature sensor (TB) and two strain gauges applied to the steel reinforcement (ARM1 and ARM2) located in a cracked section.

A more detailed data of the used sensors is presented in a technical report (Silva, 2003b). It can be seen in Figure 3 the illustration of the type of sensors used.

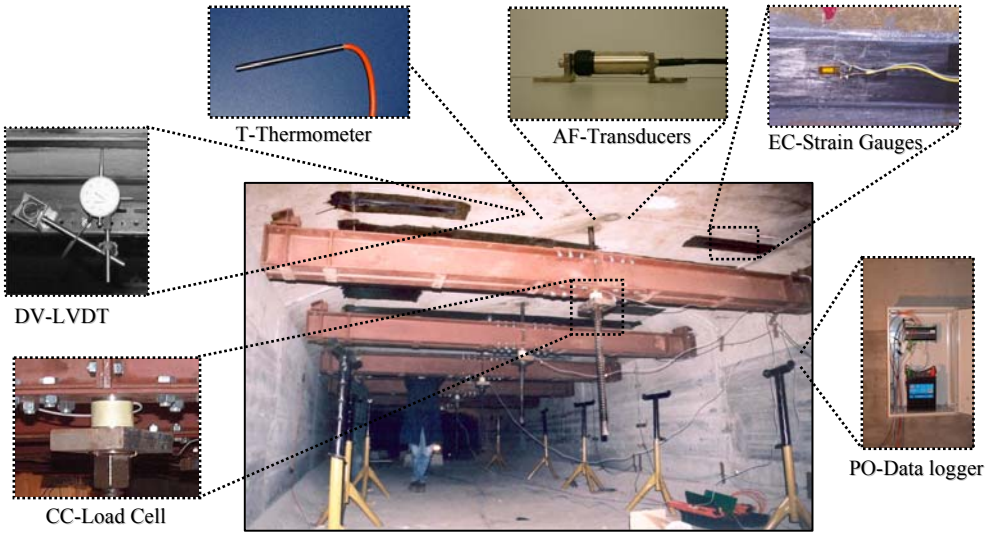



Figure 3 – Monitoring system used in N. S. da Guia bridge.

## 4. LABORATORY TESTS

At the Laboratory of Structures (LABEST) of the University of Porto is in course an experimental program where the main objective is to appraise the flexural behaviour of 2 sets of RC slabs subjected to repeated loads. The first set is formed by two reinforced concrete slabs (considered as reference) and the other include four RC slabs strengthened with two different externally bonded CFRP systems, carbon sheets (series LFBM) and carbon laminates (series LFBL).

### 4.1. Specimens and test setup

The six slab specimens presents the same characteristics as the N. S. da Guia deck slab bridge, in terms of equivalent geometry (2.85×1.0×0.2 m3), of concrete and steel reinforcement properties. The strengthening of the slabs was designed in order to double the existing strength capacity (Silva, 2003a).

Before executing the repeated load tests, the slab model LF1BM (strengthened with MBrace sheet C1-20) was submitted to a static test in order to settle the crack pattern. Afterwards, to predict the “in situ” load tests response of the CFRP systems used to strengthen a limited region of the bridge deck slab two flexure tests were carried out. The positive bending moment experimentally applied was 18 kNm/m, which correspond to the bending moment numerically attained for the field tests. The specimen general information and the test setup are illustrated in Figure 4.

### 4.2. Experimental results

The experimental results that will be presented in this section show, basically, the strain values measured in all the strain gauges placed in the CFRP system for one of the performed tests. The load setup applied in the first test and the related composite response are illustrated in Figure 5. In Figure 6 it can be seen the concrete crack influence in the CFRP strain distribution. Thus, this diagram shows, for two tests and for the maximum applied load (38 kN) the CFRP strain distribution along the system length.

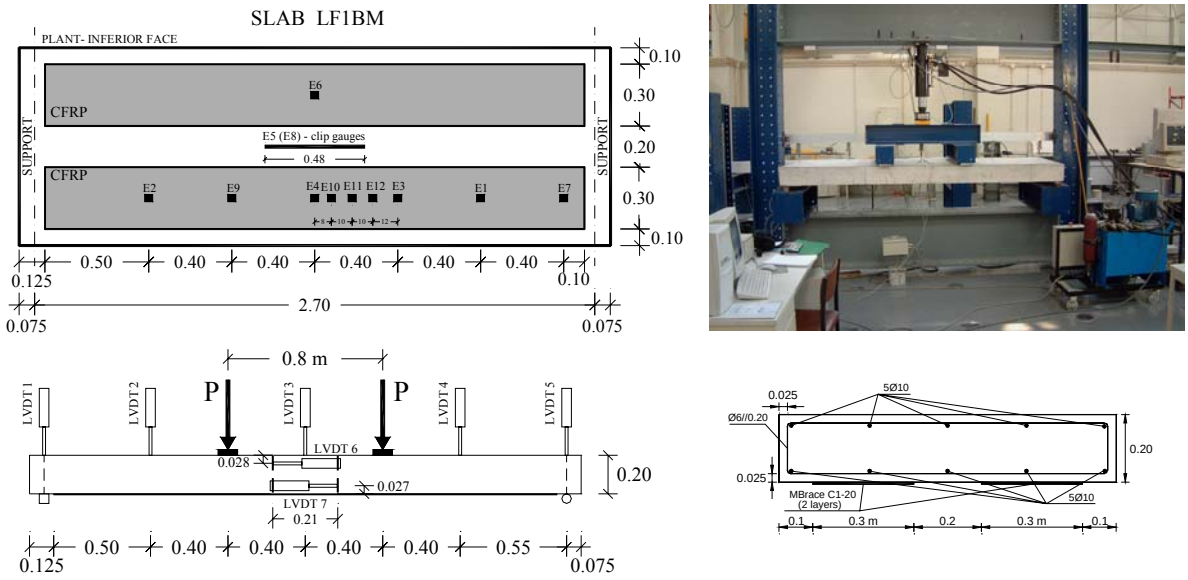
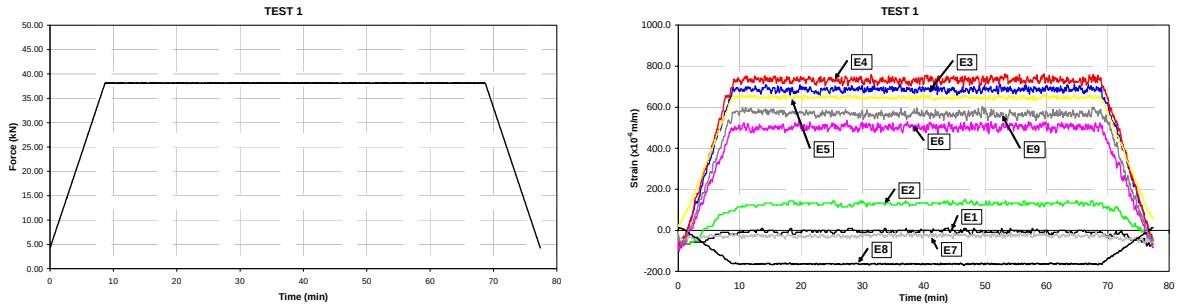



Figure 4 – Test setup and general information about slab LF1BM.




a) Test 1 – Load vs Time

b) Test 1- Strain vs Time

Figure 5 – Load and strain curves versus time of the experiment.

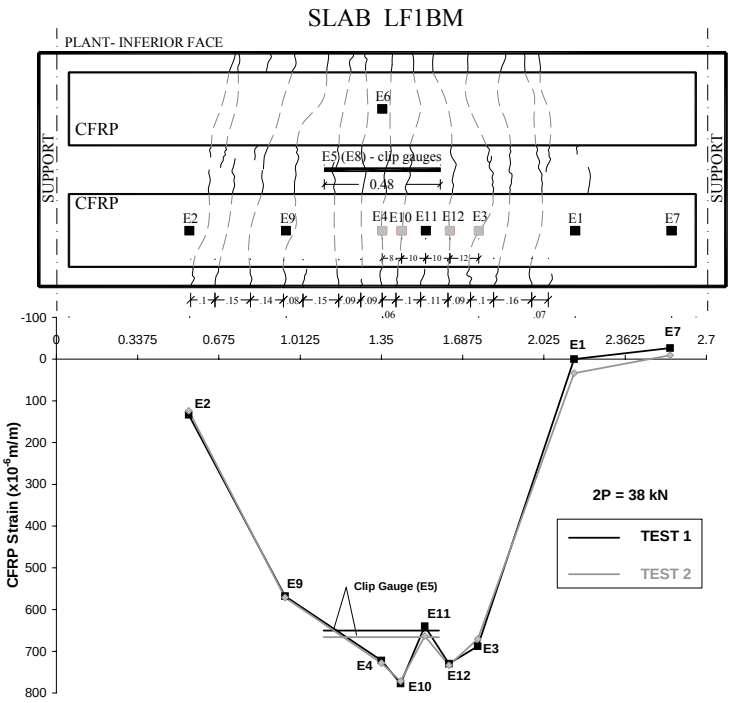



Figure 6 – Experimental strains of the CFRP plate for the slab LF1BM.

## 5. FIELD LOAD TESTS

In order to appraise the efficiency of the externally bonded CFRP systems a load test campaign was performed in the strengthened region of N. S. da Guia bridge. The applied load in all the tests is approximately 80% of the vehicle live load specified in the Portuguese code RSAEEP (Silva, 2003b). It was performed ten field load tests in a period of almost two years.

### 5.1. Test setup

The load test setup for the simulation of the vehicle live load is illustrated in Figure 7. The load is applied in the upper face of the deck slab by pulling a Dywidag rebar. The force is balanced by the mobilized reaction in the steel beam (2 UNP240) which is placed in the interior of the box girder cell. In order to distribute more uniformly the load to all the four CFRP systems we used five steel beams with 1.5 meters spacing. Each system is placed, therefore, between two steel beams. The procedure for each load test is divided into four steps. The first one is to pass over the deck slab five prestressing bars. In the next step all the steel beams are lifted until both ends reach the inner face of the deck slab. In the third step the loads are individually and incrementally applied in each beam until a predefined maximum value is reached. The applied load is kept constant for a given period of time. Finally, the last step is the incrementally unload of the deck slab and the beams return to their initial position, withdrawing all the bars.

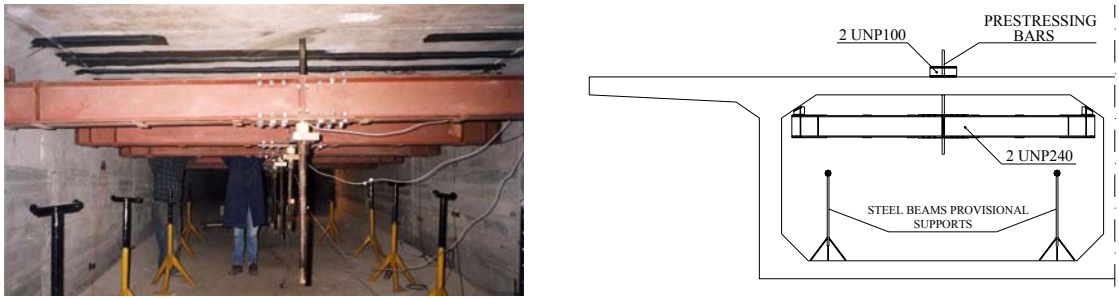



Figure 7 – Load test setup.

### 5.2. Analysis of field test results

The main results registered during the load tests were: applied load, strains in CFRP systems, steel reinforcement strains, crack widths and vertical displacements in several points of the limited region of the deck slab.

In order to increase the confidence on the measured data and to support the analysis of the results an elastic numerical study was performed. A plane frame model of the box girder cross section was used (Silva, 2003b), see Figure 8. The main purpose was to appraise the elastic bending moments in the deck slab. Afterwards, it was performed a numeric analysis of the strengthened cross section and the stress-strain distribution was obtained. In this study it was assumed perfect bonding between all materials.

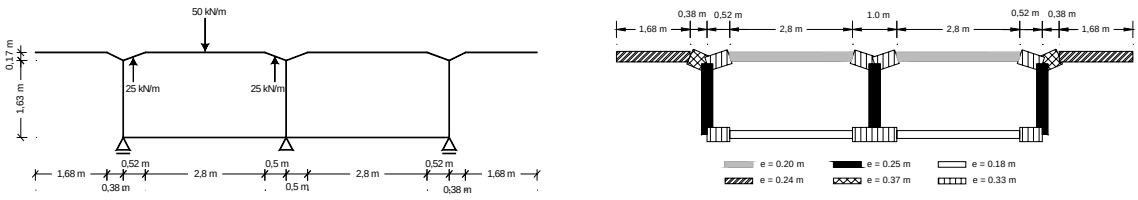
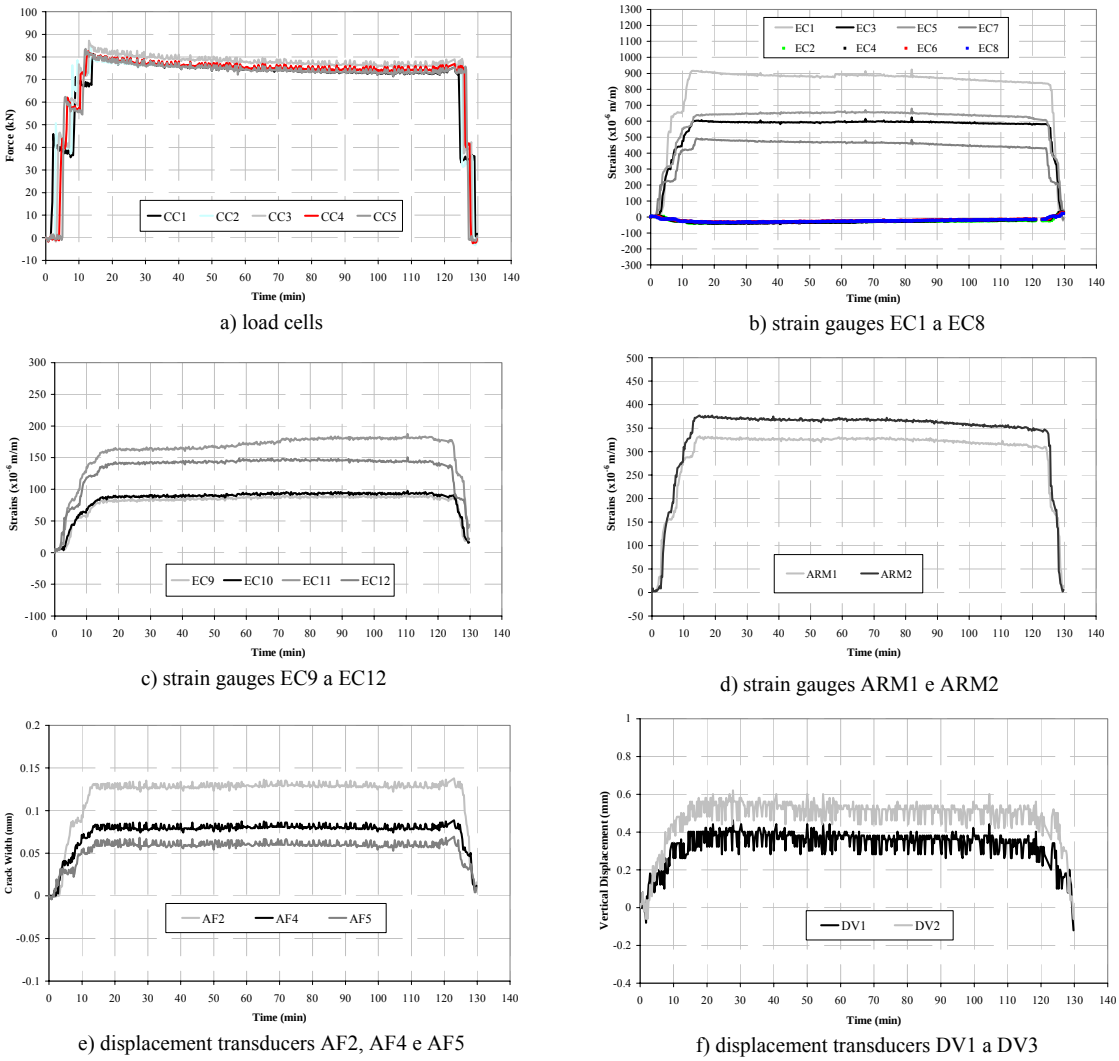



Figure 8 – Plane frame numerical model.

The last performed test, designated by "Load10", will be used to exemplify the type of measurements made, as seen in Figure 9.




a) load cells

b) strain gauges EC1 a EC8

c) strain gauges EC9 a EC12

d) strain gauges ARM1 e ARM2

e) displacement transducers AF2, AF4 e AF5

f) displacement transducers DV1 a DV3

Figure 9 - Results from the load test "Load10".

Due to the variety of the recorded data resulting from the field load tests and to the complexity of its treatment it will be presented the main aspects extracted from the load tests campaign. Thus, Table 1 shows the numerical appraised values and the mean values measured for vertical displacements and crack widths. The mean values of the CFRP systems strain recorded in the load tests carried out in N. S. da Guia bridge, in the experimental tests performed in our laboratory and the other ones appraised numerically are illustrated in Table 2. The mean values of the strain measured in the field tests were calculated from the strain values of the different systems recorded in each test in an instant when the applied load was kept approximately constant. For the strains obtained in laboratorial tests the mean value was defined from the various strain gauges located in sections of equal bending moment.

Table 1 - Mean values of crack width and vertical deflection of the Bridge deck slab.

| Measured Parameters | Field Tests | Numerical |
|---|---|---|
| Crack width – AF2, AF4 e AF5 (mm) | $w_m = 0.090$ | $w_m = 0.177$ |
| Vertical deflection – DV1 a DV4 (mm) | $\delta_m = 0.612$ | $\delta_m = 0.567$ |

Table 2 - Mean values of the CFRP strain.

| Test | Appraised Bending Moment (kNm/m) | CFRP Strain (x10$^{-6}$ m/m) | | |
|---|---|---|---|---|
| | | cracked section | uncraked section | Numerical value |
| "in situ" | 9 | - | 115.3 | 36 |
| | 15 | 626.8 | - | 834 |
| Laboratory | 10.5 | - | 72.6 | - |
| | 18 | 688.7 | - | - |

The results from the field load tests shows that the different behaviour of the various CFRP systems, quantitatively, is due to the variability of the load applied in each of the four systems and the difficulty in measuring it, to the different behaviour of the CFRP systems and to the different activity of cracks. The difference between the numeric values and the recorded ones appear to be related to the simplicity of the numerical models used. For a most precise simulation it is desirable to use more powerful numerical models, which include non-linear constitutive relationships for the material behaviour and be able to model the concrete-resin-FRP interface.

In Figure 6 it can be observed, in the pure flexion region, the local effect of cracking originating the CFRP strain variations, between cracked and uncracked sections. In the bridge load tests it was possible to compare the behaviour of all four systems either in cracked section or in uncracked section. To show those differences was selected the "Load10" test, Figure 10. It can be noticed that the system that presents the greatest strain in a cracked section show the smallest strain in an uncracked section. This behaviour is logical considering that the mean strain in the deck slab should be approximately the same in all the CFRP systems.

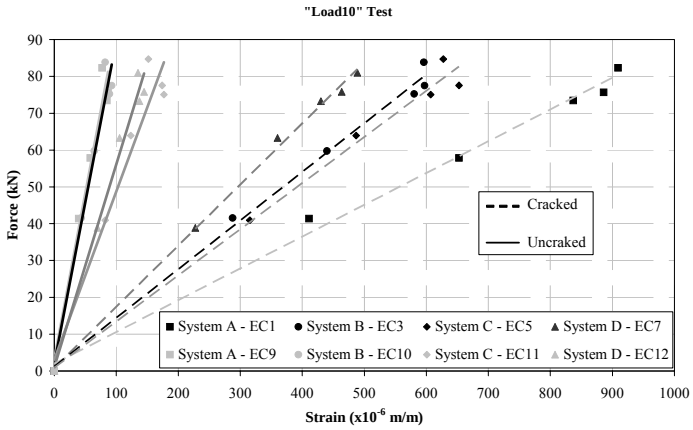



Figure 10 – CFRP systems behaviour, in cracked and uncracked sections.

## 6. HEALTH MONITORING OF CFRP SYSTEMS

The monitoring program was established in order to fulfil the following objectives: measure the daily temperature variation; appraise the CFRP systems response; and to examine the crack activity in the inner face of the slab deck to the daily actions. It included three observation periods. The first period started in 27 of July of 2001 and ended in 16 of November of 2001. In this stage the gap between readings was 4 hours. The next period occurred from January 10, 2002, to February 20. In terms of readings this stage was divided in two, the first part had a gap of 6 hours between measurements and the second had 1 hour.

The last phase was the widest and the one that gathered more relevant data. It began in 13 of May 2002 and finished in 2 of March 2004. In this final stage the interval between successive readings was 3 hours.

## 6.1. Results and discussion

It should be regarded that the gap between readings (from 1 to 6 hours) didn't allow the evaluation of the intense traffic load effects, specially, in working days. Therefore the recorded measures enable, only, the relation between CFRP systems strains or cracks width and the temperature variation. Anyhow, we didn't discard the possibility that the quantities measured can exhibit the influence of other unwanted effects.

The evolution of the external temperature, TE, the inside temperature, TI, and the temperature on the upper face of the top slab under the asphalt layer, TB, during the third observation period are illustrated in Figure 11. The recorded strain in one of the composite systems (e.g. system B) during the same period of time can be seen in Figure 12. The strain gauge EC3 is located in a cracked section and the EC4 near the end of the composite system.

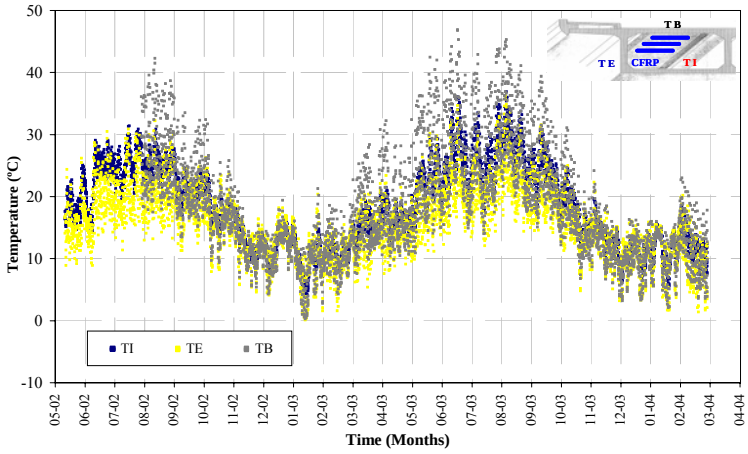



Figure 11 – Evolution of the temperature.

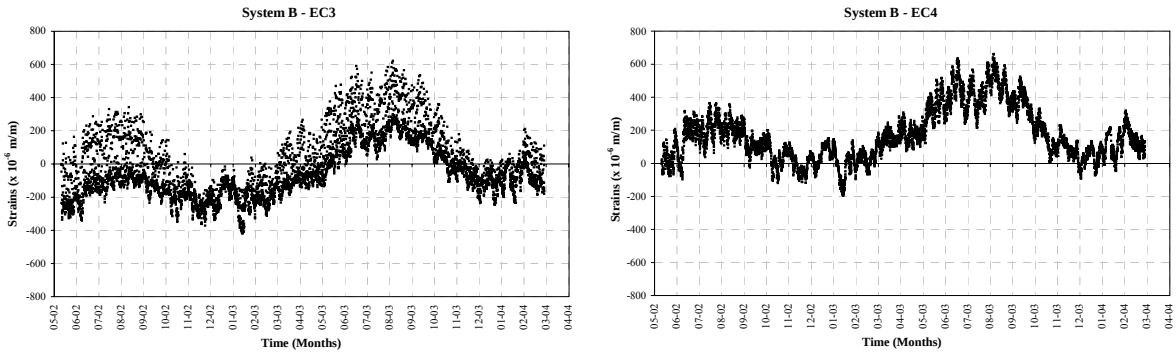



Figure 12 – Evolution of strain for CFRP system B.

## 6.2. Temperature analysis

The thermal gradient in the deck slab and in one of the three webs of the box girder was determined from the recorded data.

Considering only the last monitoring period, which include the summer of 2002 up to, practically, the end of the winter (2003/2004), it was observed that the maximum and the

minimum temperatures TE and TB were almost equals during the Autumn/Winter season. However, in Spring/Summer season the deck slab upper face temperature (TB) is higher than the exterior temperature (TE). In Figure 13 can be seen that the thermal gradient in the deck slab (black line) is greater than the one determined in the web (grey line). It is easy to understand that in winter the solar exposition is less significant and that the asphalt pavement doesn't reach a high temperature which is why the thermal gradient in this period is approximately the same either in the slab or in the web. In the others seasons the thermal gradient in the deck slab is responsible for the increase of tensile stresses in the bottom face of the slab and therefore contributing for the exhibited crack activity.

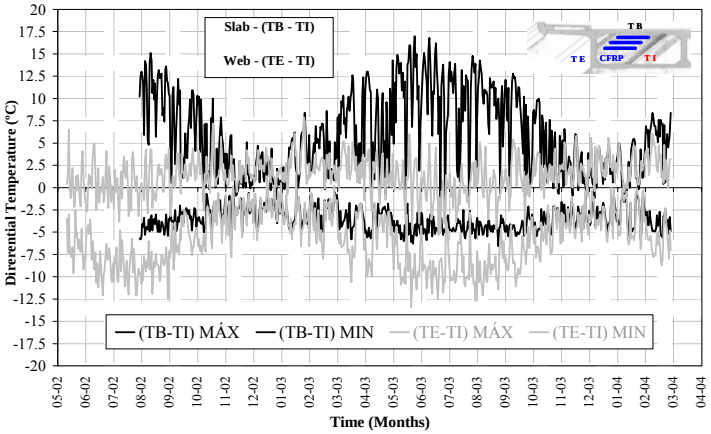



Figure 13 – Thermal gradient envelope of the box girder top slab and web.

During the year 2003, Spring/Summer season (183 days), the thermal gradient (TB-TI) in the deck slab reached the maximum value of 17ºC (27 of May) and reached values greater than 12.5ºC in 44 of those days.

Figure 14 shows the temperature measurements (TE, TI and TB) taken over two seven-day periods, one in summer and other in winter. In the warm period the daily thermal range in the slab is greater than the one registered in the box girder web. However, in the cold period those ranges are sensibly equals.

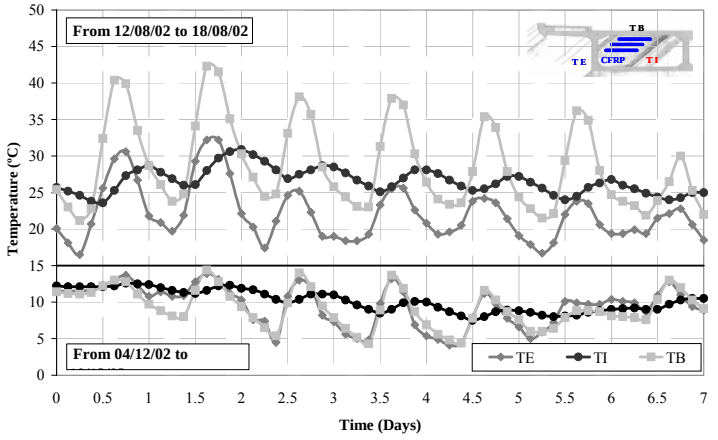
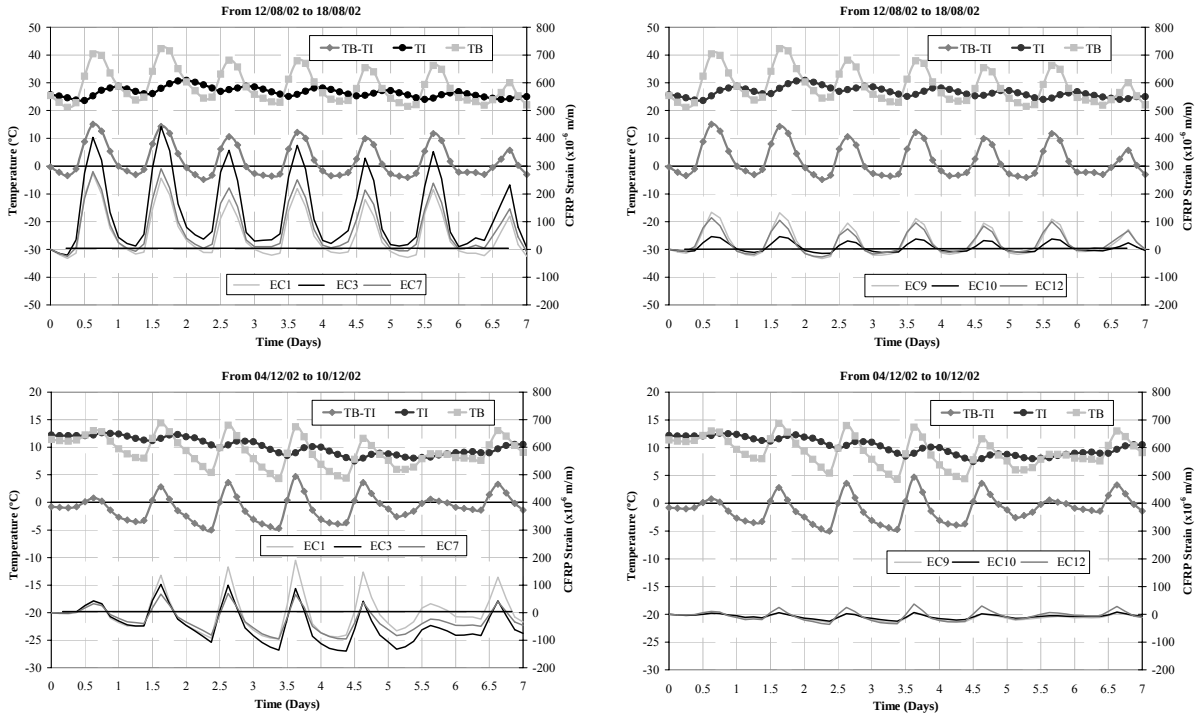



Figure 14 – Temperature variation in two different weeks (in summer and in winter).

6.3. Influence of temperature in CFRP systems response

It was also possible to register the influence of temperature in the CFRP systems response. Thus, Figure 15 illustrates, for the same weeks previously presented in Figure 14, the interior and the slab upper face temperatures variation, the deck slab thermal gradient (TB-TI) and the resulting CFRP systems deformation, measured in a cracked section (EC1, EC3 e EC7) and in an uncracked section (EC9, EC10 e EC12). The effects of temperature variation in the cracks activity can be seen in Figure 16.




a) cracked section b) uncracked section

Figure 15 –CFRP systems response to thermal action (summer and winter).

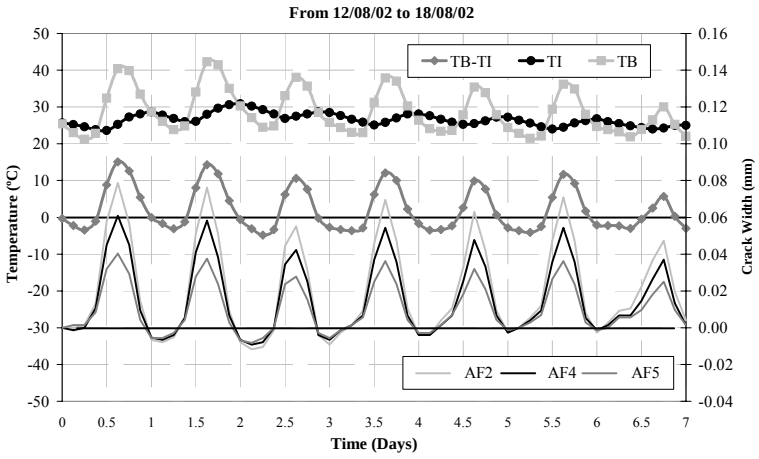



Figure 16 – Crack width due to temperature action.

After observing these figures it's unquestionable the influence of temperature in the measured strains throughout the monitoring campaign. In Table 3 are resumed the measured strain values of three CFRP systems for the same previous weeks, in a cracked and an

uncracked section, for several deck slab thermal gradients. The strain mean value was determined from the assumption that the cracked section value influences the third part of the crack spacing and that the uncracked section value influences two thirds of the crack spacing, see eq.(1). To give an example, the System A mean strain is:

$$\varepsilon_{m,\,CFRP} = 1/3 \times 256.6 + 2/3 \times 132.4 = 173.8\ \mu m/m \quad (1)$$

Table 3 - Strain values of CFRP systems due to thermal gradient in the bridge deck slab.

| **From 12/08/02 to 18/08/02** | | | | | | | | | |
|---|---|---|---|---|---|---|---|---|---|
| **Thermal Gradient (º C)** | **Strain (x10$^{-6}$ m/m) System A** | | | **Strain (x10$^{-6}$ m/m) System B** | | | **Strain (x10$^{-6}$ m/m) System D** | | |
| | EC1 | EC9 | Mean | EC3 | EC10 | Mean | EC7 | EC12 | Mean |
| 14.3 | 256.6 | 132.4 | 173.8 | 441.9 | 46.4 | 178.2 | 290.7 | 105.3 | 167.1 |
| 10.0 | 154.2 | 89.9 | 111.3 | 288.8 | 32.9 | 118.2 | 186.3 | 70.5 | 109.1 |
| -4.8 | -10.7 | -32.9 | -25.5 | 37.1 | -14.5 | 11.3 | 3.9 | -27.1 | -11.6 |
| **From 04/12/02 to 10/12/02** | | | | | | | | | |
| 4.7 | 189.3 | 5.8 | 66.9 | 87.8 | 6.8 | 33.4 | 66.3 | 36.7 | 46.6 |
| 0.0 | 11.4 | -7.7 | 3.7 | 6.8 | -10.6 | -4.8 | -4.9 | 0 | -1.6 |
| -5.0 | -92.7 | -29.0 | -50.2 | -107.3 | -24.2 | -51.9 | -81.0 | -35.8 | -50.8 |

From the values in Table 3 we can notice that the maximum thermal gradient, in this summer week, induces in all CFRP systems a strain mean value of approximately 173 μm/m. Considering that the mean value of the CFRP systems strain measured in the performed field load tests (Silva, 2003b), and treated according to the same previous assumption, is around 285.8 μm/m, it can be concluded that the deformation due to the temperature action is nearly 60% of this final one. Figure 16 shows the low effectiveness of these systems in reducing the crack width because of their low stiffness. Those crack widths values seemed to be in conformity with the mean values of the CFRP systems strain.

## 7. CONCLUSIONS

The health monitoring of the experimental strengthening of the N. S. da Guia Bridge deck slab allowed the evaluation of the efficiency of this strengthening technique. From this study we can point out the following conclusions:

- For the applied loads, corresponding to the maximum live load, the strain in the different CFRP systems is less then 1000 microstrains (1‰);
- In the period of almost three years it weren't registered any significant changes in the CFRP systems behaviour;
- In a cracked section the CFRP strain are sensitive to the crack movements;
- The laboratorial tests performed over the slab model LF1BM predicted with good approximation the CFRP systems strain.
- It's important to perform a nonlinear numerical analysis of the strengthened region of the deck slab.
- The daily temperatures in the deck slab and his effects were satisfactorily measured;
- The maximum temperatures measured were 37ºC and 47ºC in the inner face and in the upper face of the deck slab, respectively. For some types of structures (bridges, tunnels, reservoirs, silos, factory chimney) the daily temperature may come closer to the glass transition temperature of the resins used, which can cause premature failures;

- The thermal gradients measured along the total monitoring period were responsible for CFRP systems strains of approximately 0.6‰;
- The cross section geometry (bicelular box girder) is favourable for the maintenance of the internal temperature, therefore causing a little range in the internal daily temperatures;
- The deck slab thermal gradient reached a maximum value of 17ºC, having for several times reached values greater than 12.5ºC;
- The temperature action is responsible for strain distributions that have to be considered, both in service and in ultimate limit states. The cross section geometry, his redundancy level and the maintenance of the internal temperature are factors that contribute to the deformation of the structure due to temperature changes.

Finally we can say that the results obtained were satisfactory and that they are a valid contribution to a better understanding of this strengthening technique, namely, the short and long-term serviceability behaviour.

## 8. ACKNOWLEDGEMENT

The authors would like to express their thanks to the companies, STAP, SIKA, BETTOR MBT and INEGI for their collaboration and supply of the structural strengthening products. Special thanks to IEP – Portuguese Road Institute, namely, to Direcção de Estradas de Viana do Castelo for all the material means made accessible and availability during the field load tests.

## 9. REFERENCES

Figueiras, J.A., Juvandes, L.F.P. and Oliveira, L.P., Reforço experimental da laje do tabuleiro da ponte de N. S. da Guia em Ponte de Lima, *Relatório Técnico*, DECivil, FEUP, Porto, Portugal (1999). (in portuguese)

Hag-Elsafi, O., Alampalli, S. and Kunin, J., In-service evaluation of a reinforced concrete T-beam bridge FRP strengthening system, *Composite Structures*, 64, 179-188 (2003).

Mettemeyer, M. et al., Shear Load Testing of Carbon Fiber Reinforced Polymer Strengthened Double Tee Beams in Precast Parking Garage, *Proceedings of the Fourth International Symposium on Fiber Reinforced Polymer Reinforcement for Reinforced Concrete Structures*, ACI SP-188, Baltimore, November, 1063-1072 (1999).

Mayo, R. et al., Strengthening of Bridge G270 with Externally Bonded Carbon Fiber Reinforced Polymer Reinforcement, *Proceedings of the Fourth International Symposium on Fiber Reinforced Polymer Reinforcement for Reinforced Concrete Structures*, ACI SP-188, Baltimore, November, 429-440 (1999).

Nanni, A. et al., FRP Strengthening and On-Site Evaluation of a PC Slab, *Proceedings of the Second International Conference on Composites in Infrastructures – ICCI'98*, H. Saadatmanesh and MR Ehsani Editors, Tucson, 202-212 (1998).

Oliveira, L.P. and Figueiras, J.A., Análise de Esforços e Deformações Transversais do Tabuleiro da Ponte de N. S. da Guia em Ponte de Lima, *Relatório Técnico*, DECivil, FEUP, Porto, Portugal (1999). (in portuguese)

Reay, J.T. et al., Long Term Durability of Carbon FRP Composites Applied to RC Bridges: State Street Bridge on Interstate 80, *Proceedings of the Construction Materials Meeting*, Long Beach CA (2004).

Silva, P.C., Juvandes, L.F.P. and Figueiras, J.A., Determinação dos Esforços e Deslocamentos Transversais do Tabuleiro da Ponte de N. S. Guia, *Relatório Técnico*, DECivil, FEUP, Porto, Portugal (2002). (in portuguese)

Silva, P.C., Juvandes, L.F.P. and Figueiras, J.A., Reforço do Tabuleiro da Ponte de N. S. Guia, *Memória do Estudo Prévio*, DECivil, FEUP, Porto, Portugal (2003a). (in portuguese)

Silva, P.C. et al., Monitorização do comportamento do reforço experimental do tabuleiro da ponte de N. S. Guia, *Relatório Técnico*, DECivil, FEUP, Porto, Portugal, (2003b). (in portuguese)

# Session 1

International Symposium Polymers in Concrete
2 - 4 April 2006
Guimarães, Portugal

# Properties of polymer-modified mortars using hardener-free epoxy resin with nitrite-type hydrocalumite

M. OTA[1], Y. OHAMA [2]

*Department of Architecture, College of Engineering, Nihon University*
*Koriyama, Fukushima, 963-8642, Japan*

H. TATEMATSU[3]

*JR Soken Engineering Co., Ltd.*
*Kokubunji, Tokyo, 185-0034, Japan*

## ABSTRACT

The purpose of this study is to develop effective intelligent patch materials for the repair work for deteriorated reinforced concrete structures. Polymer-modified mortars using hardener-free epoxy resin with nitrite-type hydrocalumite (calumite) are prepared with various calumite contents and polymer-binder ratios, and tested for strengths, adhesion, water absorption and permeation, drying shrinkage and corrosion (of embedded reinforcing bars). As a result, increasing calumite content tends to cause a marked improvement in the corrosion-inhibiting property of the polymer-modified mortars but decreases in their compressive strength, adhesion and waterproofness, and an increase in their drying shrinkage. Their flexural strength, adhesion and waterproofness are improved to some extent with an increase in the polymer-binder ratio. Polymer-modified mortars with a self-healing function and self-corrosion inhibition function may be made by controlling the calumite content and polymer-binder ratio in the combined use of the calumite and hardener-free epoxy resin. Approach to intelligent patch materials for deteriorated reinforced concrete structures is expected by use of such polymer-modified mortars.

## 1. INTRODUCTION

In recent years, the rapid deterioration of the reinforced concrete structures due to chloride-induced corrosion, alkali-aggregate reaction and early carbonation has become a social problem in Japan and in most of the world. The polymer-modified mortar which is produced by mixing polymeric admixtures with cement mortar is currently used in large

[1] Graduate Student
[2] Professor, Ph. D.
[3] President, Ph. D.

quantities as a popular repair material for the deteriorated reinforced concrete structures because of its high tensile and flexural strengths, adhesion to cement concrete, waterproofness, airtightness and durability. In particular, it attracts notice that polymer-modified mortar using a hardener-free epoxy resin has a self-healing or self-repair function for microcracks by the self-capsuled epoxy resin formed in the mortar as Ohama (2001). Because the hardener-free epoxy resin can harden in the presence of alkali or hydroxide ions in the mortar as Ohama (1992), and cause its self-capsulation as Ohama (2001).

Nitrite-type hydrocalumite is a material or substance which can adsorb the chloride ions ($Cl^-$) causing the corrosion of reinforcing bars and liberate the nitrite ions ($NO_2^-$) inhibiting their corrosion, and provides an excellent corrosion-inhibiting property to the reinforcing bars in reinforced concrete by the addition of it to concrete as Tatematsu (2003).

Consequently, polymer-modified mortar with superior corrosion-inhibiting property and durability is expected to be made by the combined use of the nitrite-type hydrocalumite and hardener-free epoxy resin, and to be used as an effective repair material for deteriorated reinforced concrete structures. However, the properties of such polymer-modified mortar with the nitrite-type hydrocalumite have been not yet examined in detail.

In the present paper, for the purpose of developing the intelligent patch materials for the repair work for deteriorated reinforced concrete structures, polymer-modified mortars using a hardener-free epoxy resin with nitrite-type hydrocalumite are prepared with various nitrite-type hydrocalumite contents and polymer-binder ratios, and their strengths, adhesion to mortar substrates, waterproofness, drying shrinkage and corrosion-inhibiting property are discussed. In addition, the properties of the polymer-modified mortars with the nitrite-type hydrocalumite are compared to the quality requirements specified in JIS (Japanese Industrial Standard) A 6203 (Polymer dispersions and redispersible polymer powders for cement modifiers), and their quality as polymer-modified mortars are examined.

## 2. MATERIALS

### 2.1. Cement

Ordinary portland cement as specified in JIS R 5210 (Portland cement) was used as a cement. The properties of the cement are given in Table 1.

Table 1 – Physical properties and chemical compositions of ordinary portland cement.

| Density ($g/cm^3$) | Blaine specific surface ($cm^2/g$) | Setting time (h-min) | | Compressive strength of mortar (MPa) | | |
|---|---|---|---|---|---|---|
| | | Initial set | Final set | 3d | 7d | 28d |
| 3.16 | 3340 | 2-10 | 3-25 | 29.0 | 43.6 | 61.7 |
| Chemical compositions (%) | | | | | | |
| MgO | | $SO_3$ | | Loss on ignition | | |
| 1.4 | | 2.2 | | 1.8 | | |

### 2.2. Fine aggregate

ISO standard sand as specified in JIS R 5201 (Physical testing methods for cement) was employed as a fine aggregate. The properties of the ISO standard sand are given in Table 2.

Table 2 – Properties of ISO standard sand.

| Size (mm) | Bulk density (kg/l) | Density ($g/cm^3$) | Water absorption (%) |
|---|---|---|---|
| 0.08-2.00 | 1.74 | 2.63 | 0.2 |

2.3. Admixture for corrosion inhibition

Nitrite-type hydrocalumite (calumite) was used as an admixture for corrosion inhibition. The principle of corrosion inhibition by the calumite is given in the following reaction formula as Tatematsu (2003), and the properties of the calumite are listed in Table 3.

$$3CaO\cdot Al_2O_3\cdot Ca(NO_2)_2\cdot nH_2O + 2Cl^- \rightarrow 3CaO\cdot Al_2O_3\cdot CaCl_2\cdot nH_2O + 2NO_2^-$$

Table 3 – Properties of calumite.

| Appearance | Particle size (μm) | Density ($g/cm^3$) |
|---|---|---|
| White powder | <210 | 2.30 |

2.4. Polymeric admixture

A diglycidyl ether of bisphenol A (epoxy resin or epoxy) was used as a polymeric admixture. The constitutional formula of the epoxy resin is expressed in Figure 1. The properties of the epoxy resin are given in Table 4.

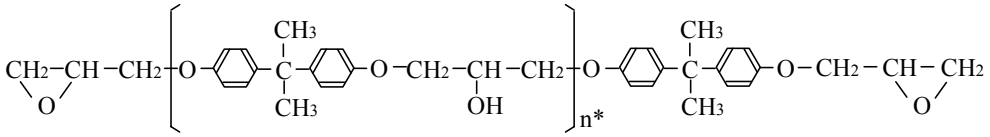


Figure 1 – Constitutional formula of diglycidyl ether of bisphenol A (epoxy resin).
Note,* : Average degree of polymerization (n=0.1~0.2).

Table 4 – Properties of epoxy resin.

| Epoxide equivalent | Molecular weight | Density ($g/cm^3$, 20 ºC) | Viscosity (mPa·s, 20 ºC) |
|---|---|---|---|
| 186 | 380 | 1.16 | 38000 |

2.5. Primer for adhesion test

A commercial two-part epoxy resin-based primer was used as a primer for adhesion test. The properties of the primer are given in Table 5.

Table 5 – Properties of primer.

| Base compound : hardener ratio (by mass) | Appearance | Viscosity (mPa·s, 20 ºC) | Coverage rate ($kg/m^2$) | Open time (min) |
|---|---|---|---|---|
| 3 : 1 | Light yellow liquid | 12500 | 0.5 | 30 |

### 2.6. Reinforcing bars for corrosion inhibition test

Steel bars (SGD3) Φ10×130mm as specified in JIS G 3108 (Rolled carbon steel for cold-finished steel bars) were used as reinforcing bars for corrosion inhibition test.

## 3. TESTING PROCEDURES

### 3.1. Preparation of specimens

Binders were previously prepared with cement : calumite ratios (by mass) of 100:0, 95:5 and 90:10, corresponding to calumite contents of 0, 5 and 10%. According to JIS A 1171 (Test methods for polymer-modified mortar), polymer-modified mortars were mixed with a mass ratio of binder to fine aggregate 1:3, polymer-binder ratios of 0, 5, 10, 15 and 20%. Their flow was adjusted to be constant at 170±5 in the water-binder ratio range of 47.0 to 53.0%. Beam specimens 40×40×160mm for flexural strength, compressive strength and water absorption tests were molded with the polymer-modified mortars, and subjected to a 2d-20°C-90%(RH)-moist plus 5d-20°C-water plus 21d-20°C-60%(RH)-dry curing. Disk specimens Φ150×40mm for water permeation test were molded with the polymer-modified mortars, and subjected to a 2d-20°C-90%(RH)-moist plus 5d-20°C-water plus 21d-20°C-60%(RH)-dry curing. Beam specimens 40×40×160mm for drying shrinkage test were molded with the polymer-modified mortars, and subjected to a 2d-20°C- 90%(RH)-moist plus 5d-20°C-water curing. Beam specimens 40×40×160mm for corrosion inhibition test were molded by embedding reinforcing bars in the polymer-modified mortars as shown in Figure 2, and subjected to a 2d-20°C-90%(RH)-moist plus 5d-20°C-60%(RH)-dry curing. Mortar substrates and special-shaped specimens for adhesion test were prepared as follows: ordinary cement mortar was mixed according to JIS R 5201 with a mass ratio of cement to standard sand 1:3 and a water-cement ratio of 50.0%. Mortar substrates 70×70×20mm were molded with the ordinary cement mortar, and given a 2d-20°C-90%(RH)-moist plus 5d-20°C-water plus 7d-20°C-60%(RH)-dry curing. Then the bonding surfaces of the mortar substrates were treated with the Aw-A-P120 abrasive papers specified in JIS R 6252 (Abrasive papers), and blown with compressed air to remove free dust particles before water wetting or primer coating. The mortar substrates were wetted with water or coated with a primer. To make special-shaped specimens, the polymer-modified mortars were bonded in the size of 40×40×10mm on the water-wetted or primer-coated mortar substrates, and then subjected to a 2d-20°C-90%(RH)-moist plus 5d-20°C-water plus 21d-20°C-60%(RH)-dry curing.

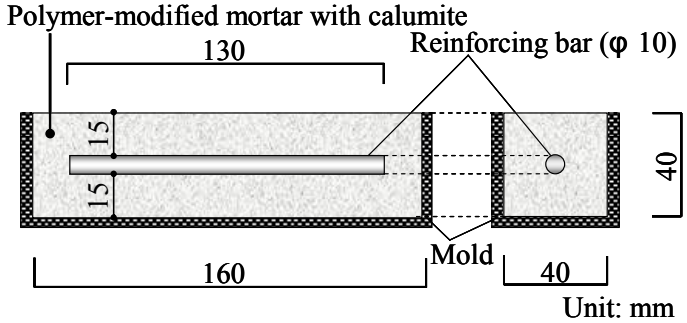



Figure 2 – Geometry of specimen.

### 3.2. Flexural and compressive strength tests

Beam specimens were tested for flexural and compressive strengths in accordance with JIS A 1171.

### 3.3. Adhesion test

Special-shaped specimens were tested for adhesion in tension to mortar substrates in accordance with JIS A 1171.

### 3.4. Water absorption test

According to JIS A 1171, beam specimens were dried at 80°C for 48h, immersed in water at 20°C for 48h, and then their water absorption was determined.

### 3.5. Water permeation test

According to JIS A 1171, beam specimens were dried at 80°C for 48h, exposed to a water pressure of 100kPa for 1h, and then their water permeation was determined.

### 3.6. Drying shrinkage test

According to JIS A 1171, after the original length of beam specimens was measured, the specimens were dried at 20°C and 60%(RH) for 28d, and their drying shrinkage was measured.

### 3.7. Corrosion inhibition test

Beam specimens with embedded reinforcing bars were tested for corrosion inhibition in accordance with JCI (Japan Concrete Institute) Standards for test methods for polymer-modified mortar (17) (Method of test for corrosion inhibition of polymer-modified mortar) as follows:

For carbonation, the specimens were placed in a sealed pressure vessel, evacuated to 667Pa or less at ambient temperature for 1h, and then exposed to pressurized carbon dioxide gas under a pressure of 1.0±0.05MPa for 24h. The carbonated specimens were dried in a circulating air oven at 30°C for 168h. After drying, the specimens were evacuated to 667Pa or less for 1h, and then impregnated with a 2.5% sodium chloride solution under a pressure of 1.0±0.05MPa for 24h in the pressure vessel for chloride ion penetration. The chloride ion-penetrated specimens were put in polyethylene bags, and heated in the circulating air oven at 80°C for 24h. After that, the specimens subjected to accelerated corrosion were removed from the polyethylene bags, and conditioned at 20°C and 60%(RH) for 24h. The conditioned specimens were split longitudinally, and the embedded reinforcing bars were removed. The surfaces of the reinforcing bars were treated with a 10% diammonium hydrogen citrate solution by using brushes for 1 min, and then cleaned with acetone. The corroded areas of the surfaces of the reinforcing bars were traced, and then measured by a suitable planimeter except the corroded areas at a distance of 20mm from both ends of the reinforcing bars. The corrosion rate of the reinforcing bars embedded in the specimens was calculated from the following equation.

$$\text{Corrosion rate (\%)} = \frac{\text{Total corroded area of reinforcing bar (mm}^2\text{)}}{\text{Total area of reinforcing bar (mm}^2\text{)}} \times 100$$

## 4. TEST RESULTS AND DISCUSSION

Figure 3 shows the calumite content and polymer-binder ratio vs. water-binder ratio of hardener-free epoxy-modified mortars with calumite. Regardless of the polymer-binder ratio, the water-binder ratio of the hardener-free epoxy-modified mortars with calumite increases gradually with increasing calumite content. This is ascribed to the increased mixing water necessary to adjust a constant consistency owing to the porous layer structures of calumite as Katsuhata (2002). With increasing polymer-binder ratio, the water-binder ratio of the hardener-free epoxy-modified mortars with calumite is gradually increased irrespective of the calumite content. The reasons for this trend are that the epoxy resin does not contain any surfactants and does not cause a marked improvement in the consistency because the epoxy resin is a liquid resin.

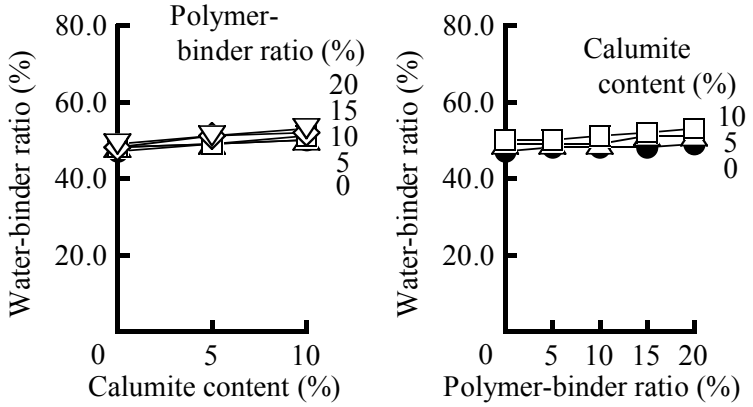



Figure 3 – Calumite content and polymer-binder ratio vs. water-binder ratio of hardener-free epoxy-modified mortars with calumite.

Figure 4 gives the calumite content and polymer-binder ratio vs. air content of hardener-free epoxy-modified mortars with calumite. Irrespective of the polymer-binder ratio, the air content of the hardener-free epoxy-modified mortars with calumite increases slightly with an increase in the calumite content. The air content of the hardener-free epoxy-modified mortars with calumite decreases gradually with increasing polymer-binder ratio regardless of the calumite content. This trend is considered to be due to a combined effect of the air-entraining action by the calumite and no inclusion of any surfactants.

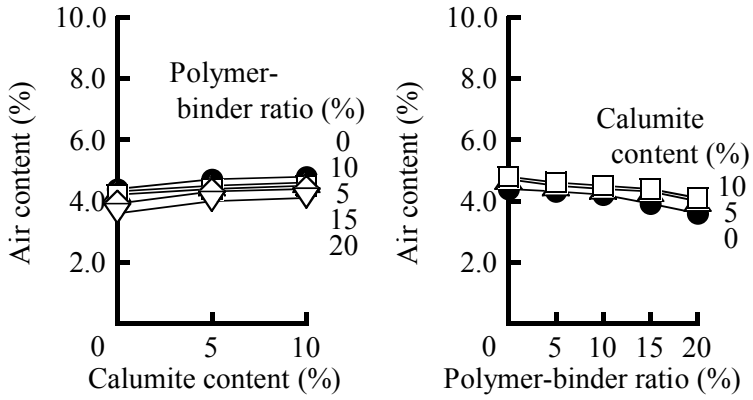



Figure 4 – Calumite content and polymer-binder ratio vs. air content of hardener-free epoxy-modified mortars with calumite.

Figure 5 exhibits the calumite content and polymer-binder ratio vs. flexural strength of hardener-free epoxy-modified mortars with calumite. In spite of the polymer-binder ratio, the flexural strength of the hardener-free epoxy-modified mortars with calumite tends to be nearly constant with increasing calumite content. Regardless of the calumite content, the flexural strength of the hardener-free epoxy-modified mortars with calumite increases with incresing polymer-binder ratio, and reaches maximums at a polymer-binder ratio of 5%. Such an improvement in the flexural strength is attributed to the synergistic effect of the reduced air content and the formation of the comatrix phases by polymer modification in the mortars. Irrespective of the calumite content and polymer-binder ratio, the flexural strength of the hardener-free epoxy-modified mortars with calumite satisfies the quality requirement (8.0MPa min.) specified in JIS A 6203.

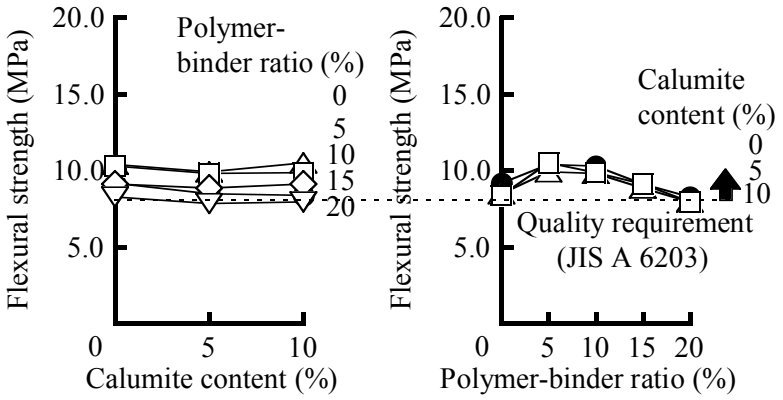



Figure 5 – Calumite content and polymer-binder ratio vs. flexural strength of hardener-free epoxy-modified mortars with calumite.

Figure 6 shows the calumite content and polymer-binder ratio vs. compressive strength of hardener-free epoxy-modified mortars with calumite. The compressive strength of the hardener-free epoxy-modified mortars with calumite decreases with increasing calumite content and polymer-binder ratio. This tendency is explained in terms of the calumite with porous layer structures in the microstructures and the inclusion of the polymer films with small elastic modulus. However, the compressive strength of the hardener-free epoxy-modified mortars with calumite satisfies the quality requirement (24.0MPa min.) specified in JIS A 6203.

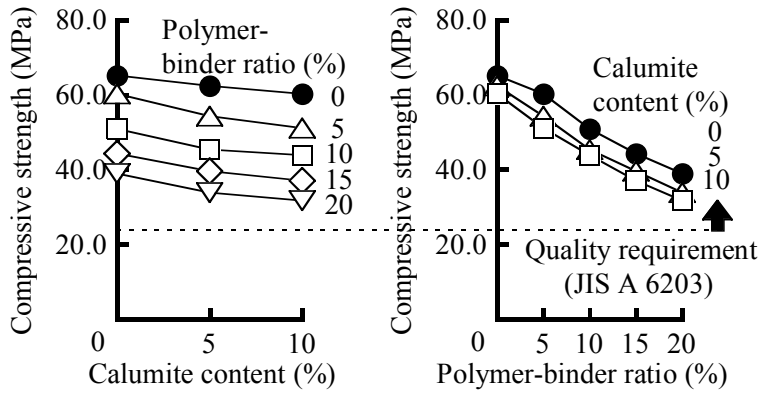



Figure 6 – Calumite content and polymer-binder ratio vs. compressive strength of hardener-free epoxy-modified mortars with calumite.

Figures 7 and 8 show the calumite content and polymer-binder ratio vs. adhesion to mortar substrates of hardener-free epoxy-modified mortars with calumite. Regardless of the type of substrate treatment and the polymer-binder ratio, the adhesion of the hardener-free epoxy-modified mortars with calumite is decreased with increasing calumite content. In spite of the calumite content, the adhesion of the hardener-free epoxy-modified mortars with calumite in the use of the primer coating as a substrate treatment increases with increasing polymer-binder ratio, and reaches maximums at a polymer-binder ratio of 5%. The adhesion of the hardener-free epoxy-modified mortars with calumite in the use of the primer coating is much larger than that of the mortars in the use of the water wetting as a substrate treatment. Irrespective of the calumite content and polymer-binder ratio, the adhesion of the hardener-free epoxy-modified mortars with calumite in the use of the primer coating satisfies the quality requirement (1.0MPa min.) specified in JIS A 6203. However, the adhesion of the hardener-free epoxy modified mortars with calumite in the use of the water wetting at polymer-binder ratios of 15 and 20% does not satisfy the quality requirement (1.0MPa min.) specified in JIS A 6203.

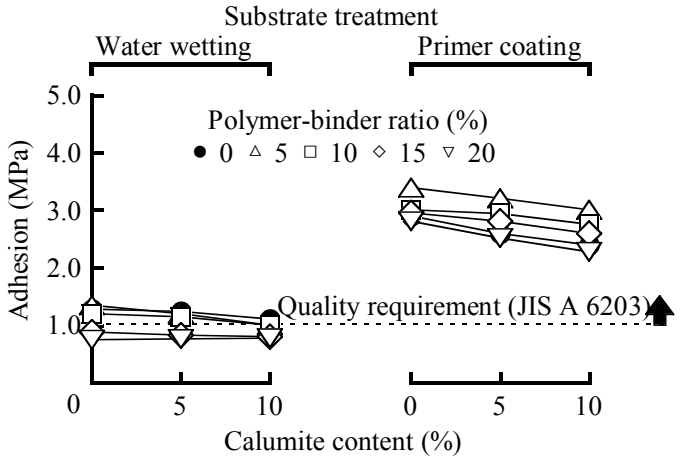



Figure 7 – Calumite content vs. adhesion to mortar substrates of hardener-free epoxy-modified mortars with calumite.

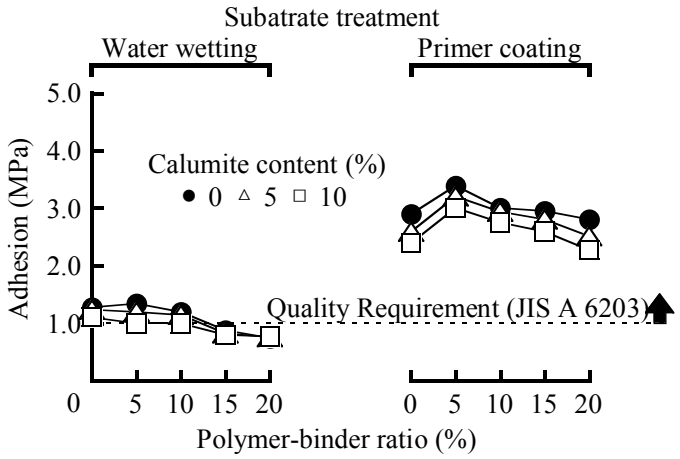



Figure 8 – Polymer-binder ratio vs. adhesion to mortar substrates of hardener-free epoxy-modified mortars with calumite.

Figure 9 illustrates the calumite content and polymer-binder ratio vs. 48-h water absorption of hardener-free epoxy-modified mortars with calumite. The water absorption of

the hardener-free epoxy-modified mortars is not largely affected by the calumite content in spite of the polymer-binder ratio. However, the water absorption of the hardener-free epoxy-modified mortars with calumite decreases sharply with incresing polymer-binder ratio, and reaches minimums at a polymer-binder ratio of 10%. The reason for this is the composite effect of the inclusion of the impervious polymer films formed and the chemical adsorption of water by the formation of the strong hydrogen bond between the water and the hydoxyl groups of the epoxy resin in the mortars. Despite the calumite content and polymer-binder ratio, the water absorption of the hardener-free epoxy-modified mortars with calumite satisfies the quality requirement (10.0% max.) specified in JIS A 6203.

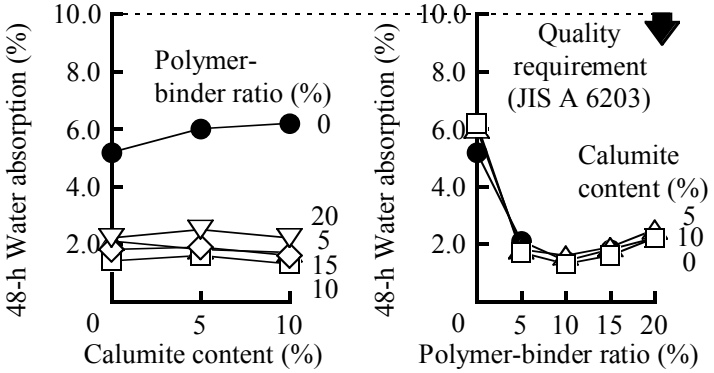



Figure 9 – Calumite content and polymer-binder ratio vs. 48-h water absorption of hardener-free epoxy-modified mortars with calumite.

Figure 10 exhibits the calumite content and polymer-binder ratio vs. water permeation of hardener-free epoxy-modified mortars with calumite. The water permeation of the hardener-free epoxy-modified mortars with calumite gives almost the same tendency to the water absorption of the hardener-free epoxy-modified mortars with calumite. This level of water permeation is not brought by complete water permeation phenomena, and appears to mainly depend on water absorption by capillary action. Irrespective of the calumite content and polymer-binder ratio, the water permeation of the hardener-free epoxy-modified mortars with calumite satisfies the quality requirement (15.0g max.) specified in JIS A 6203.

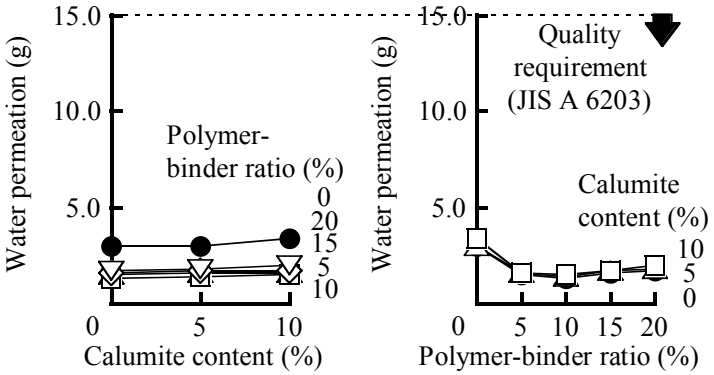



Figure 10 – Calumite content and polymer-binder ratio vs. water permeation of hardener-free epoxy-modified mortars with calumite.

Figure 11 shows the calumite content and polymer-binder ratio vs. 28-d drying shrinkage of hardener-free epoxy-modified mortars with calumite. In spite of the polymer-binder ratio, the drying shrinkage of the hardener-free epoxy-modified mortars with calumite increases with increasing calumite content. This is ascribed to the increased water-binder ratio

and air content by the addition of the calumite as represented in Figures 3 and 4. Regardless of the calumite content, the drying shrinkage of the hardener-free epoxy-modified mortars with calumite decreases gradually with increasing polymer-binder ratio because of the improved water retention by the impervious polymer films formed and the chemical adsorption of water by the formation of the strong hydrogen bond as stated above. Irrespective of the calumite content and polymer-binder ratio, the drying shrinkage of the hardener-free epoxy-modified mortars with calumite satisfies the quality requirement (0 to 0.150 %) specified in JIS A 6203.

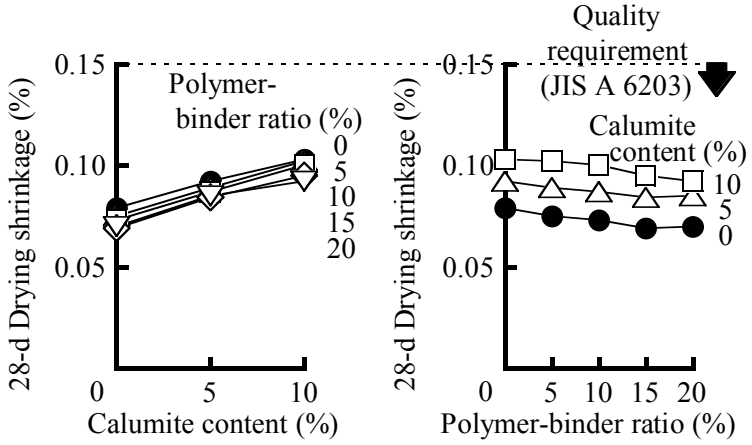



Figure 11 – Calumite content and polymer-binder ratio vs. 28-d drying shrinkage of hardener-free epoxy-modified mortars with calumite.

Figure 12 shows the calumite content and polymer-binder ratio vs. corrosion rate of the reinforcing bars embedded in hardener-free epoxy-modified mortars with calumite. Irrespective of the polymer-binder ratio, the corrosion rate of the reinforcing bars embedded in the hardener-free epoxy-modified mortars with calumite decreases sharply with increasing calumite content, and to almost 0% at calumite contents of 5% or higher. This tendency is explained by the reason that the calumite adsorbs the chloride ions causing the corrosion of the reinforcing bars and at the same time liberates the nitrite ions inhibiting it[3]. In spite of the calumite content, the corrosion rate of the reinforcing bars embedded in the hardener-free epoxy-modified mortars with calumite decreases with increasing polymer-binder ratio, and to almost 0% at polymer-binder ratios exceeding 15%.

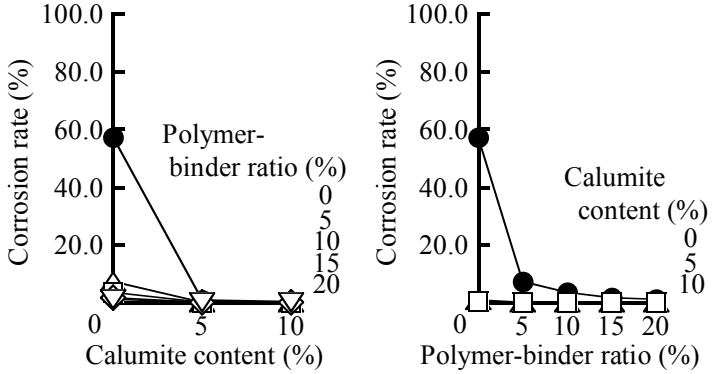



Figure 12 – Calumite content and polymer-binder ratio vs. corrosion rate of reinforcing bars embedded in hardener-free epoxy-modified mortars with calumite.

## 5. CONCLUSIONS

The conclusions obtained from the test results are summarized as follows:

1) The water-binder ratio of hardener-free epoxy-modified mortars with calumite tends to increase with increasing calumite content or polymer-binder ratio. Their air content is inclined to increase slightly with an increase in the calumite content, and to decrease gradually with an increase in the polymer-binder ratio.
2) Increasing calumite content tends to cause a remarkable improvement in the corrosion-inhibiting property of hardener-free epoxy-modified mortars with calumite but decreases in their compressive strength, adhesion to mortar substrates and waterproofness, and an increase in their drying shrinkage. Their flexural strength, adhesion to mortar substrates and waterproofness are improved to a certain extent with an increase in the polymer-binder ratio.
3) The flexural and compressive strengths, adhesion to mortar substrates, water absorption, water permeation and length change of hardener-free epoxy-modified mortars with calumite at a polymer-binder ratio of 10% satisfy all the quality requirements specified in JIS A 6203 as given in Table 6.
4) Hardener-free epoxy-modified mortars with calumite, having a self-healing function and self-corrosion inhibition function may be made by controlling the calumite content and polymer-binder ratio, and are expected to be effective intelligent patch materials for repair work for deteriorated reinforced concrete structures.

Table 6 – Quality levels of hardener-free epoxy-modified mortars with calumite at polymer-binder ratio of 10%.

| Test item | Quality requirements specified in JIS A 6203 | Test results |
|---|---|---|
| Flexural strength (MPa) | 8.0 min. | 9.8 ~ 10.3 |
| Compressive strength (MPa) | 24.0 min. | 43.7 ~ 50.8 |
| Adhesion to mortar substrates (MPa) | 1.0 min. | 1.0 ~ 1.2 |
| Water absorption (%) | 10.0 max. | 1.3 ~ 1.6 |
| Water permeation (g) | 15.0 max. | 1.3 ~ 1.5 |
| Length change (%) | 0 to 0.150 | 0.07 ~ 0.10 |

## 6. REFERENCES

Katsuhata, T., Ohama, Y. and Tatematsu, H., Properties of polymer-modified mortars using nitrite-type hydrocalumite (in Japanese), *Proceedings of the Japan Concrete Institute*, **24(1)**, 1713-1718 (2002).

Ohama, Y., Demura, K. and Katsuhata, T., Investigation of microcracks self-repair function of polymer-modified mortars using epoxy resins without hardeners, in: *Proceedings of the 10th International Congress on Polymers in Concrete (CD-ROM)*, Eds. By D.W. Fowler, G.W. DePuy and M.A. Murray, The University of Texas at Austin, Austin, Texas, USA (2001).

Ohama, Y., Demura, K. and Endo, T., Strength properties of epoxy-modified mortars without hardener, in: *Proceedings of the 9th International Congress on the Chemistry of Cement, Vol. V, Performance and Durability of Concrete and Cement Systems,* National Council for Cement and Building Materials, New Delhi, India, 512-516 (1992).

Tatematsu, H. and Sasaki, T., Repair materials system for chloride-induced corrosion of reinforcing bars, *Cement & Concrete Composites*, **25(1)**, 123-129 (2003).

International Symposium Polymers in Concrete
2 - 4 April 2006
Guimarães, Portugal

# Particulate composite materials with modulated mechanical properties

Franco Sandrolini[1], Stefania Manzi[2]

*Dipartimento di Chimica Applicata e Scienza dei Materiali (DICASM)*
*Facoltà di Ingegneria, Università di Bologna, I-40136, Italy*

## ABSTRACT

The possibility of preparing particulate composite materials with both integrated and modulated physical-mechanical properties is here investigated, using as disperse phases waste particulate materials of different Young modulus, i.e. recycled grinded rubber coming from scrap tyres, by-products coming from raw materials treatment for ceramic industry and normalized sand for reference, in order to join good mechanical properties to some deformability and damping properties.

To this aim, particulate composite materials bound by a polyester matrix have been prepared by a new laboratory moulding system and characterized. In particular, the possibilities of modulating the mechanical properties of the composite materials not only through the components mix design, but also through the set-up of the optimum particle size distribution and moulding conditions have been investigated. Experimental results are then reported and discussed.

## 1. INTRODUCTION

Particulate composite materials represent a very versatile class of materials from a double point of view. In fact, in addition to the possibility of optimizing the final physical-mechanical characteristics working on the mix-design and microstructure (Bignozzi (2000), Bignozzi (2001), Sandrolini (2002)), it is possible to better exploit waste by-products and/or residues of different origin, otherwise disposed to landfill (Bignozzi (1998), Bignozzi (1999), Sandrolini (2001), Bignozzi (2002), Bignozzi (2004/1), Bignozzi (2004/2)). However, nowadays, all new construction materials should exhibit environmental sustainability requirements, in addition to high and versatile mechanical performances.

[1] Full Professor of Materials Science
[2] DICASM Post Ph. D. grant

In this paper polyester matrix composite materials with integrated and modulated physical-mechanical properties have been prepared and characterized. Phases with a high modulus have been therefore combined with low modulus phases using rubber waste particulates together with waste ceramic particulates on a microstructural level. These materials might be a valid alternative to the present use of seismic base isolation devices, nowadays usually constituted by rubber and steel sheets.

While, in general, all materials processed by casting lead to very compact products, in composite materials a certain amount of open porosity (OP %) may be present. Composite materials are typically made by different phases sintering or binder hardening (e. g., cementitious and/or polymeric binders). So, these materials usually require a special technology for their preparation in order to obtain full contact and adhesion between the different phases as well as minimum porosity. In most technological processes, in fact, binder is hardly able to create a compact material without porosity. To improve the microstructure of these composite materials, a laboratory moulding system to control porosity has been purposely set up, which is able to control the basic technological aspects of materials microstructure through independent control of vacuum, mechanical pressure and vibration while shaping.

## 2. EXPERIMENTAL

### 2.1. Materials

Normalised silica sand (UNI EN 196-1) (NS, SISA, Torre del Lago Puccini [LI], Italy) 0.075 ÷ 2.000 mm) and commercially available calcium carbonate (S.I.S. Mineraria, Longiano [FC], Italy) with average grain size of 2.5 μm were used in samples preparation as standard aggregate and filler with high Young modulus respectively. Other high Young modulus aggregates coming from waste of the granite treatment to obtain feldspar for ceramic industry (FS, 0 ÷ 4 mm, Gruppo Minerali SpA, Novara [MI], Italy) (Bignozzi (1998), Franzoni (2004), Sandrolini (2005), Sandrolini [in press]) were used. These recycled aggregates are nowadays produced in Italy in big amounts (about 3800 t/month in the above quoted Italian plant), require large storage spaces and are currently disposed to landfill, thus negatively impacting both landscape and environment. In addition, two different tyre rubber waste, usually disposed to either incineration or landfill, were employed as low modulus dispersed phases coming from two different grinding plants. They have similar cumulative particle size distribution (Figure 1): 0.063 ÷ 2 mm (RP, Pirelli, Milano, Italy) and 0.075 ÷ 1.6 mm (RT, Isomix, Perugia, Italy) and a density of 1.16 g/cm$^3$ (determined by He pycnometer at 25°C).

The recycling of particulate waste in new composite materials helps in pursuing a reduction of the overall environmental impact, a lower exploitation of quarries and landfill disposal, thus increasing the sustainability of the global manufacturing process. The residues have been therefore optimized according to the Fuller distribution (Bignozzi (1998), Sandrolini (2002), Franzoni (2004), Sandrolini (2005), Sandrolini [in press]).

Commercially available orthopthalate unsatured polyester (UP) resin with a styrene content of 31 wt. % (FS 0956/AMV/I SIRESTER) (SIR INDUSTRIALE, Milano, Italy) was used as binder and a 50% dimethyl phthalate solution of 2-butanone peroxide ethyl-methylketon-peroxid) (Fluka) as catalyst.

In order to improve adhesion between binder and aggregates, 3-glycidoxypropyltrimethoxysilane (Aldrich) was used as coupling agent.

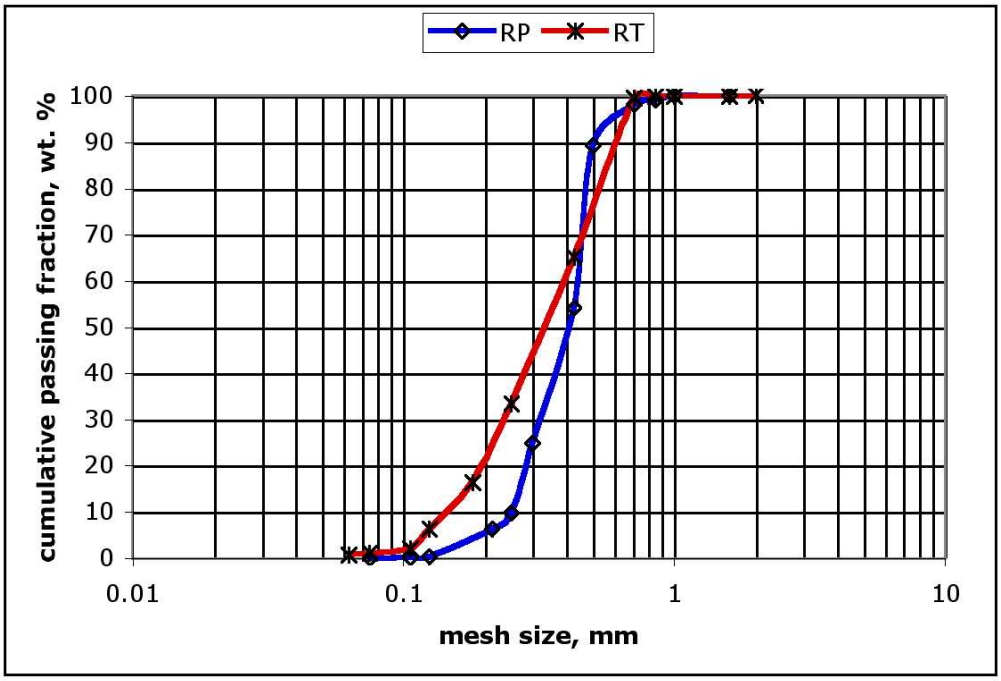



Figure 1 – Grain size distribution of tyre waste particulates

2.2. Samples preparation

The investigated mixes are listed in Table 1. All the formulations have a resin content of 8 wt. %. Reference samples S were prepared with normalized silica sand and commercially available calcium carbonate as filler (without any waste addition). Three different amounts of catalyst were added to resin in reference samples: 0.5, 1.0 and 2.0 wt. % (on resin amount) (respectively S C0.5, S C1 and S C2 samples). The same three different amounts of catalyst were also added to resin in the mix design with tyre rubber waste phase, but unfortunately some side reactions (which are at moment under study) occurred during the resin hardening, slightly decreasing the resin cross-linking rate of the samples. Only in the mix design with a catalyst content of 2.0 wt. % (on the resin amount) the resin exhibited the expected cross-linking: therefore this amount was added to all the samples containing recycled materials. Samples made with high Young modulus aggregates coming from waste of the granite treatment (FS) and commercially available calcium carbonate were named RS C2. Two different amounts of tyre by-products were added to particulate composite mixes with normalized silica sand and commercially available calcium carbonate: 1.5 and 3 wt. % (respectively RP1.5 C2, RT1.5 C2 and RT3 C2 samples). 3-glycidoxypropyltrimethoxysilane was added as coupling agent (1 wt. % on resin content).

Dispersed phases were firstly dry stirred in a Hobart mixer for 5 min. Then the UP resin premixed with the catalyst was added and the system stirred again for 1 minute. Finally, the samples were moulded in a cylindrical mould (∅ = 173 mm) of a laboratory moulding system, where vacuum up to $4 \bullet 10^{-1}$ bar, mechanical pressure (50 bar) and vibration frequency (50 Hz) were applied and controlled. After two hours samples hardening, the mould was opened and the samples extracted. After further hardening (3 days) samples were accurately cut in three specimens (40 x 40 x 120 mm) and four remains (Figure 2). Then the samples were kept at room temperature in room conditions (40 ÷ 50 R.H.) till testing.

Table 1 – Mix proportions of samples

| Samples | Binder (wt. %) | Sand (wt. %) | Sand type | $CaCO_3$ (wt. %) | Recycled tyre (wt. %) |
|---|---|---|---|---|---|
| S C0.5 | 8.0 | 77.5 | NS | 14.5 | -- |
| S C1 | 8.0 | 77.5 | NS | 14.5 | -- |
| S C2 | 8.0 | 77.5 | NS | 14.5 | -- |
| RS C2 | 8.0 | 77.5 | FS | 14.5 | -- |
| RP1.5 C2 | 8.0 | 76.5 | NS | 14.0 | 1.5 |
| RT1.5 C2 | 8.0 | 76.5 | NS | 14.0 | 1.5 |
| RT3 C2 | 8.0 | 75.5 | NS | 13.5 | 3.0 |

## 2.3. Samples characterization

Bulk density measurements ($\rho_B$) were determined by weight/volume ratio. Pore size distributions measurements were carried out by a mercury intrusion porosimeter Carlo Erba 2000 equipped with a macropore unit (Fisons 120). Three point flexural strength test, breaking deflection and compression test on the resulting part of samples (as for cement mortar samples) were determined by an Amsler testing machine (30 t): at least three measurements for each mix were made. Water absorption (WA) was measured at room temperature on one of the two parts resulting from the flexural test after accurate grinding of the fracture surface (40 x 40 x 50 mm) when constant weight was achieved (usually 1 to 3 days). Then samples were dried in an oven at about 80 °C to constant weight. Finally, after three days of water immersion at room temperature, samples subjected to WA were also subjected to compression test in order to investigate possible water effect on the binding resin.



Figure 2 – Samples after cutting in three specimens (40 x 40 x 120 mm)

## 2.4. Results and discussion

Table 2 reports the microstructural parameter bulk density ($\rho_B$) and mechanical properties (flexural, $S_F$, and compressive, $S_C$, strengths respectively) of the investigated samples. As it can be observed, the reference samples S exhibited the highest values of bulk density. Also composite materials with tyre by-products addition (RP and RT-samples) showed high values of $\rho_B$, although lower than those of the S samples. It may be observed

that an increase of tyre component in the mix causes a slight decrease in bulk density. Composite materials with recycled aggregates, on the opposite, exhibited the lowest bulk density. According to microstructural data, samples prepared with tyre by-products addition (RP and RT samples) showed compressive strength lower than reference samples S. Values of RP and RT samples are anyway very high. Of course, an increase of tyre waste content causes a decrease in both flexural and compressive strength, increasing with the tyre rubber content. No remarkable differences were observed in the properties (both physical and mechanical) of the samples with 1.5 wt. % of tyre waste (respectively RP1.5 C2 and PT1.5 C2 samples). Attention must be paid to the really high compressive strength of SC samples (up to 134 MPa) obtained using the laboratory moulding system to control porosity. In previous papers, in fact, materials prepared with similar mix design in simple gravity moulding didn't exhibit compressive strength higher than 108.8 MPa (Bignozzi (2001)). The materials obtained from the above mentioned laboratory moulding system may be therefore considered as high performance particulate composite materials. All the samples prepared with recycled aggregates (RS C2 samples) showed the lowest flexural and compressive strengths, in accordance with microstructural data. However, a tailored grain size distribution of the used industrial by-product should lead to better results: further studies are in progress. Deflection analysis at breaking stress on the samples didn't show noticeable difference among the samples; however RT3 C2 samples showed an average deflection of 0.69 mm, while RS C2 samples showed a deflection of 0.78 mm. The latter value was the highest one, clearly due to the largest porosity of the relevant samples, while the first one appears to be very low in spite of its rubber content: this means that remarkable mechanical strength may be achieved even if very low Young modulus phases are added to the particulate composite mix design, which might allow larger deflection in the elastic strain range. This seems to be promising for controlling the overall Young modulus of such particulate composite materials. Also on this point investigation are still in progress.

Table 2 – Physical and mechanical properties of particulate composite samples

| Samples | $\rho_B$ ($g/cm^3$) | $S_F$ (MPa) | $S_C$ (MPa) |
|---|---|---|---|
| S C0.5 | 2.30 | 41.2 | 134.2 |
| S C1 | 2.33 | 39.7 | 129.4 |
| S C2 | 2.36 | 36.6 | 125.6 |
| RS C2 | 2.17 | 20.1 | 67.3 |
| RP1.5 C2 | 2.31 | 39.3 | 113.0 |
| RT1.5 C2 | 2.29 | 36.9 | 113.1 |
| RT3 C2 | 2.27 | 30.3 | 88.2 |

Table 3 – Microstructural characteristics of particulate composite samples

| Samples | $\rho_B$ ($g/cm^3$) | WA (%) |
|---|---|---|
| S C0.5 | 2.30 | 0.23 |
| S C1 | 2.33 | 0.13 |
| S C2 | 2.36 | 0.17 |
| RS C2 | 2.17 | 1.55 |
| RP1.5 C2 | 2.31 | 0.27 |
| RT1.5 C2 | 2.29 | 0.31 |
| RT3 C2 | 2.27 | 0.45 |

Water absorption measurements (WA) (Table 3) showed low values, especially for reference samples S. In accordance with density values, composite materials with recycled aggregates showed the highest values of WA, even higher than those of RP and RT-samples.

Figure 3 reports the cumulative pore size distributions for the different samples. As it can be observed, in accordance with the other microstructural analysis of Table 3, only the RS-samples showed high open porosity values.

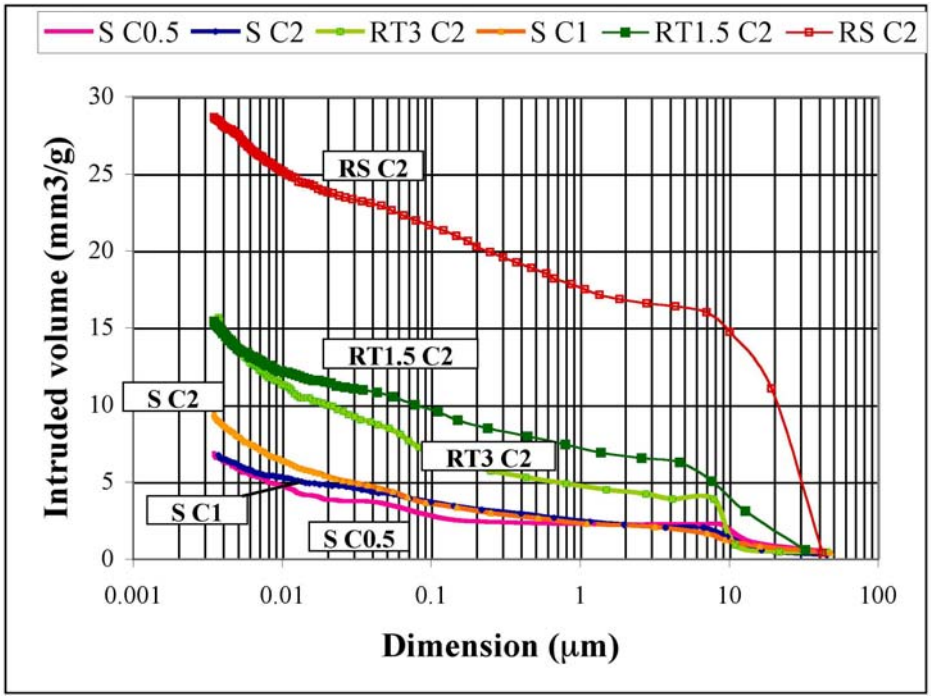



Figure 3 – Pore size distribution of the investigated samples

Table 4 – Compressive strength loss of samples after 3 days of immersion in water at 25°C (n. d.: not detectable/no difference)

| Samples | $\Delta S_C$ (%) |
|---|---|
| S C0.5 | n. d. |
| S C1 | n. d. |
| S C2 | n. d. |
| RS C2 | 8.6 |
| RP1.5 C2 | n. d. |
| RT1.5 C2 | n. d. |
| RT3 C2 | n. d. |

Finally, it was observed that the plain immersion in water lead to compressive mechanical strength loss (Table 4) in the polymer composite samples with recycled sand (RS C2 samples). This can be presumably due to a water effect on the binder resin: water could lead to some resin degradation, to be further investigated. On the contrary, reference samples and those with tyre waste addition (RP and RT samples) didn't exhibit any loss in mechanical compressive strength after three days of immersion in water. This result confirms the need of studying the possibility of preparing new mix design for the polymer composite samples

made with recycled sand in order to reduce the porosity of the material and improve the overall mechanical performances, i. e., mechanical strength, Young modulus, and durability.

## 3. CONCLUSIONS

1) Particulate composite materials with integrated and modulated physical-mechanical properties may be successfully prepared, using as disperse phases waste particulate materials of different Young modulus.

2) Particulate composite materials with high mechanical performances (compressive strength of about 130 MPa) may be prepared by proper control of grain size distributions of both low and high modulus phases and moulding factors.

3) Samples prepared with recycled aggregates showed the lowest physical and mechanical properties, but better results should come from a tailored grain size distribution of the used industrial by-product.

## 4. REFERENCES

Bignozzi, M., Saccani, A. and Sandrolini, F, Dynamic mechanical and dielectric analysis of polymer composites for machine tool basements: the effect of the polymer matrix, *Materials Engineering*, **12**, 287-299 (2001).

Bignozzi, M.C., Saccani, A. and Sandrolini, F., Glass waste valorization in advanced composites materials, in: *Proc. 11th Int. Congress on Polymers in Concrete-ICPIC 04* (Berlin, Germany, 02-04/06/2004), M. Maultzsch Ed., Berlin, 587-595 (2004/1).

Bignozzi, M., Saccani, A. and Sandrolini, F., New Polymer Mortars Containing Polymeric Wastes: Part 1. Microstructure and Mechanical Properties, *Compos Part A-Appl S*, **31**, 97-106 (2000).

Bignozzi, M., Saccani, A. and Sandrolini, F., New polymer mortars containing polymeric wastes: Part 2. Dynamic mechanical and dielectric behaviour, *Compos Part A-Appl S*, **33**, 205-211 (2002).

Bignozzi, M., Sandrolini, F., Saccani, A., Bonora, V., and Zucchetti, M., Recycling Plastics in Polymer Mortars, in: *Proc. IX ICPIC* (Bologna, Italy, 14-18/09/1999), F. Sandrolini Ed., Edizioni Casma s.r.l., Bologna, 151-162 (1998).

Bignozzi, M.C. and Sandrolini, F., Recycling tyre rubber in building materials, in *Proceedings of the International conference "Sustainable waste management and Recycling: Used/post consumer tyres"* (Kingston University, London, 14-15/09/2004), M. C. Limbachiya Ed., Thomas Telford, London, 77-84 (2004/2).

Bignozzi, M.C., Saccani, A., Sandrolini, F. and Carbonchi, C., High performance particulate composites: a new utilisation of by-products from raw materials, in: *Proc. of 2nd Nat. Congress Valorisation and Recycling of Industrial Wastes* (L'Aquila, 05-08/07/1999), Ed. M. Pelino, L'Aquila, 135-144 (1999).

Franzoni, E., Manzi, S., Sandrolini, F. and Bignozzi, M.C., High performance fully recycled materials for civil engineering as an alternative to landfill disposal, in: *Proc. First Int. Conf. on Innovative Materials and Technologies for Construction and Restoration. IMTCR'04* (Lecce 06-09/06/2004), La Tegola A and Nanni A Eds., Liguori Editore, Napoli, 395-405 (2004).

Sandrolini, F. and Manzi, S., Fully recycled particulate composite materials with outstanding properties: microstructure and durability, in: *Proc. V International Congress on Valorisation and Recycling of Industrial Waste VARIREI 2005*, (L'Aquila, Italy, 28-30/06/2005) , M. Pelino Ed., l'Aquila, 1-8 Cd-Rom (2005).

Sandrolini, F., Bignozzi, M. and Saccani, A., Scarti da raccolta urbana differenziata del vetro in materiali compositi innovativi, *Rivista della Stazione Sperimentale del Vetro*, **31** (6), 171-176 (2001).

Sandrolini, F., Franzoni, E. and Bignozzi, M., Materiali compositi particellati a proprieta' modulabili per applicazioni nelle costruzioni, in: *Atti del VI convegno nazionale AIMAT* (Modena, 08-11/09/2002), T. Manfredini Ed., Modena, 1-4, Cd-Rom (2002).

Sandrolini, F., Manzi, S. and Andrucci, A., Sulfur-polymer matrix composites from particulate wastes: a sustainable route to advanced materials, *Composites Part A*, 1-8 [in press].

International Symposium Polymers in Concrete
2 - 4 April 2006
Guimarães, Portugal

# Influence of the viscoelastic nature of the polymer concrete in its structural behaviour.

J. Tomás San-José[1]

*Labein-tecnalia, C/Geldo – Parque Tecnológico de Bizkaia. Edificio 700. 48160 Derio-Vizcaya (SPAIN). Tel. +34 94 607 3300. tomas@labein.es. Corresponding address.*

Antonio Aguado[2]

*UPC Universitat Politècnica de Catalunya. Módulo C-1, Despacho 202 B. C/ Jordi Girona Salgado, 1-3. 08034 Barcelona (SPAIN)*

ABSTRACT
This paper deals with the study of a highly durable polyester polymer concrete (PPC) reinforced with glass fibre rebars (GFRP). The paper describes the properties of this specific concrete, which were tested using different experimental techniques such as porosimetry, scanning electron microscopy and petrography. Likewise, characterisation in a macro-scale was carried out to define the mechanical properties of the material (modulus of elasticity, stress-strain curve, ultimate strength and bond). Based on the latter properties, the paper presents a relatively simple method to estimate the ultimate bearing capacity of beams under bending load. The calculation method has been verified by testing beams and full-scale elements. At the end, and due to the viscoelastic nature of the polymer, several considerations will be made in order identify safety factors dependent on the loads nature: permanent loads (deferred deformations) and live loads.

Keywords: bearing, bending, concrete, deferred, deformations, GFRP, polymer

## 1. INTRODUCTION

The PPC is a construction material comprising three phases: inorganic (aggregates), organic (thermosetting polyester resin) and inert (air porosity due to fabrication process). Most of its current applications are related to precast elements such as: crossing slabs, façade panels, drainage elements, farm components; and in situ works: overlays, flooring and rehabilitation concrete works. The properties of PPC greatly depend on the formulation, but in comparison to conventional Portland cement concrete may be generally characterised by higher compressive, tensile and flexural strength, greater impact and abrasion resistance, much lower permeability to water, dissolved salts, and industrial chemicals, greater resistance to weathering conditions such as freeze-thaw and wet-dry cycles and, finally, greater

[1] Senior Research
[2] Professor

resistance to natural environmental conditions. PC is therefore an attractive material for protecting concrete from mechanical damage, weathering, corrosion, and chemical attack. In addition to the improved strength and durability as compared to conventional concrete, PC is also easy to place, rapid curing and very fast strength developer. However, PPC has currently some drawbacks compared to cement concrete which limit their applications. Firstly, it should be understood that one of the primary limitations of polymer concrete products is cost, and especially the raw material costs. PPC does not give corrosion protection to steel reinforcement like cement concrete on account of its high alkalinity as long as the concrete is not carbonated. Steel reinforcement in polymer concrete should be therefore, if cracks can occur and corrosion causing environment prevails, provided with corrosion protection.

Nowadays, important research activities Czarnecki (1999) are being developed in the cost reduction topic of the polymer concrete, by acting in controlling the material structure to obtain specific material properties in every application.

## 2. PPC MATERIAL ASPECTS

The dosage of the PPCs analysed in the present paper is presented in Table 1. Both U-type and G-type have been made of polyester resin but with two different thermosetting resin types; namely, isophthalic and orthophthalic. During the curing period, the polymer chains of the polyester formulation are cross linked among them, as a consequence of the promoter action (curing agent). This linking effect is an exothermic process that implies a relative ordering of the polymeric chains, obviously no as clear as in the crystallographic nature of metals. Both phenomena, ordering of chains plus the exothermic effect, during the polyester resin curing, implies the shrinkage of the polymer concrete matrix along the firstly 5 to 7 hours, related to the curing period. Because of this, the polyester resin was mixed with a commercial compensated shrinkage agent. The casting process has produced two different materials, not only from a chemical point of view but also from a different internal structure, San-José (2002).

Table 1 - Polyester polymer concrete components dosage.

| **Components** | **Type U** | **Type G** |
|---|---|---|
| Polyester resin content | 12% | 12.3% |
| $TiO_2$ colour additive | 2.5%(*) | - |
| Carbonate filler | 25% | - |
| Chalk | - | 7% |
| Quartz powder | - | 6.7% |
| Quartz fine sand | 58% | 24,7% |
| Quartz sand | 17% | - |
| Quartz gravel | - | 49.3% |

(*) With regards to resin content

The microstructural analysis has been obtained through two techniques: intrusion porosimetry (Table 2) and SEM. These techniques aimed at providing information on such a different mechanical behaviour in types U and G.

Table 2 - Polyester polymer concrete intrusion porosimetry results.

| PPC types | U-isophthalic | G-orthophthalic |
|---|---|---|
| Pores Content (%) | 7.3 | 4.8 |
| Bulk Density (kg/dm$^3$) | 2.32 | 2.39 |

The internal pore distribution and pore aspect of the analysed polymer concretes can be observed in Figures 1 and 2. As referenced in San-Jose (1996), this area configuration is one of the most important aspects to understand the macroscopic performance in both types of concrete.

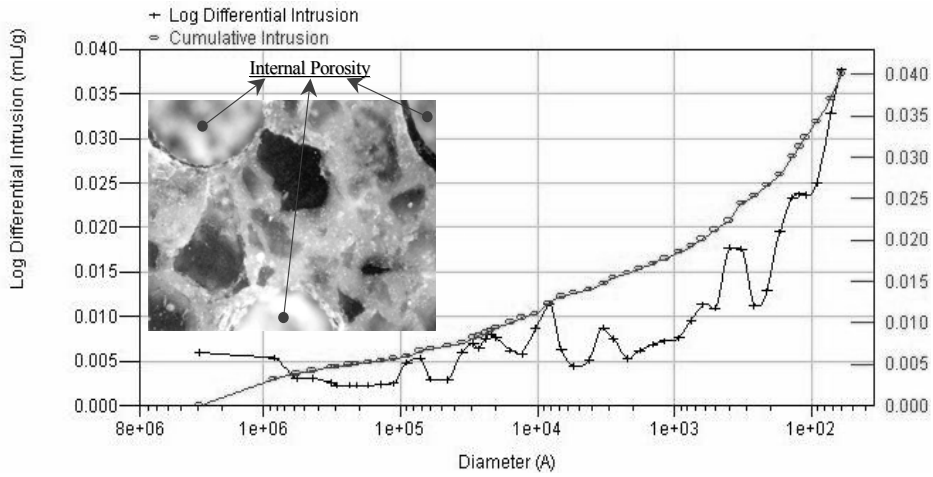



Figure - 1 Porosimetry intrusion and aspect. PPC type U.

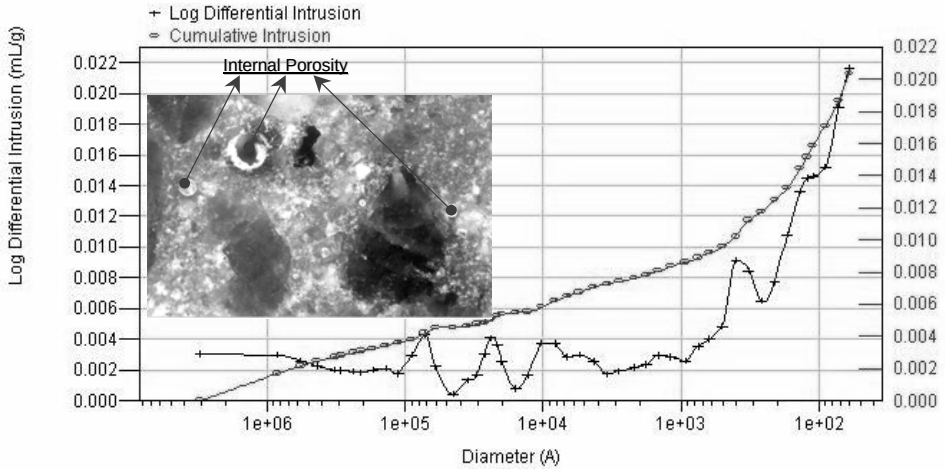



Figure - 2 Porosimetry intrusion and aspect. PPC type G.

Secondly, Scanning Electronic Microscopic (SEM), presented in Figure 3, shows a thinner resin layer (aggregate wrapping) in the PPC type U. On the other side, the most irregular shapes of the aggregates of the PPC type G and their higher size improve their anchorage effect in the resin matrix with regard to type U. It can be said, therefore, that type G is, from a microscopic point of view, a more compact material than type U. It must be also noted that there was a significant difference in size of the air voids in the two PPCs, as it was

observed through the porosimetry technique. The different pores distribution can be attributed jointly to the material (dosage ratios) and technology aspects (different casting methods, mixer machines and post-curing conditions).

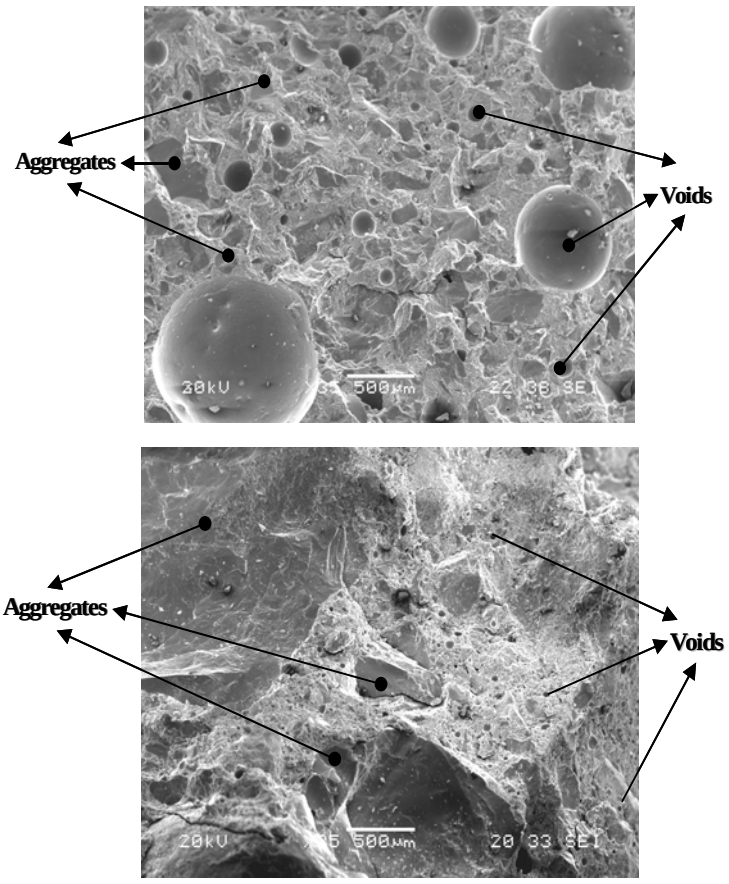



Figure 3 - SEM microphotograph (x35) of PPC type U (up) and PPC type G (down).

## 3. PPC MECHANICAL BEHAVIOUR

The most effective analysis of both PPC types, Rebeiz (2001), in compression, can be observed in their respectively stress vs strain curves (Figure 4, curves shape polynomial 2$^{nd}$ degree). As it can be shown, there are some differences, under compression loads, in the type U and G polymer concretes tackled in the present work. Stress-strain curve was plotted by using the data through out the compressive test. The Modulus of elasticity was measured by the strain gauge method, which is one of two methods stipulated in the RILEM method TC 113-CPT (PC-8). Cylindrical specimens (Ø100mm x 200mm) were used in these tests.

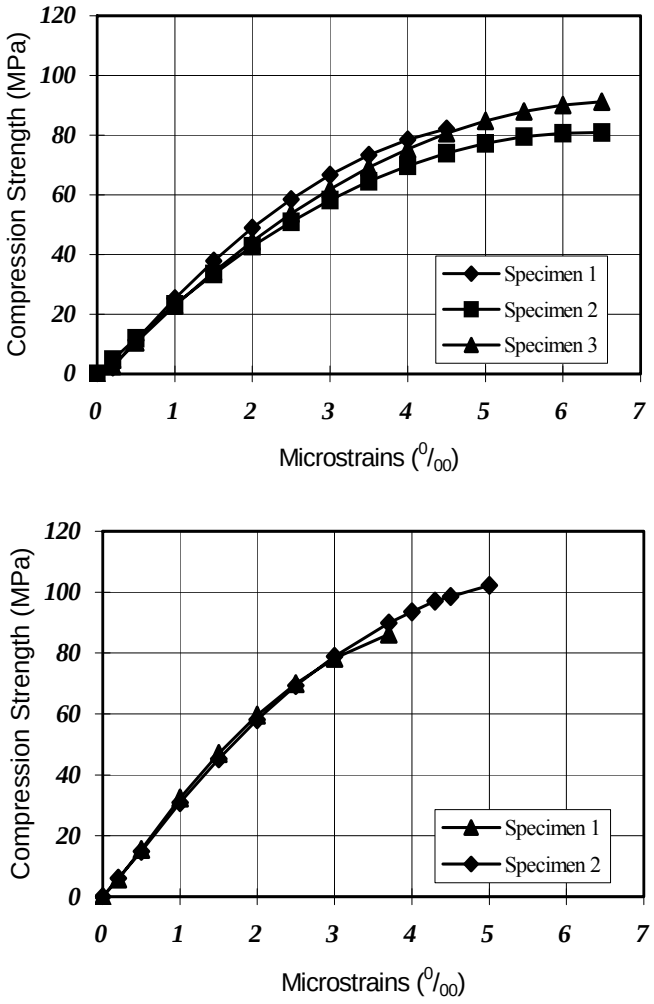



Figure 4 - Compression stress vs strain curves of PPC type U (upper) and type G (down).

Table 3 presents the fundamental stress-strain parameters in compression, jointly with bending ones.

Table 3. Compression and flexural mechanical PPCs properties

| **Properties** | **Type U** | **Type G** |
|---|---|---|
| Compression strength | 92.0 MPa | 102 MPa |
| Compression modulus (E) | 24,863 MPa | 30,492 MPa |
| Compression max. Strain | 6.5 $^{0}/_{00}$ | 5.0 $^{0}/_{00}$ |
| Poisson's ratio | 0.23 | 0.21 |
| Flexural strength | 21.5 MPa | 26.0 MPa |
| Flexural modulus E | 28,710 MPa | 37,868 MPa |
| Flexural max. Strain | 1.0 $^{0}/_{00}$ | 0.98 $^{0}/_{00}$ |

Like Portland cement concrete (CC), PPC has relatively low tensile strength compared to its compressive strength. Therefore, in many applications, it may be necessary to

add reinforcing steel to the tensile zone of PPC to increase its strength capacity, its ductility, and its toughness. In order to get the flexural stress-strain curves (Figure 5), it was conducted several tests (prismatic specimens of 40x40x160mm). With regard to measure the deformation of the specimens, a gauge were positioned at mid-span, at the lower fiber.

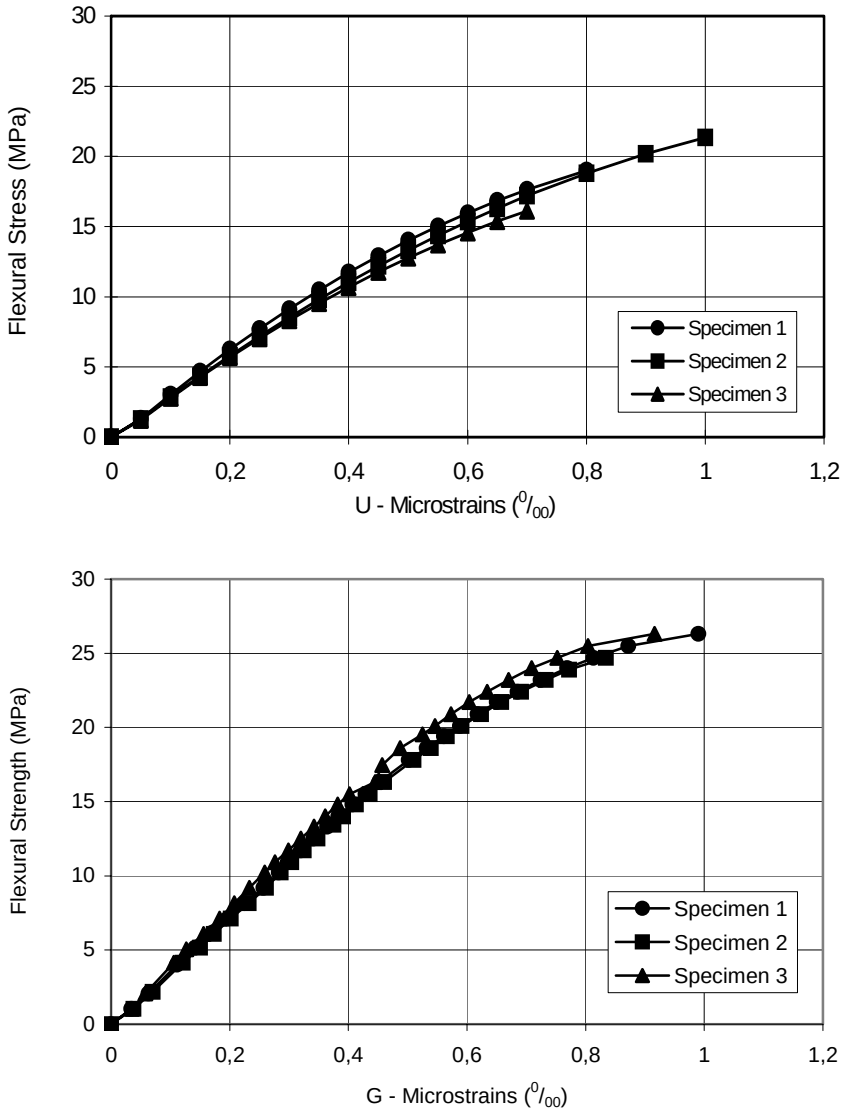



Figure 5 - flexural stress vs strain curves of PPC type U (upper) and type G (down).

The flexural tension strength value obtained in CC was very small comparing with the PPC one. Nevertheless, when designed by applying the method of ultimate strength design in PPC beams under flexural loads, as other authors' criteria such us Kwan-ho (2001), the equivalent stress block is used only over the neutral axis, that contents the flexural compression part of the cross section, accordingly to the stress distribution of polymer reinforced concrete subjected to flexural loads and affected by the required factors, as presented in last chapter.

It could be concluded that the differences among the flexural parameters (strength, strain and E modulus) are higher than in the compression study. Therefore, the flexural test is a better suited procedure for ranking, mechanically, the different PPC types, in comparison with the compression one.

## 4. BOND BEHAVIOUR OF REINFORCING BARS IN PPC

The bond mechanism of bars concrete reinforcement is the basis phenomenon which determines the structural behaviour of reinforced PPC. Table 4 shows the fundamental properties of square FRP (fiber reinforced polymer) rods in comparison with the most commonly round steel re-bars used in traditional reinforced cement concrete (CC).

Table 4 - Mechanical properties for metallic and GFRP reinforcing bars

| Property | Steel bar | GFRP square bar |
|---|---|---|
| Tensile strength | 550 MPa | 1100 MPa |
| Tensile modulus | 200 GPa | 45 GPa |
| Failure strain | 22 % | 2.5 % |
| Interlaminar shear strength | --- | 45 MPa |

Bond behaviour of different reinforced PPCs subjected to both monotonic and cyclic loading was presented by San-Jose (2002) in previous works. The results in monotonic bonding tests, taking into consideration the ACI 440.1R-01 (2001) recommendations, presents a high performance of PPC in comparison with CC, taken as reference material. Table 5 shows the monotonic bonding results between orthophthalic PPC referred in table 1 and the reference CC designed as follows:

Table 5 - Monotonic bond strength between PPC and CC.

| Concrete type | Steel bar | GFRP bar |
|---|---|---|
| Orthophthalic PPC | 24.4 MPa | 14.0 MPa |
| CC | 12.5 MPa | 9.7 MPa |

## 5. APPROACH TO GENERAL CALCULUS CURVES IN FLEXURAL REINFORCED PPC

Researches achieved for the material and mechanical properties of polymer concrete have been widely conducted by many researcher groups in Japan, U.S.A. and E.U. Previous studies by Ramírez (2001) have concluded by pointing out the large scatter on the other properties values of PPC of identical 100 MPa compression strength, which also influence the structural behaviour; and the difficulty of the actual formulations for a precise forecast of those property values. This fact also supports the idea of standardization.

One of the main reasons from above considerations arise from the viscoelastic properties of the polymer, which results in creep and sensitivity to temperature, jointly with the adversely influence of continuous exposure to humidity. With regard to consider the viscoelastic nature of the PPC, the concept of permanent and live loads will be managed, besides the temperature influence.

In the light of the previously determined material stress-strain curves in PPC (figures 4 and 5, obtained at room temperature) under live loads, different safety factors will be

presented regarded to consider the effect of higher temperatures (60ºC) and permanent loads, as occurs in real structures. At this respect, the PPC performance shown in figures 4 and 5 could be simplified to Figure 6.

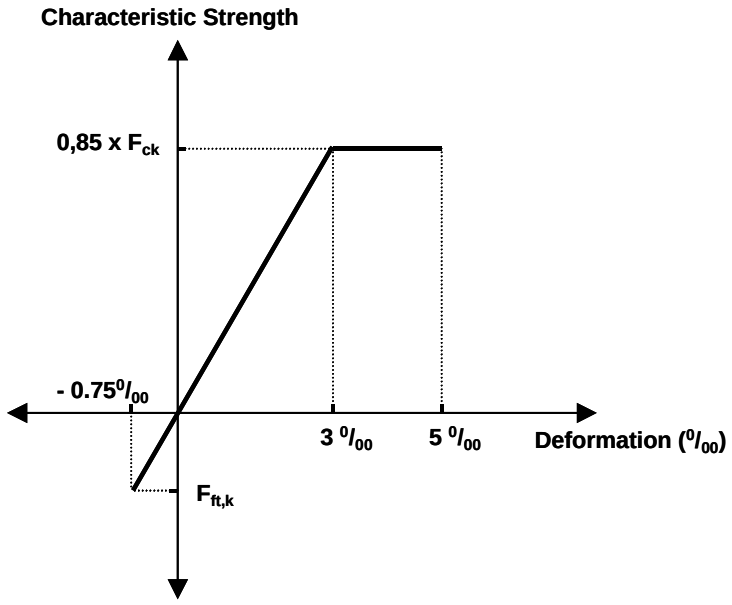



Figure 6 - Stress - Strain simplified diagram in polyester PC.

Above diagram represents, respectively, the behaviour of the compression (positive strains) and tension stress blocks of a beam cross section under flexural loads. In the first case, the linear–rectangular shape is a simplification of the Figure 4 polynomial 2$^{nd}$ degree curves, by using the 0,85 factor (nothing to see with the significance of the 0,85 factor in CC) in the rectangular part of the diagram. On the other hand, the tension stress block is a linear curve, as represented in Figure 5. Both cases, the strength limit ($F_{ck}$ - compression and $F_{ft,k}$ - tension in bending) are the characteristic one that means a 0,95 probability of obtaining higher values, instead the average one adopted initially in figures 4 and 5. This fact, as traditionally made in CC, permits to calculate the reinforced PPC sections by avoiding different safety factors depending on concrete manufacturing conditions.

From a detailed literature revision of Fowler (2001) and San-José (1996-98), several calculation curves have been produced (Figures 7). These calculus diagrams correspond to compression and tension stress blocks based in Figure 6 by considering the time of applying loads and the temperature conditions of the structure. As it can be observed, the Figure 6 has been divided in two separately figures with regards to present more clearly how the time and temperature effect could affect the PPC structural response. The four presented curves, in each one the following figures, are referred to the live (instantaneous) and permanent loads (that produces deferred deformations) under different temperatures:

*(1) Live (static) loads 22 ºC* *(3) Permanent loads 22 ºC*

*(2) Live (static) loads 60 ºC* *(4) Permanent loads 60ºC*

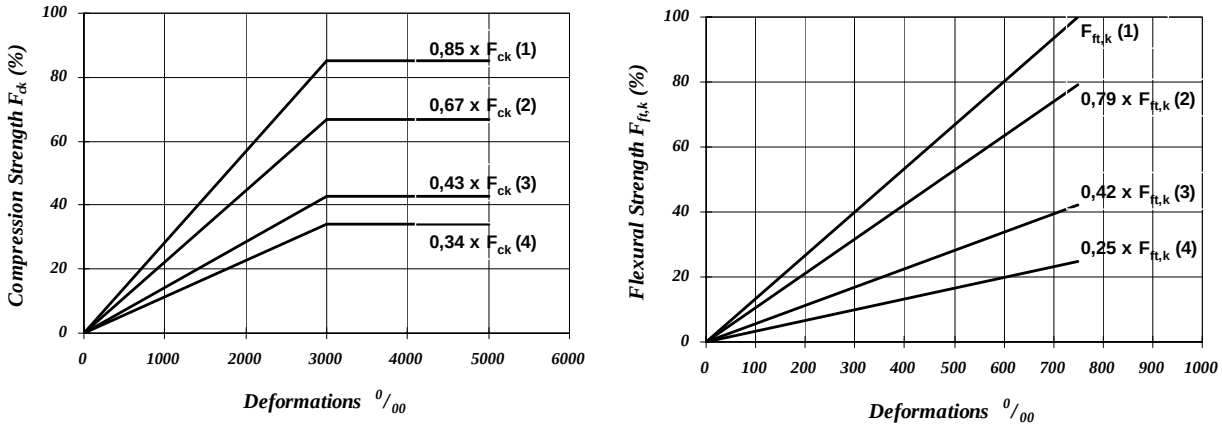



Figure 7 - Flexural - compression (left) and tension (right) calculation diagrams.

A linear combination between the live and permanent loads, joined with the thermal conditions, will be established in relation to the above (1) to (4) curves. Therefore, it will be obtained the PPC stress-strain calculus curve to be applied to the specific reinforced cross section, based on the load hypothesis of the problem.

On the other hand, in order to define the calculus diagrams, as traditionally made in CC, several safety factors have to be defined. Firstly, the loads to be considered, for the thermal ranges analysed (22ºC to 60ºC) are: Live loads (L), applied by $\gamma_L$ safety factor and Permanent loads (P), applied by $\gamma_P$ safety factor. In pure flexural, Kaeding (1998) proposes the values of 1.3 and 1.6 for $\gamma_L$ and $\gamma_P$, respectively. However, these safety factors are different than commonly used for majoring the normal controlled CC. The proportion of the permanent and life loads in the specific hypothesis of the problem will be:

$$P[\%] = \frac{100 \cdot P}{(P + L)} \qquad \text{and} \qquad L[\%] = \frac{100 \cdot L}{(P + L)}$$

The following step, involves the establishment of two parameters: alpha and beta. Both coefficients will depend on the proportions in which the permanent and live load are presented:

$$\alpha = \frac{P[\%] \cdot K_B}{100} + \frac{L[\%] \cdot K_A}{100} \quad \text{and} \quad \beta = \frac{P[\%] \cdot K_D}{100} + \frac{L[\%] \cdot K_C}{100}$$

Where:

- $\alpha$ applies to the compression in bending stress block
- $\beta$ applies to the tension in bending stress block

The above parameters, named as $K_A$ , $K_B$ , $K_C$ and $K_D$ , are the applied factors to $F_{ck}$ and $F_{ft,k}$ in the respective (1) to (4) diagrams, at Figure 7. These K-factors were determined from extensive literature review with the following meanings and values (Table 6):

$K_A$: Factor to be applied to $F_{ck}$ when bending in compression stress block is produced only by live loads at 22ºC and 60ºC, respectively, as is shown in curves (1) and (2).

$K_B$: Factor to be applied to $F_{ck}$ when bending in compression stress block is produced only by permanent loads at 22ºC and 60ºC, respectively, as is shown in curves (3) and (4).

$K_C$: Factor to be applied to $F_{ck}$ when bending in tension stress block is produced only by live loads at 22ºC and 60ºC, respectively, as is shown in curves (1) and (2).

$K_D$: Factor to be applied to $F_{ck}$ when bending in tension stress block is produced only by permanent loads at 22ºC and 60ºC, respectively, as is shown in curves (3) and (4).

If other temperatures (comprehended between +22 and +60ºC) should be used for designing conditions, a linear interpolation could be done among the Table 6 respective k-values.

Table 6 - K-factors to be applied to the characteristic PPC strengths in (1) to (4) curves.

| Temperature | Compression in bending | | Tension in bending | |
|---|---|---|---|---|
| | $K_A$ (live loads) | $K_B$ (permanent loads) | $K_C$ (live loads) | $K_D$ (permanent loads) |
| + 22 ºC | 0.85 | 0.43 | 1.0 | 0.42 |
| + 60 ºC | 0.67 | 0.34 | 0.79 | 0.25 |

Therefore, as partial conclusion, it could be point out that in the case of only permanent loads at 60 ºC, the PPC compression and flexural strengths should be reduced to the 34% ($K_B$) and 25% ($K_D$) from the initial obtained values in Table 3. In other words, rectangular sections of reinforced PPC under a specific combination of live and permanent loads could be analysed by following the Figure 8:

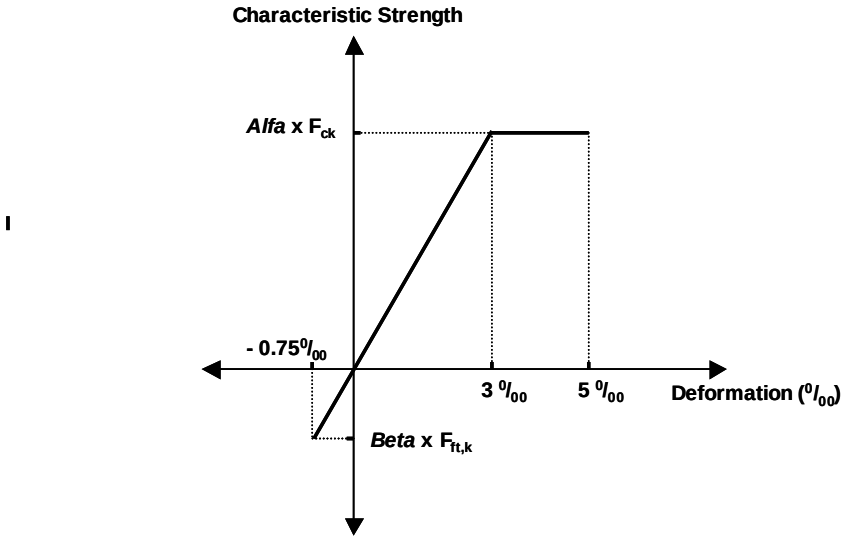



Figure 8 - Calculation diagram for polyester polymer Concrete PPC.

In the case of rectangular cross sections of reinforced PPC, the equilibrium of loads, jointly with the strains compatibility, results in the following Figure 9 internal loads ($F_c$ plus $F_a$) configuration. Due to the maintenance of the planarity of the reinforced PPC cross section, the neutral axis depth "**x**" covers the following range of values (being "**d**" the bars depth): $0.333 \cdot d < x < d$

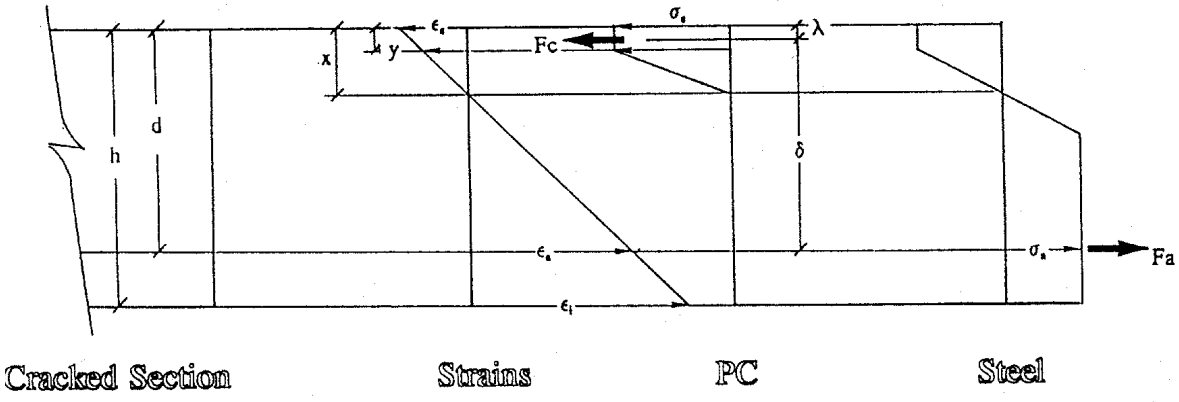



Figure 9 - Internal loads equilibrium in reinforced PPC in pure bending

$$0 = F_c - F_a \qquad M_d = F_c \cdot \delta \qquad y = 0{,}4 \cdot x$$

$$F_c = 0{,}5 \cdot b \cdot (\alpha \cdot F_{cd}) \cdot (x + y) \qquad A_a \cdot f_{yd} < F_a < 0{,}75 \cdot (A_a \cdot f_{yd})$$

$$\lambda = \frac{(x^2 + y^2 + x \cdot y)}{(3 \cdot [x + y])} \qquad \varepsilon_a\,(‰) = \frac{5 \cdot (d - x)}{x}$$

$$F_{cd} = \frac{F_{ck}}{\gamma_c} \quad \text{and} \quad f_{yd} = \frac{f_{yk}}{\gamma_s}$$

where:

$F_{ck}$ is the characteristic compression strength of PPC
$f_{yk}$ is the characteristic tension strength of reinforcing bars
$F_{cd}$ is the calculus compression strength of PPC
$f_{yd}$ is the calculus tension strength of reinforcing bars
$\gamma_c$ is the reducing strength safety factor in PPC
$\gamma_s$ is the reducing strength safety factor in the reinforcing bar

Substituting:

$\lambda = 0{,}371 \cdot x$
$F_c = b \cdot x \cdot F_{cd} \cdot (0.7 \cdot \alpha) = b \cdot x \cdot F_{cd} \cdot (\Psi)$
$\delta = d - \lambda = d - (0.371) \cdot x = d - (\lambda') \cdot x$

$\lambda'$ and $\Psi$ values are constant in CC and equal to 0.416 and 0.6681, respectively. However, in PPC $\Psi$ depends from $\alpha$, linked to: proportion of permanent loads, proportion of live loads and temperature, as referred above.

5.1. Simplified calculus diagram under live loads

In order to simplify the calculus method, as traditionally made in CC, the linear–rectangular diagram designed before, in compression, could be turned into rectangular stress block. After establishment of the calculation procedures a number of test beams were produced and loaded (100% live loads) to failure in order to verify the calculations (Figure 10): Beam 0 (two orthophthalic plain PPC beams), Beam 1 (reinforced with 2Ø8 mm steel bars) and Beam 2 (reinforced with 3Ø8 mm plain GFRP bars). More details in Table 7.

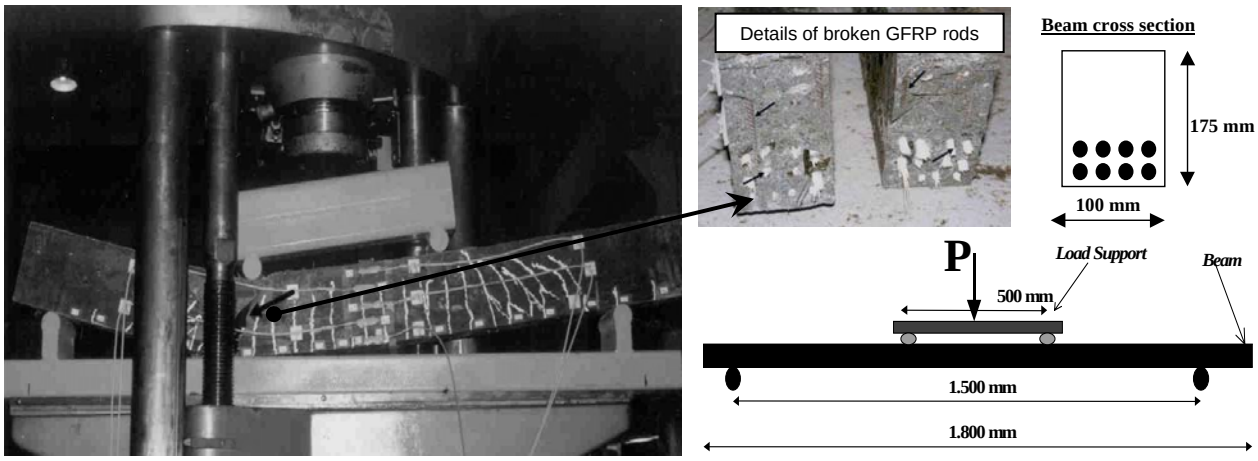



Figure 10 - Beam test configuration in GFRP and steel bars reinforced orthophthalic PC.

Table 7 - Experimental results of bending orthophthalic PPC beams.

| **Observed aspects** | **BEAM 0** | | **BEAM 1** | | **BEAM 2** | | |
|---|---|---|---|---|---|---|---|
| Section (mm) | 100 × 175 | | 100 × 175 | | 100 × 175 | | |
| Reinforcement | --- | | 10 Ø8 steel | | 12 Ø8 GFRP | | |
| $A_s$ ($mm^2$) | 0 | | 502.6 | | 603.2 | | |
| Stirrups | Ø6 steel $f_y$ = 510 MPa, c/c 100 mm | | | | | | |
| Reinforcement degree | under | | normal | | over | | |
| Mid span deflection (mm) | 20 | 20 | 103 | 112 | 233 | 215 | 255 |
| Failure load P (kN) | 41.0 | 39.5 | 160.0 | 156.5 | 145.0 | 160.0 | 169.0 |
| Failure moment (kNm) | 10.3 | 9.9 | 40.0 | 39.1 | 36.3 | 40.0 | 42.3 |
| Mode of failure | bending | | Concrete crushing (bending failure) | | Concrete rupture (bending/shear failure) | | |

Using approaches in Eurocode (EC2-1-1, par 4.2) for traditional reinforced cement concrete, the process of transforming real stress-strain graphs (Figure 4) into rectangular diagrams could, of course, be made in one operation. As the first step in converting the stress-strain diagrams for axial compression, (e.g. those shown in Figure 4) into easily manageable mathematical expressions, the curves were transformed into the best-fitting simple $n^{th}$ degree parabolas, having maximum value corresponding to the recorded ultimate strain. The reason to introduce this intermediate step - towards a rectangular representation - was to investigate the effect of various degrees of curvature of the graphs.

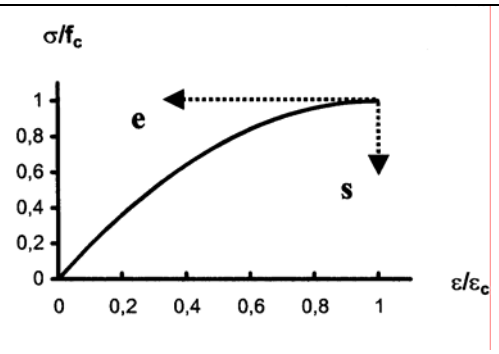
Considering the shapes of the graphs in Figure 4 it appears – comparing with typical cement concrete graphs – the maximum stress point and maximum strain point are coinciding. This means that up to now the documented degree of plasticity of polymer concrete is restricted. Higher degrees might be determined by more sophisticated procedures and equipment. Introduction of a simple $n^{th}$ degree parabola approximation (Figure 11) appeared to be a viable and realistic step further towards the final simplification.

$$\sigma = f_c \cdot \left[ 1 - \left( \frac{\varepsilon_c - \varepsilon}{\varepsilon_c} \right)^n \right]$$

or, when substituting:

$1 - \varepsilon / \varepsilon_c = e$
$1 - \sigma / f_c = s$

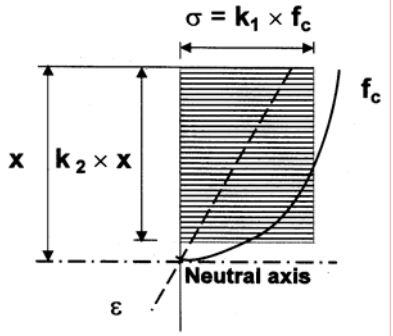
we have the simple expression: $\mathbf{s = e^{\,n}}$




Parabolic Stress-strain graph

Figure 11 - Parabolic representation of stress-strain graph.

The curve fitting was defined on basis of minimum deviations between the real stress-strain curve and the $n^{th}$ degree parabola at a number of points. Parabolas of degree n = 1.6 – 2.1 were very close to the real curves shown in Figure 4. By means of the parabolic expression for the stress-strain relationship it was possible to calculate the following conversion factors $k_1$ and $k_2$, which describe the transformed rectangular stress block shown in Figure 12, ref EC2-1-1 Fig 4.4. The $k_1$ and $k_2$ formulas and values refer to rectangular cross sections of beams, for other section shapes they are different.




$$k_1 = \frac{n \cdot (n+2)}{(n+1)^2}$$

$$k_2 = \frac{n+1}{n+2}$$

- n is the degree of the parabola. For the graphs
- in Figure 4 the factors are:

n = 1.6: $k_1 = 0.85$ $k_2 = 0.72$

n = 2.1: $k_1 = 0.89$ $k_2 = 0.76$

Figure 12 - Factors for converting stress-strain curves into rectangular stress blocks

The ultimate moment capacity at pure flexure for static loads depends i.e. on the percentage of reinforcement, ρ. The cross section can be under-reinforced, balanced or over-reinforced. As a start the calculation procedures were verified against the obtained failure moment for the full-scale beams referred to in Table 7. The results are shown in Table 8 and it appears that the differences are less than 10%. On average the measured moments are above the calculated.

Table 8 - Measured versus calculated ultimate moment

| **Observed aspects** | **BEAM 0** | | **BEAM 1** | | **BEAM 2** | | |
|---|---|---|---|---|---|---|---|
| Section (mm) | 100 x 175 | | 100 x 175 | | 100 x 175 | | |
| Reinforcement | --- | | 10 Ø8 steel | | 12 Ø8 GFRP | | |
| Reinforcement degree | under | | normal | | over | | |
| Measured Failure moment (kNm) | 10.3 | 9.9 | 40.0 | 39.1 | 36.3 | 40.0 | 42.3 |
| Calculated ultimate moment (kNm) | --- | --- | 35.1 | 35.1 | 36.6 | 36.6 | 36.6 |
| Mode of failure | bending failure | | Concrete crushing (bending failure) | | GFRP rupture (bending/shear failure) | | |

## 6. CONCLUSIONS

- With regard to the PPC properties, the casting procedure is one of the most important factors in order to establish the different microscopic and macroscopic behaviour. Porosity, interface aggregates-matrix configuration, strength and deformability, are closely linked. The mechanical properties advantages compared to those of ordinary cement concrete are very optimistic for future construction trends (compression strength three times higher than CC and a minimum bending strength of 25 MPa).
- The differences among the flexural parameters (strengths, strains and E modulus) are higher than in the compression study. Therefore, the flexural test is a better suited procedure for ranking, mechanically, the different PPC types in comparison with the compression strength, most adjusted for developing this purpose in the ordinary cement-concrete.
- The sand-coated GFRP reinforced polymer concrete provides values of the bond strength similar to traditional steel bars in reinforced concrete. In polymer concrete, steel bars develop bond strength about 70% greater than GFRP rods. In cement concrete, steel bars exhibit bonding strength about 25% greater than GFRP rods.
- The viscoelastic properties of the polymer resin results in creep and sensitivity to temperature. Because of the viscoelastic nature of the PPC, the concept of permanent loads (deferred deformations) and live loads (instantaneous deformations) have been managed, besides the temperature influence, by building several calculus diagrams based in linear-rectangular geometries.
- Various safety factors were concluded with regard to consider the effect of temperature (60ºC) and permanent loads. It could be point out that the PPC is extremely sensitive to deferred deformations, being necessary to reduce its high initial strengths to less than a third part, in the case of only permanent loads applied at 60 ºC.
- Flexural failure in reinforced PPC beams occurred when the ultimate compressive strain in the concrete reached a value of 0.005 or more. The cracking patterns and the modes of failure of reinforced PPC beams were similar and generally typical to those observed in reinforced Portland cement concrete. However, reinforced PPC beams exhibited higher strength and more ductility than reinforced Portland cement concrete beams. In addition, PPC requires less cover for the tensile reinforcing steel than Portland cement concrete because of its inherent high flexural strength, low permeability, and good chemical resistance.
- The nominal moment strength obtained from these experiments were in good agreement with the theoretical values computed from applying the method of ultimate strength design in the case that the stress distribution of polymer concrete beam, subjected to the flexural moment, was assumed as the equivalent rectangular.
- In order to design the polymer concrete beams more accurately, it is necessary to accumulate much more experimental data from other cross section shapes and other rectangular cross section specimens based on the variation of the compressive strength and the size effect, and the data about the flexural behavior of polymer concrete beams.

## ACKNOWLEDGEMENTS

The work presented in this paper has been financed by European Commission under the Contract number BRPR-CT98-0708 (1998-2002) and the Spanish Government, as a national project, under the Contract number MAT98-1734-CE (1999-2001).

REFERENCES

ACI 440.1R-01: Guide for design and construction of reinforced concrete with FRP bars. ACI Committee 440. 2001.

Czarnecki, L.; Garbacz, A.; Lukowski, P.; Clifton, J.: Optimization of polymer concrete composites. NISTIR 636, Maryland (USA). August 1999.

Fowler, D.W. (1997) Structural design of polymer concretes. Third Southern African Conference on Polymers in Concrete. Johannesburg (South African).

Kaeding, A.O. Predicting the in-service performance of precast reinforced polymer concrete. 43rd Annual Conference, Composites Institute, The Society of the Plastics Industry, Inc. February, 1-5, 1998.

Kwan-ho kim, Kyu-seok yeon, Nan-ji jin, Kwang-soo park: the investigation of the equivalent rectangular stress block for high-strength polymer concrete beams. ICPIC'01 Hawai (USA). 2001.

San-José, José T. Structural and ornamental polymer concrete. Application to building composites. Thesis presented at the Basque Country University (UPV-EHU), Bilbao (Spain), Dec. 1996.

San-José, JT. Highly durable precasted special concrete reinforced with non-metallic rebars –Plasticrete, European Project contract BRPR-CT98-0708, Bilbao, Fundación Labein, 2002.

San José, J.T., Ramírez, J.L. and Cano, M. Pure bending in polymer reinforced concrete. Design guidelines Polyester Polymer Concrete. ARQUIMACOM'98, Bordeaux (France), 1998.

San José, T., Vegas, I, Ramírez, J.L.: Static and dynamic bond behaviour between rebars and polymer concrete. International conference on polymer concretes, mortars and asphtals. Porto (Portugal). October 2002.

Ramírez, Jose L. and San-José, J.Tomás. Predictability of structural calculation values in a 100 MPa polymeric concrete. ICPIC'01 Hawai (USA), 2001.

Rebeiz, K.S.; Fowler, D.W.: Flexure for reinforced polymer concrete using recycled pet. ICPIC'01 Hawai (USA). 2001.

International Symposium Polymers in Concrete
2 - 4 April 2006
Guimarães, Portugal

# Water-soluble polymers for modification of cement mortars

E. Knapen[1], D. Van Gemert[2]

*K.U.Leuven, Departement Burgerlijke Bouwkunde, Kasteelpark Arenberg 40, 3001 Heverlee, Belgium*

## ABSTRACT

The influence of small amounts of water-soluble polymers (polyvinyl alcohol, methylcellulose, hydroxyethyl cellulose and polyethylene oxide) on the microstructure building and on the cement hydration reactions is studied. The polymer molecules are supplied on a molecular scale, improving the approach of the relatively large cement grains by the polymers. In the absence of surface active agents, these water-soluble polymers tend to require a lower proportion in order to be comparably effective as polymer dispersions. The addition of very small amounts of water-soluble polymers results in an improvement of the durability and the adhesion strength of the cementitious materials, which makes them appropriate as repair materials. XRD and SEM are used to characterize the morphology and nature of the hydrate crystals. An abundant crystal growth is noticed at the air void surfaces of the modified mortars where the presence of water-soluble polymers is expected because of their strong affinity to the gas-water phase. Possible film formation is studied by examining the influence of the curing conditions on the flexural strength of mortar beams. If film formation takes place, the contribution of the polymer film to the mechanical properties and the durability of the polymer film is studied in view of practical applications.

## 1. INTRODUCTION

Usually, polymer-modified cement concrete or mortar is prepared by mixing polymer dispersions or redispersible polymer powders with the fresh mixture. The surface active agents, added to allow emulsification and stabilization of the dispersion during storage, hinder the cement hydration and the polymer film formation (Beeldens 2002). Therefore, the addition of polymers in aqueous solution is aimed for. Water-soluble polymer molecules are supplied on a molecular scale, improving the approach of the relatively large cement grains by the polymers. In the absence of surface active agents, the film formation on the hydrate crystals may proceed more easily and uniformly and the material properties can be better tuned and modelled (Knapen 2004). In the absence of surface active agents, water-soluble polymers tend to require a lower proportion in order to be comparably effective as polymer dispersions (Chung 2004). The addition of very small amounts of water-soluble polymers results in an improvement of the durability and the adhesion strength of the cementitious

[1] Research Assistant
[2] Professor

materials, which makes them appropriate as repair materials (Chung 2004). A disadvantage of the use of water-soluble polymers may be their sensitivity to humidity and water.

In this paper, the use of water-soluble polymers in cement concrete and mortar is discussed. Research on the influence of water-soluble polymers on the microstructure building and on the cement hydration reactions is running at the Katholieke Universiteit Leuven (Belgium) and the first results are presented here. The effect of the addition of water-soluble polymers is twofold: the cement hydration reactions may be influenced and polymer film formation may take place. The microstructure building and the influence on the cement hydration reactions is studied by SEM investigation and XRD-analysis. Possible film formation is studied by examining the influence of the curing conditions on the flexural strength of mortar beams. Cement hydration requires a wet or moist curing, while a dry curing promotes polymer film formation. If film formation takes place, the contribution of the polymer film to the mechanical properties and the durability of the polymer film is studied in view of practical applications, in particular their resistance to re-dissolution in humid environment.

## 2. WATER-SOLUBLE POLYMERS IN CEMENT MORTAR AND CONCRETE

Polymer modification of mortars or concrete by adding water-soluble polymers to the fresh mixture is less frequently applied, although recent studies list some advantages. Water-soluble polymers are generally used at very low polymer-cement ratios. The addition of small amounts of water-soluble polymers changes the properties of the fresh mortar mixture. The workability of the fresh mixture is markedly improved over that of ordinary cement mortar and concrete, because of plasticizing and air-entraining effects of the polymers. The modified system shows higher water retention than the ordinary cement systems. This may contribute to an improvement in the workability and the prevention of dry-out, and it also leads to superior adhesion to porous substrates such as ceramic tiles, mortars and concrete (Ohama 1995). Addition of water-soluble polymers reduces bleeding and improves the homogeneity of mortar or concrete by controlling segregation of fresh mixtures (Soshiroda 1986). Also, a better dispersion of carbon fibers in the cement paste is realized (Chen 1997).

On the other hand, water-soluble polymers have often been found to decrease the mechanical properties of mortar and concrete because of the increased air entrainment (Ohama 1995). Although, an increase of the tensile strength (Fu 1996b) and an increase of the bond strength between cement paste and aggregate (Hayakawa 1986, Kim 1998), between cement paste and steel fibers (Najm 1994, Fu 1996a) and between cement paste and carbon fibers (Fu 1996c) have been reported.

Fu and Chung studied the effect of small additions of methylcellulose (0.2% - 0.8% by weight of cement) (Fu 1996a, Fu 1996b, Fu 1996c). The tensile strength was found to be increased by up to 72%, the tensile ductility by up to 620%, while the compressive strength was decreased by up to 30% and the compressive ductility by up to 34% (Fu 1996b). The addition of methylcellulose (0.4% by weight of cement) or latex (20% by weight of cement) to cement paste gave similarly significant increases of the shear bond strength between stainless steel fibers and cement paste, in spite of the low concentration and therefore lower cost of methylcellulose compared to latex (Fu 1996a).

The microstructure of the interfacial transition zone (ITZ) is influenced by modification with water-soluble polymers. Because of the alteration of the microstructure of the ITZ, the admixing of small amounts of water-soluble polyvinyl alcohol was reported to have doubled the pullout strength and friction of steel fibres in cement paste by Najm et al. (Najm 1994). Kim and Robertson (Kim 1998) found an increase of the aggregate-paste bond strength after the addition of polyvinyl alcohol. They noticed a significant reduction in the

thickness of the ITZ around sand grains and coarse aggregates and a significant reduction or even elimination of the $Ca(OH)_2$ crystals that normally coat the aggregate surface and their possible replacement by C-S-H phases. After addition of methylcellulose, Hayakawa et al. (Hayakawa 1996) also found an improved bond strength between cement matrix and aggregate. They attributed this to a decreased bleeding and a subsequent decreased defect under aggregates caused by bleeding.

Singh and Rai (Singh 2001) report a possible chemical interaction between polyvinyl alcohol and cement which results in the formation of some new compounds. The compounds are thought to be amorphous in nature, because they are not detected by X-ray diffraction techniques, only by the UV-visible spectra and differential thermal analysis. Singh et al. (Singh 2003) also report a possible interaction of hydroxyethyl cellulose with the ettringite phase and with the C-S-H phases of the hydrated cement and an indication of the formation of a new product. Their results are obtained by IR spectra and X-ray diffraction.

As illustrated above, polymer modification with water-soluble polymers improves some properties of mortars, such as the workability and the adhesiveness, rendering them appropriate as adhesive mortars. There still needs to be carried out a lot of research on the influence of these polymers on the cement hydrates that are formed, on the microstructure building and on the durability of the modified systems.

## 3. RESEARCH PROGRAM

Polymer film formation and cement hydration reactions are studied by means of mechanical strength tests on mortar beams, SEM investigation on fracture surfaces and XRD-analyses on cement pastes that have been hydrating for 24 hours, 2, 7 and 28 days.

### 3.1. Materials

An ordinary Portland cement (CEM I 52.5 N) and CEN-Standardsand DIN EN 196-1 are used. Different types of polymers are added to the fresh mortar mixtures: a polyvinyl alcohol (PVAA) which is a 87-89% hydrolyzed polyvinyl acetate; two cellulose derivatives, methylcellulose (MC) or hydroxyethyl cellulose (HEC); or a polyethylene oxide (PEO).

### 3.2. Specimen preparation

For the mechanical strength tests and the SEM investigation, mortar beams (40*40*160mm) are prepared with a polymer-cement ratio (p/c) of 1%, a water-cement ratio (w/c) of 0.45 and a sand-cement ratio (s/c) of 3. The polymer powders are first dissolved in the mixing water before adding to the sand and cement in the mixer. The mortar beams are covered for two days before demoulding. Standard curing implies storage, after demoulding, in a moist room for 5 days (20°C, 85-90%), followed by a dry curing for 21 days (20°C, 63% RH). The mixing procedure and proportions are not optimized with respect to the mechanical properties and this should be taken into consideration when analyzing the results. First aim of this research was to study the influence of water-soluble polymers on the microstructure building of cement mortars. However, by controlling the air entrainment, mechanical properties should be improved in future research projects. A pre-wetting mixing procedure in combination with simultaneous shocking of the mixture (Kim 1997) or the addition of anti-foaming agents (Fu 1996b) may improve these properties.

For the XRD-analyses, cement pastes with a polymer-cement ratio of 1% and a water-cement ratio of 0.45 are prepared. The polymer powders are first dissolved in the mixing water before adding to the cement in the mixer. The pastes are stored in closed recipients until

the moment of testing (24h, 2, 7, 28 days). Before the XRD-analyses are carried out, the hydration is stopped. The cement pastes are crushed with a hammer and ground to fine powder in a mortar. The prepared powders are thrice centrifuged for 20 minutes with pure ethanol to remove the excess water and to stop hydration. At the end of every cycle, the ethanol is removed and replaced by fresh one. To remove the remaining ethanol, the powders are once centrifuged with diethyl ether. Finally, they are dried at 50°C under vacuum. This solvent replacement is a common technique to stop the hydration prior to XRD-analysis. Nevertheless, the use of organic liquids is criticized (Beaudoin 1998) because of the possible interaction with the cement hydrates and the formation of carbonate-like materials (Day 1981). Hansen et al. (Hansen 1996) noticed an extensive exchange between water and ethanol and no signs of chemical interaction between the solvent and the solid by $^{13}$C-NMR spectroscopy. In the continuation of the research project, possible interaction between the solvent and cement hydrates will be studied by thermal analysis at the Katholieke Universiteit Leuven.

### 3.3. Mechanical strength tests

*Influence of the curing conditions*

Cement hydration requires a wet or moist curing, while a dry curing promotes polymer film formation. Generally, polymer film formation improves the flexural strength, while the compressive strength is rather influenced by the degree of cement hydration and the air entrainment. To study the influence of the curing conditions on the mechanical strength, mortar beams subjected to the standard curing, as described above, and beams subjected to a 26-day wet curing (85-90% RH) after demoulding are prepared. The compressive strength is hardly influenced by the curing conditions. Figure 1 shows the flexural strength of mortar beams subjected to the standard and to the wet curing. The flexural strength of the mortars modified with PEO and HEC is not influenced by the curing conditions. On the other hand, the flexural strength of the mortars modified with PVAA and MC is increased with 21% and 27% resp. if a dry curing period is included (standard curing). This is an indication of the formation of a PVAA- and MC-film which contributes to the flexural strength of the mortars. In the HEC- en PEO-modified mortars, no polymer film is formed or the polymer film does not contribute to the tensile properties of the mortars.

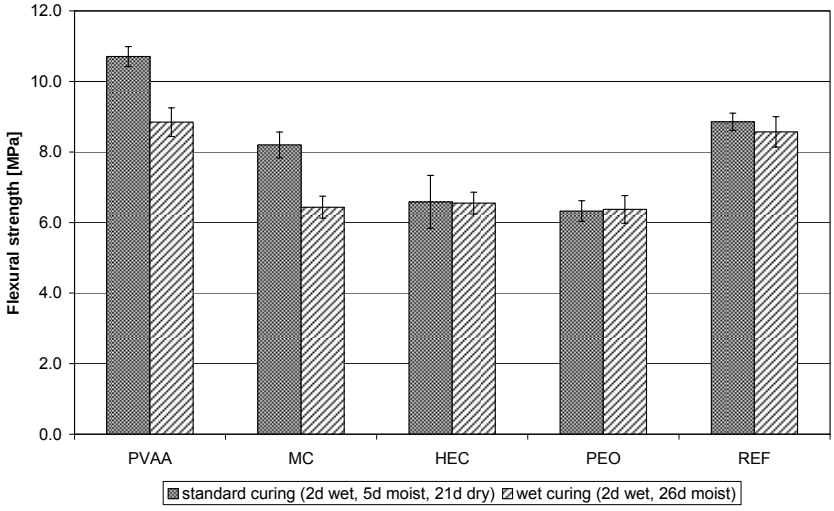



Figure 1 - Influence of the curing conditions on the flexural strength of unmodified mortars (REF) and mortars modified with 1% PVAA, 1% MC, 1% HEC and 1% PEO.

*Influence of moisture and water*

To investigate the influence of moisture on the mechanical properties, mortar beams modified with water-soluble polymers are subjected, after standard curing, to a moist curing of 7 days (85-90% RH) or a moist curing of 14 days (85-90% RH). No influence of the moist curing on the splitting tensile strength of the mortar beams is noticed. Further research is planned to study the influence of longer storage at a high relative humidity (> 95%).

Additionally, splitting tensile tests are carried out on 90-days old mortar beams before and after vacuum saturation and storage under water for 7 days. The results are shown in Figure 2. The splitting tensile strength of PVAA-modified mortars decreases with almost 40% after storage under water. The decrease in splitting tensile strength of HEC-modified mortars is not significant. These results indicate the formation of a PVAA-film which contributes to the tensile strength of the mortar beams. A contribution of a HEC-film to the strength properties is not noticed.

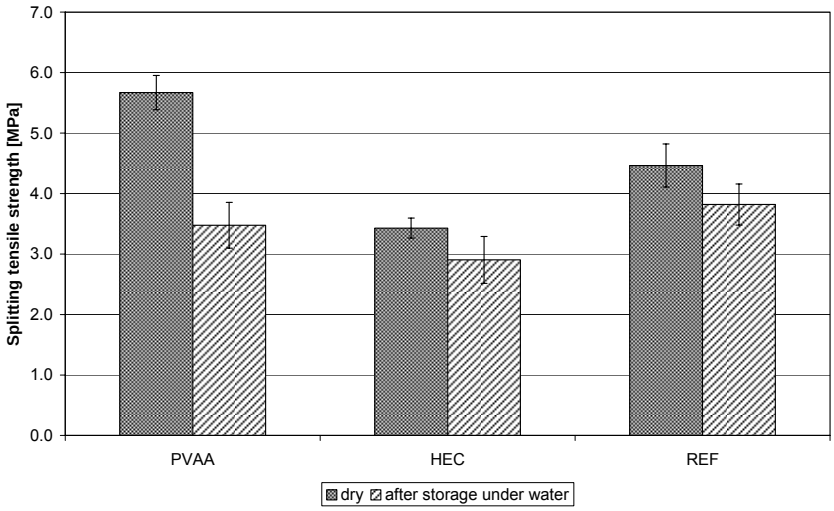



Figure 2 - Influence of storage under water for 7 days on the splitting tensile strength of unmodified mortar beams (REF) and mortar beams modified with 1% PVAA and 1% HEC.

*Influence of hydration time*

To study the mechanical properties with respect to the hydration time, mortar beams are standard cured and stored afterwards at 63% RH. The compressive and flexural strength is determined after 2, 7, 28 and 90 days. The development of the compressive strength with hydration time is almost similar for all mortar beams. When analyzing the flexural strength (Figure 3), the curing conditions should be borne in mind. During standard curing, a dry curing is applied after 7 days of moist curing. The increase of the flexural strength of the PVAA- and MC-modified mortars between 7 and 28 days of hydration is larger than that of the HEC-modified and unmodified mortar. The development of the flexural strength of the PVAA-modified beams also seems to be retarded with still a major increase of the flexural strength after 28 days.

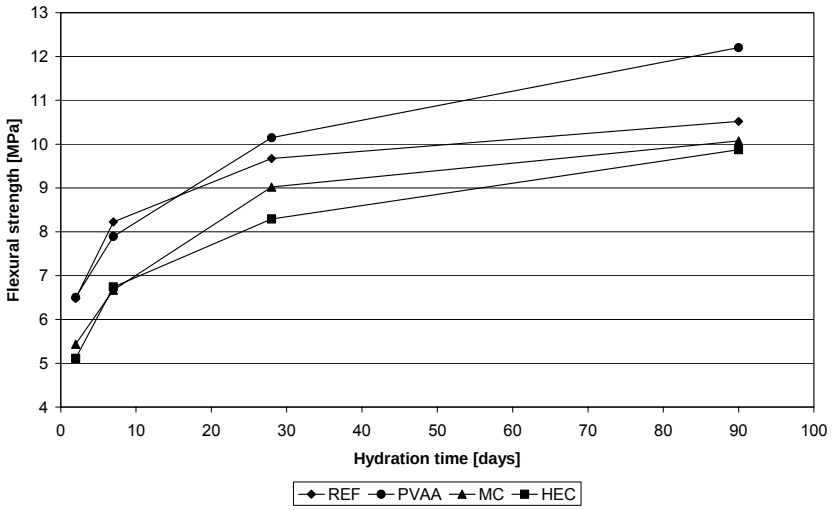



Figure 3 - Flexural strength after 2, 7, 28 and 90 days of hydration for the unmodified (REF), PVAA-, MC- and HEC-modified mortars (standard curing, p/c=1%).

### 3.4. X-Ray Diffraction

XRD-analyses of the cement pastes are carried out on a Philips Analytical PW1710 Diffractometer with $CuK_\alpha$ radiation ($\lambda$ = 1.54Å). In Figure 4, XRD-patterns are shown for unmodified pastes and pastes modified with 1% PVAA, MC and HEC and hydrated for 24 hours, 2, 7 and 28 days. All pastes have a similar XRD-pattern, dominated by $Ca(OH)_2$ peaks, and a decreasing amount of unhydrated cement phases with time. No new crystalline hydration products are detected. Nevertheless, small differences in hydration rate are present. Figure 4 shows the retardation of the hydration reactions for the HEC-modified cement pastes. After 24h of hydration, the XRD-pattern is very similar to the one of the unhydrated cement. This delay is almost eliminated after 48h of hydration. The $Ca(OH)_2$ formation in the PVAA-modified paste is slightly delayed. Cement pastes modified with MC show an abundant $Ca(OH)_2$ formation.

### 3.5. SEM investigation

Fresh fracture surfaces of mortar beams, subjected to the standard curing, are investigated using a JEOL JSM-6400 type of Scanning Electron Microscope (SEM) in the SEI mode. Samples are coated by evaporation with gold. Special attention was paid to the air void surfaces in the mortar specimens. At these surfaces, the presence of water-soluble polymers is expected because of their strong affinity to the gas-water phase. The polymers serve as surface-active agents that are initially dissolved in the mixing water. During mechanical mixing, they become attached to the air void interface and start to stabilize the entrained air voids in the fresh mixture. So, an enrichment of polymer at the interface between air void and wet cement paste may be detected (Jenni 2005), depending on the surface activity of the polymer.

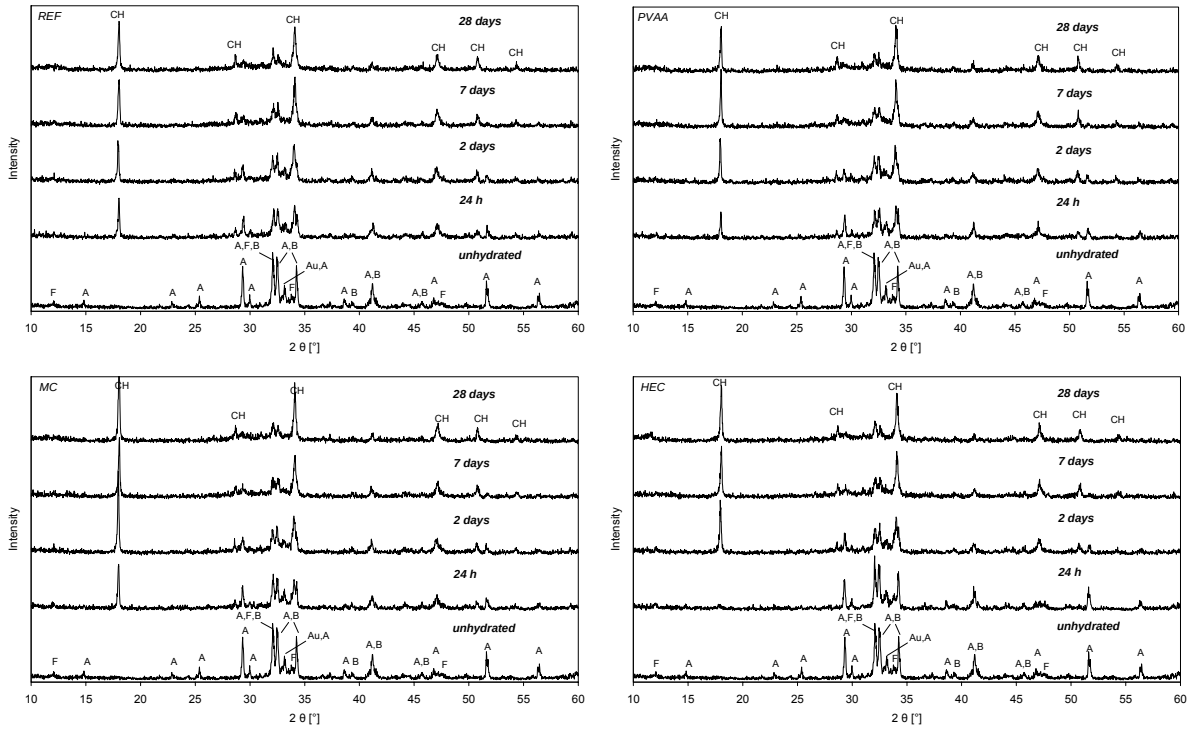



Figure 4 - XRD-patterns for unmodified cement pastes (REF) and pastes modified with 1% PVAA, 1% MC and 1% HEC (unhydrated and hydrated for 24h, 2, 7 and 28 days) – CuKα radiation, A = alite, B = belite, Au = aluminate, F = ferrite, CH = calcium hydroxide

The microstructure of cement hydrates formed at the air void surfaces is strongly influenced by polymer modification, as shown in Figure 5, although polymer film formation is not detected. The air void surfaces of unmodified mortar beams have a smooth surface at the micrometer scale. In the case of polymer modification, Figure 5-b and Figure 5-c show a similar microstructure at the air void surface for the PVAA-modified and the HEC-modified mortar. C-S-H fibres cover the walls of the air voids, disturbing the smooth surface that was found in unmodified mortars. The presence of polymer particles or polymer films is expected at the air void surfaces. Water molecules are bounded to the polymer particles until sufficient forces are exerted, e.g., by cement hydration. In this aqueous environment, crystal formation is possible.

The air void surface of the MC-modified mortar (Figure 5-d) is characterized by an abundant efflorescence of $Ca(OH)_2$ crystals, surrounded by C-S-H fibres. The $Ca(OH)_2$ plates are formed parallel towards each other and they are almost undistorted. Methylcellulose has a high swelling capacity and can swell to forty times its dry volume in water (Bikales 1971). The presence of methylcellulose at the air void surfaces results in a very aqueous environment which promotes crystal formation.

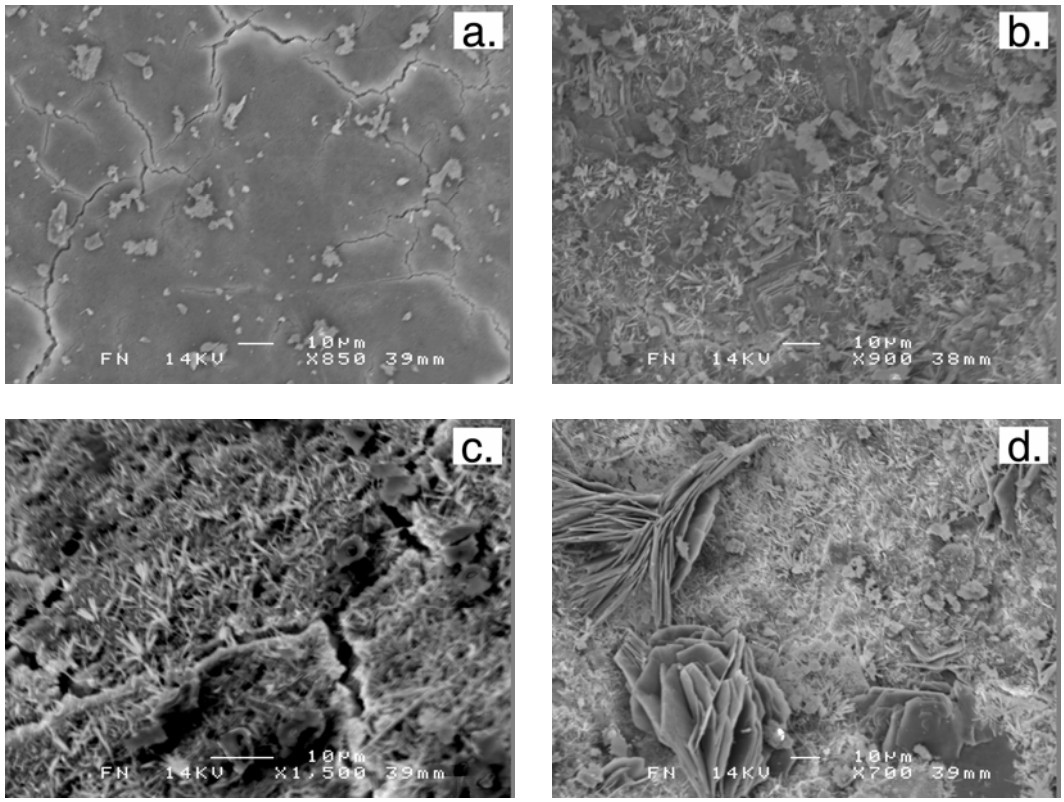



Figure 5 - SEM images at the air void surfaces: unmodified mortar (a), mortar modified with 1% PVAA (b), 1% HEC (c) and 1% MC (d).

## 4. DISCUSSION

The presence of polymers in the mortar mixture can influence the microstructure building in several ways. The rate of cement hydration and the nature and morphology of the hydrate crystals can be changed. Furthermore, polymer film formation can take place. Until now, little information is available on the effects of water-soluble polymers on the microstructure of polymer-modified cement mortars, and particularly on the polymer film formation. For polymer dispersions, a polymer-cement ratio higher than 5% is necessary for an adequate film formation throughout the cement matrix. If the polymer-cement ratio is lower than 5%, the polymer acts as an admixture for the ordinary cement mortar or concrete and no continuous polymer film is formed. Because of the low amounts of water-soluble polymers added to the fresh mixture, these polymers are generally considered as rheological additives and polymer film formation is not mentioned. However, in contrast to polymer dispersions, water-soluble polymers are added on a molecular scale, allowing the polymer film formation to proceed more easily and possibly at lower polymer-cement ratios.

Visual detection of water-soluble polymer films by SEM investigation is not easy because of the very low concentrations of the polymers in the cement paste, their possible integration in the polymer-cement matrix at a submicron scale and their sensibility to electron beam damage. In this paper, polymer film formation is studied by means of mechanical strength tests.

For an adequate film formation, a wet curing period should be followed by a dry curing period (Beeldens 2002). For the PVAA- and MC-modified mortars, an increase of the flexural strength is noticed when a dry curing period is introduced and therefore film formation may take place (Figure 1). No influence of the curing conditions on the flexural

strength of the HEC- and PEO-modified mortars is noticed. Similar results are obtained by studying the influence of water on the splitting tensile strength (Figure 2). The tensile strength of the PVAA-modified mortars decreases dramatically after immersion and storage under water, while the tensile strength of the HEC-modified mortars remains almost constant. In addition, these results are confirmed by studying the influence of the hydration time on the flexural strength (Figure 3). The standard curing consists of a moist curing for 7 days, followed by a dry curing. Due to this, polymer film formation will probably start after 7 days of curing. The PVAA-modified and MC-modified beams show a larger increase of the flexural strength after 7 days than the unmodified and HEC-modified mortars.

These mechanical strength tests elucidate the formation of a PVAA- and MC-film which contributes to the tensile strength of the mortars and redissolves in water during vacuum saturation and immersion under water for 7 days. In the HEC- and PEO-modified mortars, no polymer film is formed or the polymer film does not contribute to the tensile strength properties of the mortars. Because the water-soluble polymer films have a major contribution to the tensile strength of the mortar beams, the durability of these films in the cement matrix is important. Films of water-soluble polymers are quite hygroscopic. The equilibrium moisture content of e.g. a polyvinyl alcohol film increases exponentially with increasing relative humidity. The mechanical properties of these films are again very much a function of the water content of the film. At high values of the relative humidity, the mechanical properties of water-soluble polymer films decrease dramatically (Bikales 1971). Further research is planned at the Katholieke Universiteit Leuven (Belgium) to study the influence of a long storage at a high relative humidity and of subsequent moist-dry cycles on the mechanical properties.

Polymer modification can influence the degree of cement hydration and the nature and morphology of the hydrates that are formed. When mixing polymers with the fresh mortar mixture, the mixing water is often retained. In polymer dispersions, the surfactants hold the water, needed for hydration, more thoroughly than in the case of the unmodified mixtures; in polymer solutions, the water-soluble polymers themselves cause the water retention. The water is partly bound to the hydrophilic part of the surfactants or the water-soluble polymers by hydrogen bonds. The release of water takes time, so hydration is retarded. Figure 4 shows a serious retardation of the hydration reactions after 24h of hydration for the HEC-modified mortars. After 2 days, this delay is almost completely eliminated.

No new crystalline hydration products are detected by XRD-analysis. SEM investigation (Figure 5) shows an abundant efflorescence of $Ca(OH)_2$ crystals at the air void interfaces of MC-modified mortar. Methylcellulose has a high swelling capacity and can swell to forty times its dry volume in water (Bikales 1971). The presence of MC at the air void interfaces results in a very aqueous environment which promotes crystal formation.

## 5. CONCLUSION

Polymer modification by means of polymers in solution influences the microstructure building of cement mortars in several ways. Although the water-soluble polymers are added in very low concentrations (p/c=1%), polymer film formation is assumed in PVAA- en MC-modified mortars, based on the results of mechanical strength tests. These polymer films have a major contribution to the tensile strength of the mortars. Furthermore, for the MC-modified mortars, an abundant efflorescence of $Ca(OH)_2$ crystals is noticed at the air void surface, where the presence of water-soluble polymers is expected. During the first 24h after mixing, the cement hydration reactions of HEC-modified pastes are retarded, but this delay is almost completely eliminated after 2 days.

## 6. ACKNOWLEDGEMENT

The grant offered by the Institute for the Promotion of Innovation by Science and Technology in Flanders (IWT-Vlaanderen) is gratefully acknowledged.

## 7. REFERENCES

Beaudoin, J.J., Gu, P., Marchand, J., Tamtsia, B., Myers, R.E. and Liu, Z., Solvent replacement studies of hydrated Portland cement systems: the role of calcium hydroxide, *Advanced Cement Based Materials*, **8**, 56-65 (1998).

Beeldens, A., *Influence of polymer modification on the behaviour of concrete under severe conditions*, PhD dissertation, Faculty of Engineering, Katholieke Universiteit Leuven (2002).

Bikales, N.M., *Encyclopedia of polymer science and technology*, vol 14, ed. N.M. Bikales, John Wiley & Sons (1971).

Chen, P.-W., Fu, X. and Chung, D.D.L., Microstructural and mechanical effects of latex, methylcellulose, and silica fume on carbon fiber reinforced cement, *ACI Materials Journal*, **94(2)**, 147-155 (1997).

Chung, D.D.L., Review: use of polymers for cement-based structural materials, *Journal of Materials Science*, **39**, 2973-2978 (2004).

Day, R.L., Reactions between methanol and portland cement paste, *Cement and Concrete Research*, **11(3)**, 341-349 (1981).

Fu, X. and Chung, D.D.L., Effect of polymer admixtures to cement on the bond strength and electrical contact resistivity between steel fiber and cement, *Cement and Concrete Research*, **26(2)**, 189-194 (1996a).

Fu, X. and Chung, D.D.L., Effect of methylcellulose admixture on the mechanical properties of cement, *Cement and Concrete Research*, **26(4)**, 535-538 (1996b).

Fu, X., Lu, W. and Chung, D.D.L., Improving the bond strength between carbon fiber and cement by fiber surface treatment and polymer addition to cement mix, *Cement and Concrete Research*, **26(7)**, 1007-1012 (1996c).

Hansen, E.W. and Gran, H.C., Carbon NMR used in probing the exchange of ethanol with water in water-saturated cement pastes, *Magnetic Resonance Imaging*, **14(7/8)**, 903-904 (1996).

Hayakawa, K. and Soshiroda, T., Effects of cellulose ether on bond between matrix and aggregate in concrete, Adhesion between polymers and concrete, in: *Adhesion between polymers and concrete*, Proceedings of international symposium organized by Rilem Technical Committee 52, Ed. by H.R. Sasse, 22-31 (1986).

Jenni, A., Holzer, L., Zurbriggen, R. and Herwegh, M., Influence of polymers on microstructure and adhesive strength of cementitious tile adhesive mortars, *Cement and Concrete Research*, **35(1)**, 35-50 (2005).

Kim, J.-H. and Robertson, R.E., Prevention of air void formation in polymer-modified cement mortar by pre-wetting, *Cement and Concrete Research*, **27(2)**, 171-176 (1997).

Kim, J.-H. and Robertson, R.E., Effects of polyvinyl alcohol on aggregate-paste bond strength and the interfacial transition zone, *Advanced Cement Based Materials*, **8**, 66-76 (1998).

Knapen, E., Beeldens, A., Van Gemert, D. and Van Rickstal, F., Modification of cement concrete by means of polymers in solution, in: *Proceedings of 11th Congress on Polymers in Concrete*, Ed. by M. Maultzsch, BAM, Berlin, 83-90 (2004).

Najm, H., Naaman, A.E., Chu, T.-J. and Robertson, R.E., Effects of poly(vinyl alcohol) on fiber cement interfaces. Part I: Bond stress-slip response, *Advanced Cement Based Materials*, **1(3)**, 115-121 (1994).

Ohama, Y., Handbook of polymer-modified concrete and mortars, properties and process technology, Noyes Publications, New Jersey (1995).

Singh, N.B. and Rai, S., Effect of polyvinyl alcohol on the hydration of cement with rice husk ash, *Cement and Concrete Research*, **31**, 239-243 (2001).

Singh, N.K., Mishra, P.C., Singh, V.K. and Narang, K.K., Effects of hydroxyethyl cellulose and oxalic acid on the properties of cement, *Cement and Concrete Research*, **33**, 1319-1329 (2003).

Soshiroda, T., Hayakawa, K., Yoda, K. and Tanaka, M., Effects of cellulose ether on the homogeneity of concrete in structures – relating quality variations and construction joints, in: *Adhesion between polymers and concrete*, Proceedings of international symposium organized by Rilem Technical Committee 52, Ed. by R. Sasse, 125-133 (1986).

# Session 2

International Symposium Polymers in Concrete
2 - 4 April 2006
Guimarães, Portugal

# Effect of concrete substrate texture on the adhesion properties of PCC repair mortar

Luc Courard[1], Damien Schwall[2]

*Université de Liège, Département GéomaC*
*Civil Engineering Institute, Chemin des Chevreuils, 1*
*B – 4000 Liège, Belgium*

Andrzej Garbacz[1], Tomasz Piotrowski[2]

*Warsaw University of Technology, Faculty of Civil Engineering*
*Department of Building Materials Engineering*
*Al. Armii Ludowej 16, 00-637 Warsaw, Poland*

## ABSTRACT

The study of adhesion of repair materials on concrete structures implies a good knowledge of the influence of concrete surface characteristics. A large research project has been realized with regards to the influence of concrete substrate strength and preparation technique efficiency. Three types of concretes and four types of surface preparation have been combined in order to obtain twelve different concrete slabs. They have been characterized according different destructive and non destructive techniques: Schmidt hammer, compressive strength, superficial cohesion (pull-off tests), Impact Echo measurements and cracking quantification (microscopical observations). Finally, a polymer cement concrete mortar has been applied and adhesion has been evaluated by means of pull-off and laboratory tensile tests. The relationships between parameters describing surface quality (roughness, cracking), adhesion strength and stress wave propagation have been analysed.

## 1. INTRODUCTION

Before any repair operation, an effective assessment of the concrete substrate has to be performed. Usually next to the surface reparation of concrete, evaluation of the cohesion of the superficial concrete is requested for adhesion and durability reasons. Many authors describe the influence of the surface preparation technique on the superficial cohesion of concrete (Silfwerbrandt 2005, Courard et al. 2005) or the adhesion (Pretorius and Kruger 2001, Garbacz et al. 2005). However, the real effects of surface preparation technique only

[1] Assistant Professor
[2] Research Assistant

begin to be investigated in terms of superficial microcracking or roughness quantification (Czarnecki et al. 2003, Courard et al. 2005, Courard et al. 2004, Silfwerbrand 1998).

This project was performed with regards to the influence of concrete substrate strength and preparation technique efficiency. Three types of concretes and four types of surface preparation have been combined in order to obtain twelve different concrete slabs. The quality of the superficial concrete has been characterized according different destructive and non destructive techniques: Schmidt hammer, compressive strength, superficial cohesion (pull-off tests), Impact Echo measurements and cracking quantification (microscopical observations).

Finally, a self-compacting PCC mortar has been applied and adhesion has been evaluated by means of pull-off and laboratory tensile tests. The relationships between parameters describing surface quality (roughness, cracking), adhesion strength and stress wave propagation have been analysed.

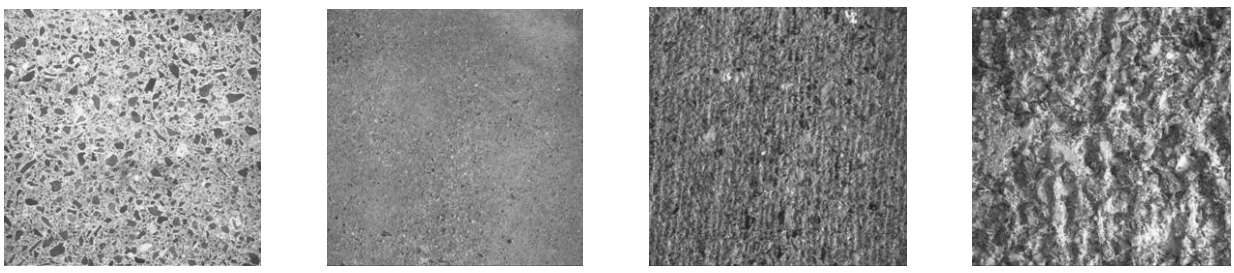
## 2. DESCRIPTION OF MATERIALS AND SURFACE PREPARATIONS

The effect of the concrete removal/preparation technique is most likely dependent upon the nature and the quality of the concrete substrate. Three types of concrete were designed in order to obtain C30/37, C40/50 and C50/60 concrete, respectively (Table 1).

Table 1 - Composition of concretes

| | C30/37 | C 40/50 | C50/60 | Unit |
|---|---|---|---|---|
| Cement CEM I 52,5 N | 275 | 325 | 375 | kg/m³ |
| Rhine Sand (0/2 mm) | 765 | 729 | 676 | kg/m³ |
| Rounded aggregate (2/8 mm) | 255 | 230 | 206 | kg/m³ |
| Rounded aggregate (8/14 mm) | 569 | 576 | 601 | kg/m³ |
| Rounded aggregate (14/20 mm) | 390 | 401 | 412 | kg/m³ |
| Water | 197 | 192 | 188 | $10^{-3}$m³ |
| W/C ratio | 0.72 | 0.59 | 0.50 | |

Four types of surface preparation techniques were investigated: sandblasting, scabbling, water jetting (250 MPa of pomp pressure during 5 min) and polishing (Schwall 2005). Polishing is obtained by means of two abrasive and rotative wearing plates until obtaining smooth touch surface. The visual observation of the concrete surfaces indicates that the high pressure water jetting technique induces a particular texture characterized by large waves mostly parallel to the water flow (Fig.1).



polishing sandblasting scabbling hydro-jetting

Figure 1 – Examples of concrete surface after preparation

The concrete slabs have been covered by a Self-Compacting commercial PCC mortars (5-cm thick) characterized by a flexural strength of 7.27 MPa and a compressive strength of 54.61 MPa (24-hours old).

## 3. MECHANICAL CHARACTERISTICS OF SUPERFICIAL CONCRETE

### 3.1. Schmidt Hammer test (before repair)

The cohesion of the superficial concrete has been first evaluated by means of Schmidt hammer. Ten measures have been taken in vertical direction; only polished surfaces strictly present adequate conditions to perform the test (Piotrowski 2005), which requires flat and leveled surface and only results on polished slabs are presented (Table 2). Other surfaces are theoretically too rough for this test method.

The Schmidt Hammer results on polished samples are lower than compressive strength evaluated through compression test on cylinders. These values can be used for calibration of Schmidt Hammer for this kind of concrete: the normative coefficient varies from 1.30 to 1.41 (Table 2).

Table 2 - Schmidt hammer test results for concretes of various strength classes after polishing

| Concrete type | Mean rebound number, R | Estimated compressive strength on the base of Producer's reference curve, $f_{ck}$, [MPa] | Compressive strength determined on the cube $f_{ck,cube}$ [MPa] | $\gamma=f_{ck,cube} / f_{ck}$ |
|---|---|---|---|---|
| C30/37 | 34.3 | 35.32 | 45.88 | 1.30 |
| C40/50 | 36.2 | 38.75 | 53.29 | 1.38 |
| C50/60 | 39.3 | 44.15 | 62.12 | 1.41 |

### 3.2. Pull-off test before repair

Pull-off test is usually performed in order to evaluate the bond strength between concrete substrate and repair material; if the test is made in absence of repair layer, it can be adopted as a cohesion measurement of the superficial concrete (Courard, et Bissonnette 2004).

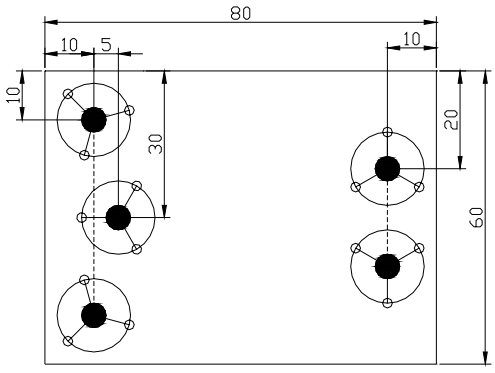



Figure 2 - Distribution of pull-off points after surface treatment

The test conditions (Fig.2) have been defined according to the practice (Courard and Bissonnette 2004):

- Diameter of the steel dolly: 50-mm;
- Depth of coring: 15-mm;

- Number of tests: 5;
- Loading rate: 0.05 MPa/s

The pull-off test results show higher strength values in comparison with the calculated values of $f_{ctm} = 0{,}3 \cdot \left( f_{ck,cyl} \right)^{2/3}$ (Table 3). Moreover, the next partial conclusions can be given:

- there seems to be a correlation between the degree of aggressiveness and the reduction of strength: while sandblasting only induces a small decrease of pull-off strength, hydro jetting and scabbling, which are more energetic surface treatments, produce a larger decrease of resistance (12 and 13 %, respectively);
- the concrete quality – in terms of characteristic compressive strength – doesn't seem to have a major influence on the cohesion of the superficial concrete. The less influence on the pull-off strength reduction was observed for the C50/60. However, the high strength rates of the concretes probably limit the influence of the surface treatment on the quality of the surface.

Table 3 - Pull-off test results after surface treatment

| pull-off strength [MPa] | | | | |
|---|---|---|---|---|
| $f_{ck,\,cyl}$ | C30/37 | C40/50 | C50/60 | Mean |
| Polishing | 4.29 | 4.07 | 3.71 | 4.02 |
| Sandblasting | 3.70 | 3.93 | 3.76 | 3.80 |
| Scabbling | 3.39 | 3.51 | 3.58 | 3.49 |
| Hydro jetting | 3.53 | 3.54 | 3.59 | 3.55 |
| Mean | 3.73 | 3.76 | 3.66 | - |
| $f_{ctm}$ | 2.90 | 3.51 | 4.07 | - |

Three types of rupture (Fig.3) have been considered in the analysis: superficial, middle and deep. The last mode means that the rupture happened at the depth coring (15-cm). In the case of polished and sandblasted slabs, main failures appeared in the middle or in the bottom of cores. Otherwise, for scabbling and hydrojetting techniques, ruptures have been observed mainly in near-to-surface area, that means 75 and 33%, respectively; this is probably due to microcracks developed in this zone during surface preparation (see chapter 5).

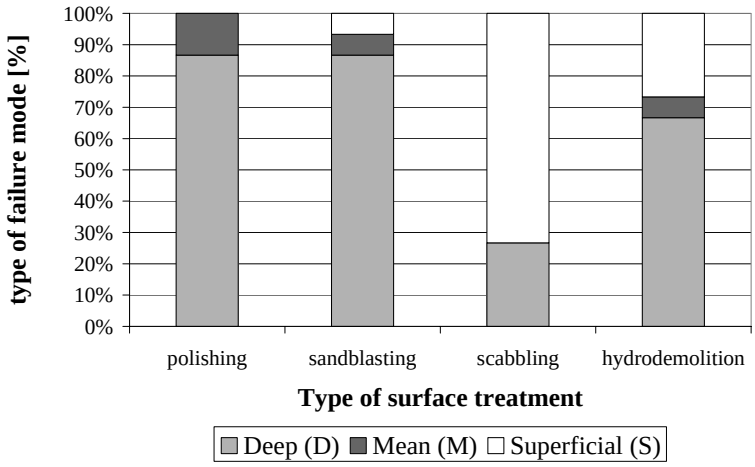



Figure 3 - Types of failure modes after pull-off cohesion test

## 4. ROUGHNESS AND WAVINESS QUANTIFICATION

A first evaluation of the surface roughness has been realized by means of Average Texture Depth test, according to prEN 13036-1 (2000): a defined volume of specific sand is sprayed on the concrete surface, the diameter of the "circle" is measured and Average Texture Depth calculated from $ATD = \frac{4 \cdot V}{\pi \cdot d^2}$. The larger the diameter, the lower ATD, the smoother the surface (Fig.4).

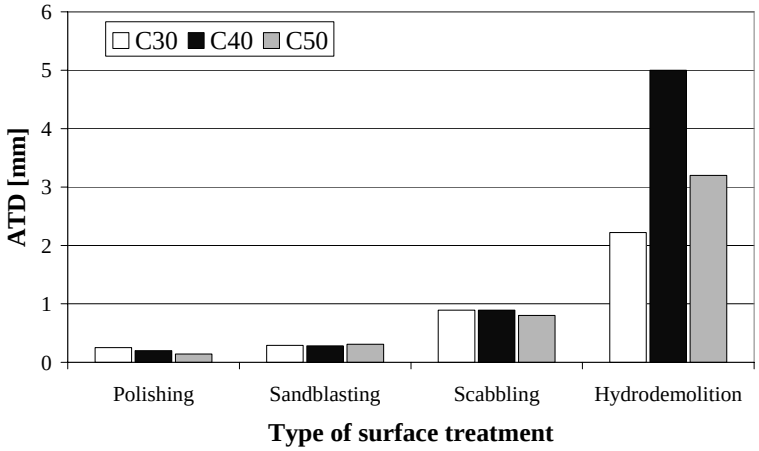



Figure 4 – Average Texture Depth values after surface preparations on different concretes

The validity of the test is between 0.25 mm and 5 mm: the results are consequently at the level of the inferior limit value for polished surfaces.

Opto-morphology technique (Perez et al., 2005) has also been used afterwards in order to calculate amplitude and statistic parameters; they have been evaluated with RugoDS program (Schwall, 2005), based on MatLab 7.0, that permits to process numeric data from representation of Moiré projection (Fig.5).

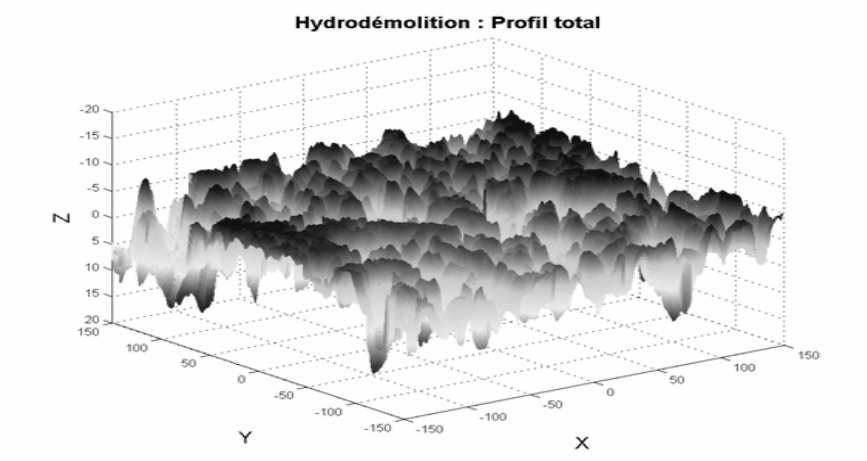



Figure 5 – total profile obtained after hydro demolition technique

One of the information coming from surface analysis is the bearing ratio and the Abbott's curve (Courard and Nélis, 2003). The surface parameters defined on the basis of this curve let us to analyse not only the depth of the holes but also the shape of the profile: $C_F$ represents the depth of the profile, excluding high peaks and holes; $C_L$ is the relative height of the holes and

$C_R$ the relative height of the peaks. The $C_F$ parameter gives an idea of the flatness of the surface: the lower it is, the more flat the profile is. Parameter $C_L$ gives an idea of the volume of voids, beneath the mean line of the profile, which could be fulfilled by the bond coat or the repair material.

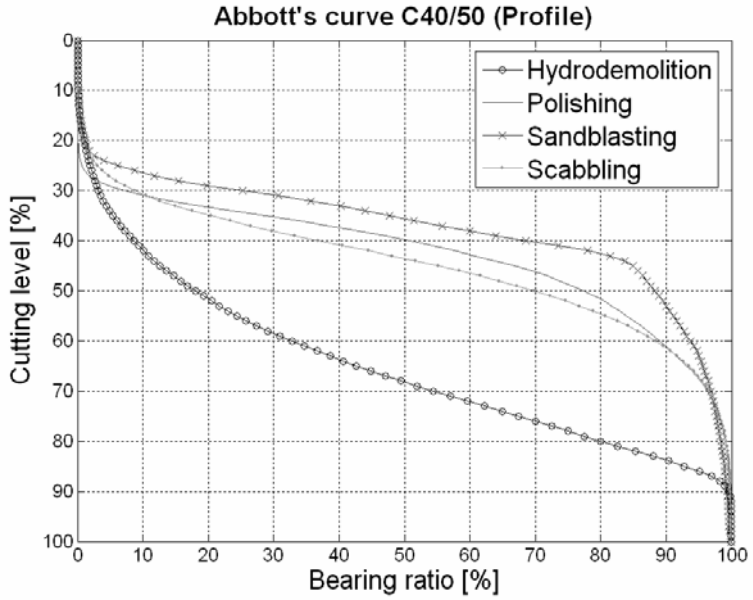



Figure 6 - Abbott's parameters for the surface preparation techniques on C40/50 concrete

Figure 6 clearly shows the effects of two groups of technique: the first group – polishing, sandblasting, scabbling – is giving surface without big peaks and deep holes, while waterjetting induces a very irregular surface, which is confirmed by the values of $C_F$ parameter (Table 4). Analysis of $C_R$ parameter also shows the larger quantity and amplitude of peaks for hydrojetting surface preparation.

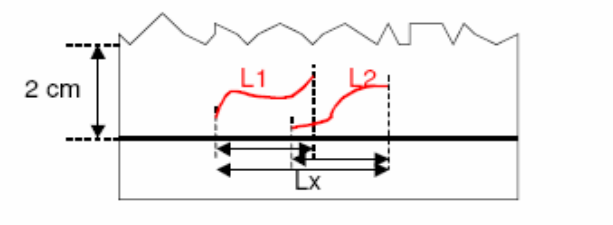
Table 4 - Abbott's parameters for the surface preparation techniques on C40/50 concrete

| Parameter [mm] | Polishing | Sandblasting | Scabbling | Hydro-jetting |
|---|---|---|---|---|
| $C_R$ | 0.34 | 0.56 | 0.87 | 5.46 |
| $C_F$ | 0.76 | 1.17 | 1.31 | 5.7 |
| $C_L$ | 0.27 | 3.1 | 1.83 | 2.61 |

## 5. MICROCRACKING

The samples used for microscope observations (80 mm in diameter and approximately 150 mm in length) were cored from the concrete substrates. The cores were sawn in two parts along their main axis. The surfaces to be observed were then polished with abrasive powders (Courard et al., 2005).

An optical binocular microscope was used for the investigation (Fig.7). The surface of investigation was delimited by drawing a straight reference line parallel to the prepared surface plane. The line was drawn approximately 20 mm from the surface, since in any case no more cracks could be observed below. The samples have been polished with a grain sand paper nr 400 (Schwall, 2005).



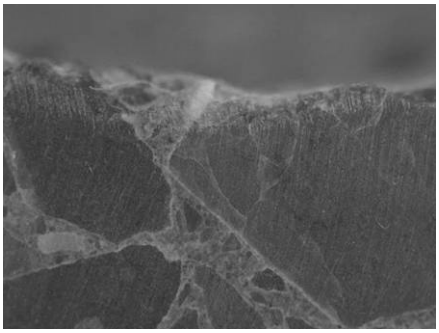



Figure 7 - Evaluation of the length ($L_i$) of the cracks and their projection on horizontal reference ($L_x$)

Number and length of microcracks have been systematically registered on the three types of concretes and four types of surface preparation (Fig.8).

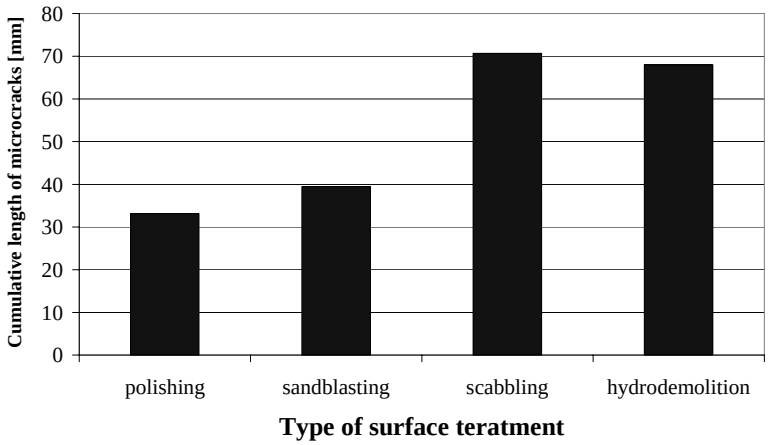



Figure 8 – The mean of microcracks cumulative length for three types of concrete after various surface treatment

The results we obtained do not allow to point out any effect of the quality of concrete; the surface preparation technique seems however to influence the length of the cracks observed on the first 2 centimetres. Scabbling induces almost 75% and 100% more cracks than sandblasting and polishing, respectively. The similar results obtained for water jetting and scabbling are more surprising, even if they show relatively low quantity of cracks. These results follow however the same classification than for the pull-off test and the Schmidt hammer test.

Another interesting information is coming from $L_{total}$ / $L_X$ ratio calculation (Table 5), where $L_{total}$ represents the cumulative length of the cracks. This parameter gives an idea of the slope of the cracks in relation to the surface. In the case of polished slabs, the cracks are more parallel to surface, while they seem more perpendicular oriented for scabbling. The conclusion is aggressive type of surface preparation, with the highest number of cracks, have the lowest $L_{total}$ / $L_X$ ratio.

Table 5 – Evaluation of the slope of the cracks

| Technique | L total/ Lx |
|---|---|
| Polishing | 0.653 |
| Sandblasting | 0.527 |
| Scabbling | 0.439 |
| Water jetting | 0.527 |

# 6. BEHAVIOUR OF CONCRETE REPAIRED SLABS

## 6.1. Pull-off test after repair

When repair was 28 days old, pull-off tests were performed in order to evaluate the bond strength between concrete substrate and repair layer. The test conditions were the same as for cohesion test. Surface preparation effect can be again divided in two groups with regards to EN 1504-10: bond strength after hydrodemolition and sandblasting is greater than the threshold minimum values for laboratory performance: 2.0 MPa for structural repair, 1.5 MPa for non structural. The bond strength for polishing and scabbling is close to or below the limit (Table 6).

Table 6 - Pull-off test results after repair

| pull-off strength [MPa] | | | | |
|---|---|---|---|---|
| $f_{ck,\ cyl}$ | C30/37 | C40/50 | C50/60 | Mean |
| Polishing | 1.91 | 2.36 | 0.86 | 1.71 |
| Sandblasting | 2.04 | 2.19 | 2.16 | 2.13 |
| Scabbling | 1.02 | 1.42 | 1.66 | 1.36 |
| Hydro jetting | 2.51 | 2.54 | 2.30 | 2.45 |
| Mean | 1.87 | 2.13 | 1.74 | - |

It can be also concluded from pull-off results that sandblasting and hydrodemolition techniques produce a better surface preparation, taking into consideration the bond strength criteria (Fig.9). Moreover, the class of concrete has no influence on bond strength for sandblasting or hydrodemolition but it could have an effect in case of polishing and scabbling.

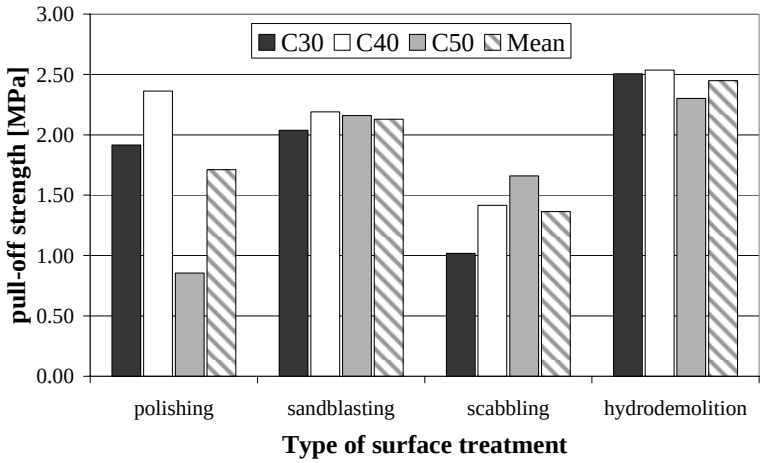



Figure 9 - Pull-off strength for tested repair systems

On the base of a visual assessment, the type of failure was registered for each specimen. In case of slabs treated by polishing, all failures appeared at the interface between concrete substrate and repair mortar. Scabbled surfaces present ruptures near to interfacial zone, due to microcracks. Situation is more unclear for sandblasting and hydrodemolition techniques: in both cases, cohesive A and interface A/B failures were observed (Fig.10).

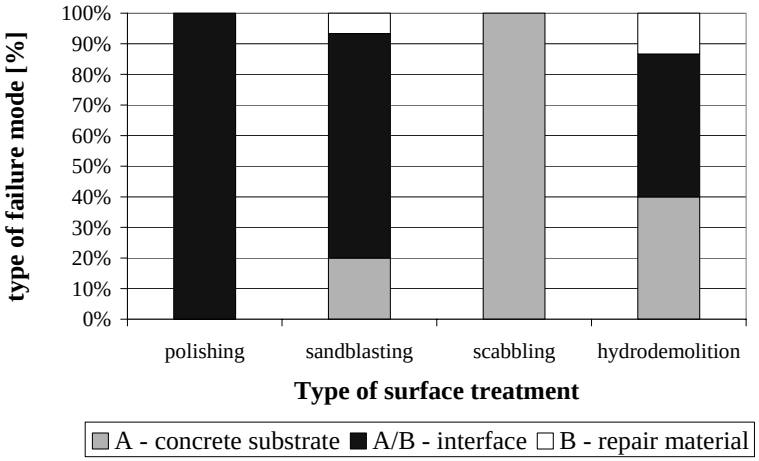



Figure 10 - Types of failure modes after pull-off adhesion test

## 6.2. Schmidt Hammer test (after repair)

The Schmidt Hammer test was performed on repaired slabs (three classes of concrete and four types of surface preparation) - Table 7. These results of rebound number measurements obtained for polished samples before repair were treated as the reference ones.

Table 7 – The mean rebound number for samples (after repair)

| Rebound number | Type of concrete substrate | | | | | | | | | | | |
|---|---|---|---|---|---|---|---|---|---|---|---|---|
| | polishing | | | sandblasting | | | scabbling | | | hydrodemolition | | |
| | C30 | C40 | C50 | C30 | C40 | C50 | C30 | C40 | C50 | C30 | C40 | C50 |
| $R_{after}$ | 34.7 | 35.5 | 35.0 | 36.1 | 34.7 | 35.5 | 34.9 | 34.8 | 33.1 | 34.5 | 34.9 | 33.3 |
| Comparison | | | | | | | | | | | | |
| $R_a/R_b$ | 1.01 | 0.98 | 0.89 | 1.05 | 0.96 | 0.90 | 1.02 | 0.96 | 0.84 | 1.01 | 0.96 | 0.85 |

The results obtained showed that surface treatment influenced the rebound number value for repair systems with concrete substrate of higher strength – the rebound number decreased about 15% in the case of more aggressive treatments like scabbling or hydrodemolition. However this decrease did not correspond to pull-off strength. This indicates that a rebound number method is not suitable for an assessment of bond quality in repair systems.

## 6.3. Impact-echo test

Impact-Echo method is based on mechanical, high energy impact of a steel ball of given diameter used to generate the stress waves that penetrate the concrete. The displacement of the surface of the element is registered by a piezoelectric oscillation converter set next to the impact point. The amplitude vs time is generated and transformed by Fast Fourier Transformation (*FFT*) into the frequency spectrum. Analysis of this spectrum allows for inside discontinuity of concrete structure detection.

The analysis of graphics coming from repaired concrete slabs shows that there is one clear and high peak in area of frequencies from interface (around 75 kHz) in case of polishing (Fig.11). Spectrums of sandblasted samples do not have any peak apart from the bottom one. For scarification, there is no specific peak at the level of interface frequencies but a wide plateau located on depth < 10 mm from the interface – probably an effect of near-to-surface highly cracked area. Finally, for hydrodemolition, there are a lot of medium high peaks

corresponding to the depth from 29 to 50 mm, what is probably due to very rough surface and air voids in this area.

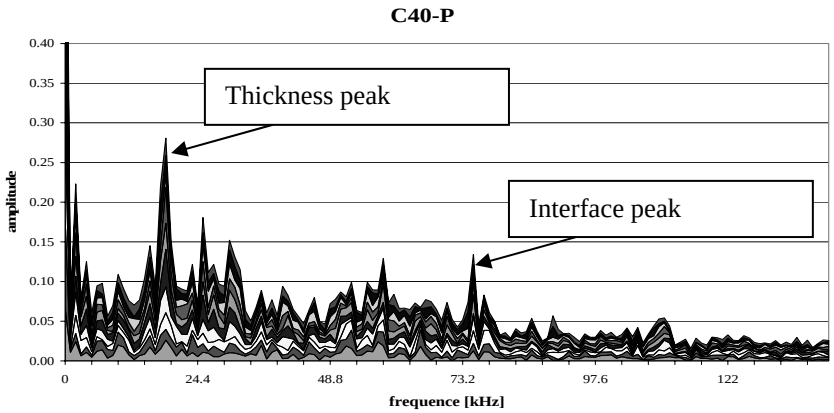



Figure 11 – Impact-echo principle and frequency spectrum for polished slab of C40/45

## 7. CONCLUSIONS

The following conclusions may be reached from the present investigations concerning the concrete substrate evaluation and the adhesion of repair systems:

- polishing, sandblasting, scabbling give surfaces without big peaks and deep holes, while hydrojetting induces a very irregular surface, which is confirmed by the values of $C_F$;
- surface preparation technique influence microcracking observed in superficial zone of concrete (2-cm): scabbling and hydrodemolition induce almost two times higher number of microcracks than sandblasting and polishing and they are more perpendicular to the surface;
- the concrete quality did not have a major influence on the cohesion of the superficial concrete;
- bond strength after hydrodemolition and sandblasting is greater than the threshold minimum values for laboratory performance, while it is close to limit for polishing and scabbling;
- in the case of polishing, all failures during pull-off test appeared at the interface between concrete substrate and repair mortar. Scabbled surfaces present ruptures near to interfacial zone, due to microcracks;
- the class of concrete has no influence on bond strength for sandblasting or hydrodemolition but it could have an effect in case of polishing and scabbling;
- quality of interface had effect on the character of high frequency part (corresponding to interface frequency peak) of frequency spectrum specific for a given type of surface treatment;
- surface treatments influence the rebound number value for repair systems – the rebound number decreased about 15% in the case of more aggressive treatments like scabbling or hydrodemolition for concrete substrate of higher strength. However this decrease did not correspond to pull-off strength.

These conclusions lead to the next consideration: microcracking is really an essential parameter in the evaluation of the quality of concrete substrate before repairing. However, it remains a very difficult property to clearly evaluate, which necessitate long preparation and

laboratory investigations: on-site test like surface permeation should be soon developed in order to help concrete surface assessment.

## 8. REFERENCES

Courard L., Bissonnette B., Essai dérivé de l'essai d'adhérence pour la caractérisation de la cohésion superficielle des supports en béton dans les travaux de réparation : analyse des paramètres d'essai.. *Mater. Struct.*, 37, 342-350 (2004).

Courard, L., Bissonnette, B. and Belair, N. Effect of surface preparation techniques on the cohesion of superficial concrete: comparison between jack-hammering and water-jetting. In: ICCRRR 2005 International Conference on Concrete Repair, Rehabilitation and Retrofitting (Eds. H. Beushausen, F. Dehn and M.G. Alexander), Cape Town, South Africa, 1027-1031 (2005).

Courard, L. and Nélis, M. Surface analysis of mineral substrates for repair works: roughness evaluation by profilometry and surfometry analysis. *Magazine of Concrete Research.* **55**(4), 355-366 (2003).

Courard L., Garbacz, A. and Gorka, M. Concrete surface treatments quantification by means of mechanical profilometry. in: ICPIC, XIth International Congress on Polymers in Concrete (Ed. M. Maultzsch, Federal Institute for Materials Research and Testing), Berlin, Germany (2-4 June 2004), 125-132 (2004).

Czarnecki, L., Garbacz, A., Kostana, K., "The Effect of Concrete Surface Roughness on Adhesion in Industrial Floor Systems", 5th Colloquium Industrial Floors, Esslingen, 2003.

Garbacz, A., Gorka, M. and Courard, L. Relationship between surface characteristics and superficial cohesion of concrete. In: ICCRRR 2005 International Conference on Concrete Repair, Rehabilitation and Retrofitting (Eds. H. Beushausen, F. Dehn and M.G. Alexander), Cape Town, South Africa, 1021-1026 (2005).

Garbacz, A., Courard, L., and Gorka, M. On the effect of concrete surface treatment on adhesion in repair systems. *Magazine of Concrete Research*. **57**(1), 49-60 (2005).

Perez, F., Bissonnette, B. et Courard, L. Outils de caractérisation paramétrique de la rugosité des surfaces en béton : nouveaux développements. In : Journées scientifiques du RF²B, 25-26 août, Sherbrooke, Canada (2003).

Pretorius, J. and Kruger, D. The influence of surface roughness on the bond strength of concrete repairs. In: Xth International Congress on Polymers in Concrete (ICPIC 01, Ed. D. Fowler), Honolulu, Hawaï, p13 (2001).

Perez, F., Courard, L., Bissonnette, B., Garbacz, A. and Gorka, M. Comparison of two different techniques for the evaluation of concrete surface roughness. In: ICCRRR 2005 International Conference on Concrete Repair, Rehabilitation and Retrofitting (Eds. H. Beushausen, F. Dehn and M.G. Alexander), Cape Town, South Africa, 1015-1020 (2005).

Piotrowski, T. Effect of concrete quality on stress wave propagation in repair systems. M.Sc. Thesis at the Warsaw University of Technology (2005).

Silfwerbrand J., Beushausen H., Bonded concrete overlays – bond strength issues, In: ICCRRR 2005 International Conference on Concrete Repair, Rehabilitation and Retrofitting (Eds. H. Beushausen, F. Dehn and M.G. Alexander), Cape Town, South Africa, 53-61 (2005).

Silfwerbrand J. and Paulsson J., Better bonding of bridge deck overlays, Concrete International, 20, 56-61 (1998).

Schwall, D, "Analyse de l'effet des techniques de préparation sur la rugosité des surfaces en béton", Travail de fin d'études en vue de l'obtention du grade d'Ingénieur civil des constructions, 2005 (in French).

## 9. ACKNOWLEDGMENTS

The authors are thankful to Professor L.Czarnecki, Head of the Building Materials Engineering Department at the Warsaw University of Technology for his valuable discussion and remarks. The research project was financially supported by the Government of Poland (KBN) and the Regional Government of Wallonia (DRI), Belgium, through the Scientific Cooperation Project “Etude des mécanismes et caractérisation de l’adhésion au moyen de méthodes destructives et non-destructives” (2005). Part of experiments have been done in the framework of project granted by Polish Scientific Research Committee - grant number KBN 4T07E02727 (2004-2006)

International Symposium Polymers in Concrete
2 - 4 April 2006
Guimarães, Portugal

# Application of percolation theory for explaining of microstructure forming in polymer-cement concretes

Paweł Łukowski[1]

*Warsaw University of Technology, Faculty of Civil Engineering, Warsaw, Poland*

ABSTRACT

Polymer-cement composites (PCC) are quick developing and largely used group of the building materials. The problem of the quantitative definition of continuity threshold of the polymer phase in the composite is one of the problems involved with PCC. The subject of the paper is verification and justification of the continuity threshold of the polymer phase in polymer-cement composites. Analysis of experimental data concerning changes of various PCC properties along with content of polymer, as well as SEM photographs shows that the threshold can be found at the level close to 5% of polymer w/w cement content. Theoretical calculations have been carried out using sterical considerations and percolation theory. The results obtained have confirmed the possibility of the threshold value being equal to 6% of polymer. Good agreement between theoretical and experimental values is confirmation of the models used. Performed computer simulations point also to the geometrical aspects as more significant for polymer film creation than the chemical nature of the polymer. In spite of the numerous limitations, the proposed course of consideration is promising way to justify the continuity threshold of the polymer phase in the polymer-cement composites. Application of the percolation theory seems to be effective method for analysis of the microstructure of the building composites.

## 1. INTRODUCTION

Polymer modifiers for cement composites can be divided in two quantitative categories – admixtures and additions (Łukowski, 2003). Amount of admixture is too small for creation the separate, continuous phase in the hardening concrete mix. Polymer additions are able to form additional continuous structure. The polymer and hydration products form two interpenetrating and co-existing matrices (Beeldens, 2002 and Su, 1995). This is called a polymer-cement binder – Portland cement and polymer are equivalent co-binders.

Polymer-cement composites (PCC) are the materials containing the polymer as additions. They are quick developing group of the building materials, used mainly for repair and protection of the concrete structures, for manufacturing of pre-cast elements, road pavements, including those of bridges as well as for making industrial floors (Czarnecki, 2002 and Kardon, 1997). In spite of the high interest of the researchers and engineers, many

[1] Ph.D.

problems involved with PCC are not resolved yet. The problem of the quantitative definition of continuity threshold of the polymer phase in the composite is one of them. Most often, five per cent of the polymer in relation to the cement mass is accepted (EN 934-2, 2001 and Czarnecki, 2004). However, there is no theoretical justification of that value. The value has been verified in the paper on the basis of the analysis of the experimental data. The justification, using stereological considerations and percolation theory, has also been proposed.

## 2. VERIFICATION OF THE POLYMER PHASE CONTINUITY THRESHOLD ON THE BASIS OF EXPERIMENTAL DATA

The properties of the composite involved with its impermeability are particularly useful for the analysis. Gas diffusion through the hardened material or capillary suction of water are determined by the pore structure of the composite (Ohama, 1991). Volume of the capillary pores in PCC are usually less than in non-modified material. The pores are also less accessible for water due to their blocking by the polymer film and hydrophobicity. Therefore, the substitution of the part of the Portland cement by the polymer phase should result in limitation of the above mentioned phenomena. The biggest quantitative change can be expected, when the amount of the polymer phase is sufficient to form the continuous film. This is observed, in fact, when analysing the test results of the barrier properties of PCC (Fig. 1- 4).

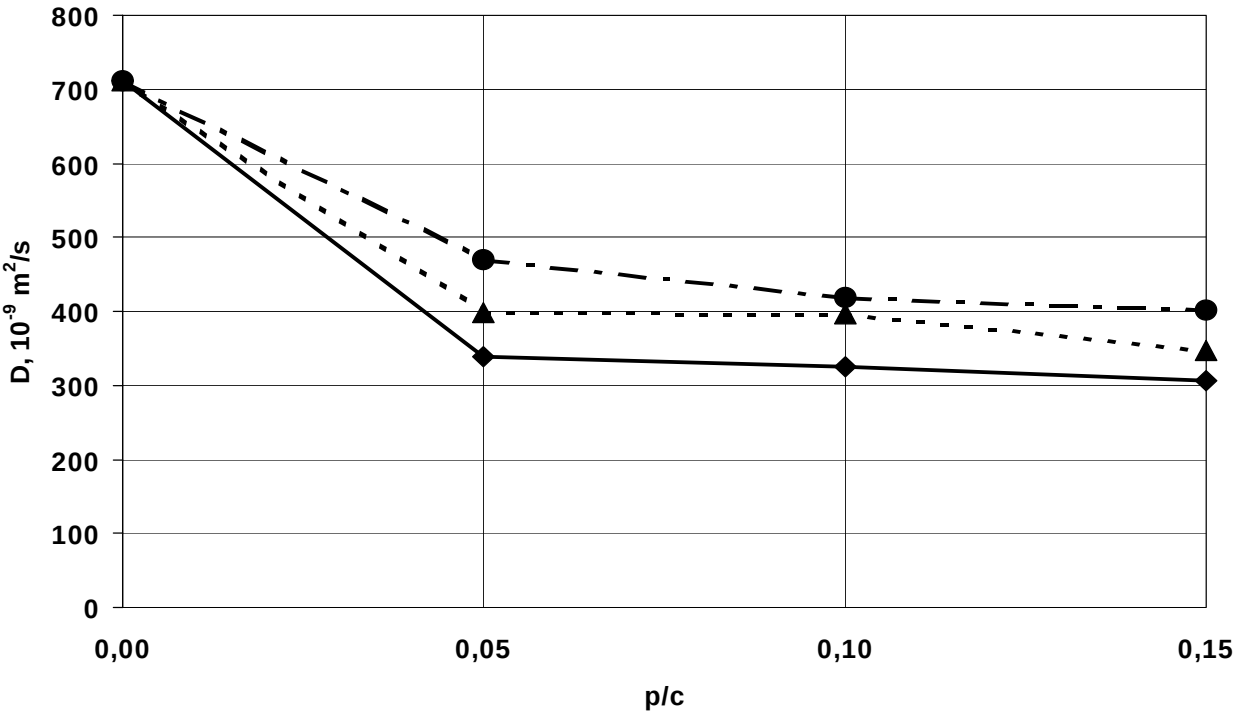



Figure 1 – Water vapour diffusion coefficients for polymer-cement composites; modifiers: acrylic co-polymers with various proportions of the components (Justnes, 1998)

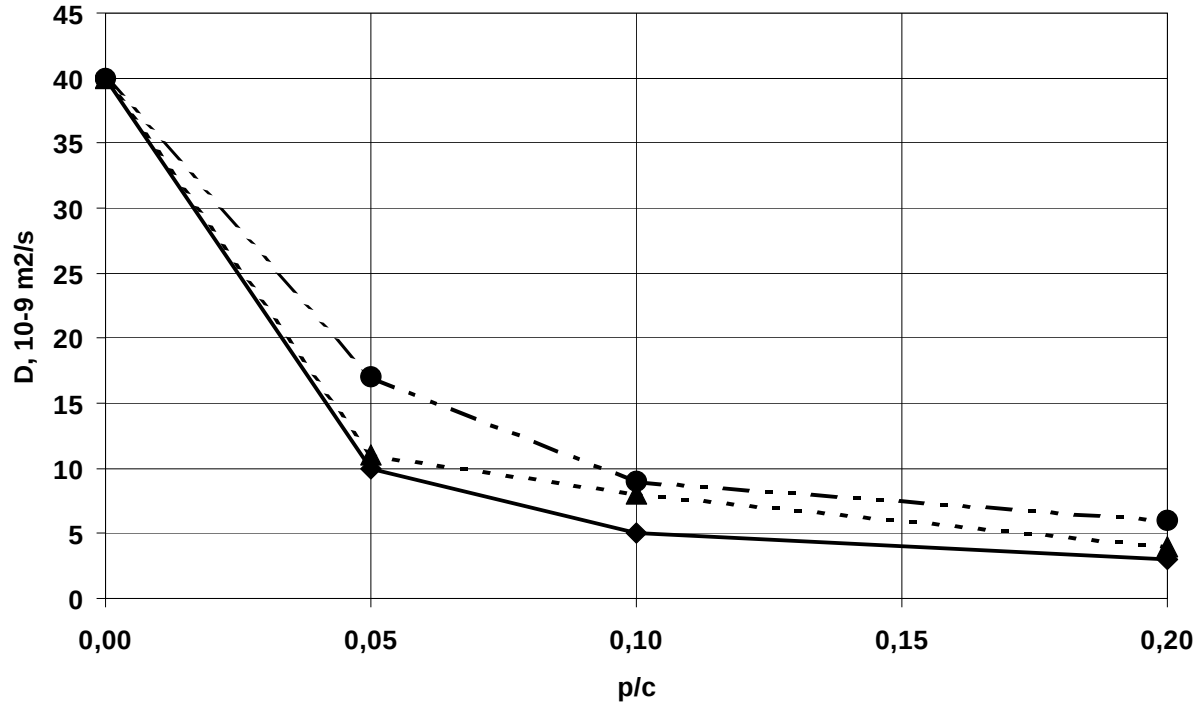



Figure 2 – Oxygen diffusion coefficients for polymer-cement composites; modifiers: styrene-butadiene rubber (- - -), polyacrylates dispersion (- — -), ethylene-vinyl acetate co-polymer (——) (investigated by the author)

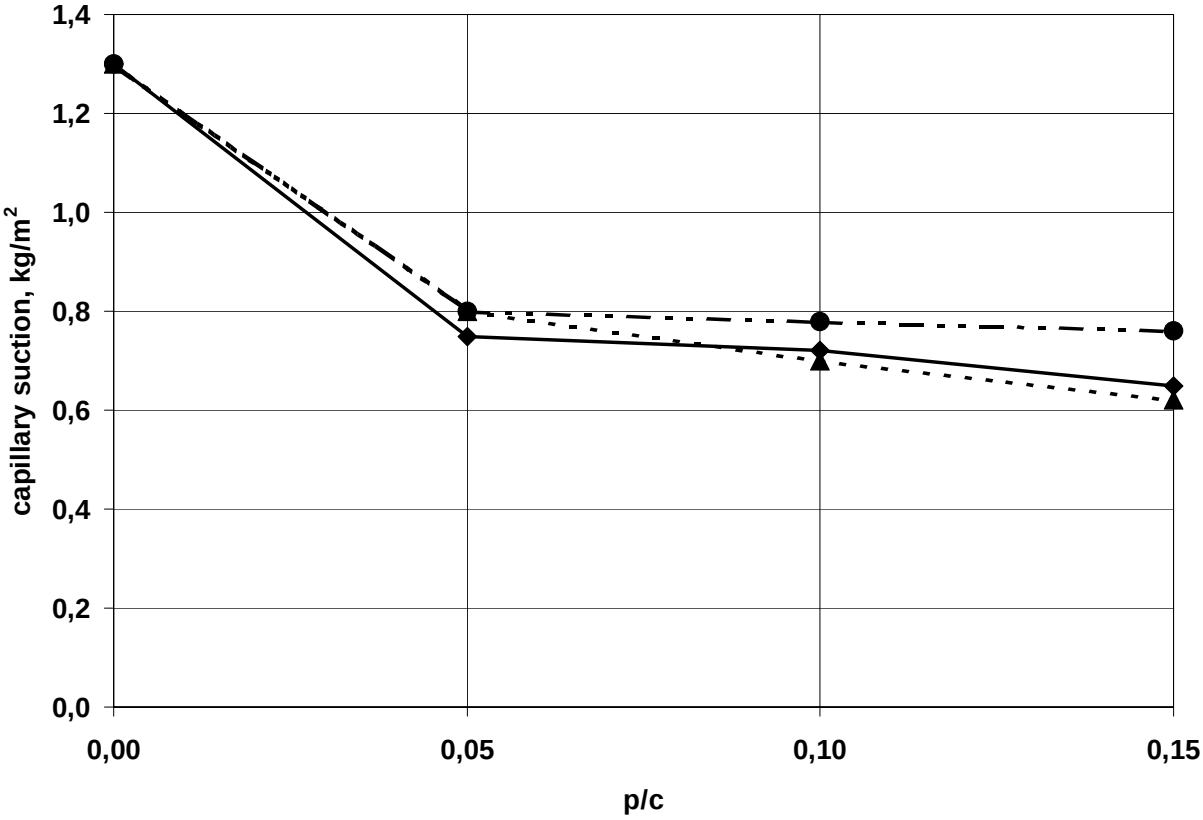



Figure 3 – Capillary suction of water by PCC; modifiers: acrylic co-polymers with various proportions of the components (Justnes, 1998)

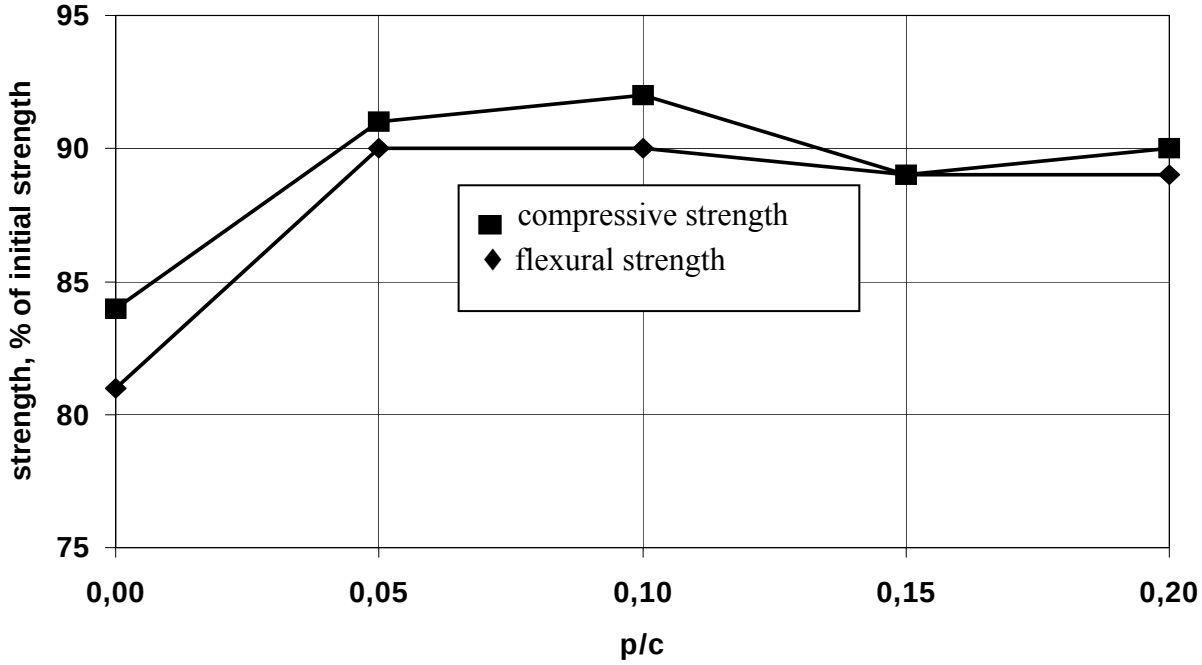
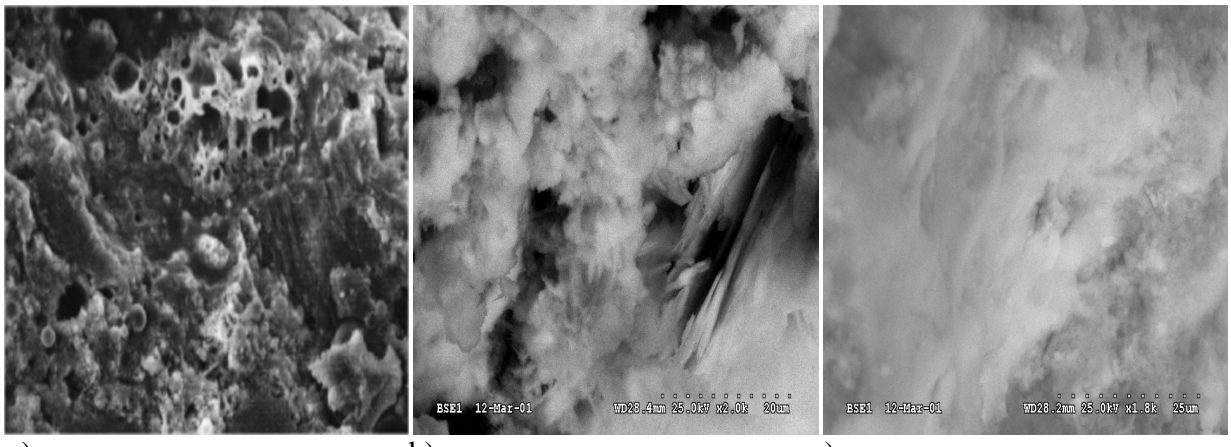



Figure 4 – Freeze-thaw resistance of epoxy-cement composites: flexural and compressive strength after 50 cycles of freezing/thawing (investigated by the author)

Significant diminishing of the diffusion coefficients and capillary suction as well as improvement of freeze-thaw resistance is observed for the amount of the polymer modifier equal to about 5% in relation to the cement mass. The changes are only slight for the bigger amounts of polymer. This indicates that the limiting amount, for which the composite microstructure undergoes the beneficial change, could be near to 5%. Similar conclusions can be drawn out from the microscopic observations (Fig. 5).




a) b) c)

Figure 5 – Microstructure of acrylic-cement composite;
polymer amount: a) 0%, b) 5%, c) 10%; SEM 2000x (photos by the author)

## 3. THEORETICAL JUSTIFICATION OF THE CONTINUITY THRESHOLD

Theoretical estimation of minimum polymer amount, necessary for forming continuous phase in the polymer-cement paste, can be carried out using stereological considerations. According to (Cherkinsky, 1984), continuous polymer phase can be defined as the structure, the thickness of which exceeds four times the size of the polymer particle. Using this definition, it is possible to estimate the volume of the polymer necessary for complete covering of the surface of the hydrated cement grains. Assuming the least lateral size of the polymer particle as 0.15 nm (Cherkinsky, 1984 and Laczynski, 1982), the thickness of the polymer layer adsorbed on the hydrated cement surface can be estimate as approximately $4 \times 0.15 = 0.6$ nm. The average specific surface of hydrated cement is 100000 $m^2/kg$, Neville (1995) and average density of polymer is 1000 $kg/m^3$. Thus, 100000 $[m^2] \cdot 0{,}6 \cdot 10^{-9}$ $[m] \cdot 1000$ $[kg/m^3] = 0{,}06$ kg of polymer is needed for covering of 1 kg of hydrated cement (Fig. 6). Therefore, the minimum amount of polymer is equal to about 6%; the value is in good agreement to the experimental data.

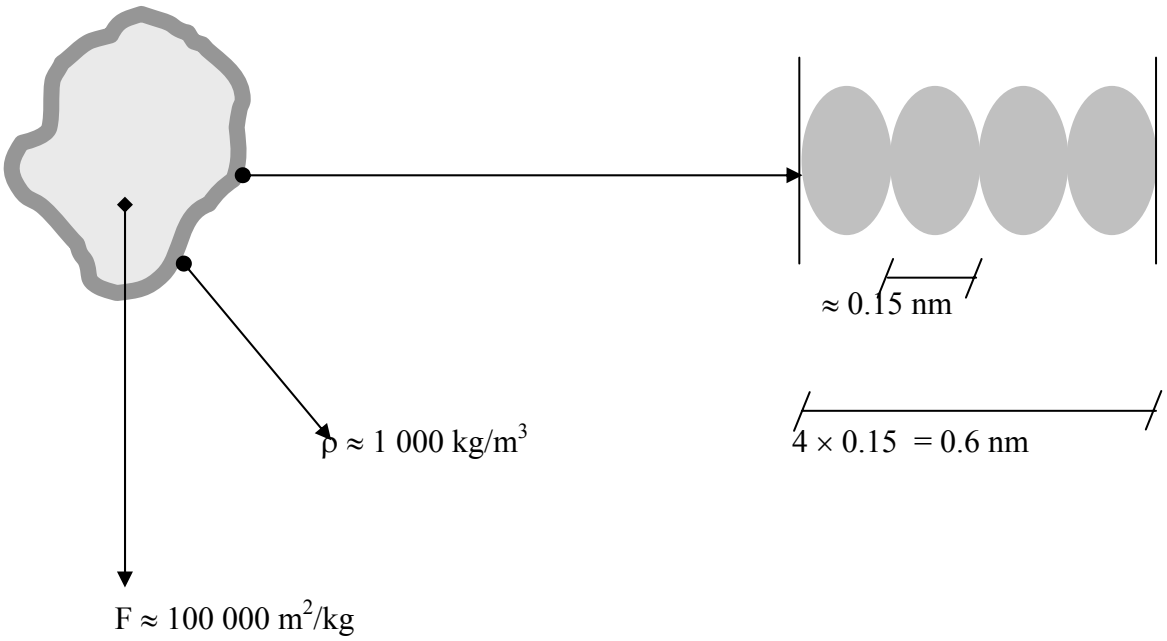



Figure 6 – Assumptions for stereological estimation of the continuity threshold: hydrated cement grain covered by the continuous polymer film and structure of the continuous polymer layer

The above estimation is not free from weak points: the values are averaging, some of them are not strongly documented, and accepted definition of "continuous polymer phase" can be the subject of discussion. In spite of that, presented considerations can be treated as interesting proposal of formulation of the theoretical background for quantitative description of polymer film forming in polymer-cement binder.

Another promising approach is using the percolation theory (Czarnecki, 1998). Percolation change generally means the transformation of a discontinuous structure into continuous one (Sahimi, 1994) (Fig. 7).

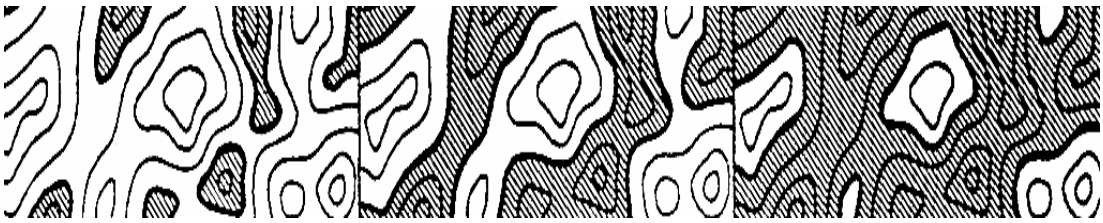


Figure 7 – Schematic presentation of percolation transformation; the shaded areas means the elements forming continuous connection , based on (Neubauer, 2000)

The basic assumption of the percolation theory is existing of the *percolation threshold* or continuity threshold. In general, it is any quantitative condition that should be met for enabling the percolation transformation. Polymer-cement paste can be treated as the system, in which the percolation transformation can be observed when the polymer amount increases. In that case the continuity threshold can be defined as minimum amount of polymer necessary for forming the continuous structure. The value of the continuity threshold is possible to estimate using suitable computer simulations and calculations.

The microstructure of the polymer-cement binder can be analysed using hcss model (hard core/soft shell) (Neubauer, 2000). The hydrated cement grains are represented by the cores and the polymer covers, adsorbed on the cement grains, are represented by the shells. When the core size is equal to 0, the shell represents the non-adsorbed polymer particle. The cores may not overlap, while the shells may (Fig. 8). The simulations for to the estimation of the continuity threshold are possible to carried out using the computer programme (Bentz, 1993), developed by National Institute of Standards and Technology (NIST), Gaithersburg, USA, which is one of the leading research centres involved with application of the percolation theory in the sector of building materials engineering (Garboczi, 1999).

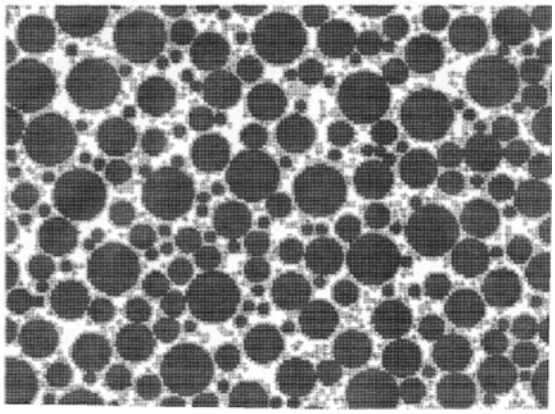


Figure 8 – Model of the microstructure of polymer-cement paste, obtained by the author when modelling the percolation transformation using Pershell computer programme developed by NIST; hcss model

The result of performed simulations is the determination of minimum amount of the polymer necessary for the percolation transformation (Fig. 9). The simulation is based on idealised model of the microstructure; for example, quantitative conclusions are possible to drawn when general homogeneity of the structure is assumed.

The minimum amount of the polymer is the lesser, the bigger the cement grain's diameter; this is due to the fact that the bigger grains have the lesser specific area. The amount of the polymer approaches asymptotically a limit of 18% by volume of the cement.

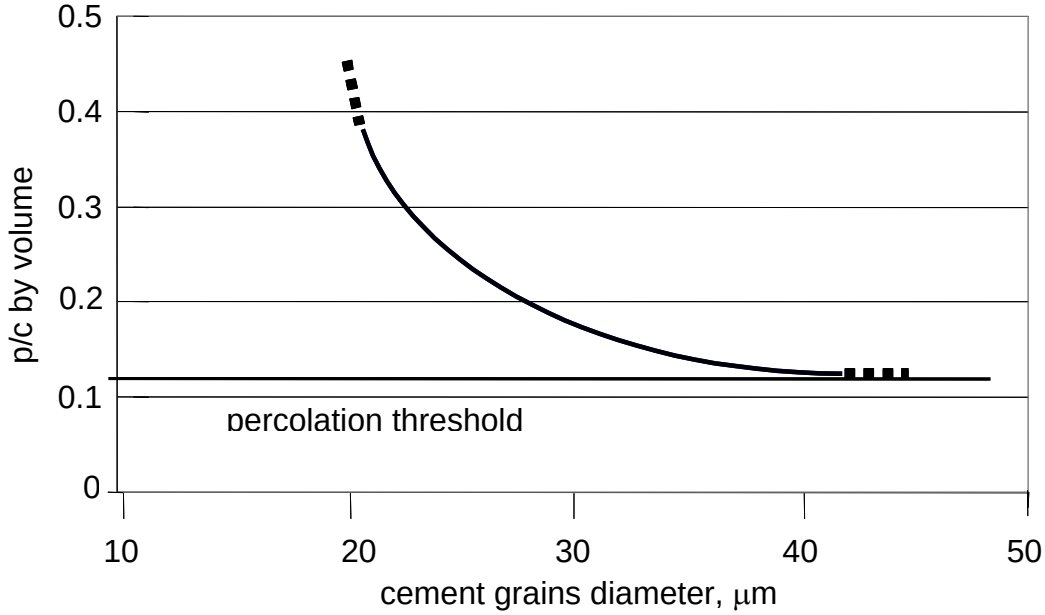



Figure 9 – Minimum amount of polymer making possible forming the continuous structure in the polymer-cement paste vs. maximum size of the cement grains; values determined using simulation of the percolation transformation (see Fig. 8).

Assuming the densities of the hydrated cement and polymer as 3000 kg/m$^3$ and 1000 kg/m$^3$, respectively, it is possible to estimate the minimum amount of the polymer in relation to the cement as equal to 6% by mass. This result is in very good agreement to both experimental and stereological estimations.

## 4. CONCLUSIONS

A way to verification and justification of the value of the continuity threshold of the polymer phase in the polymer-cement composites has been proposed.

Analysis of the experimental data, including the observations of the PCC microstructure, allows to expect the continuity threshold at the level of about 5% of the polymer in relation to the cement mass. Theoretical considerations and computer simulations, carried out using the stereological approach and elements of the percolation theory, indicate the possibility of the threshold value being equal to about 6%. Good conformity of those estimations can be a confirmation that the real value of the threshold is near to the obtained values.

The presented considerations are still tentative. There are a number of simplifications influencing the results. For example, the results are dependent on geometrical aspects. The influence of the chemical nature of the polymer can be only represented by the size of the polymer particle. This results from the assumption that above minimum film-forming temperature (MFFT) the polymer particles coalesce completely in every case. A rational method to introduce the chemical aspects in more complex way into the considerations should be found. Also, the used models of the PCC microstructure are simplified. And, last but not least, the results of estimations should be less sensitive for the initial assumptions.

In spite of the above listed limitations, the proposed course of consideration is promising way to justify the continuity threshold of the polymer phase in the polymer-cement composites. Application of the percolation theory seems to be effective method for analysis of the microstructure of the building composites.

## 5. ACKNOWLEDGEMENTS

Author wish to thank to Professor Lech Czarnecki Ph.D., D.Sc. for his valuable remarks and discussion. The paper has been granted by Warsaw University of Technology.

## 6. REFERENCES

Beeldens A., *Influence of polymer modification on the behaviour of concrete under severe conditions*, Ph.D. Thesis, Katholieke Universiteit Leuven (2002).

Bentz D.P., Garboczi E.J., Coverdale R.T., Computational materials science of cement-based mateials: an education module, *NIST Technical Note 1405*, United States Department of Commerce, National Institute of Standards and Technology, Gaithersburg MD (1993).

Cherkinsky J., *Polymer-cement concrete*, Stroyisdat, Moscow (1984) [in Russian].

Czarnecki L., Sandrolini F., Paradigms in polymers in concrete. *Proc. of 9th International Congress on Polymers in Concrete ICPIC '98*, Bologna, 21-33 (1998).

Czarnecki L., *Repair and protection of concrete structures*, Polski Cement, Cracov (2002) [in Polish].

Czarnecki L., Łukowski P., Influence of polymer admixtures and additives on durability of concrete, *Cement Wapno Beton*, **1**, 38-47 (2004).

EN 934-2:2001: Admixtures for concrete, mortar and grout – Part 2: Concrete admixtures – Definitions, requirements, conformity, marking and labelling.

Garboczi E.J., Bentz D.P., Percolation Aspects of Cement Paste and Concrete: Properties and Durability, High-Performance Concrete: Research to Practice, American Concrete Institute Spring Convention, *ACI Special Publication SP-189*, Chicago, 147-164 (1999).

Justnes H., Reynaers T., Van Zundert W., Moisture transport in polymer cement mortars based on latices and redispersible polymer powders, *Proc. of 9th Internationa. Congress on Polymers in Concrete ICPIC '98*, Bologna, 633-645 (1998).

Kardon J.B., Polymer-modified concrete: review, *Journal of Materials in Civil Engineering*, **5**, 85-92 (1997).

Łączyński B., *Polymers – types and properties*, Wydawnictwa Naukowo-Techniczne, Warsaw (1982) [in Polish].

Łukowski P., *Admixtures to concrete and mortar*, Polski Cement, Cracov (2003) [in Polish].

Neville A.M., *Properties of concrete*, Fourth Edition, Pearson Education Limited, London (1995).

Neubauer C.M., Jennings H.M., The use of digital images to determine deformation throughout a microstructure, *Journal of Materials Science*, **35**, 5751-5765 (2000).

Ohama Y., Demura K., Kobayashi K., Satoh Y., Morikawa M., Pore size distribution and oxygen diffusion resistance of polymer-modified mortars, *Cement and Concrete Research*, **2-3**, 309-315 (1991).

Sahimi M., *Applications of percolation theory*, Taylor & Francis, London – Bristol (1994).

Su Z., *Microstructure of polymer-cement concrete*, Delft University Press, Delft (1995).

International Symposium Polymers in Concrete
2 - 4 April 2006
Guimarães, Portugal

# Effect of Plastic Reject and Natural Sand Additions on the Microstructure and Mechanical Behavior of Cellular Concrete

Itamar M. de Freitas[1], Kátia A. Allende[1], Fathi A. Darwish[2]

*Universidade Federal Fluminense, Programa de Pós-Graduação em Engenharia Civil, Rua Passos da Pátria, 156 Bloco D sala 360, Niterói, R. J., Brasil*

## ABSTRACT

The present work refers to a study of cellular concrete produced by incorporating an organic additive, which promotes foam formation. The main purpose of the study was to optimize the concrete volume for a given weight of cement without having to modify the foam/cement ratio. The foam was generated by mechanically mixing the additive with water and a reference concrete mix was obtained by adding the cement to the foam. Other mixes were also produced by adding natural sand as heavyweight aggregate and plastic reject as lightweight aggregate. Significant variation observed in both the compressive strength and specific gravity of the cured concrete was associated with the quantity of aggregates added to the reference mix. Scanning electron microscopy of the fracture surface has indicated a considerable variation in the size of individual cell voids. Energy dispersion spectroscopy analysis has shown that the inner surface of cell voids is rich in C, which is consistent with the use of organic additive as frother. Using mercury porosimetry technique, one was able to determine the volume fraction as well as the size distribution of interconnected voids contained in the concrete structure. The volume fraction of closed pores was then estimated from knowledge of the volume fraction of interconnected voids and real density of the concrete, calculated from helium picnometry measurements. Finally, the compressive strength and elastic modulus are presented and discussed in light of the density and volume fraction of pores contained in the concrete structure.

## 1. INTRODUCTION

Cellular concrete is a lightweight concrete containing a large amount of pores, 0.01 to 1 mm in diameter, uniformly distributed throughout the cement mortar. Such a structure is obtained by incorporating stable air bubbles into the cement paste, which can be achieved by adding cement to preformed stable foam before eventually incorporating aggregates such as sand to the mixture. The cellular structure thus obtained presents mechanical strength that is compatible with its use as lightweight concrete for previously molded masonry block and as

[1] Research Assistant
[2] Professor

filling material for leveling slab surfaces before applying impermeable coatings. Whereas its big advantage refers to its lightweight, cellular concrete also possesses a number of attractive characteristics such as its excellent freeze-thaw resistance as well as its good thermal and acoustic insulation.

Cellular concrete had its first register as a patent by Hoffmann in 1889. Foam production at the time was achieved by the chemical reaction between hydrochloric acid and sodium bicarbonate. In 1917, in Holland, a second patent was registered and this one was based on the use of organic ferments for the purpose of liberating gases, which are necessary to form the foam. In 1923, Bayer and Erikson managed to produce spongy cellular concrete using a mixture of vegetable glues, gelatin, formaldehydes and resin soaps (without vapor cure). Only in 1934 did cellular concrete acquire worldwide importance with the advent of Siporex, a product based on a patent by Eklung, where aeration of the concrete mixture was achieved by metallic chemical agent (with vapor cure).

The study of cellular concrete was initiated back in 1940, culminating, as referenced by Legatsky, L. A. (Legastky (1994)), in the publication by Legatsky, L. M. (Legatsky (1978)) of a chapter on the subject in ASTM STP 169 B. Other pertinent publications on cellular concrete were also made through the American Concrete Institute (for example ACI (1992)). More recently, Maire and co-workers (2003) used X-ray tomography to characterize cellular materials, focusing on the relation between their structure and their global mechanical properties. Tikalsky (2004), on the other hand, studied cellular concrete, focusing on how to improve its durability by increasing its freezing-thaw resistance.

The use of cellular concrete in Brazil started in the early seventies and the study of its properties was initiated soon after. In 1992, Teixeira Filho (1992) experimented with the addition of sand and this resulted in the improvement of the mechanical properties, especially compressive strength, consistent with the increase in the concrete density. More recently, Freitas, Allende and Darwish (2004) analyzed the influence of two different frothers on the volume as well as the mechanical properties of the produced concrete. One of the main purposes of their study also referred to the optimization of the volume produced for a given weight of cement. This involved the incorporation of polymeric reject as a lightweight aggregate and sand as a fine heavyweight aggregate.

The present work was initiated in an effort to determine the volume fraction of voids within the structure of cellular concrete produced from different concrete mixtures. These mixtures were prepared using organic frother, lightweight aggregate (plastic reject) and heavyweight fine aggregate (sand), in addition to cement. Optical and scanning electron microscopy techniques were used to study the structure of the cured concrete, and the volume fraction of voids contained in the concrete specimens was calculated from porosimetry and picnometry measurements. From the results obtained, one was able to estimate the percentages of interconnected and closed pores. Mechanical properties, specifically compressive strength, $f_c$, and modulus of elasticity, E, were determined and then correlated with pertinent aspects of the voids contained in the concrete structure.

## 2. MATERIALS AND EXPERIMENTAL PROCEDURE

The different concrete mixes elaborated in the present study were based on the weight of cement used. This was taken as 25 and 50 kg, with a water cement ratio of 0.7 and a quantity of the organic frother (Espumogen N) amounting to 1.7% of water volume. These two mixtures constituted the control mixes labeled N1 and N1G corresponding respectively to the 25 and 50 kg weight of cement. Other mixes were prepared by adding lightweight and heavyweight aggregates to the control mixes N1 and N1G. Plastic reject was used as

lightweight aggregate and it amounted to 60% of the weight of cement. On the other hand, sand was added as heavyweight aggregate in the proportions of 40, 80 and 120% of the weight of cement, thus resulting in six different mixes denominated, respectively, PN64, PN74 and PN84 (corresponding to cement weight of 25 kg), and PN64G, PN74G and PN84G (corresponding to cement weight of 50 kg). Two other mixes were also prepared by incorporating plastic reject and sand in proportions of 75 and 80% respectively of the weight of cement. These two mixes were denominated PN75 and PN75G corresponding respectively to cement weight of 25 and 50 kg.

## 2.1. Materials

The cement used was Portland type denominated CP II-E, produced with blast furnace slag and having a minimum compressive strength of 40 MPa after 28 day cure period.

The plastic reject used as lightweight aggregate consists of a mixture of thermofix and thermoplastic materials which are inert with respect to the hydration reactions of the cement paste. It was supplied by a pharmaceutical industry and had the dimensions of its individual particles limited to a maximum of 6.3 mm. The individual plastic particles, which had a density of 1.02 g/cm$^3$, are shown in Figure 1.

The sand used had an apparent density of 1240 kg/m$^3$ and was sieved, before being added to the cement-foam mix, in order to limit the maximum size of sand particles to about 1.18 mm.



Figure 1 – General aspect of the particulate plastic reject

## 2.2. Experimental procedure

A systematic control of the production process was maintained in an effort to insure maximum reproducibility of the concrete properties. More specifically, the time spent in mixing the organic agent with the water was closely monitored and kept at five minutes. Cement was then gradually added to and thoroughly mixed with the preformed foam over a period of about 5 minutes. Both mechanical and manual mixing were used so as to insure uniform distribution of air bubbles and to avoid cement sedimentation. Further, the order of adding the aggregates as well as the position of the mechanical agitator within the concrete mix were also controlled. Sand was added first and then followed by the plastic reject, with the helix agitator always in movement. The total time adopted for mixing the aggregates with the cement-foam slurry was maintained at 5 minutes.

Cylindrical specimens, 150 mm in diameter and 300 mm in height, were molded and were left after removal from the mold to cure for 56 days in water. At this point it is important to mention that the high fluidity of the concrete mix facilitated considerably the molding process as well as self densification of the specimens in the mold.

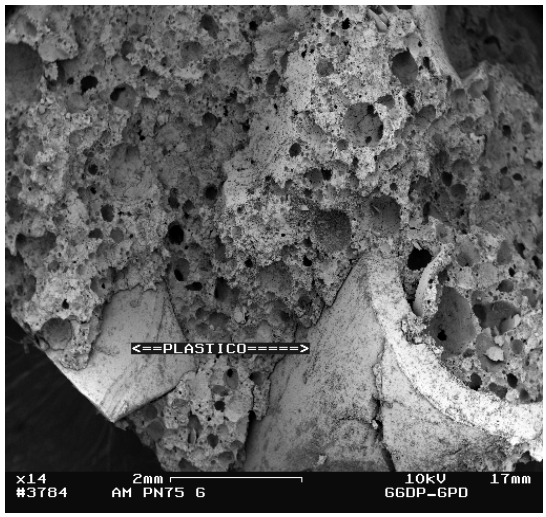
Tests for the characterization of mechanical properties of the cured concrete specimens, namely compressive strength, $f_c$, and modulus of elasticity, E, were carried out following recommendations of the Brazilian Association for Test Standards (ABNT – NBR 5739 (1994), ABNT – NBR 8522 (1984)).

Macroscopic aspects of the structure of cellular concrete produced from PN75G mix are presented in Figure 2, where one can observe the distribution of polymeric material (plastic reject) used as lightweight aggregate in the concrete mixture.



Real size photograph

(a)




(b)

Figure 2 – Macroscopic aspects of a PN75G specimen, showing the presence of particles of plastic reject; (a) optical photograph and (b) SEM micrograph of fracture surface

## 3. RESULTS AND DISCUSSION

### 3.1. Mechanical tests

The values of the compressive strength, $f_c$, secant modulus of elasticity, E, and density, ρ, are listed in Table 1, for the individual concretes produced from the mixes in question. The values of ρ in this table refer to the density as determined, in accordance with ABNT- NBR 5739 (1994), for specimens that had their surface dried in air after the cure period. The variation of $f_c$ with ρ is presented in Figure 3, where an exponential increase in $f_c$ with ρ could be detected.

Table 1 – Values of $f_c$, E and ρ for the concrete mixtures in question

| Cement weight, (kg) | Mixes | $f_c$ (MPa) | E (GPa) | ρ (kg/m$^3$) |
|---|---|---|---|---|
| 50 | N1 G | 1.78 | * | 1066 |
| | PN64 G | 2.03 | 1.47 | 1155 |
| | PN74 G | 2.73 | 2.36 | 1251 |
| | PN84 G | 3.67 | 3.07 | 1280 |
| | PN75 G | 3.47 | 2.42 | 1244 |
| 25 | N1 | 1.71 | 1.29 | 1022 |
| | PN64 | 2.05 | 1,11 | 1126 |
| | PN74 | 2.22 | 1.79 | 1196 |
| | PN84 | 3.64 | 2.99 | 1294 |
| | PN75 | 2.16 | 1.35 | 1183 |

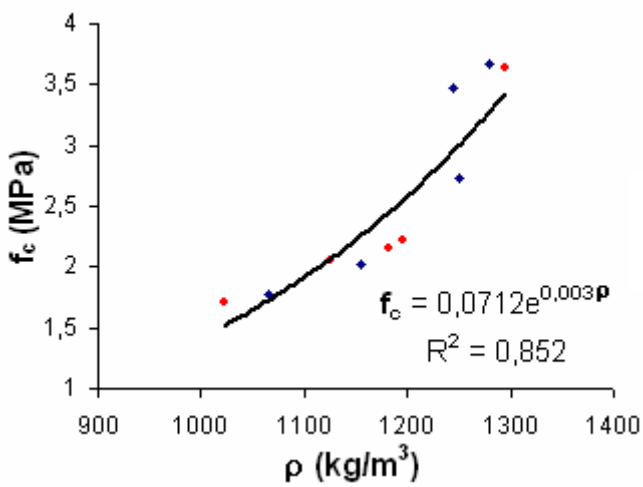
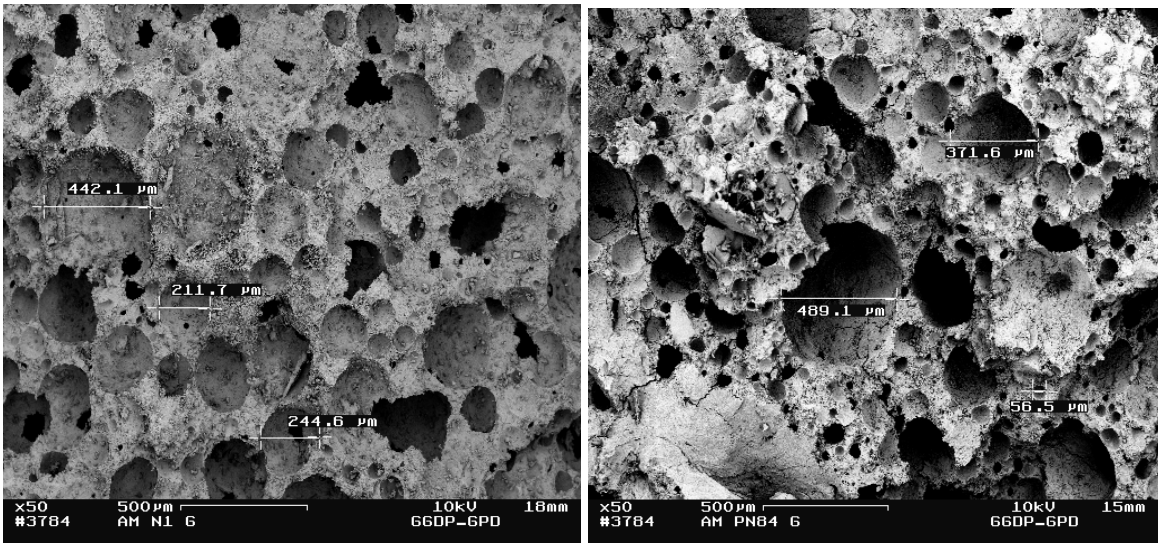



Figure 3 – Variation of $f_c$ with ρ for the different concrete mixes

## 3.2. Structural Analysis

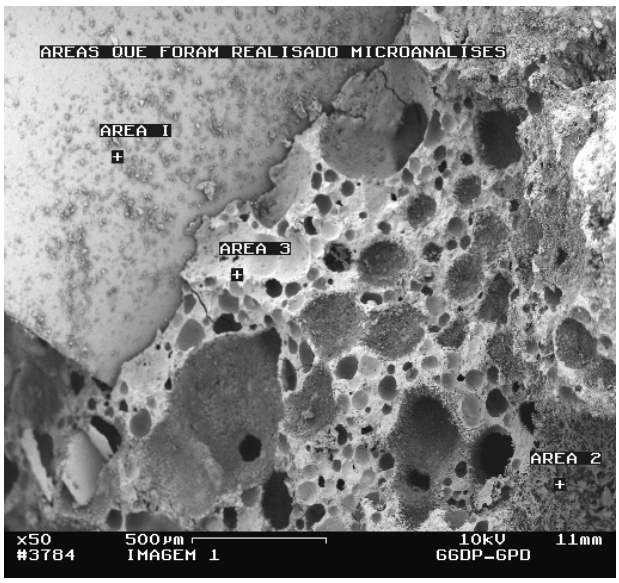
Examples of scanning electron microscopy (SEM) images of gold-coated concrete surfaces are presented in Figure 4, where one can observe the presence of macroscale voids characterizing the structure of cellular concrete. In addition, micro scale voids may be seen in cell walls.



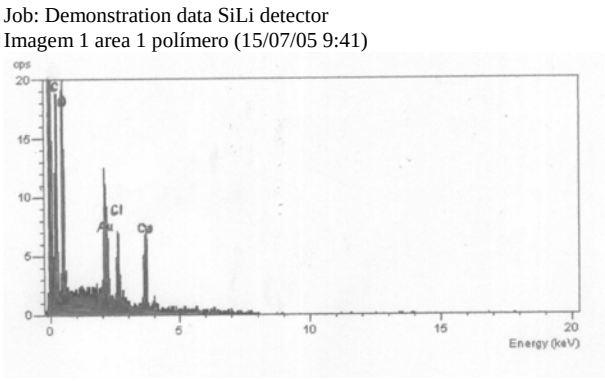

(a) (b)

Figure 4 – SEM macrographs showing the variation in the size of cell voids in (a) N1G concrete and (b) PN84G concrete

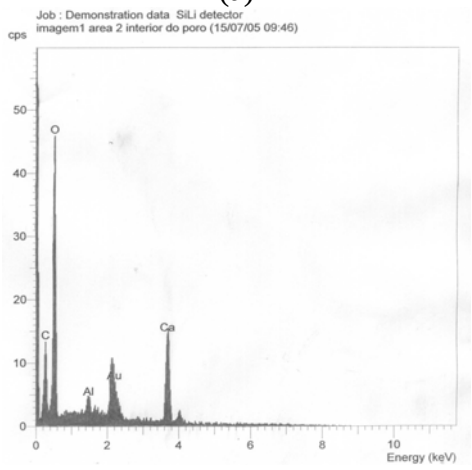
Energy Dispersion Spectroscopy (EDS) analyses were carried out in order to determine the chemical composition of both the cell walls and the plastic reject used as lightweight aggregate. The spectra obtained are shown in Figure 5, where it is verified that the plastic material is composed mainly of C, O and Cl. As to the cell walls, these are composed of Al, Ca, Si, O and C. The spectrum obtained from the inner surface of the voids did not show the presence of Si, but indicated higher carbon content in comparison with that encountered in the cell walls.



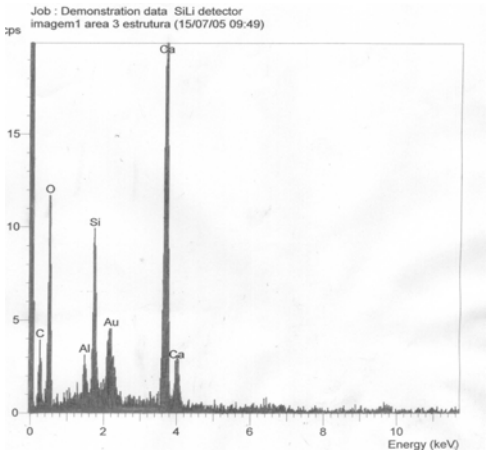

(a)




(b)




(c)




(d)

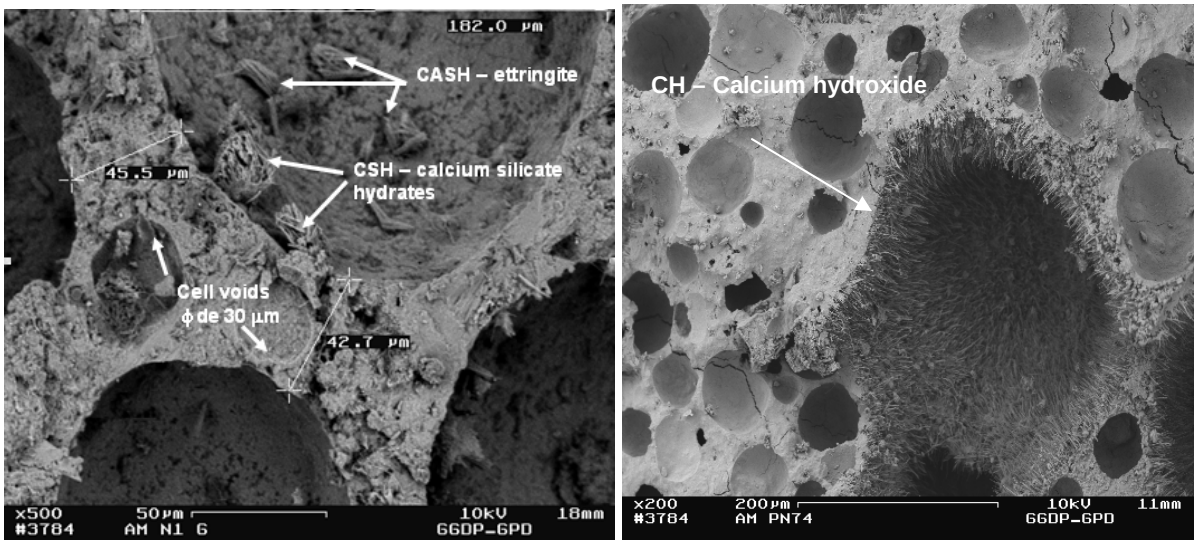
Figure 5 – (a) SEM image of the fracture surface of PN84 concrete, (b) EDS spectrum from plastic reject (area1), (c) EDS spectrum from void surface (area2) and (d) EDS spectrum from cell wall (area3)

Figure 6a represents a SEM micrograph of a N1G cellular concrete specimen, where one can observe the cell walls surrounding a 30 μm size void. One can also verify the presence in these walls of compounds such as hydrated calcium silicate and ettringite. Calcium hydroxide crystals were found on the surface of cell voids of a PN74 concrete specimen (Figure 6b). X-ray diffraction analysis of a PN75G concrete specimen has indicated that the cell walls are essentially composed of $CaCO_3$ (calcite), $Ca(OH)_2$ (calcium hydroxide), $SiO_2$ (quartz) and $Ca_6Al_2(SO_4)_3(OH)_{12}.26H_2O$ (ettringite).

### 3.3. Porosimetry and picnometry results

The volume fraction of interconnected voids was determined using mercury porosimetry technique. This was achieved by determining the volume of interconnected voids contained in small size specimens representative of the concretes considered in this study. Under low pressure, only large pores are filled with mercury and as the pressure gradually increases, the size of voids penetrated by the mercury decreases. In the pressure range from 0.0069 to 0.09 MPa., the corresponding pore diameter varies from 215.54 to 16.58 μm. At

higher pressures, in the range from 0.097 to 207 MPa, the size of voids penetrated by the mercury drops down to the range between 1.85 and 0.0072 μm. Based on this behavior, it was possible to determine the volume of interconnected voids $V_i$ as well as their size distribution. The histogram shown in Figure 8 refers to the void size distribution as obtained for a PN75G concrete. One can observe from this figure that the void size distribution is bimodal, with the first mode corresponding to void diameters between 3.5 and 215 μm, that is essentially in the macroscopic range. The other mode, on the other hand, comprises void diameters between 0.957 and 0.0072 μm. These fine voids pertain mostly to the cell walls and hence are discriminated as skeletal voids. It is to be mentioned that the bimodal pore size distribution was encountered in all of the concretes considered in this work.




(a) (b)

Figure 6 – SEM micrographs indicating compounds present in cell walls; (a) N1G concrete specimen and (b) PN74 specimen

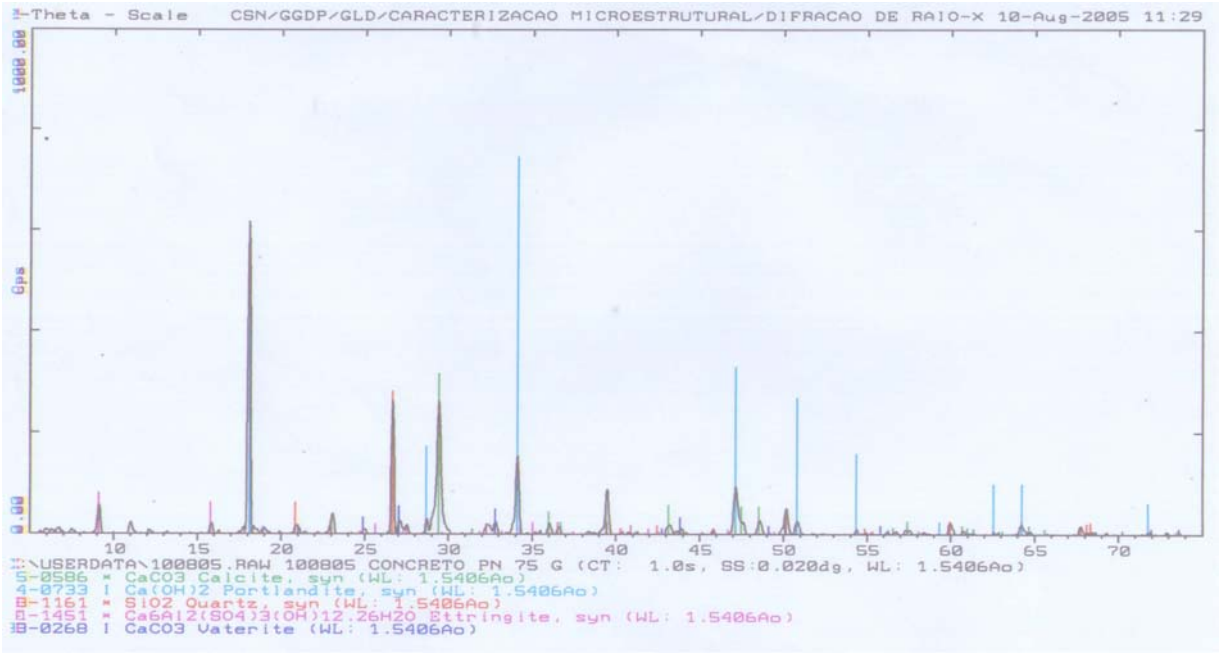



Figure 7 – X-Ray diffraction pattern indicating the presence of various phases in a PN75G concrete specimen

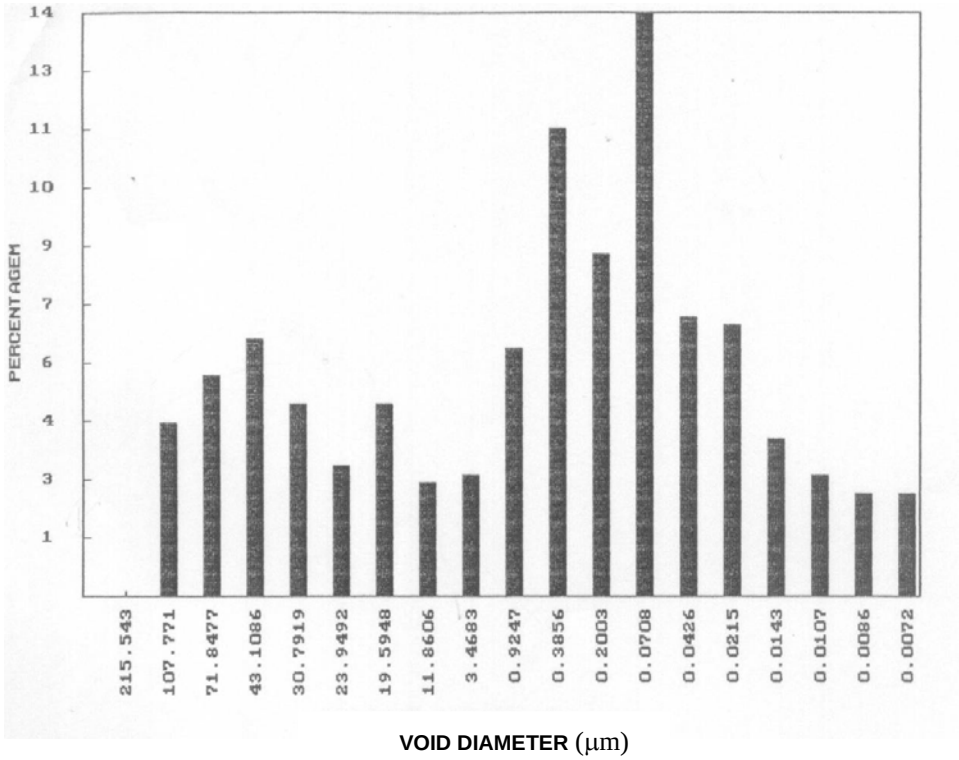



Figure 8 – Histogram representative of interconnected–void size distribution

Discounting the volume of interconnected pores from the total volume of the concrete specimens, one can calculate the skeletal density, $\rho_s$, which refers to the specific mass of the concrete yet containing the closed pores. The values of $\rho_s$ thus obtained are listed in Table 2, together with those of the respective apparent density $\rho_a$. The corresponding real density values, $\rho_r$, which were determined using helium picnometry technique, are also listed in the same table. $F_i$, $F_c$ and F in Table 2 refer, respectively, to the volume fraction of interconnected voids, closed voids and total voids. The calculation of these volume fractions is presented later in the text.

Table 2 – Values of specific mass, ρ, and volume fractional, F, for the concrete mixes

| Cement Weight (kg) | Mix | Specimen mass (g) | Specimen volume (cm3) | $\rho_a$ (g/cm$^3$) | $\rho_s$ (g/cm$^3$) | $\rho_r$ (g/cm$^3$) | $F_i$ | $F_c$ | F |
|---|---|---|---|---|---|---|---|---|---|
| 50 | N1g | 0.708 | 0.960 | 0.738 | 2.014 | 2.610 | 0.634 | 0.080 | 0,714 |
| | PN64G | 0.722 | 0.798 | 0.905 | 1.617 | 2.398 | 0.441 | 0.145 | 0.586 |
| | PN74G | 0.646 | 0.634 | 1.018 | 1.533 | 2.389 | 0.336 | 0.151 | 0.487 |
| | PN84G | 0.824 | 0.739 | 1.115 | 1.674 | 2.545 | 0.334 | 0.168 | 0.508 |
| | PN75G | 0.585 | 0.583 | 1.003 | 1.629 | 2.492 | 0.384 | 0.125 | 0.502 |
| 25 | N1 | 0.673 | 1.037 | 0.650 | 1.435 | 2.610 | 0.547 | 0.211 | 0.758 |
| | PN64 | 0.411 | 0.467 | 0.880 | 1.573 | 2.460 | 0.441 | 0.094 | 0.535 |
| | PN74 | 0.742 | 0.785 | 0.946 | 1.507 | 2.398 | 0.372 | 0.183 | 0.555 |
| | PN84 | 0.711 | 0.636 | 1.118 | 1.640 | 2.448 | 0.379 | 0.143 | 0.522 |
| | PN75 | 0.427 | 0.441 | 0.968 | 1.656 | 2.398 | 0.416 | 0.080 | 0.496 |

The volume of closed pores, $V_c$, contained in a given concrete specimen of mass, m, can be determined from the relations:

$$\rho_r = \frac{m}{V_s} \tag{1}$$

$$\rho_s = \frac{m}{V_s + V_c} \tag{2}$$

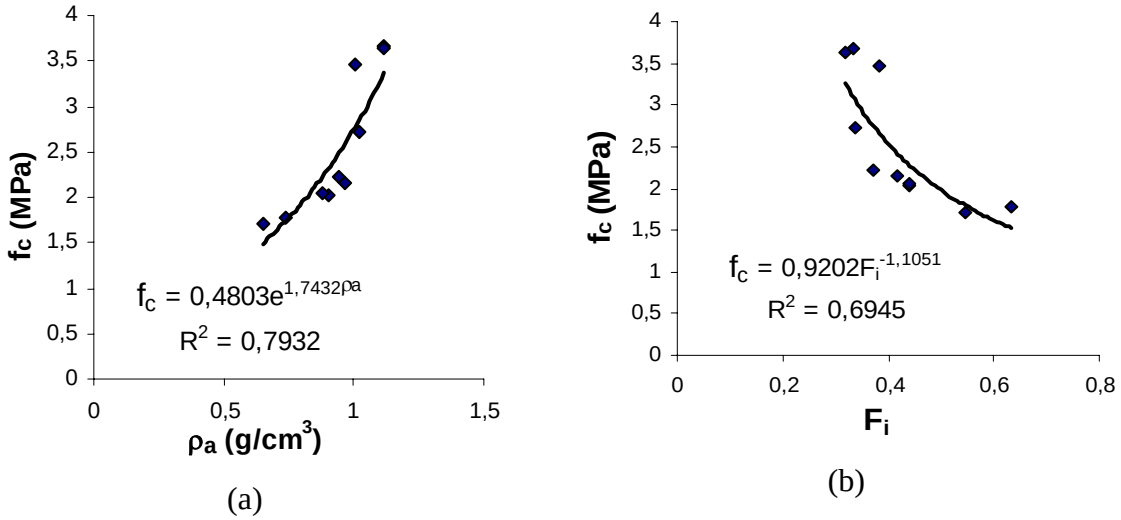
where $V_s$ represents the volume of solid material contained in the sample.

Combining equations (1) and (2), $V_c$ is obtained as:

$$V_c = m \times \left( \frac{\rho_r - \rho_s}{\rho_r \rho_s} \right) \tag{3}$$

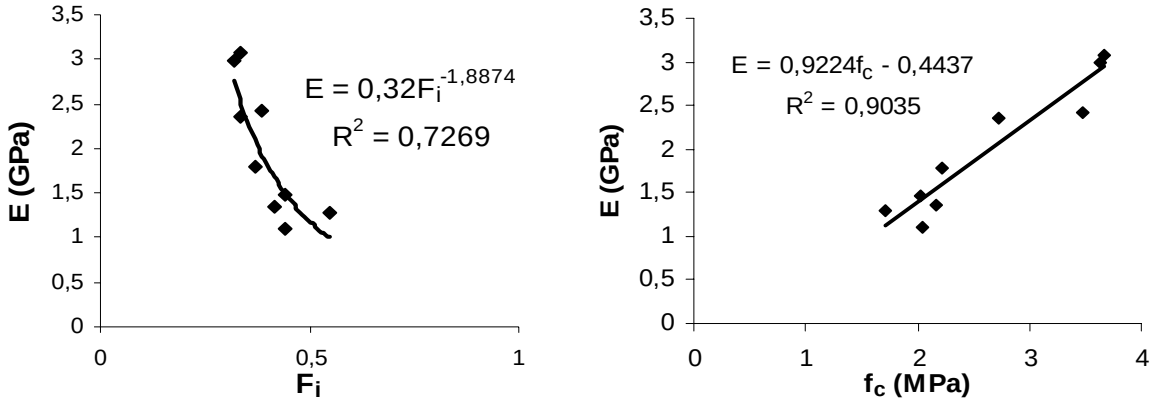
From knowledge of the specimen volume, $V_i$ and $V_c$ can be used to calculate the volume fraction of interconnected and closed pores, termed $F_i$ and $F_c$, respectively. These are presented in Table 2, where the total void volume fraction F, given by the summation of $F_i$ and $F_c$, is also listed.

Mechanical properties of cellular concrete are strongly dependent on the physical characteristics listed in Table 2. Accordingly, it seems appropriate to correlate the compressive strength $f_c$, and modulus of elasticity E, with the concrete density and/or volume fraction of pores. As examples of good correlations, one presents the variation of $f_c$ with the apparent density, $\rho_a$, and with $F_i$ as shown in Figure 9. The increase in $f_c$ with the increase in $\rho_a$ observed in this figure is attributed principally to a decrease in the volume fraction of voids. However, one should note that the increase in apparent density, which is brought about by the use of heavyweight aggregate, is accompanied by a decrease in the strength of the cement mortar. Although no attempt has been made in this work to evaluate the mortar properties, one can draw the conclusion that the decrease in the void volume fraction is the predominant structural factor in improving the concrete strength. A similar behavior to that of $f_c$ is observed for the dependence of E on $F_i$ (Figure 10a) and as shown in Figure 10b, E correlates linearly with $f_c$.




(a) (b)

Figure 9 – Variation of the concrete strength with $\rho_a$ and $F_i$




(a) (b)

Figure 10 – Correlations of the concrete elastic modulus with $F_i$ and with $f_c$

## 4. CONCLUSIONS

Large volume fraction of voids, as high as 0.76, can be achieved in cellular concrete obtained by curing cement-foam mixtures. The addition of sand and plastics as aggregates, in the proportions adopted in this study, results in a reduction in the void volume fraction that can amount to 39%.

The reduction in the void volume fraction, brought about by the use of aggregates, is accompanied by an increase in the compressive strength, $f_c$, of the cellular concrete. Such an increase can amount to about 100% of the value of $f_c$ determined for aggregate-free cement mortar.

Based on EDS analysis, one can conclude that the concentration of elements such as C and O in the surface of cell voids is much higher than that detected in areas within the cell walls, which is consistent with the use of organic frother for producing air bubbles within the concrete mixtures.

Mercury porosimetry measurements have indicated bimodal size distribution of interconnected voids.

Based on helium picnometry measurements, one can determine the real density of cellular concrete and hence estimate the volume fraction of closed voids.

## 5. ACKNOWLEDGEMENTS

The authors would like to acknowledge the help received from the Centro de Pesquisa da Companhia Siderúrgica Nacional (CSN), Brazil during the course of the present work. Thanks are also due to Dr. Protásio Ferreira e Castro for helpful discussions.

## 6. REFERENCES

American Concrete Institute - ACI, Guide for Cast-in-Place Cellular Concrete. *ACI 523.1 R-92*, Detroit, MI (1992).

American Concrete Institute - ACI, Guide for Low Density Precast Cellular Concrete. *ACI 523. 2 R-93*, Detroit, MI (1993).

Associação Brasileira de Normas Técnicas – ABNT-NBR 5739 – Concreto - Ensaios de compressão de corpos de prova cilíndricos, Rio de Janeiro, (1994).

Associação Brasileira de Normas Técnicas – ABNT-NBR 8522 – Concreto - Determinação do módulo de deformação estática e diagrama tensão-deformação - Método de ensaio, Rio de Janeiro, (1984).

Allende, K.A., Freitas, I.M., Darwish, F.A., Cellular Foam Concrete Containing Lightweight and Heavyweight Aggregates, *II Simpósio Internacional sobre Concretos Especiais*, Sobral, C.E. Brasil, Proceedings in CD ROM (2004).

Ferreira, O.A.R. Concretos Leves: O concreto celular espumoso. *A Construção*, no. **249**, 27-30, Editora PINI, São Paulo, (1987).

Freitas, I.M., Allende, K.A., Darwish, F.A., Otimização da produção e das propriedades do concreto celular espumoso orgânico e inorgânico com adição de cinasita e rejeito plástico. *XXIV ENEGEP*, Florianópolis, SC, Brasil, Proceedings in CD ROM (2004).

Freitas, I.M., Allende, K.A., Darwish, F.A., Cellular Foam Concrete Containing Expanded Clay and Natural Sand, *II Simpósio Internacional sobre Concretos Especiais*, Sobral, CE. Brasil, Proceedings in CD ROM (2004).

Legatski, L.A. Cellular Concrete, in Significance of Testing and Properties of Concrete, *ASTM Publications Code Number* (PCN) 04-169030-07, 533-539 (1994).

Legatski, L.M., *ASTM STP, 169-B* (1978), Referenced in: Legatski (1994)

Lo, T.Y. and Cui, H.Z. Effect of Porous Lightweight Aggregate on Strength of Concrete, *Materials Letters*, **58**, 916-919, (2004).

Maire, E., Fazekas, A., Salvo, L., Dendievel, R., Youssef, S., Cloetens, P.and Letang, J.M. X-Ray Tomography Applied to the Characterization of Cellular Materials. Related Finite Element Modeling Problems, *Composites Science and Technology*, **63,** 2431-2443 (2003).

Teixeira Filho, F.J. Considerações sobre algumas propriedades dos concretos celulares espumosos. Dissertação de Mestrado, *Escola Politécnica da USP*, SP, Brasil (1992).

Tikalsky, P.J., Pospisil, J. and MacDonald, W. A Method for Assessment of the Freeze-Thaw Resistance of Prefomed Foam Cellular Concrete, *Cement and Concrete Research*, **34**, 889-893 (2004).

International Symposium Polymers in Concrete
2 - 4 April 2006
Guimarães, Portugal

# Experimental Analysis of Cork as a Concrete Aggregate

Fernando G. Branco[1], António Tadeu[2]

*Faculdade de Ciências e Tecnologia da Universidade de Coimbra,*
*Departamento de Engenharia Civil*
*Pólo II – Pinhal de Marrocos, 3030-290 Coimbra, Portugal*

Maria de Lurdes Belgas C. Reis[3]

*Instituto Politécnico de Tomar, Departamento de Engenharia Civil*
*Quinta do Contador, Estrada da Serra, 2300 Tomar, Portugal*

## ABSTRACT

Given its various interesting mechanical and physical characteristics, cork is a versatile material with a great many possible uses. In the last few decades, cork has been much more extensively used as a material in the building industry. It has helped to enhance the quality and performance of both existing and new products, mainly for thermal and acoustic insulation, but also as a vibration absorber.

The work described here analyses the possibilities of using cork as an aggregate in concrete admixtures, partly replacing sand and coarse aggregates. Different concrete compositions were studied to determine how the presence of cork influences the ultimate compressive strength of concrete. The paper addresses the problem of ensuring the homogeneous dispersion of cork in the fresh concrete. The amounts of cork in the admixture and cork particle size distribution were among the variables analyzed.

## 1. INTRODUCTION

The material known as cork comes from the outer layer of bark of the *Quercus suber L.*, a type of oak tree that is native to the western Mediterranean. Cork is composed mainly of suberin, which accounts for about 40% of its dry weight, lignin (± 20%), polysaccharides (±. 20%) and extractables (±15%). This chemical composition, together with its particular cellular structure, provides cork with excellent barrier properties against polar liquids, heat and sound (Cordeiro, 1998).

The cork industry worldwide consumes more than 280 000 tons of cork a year. However, about 20% to 30% of the raw cork received at the processing unit is rejected,

[1] Assistant Professor
[2] Full Professor
[3] Adjunct Professor

mainly as cork dust, which has low granulometry and is of no industrial interest (Carvalho, 1996).

Cork is a natural, light and organic product. It is dimensionally stable, and exhibits a considerable resistance to compressive loads. These characteristics make cork a product suitable for use in a wide spectrum of applications (Karade, 2001). It has other important characteristics, too. Cork is a natural and ecological product, it is odourless, and it can be considered imputrescible and unalterable, thus retaining its efficiency for a very long time. Considering that Portugal is the world's largest cork producer, it may well prove to be interesting economically to find alternative uses for the industrial waste from cork production.

In the building industry, cork's excellent thermal behaviour and its ability to absorb vibration make it a first-choice solution as a thermal insulator and acoustic absorptive material. Despite the wide spectrum of possible applications for cork in the building industry, there are few publications on this subject. One of the few documented studies on concrete mixtures containing cork is by Aziz *et al.* (Aziz, 1979). This work reports the results of a research project which aimed to develop lightweight concrete using cork granules. Lightweight cork concrete was compared with standard concrete and other kinds of lightweight concrete (aerated, no-fines, cellular and foamed). The results indicated that although the mechanical strength of cork concrete in compression and tension is lower than that of standard concrete, yet this kind of concrete performed better than the other types of lightweight concrete analysed. Cork lightweight concrete also exhibited better thermal and shrinkage properties than other lightweight concretes produced from organic materials.

The present paper is part of a more vast research project, presenting some preliminary results obtained up to this stage. The project intends to evaluate the mechanical and physical properties of cork dust better, and to explore its potential advantages when used as a concrete aggregate. The introduction of natural or expanded cork granules in concrete mixtures will allow concrete to benefit from some of cork's useful properties, thus leading to an improvement in that concrete's performance when compared with standard concrete. Thermal insulation, acoustic behaviour, particularly in relation to impact loads, and increased durability under freeze-thaw conditions are some parameters where the inclusion of cork could be a positive advantage to concrete.

In this preliminary paper, the authors set out to analyse the impact of the presence of cork on the compressive strength of concrete. Different concrete compositions were tested, using two types of cork as an aggregate: natural and expanded cork granules. The effect of the size of the cork granules and the amount of cork in the concrete mixture were also analysed. The results obtained for the cork concrete compositions were compared with those from a reference standard concrete.

## 2. EXPERIMENTAL WORK

The experimental work required cork granules which were provided by cork industry. A reference standard concrete was designed. Then, different concrete mixtures were produced using the reference composition as a base. In these mixtures, two types of cork granules (natural and expanded cork) were used instead of coarse primary limestone aggregates and/or river sand.

Different replacement percentages of aggregates by cork granules were tested. In each mixture, a given volume of coarse aggregate or sand was replaced by the same volume of cork granules, with a similar particle size distribution (NP 115:1994). This size distribution was controlled via the fineness module, computed as

$$MF = \frac{\sum_{i=1}^{n}(100 - p_i)}{100} \quad (1)$$

where $p_i$ represents the percentage of particles with dimensions smaller than the openings in sieve $i$. Replacements of 10%, 20%, 25% and 30% were tested. In series B3 specimens, 10% of both sand and coarse aggregate were replaced by cork granules.

The cork concrete specimens were subjected to compressive strength tests, according to the LNEC E226:1968 test specification (LNEC, 1968). Tests were conducted on specimens 3, 7, 14, 21 and 28 days old, to evaluate the variation of compressive strength over time, in relation to the amount of cork in the mixture.

Table 1 gives the mixture compositions for all the concretes tested. In this table, NCG stands for "Natural Cork Granules", while ECG stands for "Expanded Cork Granules". As the Table shows, batches of different-sized cork granules of were used for each mixture. The amount of each granule size fraction was computed to reproduce the particle size distribution of the aggregates replaced.

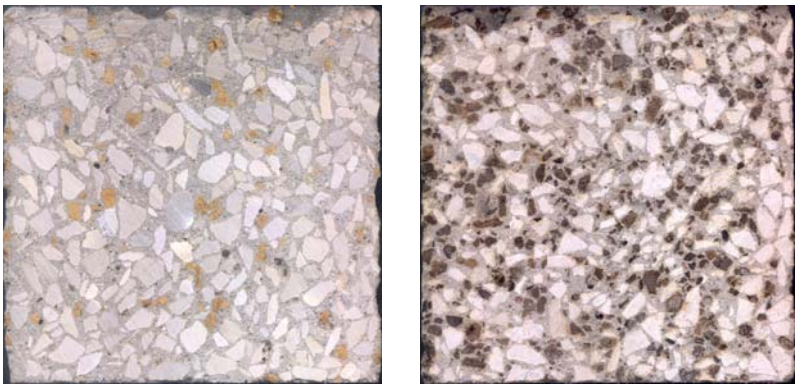
Table 1 - Concrete mix design details.

| Batch | Components (kg/m$^3$) | | | | | | | | | | |
|---|---|---|---|---|---|---|---|---|---|---|---|
| | Coarse aggreg. | Sand | Cement | Water | NCG (4/5) | NCG (0/1) | NCG (1/2) | ECG (5/10) | ECG (3/5) | ECG (0/1) | ECG (1/2) |
| BR | 1413 | 498 | 300 | 180 | - | - | - | - | - | - | - |
| B1.1 | 1271 | 498 | 300 | 180 | 6.90 | - | - | - | - | - | - |
| B1.2 | 1130 | 498 | 300 | 180 | 13.80 | - | - | - | - | - | - |
| B1.3 | 989 | 498 | 300 | 180 | 20.69 | - | - | - | - | - | - |
| BE1.1 | 1271 | 498 | 300 | 180 | - | - | - | 5.16 | 5.58 | - | - |
| BE1.2 | 1130 | 498 | 300 | 180 | - | - | - | 10.33 | 11.15 | - | - |
| BE1.3 | 989 | 498 | 300 | 180 | - | - | - | 15.49 | 16.72 | - | - |
| B2.1 | 1413 | 448 | 300 | 180 | - | 2.25 | 0.58 | - | - | - | - |
| B2.2 | 1413 | 398 | 300 | 180 | - | 4.50 | 1.15 | - | - | - | - |
| B2.3 | 1413 | 348 | 300 | 180 | - | 6.75 | 1.73 | - | - | - | - |
| B2.4 | 1413 | 373 | 300 | 180 | - | 5.61 | 1.43 | - | - | - | - |
| BE2.1 | 1413 | 448 | 300 | 180 | - | - | - | - | - | 6.54 | 2.11 |
| BE2.2 | 1413 | 398 | 300 | 180 | - | - | - | - | - | 13.08 | 4.21 |
| BE2.3 | 1413 | 348 | 300 | 180 | - | - | - | - | - | 19.62 | 6.32 |
| B3.1 | 1271 | 448 | 300 | 180 | 6.90 | 2.25 | 0.58 | - | - | - | - |
| BE3.1 | 1271 | 448 | 300 | 180 | - | - | - | 5.16 | 5.58 | 6.54 | 2.11 |

Laboratory tests were carried out to evaluate the most relevant characteristics for the aggregates used. Grading, moisture content and bulk density were determined for all aggregates and cork granules (NP 605:1996; NP 606:1995) used. Slump tests were performed to measure the workability of the fresh concrete for all mixtures.

Laboratory tests were carried out on hardened concrete to determine its mechanical strength under compressive loads (LNEC, 1968). Specific density and water absorption (NP 591:1969) were the physical parameters measured in specimens of hardened concrete.

In order to see whether the cork granules exhibited a homogeneous dispersion within the concrete mass, some specimens were divided into two, and the distribution of cork granules in the sawn surface was analysed. Figure 1 shows the cork distribution for the series B1.1 and BE 1.3 specimens. This procedure made it possible to see that good cork dispersion was obtained in all the concrete series analysed.

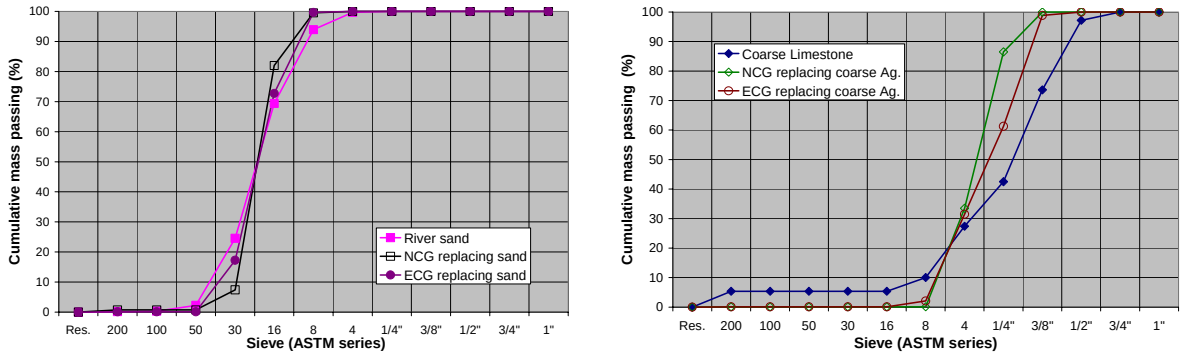


a) b)

Figure 1 - Cork granule dispersion in concrete specimens: a) series B1.1; b) BE1.3.

## 2.1. Characterization of the materials

Figure 2 gives the grading test results for the aggregates and cork granules. A good approximation between the particle size distribution of each aggregate and the corresponding cork granule mixtures can be seen. The fineness modules for sand and the coarse aggregate are 3.10 and 5.67, respectively. The cork granule replacement mixtures exhibited the same fineness modules as the material that was replaced.




a) b)

Figure 2 - Grading curves. a) River sand and replacement cork granule mixtures; b) Coarse aggregate and replacement cork granule mixtures.

Table 2 gives the bulk densities determined for all the aggregates and replacement cork granules. It can be seen that the cork granules are much lighter than the aggregates they replace, and so the concrete made with the replacement cork granules is expected to be significantly lighter.

Table 2 – Bulk densities of aggregates and cork granules.

| Aggregates | River sand | Coarse limestone | NCG (4/5) | NCG (0/1) | NCG (1/2) | ECG (5/10) | ECG (3/5) | ECG (0/1) | ECG (1/2) |
|---|---|---|---|---|---|---|---|---|---|
| Bulk density ($kg.m^{-3}$) | 2570.0 | 2669.5 | 70.1 | 85.5 | 87.8 | 68.0 | 247.8 | 362.8 | 249.0 |

The physical parameters evaluated for the concrete mixtures manufactured are presented in Table 3. As expected, when a larger amount of aggregate is replaced by cork granules, there is a perceptible drop in weight. Concrete specimens produced with natural cork granules are heavier than those containing expanded cork granulate. One exception was

batch B1.3, which is lighter than BE1.3. When coarse aggregate was replaced by an equal volume of cork, it was possible to obtain lower weights than when there was a similar volume replacement between sand and cork. When natural cork granules were used, a replacement of 30% of the coarse aggregate led to a 25% reduction in concrete weight, but when cork replaced sand, there was only a 10% loss of weight.

Table 3 – Bulk density and water absorption for concrete.

| Batch | Bulk density ($kg.m^{-3}$) | Water absorption (%) |
|---|---|---|
| BR | - | - |
| B1.1 | 2090 | 7.2 |
| B1.2 | 1970 | 6.9 |
| B1.3 | - | - |
| BE1.1 | 2090 | 6.6 |
| BE1.2 | 1930 | 7.4 |
| BE1.3 | 1800 | 8.0 |
| B2.1 | 2230 | 5.8 |
| B2.2 | 2120 | 6.7 |
| B2.3 | - | - |
| B2.4 | 2140 | 6.4 |
| BE2.1 | 2200 | 6.4 |
| BE2.2 | 2120 | 6.7 |
| BE2.3 | 2020 | 7.4 |
| B3.1 | 2060 | 6.7 |
| BE3.1 | 2090 | 6.3 |

2.2. Mechanical behaviour of hardened concrete

Concrete cubes measuring 150 x 150 x 150 $mm^3$ were produced and subjected to compressive tests at different ages (7, 14, 21 and 28 days). The specimens were removed from their moulds 24 hours after casting, and stored in a climatic chamber (20ºC; ±95% relative humidity) until testing. At least three specimens from each batch were tested. The results for the compressive tests are given in Table 4.

As expected, as the percentage of cork granulates increased, the concrete's compressive strength fell.

The B1 series specimens, where coarse aggregates were replaced by cork granules, exhibited greater loss of strength than the B2 specimens, in which natural cork replaced part of the river sand. When comparing the B1 series with the reference concrete (BR), strength falls of between 32.6% and 74.9% were registered, as the amount of coarse aggregate replaced rose from 10% to 30%. The corresponding falls in strength when there were similar replacements for sand (series B2) ranged between 26.5% and 52.8%.

When expanded cork was used to replace the aggregates, the strength loss was generally higher than when natural cork was used. The exceptions were series BE1.3 and BE2.3, where 30% volume of aggregates was substituted by expanded cork. In these series, a 61.6% and 46.0% strength reduction, respectively, were registered, against 74.9% and 52.8% observed in series B1.3 and B2.3.

Table 4 – Average compressive strength of concrete specimens.

| Series | Average compressive strength (MPa) | | | | Strength loss against BR (%) |
|---|---|---|---|---|---|
| | 7 days | 14 days | 21 days | 28 days | |
| BR | 23.40 | 25.25 | 25.66 | 26.14 | 0.0 |
| B1.1 | 13.86 | 15.98 | 16.68 | 17.62 | 32.6 |
| B1.2 | 9.3 | 11.44 | 12.18 | 12.55 | 52.0 |
| B1.3 | 5.95 | 6.77 | 6.51 | 6.56 | 74.9 |
| BE1.1 | 12.17 | 13.51 | 14.33 | 15.16 | 42.0 |
| BE1.2 | 11.03 | 11.86 | 12.80 | 13.24 | 49.3 |
| BE1.3 | 8.68 | 9.83 | 10.26 | 10.05 | 61.6 |
| B2.1 | 16.68 | 17.79 | 18.38 | 19.21 | 26.5 |
| B2.2 | 16.05 | 17.13 | 17.78 | 18.32 | 29.9 |
| B2.3 | 10.11 | 11.09 | 12.02 | 12.33 | 52.8 |
| B2.4 | 17.21 | 18.66 | 19.26 | 19.15 | 26.7 |
| BE2.1 | 14.88 | 16.93 | 18.32 | 18.28 | 30.1 |
| BE2.2 | 14.39 | 16.21 | 16.92 | 17.65 | 32.5 |
| BE2.3 | 11.31 | 12.83 | 13.69 | 14.11 | 46.0 |
| B3.1 | 13.62 | 14.99 | 15.96 | 16.54 | 36.7 |
| BE3.1 | 13.53 | 14.73 | 15.78 | 16.61 | 36.5 |

Figure 3 displays the variation of compressive strength of the specimens with their bulk density. The results indicate that the average strength of concrete containing cork granulates as aggregate materials is closely related to its bulk density. A linear trend line represents a good approach for this relation. However, as only a small number of tests was performed, it is not possible to draw definite conclusions. Further tests will be carried out on concretes with a lower bulk density, thus containing a higher percentage of cork granulates.

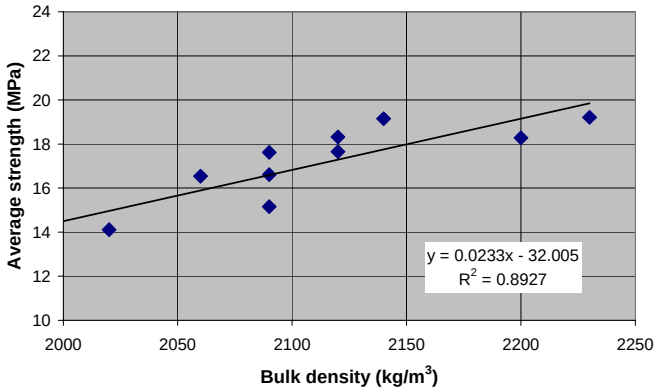



Figure 3 – Variation of the average compressive strength with the bulk mass of the specimens.

Figure 4 shows the average compressive strength variation with the amount of cork contained in the mixture. A loss of strength can be seen as the percentage of cork increases. Both types of cork studied led to similar drops in strength.

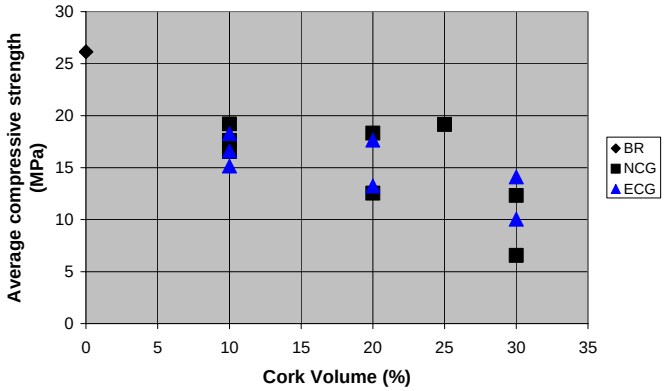



Figure 4 – Variation of the average compressive strength with the volume of cork contained in the mixture.

## 3. FINAL REMARKS

This paper presents the preliminary results of a research project that aims to assess the mechanical and physical properties of cork granules and evaluate any benefits if they are used as a concrete aggregate.

Different concrete mixtures, containing different amounts of cork granules were made up. Two types of cork (natural and expanded) were studied. Compression tests were carried out in the laboratory on the several concrete series at different ages.

The tests showed that the compressive strength of the concretes tends to fall as the amount of the cork granulates in the mixture increases. This effect is more noticeable when coarse aggregate is replaced by cork. The use of expanded cork led to high losses of strength.

The compressive strength of concrete decreases as concrete bulk density decreases. The tests carried out made it possible to conclude that this loss of strength follows a linear trend within the density range tested. Tests on lower density concrete containing cork granules are needed to check if this correlation is still valid outside the current test field.

The volume of cork in the concrete strongly influences its mechanical strength. This phenomenon is particularly important when replacing the coarse aggregates. When 10% to 30% of sand is replaced by an equivalent volume of cork granules the concrete strength drops by between 26.5 and 52.8%, while reductions ranging from 32.6 to 74.9% were registered when cork granules replaced the coarse aggregate. Expanded cork granules used as replacement material usually leads to greater strength losses than the use of natural cork granules.

## 4. ACKNOWLEDGEMENTS

The authors thank the Foundation for Science and Technology, Portugal, for the financial support granted through project POCI/ECM/55889/2004; Grupo Amorim – Portugal, for the cork granulate and CIMPOR – Cimentos de Portugal, SA, for the cement used to produce the test specimens.

## 5. REFERENCES

Aziz, M.A.; Murphy, C.K.; Ramaswamy, S.D., Lightweight concrete using cork granules, *The International Journal of Lightweight Concrete*, **2(1)**, 29-33 (1979).

Carvalho, A.P.O., Cork as a lightweight partition material. Economical and acoustical analyses, in: Proceedings of the CIB W89 Beijing International Conference, (1996).

Cordeiro, N., Belgacem, M. N., Silvestre, A. J.D., Pascoal Neto, C., Gandini, A., Cork suberin as a new source of chemicals. 1. Isolation and chemical characterization of its composition, *International Journal of Biological Macromolecules*, **22** , 71-80 (1998).

Karade, S.R.; Irle, M.A; Maher, K. – "Physico-chemical aspects of the use of cork in cimentious composites", ICWSF 2001- The Fifth International Conference on the Development of World Science, Wood Technology and Forestry in Ljubljana, Slovenia, 2001, pp. 97-103.

NP 115:1994: Granulated cork Size analysis by mechanical sieving (in Portuguese), Portuguese Standard, Lisbon, Portugal (1994).

NP 605:1996: Granulated cork. Determination of apparent density (in Portuguese), Portuguese Standard, Lisbon, Portugal (1996).

NP 606:1995: Granulated cork. Determination of moisture content (in Portuguese), Portuguese Standard, Lisbon, Portugal (1995).

LNEC E-226:1968, Concrete. Determination of compressive strength (in Portuguese), Laboratory Test Specification. LNEC - Laboratório Nacional de Engenharia Civil, Lisbon, Portugal (1968).

NP 581:1969, Aggregates for mortars and concrete. Determination of specific density and water absorption of coarse aggregate (in Portuguese), Portuguese Standard, Lisbon, Portugal (1969).

International Symposium Polymers in Concrete
2 - 4 April 2006
Guimarães, Portugal

# Study of the Resistance to Impact of Light Panels made with Residue of Expanded Polystyrene

Gisele de Oliveira Trindade[1]
*Postgraduate Program in Engineering: Energy, Ambient and Materials*
*ULBRA – Lutheran University of Brazil, Canoas/RS, Brazil*
trindarq@terra.com.br

## ABSTRACT

In this work aspects of a material composed of two concrete plates with glass fiber (GRC) filled of concrete with residues of expanded polystyrene (EPS) were analyzed on the purpose to obtain parameters and guidelines for its application in the civil construction.

Rehearsals were accomplished in samples to evaluate the influence of the composition of the mix proportions in composites impact resistance. The determination of the resistance to the impact was based on the Brazilian norm NBR - 12764 (1992). After 28 days, the samples were tested in a mounted apparel for the rehearsals.

The results have shown that samples of mix proportion 1:5 (cement:EPS) presented larger impact resistance. Once the mix proportions 1:7 (cement:EPS) and 1:9 (cement:EPS) presented smaller resistance. In the series where there is a great amount of EPS in the paste, the resistance is smaller. The difference observed among the resistance of the proportions 1:5, proportions 1:7 and 1:9 confirms that the amount of EPS in the paste influences directly in the resistance.

Therefore, the contributions of the research allow to relate the technology of the production of this panel with the context of maintainable construction and the use of residues.

Word-key: Concrete with EPS; glass fiber; panel; expanded polystyrene; Impact resistance.

## 1. INTRODUCTION

The industrial era and the change in the patterns of constructions, began to demand fast work and smaller costs. In this period, the civil construction started a new direction to the best understanding of the physical properties of the materials. The civil construction becomes an " industry of the civil " construction. Therefore, the need of codes and standardization have fastened the minimum properties that the materials should assist. This meant a great qualitative jump for the civil engineering and for the teaching institutions. The technological development in the production of the mansory components in an industrial scale brought, starting from the 60's, to the engineers and architects, the need of larger knowledge of those components and of its use in the development of a project. In that way, the professionals meet

[1] Architect, Master in Engineering

a vast field to work in the sense of the rationalization, the industrialization, the productivity and the quality of constructions.

Srilanka Ravindrarajah et al. (1994) affirmed that a natural marriage of polymeric and concrete is in the use of polystyrene expanded pearls for the production of light concrete. The combination gains profit of the intrinsic properties of both materials.

According to Cook (1983), when the polystyrene beads are combined with Portland Cement, the resulting composites offer good isolation thermal, low absorption of water, resistance to fire, and good physical properties. As filling material, the light concrete with EPS can be made easily in function of the properties to privilege, the mechanical resistance or the thermal isolation. It is possible to obtain excellent concrete in both properties.

Forlin et al. (2002) told that besides the technical factors mentioned, the largest understanding of the population in the last decades has been forcing managers and governments to invest in pro of the recovery of the environment, attracting the professionals' attention for the area. Subramanian (2000) noticed that the development technological ally to conscientiousness has been addressing the scientific community for the development of processes and methods (as recycling of residues, treatments of effluents, among others), to take advantage of the natural resources and to pollute less.

Two properties are very important for the slender components used in the civil construction: the tenacity and the ductility. The reinforcement of mortars and concrete of Portland Cement with fibers is a quite efficient way to reduce the fragility in the rupture of these materials, to increase the durability and to check mechanical properties not found in the mortars and conventional concrete, related to the deformation capacity and absorption of energy. Mehta & Monteiro (1994) affirmed that the cement composite reinforced with fibers has great variety of applications, including pavements for highways, structures of bridges, tunnels, hydraulic works, resistant structures to explosions, among others. Other important line of application of the mortars and concrete reinforced with fibers is the one of the slender elements, facade coating, panels and coverings.

The use of GRC panels is advantageous because it rationalizes the work and the reinforcement. In that case, the glass fibers are evenly dispersed in the cement matrix, reducing the mass of the panels, therefore allowing the transport of the materials in smaller equipment. PCI (1995) told that the reinforcement allows the increase of the dimensions of the panels. Yet, it’s possible to apply colors and several textures to the panels GRC, increasing the architectural potential of this component.

Thus, the characteristics of the Concrete with EPS (thermal isolation, lightness, etc.) will be guaranteed, because of the covering layers of concrete with glass fibers, facilitating the making of slender pieces.

## 2. METHODS AND MATERIALS

It is not advised the employment of the existent methods of experimental mixing for the mix proportions of concrete with residues of triturated EPS, because this is a light concrete. Thus, the mix proportions were evaluated in percentage of volume of the materials. Where the mix proportions of the concrete with glass fiber were based in PCI (1994). It was molded specific specimens for each test. In table 1 it can be observed as each mix proportions and specimens were classified, and in table 2 it can be visualized in which test each specimen was used.

Tlabe 1 – Classification of the specimens.

| | GRC | EPS | Glass Fibers | Name |
|---|---|---|---|---|
| Mix proportion | 1:1 | EPS 1:5 –w/c 0,40 | 3% | I |
| w/c | 0,33 | EPS 1:7 –w/c 0,40 | 3% | II |
| Superplastifying addictive | 0,08% | EPS 1:9 –w/c 0,40 | 3% | III |
| Dimensions (cm) | | 40 x 30 x 9 | | b |

Tlabe 2 – Tests where the specimens were utilized.

| Specimens | Tests |
|---|---|
| Series Ic (1:5)<br>Series IIc (1:7)<br>Series IIIc (1:9) | Impact Resistance<br>(based in NBR - 12764) |

As the objective was to evaluate the influence of the amount of EPS in the impact resistance, three concrete mix proportions were made with EPS. The amount of cement and the relationship water/cement were constant.

The specimens were made with the following materials:

- rejects of EPS blocks or packing, originating from the manufacturer, were received triturated, previously selected and classified by specific mass ($\lambda$ = 14 kg/m3);
- glass fibers type AR 405B - length 3,2mm;
- it was used pozolanic Portland cement CP IV-32;
- sifted sand with thinness module as 2,92;
- water originating from the net of provisioning of the city of Canoas - RS, possessing the potable characteristics.
- plastifying addictive of last generation, based in a chain of carboxylic ether modified. It is exempted of Clorets and assists the prescriptions of the norm ASTM C 494 (types THE and F), ASTM C 1017, and it is compatible with all the cements that assist the norm ASTM 150.

The compacting of the mortar with glass fiber was accomplished manually, with help of a roll of sheep wool of length 15 cm. Thus the concrete with EPS was also manually compacted, but with the help of a steel bar.

The specimens were cured for 28 days to ambient temperature without using a humid camera.

The determination of the Simple Impact Resistance was based on the Brazilian norm NBR - 12764 (1992). It was opted for using an adaptation of this norm developed in the civil engineering laboratory of CIENTEC in the city of Porto Alegre/RS. This decision was made because this method facilitates the execution of the test.

After 28 days, the Series Ib, IIb and IIIb specimens were tested in an apparel, schematized in the figure 1 and developed in the building materials laboratory of ULBRA-Canoas/RS.

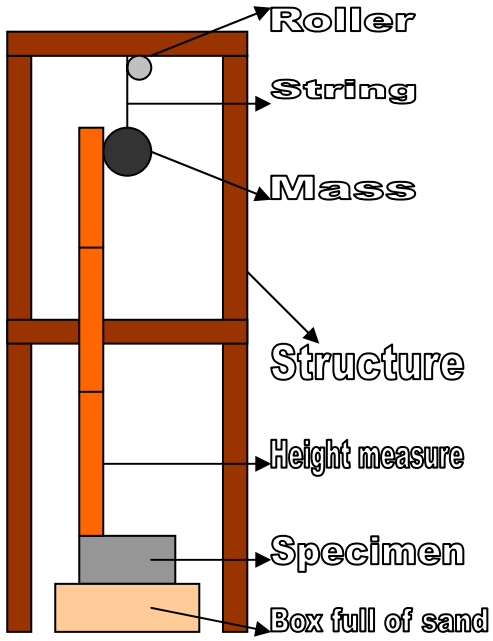



Figure 1 – Impact test apparel based in NBR – 12764 (1992).

In agreement with NBR – 12764 (1992), two masses, one of 1kg and another of 2 kg, should be thrown respectively 20 times to heights of 1 m, 1,5 m and 2 m. If, however, the rupture happened before these six impact series, it should be written down with many impacts and in which height this has happened.

Besides this annotation pictures of the broken specimens were taken to evaluate the fissure characteristics of them.

## 3. RESULTS AND DISCUSSIONS

During the test, it was taken note of the amount of impacts and in which height the rupture has happened. The results are presented on table 3.

The results of the series Ib (1:5) reached the highest values of all specimens. The resistance was kept between 313 and 392 J. The following behavior was observed: after the first fissure, the rupture was proceeded.

The specimens' resistance of the series IIb (1:7) were inferior to the results reached by the series Ib (1:5). The variation of the results among specimens of this same series was elevated. That is due to the different thickness of the layer of GRC in each specimen.

The series IIIb (1:9) reached the lower levels of impact resistance. The behavior was similar to the series IIb (1:7). However the rupture in some specimens happened without showing any fissures.

Tlabe 3 – Specimens submitted to impact resistance test according to NBR - 12764 (1992)

| Specimens | Fissure | Fracture | Impact Energy |
|---|---|---|---|
| Series Ib (1:5) CP 01 | 3 impacts with 2 kg from 2 m | Broken at 8 impacts with 2 kg from 2 m | 313,92 J |
| Série Ib (1:5) CP 02 | 5 impacts with 2 kg from 2m | Broken at 10 impacts with 2 kg from 2 m | 392,40 J |
| Série Ib (1:5) CP 03 | 8 impacts with 2 kg from 2 m | Broken at 12 impacts with 2 kg from 1,5 m | 353,16 J |
| Série IIb (1:7) CP 01 | 4 impacts with 1 kg from 2 m | Broken at 7 impacts with 1 kg from 2 m | 137,34 J |
| Série IIb (1:7) CP 02 | 7 impacts with 1 kg from 1,5 m | Broken at 5 impacts with 1 kg from 2 m | 98,10 J |
| Série IIb (1:7) CP03 | 2 impacts with 1 kg from 2m | Broken at 6 impacts with 1 kg from 2m | 117,72 J |
| Série IIIb (1:9) CP 01 | 20 impacts with 1 kg from 1m | Broken at 5 impacts with 1 kg from 1,5 m | 73,55 J |
| Série IIIb (1:9) CP 02 | _ | Broken at 7 impacts with 1 kg from 1,5 m | 103,005 J |
| Série IIIb (1:9) CP 03 | _ | Broken at 6 impacts with 1 kg from 1,5 m | 88,29 J |

From the results, it can be noticed that in the series where there is a greater amount of EPS in the paste, the resistance is lower. The difference observed among the resistance of the series Ib, the series IIb and IIIb confirms that the amount of EPS in the paste influences directly in the resistance.

The results of the impact tests showed that specimens with a great amount of cement were the ones that registered the greater values and resisted to a larger amount of impacts (as shown in figure 2).

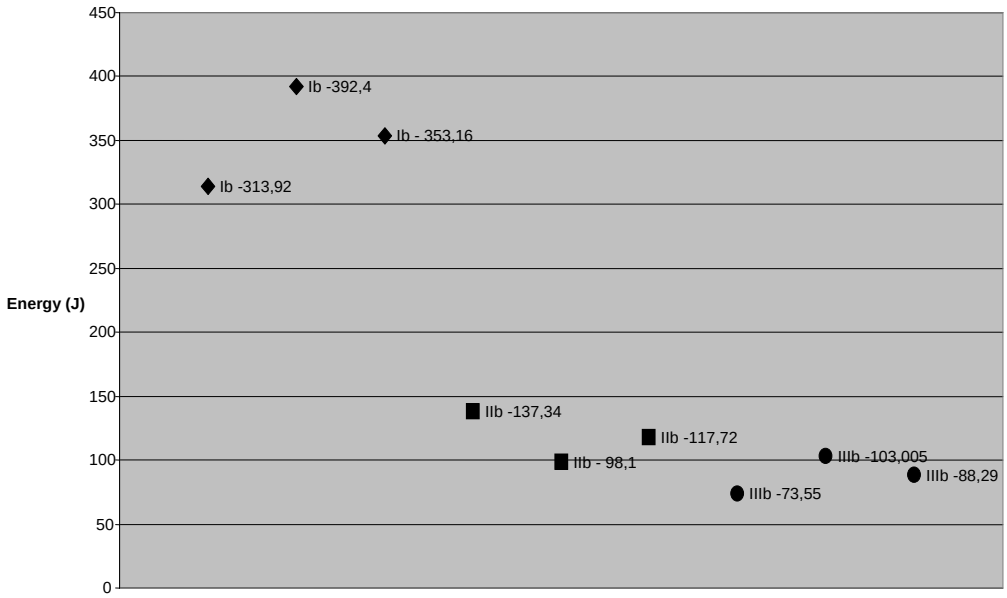



Figure 2 – Graphic - Impact Resistance of all the specimens submitted to the Impact Test according to NBR - 12764 (1992)

The following behavior was noticed in the most resistant specimens: the rupture happened associated to small fissures and crackling of the GRC's superior layer. The fractures of specimens of the series Ib, as can be observed in the figures 3 and 4, were few. However, although they were in lower amount, there was a transfer between the shear of GRC and the layer of concrete with EPS.



Figure 3 – Specimen submitted to impact test according to NBR – 12764 (1992) - Characteristics of the Fractures – Series Ib (1:5)

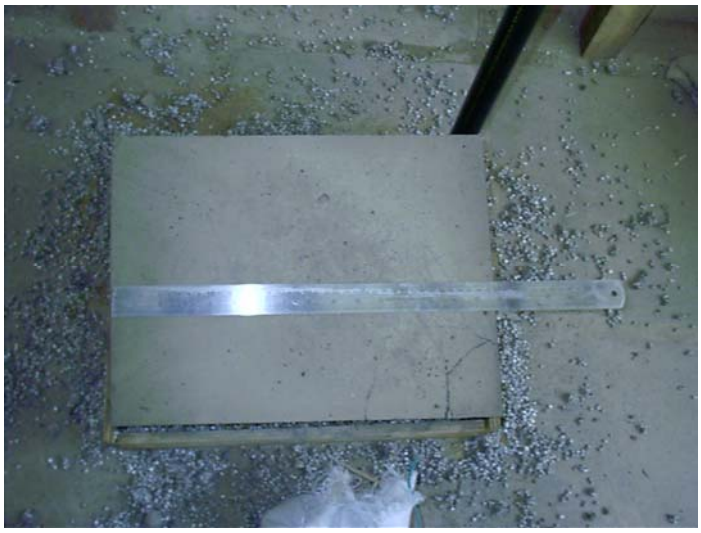


Figure 4 – Specimen submitted to impact test according to NBR – 12764 (1992) - Characteristics of the Fractures – Series Ib (1:5)

In the figures 5 and 6, the broken specimens of the series IIb (1:7) can be observed. The fractures presented were larger and with crackling of the GRC's layer. They appeared in the center and expanded until the diagonals of the specimens. The transfer of the GRC's layer was more accentuated. This behavior can be explained by the presence of a greater quantity of beads of EPS in this series' paste than in the series Ib.



Figure 5 – Specimen submitted to impact test according to NBR – 12764 (1992) - Characteristics of the Fractures – Series IIb (1:7)



Figure 6 – Specimen submitted to impact test according to NBR – 12764 (1992) - Characteristics of the Fractures – Series IIb (1:7)

In the figures 7 and 8, the specimens of the series IIIc can be observed (1:9). In those, the fractures and fissures were larger with a significant dislocament of the layer of GRC. It can be noticed that this mix is less resistant, because of the crackling of the concrete layer with EPS and the break of great parts of the GRC's layer.

It is possible to affirm that the relationship continued among the amount of cement in the paste and the resistance, influencing the type and the size of the fissures and ruptures. In the mixes that had a greater amount of EPS and, consequently, a lower amount of cement, the fissures and fractures were more frequent and larger.



Figure 7 – Specimen submitted to impact test according to NBR – 12764 (1992) - Characteristics of the Fractures – Series IIIb (1:7)



Figure 8 – Specimen submitted to impact test according to NBR – 12764 (1992) - Characteristics of the Fractures – Series IIIb (1:7)

Finally, it was noticed that, in all the mixes the fractures appeared from the center to the diagonals in 45°, breaking the specimens close to the corners. It can be considered that this type of fracture happened in the extremities because they are more fragile.

## 4. CONCLUSIONS

From the results of the impact tests it can be concluded that the amount of cement of the paste is responsible for the increment of the impact resistance, because the specimens made with stronger mixes (1:5) were the ones that registered the greater values and resisted to a greater amount of impacts (impact resistance of 313,92 J to 392,40 J). Other important factor for the resistance was the amount of EPS in the paste. The series which presented a great percentage of that material (mix proportion 1:7 - resistance to the impact of 98,10 J to 137,34 J; mix proportion1:9 - resistance to the impact of 73,55 J to 103,00 J), obtained the lower impact resistance.

In the visual evaluation of the fissures, it was noticed the crackling of the diagonals and the corners. It can be affirmed that the extremities are the weak points of the specimens.

## 5.REFERENCES

Abrapex (Associação Brasileira do Poliestireno Expandido). *Matérias diversas.* Disponível em: <http:/ www.abrapex.com.br>. Acesso em: janeiro de 2004.

American Society for Testing and Materials – ASTM C 947 – *Standard test method for flexural properties of thin-section glass-fiber-reinforced concrete (using simple beam with third-point loading)* – Philadelphia, 1997.

Bagon, C.; Frondistou-yannas, S. (1976) - *Marine Floating Concrete made with Expanded Polystyrene Beads* - Magazine of concrete research – V.28, N. 97, Dez. 1976 - M.I.T., Cambridge, MA, USA.

Balaguaru, P. N.; Shah, S.P. (1992) – *Fibre reinforced cement composites* – Mc Graw Hill International Editions – p. 311-362 , New York, 1992.

Carvalho, A. (1993) – *Fibras de vidro In: Simpósio Internacional sobre Materiais Reforçados com Fibras para Construção Civil* – Anais. EPUSP: p. 41-51, São Paulo, 1993.

Cem-FIL International ltd. *Cem-FIL Technical Data* , Merseyside, 1996. 6pp.

Cem-FIL International ltd. *Cem-FIL Technical Data* , Merseyside, 2000. 87pp

Cook, D.J. (1973) - *Expanded polystyrene beads as lightweight aggregate concrete* – Precast Concr. 4 – p. 691-693 ,1973.

Cook, D.J. in Swamy, R.N. (Ed.) (1983) - *Expanded Polystyrene Concrete* - *CONCRETE TECHNOLOGY AND DESIGN* - Volume I New Concrete Materials – Surrey University Press, p 41-69 , London ,1983.

Forlin, F.J.; Faria, J. A (2002). – *Considerações sobre a Reciclagem de Embalagens Plásticas* – Polímeros:Ciência e Tecnologia – v.12, nº1, jan/mar 2002.

Hohwiller, F. ; Kohling, K. (1968) - *Lightweight concrete filled with Styropor*,- Betonstein-Zeitung – s.d. - N. 34, 1968, p. 81-87, e p. 132-137.

Kohling, K. (1960) – *Prodution of lightweight concrete using prexpanded Styropor beads as aggregate* – BetonsteinZeitung - n. 26, 1960, p. 208-212.

Majumdar, A. J.; Laws, V. (1991) – *Glass fibre reinforced cement* – BSP Professional Books, published on behalf of the Building Research Establishment – 197p, London, 1991.

Mehta, P. K.; Monteiro, P. J. M. (1994) - *Concreto estrutura, propriedades e materiais*. Editora PINI. São Paulo. 1994.

NBR – 7221 (1992) – *Agregados – ensaio de qualidade de agregado míudo determinação* – Associação Brasileira de Normas Técnicas.

NBR – 11752 (1993) – *Materiais celulares de poliestireno para isolamento térmico na construção civil e em câmaras frigoríficas* – Associação Brasileira de Normas Técnicas..

NBR – 12764 (1992) – *Rochas para revestimento – determinação da resistência ao impacto de corpo duro* – Associação Brasileira de Normas Técnicas.

Precast/Prestressed Concrete Institute – PCI (1994) – *Recommended practice for glass fiber reinforced concrete panels* – PCI (*revised edition*)– 99 p, Chigago,1994.

Precast/Prestressed Concrete Institute – PCI (1995) – *Innovation by design: Glass Fiber Reinforced Concrete* – PCI – 15 p, Chigago,1995.

Silva, V. G.; John, V. M. (1998) – *Painéis em cimento reforçado com fibra de vidro (GRC)* – Boletim Técnico da Escola Politécnica da USP, Departamento de Engenharia de Construção Civil – 20p, São Paulo, 1998.

Silva, V.G. (1998) – *Diretrizes para o projeto de painéis de fachada em cimento reforçado com fibras de vidro* – Dissertação (Mestrado), Escola Politécnica, Universidade de São Paulo – 145p, São Paulo, 1998.

Sri Ravindrarajah, R., Tuck, A.J. (1994) - *Properties of hardened concrete containing treated expanded polystyrene beads* – Cement & Concrete Composites – V.16 - nº:4 – p. 273-277, 1994.

Subramanian, P.M. (2000) – *Plastic Recycling and Waste Management in the US* – Resources, Conservation and Recycling – v.28 – p.253-263 – 2000.

Tartuce, R. & Giovanneti, A. (1990) – *Dosagem experimental do concreto* – Ed. PINI – 115 p, São Paulo, 1990.

Vetrovex – *The reinforcement for mortars & concrete* – Vetrovex - 2p, London, 2002.

Vetrovex – *Compósitos Cem-FIL GRC* – Vetrovex –2p, London, 2001.

International Symposium Polymers in Concrete
2 - 4 April 2006
Guimarães, Portugal

# Different gradation influence of tire rubber scraps in the behavior of the high performance concrete

Israel Rodrigo de Freitas Martins [1], Jorge Luís Akasaki [2]

*São Paulo State University – Unesp – Campus of Ilha Solteira*
*Civil Engineering Department*
*Al. Bahia, n° 550 – CEP: 15385-000, Ilha Solteira – SP – Brazil. Tel:+55 18 3743-1213 – Fax: + 55 18 3743-1160.*
*e-mails: rf@dec.feis.unesp.br [1], akasaki@dec.feis.unesp.br [2].*

## ABSTRACT

The great amount of discarded idle tires annually in all globe confront strongly the ambient questions, being essential studies that define possibilities of the effective reuse of these tires.

Thus it was opted to studying the application of tire rubber scraps in the manufacture of high performance concrete, which are being each time more employees due its high capacity of compressive strength and good indices of durability.

The present work evaluates the influence of the addition of tire rubber scraps, with different grain sized bands, how much the workability and the compressive strength of the high performance concrete.

Analyzing the gotten results one observed significant alterations in the behavior of the high performance concrete, when in the fresh state, relation to the variation of the granulometry of the tire rubber scraps employed. Being that, in hardened state the influence of the tire rubber scraps granulometria was demonstrated more forceful to the measure of the increment added amount.

## 1. INTRODUCTION

In the world contemporary, where many problems are wordily, great compromise in uniting the propulsion of the development with the preservation of the environment exists, thus a real interest for the recycling is noticed of manufactured that they devastate the globe and they compromise the quality of life to world-wide population.

Having as approach the sustainable development, diverse on agencies to the preservation of the environment in some countries of the world, are becoming more

[1] Prof. MSc.
[2] Prof. Dr.

rigid the environmental laws each time.

In this context the accumulation of idle tires is fit with great representation, thus, diverse researchers of different areas of interest studies the exploitation of this potential in an enormous gamma of applications, amongst which its use in the production of asphalt and Portland cement concrete is also had.

According to Bignozzi and Sandrolini (2004), with intention to improve the behavior the changes of temperature and the resistance mechanics of the asphalt cement the rubber addition of idle tires has been investigated for more than thirty years, being such advantageous addition in diverse aspects. Still in agreement with these authors the studies of the rubber use of idle tires in Portland cement concrete exist to about one decade and amongst varied objective it is had analysis of the influence in the behavior of breaking of the concrete ones.

Olivares and Barluenga (2004) had studied the staple fiber addition of tire rubber in the behavior of high strength concrete of the how much its performance to the fire and had evidenced an advance in its capacity of resistance to the fire due to rubber addition.

Recently, Martins and Akasaki (2005) had considered the implementation of tire rubber scraps in High Performance Concrete (HPC), verifying that the values of compressive strength for high performance concrete added of low percentages of these scraps, although reduced but are remained in significant platforms, and had still presented, in relation to the HPC, profits how much to the ductile.

The HPC is that one that possess resistance mechanics high; above of 42MPa according to Shah and Ahmad (1994); which must be enough to receive the requests imposed in the project, and definitively it reveals durable to the long one of the time, characterizing itself also for the excellent election of constituent materials and rigorous controls of production.

In this line of research this work approaches on questions the influence of the tire rubber scraps granulometry added in of high performance concrete, aiming at not only contributing for the improvement of the high performance concrete ones but also to the sustainable development, to the measure that promotes the use of a harmful residue to the environment.

## 2. MATERIALS

The materials used in the development of the compositions of high performance concrete in this study had been: cement Portland CP II F (Filler) in compliance with the Brazilian norm for cements composites NBR 11578 – Associação Brasileira de Norma Técnicas - ABNT (1991), silica fume in dense form, superplasticizer to the base of policarboxilato with maximum dosage of 2 %, basaltic crushed stone with maximum particle size of 19 mm, natural sand with fineness modulus of 2,09 and tire rubber scraps (TRS) in different bands grain sized, proceeding from the process of retreading tires.

In Figure 1, are presented, on the basis of the NBR 7217 - ABNT (1993), the grain sized curves of natural aggregates and the diverse used tire rubber scraps. Where the Total TRS represents the sum of the TRS selected for sieving and then classified in Thin (25,0 %) with granular format, Medium type (27,2 %) and Rough (45,9 %) with formats type fiber, totalizing 98.1 % of the general granulometry of the tire rubber scraps in the state where it is discarded for the retreading company, being that only 1.9 % of its granulometry were excluded from this study

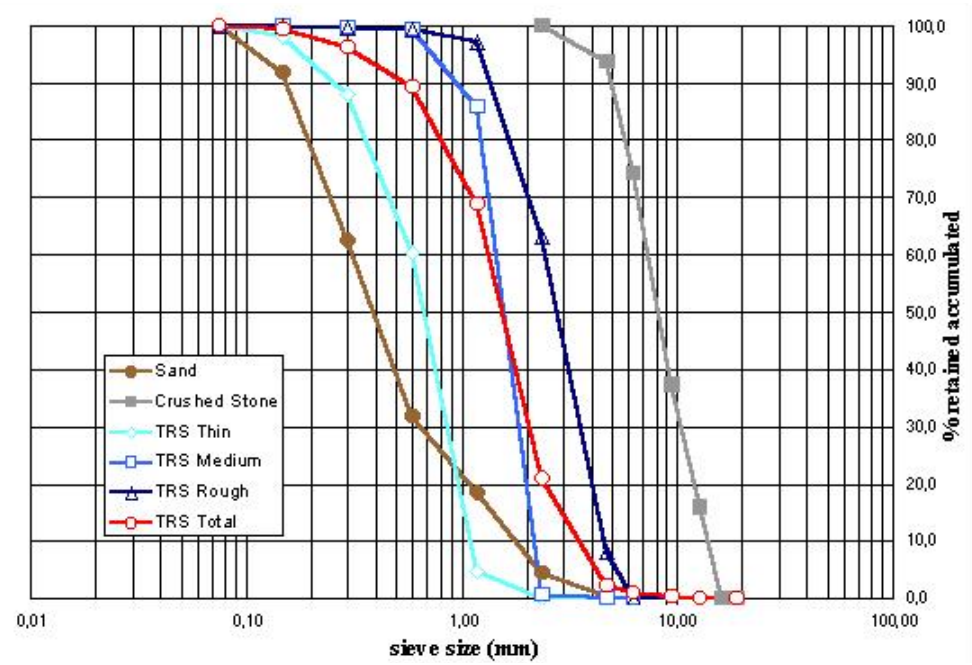



Figure 1 – Sieve analysis of aggregates and TRS ones.

## 3. EXPERIMENTAL PROGRAM

### 3.1. Mixtures

The used method of dosage was the Aïtcin method, elucidated in Aïtcin (2000), which is specific for HPC and of simplified methodology, a time that is establish in empirical results.

Thus the composition of the HPC is presented in the Table 1.

Table 1 – Composition of HPC.

| Materials | Proportioning |
|---|---|
| Water | 130,0 kg/m³ |
| Cement | 478,4 kg/m³ |
| Silica Fume | 41,6 kg/m³ |
| Water/Agglomerate | 0,25 |
| Sand | 774,3 kg/m³ |
| Crushed Stone | 1125,0 kg/m³ |
| Superplasticizer | 5,74 kg/m³ |

In the sequence, from the simple volumetric partial substitution of the TRS in the sand, in the same way that Olivares and Barluenga (2004), in the percentages of 3 % and 5 % in relation to a cubical meter, had determined the diverse mixtures of high performance concretes with addition of enumerated TRS following. Where in special the mixture had that was composed with Total TRS, in the which had ampler grain sized

band of this scraps, was opted to volumetric partial substitution in 50 % of crushed stone and 50 % of the sand, as adopted for Güneyisi, Gesoglu and Özturan (2004), having itself evaluated only in the percentage of 3 % in relation to the cubical meter.

I. Mixture HPC TRS Thin 3 %
II. Mixture HPC TRS Thin 5 %
III. Mixture HPC TRS Medium 3 %
IV. Mixture HPC TRS Medium 5 %
V. Mixture HPC TRS Rough 3 %
VI. Mixture HPC TRS Rough 5 %
VII. Mixture HPC TRS Total 3 %

### 3.2. Test Methods

The rheological behavior of the high performance concrete ones produced was evaluated through the discouragement of the slump test, in accordance with NBR NM 67 - ABNT (1998).

Had been used cylindrical specimens of 10 X 20 cm, which had been kept in humid chamber with controlled temperature until the respective ages of test.

The high performance concrete ones had been evaluated how much its compressive strength, according to NBR 5739 - ABNT (1994), in the ages of 3, 7, 28 and 91 days of age.

Previously to the tests of compressive strength the specimens had its end faces capped with a high strength sulfur mortar, aiming at exempt them of possible eccentricity.

## 4. RESULTS AND DISCUSSION

### 4.1. Fresh Properties

Aiming at to provide one better condition of visual comparison Figure 2 enters the diverse elaborated traces, presents in set the slumps all the elaborated mixtures.

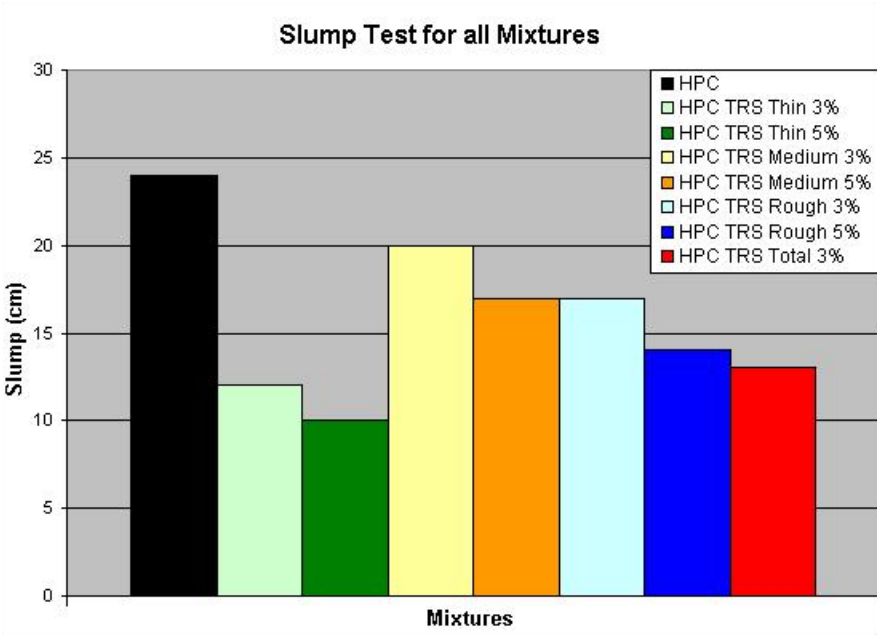



Figure 2 – Workability of all mixtures.

Analyzing Figure 2, great influence of the granulometry of the TRS employed is still observed that the workability of the HPC reveals affected due to implementation of the TRS, being distinguished.

Thus, amongst the different granulometry of TRS mixtures with Medium TRS had presented the reduction of workability of less sharp form. Being distinguished that beyond Medium HPC TRS 3 % having presented the best workability, amongst the too much added mixtures of scraps, the trace of HPC TRS Medium 5 %, it was not surpassed, how much the workability, for none another trace of HPC TRS of any granulometry, also to those with 3 % of scraps.

The traces that had presented the lesser workability had been to those with Thin addition of TRS, considering also the mixture of HPC TRS Total 3 %.

How much to the mixtures of Rough TRS, certain difficulty in the final planning of the surface of the specimens was observed, exactly had to the biggest length of such scraps.

## 4.2. Hardened Properties

Figure 3, presents in set the evolution of the compressive strength for the respective mixtures evaluated in Figure 2, being that each pointed value is resulted of the average of three specimens.

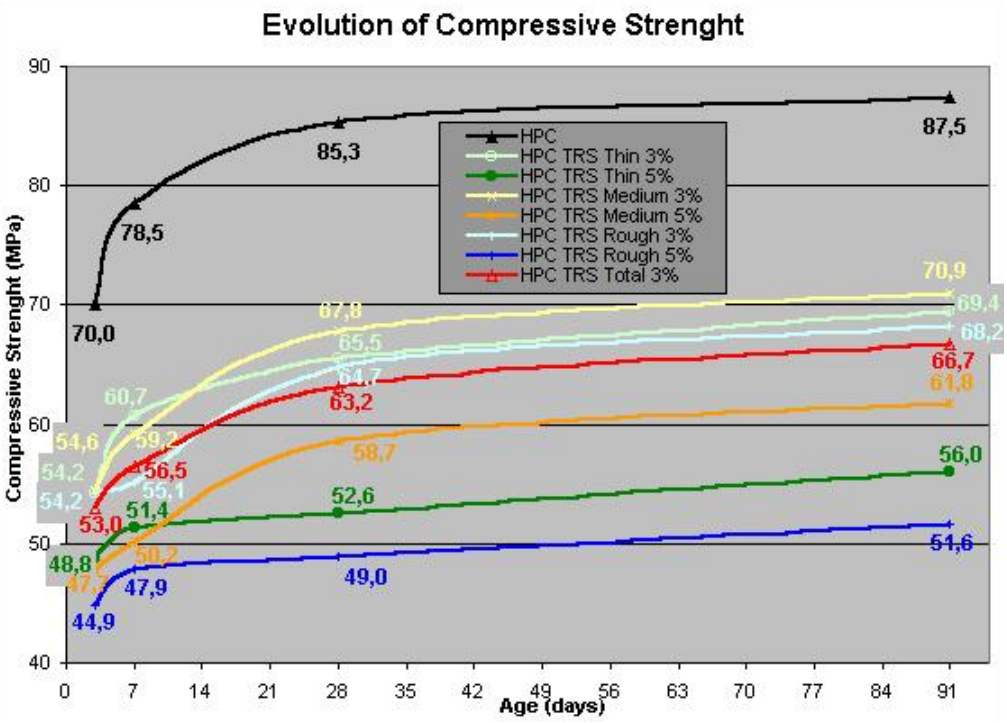



Figure 3 – Evolution of compressive strength for all mixtures.

As it is foreseen by literature occurred the reduction of the compressive strength with the implementation of the TRS, it has since the mixture with addition of 5 % rubber had presented minors values of compressive strength in comparison to the values gotten for the mixture with 3 % of addition, which in turn had been inferior to those of the HPC mixture.

In general way, the percentage of reduction of compressive strength observed in the mixture of HPC TRS 3 % in relation to the mixture of HPC, this around 20 to 25 %. However the indicative values of the compressive strength for such mixture are without pertaining doubts to the group of high performance concrete.

On the other hand to this reduction of compressive strength, it was possible to observe, in relation to the mixture of HPC, the reduction of the fragility in the behavior of rupture in all the mixtures with TRS addition. Aiming at to illustrate such fact Figure 4 presents a typical specimen of the HPC mixture after to have been tested to the compression, while one another specimen, visualized in Figure 5, represents of characteristic form the ruptures gotten for the mixtures with TRS.



Figure 4 – Typical specimens of HPC, breached after compression test.



Figure 5 – Typical specimens of HPC TRS, breached after compression test.

It is distinguished amongst the traces with addition of 5 % of TRS, to that one with Medium scraps, which was the only one to present a significant increase of compressive strength, in special, between the seventh and twentieth eighth day.

Being based on the referring results to HPC TRS Total mixture 3 %, although inferior to the mixture of HPC TRS 3 %, they demonstrate the viability of the use of the tire rubber scraps, almost that integrally, or either 98,1 %.

The comment of the reduction of the fragility in the behavior of rupture in all the traces with rubber addition, in relation to the trace standard, from the carried through tests do not have the capacity to determine a quantitative measure of the extension of such reduction. Analyzing itself only qualitatively, or either, in relative way to the mixture of HPC, the reduction it fragile behavior in the high performance concrete ones with addition of tire rubber scraps, occurred indifferently for the concrete ones added in 3 % or 5 %.

Amongst the added traces high performance concrete of 3 % TRS, to that one consisting by the Medium rubber it demonstrated to superiority how much its

workability; and still excellent evolutions of compressive strength independently of the analyzed percentage.

However, it is valid to remember that amongst other possibilities to the combat of the bad workability, observed for some types of granulometry of rubber, fast increases in the water/agglomerative relation could be tried, as for example its rise 0,28 or 0,30, however, verifying always the performance how much to the compressive strength.

## 5. CONCLUSIONS

The workability of the high performance concrete ones is affected due to implementation of tire rubber scraps, and still it suffers to significant influence how much the granulometry from this scraps. In thus high performance concrete the scraps of granular format, assigned in this study of fine TRS, result in a significantly lesser workability, then in this approach its use, mainly separately must be prevented.

The behavior of rupture of the HPC with addition of tire rubber scraps is differentiated, in that the fragility presented for the high performance concrete ones in general way says respect.

The high performance concrete ones with addition of TRS in the 3 % percentage, had presented values of sufficiently next compressive strength, independently of the granulometry of employed rubber.

With the rise of the percentage of tire rubber scraps in the HPC to the 5 % percentage, the respective values of compressive strength had demonstrated to a bigger trend of distinction due the granulometry of employed rubber.

However, as the mixtures of HPC TRS 3 % as those with 5 %, respectively, they present the same sequence, considering itself it increasing order of average values of compressive strength, how much the granulometry of the residues: Rough, Thin and Medium.

The use of pertaining tire rubber scraps to a more extensive grain sized band, as to that one used in HPC TRS Total 3 % mixture rubber, instead of more select granulometry, also revealed viable to the HPC production, and thus they extend the possibility of a bigger percentile exploitation of these residues.

## 6. ACKNOWLEDGEMENTS

The authors desire to thank the companies who had donated the materials used in this research: Votorantim Cimentos, Camargo Corrêa/CAUÊ, Sika do Brasil, Porto de Areia São Judas, Mineração Noroeste Paulista, Regigant Recuperadora de Pneus Pará and to Laboratório CESP de Engenharia Civil.

## 7. REFERENCES

Aïtcin, P. C. *Concreto de alto desempenho*. 1°ed. São Paulo: PINI, (2000). 667p.

Associação Brasileira de Normas Técnicas. *NBR 7217*: agregados – Determinação da composição granulométrica. Rio de Janeiro: ABNT, (1993).

Associação Brasileira de Normas Técnicas. *NBR 11578*: cimento Portland composto. Rio de Janeiro: ABNT, (1991).

Associação Brasileira de Normas Técnicas. *NBR NM 67*: concreto –

Determinação da consistência pelo abatimento do tronco de cone; procedimento. Rio de Janeiro: ABNT, (1998).

Associação Brasileira de Normas Técnicas. *NBR 5739*: concreto – Ensaio de compressão de corpos-de-prova cilíndricos. Rio de Janeiro: ABNT, 1994.

Bignozzi, M. C.; Sandrolini, F. Recycling tire rubber in building materials. In: *International Conference Sustainable Waste Management and Recycling: Challenges and Opportunities*, 2004, England. Anais… England: Kingston, (2004).

Güneyisi, E.; Gesoglu, M.; Özturan, T. Properties of rubberized concretes containing silica fume. *Cement and Concrete Research*. v 34, p 2309-2317, (2004).

Martins, I. R. F.; Akasaki, J. L. Avaliação da adição de fibras de borracha de pneus no comportamento do CAD. In: *Congresso Brasileiro do Concreto, 47°*, 2005b, Recife. Anais... Recife: IBRACON, (2005). CD-ROM, Trabalho 47CBC0209.

Olivares, F.H.; Barluenga, G. Fire performance of recycled rubber-filled high-strength concrete. *Cement and Concrete Research*. v. 34, p. 109-117, (2004).

# Session 3

International Symposium Polymers in Concrete
2 - 4 April 2006
Guimarães, Portugal

# Core reinforced braided composite armour as a substitute to steel in concrete reinforcement

R. Fangueiro[1], G. Sousa[2], M. de Araújo[3] and C. Gonilho Pereira[4]

*Universidade do Minho, Departamento de Engenharia Têxtil*
*Azurém, P – 4800-058 Guimarães, Portugal*

S. Jalali[5]

*Universidade do Minho, Departamento de Engenharia Civil*
*Azurém, P – 4800-058 Guimarães, Portugal*

## ABSTRACT

This paper presents the work that is being done at the University of Minho concerning the development of braided rods for concrete reinforcement. Several samples of core reinforced braided fabrics have been produced varying the type of braided fabric (core reinforced and hybrid), the linear density of the core reinforcing yarns and the type of braiding structure (with or without ribs). The tensile properties of these samples were evaluated and the results are presented. The influence of each factor on the tensile properties of braided fabrics has also been analysed. Core reinforced braided composites rods were produced and tested to evaluate tensile and bending properties. The results obtained are presented and discussed. Reinforced concrete beams, with composite armour and steel armour, were produced and were subjected to bending test and the test results are presented. The adherence between composite rods and concrete was analysed as well.

## 1. INTRODUCTION

Concrete structures are subjected to repeated loading and to aggressive environmental agents which may lead to poor mechanical and durability performance of the structures with time. One of the most serious problems affecting concrete is corrosion of the steel reinforcement. As shown in Figure 1, corrosion may occur as a result of the reaction of lime present in hydrated cement with carbon dioxide or to the action of chlorides. In the first case, the lime reaction with the carbon dioxide, existing in the atmosphere, leads to a gradual decrease in concrete alkalinity. When the concrete cover pH is lower than 9 the compact oxide layer that protects the steel is destroyed, thus leading to the formation of

[1] Professor
[2] Researcher
[3] Full Professor
[4] Researcher
[5] Associate Professor

electrochemical reactions which are responsible for the corrosion of the steel. The chloride ion attack is mainly due to the migration of chloride ions existing in the vicinity of the structure. It is accepted that when the chloride ions reach a given critical concentration the potential for steel corrosion increases significantly. This fact is particularly hazardous in marine or structures in contact with de-icing salts.

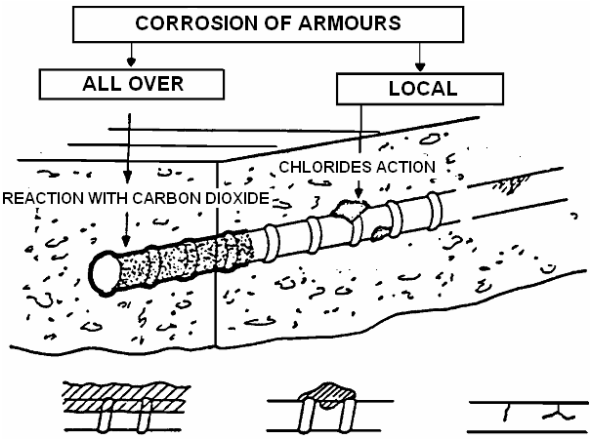



Figure 1 – Corrosion of steel armours

Composite materials are used in civil engineering as a substitute or as a reinforcement of conventional materials, like concrete and steel. The main reasons for the use of composite materials are corrosion resistance, low weight and nonmagnetic properties. In spite of these advantages, the lack of ductility and energy absorbing capabilities are a severe limitation of all these fiber systems if they are to be considered for earthquake resistant applications (Pastore 2004). The resistance to corrosion is one of the most important advantages when compared with steel. In the last years, several studies and applications have been developed using fibre reinforced polymers (FRP). Composite materials can be used in a structural way (as steel is used), as a concrete reinforcement and in rehabilitation of existing structures. The reinforcement of concrete can be done with composite materials reinforced by fibres or adding fibres and polymers to cement. Replacement of steel reinforcement in concrete structures with more corrosion resistant substitutes, such as composites, is rapidly becoming a more economical option for construction facilities worldwide. It's possible to use composite rods substituting ordinary steel armour in concrete reinforcement.

Textile materials are also widely used in civil engineering structures and it is possible to adapt some textile production techniques to produce new composite materials with structural function.

Braiding technique is probably the most ancient production process for textile structures. Normally used for ropes and cables, braided fabrics are also very interesting for composite reinforcements due to their characteristics: in-plane multiaxial orientation, conformability, excellent damage tolerance and cost. The braiding technique can produce a wide range of preforms for composite reinforcements, however, the number of yarn bobbins in the braiding machine limits the dimensions of the fabric.

## 2. STUDY ON THE MECHANICAL BEHAVIOUR OF BRAIDED FABRICS

In order to evaluate the mechanical behaviour of braided fabrics when subjected to tensile stress, different types of fabrics have been produced, i.e, core reinforcement braided fabrics with and without ribs (core yarns reinforcing axially the braided fabric) and hybrid

braided fabrics (combining different materials and without core reinforcement). Some characteristics of the materials used are summarized in Table 1.

Table1 – Types of fabrics produced.

| | Ribs | Material | Yarn Count (Tex) |
|---|---|---|---|
| Braided fabric | Without | E Glass | 204 Tex |
| Core reinforcement | | E Glass | 6-12 rovings, 900 Tex each |
| Braided fabric | With | E Glass | 204 Tex |
| Core reinforcement | | E Glass | 12 rovings, 900 Tex each |
| Braided fabric | With | E Glass | 204 Tex |
| Core reinforcement | | E Glass | 12 rovings, 900 Tex each |
| | | Carbon | 200 Tex |

Braided fabrics were produced on a vertical braiding machine and the geometrical and dimensional parameters of each material produced have been evaluated. The obtained results are shown in Table 2 according to Figure 2.

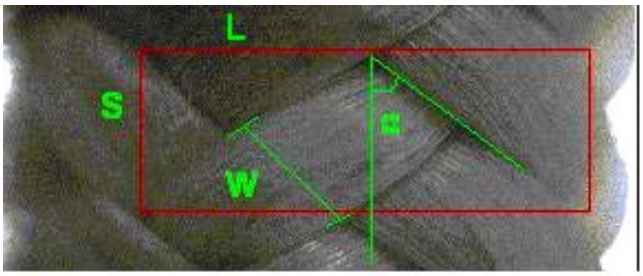



Figure 2 – Geometrical parameters of braided fabrics

Table 2 – Geometrical and dimensional parameters of each braided fabric tested.

| Braided fabric | α (º) | L (mm) | W (mm) | S (mm) | Mass (g/m) | Thickness (mm) | Area ($mm^2$) |
|---|---|---|---|---|---|---|---|
| Glass (6 rovings of glass) | 45,3 | 1,59 | 0,72 | 1,01 | 10,43 | 2,61 | 5,35 |
| Glass (7 rovings of glass) | 45,2 | 1,68 | 0,72 | 1,01 | 11,28 | 2,72 | 5,81 |
| Glass (8 rovings of glass) | 44,8 | 1,77 | 0,73 | 1,01 | 12,27 | 2,82 | 6,24 |
| Glass (9 rovings of glass) | 45,0 | 1,85 | 0,73 | 1,03 | 13,27 | 2,93 | 6,74 |
| Glass (10 rovings of glass) | 44,8 | 1,95 | 0,75 | 1,05 | 14,31 | 3,08 | 7,45 |
| Glass (11 rovings of glass) | 48,2 | 2,07 | 0,7 | 1,08 | 15,39 | 3,16 | 7,84 |
| Glass (12 rovings of glass) | 45,0 | 2,22 | 0,78 | 1,11 | 16,51 | 3,28 | 8,45 |
| Glass (12 rovings of glass) with ribs | 46,1 | 2,55 | 0,82 | 1,12 | 17,78 | 3,45 | 9,34 |
| Glass (12 rovings of glass and 1 roving of carbon) | 48,5 | 2,55 | 0,82 | 1,12 | 17,93 | 3,46 | 9,40 |

2.3 Mechanical properties

Each type of braided fabric has been tested on a Hounsfield H100 KS tensile machine according to standard ISO 2062, using a cross-head speed of 100 m/min. Due to brittleness of glass fiber, samples have been impregnated with polyester resin in the jaws contact area. The results are presented in Table 3.

Table 3 – Mechanical properties of each braided fabric tested.

| Braided fabric | Stress (MPa) | | | Extension (%) | | |
|---|---|---|---|---|---|---|
| | Mean | Stand. Dev. | C. V. | Mean | Stand. Dev. | C. V. |
| Glass (6 rovings of glass) | 336,53 | 28,86 | 8,58 | 2,75 | 0,33 | 11,82 |
| Glass (7 rovings of glass) | 356,83 | 17,75 | 4,97 | 2,72 | 0,17 | 6,11 |
| Glass (8 rovings of glass) | 391,47 | 26,67 | 6,81 | 3,16 | 0,15 | 4,74 |
| Glass (9 rovings of glass) | 413,70 | 22,74 | 5,50 | 3,26 | 0,21 | 6,28 |
| Glass (10 rovings of glass) | 444,93 | 5,74 | 1,29 | 3,79 | 0,31 | 8,11 |
| Glass (11 rovings of glass) | 454,16 | 14,15 | 3,12 | 3,93 | 0,50 | 12,71 |
| Glass (12 rovings of glass) | 477,07 | 25,04 | 5,25 | 4,18 | 0,28 | 6,66 |
| Glass (12 rovings of glass) with ribs | 522,65 | 15,88 | 3,04 | 4,00 | 0,15 | 3,74 |
| Glass (12 rovings of glass and 1 roving of carbon) | 429,96 | 8,99 | 2,09 | 5,15 | 0,63 | 12,15 |

The geometrical and dimensional parameters of each braided fabric are different and as the number of core rovings increase, the maximum load supported and the extension are also increasing. Core reinforced braided fabric with ribs presents an increase of 10% on the supported load and a decrease of 4% on the extension when compared with core reinforced braided fabric without ribs. The presence of carbon fiber reviled a decrease on mechanical properties.

## 3. BRAIDED REINFORCED COMPOSITE RODS

Braided reinforced composite rods have been produced and tested. Table 4 presents some characteristics of the rods produced. Moreover, the adhesion between concrete and composite rods has also been evaluated and discussed.

Table 4 – Types of composite rods produced.

| Braided fabric | Ribs | Material | Yarn Count (Tex) |
|---|---|---|---|
| Core reinforcement | With | E Glass | 204 Tex |
| | | E Glass | 12 rovings, 900 Tex each |
| Core reinforcement | With | E Glass | 204 Tex |
| | | E Glass | 12 rovings, 900 Tex each |
| | | Carbon | 200 Tex |

### 3.1 Production

The samples have been produced on a conventional braiding machine specially adapted to impregnate simultaneously the braided fabrics. In order to increase roughness of the braided reinforced composite material rods, and then its adhesion to the concrete, braided fabrics have been produced as a ribbed structure, as shown in Figure 3. This ribbed structure is provided by thicker yarns that are used in the braiding machine in a combination of 7 standard to 1 thicker yarn. For a stronger effect on roughness the number of thicker yarns could be increased during braiding the process.

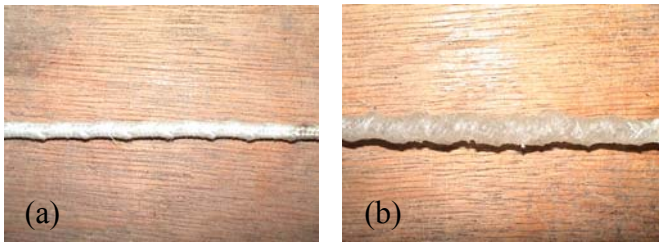



Figure 3 – Ribbed structure
(a) braided fabric (b) braided reinforced composite rod

The glass braided fabrics have been produced and simultaneously impregnated with a polyester thermosetting resin, with the reference Quires 272 THV, according to the following percentages: Resin 272 THV + 0.3% of CO accelerator + 2% of Butanox M60 catalyser. The characteristics of the composite material rods produced are shown in Table 5.

Table 5 – Characteristics of the composite material rods.

| Braided fabric type | Fibre type | Fiber volume fraction (%) | Resin volume fraction (%) |
|---|---|---|---|
| Core reinforced | Braiding yarns: 204 tex, E glass fiber and 900 tex, E glass fiber<br>Core reinforcement: 12 E glass fiber 900 tex rovings | 44,45 | 55,55 |
| Core reinforced | Braiding yarns: 204 tex, E glass fiber and 900 tex, E glass fiber<br>Core reinforcement: 12 E glass fiber 900 tex rovings and carbon fiber 200 tex roving | | |

3.2 Mechanical properties

For the evaluation of the tensile properties of the braided reinforced composite rods produced, experimental work has been undertaken using a HOUNSFIELD universal tensile tester, according to NP 2257 standard, at a cross-head speed of 1 mm/min. The results obtained are shown in Table 6 while Figure 4 shows the typical stress-strain curve.

Table 6 – Tensile properties of composite reinforced rods (mean value of 10 tests).

| Braided fabric type | Fibre type | Final Strength (MPa) | Extension at maximum stress (%) | Young´s modulus (GPa) |
|---|---|---|---|---|
| Core reinforced | Braiding yarns: 204 tex, E glass fiber and 900 tex, E glass fiber<br>Core reinforcement: 12 E glass fiber 900 tex rovings | 437,20 | 6,18 | 12,88 |
| Core reinforced | Braiding yarns: 204 tex, E glass fiber and 900 tex, E glass fiber<br>Core reinforcement: 12 E glass fiber 900 tex rovings and carbon fiber 200 tex roving | 593,95 | 8,89 | 9,60 |

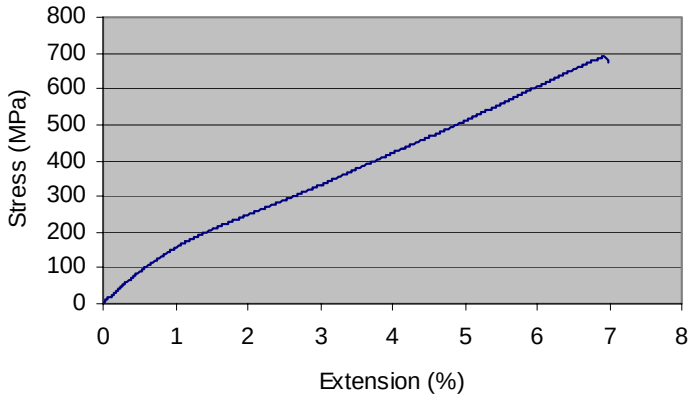



Figure 4 – Typical stress-strain curve for braided reinforced composite rods.

Bending properties were also evaluated on glass fibre composite rods, according to ISO 14125, using HOUNSFIELD H100 KS, at a cross-head speed of 1 mm/min and 100mm distance between supports. The results obtained are shown in Table 7.

Table 7 – Bending properties of composite reinforced rods (mean value of 5 tests).

| Braided fabric type | Fibre type | Final Strength (MPa) | Deflection at maximum stress (mm) | Young´s modulus (GPa) |
|---|---|---|---|---|
| Core reinforced | Braiding yarns: 204 tex, E glass fiber and 900 tex, E glass fiber<br>Core reinforcement: 12 E glass fiber 900 tex rovings | 521,12 | 15,24 | 12,31 |

Analysing tensile properties, glass/carbon composite rod presents higher final strength when compared with glass composite rods. The strength increased 36% and the deformation at final strength had an increase of 44%. The Young's modulus decreased 25%.

When analysing bonding properties, it is concluded that the values of final strength and Young's modulus are not so different when compared with the results obtained with tensile test.

3.3 Adhesion to the Concrete

In order to evaluate the adherence between the braided composite rods and the concrete, 8 samples have been prepared, as shown in Figure 5. The samples have been tested on a universal tensile tester (Figure 6), at a cross-head speed of 0.1 mm/s, according to standard NP EN 10002-1 usually used for steel. The braided composite rods have completely adhered to the concrete up to the breaking point.



Figure 5 – Samples for adherence test

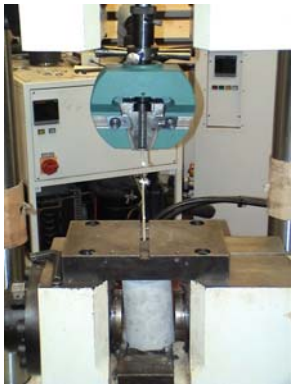


Figure 6 – Adherence test

## 4. CONCRETE BEAMS REINFORCED BY BRAIDED REINFORCED RODS

### 4.1 Samples preparation

Three concrete beams reinforced by an armour of braided composite rods (Figure 7) and three concrete beams reinforced by an armour of steel were prepared with the configuration presented in Figure 8. The dimensions of the beams are presented in Figure 9.

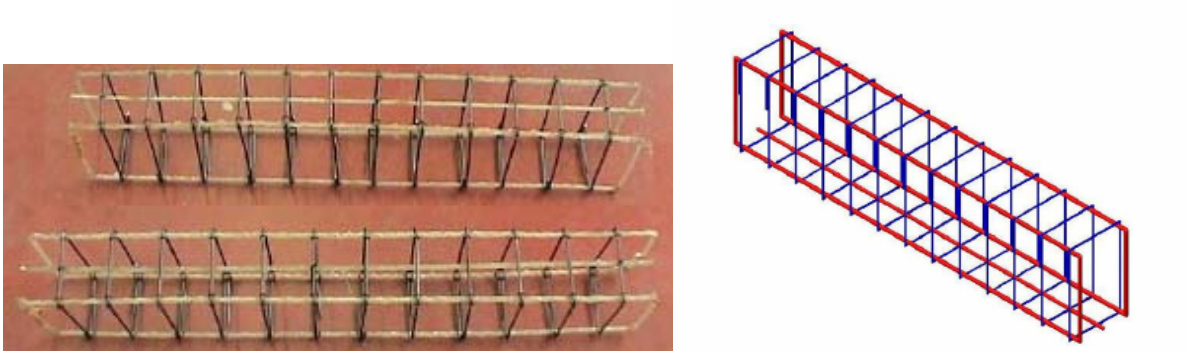


Figure 7 – Composite rods reinforcements used.

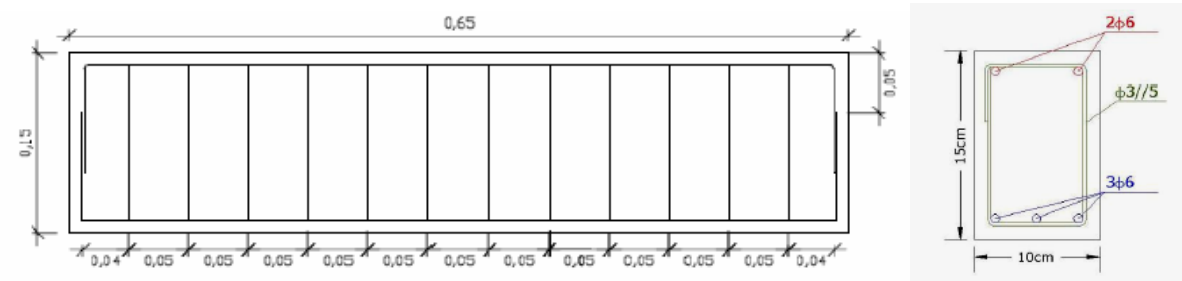



Figure 8 – Configuration of reinforcement used.

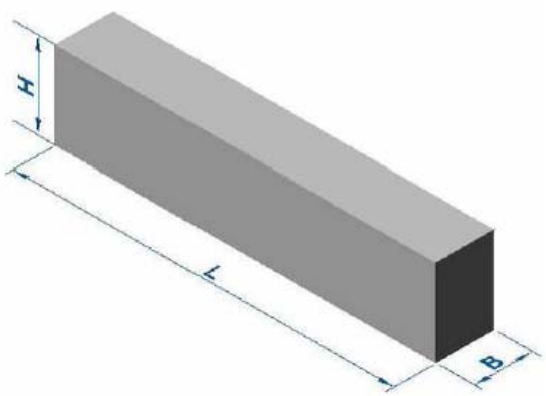



Figure 9 – Beam dimensions (B=10 cm; H=15 cm; L=65 cm)

Were produced 60 L of concrete according to the Table 8.

Table 8 – Constitutes and quantities of concrete.

| Constitutes | Quantity per $m^3$ of concrete |
|---|---|
| Cement (CEM I 42,5R) [kg] | 339,9 |
| Sand [kg] | 868,0 |
| Aggregates [kg] | 864,6 |
| Water [L] | 201,6 |

The concrete curing process occurred in three different steps: 24 hours in the place where the beams were made (Laboratory of Civil Engineering, University of Minho); 20 days in water at a temperature of 20 ºC; 6 days at a room temperature of 20ºC and 100% relative humidity. (Figure 10)



Figure 10 – Concrete beams reinforced by composite rods-

3.2 Testing and results

The beams were tested in bending in a hydraulic press with a speed of 10 μm/s. The displacements and the corresponding loads were registered (Figure 11).



Figure 11 – Three point bending test for concrete beams reinforced by composite rods.

Table 9 and 10 present the results obtained for each type of beam tested.

Table 9 - Bending test results for beams reinforced by steel (mean values of 3 tests).

| Concrete reinforced with steel armour | Strength (kN) | | Elongation at failure (mm) | |
|---|---|---|---|---|
| | Mean | C. V. | Mean | C.V. |
| | 60,50 | 4,30 | 3,43 | 28,72 |

Table 10 - Bending test results for beams reinforced by composite rods (mean values of 3 tests).

| Concrete reinforced with composite rods armour | Strength (kN) | | Elongation at failure (mm) | |
|---|---|---|---|---|
| | Mean | C. V. | Mean | C. V. |
| | 30,80 | 4,04 | 6,57 | 21,29 |

Figure 12 presents a beam after testing. The broken braided reinforced composite rods are shown.



Figure 12 – Beam produced with braided reinforced composite rods after testing.

Figure 13 presents the load-deformation curves for each type of beam tested.

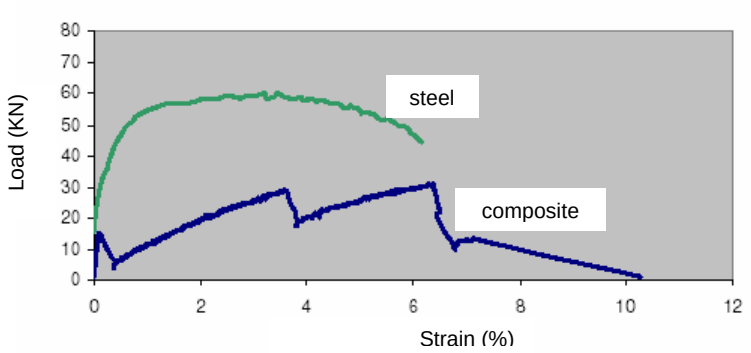



Figure 13 – Load-strain curves for concrete beams reinforced by composite rods and steel.

Analysing the results obtained and the correspondent load-extension curves it is possible to detect different performances between both types of beams tested. The steel reinforced beams carry twice as much load compared to composite reinforced beams. Moreover, strain values of the steel reinforced beams are lower than those obtained for beams reinforced by the composite rods.

In the load-strain curves obtained for the composite reinforced beams, three peaks are visible that correspond to the breaking point of each of the composite rods used. These peaks show that the rods in the reinforcement are not stressed simultaneously. Moreover, the first peak indicates that the reinforcement is not bearing the full load at the initial stage of testing. This behaviour is probably due to the rather loose state of the composite rods that are tensioned only after some considerable deformation of the beam.

## 4. CONCLUSIONS

In order to evaluate the mechanical behaviour of braided fabrics when subjected to tensile stress, core reinforced braided fabrics were subjected to tensile stress. Based on tensile test results, it can be concluded that as the number of core rovings increase, the maximum load supported increases also, as well the extension value. The results of tensile test shows that core reinforced braided fabric with ribs present higher final strength and lower extension at final strength.

Composite rods were subjected to tensile stress and bending. Based on tensile test results, it can be concluded that glass/carbon composite rod presents higher ultimate strength, higher deformation at ultimate strength and lower Young's modulus when compared with glass composite rods.

When analysing bonding results on composite rods, it is concluded that the values of final strength and Young's modulus are not so different when compared with the results obtained with tensile test.

Concrete beams reinforced by composite rods carried half load compared to steel reinforced beams and strain values are higher than those obtained for beams reinforced by steel rods.

The composite rods used to reinforce concrete beams were not stressed simultaneously, then the behaviour of concrete beam when subjected to bending present three peaks that correspond to the breaking point of each of the composite rods that were used.

## REFERENCES

Coutinho, A. de Sousa, Gonçalves, Arlindo, Production and properties of concrete, vols I, II e III, Lisbon, (1988) (only available in portuguese).

Fangueiro, R., Soutinho, F, Jalali, S. and Araújo, M., Development of Braided Fabrics For Concrete Reinforcements, Proceedings of 4rd AUTEX CONFERENCE, Roubaix, France, 22-24 June, (2004).

Fangueiro, R., G. Sousa, Soutinho, F, Jalali, S. and Araújo, M., Braided Fibre Reinforced Composite Rods for Concrete Reinforcement, Proceedings of 5rd AUTEX CONFERENCE, Portorož, Slovenia, 27-29 June, (2005).

Ko, F.K., Three dimensional Fabrics for composites, Textile Structural Composites: Series 3, Chou, T.W. and Ko, F.K., Editors, Elsevier, New York, (1989).

Mendes, M T., Gonçalves S. C., Alves, S. M., Braided structural elements for concrete reinforcement, Graduation Project, University of Minho, Guimarães, Portugal, (2004) (only available in portuguese).

Olcina, S., Braiding Structures to Substitute Steel in Civil Engineering Construction, Graduation Project, University of Minho, Guimarães, Portugal, (2005) (only available in portuguese).

Pastore, C., Ko, F. and Harris, Harry, Braided Hybrid Composites for Bridge Repair and Construction, (2004),

Somboonsong, W., "Development of ductile hybrid fiber reinforced polymer (D-H-FRP) for concrete structures", Ph.D.Thesis, Department of Civil and Architectural Engineering, Drexel University, Philadelphia, PA, December, (1997).

Sousa, G., Braided structures for concrete reinforcement, Master Thesis, University of Minho, Guimarães, Portugal, (2004) (only available in portuguese).

International Symposium Polymers in Concrete
2 - 4 April 2006
Guimarães, Portugal

# Bond behaviour of polymer impregnated AR-Glass textile reinforcement in concrete

Butler, M.[1]; Hempel, R.[1] and Schorn, H.[2]

*Technische Universität Dresden, Building Materials Institute*
*D 01062 Dresden, Germany,*

## ABSTRACT / INTRODUCTION

The formation of the interface zone between the filaments of a multi filament yarn (i.e. Roving) and cement matrix significantly determines the bond behaviour of the compound material Textile Reinforced Concrete (Schorn 2004/A).

The outer filaments of the roving (sleeve fibres) are well bonded to the matrix, the inner filaments (core fibres) are hardly reached by hydration products. Therefore, only few inner filaments contribute to load carrying behaviour. This contribution is mainly based on friction bond. Hence, the load transfer at small crack widths is basically realised by the sleeve fibres (Schorn 2003).

A higher utilisation factor of the entire multi filament yarn can be achieved by an additional impregnation of the roving with aqueous polymer dispersions. Due to their small diameter (150 – 200nm) the polymer particles better penetrate into the core region of the roving than cement particles (Schorn 2002). Using this polymer modified reinforcement in cement matrix the bond of fibre-matrix-interface is primarily realised by hydration products. Forthcoming hydration products can interact with polymer particles improving the bond behaviour. In this case forces can be better transmitted into the core of the roving even at small cracks via the polymer particles among the filaments.

Some selected results of the influence of polymer impregnated textile or polymer modified matrix on the bond behaviour will be discussed in the following paper.

## 1. USED MATERIALS

### 1.1. Characterisation of Used Polymers

Two polymers with different film forming temperatures were used. They are available under the trade name ACRONAL produced by BASF-AG.

[1] Dipl.–Ing.
[2] Professor

1.1.1. State before film forming (Uncured state)

*polymer 1 (Acronal A969)*

- The film forming temperature is 55°C.
- The effused polymer dispersion is brittle. Under marginal loading or decreasing water content it breaks to clods or pulverises (Fig. 1).
- The hydrophilicity is very good (Fig. 2). Due to addition enough water the effused polymer dispersion gets mellow again and a re-dispersion of the polymer occurs.




Fig.1: Effused polymer 1 (A969) after drying at 20 °C



Fig. 2: Drop test on effused polymer 1 after drying at 20 °C [top, bellow]

*polymer 2 (Acronal S400)*

- Because of the low film forming temperature at only 1°C the uncured state did not be evaluated under practical aspects.

1.1.2. State after film forming (Cured State)

*polymer 1 (Acronal A969)*

- Exceeding the minimum film forming temperature at 55°C the cross linking of polymer particles begins, after storage about 2 hours it forms a transparent-glossy and brittle film (Fig. 3). Under load the film tends to disruption.
- The water doesn't penetrate into the film and the film doesn't re-disperse (Fig. 4).
- The film shows a clearly better alkali resistance in NaOH-Base than the uncured product.

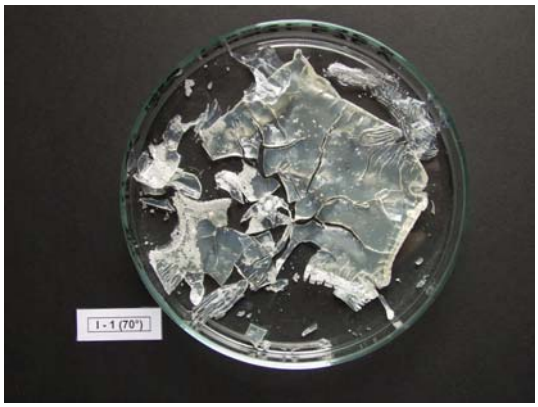



Fig. 3: Effused polymer 1 (A969) after drying at 70 °C

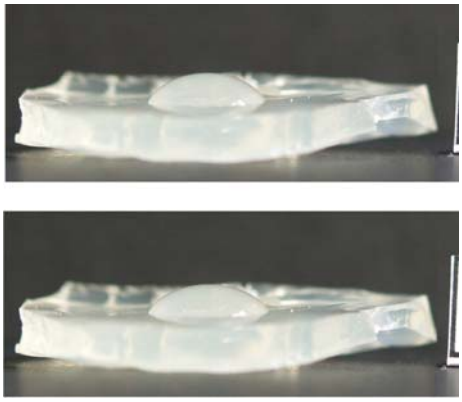


Fig. 4: Drop test on effused polymer 1 after drying at 70 °C [top, bellow]

[top] : 2 seconds after drop up
[bellow]: 90 seconds after drop up

*polymer 2 (Acronal S400)*

- After evaporating the dispersion water the polymer particles are forming a mellow, very elastic and transparent film (Fig. 5).
- The film shows at nearly all surfaces a good adhesion.
- The water doesn't penetrate into the film and the film doesn't re-disperse (Fig. 6).
- The film primary shows a high alkali resistance in NaOH-base. With increasing duration of storage maceration and whitening of polymers can be observed due to the alkali attack.




Fig. 5: Effused polymer 2 (S400) after drying at 20 °

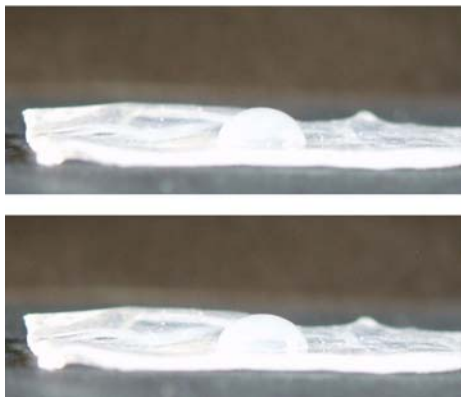


Fig. 6: Drop test on effused polymer 2 after drying at 20 °C [top, bellow]

## 1.2. Characterisation of Textile Reinforcement

### 1.2.1. Base material

AR-glass fibre rovings with a yarn count of 1100 tex from NEG-company were used as reinforcement. The concrete specimens were reinforced by 7 rovings, so that multi crack formation regularly doesn't occur but strain behaviour appears only at one crack. The fibre volume content of the specimens is 0.35 % Volume. Table 1 specifies the characteristics of reinforcement material.

Table 1: Characteristics of reinforcement

| | | filament | roving |
|---|---|---|---|
| density | [g/cm³] | 2,8 | — |
| yarn count | [tex] | 0,504 | 1114 |
| diameter | [µm] | 15,14 | — |
| breaking elongation | [%] | 2,73 | 0,74 |
| strength | [N/mm²] | 2061 | 574 |
| elastic modulus | [N/mm²] | 79510 | 81170 |

### 1.2.2. Impregnation of reinforcement and their modification

The rovings used as reinforcement were impregnated with polymer dispersion before mounting in concrete. In contact between roving and polymer dispersion, the roving can fill all filament interspaces with dispersion, due to capillary suction.

[top] : 2 seconds after drop up
[bellow]: 90 seconds after drop up

After drying of the impregnated reinforcement elements the polymer particles close ranks. Exceeding the minimum film forming temperature the cross linking of particles occurs depending on characteristics of the polymer solid.

For minimum film forming temperatures about room temperature the start of film forming can be influenced by heat treatment of reinforcement. So the bond behaviour between impregnated reinforcement and matrix can be modified. Table 2 gives an overview for used elements of reinforcement (impregnations) and their different heat treatment (modification).

Table 2: Variations of fibre impregnations and their modifications

| Used fibre impregnations *(type of polymer)* | Modification of fibre impregnation *(point in time of film forming)* |
|---|---|
| without polymer (unprocessed yarn) | not applicable |
| roving with polymer 1 (A969) | **Before mounting** in concrete the roving is impregnated and **uncured by no heating**. |
| | **Before mounting** in concrete the roving is impregnated and **cured by heating**<br>The impregnated reinforcement is cured by heating about a period of 2 hours up to 70 degrees. |
| | Before mounting in concrete the roving is impregnated and **after mounting** in concrete the roving is **cured by heat treatment**.<br>After hardening the specimens were stored in a climatic chamber with controlled 2-steps program of temperature and humidity. The maximum temperature was 65 degrees.<br>Due to heat treatment the hydration kinetics of concrete is different from unheated concrete specimens. The changed microstructure of heat-treated concrete results in a coarsening of hydration products. |
| roving with polymer 2 (S400) | The roving is impregnated and **directly cured before mounting** in concrete<br>The crosslinking happens before casting in concrete because of evaporation of the dispersion medium at room temperature without extra heating. |

## 1.3. Characterisation of Concrete Matrices

The composition of the used matrix (M1) is typical for AR-glass textile reinforced concrete with a powerful attenuation of alkalinity. Based on this composition 3 polymer-modified fine concretes M1-05, M1-10, M1-15 were deduced with polymer content of 5%, 10% and 15% polymer-solid relating to cement content. In table 3 the compositions of all matrices are specified.

Table 3: Compositions of used Matrices in kg/m³ concrete

| matrix | M1 | M1-05 | M1-10 | M1-15 |
|---|---|---|---|---|
| CEM III 32,5 NW-HS-NA | 598 | | | |
| fly ash | 269 | | | |
| micro-silica suspension | 60 | | | |
| sand 0-1 | 1196 | | | |
| water | 269 | 247 | 226 | 299 |
| polymer dispersion 2: S400 | — | 48 | 95 | 145 |

## 2. GEOMETRY OF SPECIMENS AND METHODS

### 2.1. Geometry

The investigated specimens were produced dividing large platters into single bars with the dimensions length x width x hight = 260 x 60 x 12mm³. The reinforcement consisting of unidirectional glass fibre rovings is located 10 mm under bottom surface (Fig. 7).

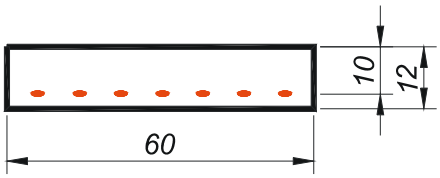



Fig. 7: Cross section of specimen

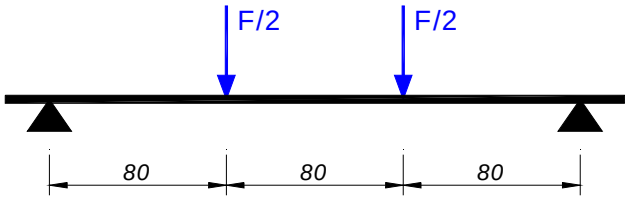



Fig. 8: Schematic drawing of supporting and loading points

### 2.2. Methods

All investigations were carried out at series each covering 10 bending test specimens. After production, the specimens were stored under standard conditions and tested after a storing time of 28 days using 4-point–bending test (Fig. 8). The tests were performed path-controlled with deformation speed of 3 mm/min and stopped at a maximum deformation of 12 mm. Force and deformation were recorded both in the plate centre and in the third points of the sample during testing.

Additionally to bending tests, the bond between filaments-matrix or filament-filament of selected specimens has been inspected using an electron microscope (ESEM).

## 3. RESULTS

### 3.1. Yarn Impregnation Using Rovings with Constant Thickness of 1100 tex

Load-deformation-curves of 28 days aged specimen are presented in Fig. 9. They are obtained by using different reinforcement impregnations and impregnation modifications. The bending test curve of the untreated reinforcement (curve 1) shows the characteristic behaviour for multi filament AR-glass yarns: Only the filaments in the fill-in-zone are loaded after cracking of the matrix. They are stretched with increasing crack width and successively fail.

This phase is characterized by a decreasing load due to the small number of participated filaments (unfavourable perimeter/ cross section ratio).

The filaments of the core region contribute to total load transfer only by friction or adhesion. Most of them are pulled out.

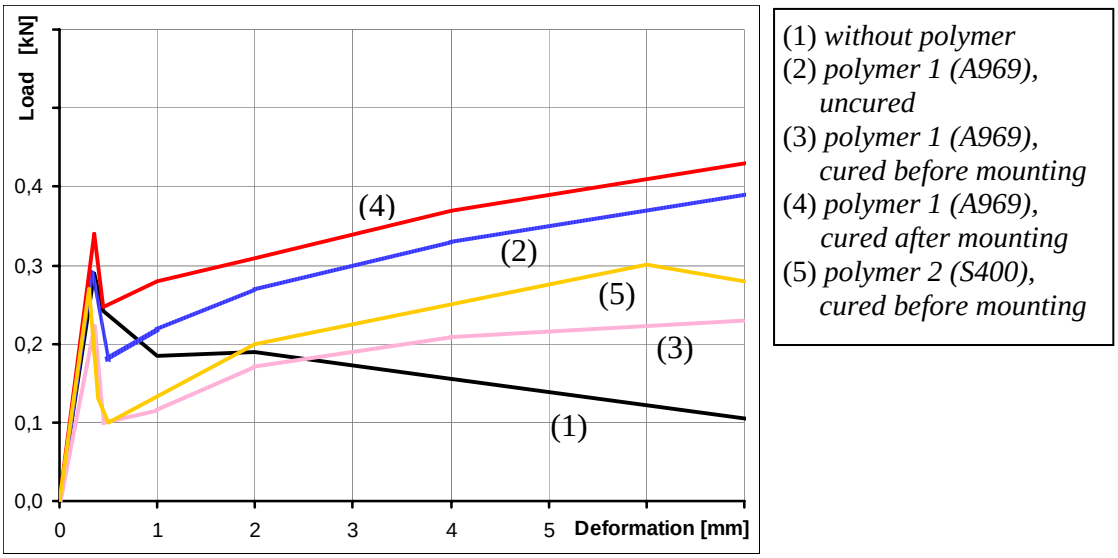



Fig. 9: Load-deflection-curves of bending test samples from matrix M1 with different impregnation of reinforcement

Impregnating the reinforcement with an uncured polymer, the friction and adhesion between all filaments in the roving is increased due to the presence of the polymer particles and consequently the load transfer capability increases, too. The load capacity considerably exceeds that of the untreated reinforcement.

The impregnated uncured reinforcement is strongly hygroscopic. After mounting in the fresh concrete the rovings suck in water and fine particles of the cement paste. A small part of the polymer particles re-disperses and migrates into the concrete that encircles the roving. With advancing hydration the generated CH- and CSH-phases penetrate in this dispersion liquid and use the stored water for further hydration product formation. Loosing this water the polymer particles once more converge and coagulate by cohesion between the particles forming compact clusters or they accumulate as single small polymer spheres at the surfaces of the filaments. Both effects result in a more effective and larger fill-in-zone and also a better compound is obtained between fibre and matrix by the intermix of polymer particles and cement constituents (Fig. 10).

The higher retrace of the load immediately after concrete cracking compared to the unimpregnated roving is due to the changed geometrical cross section of the roving after impregnation. Originally the roving shows a flat elliptical cross section. This cross section changes into a rather circular one due to the aqueous dispersion liquid. Hence, the perimeter of the roving and resulting from this the compound area to the matrix is reduced. Also the stiffness of the matrix-fibre interface decreases as a result of the infiltration of polymer particles.

The load capacity can be further increased by subsequent film forming of polymer 1 in the concrete matrix (curve 4 in Fig. 9). Heating them, the formerly only by cohesion linked polymer particles are now forming a network and more stable complexes with higher stiffness (Fig. 11). Both the adhesion between polymer and filament and polymer and matrix increases. As an effect of this more intensive adhesion a clearly reduced value of the test load retrace after concrete cracking is obtained as seen in Fig. 9.

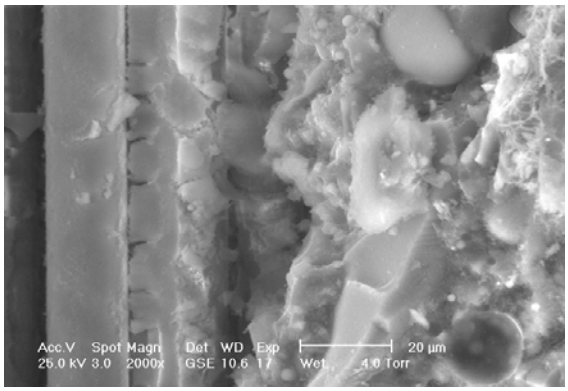



Fig.10: Fill-in-zone with polymer 1 (A969) without film forming (magn. 2000x)

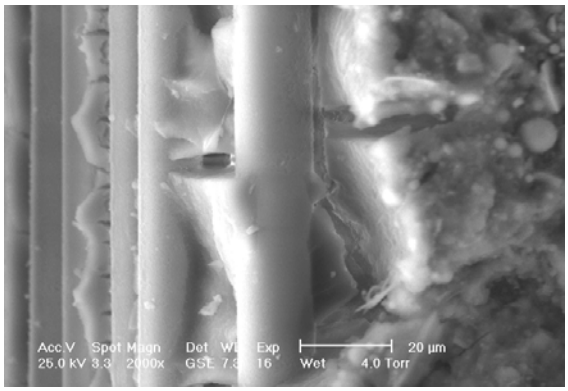



Fig 11: Fill-in-zone with polymer 1 (A969) after film forming at 65 °C (magn.2000x)

The reinforcement, impregnated with polymer 1 (A969) and cured before mounting in the matrix, shows a significantly smaller loading capacity as the untreated reinforcement. This is a result of the weak bond between the (now compact) roving surface and the matrix, for the generated hydration products are not able to penetrate into the border zone of the roving due to the compact surface of the roving and the hydrophobic character of the cured polymer. As an additional effect at the beginning of the matrix hydration the cured polymer swells in contact with the water of the cement paste. Forthcoming hydration needs more water and so the swelled roving dehumidifies and shrinks down to its original cross section. The arising shrinkage cracks between roving and matrix disturb the bond in the fibre matrix interface (Fig. 12). As a minor effect a reduced anchorage of the roving in the matrix can be obtained by a discontinuity of the roving cross section due to varying polymer thickness.

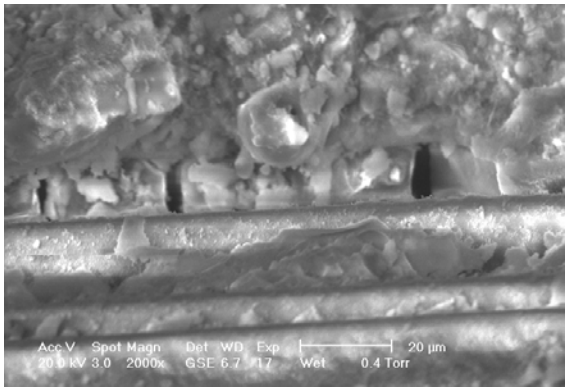



Fig.12: Fill-in-zone with Polymer 1 (A969) cured before mounting in matrix (magnification 2000x)

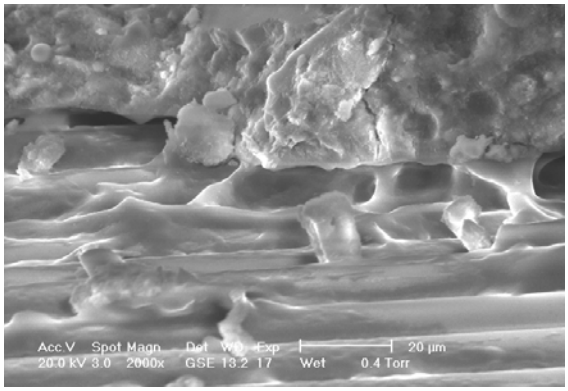



Fig.13: Fill-in-zone with Polymer (S400) (magnification 2000x)

Impregnating the textile reinforcement with polymer 2 (S400) the effects are similar to those of polymer 1 (see curve 5 in Fig. 9). Because of the minor swell capability the shrinkage in the contact zone has no great importance. But the bond situation in the interior of the roving changes. The core fibres are more intensively affected due to a better adhesion caused by the different mechanical properties of polymer 2 (Fig. 13), giving a small higher load capacity of these specimens.

### 3.2. Yarn Impregnations Using voluminous Rovings

The efficiency of polymer impregnation by using thick rovings (e.g. high count of yarn) has also been investigated. For this purpose two glass fibre strands each 1100 tex had been integrated and built-in as reinforcement with the double count of yarn from 2x1100 = 2200 tex/roving.

The double reinforced samples without any impregnation (curve 1 in Fig. 14) show a behaviour which resembles the test pieces with single reinforcement. In spite of a greater reinforcement concentration only an insignificant increase of the load capacity can be achieved because of the disproportionately increasing of core fibres fraction compared to the perimeter of the roving.

Impregnation of the doubled roving with polymer 1 without film forming (curve 2 in Fig. 14) significantly enhances the working capability. The largest increase, indeed, is achieved again by impregnation with polymer 1 and late film forming in the hardened concrete (curve 4 in Fig. 14).

This behaviour allows an increase in the mesh aperture size of the textile reinforcement, using rovings with higher tex number. As a consequence aggregates with large diameter can be applied, too. Higher dimensioned grains, however, require less mixing water, so reducing shrinking potential of the matrix and increasing the durability of the composite material.

As in the case of thin rovings the test samples, the reinforcement of which is cured before installation in the concrete, show only an insignificant increase of the load capacity (curves 3 and 5 in Fig. 14). Although the reinforcement has a good interior bond in the roving, swelling, shrinkage and hydrophobia remain the reasons for the weak fibre matrix interface.

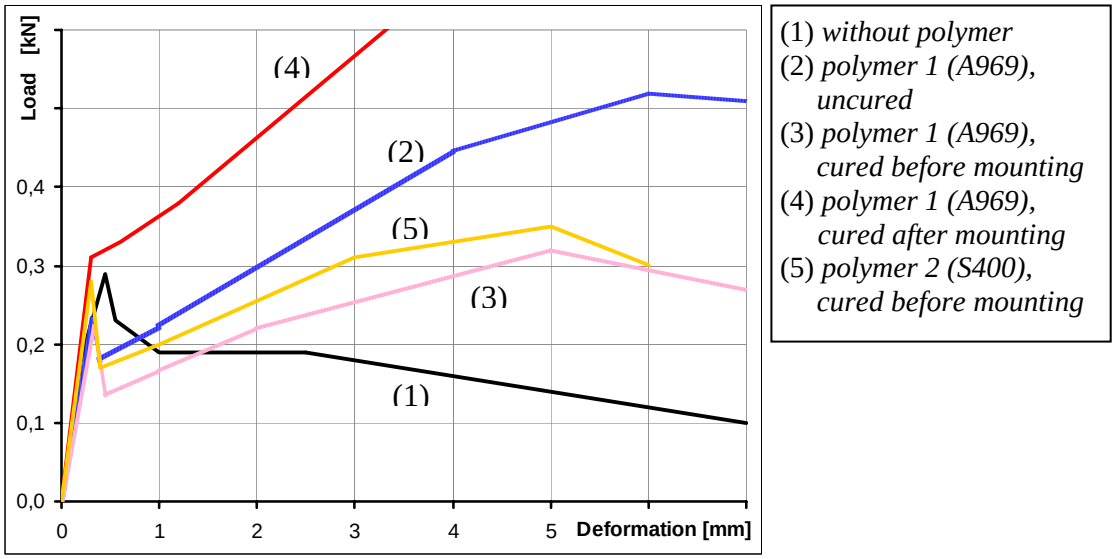



Fig. 14: Load-deflection-curves of bending test samples from matrix M1 with doubled roving and different impregnations of reinforcement

### 3.3. Polymer Impregnation of Matrix

The local deformation behaviour of polymer modified concrete with different mixtures (see table 3) has been investigated, only using unimpregnated reinforcements.

Matrix M1 was used for the sample production with 0, 5%, 10% and 15% polymer content, respectively. The obtained load deformation curves are shown in Fig. 15. The

breaking load of concrete as well as the working capacity during fibre pull out increases with increasing polymer content. Two effects are responsible for this behaviour.

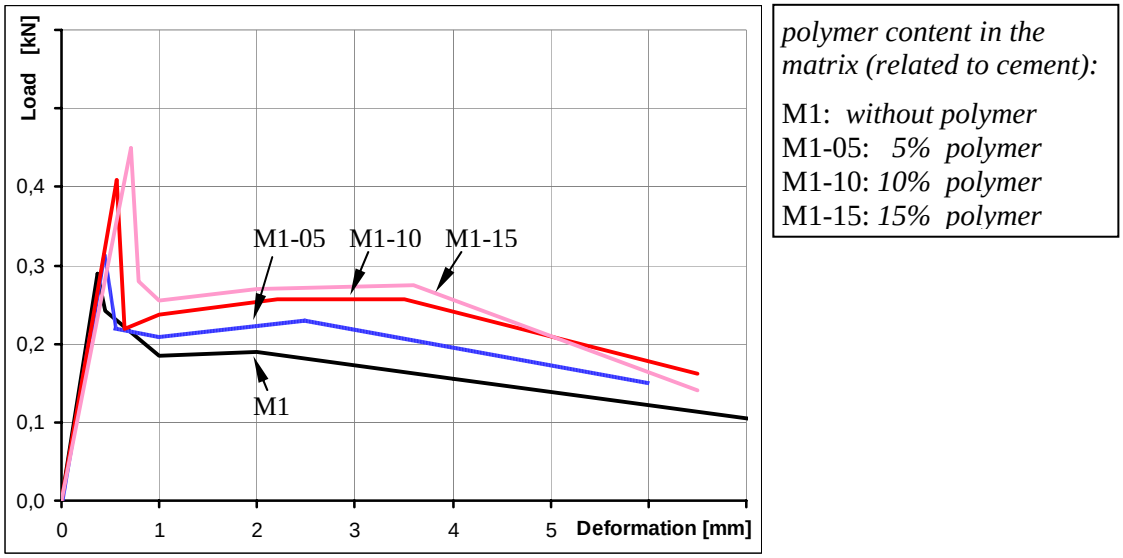



Fig. 15: Load-deflection-curves of bending test samples made of matrices M1, M1-05, M1-10 and M1-15 reinforced with not impregnated rovings

The polymer particles are dispersed in the concrete mixing water. In the matrix the polymer is nearly uniformly distributed forming a network, which will be penetrated by hydration products. Therefore the polymers can bridge the micro cracks, resulting in higher bending strengths of the concrete (Schorn 2004/B). Preparing the concrete specimen, the unimpregnated rovings get contact to the wet concrete. At once, from this moment, parts of the mixing water together with cement and polymer particles as well as first hydration products are sucked into the roving. The large cement particles can only penetrate in the border area of the roving due to a filtering effect of the tight-knit filaments. However, the smaller polymer particles and the water molecules are also capable of entering the core region of the roving, so adhesive linking the core filaments (see Fig. 17). Their penetration rate significantly decreases from surface to roving depth.

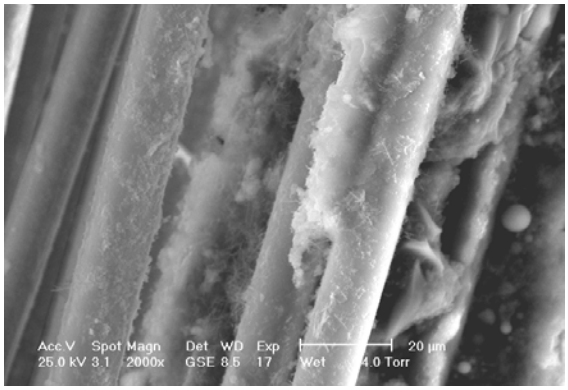



Fig. 16: Filaments in the fill-in-zone embedded in matrix M1-15 (magnification 2000x)

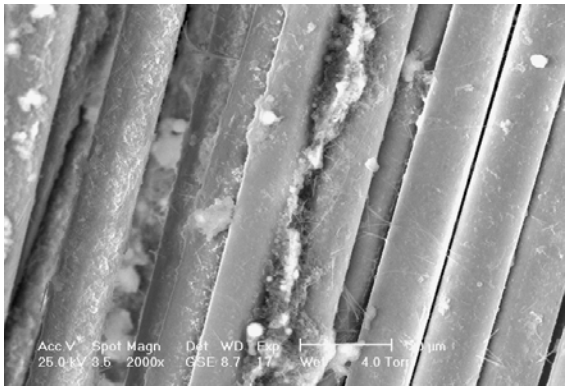



Fig. 17: Filaments in the core zone embedded in matrix M1-15 (magnification 2000x)

The hydration process in the fibre-matrix interface makes use of the weakly stored water in the filaments, in consequence the roving dehumidifies, especially by an advanced

hydration. Losing water the polymer particles are accumulated on the surface of the fibres and cure, forming a hardened film on the roving surface and intensifying the bond between hydration products and filaments (Fig.16). But the gain of working capacity is relatively small compared to samples with impregnated reinforcement (see Fig. 1 and 2).

These benefits are marginal also considering the material usage under a more economical point of view. Only a small fraction of the totally added polymer penetrates into the roving to intensify fibre-fibre or fibre-matrix bond. The greater fraction of the polymer remains in the matrix and does not perform a contribution to improve the load transfer during fibre pull out.

### 3.4. Combination of Polymer Modified Matrix and Impregnated Reinforcement

In addition to the above described experiments the combination of impregnated roving and polymer modified matrix was studied, too. In this case the bond behaviour is mainly determined from the impregnation of the fibre and their modification. The influence of the polymers in the matrix on the working capacity of these composites is nearly negligible.

## 4. CONCLUSIONS

Polymer modification of the matrix or polymer impregnation of textile reinforcements made from AR-glass allows specific influencing of the working characteristic of the composite material Textile Reinforced Concrete.

Only a small improvement of bond and working capacity is achieved using multi filament yarns with a polymer impregnation cured outside the concrete matrix. The fibre-matrix-interface becomes the weak point of the composite caused by the relatively closed surface of the roving, the hydrophobic surface reaction and the swelling and shrinking behaviour of the polymers.

The application of polymers in the matrix (PMC) only insignificantly improves the bond behaviour compared to multi filament yarns without impregnation. This is a result of the competing processes leading to changes in the water balance of the fibre-matrix-interface.

Favourable effects were achieved by impregnation of the textile reinforcements using polymers possessing a significant higher film forming temperature than the processing temperature and inducing a film forming of reinforcement in the built-in state by subsequent heat treatment of the composite. In this way the working capacity can be nearly enhanced by a factor of two. The effect slowly increases by increasing count of yarn of the roving (e.g. thicker roving). Strong adhesive bridges were formed by the polymer in the core region of the rovings, enabling an activation of the core fibres already at small crack widths and increasing the specific glass utilization.

Rovings with higher counts of yarn make it possible to increase the aperture size of the textile reinforcement and to reduce the required water amount due to possible larger maximum diameters of grain. Thus shrinking can be reduced and the durability of the composite is increased. Also higher loads can be transferred by this composite. Consequently this textile reinforced concrete with enlarged effective cross section of reinforcement will help to expand the fields of application of this composite material.

## 5. REFERENCES

Schorn, H., Schiekel, M., Hempel, R.: Durability of textile glass reinforcement in concrete. (in German). *Bauingenieur 79* (2004/A) H. 2, S.86-94

Schorn, H.: An adhesive cross-linkage model for textile glass fibre reinforcement in concrete. (in German). *Bautechnik 80* (2003) H. 3, S.174-180

Schorn, H., Puterman, M.: Textile glass fibres with polymer dispersion as reinforcement in concrete. (in German). *Bautechnik 79* (2002) H.10, S. 671-675

Schorn, H.; Butler, M.; Hempel S. (2004/B): Polymers as Microcrack Stopper in Concrete observed in ESEM. *Proceedings of the 11th International Congress on Polymers in Concrete (ICPIC '04)*, Published by the Federal Institute for Materials Research and Testing, Berlin, Germany, 2004

International Symposium Polymers in Concrete
2 - 4 April 2006
Guimarães, Portugal

# Composite Improvement of Textile Reinforced Concrete by Polymeric Impregnation of the Textiles

U. Dilthey[1], M. Schleser[2]

*RWTH Aachen University, ISF - Welding and Joining Institute*
*Pontstrasse 49, 52062 Aachen, Germany*

## ABSTRACT

The building material „textile reinforced concrete“ enhances the possibilities in the design of high-strength thin-walled structures. The utilisation of the technical textiles, made of glass, carbon, basalt or high-module polymers is, however, still far below the material strength potentials. Within the scope of this paper, the application of polymer-impregnated, alkali-resistant glass textiles for the improvement of a component's load-bearing behaviour has been examined. The mechanical properties of the polymers were tested by tensile tests of polymer films. The interaction between glass filaments, polymer and concrete matrix was investigated by means of wetting tests, yarn-tensile tests, pull-out and pull-off tests and tensile tests of reinforced components. Through the application of suitable polymeric impregnations the reinforcement utilisation in the component was more than tripled and the corrosion protection against chemical attack of the textiles in the interstitial water was improved.

## 1. INTRODUCTION

As a result of its good workability and formability the construction material „concrete“ is widely-used in the field of structural design. Cementitious concrete is, moreover, the cheapest construction material for the transmission of compressive forces. Due to its low tensile strengths, structures which are subjected to bending and tensile stresses are usually reinforced with a steel bars, which, for reasons of corrosion protection, demand a minimum concrete cover of several centimetres. The application of textiles made of corrosion resistant high-efficiency filament yarns for the reinforcement of concrete components allows the production of particularly thin and high-strength components. The focus has been put on textiles made of glass, basalt, carbon or high-module polymers. In this connection, many questions are raised about the bond behaviour, the load-bearing behaviour, the durability and the handling of the construction material textile reinforced concrete. The contribution of the reinforcement in the composite shows, compared to its material strength, considerable potential for optimisation. The main reason for the bad efficiency is founded in the inhomogeneous force transmission between the filaments. While the outer filaments are

[1] Univ.-Prof. Dr.-Ing.
[2] Research Assistant

embedded in the cemetitious matrix and transfer most of the load, the inner filaments of the textile contribute only minor to the load transmission, presumably by friction.

In this context, different strategies for the improvement of the bond behaviour have been elaborated. Those include the increase of the cementitious penetration of the textiles, the development of hybrid yarn structures as shown in Kolkmann (2005) and the application of polymers. Within the scope of this paper,

Therefore textiles which are made of alkali-resistant (AR) glass were impregnated with liquid polymers and embedded into the concrete after the polymers were completely cured. Glass as a reinforcement material is comparatively cheap and shows a good strength. It was the aim to improve the force transmission between the filaments in the roving core and to maintain or even improve the good properties of the interaction-zone with the cementitious matrix. This comprises the testing of the mechanical properties of the concrete, the glass fibers and the polymers as well as the interaction of these materials in the composite. For the evaluation of the composite, concrete specimens reinforced with single impregnated rovings as well as with impregnated textiles have been tested.

## 2. MATERIALS

### 2.1. Roving and textile

The basic component of the alkali-resistant glass textiles that were used for the reinforcement of the concrete is the single filament. In the nozzle pulling process several hundred up to several thousand of parallel filaments are produced and bundled into rovings with different yarn counts. Each filament is already coated with an organic sizing during production, which facilitates further processing and reduces filament damage. The rovings which have thus been treated are further processed into two or three-dimensional textiles for the manufacturing of textile reinforced concrete components.

Since common glass fibres known from the field of fibre reinforced plastics, e.g. E-glasses or C-glasses, do not show sufficient durability in the alkaline environment of the concrete, special, alkali-resistant (AR) glasses were used. The improved alkali resistance is a result of the increased zirconium dioxide content. The basic reinforcement material used in this project, was a sized AR-glass-roving of the Vetrotex company with a yarn count of 2400 tex (1tex = 1g/km) and a medium filament diameter of approximately 27 µm (VET-RO-ARG-2400-1-03). This roving was then applied by the ITA Institute of Textile Technology, RWTH Aachen University, for the production of a two-dimensional textile. The lattice spacing is 8 mm, in the 0° (direction of tensile load) and as well as in the 90° direction. This results in a weight per area of 600g/m². The characteristics of filament and roving are shown in Table 1.

Table 1 - Properties of alkali resistant filament and roving

| | Filament | Roving |
|---|---|---|
| Label | VET-FIL-ARG-1-03 | VET-RO-ARG-2400-1-03 |
| Density [g/cm³] | 2.69 | - |
| Yarn count [tex] | 1.55 | 2400 |
| Tensile strength [N/mm²] | 1700 | 700 |
| Young's modulus [N/mm²] | 67890 | 55400 |
| Elongation at rupture [%] | 2,9 | 1,7 |

## 2.2. Concrete

The concrete matrix has to fulfil the special demands of the composite textile reinforced concrete with regard to strength, processability and durability. The most important prerequisite for good bonding is the sufficient penetration of the textiles. Therefore, a matrix which is capable of flowing and which exhibits an aggregate adapted to the textile geometry is demanded. In order to guarantee sufficient durability of textile reinforcements a low alkalinity of the concrete is aimed for, particularly when glass is applied. With regard to the production of thin-walled components the concrete must exhibit a high strength to ensure proper demoulding. Moreover, the fresh-concrete properties have to be adapted to the production process.

In consideration of the above-mentioned requirements, the ibac Institute of Building Materials Research, RWTH Aachen University, has developed a fine concrete formulation (PZ-0899-01) which is based on Portland cement, Table 2.

Table 2 - Fine concrete prescription PZ-0899-01

| Material | Unit | PZ-0899-01 |
|---|---|---|
| Binder | | |
| Cement (CEM I 52.5 R) | kg/m³ | 490 |
| Additives | | |
| Fly ash | kg/m³ | 175 |
| Silica fume | kg/m³ | 35 |
| Admixtures | % c+sfa+sf | 1.5 |
| Superplastiziser | | |
| Aggregate | kg/m³ | 499 |
| Quartz flour | kg/m³ | 714 |
| Sand < 0,6 mm | | |
| Additional Notes | | |
| Quartz flour/Sand-ratio | - | 0.7 |
| Amount of Binder | kg/m³ | 700 |
| w/b = w/(c+sfa+sf) | - | 0.4 |

## 2.3. Polymers

Within the scope of the project various different polymeric systems have been investigated for the impregnation of rovings and textiles. The tests that are described in this paper were done with dispersions based on acrylates and reactive resins based on epoxy. The chosen polymers cover a wide range in mechanical and processing properties. The acrylic dispersion AD1 has a minimum film forming temperature (MFT) of 14°C and forms a homogeneous film below room temperature. The MFT of the acrylic dispersion AD2 is 40°C and hence no film is being produced upon room temperature curing. The properties of the liquid polymers are displayed in Table 3.

Table 3 - Properties of liquid polymers

| Polymer | Chemical base | Solid content | pH-value | Particle diameter | Minimum film forming temperature |
|---|---|---|---|---|---|
| | | wt.-% | - | µm | °C |
| AD1 | Pure Acrylic | 52,9 | 7.5 | 0.15 | 14 |
| AD2 | Pure Acrylic | 53,4 | 7.0 | 0.15 | 40 |

The mechanical properties of the polymer films were tested according to DIN 53455/EN 61. Table 4 shows their tensile strength and the strain at failure. The dispersion AD1 and the epoxy EP1 were cured at room temperature. The dispersion AD2 and the epoxy resin EP2 were cured at 120°C.

Table 4 - Tensile strength and strain at failure of the impregnation polymers

| | Tensile strength [N/mm²] | Strain at failure [%] |
|---|---|---|
| Acrylic dispersion AD1 | 4.7 | 580.2 |
| Acrylic dispersion AD2 | 27.2 | 4.0 |
| Epoxy resin EP1 | 72.1 | 4.3 |
| Epoxy resin EP2 | 79.5 | 3.8 |

## 3. COMPOSITE BEHAVIOUR

The composite of textile reinforced concrete is determined by the interaction between the inner filaments themselves and the outer filaments which are in contact with the concrete matrix.

In textile reinforced concrete the outer filaments of non-impregnated multi-filament yarns are penetrated with hydration products (fill-in zone). Thus, they possess a good bond with the matrix and contribute substantially to the load transfer. The inner filaments in the core of the roving, however, are not penetrated with hydration products. The forces between the filaments are transmitted presumably by friction. Their contribution to the load transfer is of little account.

For the improvement of the force transmission between the filaments in the roving core it is a precondition that the polymers wet the filaments well. To investigate the wetting of single filaments they were immersed a couple of millimetres into the liquid polymers with a speed of 1 mm/min. The resulting wetting forces were measured with a tensiometer and the dynamic contact angle was calculated according to eq. (1).

$$\cos\Theta = \frac{F_T - F_b}{\sigma_l \cdot L_w} \tag{1}$$

$\Theta$ dynamic contact angle [°]
$F_T$ measuring force tensiometer[N]
$F_b$ buoyant force of fiber[N]
$\sigma_l$ surface tension of liquid polymer [mN/m]
$L_w$ wetted length [µm]

This test was done with sized and unsized filaments. The polymers showed a good wetting behaviour as published in Dilthey (2004).

The impregnation of textiles with polymers improves the inner bond substantially through the increased force transmission between the filaments. Figure 1 shows the results of tensile tests with the impregnated rovings compared to the non-impregnated reference. The acrylic dispersions AD1 and AD2 improve the material strength after film forming through cohesion and adhesion. When the dispersion AD2 is applied at room temperature no film is formed. The improvement of the maximum tensile tension in the roving is caused by hard polymer particles between the filaments themselves as well as between the filaments and the concrete. The high-module epoxy resins use the material strength almost to full capacity.

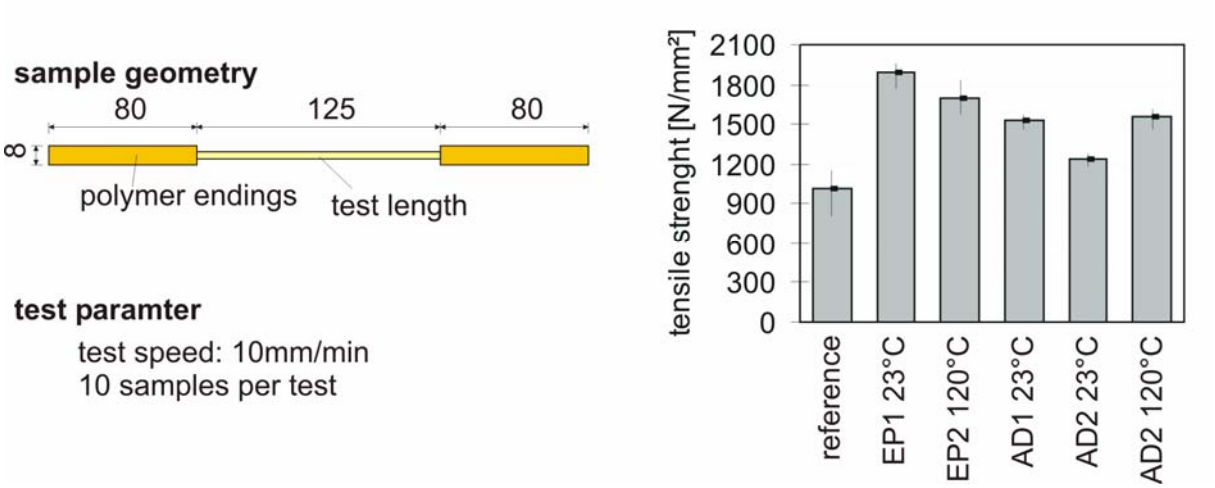



Figure 1 - Tensile test of impregnated rovings

With regard to the bond between textile and matrix, the impregnation of the rovings with polymers results in an increasingly "closed" surface. The bond behaviour is thus, in comparison with non-impregnated rovings, characterised by two substantial differences. The improved force transmission between the filaments, as proven in the yarn tensile tests, leads, on the one hand, to a reduction of the successive filament failure due to an improved load transmission between the inner filaments.

On the other hand, the interaction-zone is, as a result of the complete impregnation of the textile reduced to the enveloping surface of the roving. Its geometrical, mechanical and chemical characteristics are, due to the substantially reduced bond area between matrix and impregnated roving, particularly important for a good composite. The interaction in the contact area between impregnated reinforcement textile and the concrete matrix was investigated with pull-off and pull-out tests.

For a qualitative evaluation of the adhesive bonding of the concrete to the hardened polymer, concrete dies were cast onto polymer-coated glass panels and, after 28 days (50% relative humidity) pulled off without moment. The bond strengths of the polymers were below 0.25 N/mm². This led to the conclusion that the composite is mainly determined by micromechanical and physical effects rather than chemical effects.

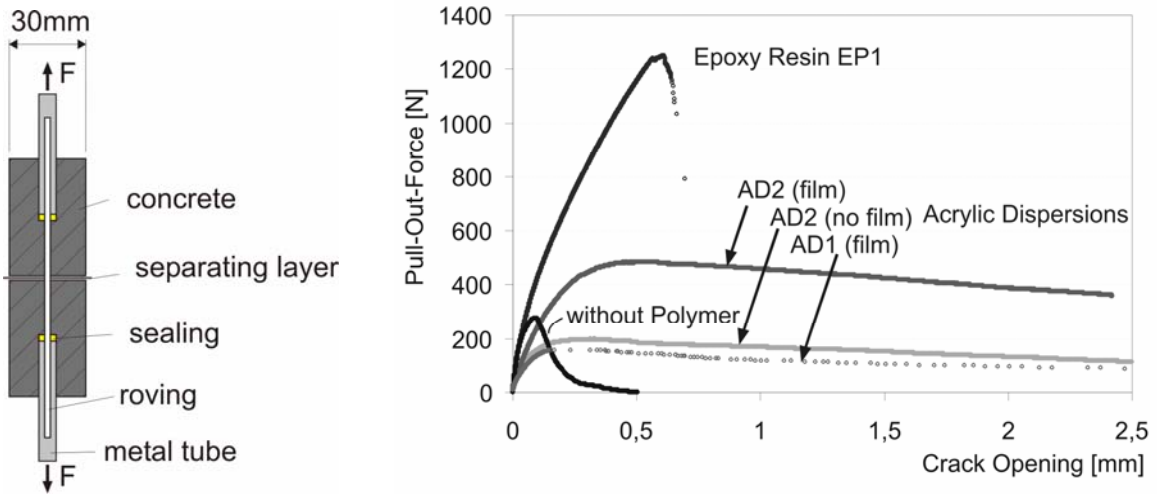



Figure 2 - Pull-out test of VET-RO-ARG-2400-1-03 rovings with different impregnation

The bond behaviour of impregnated rovings in the concrete matrix was tested by means of double sided roving pull-out tests. The embedding length of the yarns was 30 mm, the testing speed was 0.1 mm/min. Figure 2 shows the experimental set-up and the pull-out behaviour of completely impregnated rovings, in comparison with non-impregnated rovings.

The pull-out behaviour of rovings that are impregnated with film forming polymers is determined by the interaction between the polymeric film on the outside of the roving and the surrounding concrete matrix. There is no penetration of hydration products into the roving, Figure 3.

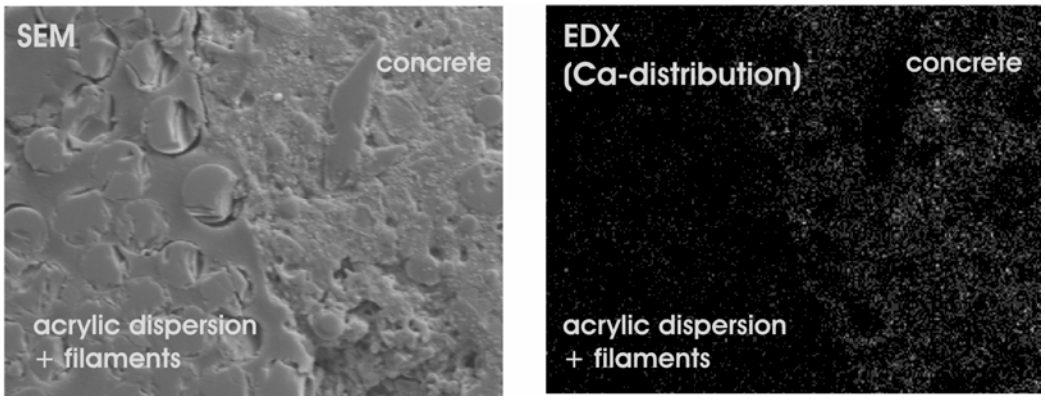



Figure 3 - Interface zone of completely impregnated rovings

Because of the high cohesive strength of the epoxy resin, comparatively high bond forces were transmitted into the concrete via the shear bond. The selected embedding length of 30 mm led to the failure of the roving when crack openings of 0.6 mm were exceeded. In contrast to this, the lower bond strengths of the film formed soft acrylic dispersion AD1 led to the complete pulling out of the impregnated roving on a comparatively low load level. The inner filaments were not damaged, because of the good load transmission between the polymer coated filaments. The film formed by the acrylic dispersion AD2 shows the same behaviour at a higher load level because of the higher adhesive and cohesive forces in comparison with dispersion AD1. Below the minimum film forming temperature (MFT) the acrylic dispersion AD2 allows, as well as the non-impregnated yarn, the penetration of the fine concrete into the roving and thus the development of a distinctive fill-in zone. Compared to the non-impregnated yarn, the friction between the inner filaments is increased through the hard polymer particles. Since the force transmission between the filaments in the roving interior is, however, limited in comparison with the adhesively and cohesively active polymer films, here also successive filament failure occurred. The achievable pull-out forces were, therefore, much lower than those of the epoxy resin.

For a defined improvement of the outer bond, in connection with the polymer impregnation, different strategies are investigated within the scope of the research project. Those include, for example, sand coating of the impregnated roving, thermoplastic profile or cavities in the impregnated roving for a better matrix penetration, Dilthey (2005).

Figure 4 shows the pull-out behaviour of an impregnated roving that was surface modified with sand. The comparison between the surface modified and the non surface modified roving shows mainly two effects. The maximum pull-out force is on the same level because of the cohesive failure of all filaments. The composite stiffness of the surface modified roving is higher because of the better mechanical interlocking with the concrete matrix.

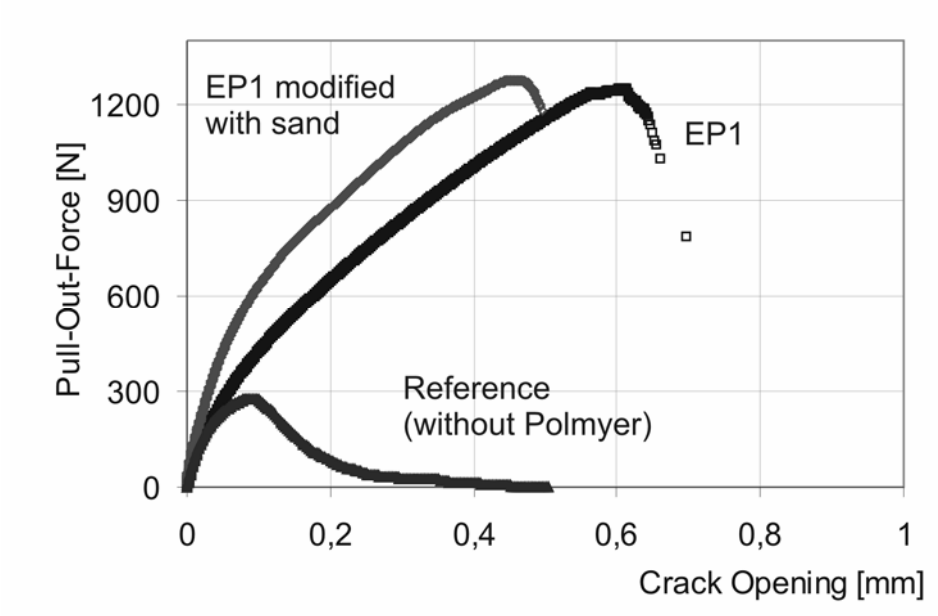



Figure 4 - Pull-out test of impregnated and surface modified rovings

The composite of textile reinforced components was tested under tensile load. Therefore specimens with dimensions of 500 x 100 x 10 mm³ were reinforced with one layer of impregnated AR-glass textiles MAG 07-03 (equal to 12 AR glass rovings of 2400tex). These specimens were tested in the tension testing machine with a free length of 400 mm and a test speed of 1 mm/min. Figure 5 shows their load bearing behaviour.

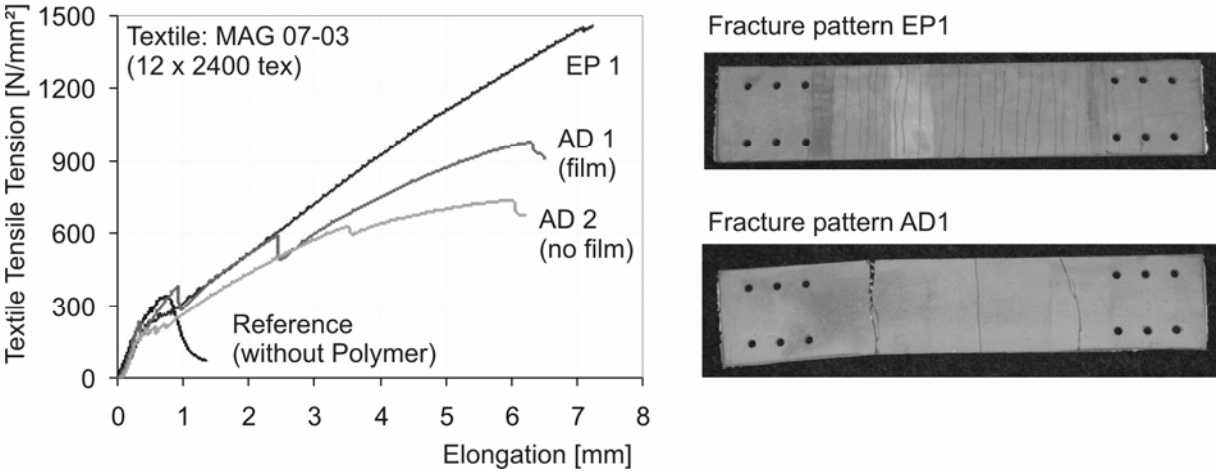



Figure 5 - Tests of textile reinforced components

The reduction of the progressive filament failure led, in the case of all applied polymers, to a substantial increase of the load carrying capacity after the crack formation in the fine concrete. The inferior bond of the acrylic impregnated textiles to the concrete results in comparatively large crack distances and crack widths. In contrast to this the good bond between epoxy-impregnated textiles and concrete led to a constant, finely distributed crack pattern, Figure 5.

The component behaviour has also been tested in the bending test with comparable polymer systems. This test combines tensile forces with radial forces. It is a more application-oriented method to evaluate the application of impregnated textiles in textile reinforced

concrete elements. The results show the same tendencies. They are presented in detail by Schorn and Puterman (2002) and by Dilthey (2005).

## 4. CONCLUSIONS

The investigations show the potential of improving the load bearing behaviour of textile reinforced concrete components by the use of liquid polymer systems. All of the used polymers improve the load bearing capacity in comparison with not impregnated textiles.

The improved load transmission between the inner filaments arises from the adhesive and cohesive properties of polymeric films as well as from an increased friction due to hard polymer particles. The interaction between the impregnated textiles and the concrete matrix is mainly determined by the mechanical and physical properties of the substantially reduced interface-zone. The best results can be achieved with high module polymers such as epoxy resin.

The different contributions of cohesion, adhesion, friction and mechanical interlocking to the load transmission in the interface-zone are currently investigated at the ISF Welding and Joining Institute, RWTH Aachen University. The impregnation improves also the durability of the reinforced components. Further investigations of the detailed corrosion mechanisms and the resistance against fire are to be done.

## 5. REFERENCES

Dilthey, U. and Schleser, M., Improvement of bond by use of a polymer phase, *in: Research proposal 2005-2008: SFB 532 Textile-Reinforced Concrete - Development of a new technology*, Eds. by J. Hegger, RWTH Aachen University (2004)

Dilthey, U., Schleser, M., Böhm, S. and Mund, F., Improvement of Textile Reinforced Concrete by Use of Polymers, *in: E-MRS Fall Meeting 2005 - Symposium G, Adhesion on macro-, micro- and nano-scale*, 5th-9th September, Warsaw University of Technology (2005)

Kolkmann, A., Gries, T., Schleser, M. and Dilthey U., Innovative yarn structures and coatings for textile-reinforced concrete, *in: Proceedings: 13th International Techtextil-Sysposium for Techical Textiles, Nonwovens and Textile-Reinforced Materials*, 6th-9th June, Frankfurt am Main (2005)

Schorn, H. and Puterman, M., Textile Glasfasergelege mit Polymerdispersionen als Bewehrung für Beton, *Bautechnik,* **79**, 671-675 (2002)

# Comparative Study with Alternative Materials for Manufacture of Machine Tool Structures

Vitor A. Ducatti[1]

*(1) Universidade Estadual de Campinas, Faculdade de Engenharia Civil, Arquitetura e Urbanismo, Campinas, Brasil.*

José M. Santos[2]

*(2) Universidade Estadual de Campinas, Faculdade de Engenharia Mecânica, Campinas, Brasil.*

Rosa C. Lintz[3]

*(3) Pontifícia Universidade Católica de Campinas, Faculdade de Ciências Tecnológicas, Campinas, Brasil.*

ABSTRACT

This paper presents a comparative study between dynamic test results achieved with some alternative materials used to manufacture machine tool structures. The part selected as a test prototype represents a lathe bed in actual scale. Based on this pattern twelve test prototypes were manufactured and dynamic tests performed by using the following materials and/or composites: polymer mortar, polymer mortar with reinforcement cage, cast iron, cast steel, ferrocement with reinforcement cage, and fiber-reinforced mortar. Dynamic tests were made to obtain natural frequencies, damping rates, and mode shapes to the firsts deformed natural vibration modes. The results are compared and discussed in the aim to reveal the advantages and disadvantages in using these alternative materials instead of the traditional ones, cast iron and cast steel, to manufacture machine tool structures.

## 1. INTRODUCTION

Properties of high flexure and torsion static stiffness, good dynamic characteristics as high natural frequency and damping ratio, long-term dimensional stability, lower coefficient of thermal expansion and fabrication simplicity at low costs are required for machine tool structures. An important issue during the machining process is the chatter generated by self-

excited vibrations. These vibrations can generate high levels of relative displacements between the part and the tool that compromise the accuracy of the final part. Such mechanism prevents higher cutting speeds and becomes an obstruction to reduce manufacturing times and costs. Traditionally, machine tool structures have been made of cast iron and cast steel, which can be cast into complex shapes, and easily machined to a high degree of accuracy. But, they also have some problems like high shrinkage rates during curing, long production lead-time, a need for special anti-corrosion treatment, high cost, etc.

Several attempts have been made either to supplement or to completely replace cast metals using mild steel welding, synthetic granite, hydraulic cement concrete [1], polymer concrete [2,3,4], ferrocement [5,6] and fiber-reinforced concrete [7].

This paper reports the effects of replacing machine tools traditional materials by ferrocement, hydraulic cement mortar reinforced with steel fiber, polymer mortar, and reinforced polymer mortar. In that sense it presents a comparative study about the dynamic tests carried out with twelve prototype of a centre lathe bed (Figure 1).

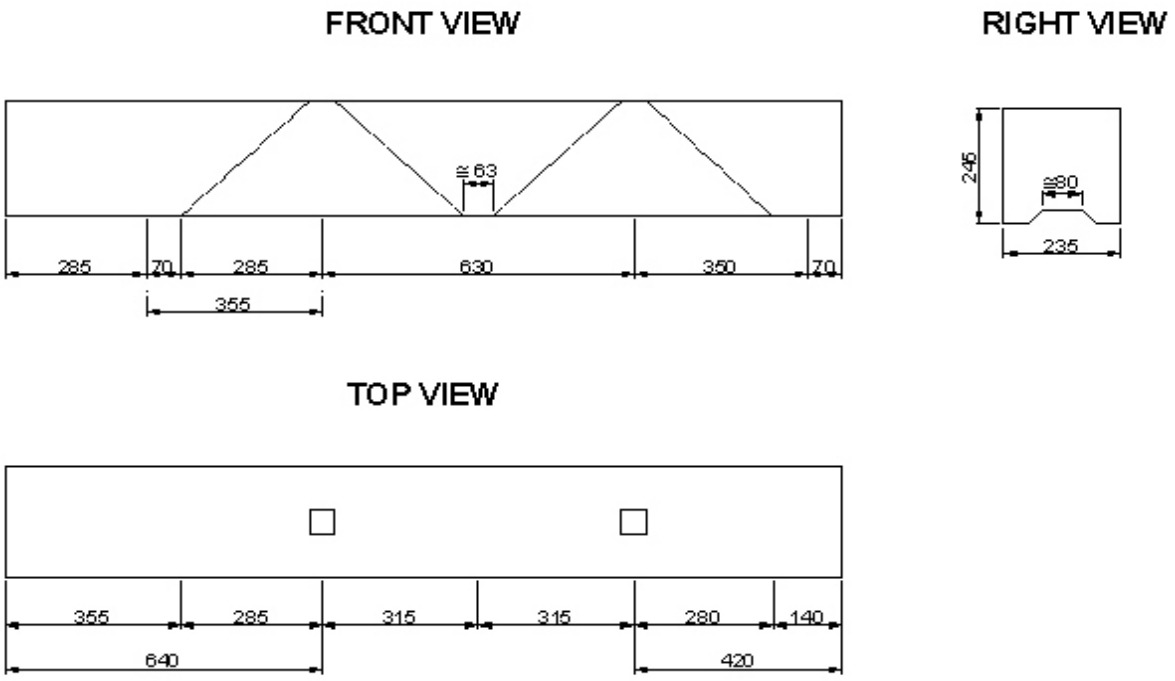



Figure 1 – Geometry and main dimensions of the lathe bed prototype (units in mm).

## 2. MATERIAL PROPERTIES AND PROTOTYPES FABRICATION

Ferrocement, as the name implies, consists of iron or steel and cement. It is defined as type of thin wall reinforced concrete commonly constructed of hydraulic cement mortar reinforced with closely spaced layers of continuous and relatively small diameter wire mesh. The mesh may be made of metallic or other suitable material. Ferrocement differs from normal reinforced concrete because it uses wire mesh rather than heavy rods or bars, and uses sand rather than a mixture of sand and stone as aggregates. Ferrocement utilized in this investigation is made up of high early strength portland cement (ASTM Type I), condensed silica fume, natural siliceous sand, and superplasticizer in the following proportion by weight: 1.00:0.20:2.00:0.26:0.02. Before mixing the ingredients, sand was passed through the 1.20 mm sieve. The fine wire mesh used in the reinforcement cages was of welded type with 12.5 mm square grids and 1.2 mm wire diameter, the yield strength of mesh reinforcement being 410 N/mm$^2$

Fiber-reinforced mortar, is the ordinary concrete (mortar) containing discrete short length and small diameter fibers. The fibers are usually added to the concrete during mixing of its ingredients, and the resulting fiber concrete is directly poured into the mould simplifying the construction process considerably. The mix proportion of this mortar was the same of the ferrocement. Collated hooked-end steel fibers with aspect ratio 65 (35 mm long / 0.55 mm diameter) were incorporated to the mortar, in volume fractions of 1%, 2% and 3%, resulting in three distinct categories of resistance of fiber-reinforced mortar.

Polymer mortar, is the polymer composite utilized in this research was a mortar made up of three components: a liquid epoxy resin, a hardening agent, and a graded fine aggregate

containing fine sand and filler. The mix proportion of aggregate and binder , by weight, was 6.75:1.00.

Reinforced polymer mortar, is the mortar with the same composition of polymer mortar which was reinforced with the same wire mesh (cage) of the ferrocement.

Cast iron, is a gray cast iron, GG 15 (lamellar graphitic) DIN 1691 with the following nominal average properties: 150 MPa tensile strength, 80 – 105 MPa yield strength, 550 – 700 MPa compression strength, 150 MPa shear strength, 230 – 370 bending strength, and 140 – 190 Brinell hardness.

Cast steel is a standard ASTM A 216 grade WCD.

Prototypes were named using the following abbreviations: AR1, AR2 and AR3 for the fiber-reinforced mortar with 1%, 2% and 3% volume fraction of fiber, respectivelly; AA for the ferrocement; AP for the polymer mortar; APA for the reinforced polymer mortar; FF for the cast iron; and AF for the cast steel. The mixes of portland cement mortar were made in one inclined axle intermittent concrete mixer. The batching procedure was as follows: (a) the cement and condensed silica fume pre-mixed was placed in the mixer; (b) then, half of the required water was mixed with a half of the superplasticizer and poured into the mixer; (c) these materials were mixed during three minutes; (d) the sand was added with the remaining water and superplasticizer; (e) with the mixer running, the fibers were sprinkled in by hand to assure even distribution. The total mixing period ranges form 10 to 15 minutes. The obtained mortars had presented consistency indexes of 253, 252, 223, and 210 mm, on the flow table, for the volume fiber of 0%, 1%, 2%, and 3%, respectivelly. These consistencies provided a ease consolidation of the mortar inside the moulds under the action of the vibratory table.

The total volume of polymer mortar needed for casting one prototype and the control specimens was separated in eight parts. Each of these parts was mixed in two stages. First, the sticky liquid phase, that is, the epoxy resin and the hardening agent were stirred with the help of a electric hammer drill whit a shovel in the end. In the second stage, with the machine running, the aggregate mix was added bit by bit, and the mix continued untill a homogeous colour of the material was reached. The polymer mortars were self-levelling and was moulded without vibration effort.

The mould to casting the cement mortar prototypes was made of fiber-glass (Figure 2a) and for polymer mortar was made of wood. Figure 2a shows the mesh of reinforcement with the cage and Figure 2b shows the reinforcement with bars and stirrups. All prototypes include a longitudinal reinforcement of four bars (10mm diameter), two for compression and two for tensile efforts. These bars were kept in position by three stirrups of 5 mm diameter.

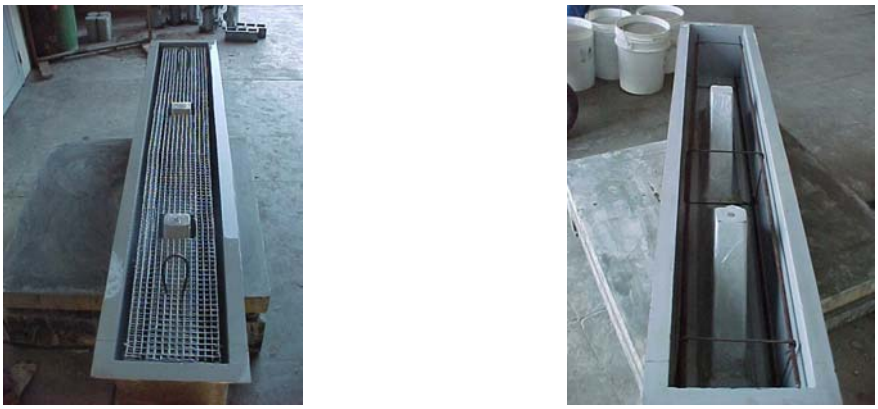
Mechanical properties results of tested prototypes are presented in the Table 1.

Table 1 – Material mechanical properties.

| Material | Compressive Strength [MPa] | Tensile Strength [MPa] | Modulus of Rupture [MPa] | Elastic Modulus [GPa] |
|---|---|---|---|---|
| AR1 | 105 | 12 | 12 | 41 |
| AR2 | 108 | 13 | 12 | 39 |
| AR3 | 119 | 15 | 21 | 39 |
| AA | 103 | 7 | 11 | 41 |
| AP | 89 | 17 | 30 | 18 |

## 3. DYNAMIC BEHAVIOR

A technique commonly used to estimate dynamic system properties at low frequency ranges is the Experimental Modal Analysis (EMA). By using this technique 8 lathe beds were tested under free boundary conditions. The beds were mounted over pneumatics springs in order to obtain free boundary conditions at the experimental setup (Figure 3b).



(a) (b)

Figure – 2 Fiberglass mold: (a) reinforcement cage and (b) reinforcement bars and stirrups.



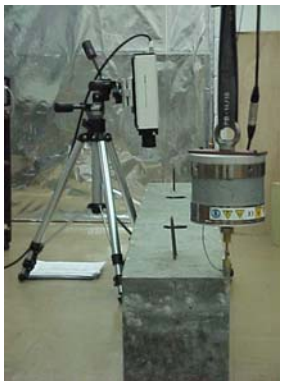
(a) (b)

Figure 3 – Dynamic experimental setup: (a) general view and (b) pneumatic springs detail.

Temperature variations during the test were neglected, because tests were made in acclimatized test room (constant environment temperature around 25ºC). Lathe beds were forced in two directions transverse to the bed length through an electrodynamics shaker. The force was applied through a stinger connected to a piezoelectric force transducer, which was screwed to a metallic insert glued with epoxy at the bed surface (Figure 4a). A random noise signal was amplified and delivered to the shaker. For each excitation degree of freedom (vertical and horizontal) velocities of beds were measured at 54 points over the frequency range from DC-1024 Hz with a point laser Doppler vibrometer – LDV (Figure 4b). In order to improve the poor reflection of bed surfaces, and to localize measurement points in different tests, these points were covered with small paper stickers.



(a)



(b)

Figure 4 – Excitation experimental setup: (a) horizontal excitation and (b) vertical excitation and velocity measurement.

The outputs of force transducer and LDV were sent to a data acquisition system (Hewllet Packard VXI-E1421B) and the signals processed in a modal analyses computational program (LMS-CAD-X3.5C) [8].

The EMA procedure requires the definition of a measurement geometry, which includes all degrees of freedom measured and excited. From the lathe bed geometry, it was used a cartesian coordinate system (*X, Y, Z*) with *X* along bed length and *Y* and *Z* in vertical and horizontal direction, respectively. Figure 5 shows the measurement points.

To the points 1 to 18 were taken velocity measurements in *Y* and *Z* directions, while to the points 19 to 36 were taken velocity measurements only in *Z* direction, and the velocities in *Y* direction were assumed as the same of point velocities for 1 to 18 in *Y* direction. It was possible due bed's mode dynamic symmetry. Although 54 point velocities have been measured, it was possible to carrier out the modal analyses with 72 point velocities and 2 point forces (references), at point 9 directions $-Y$ and $+Z$. Frequency response functions (FRFs) were obtained with 1024 time samples, averaging over 30 blocks, using a Hanning window and frequency range DC-1024 Hz.

Modal parameter estimation was performed using the LMS-CAD-X® software [8] with a time domain Polyreference Complex Exponential algorithm [9]. By utilizing simultaneously all FRFs, the method can extract natural frequencies, modal damping coefficients and vibration mode shapes for all modes in the frequency band that can be excited with the two references used. As a general rule, the 6 first deformable vibration modes were identified in a consistent way for the 8 lathe beds except to the fourth mode in the model FF. Table 2 and Table 3 shows the natural frequencies and modal damping coefficients identified, respectively.

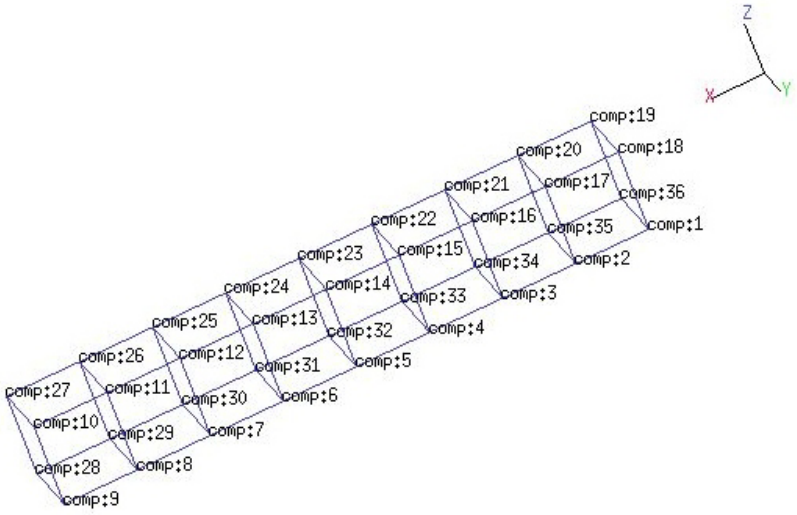



Figure 5: Measurement geometry configuration.

Table 2 – Identified natural frequencies.

| Mode | Natural Frequency [Hz] | | | | | | | |
|---|---|---|---|---|---|---|---|---|
| | AF | FF | AR1 | AR2 | AR3 | AA | AP | APA |
| 1 – 1º Horizontal Bending | 388 | 269 | 317 | 321 | 328 | 328 | 2378 | 232 |
| 2 – 1º Vertical Bending | 395 | 285 | 336 | 336 | 330 | 341 | 244 | 260 |
| 3 – 1º Torsion | 600 | 402 | 407 | 388 | 409 | 474 | 280 | 314 |
| 4 – 2º Torsion | 705 | N/I* | 495 | 510 | 508 | 516 | 339 | 412 |
| 5 – 2º Horizontal Bending | 944 | 646 | 772 | 765 | 788 | 792 | 583 | 550 |
| 6 – 2º Vertical Bending | 1011 | 711 | 821 | 841 | 855 | 871 | 628 | 626 |

- Not Identified

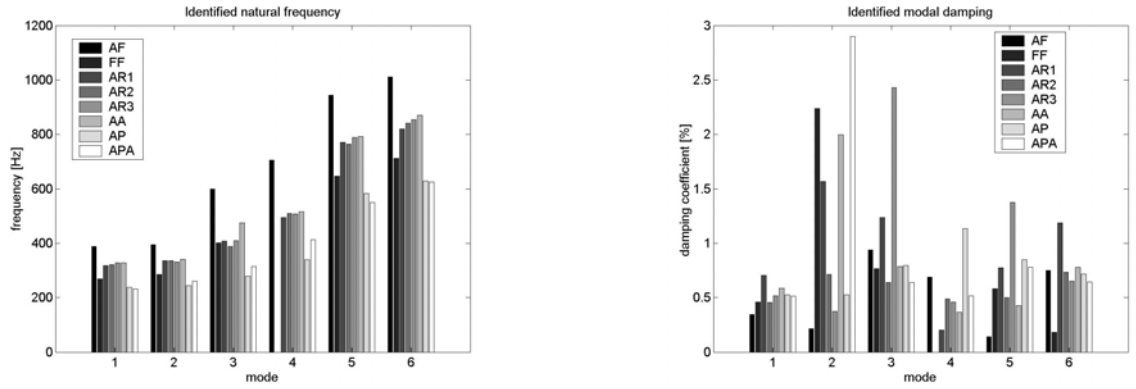
Table 3 – Identified modal damping coefficients.

| Mode | Modal damping coefficient [%] | | | | | | | |
|---|---|---|---|---|---|---|---|---|
| | AF | FF | AR1 | AR2 | AR3 | AA | AP | APA |
| 1 – 1º Horizontal Bending | 0.344 | 0.458 | 0.706 | 0.457 | 0.517 | 0.586 | 0.526 | 0.511 |
| 2 – 1º Vertical Bending | 0.216 | 2.239 | 1.568 | 0.714 | 0.376 | 1.997 | 0.526 | 2.900 |
| 3 – 1º Torsion | 0.936 | 0.767 | 1.237 | 0.640 | 2.430 | 0.788 | 0.793 | 0.641 |
| 4 – 2º Torsion | 0.687 | N/I* | 0.203 | 0.487 | 0.461 | 0.365 | 1.134 | 0.518 |
| 5 – 2º Horizontal Bending | 0.140 | 0.583 | 0.775 | 0.502 | 1.377 | 0.426 | 0.848 | 0.778 |
| 6 – 2º Vertical Bending | 0.751 | 0.183 | 1.189 | 0.733 | 0.653 | 0.778 | 0.717 | 0.642 |

* Not Identified

Plots in Figure 6 allow a better analysis of these results. Figure 6a shows that for the 6 first modes, as was expected, a clear predominance of the cast steel model (AF) at high natural frequencies could be noticed, followed by fiber- reinforced mortar (AR1/2/3) models, ferrocement model (AA), cast iron model (FF), and finally polymer cement models (AP and APA). This pattern could be verified in all modes except to the fiber-reinforced mortar models, where there were some inversions among different fiber percentage. Figure 6b shows a similar analysis to the modal damping coefficient. The cast steel model (AF) presents an

expected behavior, i.e., the smaller damping to almost all analyzed modes, exception made to the mode 6.




(a) (b)

Figure 6 – Identified results: (a) natural frequencies and (b) modal damping coefficients.

However, for the other models it is noticed that damping coefficients presents huge variations from mode to mode. For mode 1 there is no significant variations between models, where all values are lower than 0.75% and model AR1 presents the higher damping coefficient. For mode 2 damping coefficient value for APA model is very high (2.9%) followed by FF, AA and AR1 models with values higher than 1.5%, which is much higher than the others identified models. For mode 3 the AR3 model presents a damping coefficient value (2.43%) much more high than all the others. For modes 4, 5 and 6 there is predominance to the models AP, AR3 and AR1, respectively, all in the range from 1 to 1.5%, while the others present values inferior to 0.85%.

Based on this results it is difficult to get a precise criteria to choose a material that will introduce an effective structural damping, i.e., that ones with the major damping contribution to all identified modes. In order to improve the visualization of this contribution, and to minimize the bias introduced by the huge differences between the models in some modes, a median plot of modal damping coefficients was constructed (Figure 7). It is clear from this plot the AR1 model predominance followed by AP, AA, APA, AR3, AR2, FF e AF. This behavior corroborates some literature results [6,7,2], which presents ferrocement, low fiber-reinforcement mortar, and polymer cement models with structural damping characteristics more effective than that obtained by traditional materials like cast iron and cast steel.

Although, Figure 7 plot demonstrate this tendency it is necessary to reevaluate the modal damping coefficients for each mode separately in a refined experimental modal analyses. It will increase the damping coefficient identification precision and hopefully will decreases the damping coefficient dispersion observed in some modes.

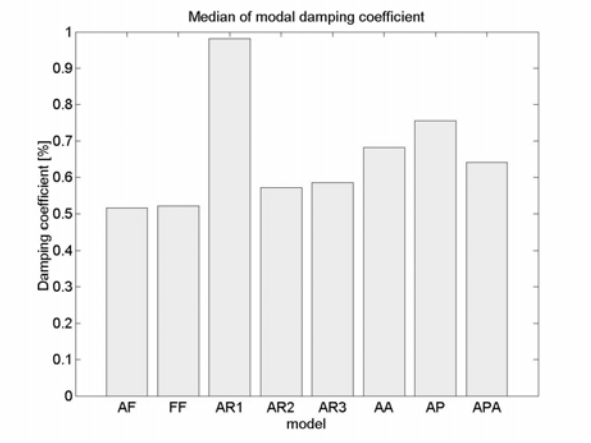



Figure 7 – Median of modal damping coefficients.

Figures 8a and 8b shows the identified mode shapes to 6 lathe beds (AF, AR3, APA, AA, FF and AP). Models AR1 and AR2 were omitted since they do not presents significant differences related to the AR3 model.

## **4.** FINAL REMARKS

Twelve lathe bed prototypes in actual scale were fabricated with the following materials/composite: cast steal (AF); cast iron (FF); fiber-reinforced mortar (AR1, AR2 and AR3), ferrocement (AA); polymer mortar (AP); reinforced polymer mortar (APA). Dynamic tests were carried out on the beds and the results discussed with the aim to substitute the traditional materials, cast iron and cast steel, for the news ones, cement and polymer mortar. Static tests results — which are not presented in the paper— showed that the ferrocement, polymer mortar, and fiber-reinforced mortar prototypes are able to perform well as a machine tool lathe bed at point of view of flexure strength, stiffness, and cyclic load.

From the dynamic behavior, it is clear the experimental identification of the 6 first vibration modes for almost all prototypes. As expected, the cast steel dominance in terms of higher natural frequencies for all the modes demonstrates that the alternatives materials will be the tendency to reduce them. Modal damping coefficients confirm some literature results related to alternative materials increase global damping when compared to the traditional ones. Of course, these are preliminary results and more research must bee done in order to clarify the contributions to the damping coefficient rise for each mode separately.

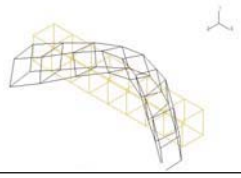
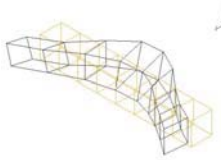
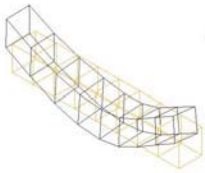
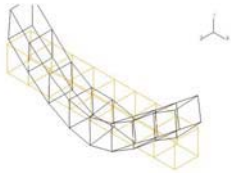
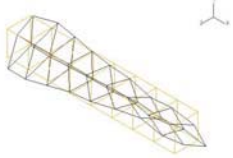
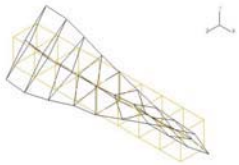
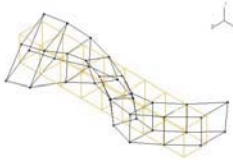
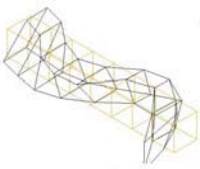
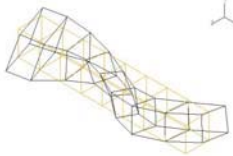
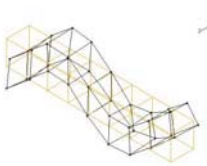
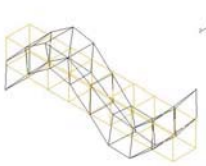
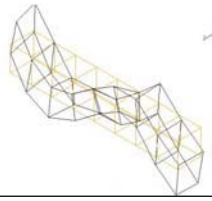
| Mode | AA | FF | AP |
|---|---|---|---|
| 1º. Horiz. Bending |  |  |  |
| 1º. Vertical Bending |  |  |  |
| 1º. Torsion |  |  |  |
| 2º. Torsion |  | **Not Identified** |  |
| 2º. Horiz. Bending |  |  |  |
| 2º. Vertical Bending |  |  |  |

Figure 8a – Lathe beds vibration mode shape.

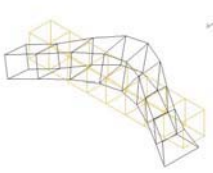
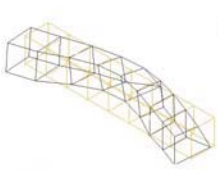
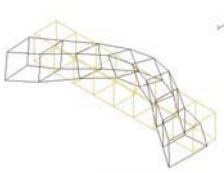
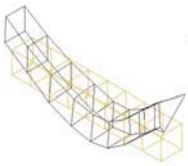
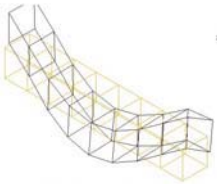
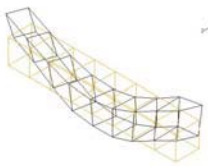
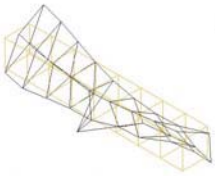
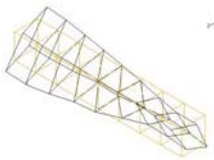
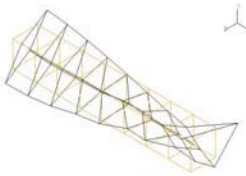
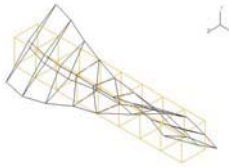
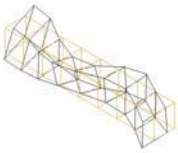
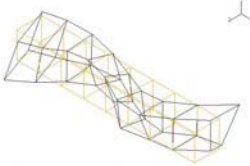
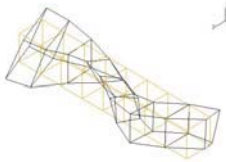
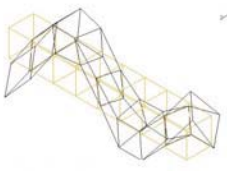
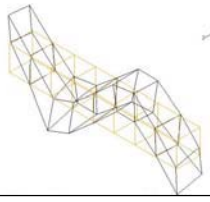
| Mode | AF | AR3 | APA |
|---|---|---|---|
| 1º. Horiz. Bending |  |  |  |
| 1º. Vertical Bending |  |  |  |
| 1º. Torsion |  |  |  |
| 2º. Torsion |  |  |  |
| 2º. Horiz. Bending |  |  |  |
| 2º. Vertical Bending |  |  |  |

Figure 8b – Lathe beds vibration mode shape.

ACKNOWLEDGMENTS

The authors are grateful to LMS and Smartthec Companies for the free-use of CADA-X3.5C and to the government research agencies CNPq, CAPES, and FAPESP for the financial support.

REFERENCES

[1] ACI Committee 544, 'Measurement of properties of fiber reinforced concrete (ACI 544.2R-89)', Detroit, MI, 1989.

[2] Kane, J.F., 'Polymer concrete machine tool components', in Polymers in Concrete, Proceedings of an International Congress, San Francisco, September, 1991.

[3] Koblischek, P.J., 'Polymer concrete as an alternative material for gray cast iron and welded steel construction in the machine tool industry', in Proceedings of the 3rd International Symposium on Brittle Matrix Composites, Warsaw, September, 1991, 529-538.

[4] Rahman, M., Mansur, M.A., Lee, L.K. and Lum, J.K., 'Development of a polymer impregnated concrete damping carriage for linear guide ways for machine tools', *International Journal of Machine Tools and Manufacture* **41**(7) (2001) 431-444.

[5] Rahman, M., Mansur, M.A., Ambrose, W.D. and Chua, K.H., 'Design, fabrication and performance of a ferrocement machine tool bed', *International Journal of Machine Tools and Manufacture* **27**(4) (1987) 431-442.

[6] Rahman, M., Mansur, M.A.and Chua, K.H., 'A study on the application of cementitious materials for machine tools structures', *Bull. Japan Soc. Prec. Engg* **23**(2) (1989) 94-99.

[7] Rahman, M. and Mansur, M.A., 'Fiber reinforced concrete — A new material for machine tools', *International Journal of Japan Society for Precision Engineering* **26**(3) (1992) 183-188.

[8] LMS CAD-X Version 3.5C (Software).

[9] Vold, H., Kundrat, J., Rocklin, G.T. and Russel, R., 'A multi-input modal parameter estimation algorithm for mini-computers', SAE paper 820194, 1982.

International Symposium Polymers in Concrete
2 - 4 April 2006
Guimarães, Portugal

# Carbonation resistance of different concrete mixtures. Effect of the presence of coatings.

M. P. Rodrigues[1], A. Bettencourt[2]

*LNEC, Departamento de Materiais*
*Av. Brasil 101, Lisboa, Portugal*

## ABSTRACT

Concrete carbonation is a natural and inevitable process. The carbonation resistance can be improved, increasing the cement content and reducing W/C, or by the use of a coating applied on the exposed surface of the concrete and acting as a physical barrier against the penetration of $CO_2$. In addition, coatings can be useful when applied on concretes containing mineral admixtures as a percentage of replacement of portland cement that have lower carbonation resistance. This study presents the results of the carbonation resistance of several painted and unpainted concretes having the same water binder ratio but with different mineral admixtures contents. An accelerated carbonation test was used to measure the carbonation resistance of the samples.

## 1. INTRODUCTION

Carbonation is one of the causes of reinforced concrete structures degradation by corrosion of the rebars. Corrosion can be initiated as soon as the carbonation front reaches the reinforcement in result of the lost of passivity given by the concrete cover to the steel. The velocity of the attack mainly depends on the open porosity and the moisture content of concrete, but the role of the binder is also significant, namely the type of cement used and its amount in the concrete, Ribeiro et al. (2001). The process can be reduced by improving the concrete mixture performance, increasing the cement content and reducing the W/C. However, the resulting cost increase may be enough to consider the protection of the concrete surface by a coating system as a competitive alternative solution.

Another way of cost reduction is the use of mineral admixtures as a significant part of the binder, which has environmental advantages. However the reduction on the amount of calcium hydroxide, due to the lower clinker content, also decreases the carbonation resistance. So, the use of binders with high amounts of fly ash or blast furnace slag in low strength concrete mixtures, for housing purposes, which is technically possible today due to the development of the chemical admixtures and the increase of the strength of portland cements, is an alternative that may be used only after testing it's carbonation resistance. If not enough

[1] Senior Research Officer
[2] Research Officer

carbonation resistance is achieved, the use of a coating system should be considered as an alternative solution.

In order to quantify the gain obtained in the carbonation strength by the use of coatings, this study presents the carbonation decrease of low strength concrete mixtures due to the presence of coatings. Type I portland cement, fly ash and slag were used as binders. A binder content of 250kg/m$^3$ of concrete, a water binder ratio W/B=0,66 and different percentages of mineral admixtures were studied. Two different coatings were applied on the studied concretes and an accelerated carbonation test was used to measure the carbonation resistance of the different concretes, with and without paint.

## 2. EXPERIMENTAL PROGRAMME

### 2.1. Constituent materials of concrete

The concrete mixtures were prepared using portland cement, CEM I 42.5 R, in accordance with EN 197-1, siliceous fly ash in accordance with EN 450, blastfurnace slag in accordance with LNEC E 375-1993, limestone coarse aggregates and natural silica sand. Concrete mixtures included a superplasticizer based on polycarboxylic molecules.

### 2.2. Mixture proportions

Table 1 presents the identification of the mixtures and their composition.

Table 1 – Identification of concrete mixtures

| Concrete codes | Binder content (kg/m$^3$ of concrete) | Water-binder ratio (W/B) | Cement replacement content, in mass | | |
|---|---|---|---|---|---|
| | | | Type I Portland cement content (%) | Fly ash FA (%) | Slag S (%) |
| A1 | 250 | 0,66 | 100 | 0 | 0 |
| C1 | | | 75 | 25 | 0 |
| E1 | | | 50 | 50 | 0 |
| F1 | | | 75 | 0 | 25 |
| H1 | | | 50 | 0 | 50 |
| I1 | | | 50 | 25 | 25 |

### 2.3. Protection coating systems

Two different coatings were used, a solvent based paint (U) and a water based paint (V), both having an acrylic resin as binder. According to the technical information given by the producers, coating U has a diffusion equivalent air-layer thickness, Sd (EN 1062-6), above 1000 m correspondent to a dry film thickness around 150 μm and coating V has a Sd of 70 m for the same film thickness. According to EN 1504-2, the minimum required value of Sd for coatings for concrete protection against carbonation is 50 m.

## 2.4. Preparation of testing specimens

For each concrete mixture, four prismatic test specimens were cast at sizes of 200x200x120 $mm^3$, demolded after 24 hours and then cured for 7 days under water and kept in a laboratory room at 20±2 ºC and 65±5 %RH for 1 day. After this 8 days period, one of the prisms was prepared for testing at 28 days of age and the other three were kept at the lab until painting.

Test specimens for carbonation resistance evaluation of concrete at the age of 28 days: Several cylindrical pieces with 50 mm diameter and 120 cm length were obtained by coring one of the prismatic concrete specimens. At 21 days, the lateral surfaces were sealed with an epoxidic resin impermeable to $CO_2$ in order to have two opposite 50 mm diameter permeation areas. These cylindrical specimens were kept at the laboratory environment until the age of 28 days, before further testing.

Test specimens for carbonation resistance evaluation of painted concrete: The three remaining concrete specimens, after the 7 days period of curing were kept for 14 days at the laboratory at 20±2 ºC and 65±5 %RH and at least two months more at 23ºC and 50% RH, in order to obtain a dry surface appropriate for the painting. Two of the concrete prisms were painted (paint U and paint V) and the other was kept as reference at the same conditions of temperature, humidity and age. Before painting, the opposite (200x200) $mm^2$ surfaces of the prisms were brushed and cleaned to eliminate laitance and dust to allow a better adherence of the coating. The paints were then applied in two coats according to the instructions of the producers and cured for at last 2 weeks. The final thickness in both paints was about 150 μm. Then, several cylinder pieces with 50 mm diameter and 120 cm length were obtained by coring both the two painted prisms and the unpainted prism kept as reference. Again the lateral surfaces were sealed with an epoxidic resin in order to have only the two opposite 50 mm diameter permeation areas.

The total time spent from the casting of the concrete to the beginning of the carbonation test was about 5 months.

## 2.5. Test method

The cylindrical test specimens of concrete mixtures having 28 days of age were submitted to the $CO_2$ attack in a chamber at 23ºC, relative humidity ranging between 60% and 70 % and $CO_2$ concentration between 5 and 6%.

The painted specimens were tested simultaneously with the unpainted reference concrete specimens having the same age (about 5 months), in order to compare their carbonation resistance with the carbonation resistance of the 28 day aged concretes previously tested.

Test specimens were taken from the carbonation chamber after 30, 60 and 90 days and the carbonation depth was measured after broken the specimen, by using the phenolphthalein test [RILEM CPC-18]. Tests specimens of the reference unpainted concretes aged 5 months were taken from the chamber after 30 and 90 days and compared with the 28 days aged concretes previously tested, in order to evaluate the possible influence of the age on the carbonation resistance of the concretes.

## 3. RESULTS AND DISCUSSION

### 3.1. Carbonation resistance of unpainted concretes

Figures 1 and 2 present the carbonation depth of the unpainted 28 day and 5 months aged concretes, after 30, 60 ad 90 days of exposure in a carbonation chamber.

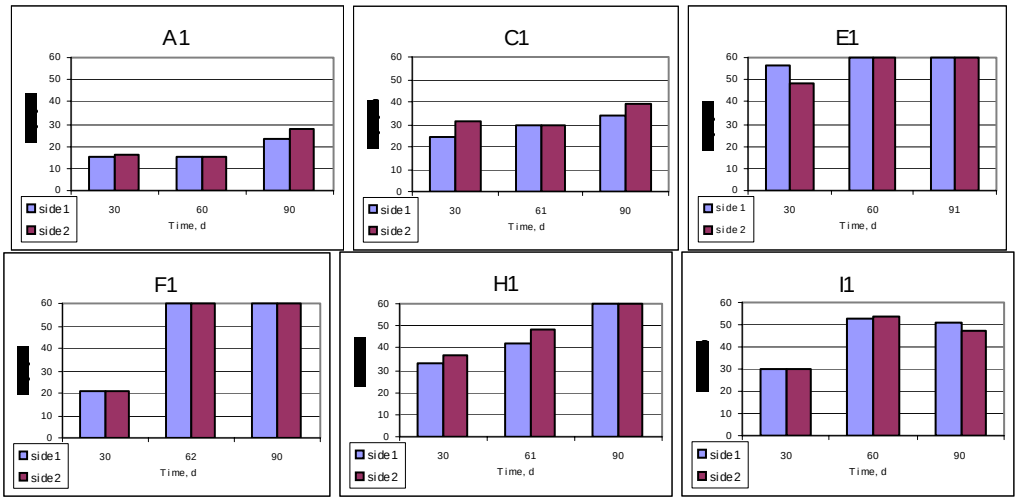



Figure 1 – Carbonation depths (mm) of different concretes aged 28 days, after accelerated carbonation during 30, 60 and 90 days.
A1 – 100% Type I Portland cement concrete; C1 – 25% Fly ash (FA) content;
E1 – 50% FA content; F1 –25% Slag (S) content; H1 – 50% S content;
I1 – 25% FA content + 25% S content.

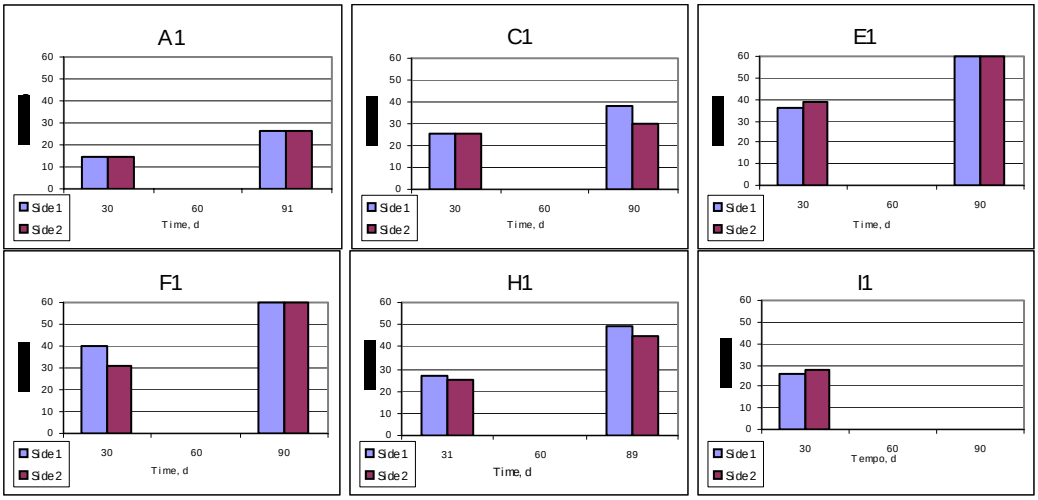



Figure 2 – Carbonation depths (mm) of different concretes aged 5 months, after accelerated carbonation during 30 and 90 days
A1 – 100% Type I Portland cement concrete; C1 – 25% Fly ash (FA) content;
E1 – 50% FA content; F1 –25% Slag (S) content; H1 – 50% S content;
I1 – 25% FA content + 25% S content

The higher carbonation resistance was presented by the concrete mixture A1, having only type I portland cement as binder (due to the higher availability of calcium hydroxide, $Ca(OH)_2$).

The concrete mixtures having mineral admixtures in the binder showed poorer performance against the $CO_2$ attack than A1. In the case of the fly ash increase from 25% to 50% (C1 and E1 mixtures) there is a decrease in the carbonation resistance, as should be expected due to the lower availability of $Ca(OH)_2$.

The same did not happened in the case of the slag increase – F1 (25% S) and H1 (50% S) mixtures – since mixture H1 performed better than mixture F1, whatever the age (28 days or 5 months). This was unexpected since the portland cement has higher lime content (Bijen (1996)). However, since the substitution of cement by slag was weight replacement, the volume of binder is higher in 50% mixture, due to the lower density of slag, which may be responsible for the better performance of H1 mixture.

Comparing the carbonation resistance of different ages of the same concrete mixtures we can see that no appreciable difference are presented by mixture A1 (100% Tipe I Portland cement) and by the concretes with 25% content of admixtures – C1 (25% FA) and F1 (25% S). However on concretes with 50% content – E1 (50% FA) and H1 (50% S) – a slight improvement was verified from 28 days to 5 months cure. The improvement of 50% mixtures may be explained by the later hydration of the mineral admixtures, which becomes more evident when the percent of cement replacement is higher.

## 3.2. Carbonation resistance of painted concretes

Figures 3 and 4 present the carbonation depths of the painted 5 months aged concretes, compared with the unpainted concretes with the same age.

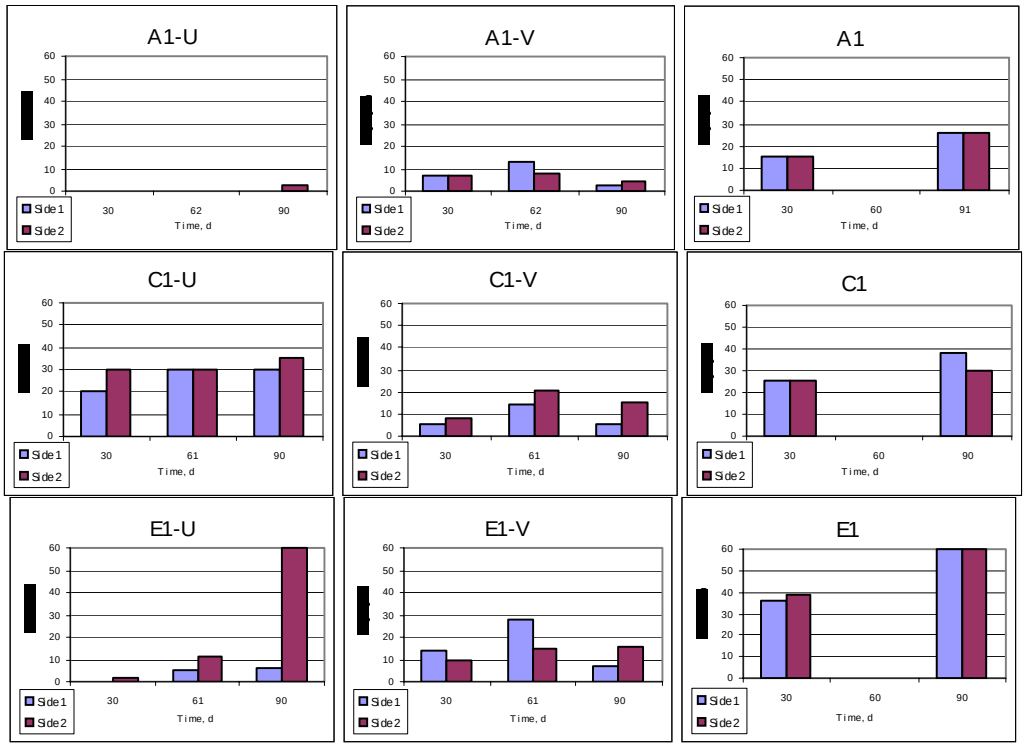



Figure 3 – Comparison of carbonation depths (mm) of painted (paints U and V) and unpainted concretes (concretes age: 5 months)
A1 – 100% Type I Portland cement concrete; C1 – 25% Fly ash (FA) content;
E1 – 50% FA content;

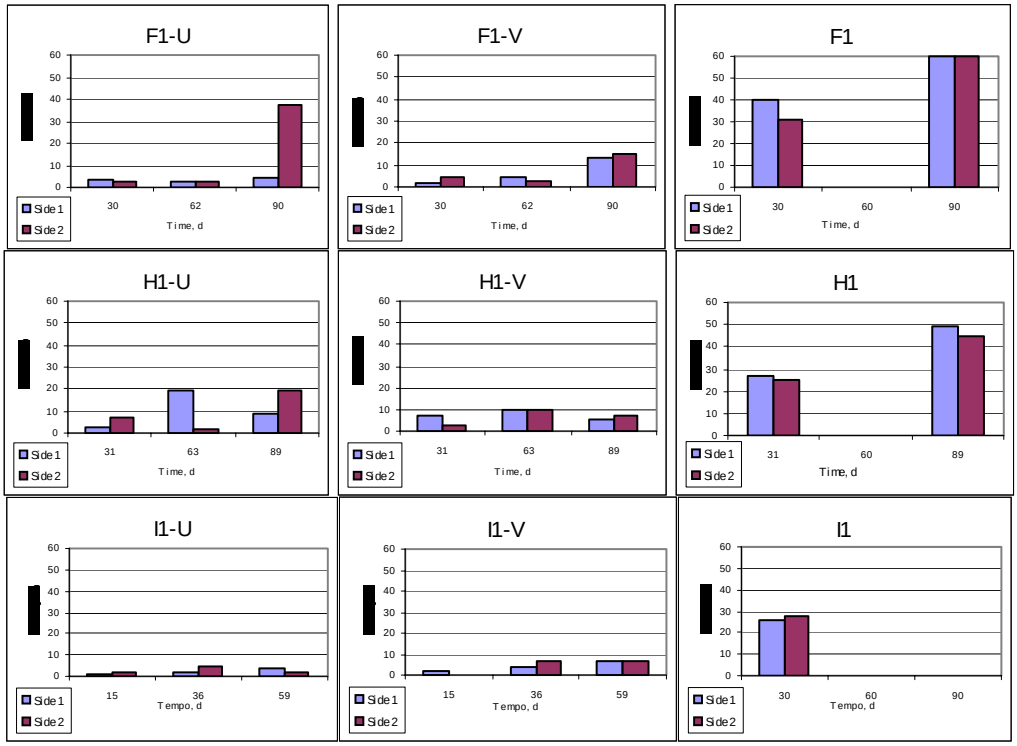



Figure 4 – Comparison of carbonation depths (mm) of painted (paints U and V) and unpainted concretes (concretes age: 5 months)
F1 –25% Slag (S) content; H1 – 50% S content; I1 – 25% FA content + 25% S content

In general the presence of coatings reduces substantially the carbonation of the concrete. However the performance of the coatings depends on the continuity of the film, which is affected by the quality of the substrate – the presence of voids and the missing of smoothness can compromise the formation of a continuous film and lead to the presence of areas of lower thickness. This was the case for some of the studied concretes and explains the irregularity of carbonation depth obtained at the opposite faces of some painted specimens – see for instance F1-U and E1-U after 90 days of carbonation presenting total carbonation at one face and only some millimetres at the opposite face and C1-U that presents no appreciable improvement against the unpainted concrete C1.

As to the evaluation of the performance of paint U against paint V, although the first is more resistant to $CO_2$ permeation as can be seen by the higher Sd (EN 1062-6), both have in general a similar behaviour as to the protection against the carbonation of the concretes. Again this can be explained by the irregularity of the films due to the missing of smoothness of the substrates.

## 4. CONCLUSION

Based on the results of this study as to the carbonation protection, the following conclusions can be drawn:

- The use of slag or fly ash reduces the carbonation resistance of the binder;
- Coatings can reduce appreciably the carbonation of concrete so they can be an useful way of increase the carbonation resistance of poorer portland cement mixtures. However their behavior depends mainly on the continuity of the film and to profit from the use of a coating

with a lower permeability to $CO_2$ is necessary to prepare de substrate before paint, for instance by using a mortar;

- The improvement on concrete carbonation resistance by the use of coatings is much higher when using high W/C in result of the cement replacement by mineral admixtures.

## 5. ACKNOWLEDGMENTS

This study was performed with the collaboration of JOMATEL, a ready-mixed concrete producer, which was responsible for the supply of the concrete constituents and the preparation of all concrete specimens. The authors also wish to thank to JOMATEL, namely the technicians Mr. José Fernandes and Mr. José Cunha, for the technical support in the definition of the concrete mixtures. A final acknowledgment is given to the experimental tests coordination by João Milharadas (LNEC).

## 6. REFERENCES

Ribeiro, A.B., Machado, A., A. Gonçalves, A., Salta, M., A Contribution to the Development of Performance-Related Design Methods, RILEM Proceedings, PRO 29, Life *Prediction and Aging Management of Concrete Structures*, 2nd International RILEM Workshop, Paris, 5-6 May, 223-236 (2003).

Bijen, J, Blast Furnace Slag Cement, *Association of the Netherlands Cement Industry*, Netherlands (1996).

EN 1504-2, Products and systems for the protection and repair of concrete structures. Definitions, requirements, quality control and evaluation of conformity - Part 2: Surface protection systems for concrete.

EN 1062-6, Paints and varnishes – Coating materials and coating systems for exterior masonry and concrete – Part 6: Determination of carbon dioxide permeability.

International Symposium Polymers in Concrete
2 - 4 April 2006
Guimarães, Portugal

# Mechanisms of Blistering of Coatings on Concrete

L. Wolff[1], Kidist Hailu[2], M. Raupach[3],

*Institute of Building Materials Research of Aachen University*
*Schinkelstrasse 3, 52064 Aachen, Germany*

## ABSTRACT

The phenomenon of the so-called osmotic blistering in polymer coatings on concrete is known since the early 1970s. Liquid-filled blisters in a diameter-range from a few mm to cm can appear immediately or certain weeks or months after coating.

In an ongoing research project, carried out at Institute for Building Materials Research of Aachen University, as a start all raw materials of epoxy formulations, which may cause blistering on industrial floors, have been investigated. Thereby several epoxy systems with known formulation have been provided by chemical industry or, in view of separation of influence parameters, produced in own laboratories. Existing market products have been used as reference materials.

Achieved results seem to be in contradiction to existing theories of the so-called semi permeable membrane. The contact zone of concrete and base coat is likely to form a blister permeable to dissolved ions of potassium and sodium. The mechanism of blistering may therefore be described as a directed diffusion process and not as an osmotic process.

## 1. INTRODUCTION

The so called osmotic blistering of thermosetting resins like epoxy resin on cementitious substrate is a phenomenon which has not yet been explained in detail, Ignoul (2004), Stenner (2003). The requirements on a coating as protection of concrete against aggressive substances, easy cleaning, high abrasion resistance or functionality of clean rooms are no longer fulfilled after blistering, resulting in the need for extensive repair.

The common reason of this blistering is seen within the framework of osmotic transport processes. Osmosis is chemically described as a transport of solvent between two liquids containing different concentrations of dissolved ions or molecules separated by a semipermeable membrane. If the dissolved substances can penetrate the membrane, the equilibrium of concentration is achieved by diffusion processes. Within osmosis only the solvent, e.g. water can penetrate the membrane, dissolved ions are hindered, see also figure 1.

[1] Dipl.-Ing.
[2] Dr. rer. nat.
[3] Prof. Dr.-Ing.

The majority of publications locate this membrane either in the epoxy base coat, the contact zone between base coat and concrete or, depending on porosity of concrete, in the concrete (e.g.. Stenner (2003), Pfaff (1997), Hensel (1995)).

According to actual perceptions, the following assumptions are necessary for osmotic blistering (e.g. Stenner (2003)):

- existence of an adequate amount of movable water inside the concrete
- a mostly water pressure tight top layer of the coating
- existence of *dissolved* compounds with a concentration gradient between concrete surface and the inside of the concrete
- Formation of a semipermeable membrane

If one of the named postulates is missing, osmotic blistering is, based on common understanding, not possible. In figure 1 the transport processes between concrete and blister based on osmotic principles are schematically shown.

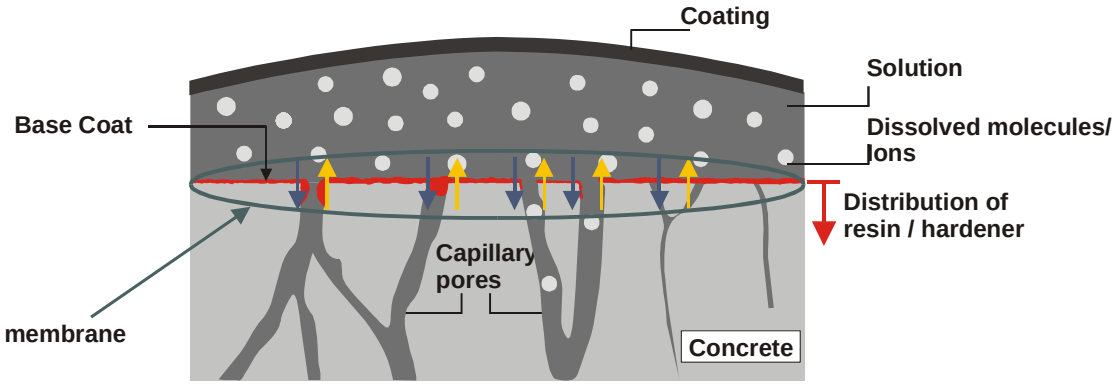



Figure 1 – Schematic view of transport processes in an osmotic blister

Some authors explain the occurrence of blisters mainly with the so called chromatographic effect, which means that the epoxy formulation is partially separated by capillary suction of the concrete. According to literature mainly aliphatic amines as part of the hardener undergo this effects which may lead to uncompleted crosslinking of the different components. (e.g. Stenner (2003), Dively (1994))

According to /2/ a dense concrete, e.g. a C50/60, which contains in practical view no capillary pores, showed no blistering at all, as neither a chromatographic effect nor a relevant water transport occur. However, according to Dively (1994), blistering was also observed on concrete surfaces with comparable higher compressive strength. This effect might therefore exist on all types of concrete substrates.

## 2. RESEARCH PROGRAMME

### 2.1. General

Earlier investigations about “osmotic blistering” were mainly based on ready for use epoxy formulations from different producers. The knowledge about the composition of these formulations was therefor limited to the contents of usual safety data sheets. Some components, which might essentially influence the properties of the polymer system, may not be listed at all. By means of production of different resin and hardener compositions in the own laboratory most investigations could be carried out with epoxy formulations of known

composition. In this research mainly the composition of the hardener was varied, while the composition of the resin component containing reactive diluents was held constant.

The selection of subjects was mainly based on the existing contradiction between assumed transportation process by osmosis and the composition of the blister fluid containing the coating solvent and dissolved ions or molecules.

- Reaction kinetics of epoxy base coats
- Water uptake of epoxy base coats
- Diffusion properties of epoxy resins
- Investigations on the chromatographic effect
- Blistering versus formulation of base coat and type of concrete substrate

## 2.2. Composition of Hardener Components of Epoxy Base Coats

The composition of epoxy formulations for base coats for concrete elements is only roughly described hence many publications on this topic exist, e.g. Stenner (1995). Therefore this introduction concentrates on the composition of the hardener, which was systematically investigated within this work.

Typical hardener systems for epoxy resins for application on site are mixtures of the following components.

- Amine based hardener, e.g. Isophorondiamine IPD, Methaxylendiamine or Diethylentriamine DETA
- Bisphenol A/F as adduction partner
- Catalysts, e.g. salicylic acid
- Reactive diluents, e.g. benzyl alcohol or nonyl phenol
- Solvent, e.g. ethyl alcohol
- Additives and pigments

Fundamentally two groups of hardeners are distinguished, blends and adduct hardeners. While blends are only a mixture of the mentioned components, adduct hardeners are characterised by a partial reaction between a small amount of the resin component with the hardener. The complete crosslinking is in both cases fulfilled after mixture of both components and application on site.

Furthermore, the results of different epoxy formulations are presented and described. The formulations used differ on the type of aminic hardener, concentration of benzyl alcohol or nonyl phenol and on the degree of adduction. Parallel to formulations produced in laboratory, pre-formulated systems of the chemical industries and for comparison ready to use systems have been investigated.

## 2.3. Reaction Kinetics of Epoxy Formulations

The reaction of epoxy formulation runs by polyaddition. Due to the stoichiometric relationship between resin and hardener a complete crosslinking is, theoretically, ensured. The developing of crosslinking is however influenced by many factors. First of all temperature during chemical reaction plays a decisive role. Also impact of moisture before and during crosslinking influences the degree of crosslinking. If parts of the epoxy base coat remain unreacted, blistering might be enabled.

The degree of crosslinking of epoxy resins can be characterised by both the glass transition temperature $T_g$ and the amount of residual enthalpy. The glass transition temperature defines the transition between the glassy and the viscoplastic state. By means of the ratio between existing glass transition temperature of a partially crosslinked specimen and

the one of a completely crosslinked probe, the current degree of crosslinking can be calculated UserCom (2004). The residual enthalpy is a measure for the remaining capacity of reaction of a partially reacted epoxy system.

The determination of glass transition temperature and remaining enthalpy was achieved by Differential Scanning Calorimeter DSC. Using this method a probe is heated in a temperature range of e.g. –50 °C and +250 °C while the heat energy is measured comparatively to a reference probe that is thermally inert.

The tested epoxy resins have been prepared as free films after application on Teflon foil. Afterwards the specimens were stored in laboratory climate of 23 °C and 50 % relative humidity. In figure 2 different plots of DSC measurements are presented. Specimens of different ages as well as a tempered and therefore completely crosslinked probe have been investigated. The different glass transition temperatures of the probes are simplistically marked at the inflexion point of the plot. The shaded area is the remaining enthalpy of the examined probe.

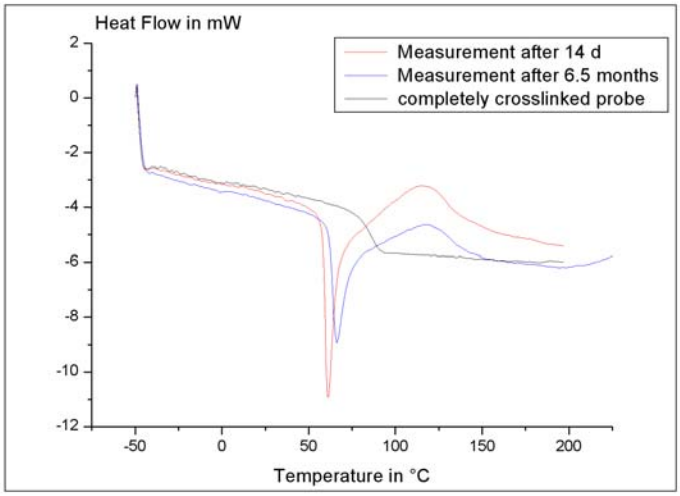



Figure 2 – Comparison of DSC measurements of an epoxy system showing the glass transition temperature (adduct hardener without solvent or benzyl alcohol)

Relating to the maximum achievable glass transition temperature a crosslinking degree of 71 % was calculated after 14 d and of 79 % after 6.5 month, respectively. Looking at usual industrial floors with temperatures of not more than 10 °C a significant lower degree of crosslinking can be expected in practice. It can be assumed that a complete crosslinking cannot be achieved within practical conditions, e.g. UserCom (2004)

## 2.4. Water Uptake of Epoxy Base Coats

The water uptake of hardened epoxy systems for application on cementitious substrates is usually not tested. In Germany this parameter is only tested within the suitability test for sealing of concrete bridges. Hereby the maximum water uptake of free epoxy films with a thickness of 1 mm is limited to an amount of 2.5 M.-% after a storage in water for 14 d.

Within this research work each of the 11 different epoxy formulations were stored in tap water and artificial pore solution of concrete with an pH of 13.8 over a time of 6 month. The production of the polymer films with a thickness of about 0.7 mm was carried out

analogue to chapter 2.3. The change of mass was determined by weighing. In figure 3 water uptake is plotted against time under storage in tap water.

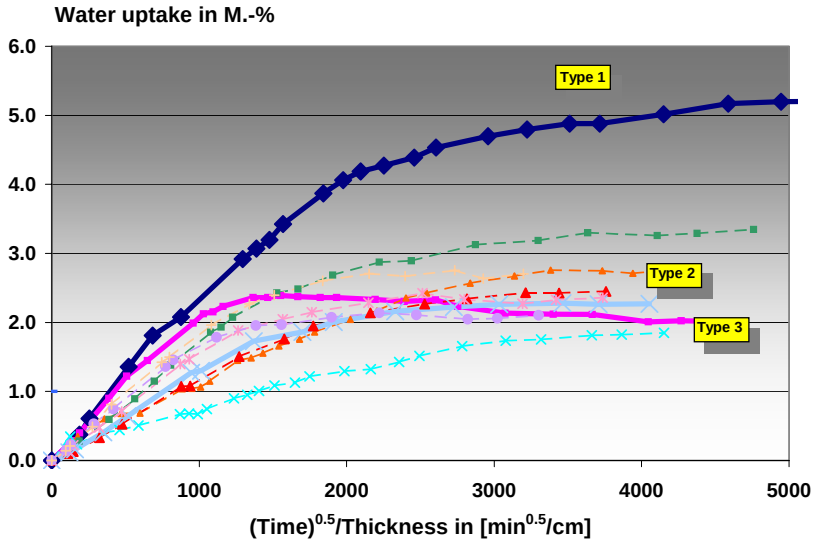



Figure 3 – Water uptake of free epoxy films under storage in tap water

The eleven measured probes can be divided in three different types based on the character of the plot (Type 1, Type 2, Type 3). Correspondingly to these types, three different epoxy formulations are discussed in detail.

Type 1 is characterised by a comparable high water uptake of more than 5 M.-%. Also after a storage time of 6 month an increasing water uptake is measured. The labelled epoxy formulation is based on a commercial available blend hardener with an amount of benzyl alcohol of about 20 M.-%.

The majority of the formulations tested are characterised by type 2 with a water uptake varying between 2 and 3 M.-%. This type of epoxy formulation reaches a constant value of water uptake after a storage time of about 3 to 4 months. Both adduct and blend hardeners with different aminic components and solvent degree of about 3 to 35 M.-% show this tendency.

Type 3 shows initially increasing weight as type 1 and type 2 formulations. After a certain storage time of some weeks these probes show decreasing weights. This decrease is probably caused by leaching of soluble components, which are not completely bounded in the polymeric network /5/. These arising microholes might be filled with water. The marked formulation is an adduct hardener with a content of benzyl alcohol of about 35 M.-%.

Storage in artificial concrete pore solution showed similar results. A loss of resistance of some epoxy formations in alkaline solution was not found at all.

## 2.5. Diffusion properties of epoxy formulations

In previous investigations of damage events regarding osmotic blistering analysis of the liquid inside the blisters showed identical compositions. The main components were sodium and potassium. Calcium was only found in crystalline formation, e.g. as calcium carbonate. The detected organic substances were mostly part of the base coat or other coating layers. Hereby benzyl alcohol, phenol, BisphenolA/F or amines were detected in the watery blister solution. The pH was in range of 12 to 13, e.g. Ignoul (2004), Stenner (2003).

By reason of the high amounts of sodium and potassium is has to be questioned, how these ions can penetrate the epoxy base coat and accumulate inside the blisters.

Water soluble sodium or potassium are neither part of the coating products nor can these amounts originate from atmosphere. Only the concrete pore solution can be the origin of such high concentration of alkalis. An additional application of the so-called sodium silicates does only play a minor role in practice and can be neglected within this research project. If therefore alkaline ions penetrate through the base coat into the blisters, which are usually between base coat and top coat layers, no semipermeable membrane can exist at all as not only the solvent but also dissolved ions penetrate the base coat.

For detailed investigation of the diffusion and transport behaviour of epoxy formulations both free polymer films as well as concrete slices coated with different epoxy formulations have been tested in diffusion cells, see figure 4. Hereby the following parameters besides formulation of the epoxy systems have been considered:

- Composition of concrete substrate by means of size of capillary porosity
- Condition of concrete immediately before coating (dry, water saturated)
- Blasting of the base coat with quartz sand

The diffusion cells consist of two chambers. One chamber is filled with artificial pore solution with an pH of 13,8, consisting of sodium, potassium and calcium hydroxide. The second chamber was filled with demineralised water. In case of the coated concrete slices the uncoated side was exposed to pore solution, the coated side was exposed to demineralised water. Measurement of diffusion properties of both the free polymer films and the coated concrete slices was carried out by determination of electrolytic resistivity as reciprocal of the electrolytic conductivity in the chamber filled with demineralised water. If diffusion of ions into this chamber occurs, falling electrolytic resistivity and rising conductivity, respectively are determined. The plot of rising electrolytic conductivity enables calculation of the diffusion coefficient by means of Fick's second law of diffusion.

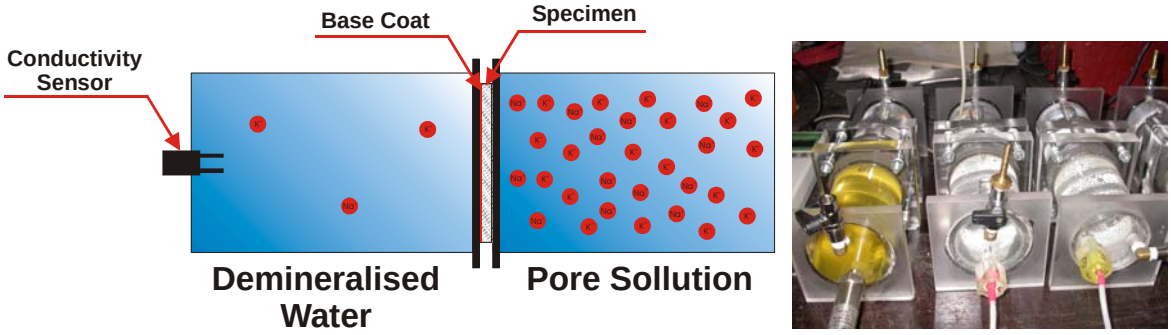



Figure 4 – Diffusion cells for epoxy coated concrete slices and free polymeric films

In figure 5 the plots of conductivity inside the diffusion cell with free polymeric films based on different epoxy resin and hardener formulations are represented. Over the measurement time of about 11 weeks, an increase in conductivity of one order of magnitude, at a maximum,was observed.

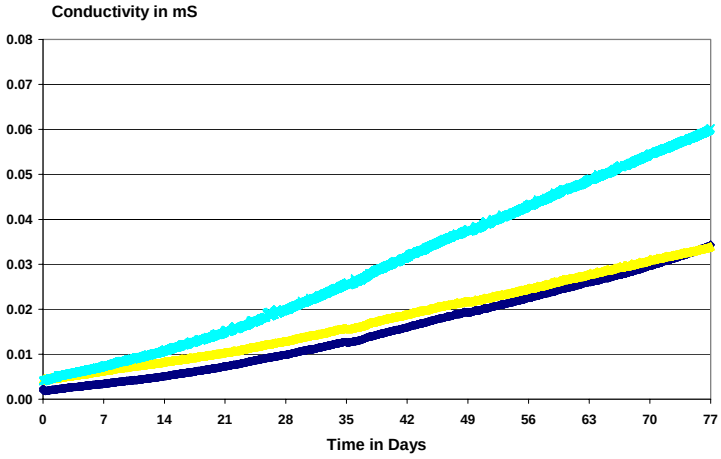



Figure 5 – Change of conductivity inside the diffusion cell “demineralised water” with different free films

Measurements of concentration of potassium and sodium showed no detectable concentration inside the cell filled with demineralised water. The light increase of conductivity seemed therefore to be caused by shifting of charging inside the diffusion cell.

In further tests coated concrete slices have been mounted inside the diffusion cells. The coating of these slices was carried out according to the procedure described in chapter 2.7. In the following figure 6 the changes of conductivity of the diffusion cells “demineralised water” are plotted in dependence of the moisture content of the concrete before application of the base coat. While in case of the water saturated concrete only a light increase of onductivity was detected due to lower diffusion rates of alkalis, on dry coated concrete slices a significant higher change of conductivity was observed. The diffusion rates of the uncoated reference concrete are about six times higher than the rates of the dry coated concrete slices.

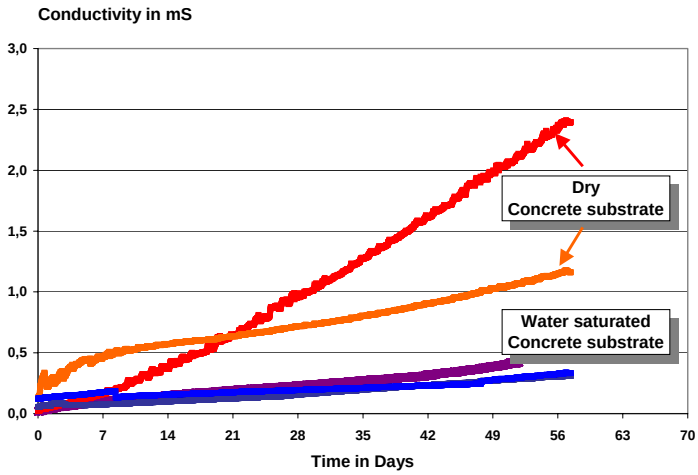



Figure 6 – Change of conductivity inside the diffusion cell “demineralised water” with base coated concrete slices against different moisture conditions of the concrete substrate

In contrast to the investigation of the free films, significantly increased concentrations of potassium and sodium were detected inside the diffusion cell “demineralised water”. In the following table, the maximum concentrations of potassium and sodium inside the diffusion cell “demineralised water” are presented after a measurement time of 5 weeks.

Table 1 – Maximum Alkali Concentration inside the Diffusion Cell “demineralised Water” after a measurement time of 5 weeks

| Moisture condition of concrete substrate | Alkali concentration in mg/l | |
|---|---|---|
| | $Na^+$ | $K^+$ |
| Water saturated | 11,4 | 8,2 |
| dry | 7,8 | 42,3 |

## 2.6. Investigations on the chromatographic effect

Further investigations on the formation of blisters within reactive resin coatings at ibac deal with the already described chromatographic effect, see chapter 1. This effect is now being investigated using the confocal Raman microscopy, which allows a detection of organic substances along the concrete depth under a coating.

With this method a quantification of the chromatographic effect is possible in dependence of the type and formulation of the epoxy resin and the hardener. The so far phenomenologically described effect of chromatography of the epoxy formulation inside a cementitious substrate can now be described in detail. The results of these actual running research will be published later.

## 2.7. Blistering versus formulation of base coat and condition of concrete substrate

The dependence of formation of blisters on the type and condition of the cementitious substrate has already been investigated in various research projects, Stenner (2005), Ignoul (2004), Schäper (2003). Within this research work two different concrete substrates have been used. Selection characteristics for the substrate were not as usual the strength class but the hereby more important size of capillary pore volume. Thus a concrete with a large capillary pore volume of about 8 % with a true porosity of 15 % and a comparable dense concrete with a capillary volume of 3 % with a true porosity of also 15 % have been used (determination of capillary pore volume by mercury pressure porosimeter, determination of true porosity by water uptake under pressure of 150 bar)

The coating of the concrete slabs with the base coat was either executed on dry concrete (storage of the concrete slabs in laboratory at a climate of 23 °C and 50 % r. h.) or on water saturated concrete (storage under water) which was taken from the water bath 15 min before application of the coating. The application of the epoxy formulation on the partially blasted and unblasted concrete slabs was carried out at a temperature of 8 °C. Afterwards all specimens have been stored in a water bath with a water level 1 cm bellow the upper side of the specimens. Epoxy formulation produced in laboratory with known composition have been used. The application rate of the base coat was held constant at 400 g/m².

Formation of blisters was both detected on dry and wet coated concrete slabs after a storage time between some weeks and about three months. A higher density of blisters was detected on the concrete substrate with the large capillary pore volume. The possible reasons for the occurrence of blisters are discussed in the next chapter.

## 3. DISCUSSION

The formation of blisters depends significantly on the conditions of the concrete substrate under application of the epoxy formulation which leads to interaction of the liquid epoxy resin and the substrate itself.

An application of the base coat on water saturated substrate leads to a change of reaction of the epoxy resin, which might interfere the crosslinking. This effect which is strongly dependent on the formulation of the epoxy base coat, was already quantified by differential scanning calorimeter DSC, User Com (2004). The plot of heat flow shown in figure 2 would in this case significantly change in the temperature range up to about 100 °C,.

At the same time imperfections may occur inside the base coat resulting in a penetration of alkaline ions through the base coat. This effect, which is schematically shown in figure 7, was already indicated by the results presented in figure 6.

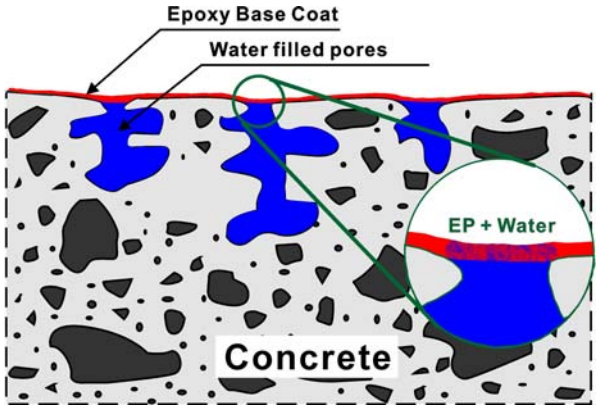



Figure 7 – Schematic view of occurrence of imperfections in a base coat applied on wet concrete substrate

Formation of blisters on dry coated concrete substrate however is caused by two parallel running effects. Firstly the chromatographic effect may lead to a partial separation of resin and hardener causing a disturbance in crosslinking of the reactive resin. Additionally a rough surface with a large specific surface area compared to a water saturated concrete may lead to the so called geometric effect. A part of the applied base coat may be drawn inside larger pores of the concrete, where small imperfections occur. These imperfections enable, similarly to wet coated concrete, the diffusion of alkaline ions, leading to the formation of blisters.

The results presented in chapter 2.5 have shown the large diffusion rates of potassium and sodium through a dry coated concrete slice. Due to the geometric effect, as well as the chromatographic effect, the amount of imperfections is clearly higher at dry coated substrates than at wet coated substrates.

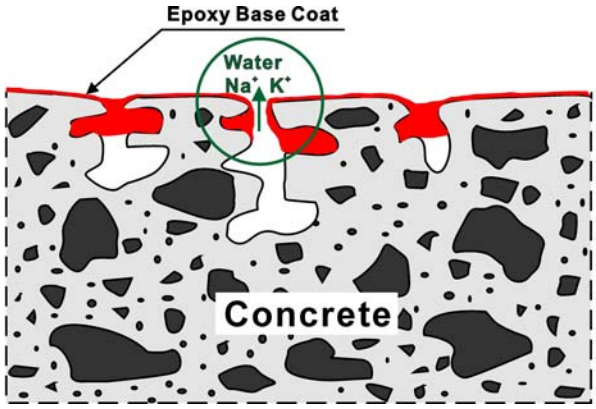



Figure 8 – Occurrence of imperfections inside the base coat applied on dry concrete as a result of the geometric effect

The presented results indicate that no semipermeable membrane is located in the contact zone between concrete and base coat. Therefore no osmotic transport process should occur in this region. The phenomenon described former as osmosis seems rather to be a directed diffusion phenomenon.

## 4. CONCLUSION AND OUTLOOK

Within the presented research project, the fundamentals of the so-called osmosis on blister formation have been investigated in detail. It could be shown that the reason for the formation of blisters may be seen as a consequence of diffusion transport processes instead of osmotic effects. In a forming blister, a semipermeable membrane which is required for osmotic processes does not seem to exist, being rather. the contact zone of substrate and base coat permeable to dissolved ions.

The presented research project is to be continued with the support of the DFG. The focus of further research is the investigation of the mechanisms leading to the pressure inside the growing blisters.

## 5. Acknowledgement

The presented investigations were carried out with financial support by the German Research Foundation DFG. The authors would like to thank for this support.

## 6. REFERENCES

Dively, R.W.: Osmotic Blistering of Coatings and Linings Applied to Concrete Surfaces. In: *Materials Performance* 33 (1994), Nr. 5, S. 42-44

Fiebrich, M.: *Kunststoffbeschichtungen auf ständig durchfeuchtetem Beton*. Aachen : Institut für Bauforschung der RWTH Aachen, 1987. - Forschungsbericht Nr. F 184

Hensel, W.: Blasenbildung bei organischen Beschichtungen auf zementgebundenen Baustoffen. In: *Betonwerk und Fertigteil-Technik* 61 (1995), Nr. 2, S. 106-108,110-114

Ignoul, S. ; Van Ricjstal, F. ; Van Gemert, D.: Blistering of Epoxy Industrial Floors on Concrete Substrate: Phenomena and Case Study. Berlin. International Conference on Polymers in Concrete, 1. – 4.6.2004

Pfaff, F.A. ; Gelfant, F.S.: Osmotic Blistering of Epoxy Coatings on Concrete. San Diego: SSPS, 1997. - In*: Expanding Coatings Knowlegde Worldwide, Proceedings of the SSPC*, San Diego, November 16-20, 1997, S. 146-158

Rheinwald, G.: Blasenbildung an Beschichtungen durch Substratreaktion. Ostfildern : Technische Akademie Esslingen, 2003. - In: *Industrieböden '03, Internationales Kolloquium*, 21. - 23. Januar 2003, (Seidler, P. (Ed.)), Vol. II, S. 733-740

Schäper, M. ; Kreye, J. ; Hiess, T.: Hinterfeuchtete Betonbeschichtungen - Untersuchungen zur Vermeidung von Osmoseschäden. Wiesbaden : Fachhochschule Wiesbaden. - In: *Veröffentlichungen aus Lehre, angewandter Forschung und Weiterbildung* (ca. 2003), Nr. 40

Soles, C.L. ; Chang, F.T. ; Bolan, B.A. ; Hristov, H.A. ; Gidley, D.W. ; Yee, A.F.: Contribution of the Nanovoid Structure to the Moisture Absorption Properties of Epoxy Resins. In: *Journal of Polymer Science Part B* 36 (1998), Nr. 17, S. 3035-3048

Stenner, R. ; Machill, N.: Adhäsion und Blasenbildung von Beschichtungen bei rückseitiger Feuchteeinwirkung. Ostfildern : Technische Akademie Esslingen, 2003. - In: *Industrieböden '03*, Internationales Kolloquium, 21. - 23. Januar 2003, (Seidler, P. (Ed.)), Vol. I, S. 79-102

Stenner, R. ; Magner, J.: Influence of Moisture from Substrate to Blistering. Leuven : Katholieke Universiteit, 1995. - In*: VIIIth International Congress on Polymer in Concrete, ICPIC Congress*, Oostende, July 3-5, 1995, S. 215-220

User Com ; Wagner, M. ; Bottom, R. ; Larbonois, P. ; Schawe, J.: Messen mit hohen Heizraten - Vorteile und Grenzen. Schwerzenbach CH : Mettler Toledo GmbH. - In: *User Com Informationen für Anwender von METTLER TOLEDO Thermoanalysen-Systemen* (2004), Nr. 19, - Firmenschrift

International Symposium Polymers in Concrete
2 - 4 April 2006
Guimarães, Portugal

# Systems for superficial protection of concretes

Pedro M. Moreira[1], José B. Aguiar[2], Aires Camões[3]

*University of Minho, Department of Civil Engineering*
*Azurém, P - 4800-058 Guimarães, Portugal*

## ABSTRACT

Nowadays, it is consensual that the biggest degradation of concrete happens from outside to inside actions, due to the penetration of moisture, active gases and aggressive ions, by mechanical, physical and chemical causes that frequently act together. A low porosity, permeability and concrete penetration to moisture and gases are the first lines of defence against several deterioration mechanisms. The durability of concrete depends largely on how hard or easy fluids (water, carbon dioxide, oxygen) in liquid or gas form can migrate through the concrete hardened mass. When selecting the paint coating for concrete protection, importance is given to the properties of diffusion and permeability resistance, besides the properties of durability and chemical resistance. The paint coatings must stop the penetration of water and delay the influence of aggressive agents ($CO_2$, $SO_2$, $Cl^-$ ions), allowing the structure to breathe by a water vapour diffusion mechanism. Through tests of capillarity absorption, immersion absorption, porosity, water and oxygen permeability, a comparison was made between painted and non painted concrete specimens. Three different coating types were tested: silicon varnish; acrylic and epoxy paints. The results showed that, in general, all coatings reduce the porosity and the permeability. The epoxy paints proved to be the best ones.

## 1. INTRODUCTION

Concrete can be a highly durable construction material as long as care and quality control are enforced at all stages of the design, production and construction processes. However, experience has demonstrated that its potential long-term durability is not always achieved, leading to early failure of reinforced concrete structures (Rodrigues, 2000). It should be recognized that concrete is intrinsically a porous material, despite the improvements on its formulation and quality control to the best possible extent, it is not possible to prevent completely the ingress of potentially harmful agents into it. Micro-cracks and macro-pores will always exist on the concrete surface, providing a path for the transportation of aggressive ions into the interior of concrete (Swamy, 1998).

[1] MSc student
[2] Associate Professor
[3] Assistant Professor

It is now accepted that the durability of the reinforced concrete depends mainly on the composition and properties of the concrete surface layer (Kreijger, 1984). This layer, sometimes with a thickness close to the cover of the reinforcement, is most of the times the only responsible for the corrosion protection of the reinforcement. Surface treatments act as a barrier between the environment and the concrete. They prevent or retard the entry of harmful substances such as water, chlorides, etc. (Pfeifer, 1981). Surface coatings with appropriate "barrier" characteristics can cut off the transportation path into concrete. The standard EN 1504-2, establishes as a minimum requirement for the coated concrete ingress that the water permeability coefficient should not exceed 0.1 $kgm^{-2}h^{-0.5}$ and the $CO_2$ permeability should exceed 50 m.

Swamy and Tanikawa (1990) evaluated the effect of concrete coatings to preserve concrete durability and concluded that the application of an impervious surface coating to concrete is a very attractive solution to protect new and existing concrete structures.

Water is the most critical agent because it lies on the root of many important degradation processes: it is related to freeze-thaw durability, it provides the transport path for chloride ions and establishes electrolytic continuity inside concrete. Besides, in order that the carbonation reaction can take place, the presence of a certain amount of water is required (Duval, 1992).

This work intends to contribute to a better understanding of this issue, by presenting data of water and gas permeability of several coatings used to protect concrete. The effect of organic coatings on water and chloride transport in reinforced concrete was studied by Fluckiger *et al* (1990). They concluded that the concrete coatings strongly reduced the water and chloride uptake in concrete.

Concrete coatings have the unique advantage that they can be applied to protect either the existing or the new structures. However, with a wide range of coatings available in the market, it becomes extremely difficult to choose the right type of coating, since coatings of similar generic types are known to possess considerably different diffusion characteristics (Hawkins, 1985).

The performance of the available generic types under varying service conditions needs to be studied. There is also a need to develop performance criteria for evaluation of concrete coatings guidelines for the selection of coatings appropriate for various exposure conditions (Almusallam, 2002).

## 2. EXPERIMENTAL PROGRAM

### 2.1. Materials

To evaluate the influence of cement, two types of cement were used: Portland Type I 42.5R and Type IV/A (V) 32.5R. Crushed granite with a density of 2566 $kg/m^3$, water absorption of 2.1% and a maximum size of 9.53 mm was used as a coarse aggregate, while crushed sand with a density of 2477 $kg/m^3$ and water absorption of 1.36 % was used as a fine aggregate in the preparation of concrete specimens.

Concrete coatings were selected to represent the following three generic types:

i. Silicone varnish (S);
ii. Acrylic coatings (A);
iii. Epoxy resin coatings (E).

Each generic type was represented by two coatings from different manufacturers. Table 1 shows the properties of the selected concrete coatings. All coatings were applied on the substrate by brush following the recommendations of the manufacturers and after a good drying of the specimen.

2.2. Preparation of specimens

Cylinder concrete specimens 110 mm in diameter and 230 mm in eight (ø110 x 230) were cast to evaluate the absorption by capillarity of the selected concrete coatings. Cubic concrete specimens 100x100x100 $mm^3$ were cast to evaluate the absorption by immersion of the selected concrete coatings. Disk concrete specimens 50 mm in diameter and 40 mm in thickness (ø50 x 40) were cast to evaluate the permeability to oxygen, the permeability to water and the porosity of the selected concrete coatings.

The concrete specimens were proportioned for an effective water-to-cementitious materials ratio of 0.60 and a cement content of 320 $kg/m^3$.

Table 1 – Description of the selected coating

| Coating type | Generic type | Coverage rate $m^2/dm^3$ | Specific weight $Kg/dm^3$ |
|---|---|---|---|
| Silicone, SA | Siloxane resin-based water repellent | 2.8 | 0.83 |
| Silicone, SB | Siloxane resin-based water repellent | 4.0 | 0.80 |
| Acrylic, AA | Water-based acrylic resin | 3.5 | 1.40 |
| Acrylic, AB | Water-based acrylic resin | 5.0 | 1.30 |
| Epoxy, EA | Two-component epoxy resin | 2.2 | 1.30 |
| Epoxy, EB | Two-component epoxy resin | 4.0 | 1.60 |

2.3. Test procedures for evaluation of concrete coatings

The selected concrete coatings were applied to concrete. The coverage rate is shown in Table 1. The purpose of the tests performed in laboratory was the evaluation of the "barrier" properties of the coatings against water and gases, by determining their absorption by capillarity and immersion, porosity and permeability to water and oxygen.

2.3.1. Absorption by capillarity

The selected concrete coatings were applied on one face of the cylindrical concrete specimens measuring ø110 x 230 after drying. A rapid set epoxy resin coating with 20 mm was painted in the curved surfaces of the concrete specimens to ensure the absorption by capillarity. One week later, the specimens were then placed in a tank with 5±1mm height of water and weighted in time intervals outlined in LNEC E393 (1993), which is based on the RILEM CPC11.2 (1974) draft recommendation. Dividing the increase of mass by the area in contact with the water, we can obtain the absorption of water by capillarity, in each interval.

$$Kc_M = \frac{\left(M_i - M_0\right)}{A} \tag{1}$$

$Kc_M$ – absorption of water by capillarity ($g/mm^2$);
$M_i$ – specimen mass in time $t_i$ (g);
$M_0$ – specimen initial mass (g);
$A$ – specimen inferior surface area ($mm^2$).

2.3.2. Absorption by immersion

After painting all the faces of the concrete specimens measuring 100x100x100 $mm^3$ with the selected concrete coatings, they were placed in a tank filled with water in a room with a controlled environment. Before the beginning of the test at least one week should pass to ensure a good cure of the coatings. When the specimens mass becomes stable, following the procedure outlined in LNEC E394 (1993), they were weighted. Then the specimens were placed in an oven at a temperature of 105±5 ºC, until the mass becomes constant, after that they were weighted again. The absorption of water by immersion at atmospheric pressure was calculated using the following equation:

$$Ai_M = \frac{m_1 - m_3}{m_1 - m_2} \times 100 \quad (2)$$

$Ai_M$ – absorption of water by immersion (%);
$m_1$ – saturated specimen mass (g);
$m_2$ – specimen hydrostatic mass after saturation (g);
$m_3$ – dry specimen mass (g).

2.3.3. Porosity

After painting all the faces of the concrete cylindrical specimens ø50x40 with the selected concrete coatings, they were placed in an excicator, respecting the cure time. After keeping the specimens in vacuum state during 3 hours, the specimens were immersed in distilled water and kept in vacuum state for another 3 hours, following LNEC E395 (1993).

The porosity was calculated using the following equation:

$$P_{AM} = \frac{m_1 - m_2}{m_1 - m_3} \times 100 \quad (3)$$

$P_{AM}$ – porosity (%);
$m_1$ – specimen saturated mass (g);
$m_2$ – specimen dry mass (g);
$m_3$ – specimen immerse mass (g).

2.3.4. Permeability to oxygen

After porosity test, the cylindrical specimens ø50x40 were subjected to permeability to oxygen test using the apparatus developed at Leeds University (Cabrera, 1999). This device (Figure 1) ensures that the specimen is subjected to a steady state flow of the fluid that passes through the sample under a given pressure during a certain period of time. The specimens were inserted under pressure in a rubber ring and then inside the test cell, which was closed with a torque wrench. Then all the valves were closed and the oxygen-holder was open. The test pressure was selected in a way that time of the soap-bubble route for a distance of 10 cm would be greater than 45 seconds after 30 minutes of test. The permeability to oxygen was calculated using the following equation:

$$K_{GM} = \frac{4{,}04 \times v \times L \times 10^{-16}}{A \times (P_1^2 - 1)} \quad (4)$$

$K_{GM}$ – permeability to oxygen (1E-16 $m^2$);
$v$ – determinated flow, pipette reading ($cm^3/s$);
$A$ – cross-sectional area of the specimen ($m^2$);
$L$ – specimen height (m);
$P_1$ – test pressure (bar).



Figure 1 – Permeability device

2.3.5. Permeability to water

The same specimens used in the porosity test were afterwards subjected to oxygen permeability and then to water permeability test. The apparatus developed at Leeds University were also used. The test procedure is similar to the described oxygen permeability test except that after the closing of the test cell, an alcohol, water and fenolftalein solution was introduced in the valve of the cell. Then, all the valves were closed and the oxygen-holder was open. The test pressure was selected and after 3 hours the test was finished. The specimen was then broken in half and the penetration of the solution was measured. The permeability to water was calculated using the following equation:

$$K_{WM} = \frac{d_p^2 \times \delta}{2 \times h \times t} \times 1.3 \times 10^{-7} \quad (5)$$

$K_{WM}$ – permeability to water (1E-16$m^2$);
$d_p$ – penetration depth (m);
$\delta$ – specimen porosity;
$t$ – time to reach $d_p$ depth (s);
$h$ – height of water ($H_2Om$); 1 bar = 10.207 $H_2Om$.

## 3. EXPERIMENTAL RESULTS AND DISCUSSION

### 3.1. Water absorption by capillarity

In Figure 2 one can observe the obtained capillary water absorption tests results. This figure shows that the use of the selected coatings decreases the absorption by capillarity, specially the silicone varnish and the epoxy resin. In the case of the silicone varnish the

results were surprisingly good, reducing the absorption in 99.2% to the uncoated conventional cement specimens and 99.6% to the uncoated specimens with Type IV cement, which had the worst result of all, due to a bigger porosity. The two products seem to be very similar and to have the same behaviour.

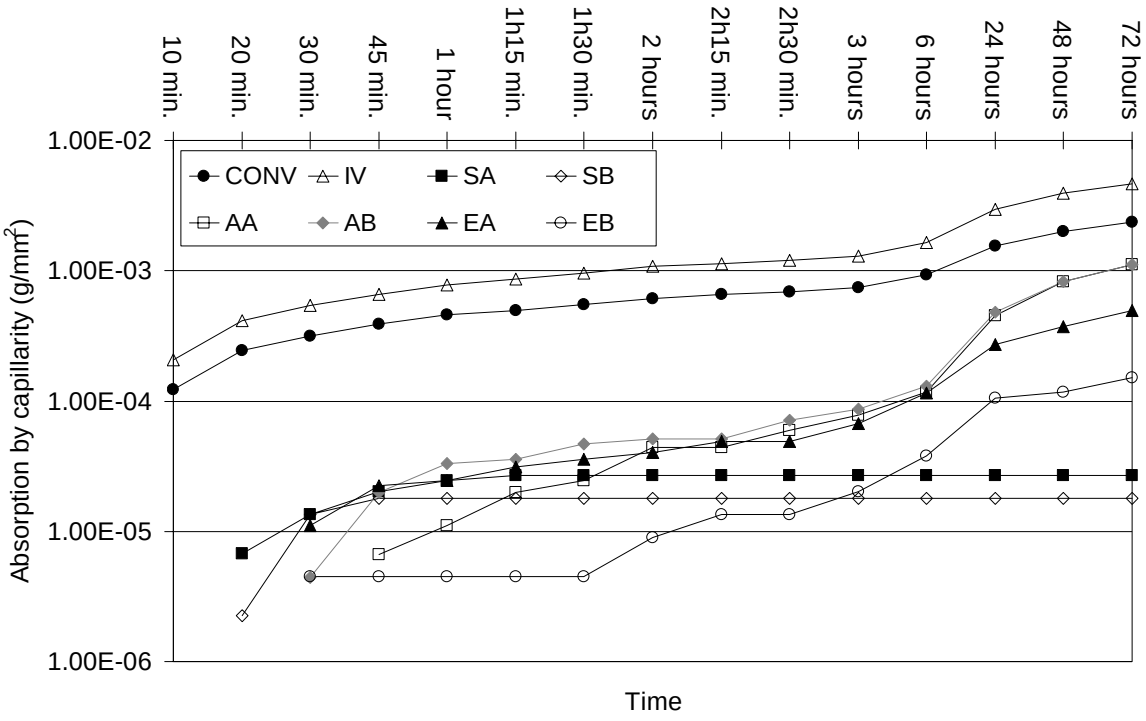



Figure 2 – Water absorption by capillarity in the coated and uncoated specimens

Concerning the acrylic paints, they had the worst performance of all the selected coatings. They had a good start, absorbing even less than the silicone varnish in the first 30 minutes, but then they never stop to increase. Nevertheless, the best product reduced the absorption in 53.0% to the uncoated conventional cement specimens and 76.0% to the uncoated Type IV cement specimens. The two products seem to be very similar, having product B a bigger absorption in the first two hours.

The epoxy paints had the best results next to the silicones varnishes, although the two products had the same behaviour. In the 24 hour interval measures, the two products had the same behaviour, but with less intensity than before and always with bigger absorption of the product A. The use of the best epoxy paint allowed a reduction in the absorption by capillarity of 93.6% to the uncoated conventional cement specimens and 96.7% to the uncoated Type IV cement specimens.

### 3.2. Water absorption by immersion

Figure 3 shows that the use of the selected coatings diminishes the absorption by immersion, specially the epoxy resins. The best epoxy resin reduced the absorption of water by immersion in 80.3% to the uncoated conventional cement specimens and 80.1% to the uncoated Type IV cement. Product B proved to be better than product A.

The acrylic resins had a similar behaviour, with a slight advantage of product B, reducing the absorption by immersion in 29.7% to the uncoated conventional cement specimens and in 28.9% to the uncoated Type IV cement specimens.

The varnishes of silicone didn't improve significantly the specimen's behaviour. The best product only reduces 6.8%, showing that this coating isn't appropriate to protect concrete against this type of water absorption.

Between the uncoated specimens with conventional cement and Type IV cement, one couldn't see significant differences, showing that the Type IV cement is not an improved choice to reduce the water absorption by immersion in concrete.

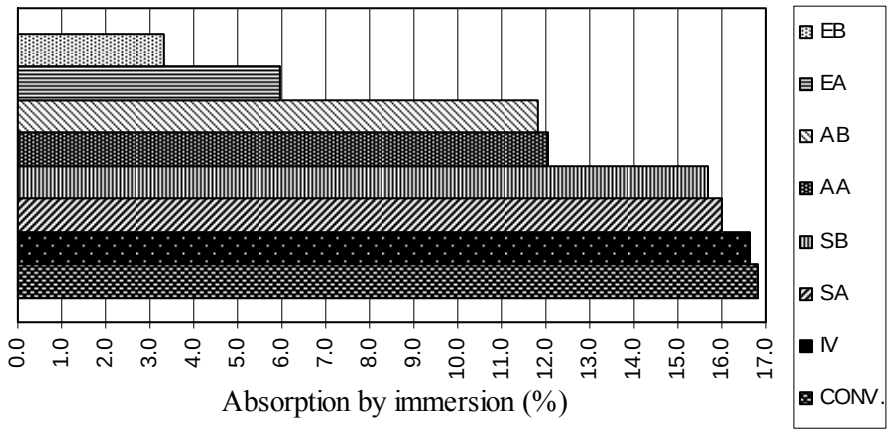



Figure 3 – Water absorption by capillarity in the coated and uncoated specimens

3.3. Porosity

By observing Figure 4, we can conclude that the use of the selected coatings decreases the porosity, specially the epoxy resins. The specimens painted with the best epoxy resin (product B) had 96.6% less porosity than the uncoated specimens with conventional cement and 96.8% less than the uncoated specimens with Type IV cement.

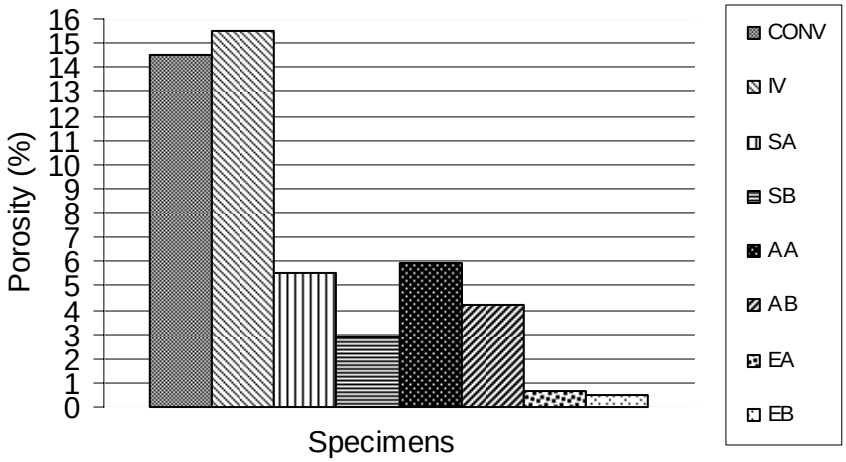



Figure 4 – Porosity in the coated and uncoated specimens

The acrylic resins and the silicone varnishes had a very similar performance. The silicone varnish B behaved even better than the two acrylic resins and the silicone varnish A was better than the acrylic resin A, which was a surprise. This excellent behaviour of the silicone varnishes can be explained by its hydrophobic impregnation responsible by the pores and capillaries internal coating.

The acrylic resin B allowed a reduction of the porosity in 71.1% to the uncoated specimens with conventional cement and 73.1% to the uncoated specimens with Type IV cement.

The specimens coated with varnish silicone B had less 80.0% porosity then the uncoated specimens with conventional cement and less 81.4% than the uncoated specimens with Type IV cement. The uncoated specimens with Type IV cement had 6.8% more porosity than the uncoated specimens with conventional cement, although they had the same cement content and the same water-to-cementitious materials ratio and addictions.

3.4. Oxygen permeability

From Figure 5 we can conclude that the use of the selected coatings decreases the permeability to the oxygen, specially the epoxy and acrylic resins.

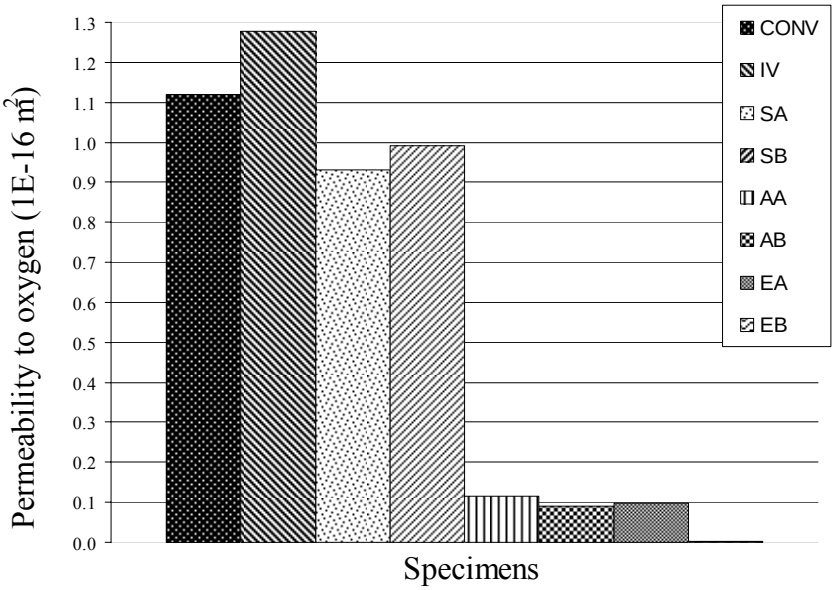



Figure 5 – Oxygen permeability in the coated and uncoated specimens

In the epoxy resins product B had by far the best performance, reducing the permeability to oxygen in 99.7% to the uncoated specimens with conventional cement and 99.8% to the uncoated specimens with Type IV cement. Surprisingly product A had a bigger permeability than the one of the acrylic resins. In the test were used pressures of 9.5 bar for product B and 6.3 to 9.3 bar for product A, using pipettes with 2,9 mm of diameter, due to the low permeability of these products, specially of product B.

The acrylic resins had the best results next to the epoxy resins, in the case of the acrylic resin B the behaviour was even better than the epoxy resin A. Product B allows a reduction of the permeability in 91.2% to the uncoated specimens with conventional cement and 92.2% to the uncoated specimens with Type IV cement. In the test were used pressures of 5.8 to 6.8 bar for product B and 5.7 to 7.1 bar for product A using pipettes with 2.9 mm and 4.8 mm of diameter. The reduction in the diameter was made to allow the measuring of the soap-bubble with more precision and speed.

The varnishes of silicone had the worst behaviour, the best product (A) was only able to reduce the permeability in 17.0% to the uncoated specimens with conventional cement and 27.2% to the uncoated with Type IV cement, which indicates that this product is not the most indicated to decrease the permeability of concrete to oxygen.

The uncoated specimens with Type IV cement had a permeability 12.3% bigger than the uncoated specimens with conventional cement, due to its bigger porosity, despite having the same cement content, the same water-to-cementitious materials ratio and addictions.

### 3.5. Water permeability

Figure 6 show that the use of the selected coatings decreases the permeability to water, specially the epoxy and acrylic resins.

Product B of epoxy resins proved to be completely impermeable to the penetration of water. Product A had a very good performance reducing the permeability to water in 99.5% to the uncoated specimens with conventional cement and 99.7% to the uncoated specimens with Type IV cement. In the test were used pressures of 5.5 to 5.8 bar in product B and 5.3 to 5.6 bar in product A.

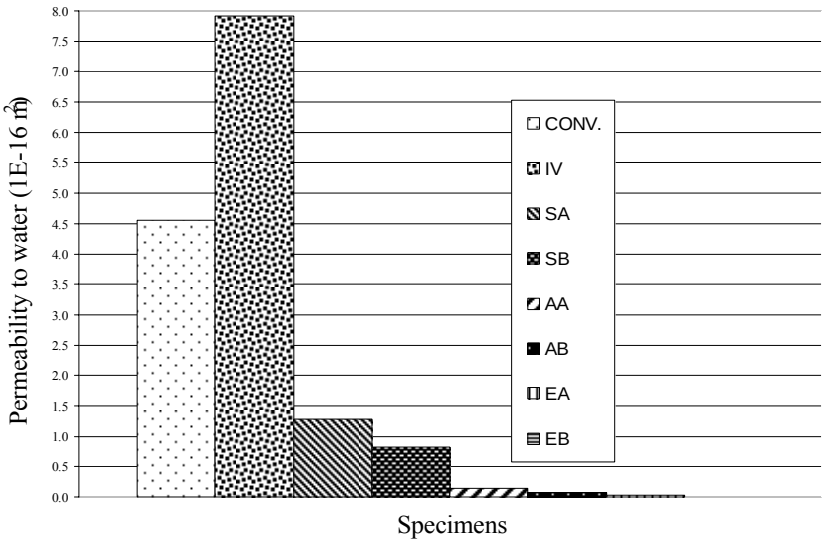



Figure 6 – Water permeability in the coated and uncoated specimens

The acrylic resins had the best performance next to the epoxy resins reducing, in the case of product B, the permeability in 98.5% to the uncoated specimens with conventional cement and 99.2% to the uncoated specimens with Type IV cement. In the test were used pressures of 5.2 to 5.98 bar in product B and 4.6 to 5.4 bar in product A.

The varnishes of silicone had the worst results reducing (for product B) the permeability in 81.9% to the uncoated specimens with conventional cement and 89.5% to the uncoated specimens with Type IV cement, which indicates that this material is still effective protecting the concrete from water.

The uncoated specimens with Type IV cement had a permeability 42.4% bigger than the uncoated specimens with conventional cement, due to its bigger porosity, despite having the same cement content, the same water-to-cementitious materials ratio and addictions.

## 4. PERFORMANCE RANKING OF CONCRETE COATINGS

The performance of the selected concrete coatings under the test regimes evaluated in this research work is summarized in Table 2. First, it was given a degree of importance to each test, based on the element tested, gas or water. Since the water is the main agent of degradation in concrete, (Li, 2000) a bigger weight (1.5) was given to the tests that study the

behaviour of this element in concrete: absorption by immersion, capillarity and permeability to water. A lower weight (1.0) was given to the other tests. Afterwards it was attributed a classification for every test and for each selected coating based on their performance.

Based on the results obtained in this study the overall ranking of the performance of the selected coatings in the descending order of importance is as shown below:

EB → EA → AB → SB → AA ,SA → CONV → IV

The results obtained in this study have also indicated that there is a variation in the performance of coatings of similar generic types. That was shown with silicone varnishes and with the acrylic resins. It is, therefore, recommended that whenever a coating is selected for use in aggressive environments, it should be tested under conditions similar to those it will be exposed to during its service life.

Table 2 – Performance ranking of selected coatings

| Specimen | Absorption by capillarity | Absorption by immersion | Porosity | Permeability to oxygen | Permeability to water | **Total** |
|---|---|---|---|---|---|---|
| CONV | 1X1.5 | 2X1.5 | 2X1.0 | 2X1.0 | 2X1.5 | **11.5** |
| IV | 2X1.5 | 1X1.5 | 1X1.0 | 1X1.0 | 1X1.5 | **8.0** |
| SA | 3X1.5 | 7X1.5 | 4X1.0 | 4X1.0 | 3X1.5 | **27.5** |
| SB | 4X1.5 | 8X1.5 | 6X1.0 | 3X1.0 | 4X1.5 | **33** |
| AA | 5X1.5 | 3X1.5 | 3X1.0 | 5X1.0 | 5X1.5 | **27.5** |
| AB | 6X1.5 | 4X1.5 | 5X1.0 | 7X1.0 | 6X1.5 | **36** |
| EA | 7X1.5 | 5X1.5 | 7X.10 | 6X1.0 | 7X1.5 | **41.5** |
| EB | 8X1.5 | 6X1.5 | 8X1.0 | 8X1.0 | 8X1.5 | **49** |

## 5. CONCLUSIONS

The selected coatings proved to be effective protecting the concrete against the action of water and gas (oxygen). The silicone varnishes exhibited the lowest absorption by capillarity, followed by epoxy and acrylic resins. The acrylic resins were not effective in protecting the concrete against absorption of water by capillarity and should not be used in situations where this is the basic requirement. The ability of the epoxy resins to prevent the absorption by immersion was better than that of acrylic resins and silicone varnishes. The silicone varnishes were not effective reducing the absorption of water by immersion.

The epoxy resins were highly effective in reducing the porosity of concrete, which was almost negligible. The epoxy resins were followed by the silicone varnish and the acrylic resin B. The silicone varnish and the acrylic resin A were the most porous of the selected coatings. Nevertheless, they reduced significantly the porosity of concrete.

The permeability to oxygen of the epoxy resin B was negligible. It was followed by the acrylic resin from the same fabricant and the epoxy and acrylic resins A, all with identical permeability. Both silicone varnishes were ineffective in controlling the permeability of concrete to oxygen and should not be used in situations where this is the basic requirement.

The permeability to water of the epoxy resins was negligible, especially product B which was impermeable. They were followed by the acrylic resin B whose permeability to water was also negligible and by the acrylic resin A with a very low permeability. Both

silicone varnishes were less effective in controlling the permeability of concrete to water, despite controlling very well the permeability of the concrete to water.

As an overall evaluation, the performance of epoxy resins was much better than that of other concrete coatings studied in this research work. The acrylic resin A followed by the silicone varnish A proved to be very similar quality products, although with a much smaller performance than the epoxy resins.

The acrylic resin and the silicone varnish B had the worst results of the selected coatings with the same place in the ranking. This means that the quality of the acrylic resin A seems to be inadequate and the quality of the silicone A is much worst than the one of product B.

From the ranking we can conclude that the economic comparison between some products should be done. For example, between the acrylic A and the silicone varnish A with the same ranking and between the acrylic B and the silicone varnish B with a very close ranking.

The results obtained in this study indicate that the performance of coatings varies with the exposure conditions. While the performance of a certain coating is better under certain exposure conditions, it does not perform better than others in another environment. Therefore, the selection of the coatings should be case specific.

## 6. REFERENCES

Almusallam, A., Khan, F. M. and Maslehuddin, M., Performance of concrete coatings under varying exposure conditions, *Materials and Structures*, vol. 35, September-October, 487-494 (2002).

Cabrera, J.G., Design and Production of High Performance Concrete, *Proceedings of International Conference, Infrastructure Regeneration and Rehabilitation Improving the Quality of Life Through Better Construction*, Sheffield, U.K., 1-14 (1999).

Duval, R., La durabilité des armatures et du béton dénrobage in *La durabilité des betons*, cap. 6, Presses de l´École Nationale des Ponts et Chaussés, Paris (1992).

EN 1504-2, Products and systems for the protection and repair of concrete structures. Definitions, requirements, quality control and evaluation of conformity. Part 2: Surface protection systems for concrete, *CEN* (2004).

Fluckiger, D. Elsener, B. ,Studer, W. and Bohni, H., Effect of organic coatings on water and chloride transport in reinforced concrete, *Corr. & Corr. Prot. Of Stl. In Conc. 2,* 1017-1027 (1990).

Hawkins, P. J., The use of surface coatings to minimize carbonation in the Middle East, Proceedings of *1st International Conference on Deterioration and Repair of Reinforced Concrete in the Arabian Gulf*, Bahrain, 273-285 (1985).

Kreijger, P. C., The skin of concrete. Composition and properties, *Materials and. Structures* 17**,** 100, 275-283 (1984).

Li, Z., Chau,, C., New water permeability test scheme for concrete, *ACI Materials Journal*, January-February, 84-89 (2000).

LNEC E 393, Evaluation of the water absorption by capillary suction, Lisbon, Portugal (in Portuguese)(1993).

LNEC E 394, Evaluation of the water absorption by immersion. Atmospheric pressure test, Lisbon, Portugal (in Portuguese)(1993).

LNEC E 395, Evaluation of the water absorption by immersion. Vacuum test, Lisbon, Portugal (in Portuguese)(1993).

Pfeifer, D.W., Scali, M.J., Concrete Sealers for Protection of Bridge Structures, *Department of Transportation,* NCHRP 244, Washington D.C., 138 p. (1981).

RILEM Tentative Recommendation Nº. 11.2, Absorption of water by capillarity, National Inf. Service, Springfield, Virginia, 22161, (1974)

Rodrigues, M. P. M. C., Costa, M. R. N., Mendes, A. M. and Marques, M. I. E., Effectiveness of surface coatings to protect reinforced concrete in marine environments, *Materials and Structures*, Vol. 33, 618-626, December (2000).

Swamy, R. N., Suryavanshi, A. K. and Tanikawa, S., Protective ability of an acrylic-based surface coating system against chloride and carbonation penetration into concrete, *ACI Materials Journal*, March-April, 101-112 (1998).

Swamy, R.N. and Tanikawa S., Surface coatings to preserve concrete durability, Proceedings of *International Conference on Protection of Concrete*, edited by R.K. Dhir and J. W. Green (E & FN Spon, London), 149-165 (1990).

International Symposium Polymers in Concrete
2 - 4 April 2006
Guimarães, Portugal

# UV Curing behaviour of a vinylester resin for concrete restoration

R. Serrano[1], A. Maffezzoli [2]

*Department of Innovation Engineering University of Lecce,*
*Via Monteroni, 73100 Lecce, ITALY.*

A. Tarzia [3], C. Stifani [4]

*Fibrover Coop. S.c.r.l*
*Zona Industriale -Via Belgio, n° 8 - 73100 Lecce, ITALY*

## ABSTRACT

In this work the UV polymerisation of a vinylester resin for infusion processes of composites for restorations of civil engineering structures was studied. The curing reaction of the vinylester resin was analysed taking into account the solar radiation and the UV lamp effects by a differential scanning calorimeter (DSC) and rheological measurements. In order to reproduce the solar radiation a solar simulator has been used. A photoinitiator, with extinction coefficient near to zero in the visible region of the solar spectrum was selected.

The curing behaviour of the vinylester resin was modified varying the photoinitiator amount. At low percentages of photoinitiators (0,5%$_{wt}$ ), the solar radiation lead to a very fast curing rate, resulting in a viscosity increase out of the range for an optimal resin infusion process.

The resin formulation was optimized in order to reduce solar effects on the polymerisation rate using an UV absorber (UVA) and a radical scavenger (HALS). A kinetic study by DSC has shown that HALS don't affect the cure rate, whereas UV absorbers slow down the cure process.

## 1. INTRODUCTION

The use of fiber reinforced plastics (FRP) for concrete columns or beams restoration has already shown a strong potential with respect to traditional techniques thanks to the high strength/stiffness to weight ratio and excellent corrosion resistance of FRPs.

Currently resin cured at room temperature is used to repair damaged concrete structures by hand lay-up techniques. The problems concerning this reactive materials are, by

[1] PhD Student
[2] Professor
[3] Research manager
[4] Assistant technician

one side, their too long curing time, by the other side, the different environmental conditions in which they could be polymerized (Toutanji (2001), Li (2002), Guoquiang (2003)). The extended curing time could lead to a delay in the structure re-opening to service resulting in significant cost increase for the customer (Mukai (2002)). For these reasons, fast curing resins with controlled and reproducible curing conditions can be conveniently applied. The ultraviolet (UV) curing resin represents a suitable alternative to the traditional resins to get a faster polymerization reaction activated "on demand" simply by a proper illumination of the lay up.

During the cure process of a thermosetting resin the initial growth of molecular weight is associated with a viscosity increase of the reactive mixture until gelation event is reached. Then the curing mixture undergoes a transition from a viscous liquid to an elastic gel, and its viscosity suddenly becomes infinity. At the gel point the reactive mixture cannot be anymore processed. In order to obtain a homogenous reinforcement impregnation resin infusion processes are compatible with a viscosity lower than 500 mPa s.

Usually UV curable resins are processed indoor, and the polymerization reaction starts when the reactive mixture is illuminated with an UV lamp. Since the civil engineering structures such as bridges are repaired under direct or indirect sunlight exposure, the resin infusion processes can be applied only if the viscosity of the resin is not significantly altered by sunlight induced polymerization.

In this work the UV polymerisation of a vinylester resin for infusion processes of composites for restorations of civil engineering structures was studied, evaluating the solar radiation effects on the kinetic reaction and on the processing times. The curing reaction of the vinylester resin was analysed taking into account the solar radiation and the UV lamp effects by a differential scanning calorimeter (DSC) and rheological measurements. In order to reproduce the sunlight spectrum a solar simulator has been used.

The obtained results show that also a low amount of photoinitiator, such as $0{,}5\%_{wt}$ , lead to a too fast curing rate under solar irradiation, resulting in a viscosity increase out of the range for an optimal resin infusion process. In order to reduce solar effects on the polymerisation rate, the influence of light stabilizers, like UV absorbers (UVA) and hindered amine light stabilizers (HALS) was also studied. Light absorbers are commonly use to reduce the degradation effects of organic materials upon outdoor exposure, due to the combination of solar radiation, atmospheric oxygen, humidity, pollutant and heat, responsible of changes in physical, optical and mechanical properties (Schmidt (1988), Bauer (1990)).

UVA, acting as UV shield, absorbs the light in a given spectral range, preventing a fast initiation of the radical curing of the resin. The penetration of the light in a material is governed by the Lambert-Beer Law:

$$I_t = I_0 \exp(-2/3\varepsilon lc) \qquad (1)$$

Where $I_0$ is the intensity of the incident light and $I_t$ the intensity of the light transmitted by a sample of thickness l containing an absorbing chromophore at a molar concentration c, being ε its extinction coefficient. On the other hand HALS generates radical scavengers upon UV irradiation that, reacting with the free radicals produced by the photoinitiator, should delay the beginning of the curing reaction (Fouassier (1995)).

## 2. EXPERIMENTAL

### 2.1. Materials

The vinyl ester resin used was a commercial thermosetting resin, Distitron VE 100 SC, supplied by Lonza S.p.A with a styrene content of 48 $_{wt}$%, for resin infusion processes. A 2-Hydroxy-2-methyl-1-phenyl-propan-1-one (Darocure 1173 from Ciba Specialty Chemicals) photoinitaitore was used to generate the free radicals upon UV light exposure.

The selected photoinitiator has an extinction coefficient near to zero in the visible region of the solar spectrum. In this region the sun radiation intensity is the highest, and an extinction coefficient considerably different to zero, may lead to high rate of reaction with a consequent reduction of the available time for technological operations.

A hindered-amine light stabilizer (HALS), a bis (1,2,2,6,6-pentamethyl-4-piperidinyl) sebacate (Tinuvin 292 from Ciba) and an UV absorber (UVA), a 2-hydroxyphenyltriazine (Tinuvin 400 from Ciba), was selected.

The chemicals used to adapt the resin to the outdoor resin infusion process are reported in Figure 1. The studied formulations are reported in Table 1.

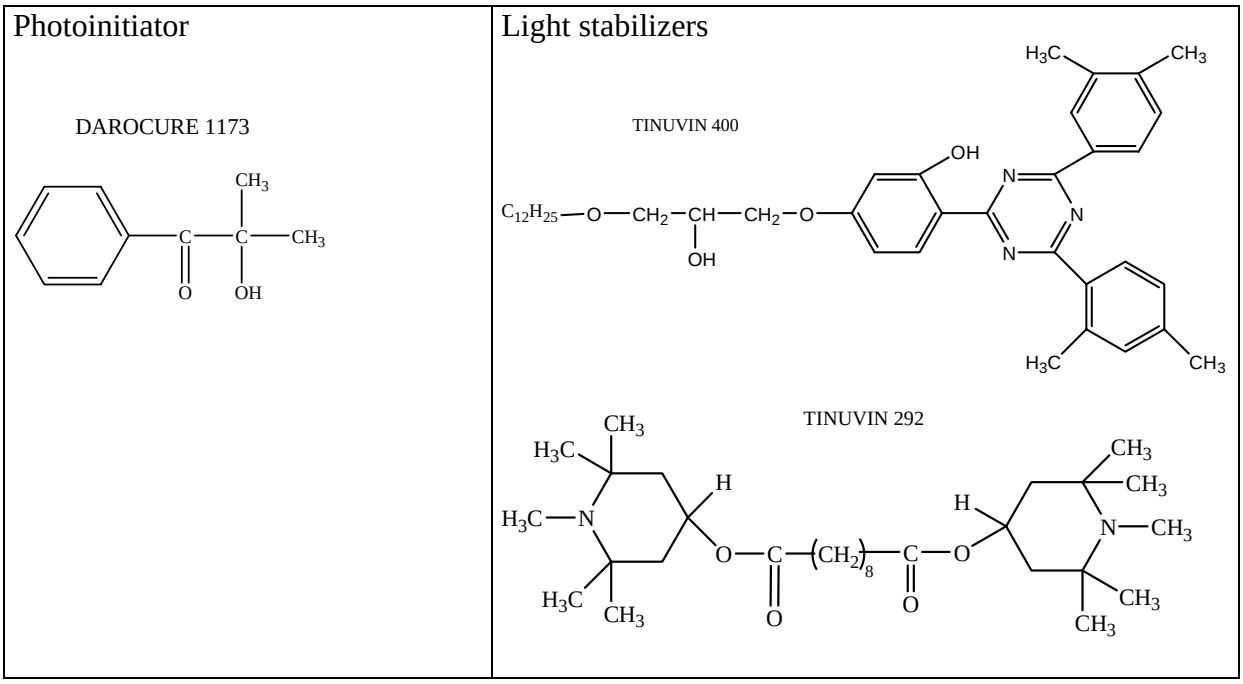



Figure 1 – Formulas of photoinitiator and light stabilizers used

Table 1 – Summary of the formulations studied

| | Photoinitiator (%wt) | UVA (%wt) | HALS (%wt) |
|---|---|---|---|
| A1 | 0,5 | 0 | 0 |
| A2 | 0,5 | 0,1 | 0 |
| A3 | 0,5 | 0,3 | 0 |
| A4 | 0,5 | 0,6 | 0 |
| A5 | 0,5 | 0 | 0,5 |
| A6 | 0,5 | 0 | 2 |

## 2.2. Methods

### 2.2.1 Differential scanning calorimetry

The photopolymerisation process was studied by a differential scanning calorimeter (DSC 7 Perkin Elmer). The DSC was modified to allow uniform illumination of both the sample and reference pans. In place of the standard DSC covers, two transparent quartz windows, placed directly above the pan holders, were used to let the light to irradiate the photoreactive resin samples. In order to minimize styrene losses by evaporation during the DSC experiments, isothermal conditions (25 °C) were used in nitrogen atmosphere (flow rate 20 $cm^3$/min) to prevent the detrimental effects of $O_2$ inhibition on the radical curing.

The polymerization reaction was started by the UV radiation emitted from a medium pressure mercury lamp (180 $W/m^2$), supplied by Jelosil s.r.l. The emission spectrum of the lamp range from 330 to 400 nm.

A typical DSC sample weight was 1 mg, corresponding to a thickness of about 0.1 mm; as reference was used a vinyl ester resin sample (without photoinitiator) in order to balance in the sample ad reference ovens the eventual effects related with styrene evaporation during the measurements.

After loading the sample in the DSC, it was exposed to the nitrogen for 2 minutes, and after the DSC signal stabilization, a shutter was opened to allow the exposition to the UV radiation. Additional temperature measurements were carried out in order to verify the absence of significant heating effects caused by the radiation source.

The samples were kept in the dark for the time elapsed between the sample preparation and the UV radiation exposure. Moreover, in order to have a uniform sample thickness, it was necessary to minimize the meniscus effect due to the surface tension between the aluminium pan and the liquid resin. To this purpose, the DSC aluminum pans were modified, pressing the bottom surface to obtain a little cavity of 2 mm of diameter and 0.2 mm of depth.

### 2.2.2. Solar simulator

A LOT ORIEL solar simulator was used, equipped of a xenon lamp from 100 W, emitting a radiation above 260 nm.

All samples were irradiate by a collimated square beam on a surface of 100 X 100 $mm^2$. The emission spectrum of the xenon lamp was modified by two filters:

- air mass zero filter: using this filter is possible to simulate the solar radiation to the outside of the terrestrial atmosphere;
- air mass 1 filter: the radiation reaching the terrestrial surface is attenuated from the atmosphere because of reflection, diffusion and absorption effects. Moreover the attenuation effects depend on the solar light travelling trough the atmosphere. The filter Air mass 1 is used to simulate the solar radiation when the sun is to the zenith, corresponding to the shortest light travel trough the atmosphere.

The resin was poured into alumina pans, 30 mm in diameter and 5 mm in depth, resulting in a layer thickness of 5 mm. The pans were sealed by an 80 μm thick nylon film, supplied by AIRTECH with the trade name of Econolon 0015, used as vacuum bag in resin infusion processes. The vacuum bag was selected for its high light transmission properties in the UV range. The samples sealed by the vacuum bag were protected either by oxygen diffusion inhibiting the radical polymerisation reaction either from the styrene losses by evaporation. Moreover the use of a vacuum bag reproduces the film filtering effects occurring during UV irradiation of the resin, after the infusion process is completed. All samples were

kept in dark conditions for the time elapsed between the sample preparation and the solar simulator exposure.

The samples were exposed to the solar simulator for 15, 30 and 45 minutes; the irradiation intensity, measured by a radiometer, was 1087 W/cm$^2$. The selected intensity value, kindly supplied from climatology lab of University of Lecce, represents the most severe illumination condition in Italy, relative to the Pantelleria Island in June.

### 2.2.3. Rheological analysis

Rheological analysis was performed on the formulations and compositions reported in Table 1 in steady shear after exposition to solar simulator, in order to determine the viscosity increase of the curing mixture. A parallel plate rheometer (ARES, Rheometric Scientific) was used in isothermal experiments carried out at room temperatures The steady rheological study was performed at shear rates ranging from 0,1 $s^{-1}$ to 100 $s^{-1}$.

## 3. RESULTS AND DISCUSSION

### 3.1 UV radiation curing

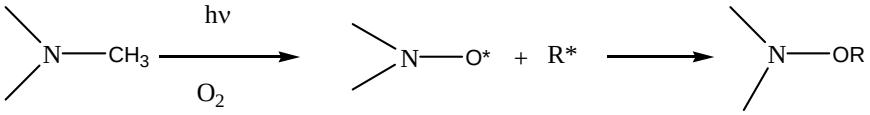
A DSC study was devoted to the analysis of the effects of the light stabilizer on the cure kinetic of the UV curable vinyl ester resin. A typical DSC result obtained in isothermal conditions is shown in Figure 2: as the shutter was opened and the sample is exposed to light illuminated, the heat flow goes through an exothermic minimum and then returns to a plateau value, corresponding to the end of the polymerization reaction. The peak area of DSC curves are a measure of the enthalpy involved in the cure, calculated by drawing a straight line extension from both side of each exothermic peak. These calculations and the normalization procedures were performed by the DSC software.

The results obtained from DSC measurements on a reactive mixture of vinyl ester resin containing 0,5%$_{wt}$ of photoinitiator Darocure 1173, varying the amount of the UV absorber (Tinuvin 400 ) and of the HALS (Tinuvin 292) are reported in Figure 3 and Table 2.

The peak of the DSC curves (proportional to the maximum rate of reaction) decreases as the UV absorbers amount increases. The UV absorber extinction coefficient is different from zero in the UV lamp emission range, i.e. 330 – 400 nm. Therefore the photoinitiator and the UV absorber compete in the absorption of the incident photons, leading to a slower rate of photoinitiation. Moreover as the UV absorber amount increases, the enthalpy of reaction decreases. This is attributed to the radiation filtering of the UV absorber, leading to a profile of degree of cure through the sample thickness.

The magnitude of the effects above described is directly related to the relative ratio of both, the concentration and the absorbance of photoinitiator and UV absorber. On the other hand, the addition of HALS Tinuvin 292, does not affect the kinetics of radical-induced polymerisation as shown in Table 3.

This behaviour may be explained considering that the radical scavenging species, i.e. the nitroxyl radicals, are formed by photooxidation of the HALS molecule. However DSC experiments were carried out in nitrogen atmosphere and under these conditions the nitroxyl radical scavenger species cannot be longer formed by the oxygen dissolved in the sample during its preparation. Consequently the polymerisation of the vinyl ester resin proceeds unperturbed.




(2)

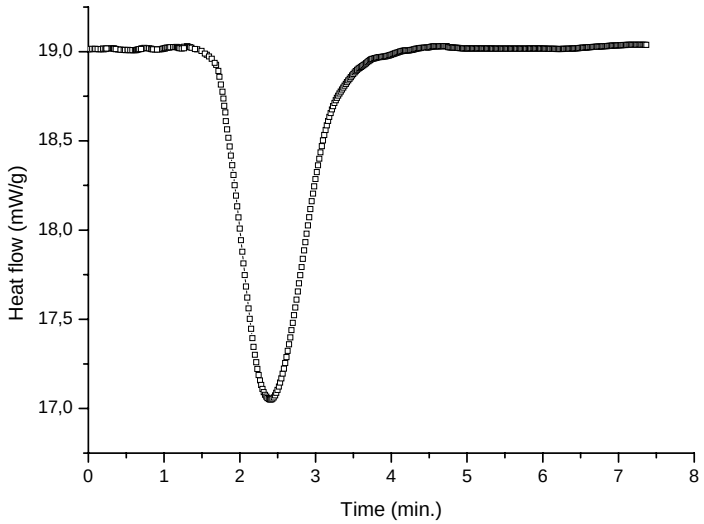



Figure 2 – Isothermal DSC scan obtained during photopolymerization at 25 °C

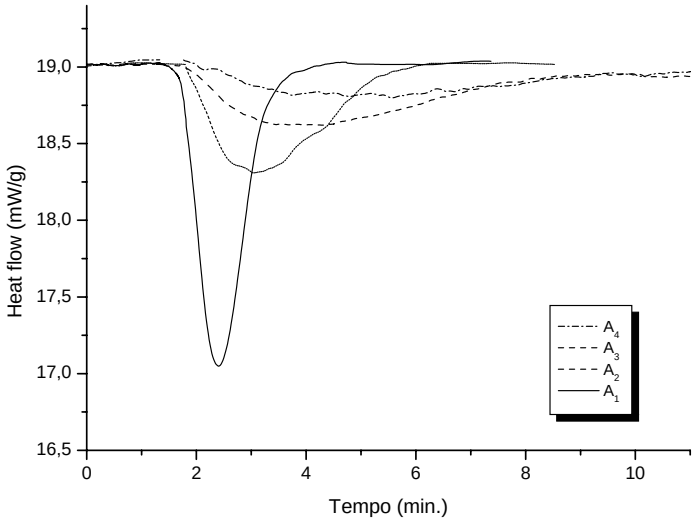



Figure 3 – Influence of the UV absorber (Tinuvin 400) on the UV curing kinetics on a vinyl ester resin containing 0,5%$_{wt}$ of photoinitiator (Darocure 1173) monitored by DSC.

Table 2 – Summary of results from isothermal photo-DSC of a vinyl ester resin containing 0,5%$_{wt}$ of photoinitiator (Darocure 1173), varying the UV absorber amount (Tinuvin 400).

| | Enthalpy of reaction (J/g) | Peak of reaction (min.) |
|---|---|---|
| A1 | 130,11 | 2,4 |
| A2 | 83,03 | 3 |
| A3 | 67,77 | 4 |
| A4 | 39,11 | 5,3 |

Table 3 – Summary of results from isothermal photo-DSC of a vinyl ester resin containing 0,5%$_{wt}$ of photoinitiator (Darocure 1173), varying the HALS amount (Tinuvin 292).

| | Enthalpy of reaction (J/g) | Peak of reaction (min.) |
|---|---|---|
| A1 | 130,11 | 2,4 |
| A5 | 127,32 | 2,6 |
| A6 | 134,41 | 2,2 |

3.2. Solar radiation curing

In outdoor infusion processes, the reactive mixture is inevitably exposed to the sunlight, characterized by emission lines from 250 nm to 400 nm in the UV range. Since the selected photoinitiator absorbs strongly in the far UV region, the solar radiation can therefore start the polymerisation reaction so increasing the resin viscosity. In order to understand the solar radiation effects on the radical polymerisation reaction, samples of vinyl ester resin containing 0,5%$_{wt}$ of photoinitiator Darocure 1173 were illuminated with the solar simulator for 15, 30 and 45 minutes and then analysed by the photo-DSC, equipped with the UV lamp above described.

The samples illuminated for 15 and 30 minutes, were in a gelled and glassy state respectively: the solar radiation lead to a too fast curing rate, resulting in a physical state of the resin inadequate for the resin infusion process. Therefore, samples containing different amounts of UV absorber (see Table 1) were prepared in order to reduce the rate of reaction under sunlight and in particular to cut the wavelength spectrum below 330 nm, the lower emission limit of the UV lamp. Both resin samples containing the UV absorber, i.e. A5 and A6 in Table 1, were in a liquid state after every solar irradiation cycle.

The residual enthalpy of reaction measured by DSC, reported in Table 4, indicates that for the composition with 0,6%$_{wt}$ of Tinuvin 400 it rises as the exposure time increases. This indicates that during the solar simulator exposure, an UV absorber portion is consumed, reducing during the next DSC experiments the filtering effects above described.

For mixtures containing 0,3 %$_{wt}$ of Tinuvin 400 an inversion in the trend of the residual enthalpy was observed after 30 minutes: the enthalpy decreases is explained assuming that the UV absorber is consumed in the first 30 min of exposure and consequently the polymerisation reaction starts during the solar simulator irradiation.

Table 4 – Summary of results from isothermal photo-DSC after exposure to solar simulator of a vinyl ester resin containing 0,5%wt of photoinitiator (Darocure 1173), varying the UV absorber amount (Tinuvin 400)

| | Solar simulator exposure time (min.) | Residual enthalpy of reaction (J/g) |
|---|---|---|
| A3 | 0 | 67,77 |
| | 15 | 89,56 |
| | 30 | 113,12 |
| | 45 | 92,45 |
| A4 | 0 | 39,11 |
| | 15 | 57,41 |
| | 30 | 78,15 |
| | 45 | 107,41 |

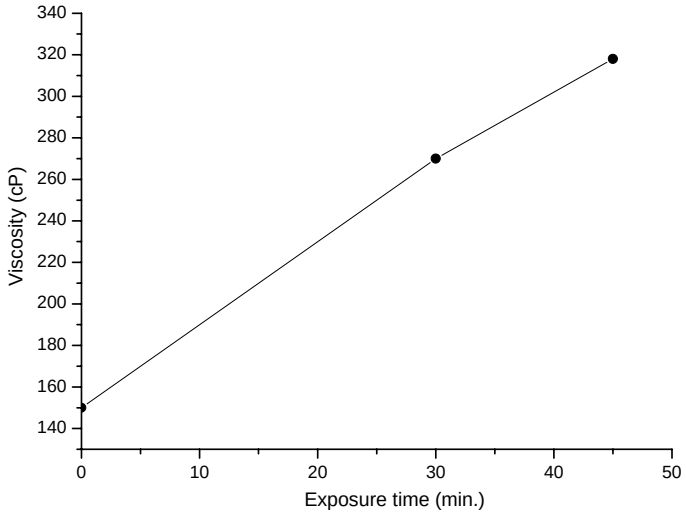



Figure 4 – Rheological results after solar simulator exposure of the reactive mixture A4 at a shear rate of 100 $sec^{-1}$

Rheological analysis were carried out on a resin containing 0,5%$_{wt}$ of Darocure 1173 and 0,6%$_{wt}$ of Tinuvin 400 in order to evaluate the viscosity increase after exposure to solar simulator. The results reported in Figure 4, show that after 45 minutes of solar radiation exposure the viscosity is doubled but its value is still suitable for resin infusion process.

## 4. CONCLUSIONS

In this study the development of a resin formulation for resin infusion in outdoor conditions is presented. Sun irradiation typical of outdoor environmental conditions occurring during restorations of civil engineering structures must be taken into account in order to use a UV curing resin. The sun radiation is able to initiate and propagate the radical induced polymerisation, leading to a gelled or glassy resin state in few minutes so preventing any process involving resin flow. Therefore, in order to repair damaged concrete structures in outdoor conditions with UV curing resins, it is necessary to modify the typical formulations used in indoor processes employing UV absorbers. The UV absorber, depending on its quantity, slow down the cure speed keeping the viscosity in a range of values compatible with resin infusion or other composite manufacturing processes involving resin flow.

## 5. ACKNOWLEDGEMENTS

The authors would like to acknowledge Dr. Antonella Rizzo of ENEA for solar simulator measurements and the climatology lab of the University of Lecce for sunlight intensity data.

## 6. REFERENCES

Bauer, D.R., Gerlock, J.L., Mielewsky, D.F., Caputa Peck, M.F., and Carter, R.O., *Polymer Degradation Stabil.*, **27**, 271 (1990), **28**, 39 (1990).

Fouassier, J. P., *Photoinitiation, photopolimerization, and photocuring*, Hanser/Gardern Publications, Inc., Cincinnati, (1985).

Guoquinag, L., Pourmohamadian, N., Cygan, A., Peck, J., Helmes, J. E., and Pang, S.S., *Composite Structures*, 60, 73-81 (2003).

Li, G., Mukai, D., Pang, S.S., Helms, J.E., Ibekwe, S.I., Alaywan, W., Structural Degradation of FRP Strengthened RC Beams Subjected to Hygrothermal and Aging Attacks, *Journal of Composite Materials*, **36**, No. 7, 795-812 (2002).

Schmidt, E.V., *Exterior Durability of Organic Coatings*, FMJ Inter.,Redhill, Surrey, England (1988).

Toutanji, H., Deng, J., Performance of Concrete Columns Strengthened with Fiber Reinforced Polymer Composite Sheet, *Advanced Composite Materials*, **10**, No. 2-3, , 159-168 (2001).

# Session 4

International Symposium Polymers in Concrete
2 - 4 April 2006
Guimarães, Portugal

# FRP Reinforcement for Damaged R/C Bridge Decks

Alessandra Aprile[1],

*University of Ferrara, Engineering Dept., Via Saragat 1, 44100 Ferrara, Italy*

Domenico Capuani [2]

*University of Ferrara, Architecture Dept., Via Quartieri 8, 44100 Ferrara, Italy*

## ABSTRACT

This paper reports the results of an extensive experimental investigation carried out on damaged R/C bridge decks removed from the "Fornello" viaduct of the Orte-Ravenna highway, Italy. The study was conducted in order to evaluate the concrete damage level and to assess a possible strengthening technique for repair making use of fibre reinforced polymers (FRP). In particular, the problem of the FRP debonding and concrete cover separation in the presence of damaged concrete is addressed and the effectiveness of different practical approaches to improve the composite-concrete interface is investigated.

## 1. INTRODUCTION

Damage of reinforced concrete in structures like bridges and highways is related to factors like environmental aggression, service loads, construction technologies and, exceptionally, seismic events. Chemicals and physical agents may induce a gradual increase in the concrete porosity and permeability, causing loss of the material integrity. In bridge decks, damage is also dependent on low fatigue level due to cyclic loads, on thermal loads and corrosion of steel bars.

The object of the present study is a viaduct of the Orte-Ravenna highway, built in the first seventies. The reinforced concrete slab of the viaduct exhibited serious structural deficiencies and, therefore, was destined to demolition and subsequent reconstruction. Parts of the removed slab were carried to the Ferrara University Laboratories in order to evaluate the concrete damage level and to assess a possible strengthening technique for repair.

In the paper, the investigation results are reported. The investigation consists of non destructive evaluation as well as experimental tests on concrete specimens (Basheer, 1996). At the structural scale a thermography is carried out in order to observe homogeneity of concrete and to point out anomalous zones with cracks, cavities or incoherent aggregates

[1] Assistant Professor
[2] Assistant Professor

(Shubinsky, 1994). Thermography is based on the emission of thermic radiation and, according to Wien law, the range of medium and far IR (2-15 μm) turns out to be suitable to characterise thermic emission of objects at ambient temperature. Surface temperature difference corresponds to different intensity of infra-red rays and this produces, in the radiographic apparatus, contrast of the thermographic image. At the specimen scale, the investigation is carried out by mercury porosimetry, compression test, three-point bending test, ultrasound measurements, scanning electron microscope equipped with an energy dispersive X-ray (EDX) analyser.

Concerning the strengthening techniques, the application of fibre reinforced polymers (FRP) is considered. In particular, the problem of fibre debonding and concrete cover separation (Li, 2001), in the presence of damaged concrete, is addressed and experimental results are reported showing the effectiveness of different practical approaches to improve the composite-concrete interface.

## 2. EXPERIMENTAL INVESTIGATION FOR CONCRETE CHARACTERISATION

The object of the present study is a viaduct, known as "Fornello", of the highway Orte-Ravenna (E45), Italy, managed by the National Organization for Highways (ANAS). This study was developed in co-operation with ANAS, Division of Emilia-Romagna.

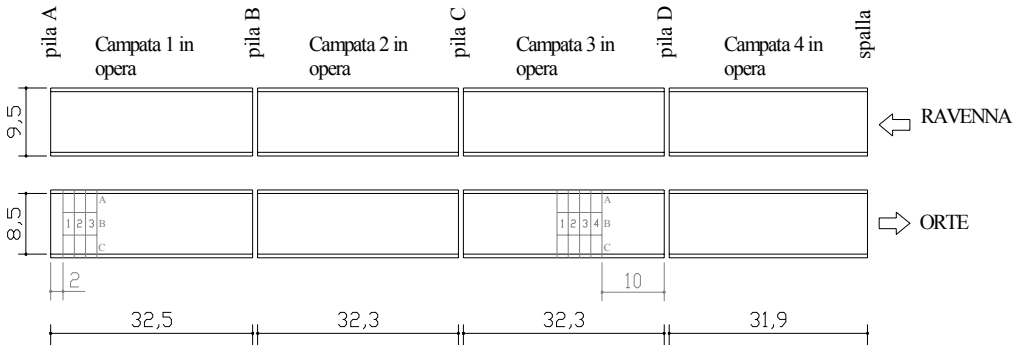



Figure 1 - Plan view of the viaduct.

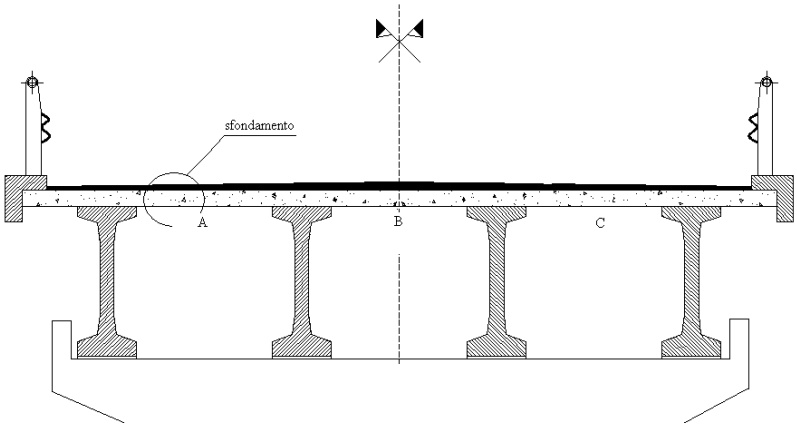



Figure 2 - Cross-section of the viaduct deck.

The highway winds along a mountain route and the structure, built in the early seventies, presents damage problems due to freeze-thaw cycles and to abundant use of salt during the winter season, together with lack of maintenance. In the particular case of the

Fornello viaduct, the slabs showed very poor conditions of preservation and they needed urgent interventions of structural rehabilitation. The viaduct slab was bound to demolition and part of it was transferred to the research laboratory for experimental investigation.

The viaduct has 4 spans of length 32 m, and width 9.5 m in each direction (Fig. 1). The deck consists of 4 pre-stressed reinforced concrete girders and a R/C slab with average thickness of 200 mm (Fig. 2). A series of 21 samples of size 500 mm x 1800 mm were extracted from the slab. The position of samples is reported in Fig. 1. Bars with round and square cross section constitute the steel reinforcement in the longitudinal and transversal direction. This is visible in Fig. 3 where a portion of deck slab with spalling and heavy corrosion is shown.

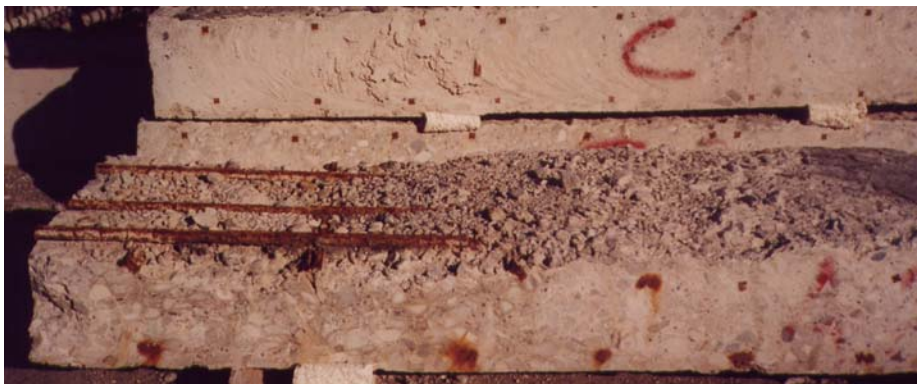


Figure 3 - Slab sample.

On the slab samples, infrared thermography was carried out. This is a non-destructive evaluation technique which uses differences in heat transfer through the structure to reveal the locations of hidden defects. Typical defects that can be located by means of infrared thermography are voids, delaminations, coating defects, such as blistering and subsurface corrosion spots. In our case, two lamps of 250 W were used as heating sources, located 1 m far from the slab surface (heated surface) (Fig. 4). The resulting thermographic images are reported in Fig. 5 where red zones, visible after heating, correspond to coating defects. The images show that defects can be detected in infrared images as a result of the differences in the thermal diffusivity of the defective and nondefective areas. In particular, when the defects are near to the surface, they restrict the cooling rate due to an insulation blocking effect, and therefore produce “hot spots”. Of course, the amount of contrast observed at the surface depends of the defect dimensions and depth from the observed surface, the initial temperature rise and the material thermal properties (Shubinsky, 1996).



Figure 4 - Equipment for thermography: the heating source and the thermal imaging system.

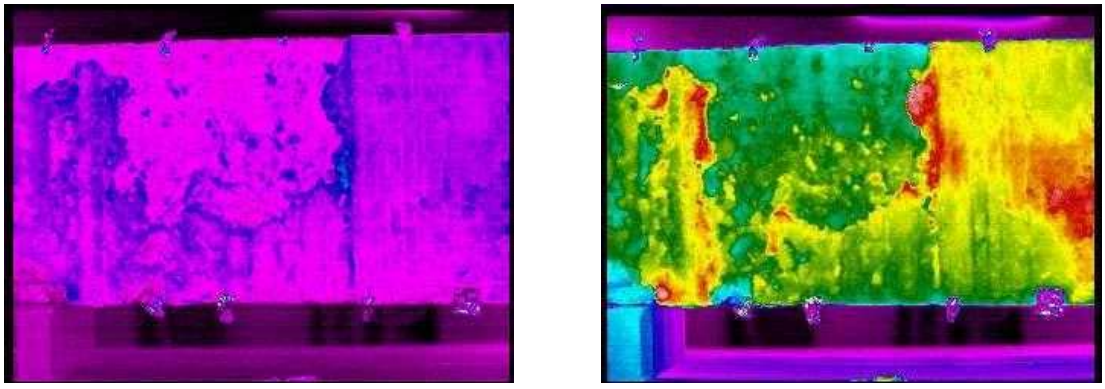


Figure 5 - Thermographic images: before and after heating

For laboratory testing, concrete cores of 100 mm diameter were drilled from the slab (Fig. 6). A significant percentage of coarse aggregates was noticed with characteristic size up to 50 mm. Mercury porosimetry, used to detect changes in the pore structure of the cement paste, revealed a total porosity ranging between 9% and 11% with prevailing micropores of 0.01 μm (Fig. 6).

For strength estimation, the concrete specimens were subjected to compression tests, showing compressive strength values between 23 and 33 MPa. The behaviour of concrete under cyclic loading, at different levels of maximum load, was also investigated. To this purpose, the specimen was subjected to 13 load cycles: cycles 1-4 up to a load giving a maximum nominal stress of 9.5 MPa; cycles 5-8 up to a maximum nominal stress of 14.4 MPa; cycles 9-12 up to a maximum nominal stress of 18.7 MPa and cycle 13 up to the specimen ultimate strength. Results are plotted in Fig. 7 showing the slope variation of the stress-strain loading branch consequent to the change of the maximum load in load cycles.

For indirect evaluation of tensile strength, prismatic specimens (100 mm x 180 mm x 500 mm) were cut from the concrete slab and the schematic test apparatus of Fig. 8 was employed. On the same specimens, ultrasonic pulse velocity tests (Achenbach, 1999) were made using piezo-electric pulse generator and pulse receiver, and measuring the travel time of an ultrasonic pulse passing through the concrete. Pulse velocity ranging from 3800 m/s to 4600 m/s were recorded.

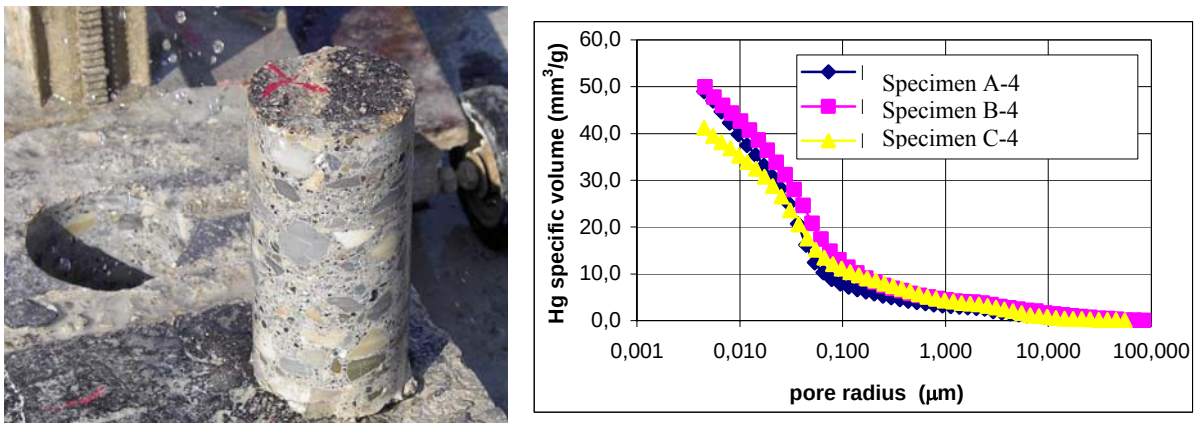



Figure 6 - Concrete specimen drilled from the slab and porosimetry of the cement paste for three different specimens.

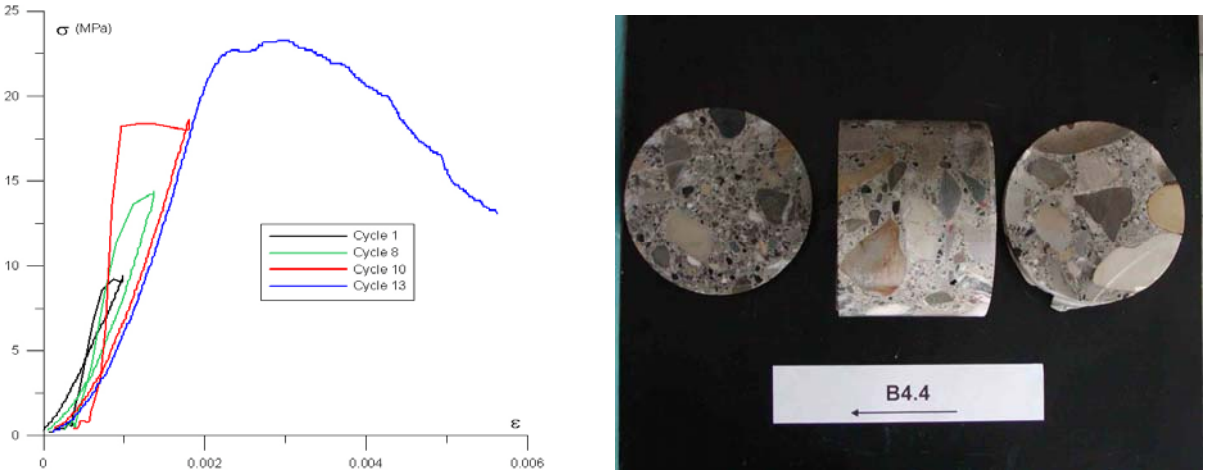



Figure 7 - Stress-strain curves for cycles at different load levels and typical inert distribution.

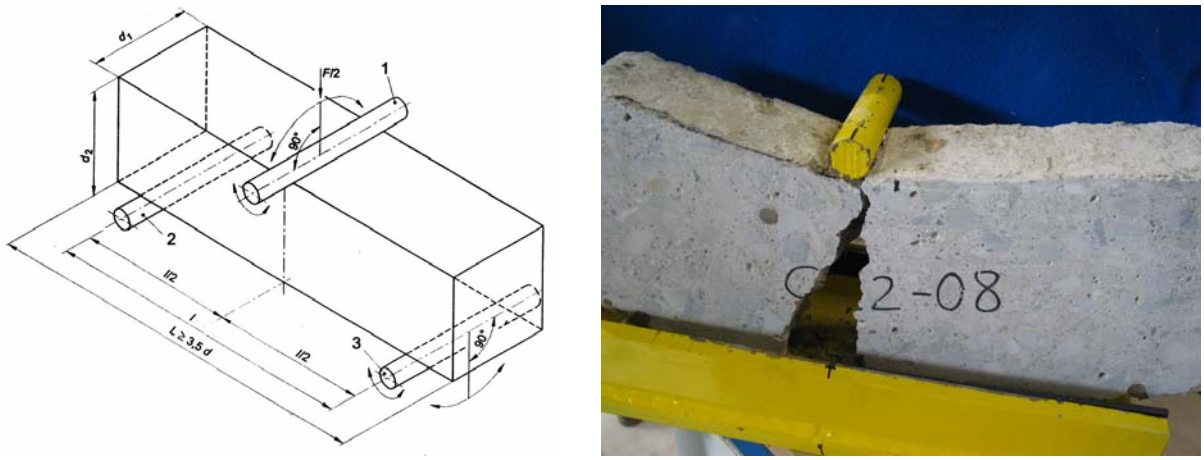



Figure 8 - Testing apparatus (UNI EN 12390-5) for indirect evaluation of tensile strength.

As for the analysis of steel reinforcement (Fig. 9), a scanning electron microscope (SEM) equipped with an energy dispersive X-ray (EDX) analyser was employed. In different points of the steel bars, a high percentage of chlorides and corrosion products has been observed. The EDX spectrum recorded on the bar cross section (at the point indicated as "spectrum 1" in the figure) is reported in Fig. 10, indicating the presence of chlorides and agents of chemical attack (Na, Ca, S).



Figure 9 - Cross section of a reinforcing steel bar.

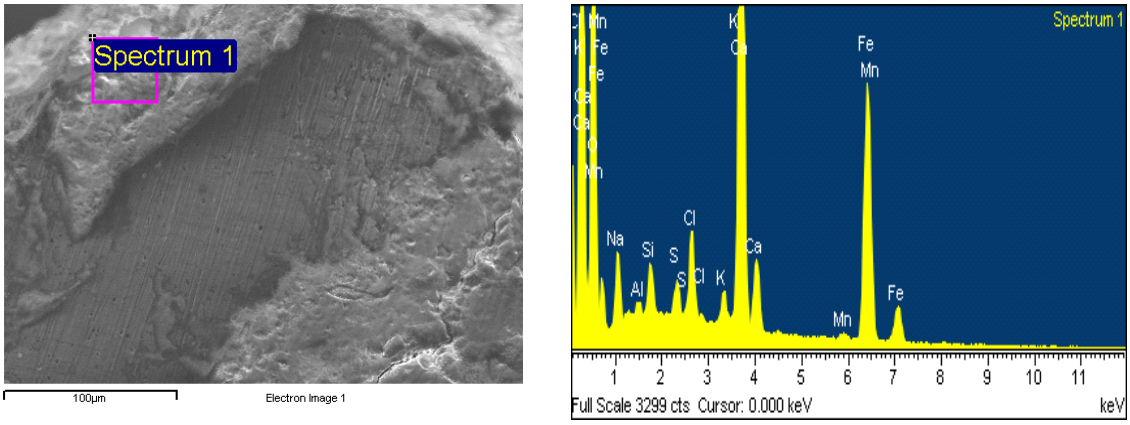



Figure 10 - SEM micrograph of bar cross section and EDX spectrum.

## 3. BONDING OF FRP REINFORCEMENT

The performed experimental tests enlightened that the concrete damage is wide but superficial, limited to the concrete cover depth of the slab upper side. Except than in this area, the actual mechanical properties of the concrete are rather constant along the slab height and consistent with the original concrete quality. The good preservation of the slab lower side concrete suggests the possibility to strengthen the slab by bonding external FRP reinforcement on this side while replacing the upper side damaged concrete and rebars. An interesting issue concerns the possibility of bonding the FRP reinforcement on restored concrete. In this study, this particular feature of the problem was investigated.

A number of 78 prismatic specimens (100 mm x 180 mm x 500 mm) were cut from the concrete slab in order to try different repair techniques based on the restoration of the wasted superficial concrete and bonding of the FRP reinforcement on both the original (lower side of the slab) and the restored (upper side of the slab) concrete surfaces. As Fig. 11 shows, the typical specimen extracted from the slab exhibited deep cracks at the rebar level; the damaged concrete was then completely removed by means of a needle hammer and the rasted steel rebars were extracted.




Figure 11 - Typical prismatic specimen cut from the concrete slab and specimen preparation

The concrete restoration was carried out making use of two different mortar qualities. A single component mortar with limited shrinkage and hight strength named Sika Monotop-624 A was applied to 12 of the cured specimens. As certified by the technical notes of the producer, the 28-day average strength of this mortar is around 60 MPa. A standard mortar

with 3 parts of mixed 325 K cement, 2 parts of sand and 1 part of acrilical emulsion in water dispersion was applied to 12 of the cured specimens. The average 28-day concrete cilindrical strength was extimated around 32 MPa.

Finally, the FRP reinforcement was applied on the cured concrete surfaces. For this application, 50 mm x 400 mm strips of SikaWrap-230C were glued by means of Sikadur-330 epoxy. As certified by the technical notes of the producer, the average tensile strength and elastic modulus of this carbon tissue are respectively around 3500 MPa and 230 GPa. Also, identical CFRP strips were applied on 12 lower side concrete surfaces, where the original concrete support was arranged with a simple surface brushing before the FRP strip was glued The application was executed by expert workmanship, following the recommended application procedure (Fig. 12).



Figure 12 - Specimen's upper side restoration and FRP bonding.

One half of the arranged specimens were subjected to artificial ageing treatmens before the bond tests were executed. The ageing treatmens consisted on 10 days of sun-rain cycles (2 and ½ hours of ultraviolet radiation and ½ hour of rain) and of freeze-thaw cycles (2 hours at -20° C and 2 hours at +20° C) (Fig. 13).



Figure 13 - Specimens subjected to artificial ageing treatments.

The fabricated specimens were employed to execute direct bond tests, making use of a force controlled hydraulic jack (MTS 810) with 250 kN load cell. The specimens were positioned thanks to a fitting steel case that allowed reducing normal stresses (peeling) due to the imperfect alignment of the FRP strip with the loading grips (Fig. 14). All of the experimental tests were performed at the Laboratory of Material Testing of the University of Ferrara.



Figure 14 - Specimen's testing devices.

The performed bond tests evinced very interesting results. Superficial debonding (SD) due to the detachment of the FRP strip from the concrete support (Fig. 15) and deep deboning (DD) due to shear failure within the original concrete (Fig. 16) were observed during the bond tests of the restored concrete joints executed at the upper side of the slab. This last bond failure mode was much less frequent than the previous one.

On the other side, superficial debonding due to the detachment of the FRP strip from the concrete support with coarse aggregates fracture was typically observed during the bond tests of the original concrete joints executed at the lower side of the slab (Fig. 17).



Figure 15 - Superficial debonding due to the detachment of the FRP strip from the concrete.




Figure 16 - Deep debonding due to shear failure within the original concrete.



Figure 17 - FRP strips debonding with coarse aggregates fracture.

In order to evaluate the efficiency of the executed concrete restoration and to assess the validity of this strengthening technique, the experimental values of the bond forces are compared with the theoretical values extimated by means of the Italian CNR-DT 200 (2004). In accordance with the above mentioned recommendations, the maximum bond force that can be transferred by the FRP-concrete interface is given by the following expression:

$$F_{\max} = b_f \cdot \sqrt{2 E_f t_f \Gamma_{Fm}} \tag{1}$$

where $b_f$, $t_f$ and $E_f$ are respectively the FRP strip width, thickness and elastic modulus. $\Gamma_{Fm}$ is the specific fracture energy mean value of the FRP-concrete bond law, given by:

$$\Gamma_{Fm} = 0.064\, k_b \sqrt{f_{cm} f_{ctm}}\,, \tag{2}$$

where $f_{cm}$ and $f_{ctm}$ are respectively the mean values of the concrete compression and tensile strength, while $k_b \geq 1$ is a shape coefficient depending on the ratio between the bonded FRP strip width and the supporting concrete surface width.

It is to recall that the maximum bond force given by Eq. (1) holds when the optimal bond length $l_e$ is available, i.e. when the effective bond length $l_b$ satisfies this condition:

$$l_b \geq l_e = \sqrt{\frac{E_f t_f}{2 f_{ctm}}}\,. \tag{3}$$

Of course, the experimental bond length was widely overestimated assuming $l_b$ ~200 mm. In this study, the following Efficiency Factor is considered in order to analyse the experimental results:

$$EF = \frac{F_{\exp}}{F_{\max}}, \tag{4}$$

where $F_{exp}$ is the bond force experimentally detected.

In Figs. 18 and 19, the obtained efficiency factors are reported for the bond tests performed on the upper side of the slab, respectively when the Sika Monotop 624 A mortar and the standard mortar are employed for restoration. For both of the cases, an average efficiency factor very close to 1 was found (0.98 and 0.93 respectively), despite 4 of the 12 bond tests underwent failure with a deep debonding failure mode (Fig. 16). In this case, a shear failure occurred within the original concrete support, as attested by the measured value of the bond forces. Unfortunately, 1 of the 12 bond tests was interrupted due to the strip failure, probably caused by the imperfect axiality of the applied load. The restored joints exhibit bond forces at failure that are in good agreement with the theoretical previsions i.e. the

loss of joint efficiency due to the concrete restoration is not appreciable.

In fact, the standard deviation of the obtained values is around 12%, which is included within the admitted uncertainty due to the rought modality of execution (CNR-DT 200, 2004). It is to recall that the executed application tried to reproduce the actual working site conditions.

In Fig. 20, the experimental bond forces of both the previous cases are compared. The bond forces of the joints where the special mortar was applied are bigger of around 40% than where the standard mortar was applied. This result seems to address this special mortar as much more effective than the standard one; however, if the very high cost of the special product is considered (around 6:1 in weight), this simple effectiveness comparison is meaningful without an accurate analysis of the global cost to benefit ratio.

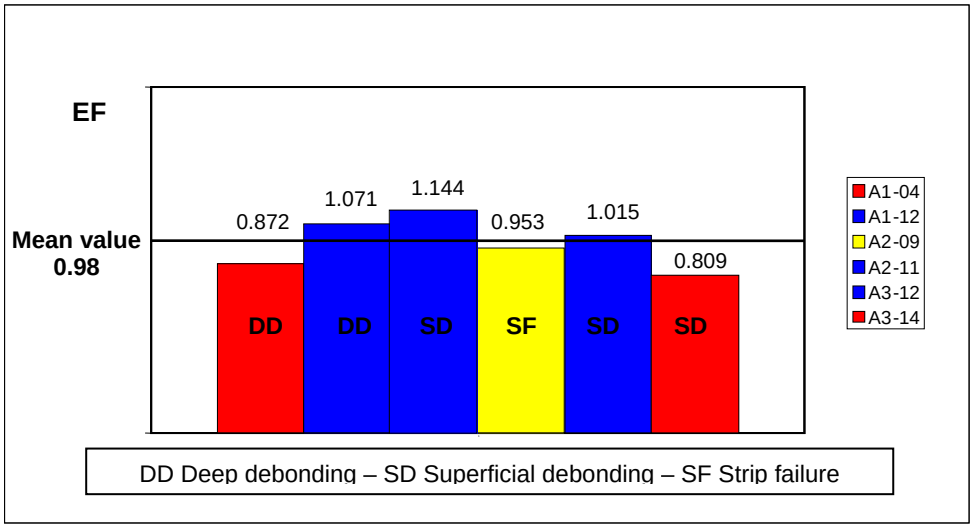



Figure 18 – EF of the bond tests on restored concrete joints (Sika Monotop-624 A mortar).

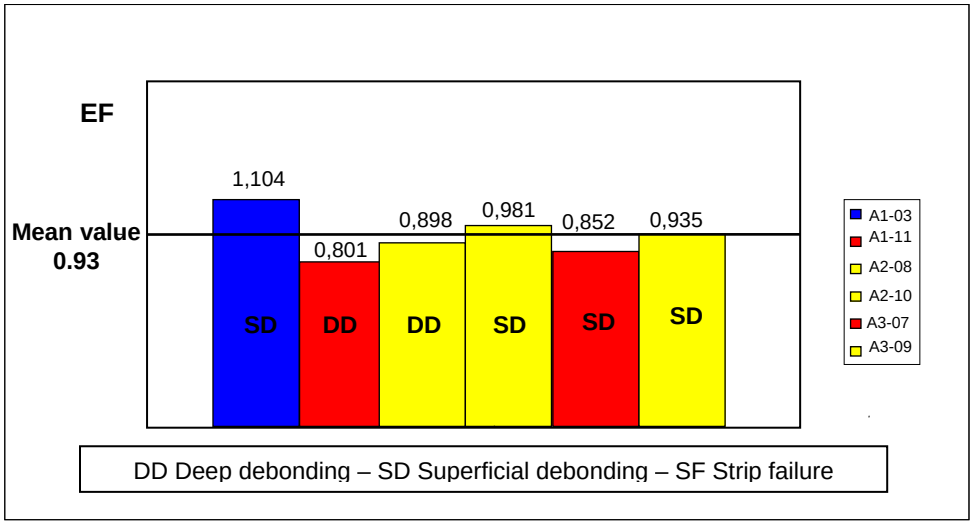



Figure 19 - EF of the bond tests on restored concrete joints (Standard mortar).

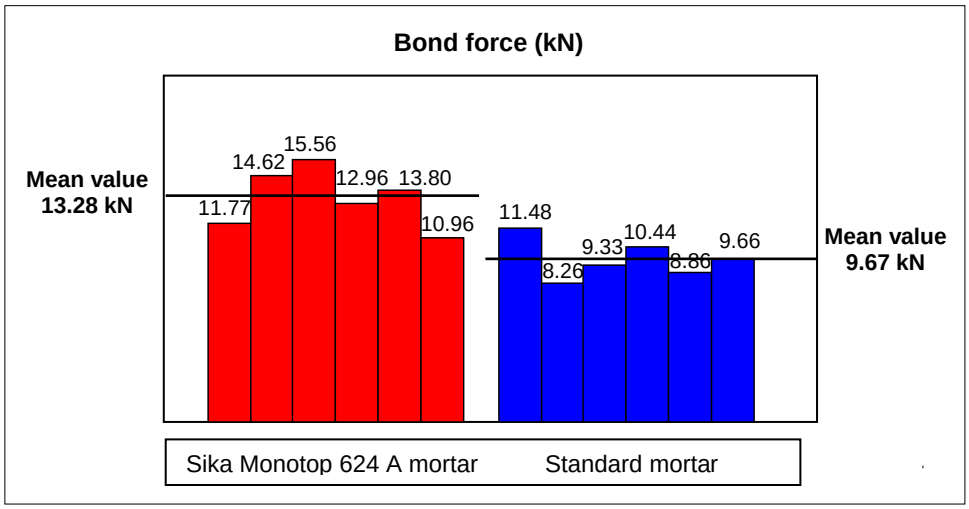



Figure 20 - Bond forces of restored concrete joints in comparison.

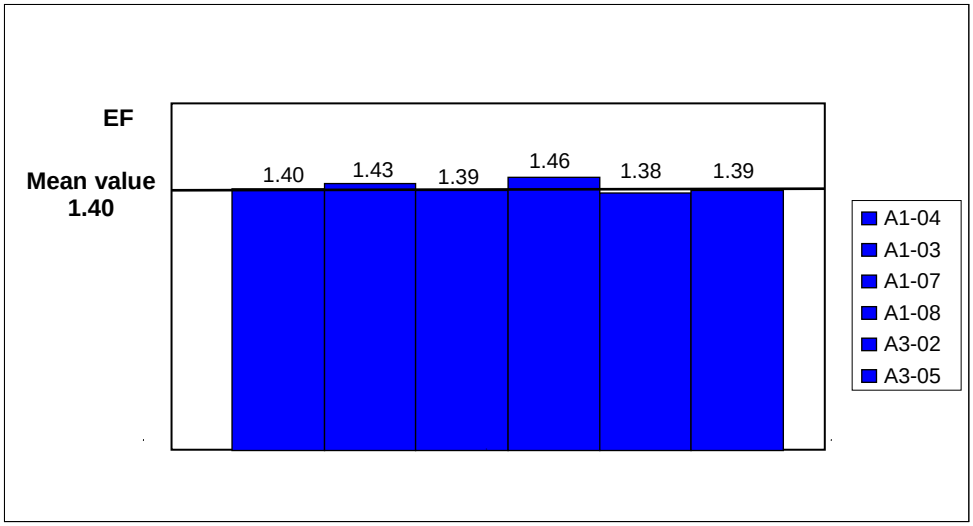



Figure 21 - EF of the bond tests on original concrete joints (lower side of the slab).

Finally, 6 bond tests were executed on FRP-concrete joints realized on the lower side of the slab. The obtained results in terms of efficiency factor are reported in Fig. 21. In this case, a surprising high value of the efficency factor is found, with mean value 1.4 and standard deviation 3%.

In order to better understand these results, it is necessary to recall the uncommon particle-size of the concrete aggregates, with a significant percentage of coarse aggregates mainly settled in the lower part of the slab due to gravitational effects during the concrete casting. As shown in Fig. 17, the bond surface at failure is marked by several wide-size fractured aggregates, which probably contributes to increase the bond strength of the joint with a sort of "strut" effect. This particular effect is not accounted by the theoretical prevision given by Eq. (1) but it is worth being investigated in the future.

Bond tests were also executed on specimens subjected to ageing treatments. The obtained results did not put in evidence any appreciable damage effect.

## 4. CONCLUSIONS

This paper reports the results of an extensive experimental investigation carried out on

samples of damaged concrete slab demolished from a viaduct of the Orte-Ravenna highway (E45). The study allowed to enlight the following main results:

- The damage state of the considered viaduct slab is wide but superficial, limited to the concrete cover depth of the slab upper side; however, the slab thickness reduction due to concrete damage and the loss of the concrete-steel rebar bond are such to produce serious structural deficiencies.
- Except than in the upper part of the slab, the actual mechanical properties of the concrete are rather constant along the slab height and consistent with the original concrete quality.
- The concrete cover restoration turns out to be adequate in order to strengthen the slab by means of FRP external reinforcements and guarantees an acceptable efficiency of this strengthening technique.
- The FRP reinforcement applied to the lower part of the slab reveals to be particularly effective, producing bond forces +40% than the theoretical expectations.

Further experimental investigations are still in progress. A number of restored slab pieces have been strengthened with FRP on both the upper and the lower side and will be shortly subjected to four point bending tests up to failure. The authors expect to confirm this strengthening technique suitable for practical applications making use of real scale specimens.

## 5. ACKNOWLEDGEMENTS

The experimental investigations reported in this paper are the result of an extensive applied reaserch carried out by the authors over the last few years, which involved the help of many researchers and contractors. The authors gratefully acknowledge: Antonio Simone, Michele Adiletta and Pietro Gualandi (ANAS – Compartimento Emilia-Romagna, Bologna), Fabio Toni (EDILTURCI SRL, Mercato Saraceno, FC), Alberto Grandi (Sika Italia SPA, Milano), Massimo Bugnoli (BUGNOLI SAS, Ferrara), Arlen Ferrari and Marco Danieli (GFC Chimica SRL, Ferrara). The contributions of Luis Filippo Lanza (Laboratory of Material Testing of the University of Ferrara), Gianluca Garagnani, Roberto Tovo and Carmela Vaccaro (University of Ferrara), Veronica Redaelli (TERMOLAB, Milano) and the financial support of PRIN 2005/2005085158 are also gratefully acknowledged.

## 6. REFERENCES

Achenbach J.D., Popovics J.S., Song W.J., Application of new ultrasound and sound generation methods for testing concrete structures. *Magazine of Concrete Research*,, **51(1),** 35-44 (1999).

Basheer P.A.M., Chidiac S.E., Long A.E. Predictive models for deterioration of concrete structures. *Construction and Building Materials*;**10(1)**, 27-37 (1996).

CNR-DT 200/2004, *Istruzioni per la Progettazione, l'Esecuzione ed il Controllo di Interventi di Consolidamento Statico mediante l'utilizzo di Compositi Fibrorinforzati,* (2004).

Li G., Xie H, Xiong G. Transition zone studies of new-to-old concrete with different binders. *Cement and Concrete Composites*, **23**, 381-387 (2001).

Shubinsky G., Jan K.H., Bernecki T. Application of infrared and visual imaging for inspection and evaluation of protective coatings. *SSPC Conference on Evaluating Coatings for Environmental Compliance* (1994).

International Symposium Polymers in Concrete
2 - 4 April 2006
Guimarães, Portugal

# CFRP-based Confinement Strategies for RC Columns - Experimental and Analytical Research

Débora Ferreira[1]

*University of Minho, Department of Civil Engineering*
*Azurém - 4810-058 Guimarães, Portugal*

Joaquim Barros[2]

*University of Minho, Department of Civil Engineering*
*Azurém - 4810-058 Guimarães, Portugal*

## ABSTRACT

The present work aims to compare the confinement effectiveness of full and partial wrapping of concrete elements under compression loads. The main results of the experimental program are presented and analysed. The Lam and Teng analytical model was applied to predict the compression stress-strain behaviour of concrete column elements partially confined by strips of CFRP lay-up sheets. The model performance is assessed using the experimental results.

## 1. INTRODUCTION

It is well recognized that both the strength and ductility of concrete compressive members can be greatly enhanced using transverse carbon fiber reinforced polymer (CFRP) wraps. These non-corrosive and lightweight wraps, which are easy to install, can be used to rehabilitate damaged concrete columns, increase the load capacity of under strength members, and retrofit seismically inadequate bridges and buildings. Among many possible applications of CFRP materials, one of the most attractive is their use as confining systems for concrete columns, which may results in remarkable increase of strength and ductility. The current CFRP-based confinement strategy is wrapping the exposed area of the concrete column. Preliminary tests with concrete elements submitted to direct compressive loading have, however, revealed that partial wrapping (strips of CFRP sheets) is also a promising confinement technique, since significant increments on the load carrying capacity and energy absorption capacity were obtained using this type of discrete confinement Barros and Ferreira (2005), Ferreira and Barros (2004). Saadatmanesh (1994, 1996) found that the strength and

[1] PhD Student
[2] Associate Professor

ductility of bridge concrete columns can be significantly increased by wrapping FRP strips around the columns due to the concrete confinement and prevention of the buckling of longitudinal reinforcement bars.

To assess the effectiveness of the partial wrapping technique, 108 prototypes of reinforced concrete (RC) columns were confined by distinct CFRP arrangements and tested under direct compression. The experimental program was designed to evaluate the influence of the concrete strength class, the stiffness of the wet lay-up CFRP sheet, the distance between strips, the width of the strip, and the number of layers per each strip. The present work describes the experimental program and analyses the main obtained results, especially those related to the load carrying capacity and deformation capacity of the tested RC elements, provided by the considered confinement arrangements.

The Lam and Teng (2003) analytical model was adopted to predict the compression stress-strain behaviour of the RC elements partially confined. Some of the parameters of this model were calibrated from the results obtained in the present experimental program.

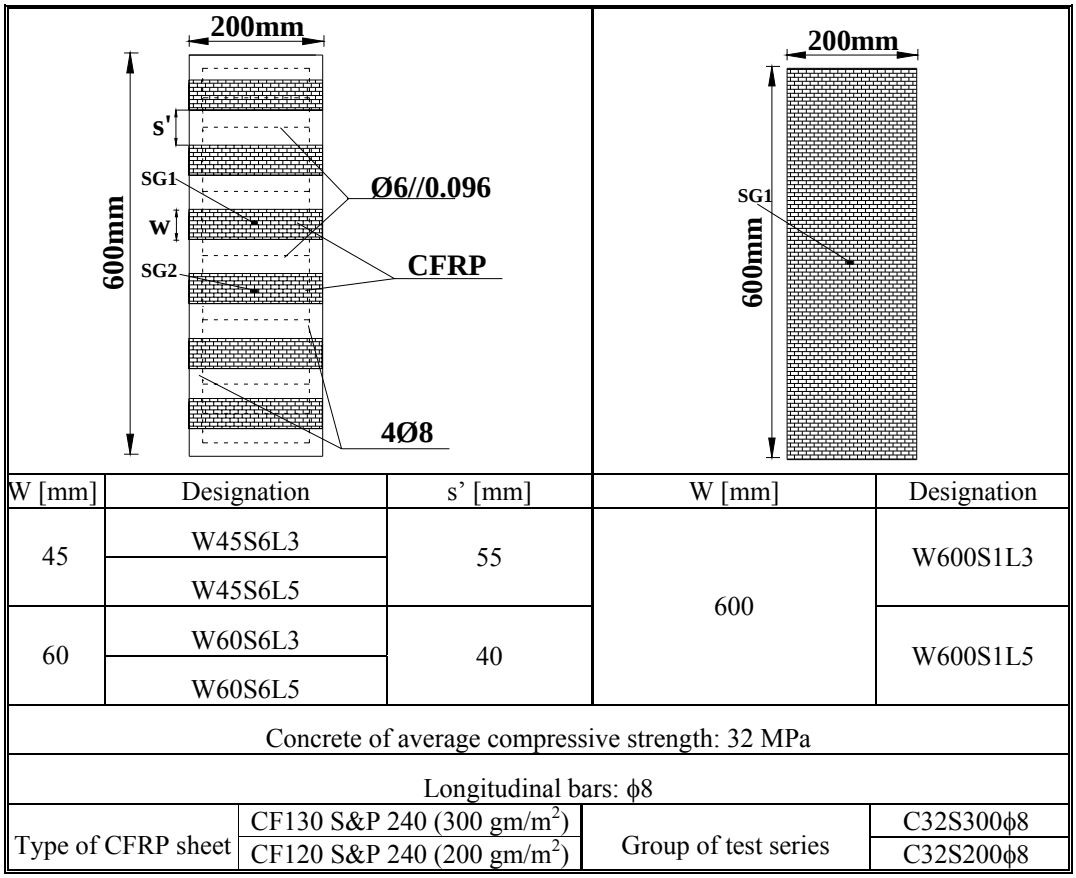
## 2. CONFINEMENT ARRANGEMENTS AND EXPERIMENTAL PROGRAM

The experimental program deals with direct compression tests with reinforced concrete column elements of 600 mm length and 200 mm diameter. This program is composed by several groups of tests in order to evaluate the influence of the following parameters on the compressive strength and deformation capacity of RC elements submitted, predominantly, to compression loading: concrete strength class (two compressive strengths, 16MPa and 32MPa); stiffness of the confinement CFRP system (two CFRP sheets, one of 300 g/m$^2$ of fibers and the other of 200 g/m$^2$ of fibers); width (W) and spacing (s') of the CFRP strips; number of CFRP layers per strip (L); percentage of the longitudinal, $\rho_{sl}$, and transversal, $\rho_{st}$, steel reinforcement ratio. Due to lack of space, only the groups of tests C32S200Φ8 and C32S300Φ8, indicated in Table 1, are analyzed in the present paper. In this designation, C32 means specimens of a concrete of average compressive strength of 32 MPa, while S200 and S300 indicate the type of CFRP sheet, 200 g/m$^2$ and 300 g/m$^2$, respectively. Finally, Φ8 indicates the diameter, in mm, of the steel longitudinal bars.

One group was confined with a CFRP sheet of 300 g/m$^2$ of fibers, with the tradename of CF130 S&P 240, while the specimens of the other group were confined with a CFRP sheet of 200 g/m$^2$ of fibers, with the tradename of CF120 S&P 240.

The specimens of the two groups were manufactured with a concrete of average compressive strength of 32MPa, and were reinforced longitudinally and transversally with four steel bars of 8 mm diameter and steel hoops of 6 mm diameter at 96 mm, respectively. The groups dealing with a concrete of average compressive strength of 16 MPa were analyzed in another paper, Barros and Ferreira (2005). Each group is constituted of three test series, being distinguished by the width of the CFRP strip: 45 mm (W45), 60 mm (W60) and 600 mm (W600 – fully-wrapped). As Figure 1 shows, the partially-wrapped specimens are confined by six strips (W45S6 and W60S6). These three test series have two sub-series, one of three layers per strip (L3) and the other with five layers per strip (L5). Previous research revealed that, above five layers per strip, the benefits in terms of specimen load carrying capacity and energy absorption capacity are marginal Ferreira and Barros (2004).

Table1 – Experimental program




| W [mm] | Designation | s' [mm] | W [mm] | Designation |
|---|---|---|---|---|
| 45 | W45S6L3 | 55 | 600 | W600S1L3 |
| | W45S6L5 | | | |
| 60 | W60S6L3 | 40 | | W600S1L5 |
| | W60S6L5 | | | |
| Concrete of average compressive strength: 32 MPa | | | | |
| Longitudinal bars: ϕ8 | | | | |
| Type of CFRP sheet | CF130 S&P 240 (300 gm/m$^2$) | | Group of test series | C32S300ϕ8 |
| | CF120 S&P 240 (200 gm/m$^2$) | | | C32S200ϕ8 |



W45S6 W60S6 W600S1

Figure 1 - Confinement arrangements

## 3. MATERIALS

From direct compression tests carried out at 28 days with three concrete cylinder specimens of 150 mm diameter and 300 mm height, average compression strength of 32 MPa was obtained.

The CFRP sheets used have the trade name of Mbrace CF-130 (300 g/m$^2$ of fibers) and CF-120 (200 g/m$^2$ of fibers). According to the supplier, CF-130 and CF-120 sheets have a thickness of 0.176 mm and 0.117mm, respectively, and have a tensile strength higher than 3700 MPa, and an elasticity modulus and an ultimate strain in the fibre direction of about 240 GPa and 15‰, respectively, (degussa 2003). To check the values of these properties, samples of CFRP were tested according to ISO recommendations (2003), see Barros and Ferreira (2005). The obtained results are presented in Table 2. The values determined experimentally for the thickness, included in Table 2, were used in the evaluation of the elasticity modulus and tensile strength of the CFRP sheets.

Table 2 – CFRP properties (average of five tests)

| CFRP Sheets | Thickness (mm) | Tensile strength (MPa) | Ultimate strain (%) | Elasticity modulus (GPa) |
|---|---|---|---|---|
| CF120 | 0.113 | 3535 | 1.52 | 232 |
| CF130 | 0.176 | 3070 | 1.33 | 230 |

## 4. TEST SETUP

Three displacement transducers were positioned at 120 degrees around the specimen and registered the displacements between the steel load plates of the equipment (see figure 2). This test setup avoids that the deformation of the test equipment is added to the values recorded by the LVDTs. Taking the values registered in these displacement transducers, the displacement at the specimen axis was determined for each scan reading (Ferreira and Barros 2004), and the corresponding strain was obtained dividing this displacement by the measured specimen's initial height. To decrease the restriction imposed by the machine load plates to the radial expansion of the specimen's extremities, a system of two sheets of teflon with oil between them was applied in-between the bottom plate of the test machine and the bottom specimen's extremity. The Teflon system was not applied in-between the top plate and the top specimen's extremity, since this plate was connected to a spherical steel hinge. Strains in the CFRP fiber direction were measured by strain gauges (SG1 and SG2) fixed on the specimen according to the arrangements indicated in the figures into Table 1. A detailed description of the test equipment and test procedures can be found elsewhere (Ferreira and Barros 2004).

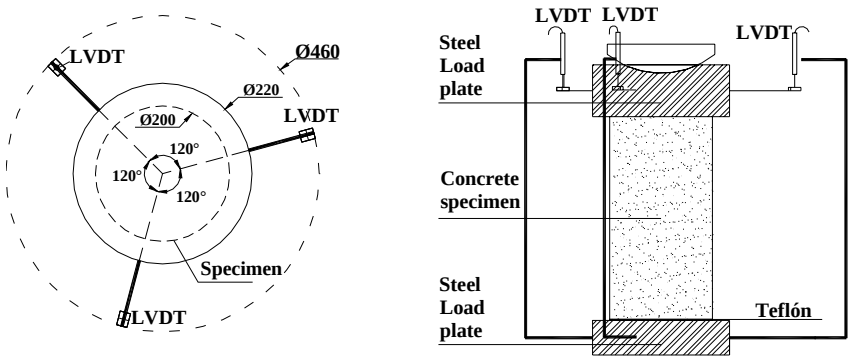



Figure 2 – Position of the LVDTs

## 5. EXPERIMENTAL RESULTS

Figures 3 and 4 show the relationships between concrete stress and both the concrete axial strain and the CFRP strain in the fiber direction for the groups of tests C32S200Φ8 and C32S300Φ8 confined with strips of 45 mm, 60 mm and 600 mm of width. Each curve represents the average response registered in the two specimens that compose each series. The concrete stress is the ratio between the applied load and the specimen cross section.

In these figures, UPC represents the unconfined plain concrete specimens, URC_ϕ8 the unconfined reinforced (longitudinally and transversally) concrete specimens. In each graph, the CFRP confinement ratio is also included, where $\rho_f = A_f/A_{c,t}$, with $A_f = 2 \times S \times W \times L \times t_f$ mm$^2$ being the cross sectional area of the confinement system ($t_f$ is the thickness of the CFRP sheet), and $A_{c,t}$ is the area of specimen longitudinal cross section ($A_{c,t} = 200 \times 600$ mm$^2$). In general, the stress-strain relationship of the confined specimens is composed by two quasi-linear branches, connected by a nonlinear transition branch.

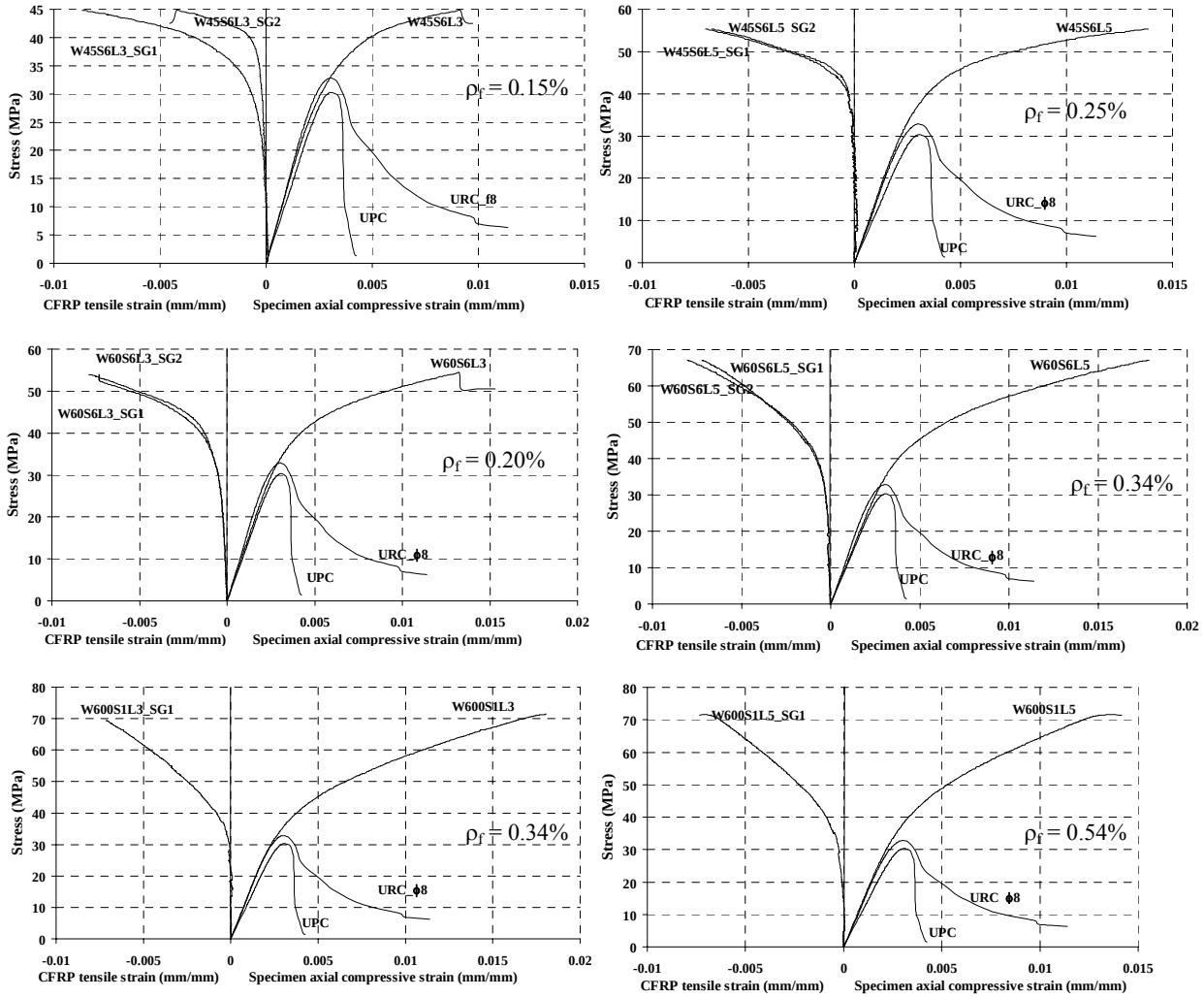



Figure 3 - Test group C32S200ϕ8.

Tables 3 and 4 include de main indicators of the effectiveness provided by the applied confinement arrangements. In these tables, $f_{co,UPC}$ and $f_{co,\phi 8}$ are the compressive strength of UPC and URC_ϕ8 specimens, respectively, $\varepsilon_{co,UPC}$ and $\varepsilon_{co,\phi 8}$ are the specimen axial strain at

$f_{co,UPC}$ and $f_{co,\phi 8}$, respectively, $f_{cc}$ is the maximum compression stress of the confined specimens, $\varepsilon_{cc}$ is the confined-specimen axial strain at $f_{cc}$, $\varepsilon_{fmax}$ is the maximum tensile strain in the CFRP fiber's direction and $\varepsilon_{fu}$ is the CFRP failure strain indicated in Table 2. Each value of Tables 3 and 4 is the average of the values obtained in the two specimens of each series.

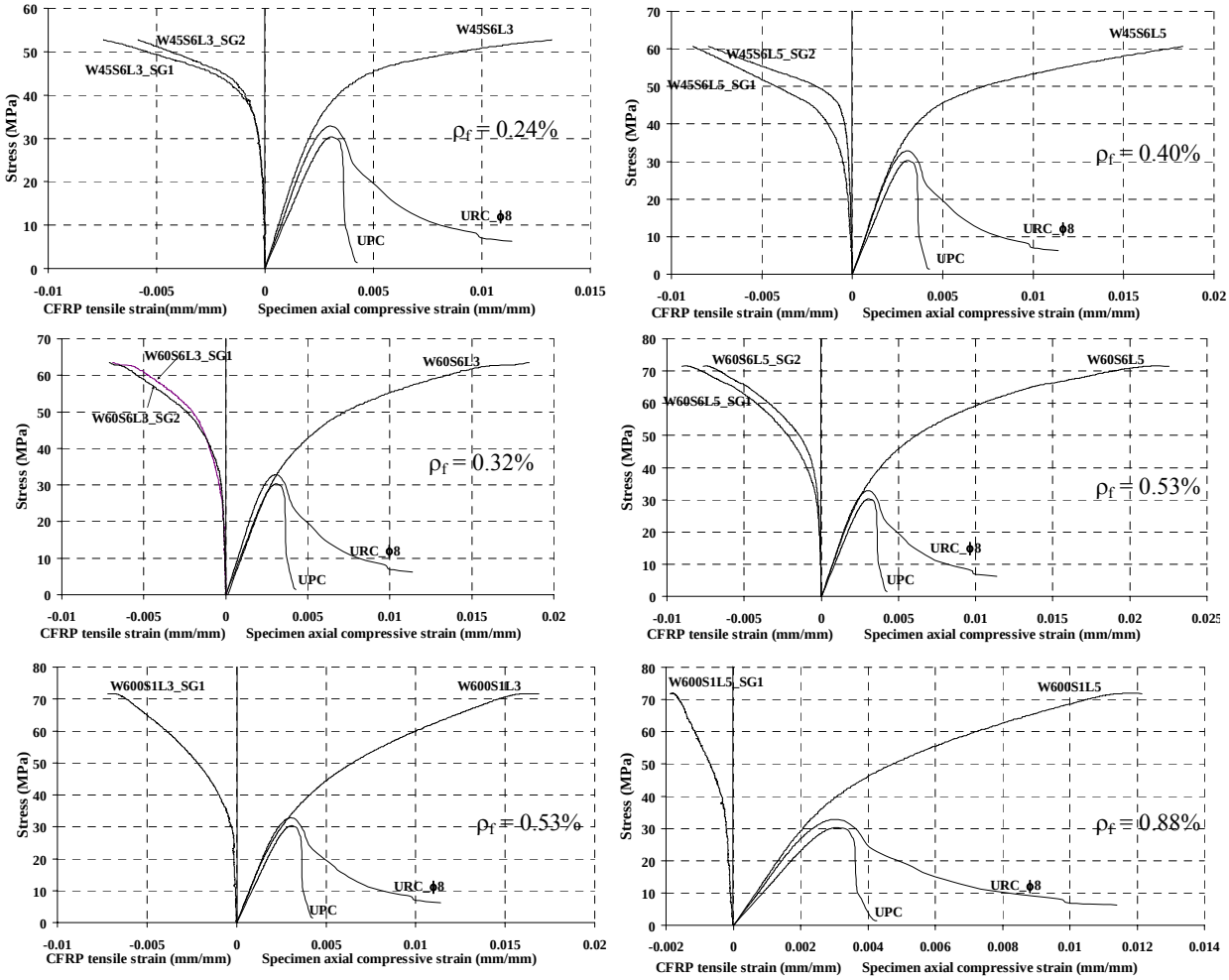



Figure 4 - Test group C32S300ϕ8.

The load carrying capacity of the test equipment was attained in the W600S1L5 series of C32S200Φ8 group and in the W60S6L5, W600S1L3 and W600S1L5 series of C32S300Φ8 group, without the occurrence of the rupture of the specimens. Since the load carrying capacity of equipment can be doubled if the tests are carried out in a non-closed loop control, the specimens of these series were again tested, up to its failure, and the attained $f_{cc}$ values are indicated in Tables 3 and 4, in square brackets. The relationship between the normalized strength of the confined specimens ($f_{cc}/f_{co}$) and $\rho_f$, represented in Figure 5, shows a linear increasing trend between these two parameters. In this figure, the $f_{cc}$ corresponds to the compressive strength at the failure of the specimens. Figure 6 shows that $\varepsilon_{cc}/\varepsilon_{co}$ has also a linear increase trend with the increase of $\rho_f$. Since in the manually controlled tests the strains were not measured, this figure only includes the results obtained in the specimens that failed when the tests were carried out under closed loop control.

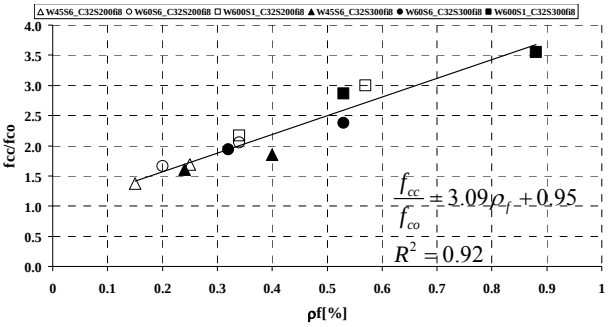



Figure 5 - $f_{cc}/f_{co,\phi 8}$ versus $\rho_f$ for all the specimens

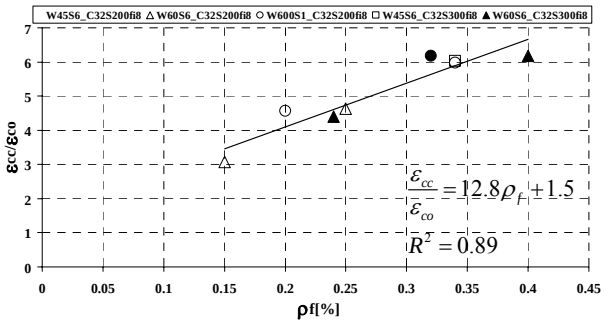



Figure 6 - $\varepsilon_{cc}/\varepsilon_{co,\phi 8}$ versus $\rho_f$

In series of equal $\rho_f$, such is the case of series W60S6L5 and W600S1L3, the confinement was a little bit more effective in the specimens fully wrapped, but the time consumed in the confinement procedures was higher and the failure modes were more violent. The last column of Tables 3 and 4 shows that, at the failure of the specimens, which always occurred by the CFRP tensile rupture, the maximum tensile strain in the direction of the fibers, $\varepsilon_{fmax}$, varied from 27% up to 85% of the CFRP ultimate tensile strain, $\varepsilon_{fu.}$ These values are just for specimens that have failed up to the load carrying capacity of the equipment working in closed-loop control. As Lam and Teng, (2003) have already reported, the variation of the strain field in CFRP depends considerably on the distribution of the damage in the concrete specimen. Taking this into account and considering that only one or two strain gauges were applied, per specimen, for recording the CFRP strain variation, it is not surprising that a tendency was not determined for the $\varepsilon_{fmax}/\varepsilon_{fu}$ ratio. A high scatter was registered on the maximum strain values in the CFRP, since the recorded values only represent the areas where the strain gauges are placed, and are too dependent on specimen failure mode configuration.

Table 3 - Main indicators of the efficacy of the confinement systems in the C32S200ϕ8 test group.

| Specimen designation | S | L | $\rho_f$[%] | $f_{cc}$ (MPa) | $\varepsilon_{cc}$ (μm/m) | $f_{cc}/f_{co}$, ϕ8 | $\varepsilon_{cc}/\varepsilon_{co}$ | $\varepsilon_{fmax}$ (μm/m) | $\varepsilon_{fmax}/\varepsilon_{fu}$ |
|---|---|---|---|---|---|---|---|---|---|
| Uncon. Plain Concrete (UPC) | | | | 30.31 ($f_{co,UPC}$) | 0.0031 ($\varepsilon_{co,UPC}$) | - | - | - | - |
| Uncon. ϕ10 Reinf. Concrete | | | | 32.80 ($f_{co,\phi 8}$) | 0.0030 ($\varepsilon_{co,\phi 8}$) | - | - | - | - |
| W45S6L3 | 6 | 3 | 0.15 | 44.80 | 0.0092 | 1.37 | 3.07 | 0.00867 (SG1) | 0.56 (SG1) |
| | | | | | | | | 0.00422 (SG2) | 0.27 (SG2) |
| W45S6L5 | | 5 | 0.25 | 55.36 | 0.0139 | 1.69 | 4.63 | 0.00702 (SG1) | 0.45 (SG1) |
| | | | | | | | | 0.00672 (SG2) | 0.43 (SG2) |
| W60S6L3 | | 3 | 0.20 | 54.37 | 0.0137 | 1.66 | 4.57 | 0.00731 (SG1) | 0.47 (SG1) |
| | | | | | | | | 0.00822 (SG2) | 0.53 (SG2) |
| W60S6L5 | | 5 | 0.34 | 67.09 | 0.0179 | 2.05 | 5.97 | 0.00721 (SG1) | 0.47 (SG1) |
| | | | | | | | | 0.00804 (SG2) | 0.52 (SG2) |
| W600S1L3 | 1 | 3 | 0.34 | 71.37 | 0.0181 | 2.17 | 6.03 | 0.0131 (SG1) | 0.85 (SG1) |
| W600S1L5 | | 5 | 0.57 | 71.51 [98.36] | 0.014 | 2.18 [3.0] | 4.67 | 0.00735 (SG1) | 0.47 (SG1) |

Table 4 - Main indicators of the efficacy of the confinement systems in the C32S300ϕ8 test group.

| Specimen designation | S | L | $\rho_f$[%] | $f_{cc}$ (MPa) | $\varepsilon_{cc}$ (μm/m) | $f_{cc}/f_{co}$, ϕ8 | $\varepsilon_{cc}/\varepsilon_{co}$ | $\varepsilon_{fmax}$ (μm/m) | $\varepsilon_{fmax}/\varepsilon_{fu}$ |
|---|---|---|---|---|---|---|---|---|---|
| Uncon. Plain Concrete (UPC) | | | | 30.31 ($f_{co,UPC}$) | 0.0031 ($\varepsilon_{co,UPC}$) | - | - | - | - |
| Uncon. ϕ10 Reinf. Concrete | | | | 32.80 ($f_{co,\phi8}$) | 0.0030 ($\varepsilon_{co,\phi8}$) | - | - | - | - |
| W45S6L3 | 6 | 3 | 0.24 | 52.76 | 0.0132 | 1.60 | 4.40 | 0.00743 (SG1) | 0.47 (SG1) |
| | | | | | | | | 0.00585 (SG2) | 0.38 (SG2) |
| W45S6L5 | | 5 | 0.40 | 60.70 | 0.0185 | 1.85 | 6.17 | 0.00883 (SG1) | 0.57 (SG1) |
| | | | | | | | | 0.00796 (SG2) | 0.51 (SG2) |
| W60S6L3 | | 3 | 0.32 | 63.50 | 0.0185 | 1.94 | 6.17 | 0.00689 (SG3) | 0.44 (SG1) |
| | | | | | | | | 0.00711 (SG4) | 0.46 (SG2) |
| W60S6L5 | | 5 | 0.53 | 71.52 [77.98] | 0.0225 | 2.18 [2.38] | 7.50 | 0.00902 (SG1) | 0.58 (SG1) |
| | | | | | | | | 0.00764 (SG2) | 0.49 (SG2) |
| W600S1L3 | 1 | 3 | 0.53 | 71.56 [93.59] | 0.0168 | 2.18 [2.86] | 5.60 | 0.00718 (SG1) | 0.46 (SG1) |
| W600S1L5 | | 5 | 0.88 | 71.88 [116.22] | 0.0121 | 2.19 [3.55] | 4.03 | 0.00188 (SG1) | 0.12 (SG1) |

## 6. ANALITICAL MODEL

To simulate the behavior of concrete specimens fully wrapped with CFRP sheets, submitted to direct compression loading, several analytical models have been proposed Saaman et. al. (1998), Toutanji (1999), Xiao and Wu (2000), Untiveros (2002), Lam and Teng (2003). To simulate the behavior of the partially confined concrete specimens tested in the present work, the model developed by Lam and Teng (2003) was adopted. According to this model, the stress in the confined concrete ($\sigma_c$) is determined by the following expressions (see Figure 7):

$$\sigma_c = E_c\varepsilon_c - \frac{(E_c - E_2)^2}{4 f_0}\varepsilon_c^2 \text{ for } 0 \le \varepsilon_c \le \varepsilon_t \quad (1)$$

$$\sigma_c = f_0 + E_2\varepsilon_c \text{ for } \varepsilon_t \le \varepsilon_c \le \varepsilon_{cc} \quad (2)$$

where $f_o$ was assumed equal to $f_{co}$, $\varepsilon_t$ is the strain at the transition between the domain of these two equations,

$$\varepsilon_t = \frac{2 f_0}{(E_c - E_2)} \quad (3)$$

with $E_2$ being the slope of the equation (2):

$$E_2 = \frac{f_{cc} - f_0}{\varepsilon_{cc}} \tag{4}$$

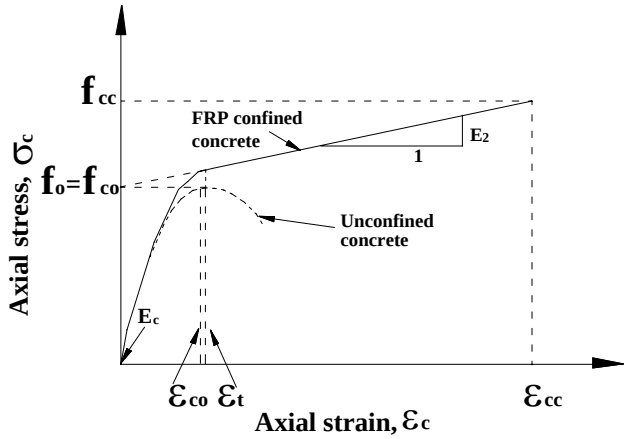



Figure 7 – Proposed stress-strain Lam and Tend model for FRP confined concrete.

To simulate the behavior of the specimens partially confined, the $f_{cc}/f_{co,\phi 8}$-$\rho_f$ and $\varepsilon_{cc}/\varepsilon_{co,\phi 8}$-$\rho_f$ relationships registered experimentally were used (see Figures 5 and 6):

$$\frac{f_{cc}}{f_{co}} = 3.09\rho_f + 0.95 \quad \text{for} \quad 0.15 \le \rho_f \le 0.88 \tag{5}$$

$$\frac{\varepsilon_{cc}}{\varepsilon_{co}} = 12.8\rho_f + 1.5 \quad \text{for} \quad 0.15 \le \rho_f \le 0.34 \tag{6}$$

Using the $E_c = 14166$ MPa obtained from the stress-strain curves of the URC_ϕ8 specimens, the analytical and experimental stress-strain axial relationships ($\sigma_c$-$\varepsilon_c$) of the series of specimens partially confined are compared in Figure 8. For the series confined with CFRP sheets of 200 g/m$^2$ of fibers, the analytical model predicted the experimental stress-strain response with high accuracy, mainly the compressive strength. However, for the series confined with CFRP sheets of 300 g/m$^2$ of fibers, the analytical model shows a tendency of predicting a load carrying capacity higher than the one registered experimentally. Furthermore, in the $\varepsilon_t \le \varepsilon_c \le \varepsilon_{cc}$ strain field the experimental $\sigma_c$-$\varepsilon_c$ relationship was not as linear as estimated by the analytical model, which indicates that the plastic deformation of the steel bars has influence in the $\sigma_c$-$\varepsilon_c$ shape.

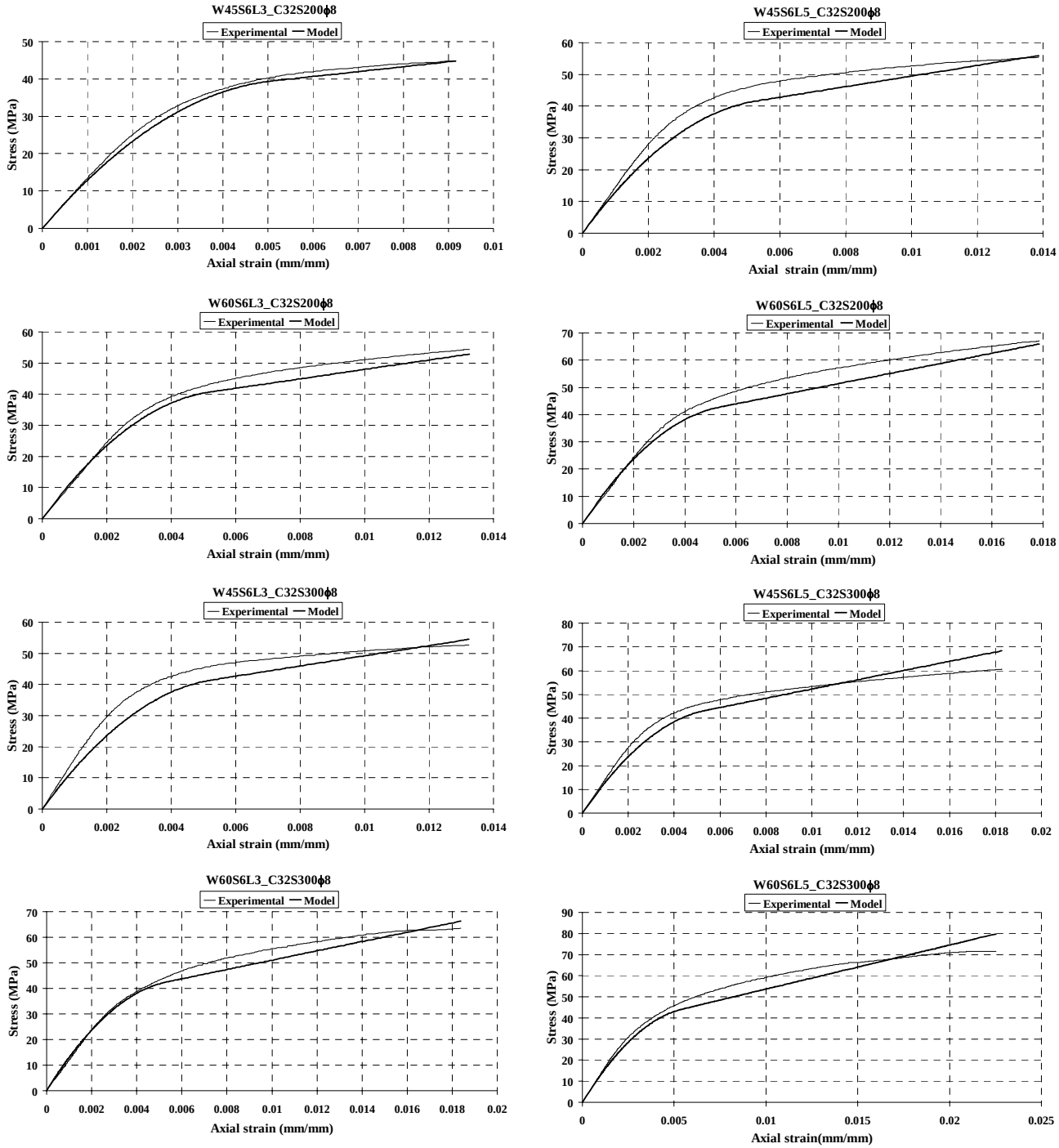



Figure 8 – Comparison between analytical model and experimental results for the group of series C32S200ϕ8 and C32S300ϕ8.

## 7. CONCLUSIONS

The present work dealt with an experimental and an analytical research involving the use of carbon fiber reinforced polymer (CFRP) wet lay-up sheets to increase the load carrying capacity and the deformation ability of reinforced concrete (RC) elements submitted to direct compression loading. The experimental program was conceived to evidence the influence of full and partial wrapping confinement arrangements in the compression behavior of this type of elements. In the partial wrapping systems, the distance and width of the CFRP strips and

the thickness of the CFRP were also parameters considered in the experimental program. The RC elements had 200 mm diameter and 600 mm length, were manufactured by concrete of average compressive strength of 32 MPa, were reinforced longitudinally by four steel bars of 8 mm diameter and were confined by steel hoops of 6 mm diameter, spaced at 96 mm.

The experimental results showed that, the load carrying capacity of CFRP-confined elements has a linear increasing tendency with the increase of the CFRP confinement ratio, $\rho_f$. The normalized maximum compressive strength ($f_{cc}/f_{co,}$ where $f_{co}$ is the compressive strength of unconfined elements) varied from 1.37 for $\rho_f$=0.15% up to 3.55 for $\rho_f$=0.88%. A linear increasing trend was also observed for the $\varepsilon_{cc}/\varepsilon_{co}$-$\rho_f$ relationship, having $\varepsilon_{cc}/\varepsilon_{co}$ ranged from 3.0 for $\rho_f$=0.15% up to 7.5 for $\rho_f$=0.53%. For the specimens that, when failed, the strains in the fiber direction of the CFRP were registered, the maximum strain varied from 27% up to 58% of the CFRP ultimate tensile strain. For the specimens of equal $\rho_f$, the load carrying capacity of partially confined specimens was a little bit lower than the one of the fully confined specimens. However, partial confinement arrangements were easier and faster to apply than full confinement arrangements.

From the experimental results, two equations were derived, one to evaluate $f_{cc}/f_{co}$ and the other to determine $\varepsilon_{cc}/\varepsilon_{co}$, both in function of the confinement ratio, $\rho_f$. These two equations, plus the initial concrete Young's Modulus, provide the basic data of an analytical model used to predict the stress-strain diagrams registered in the partially confined specimens. The accuracy of the simulation was reasonable, but it can be improved if a nonlinear equation was assumed for the phase when plastic deformation occurs in the longitudinal steel bars and/or in the transversal steel hoops. For the sake of simplicity, in the present model a linear relationship was assumed for the $f_{cc}/f_{co}$-$\rho_f$ and $\varepsilon_{cc}/\varepsilon_{co}$-$\rho_f$. However, the increase ratio of $f_{cc}/f_{co}$ and $\varepsilon_{cc}/\varepsilon_{co}$ should decrease with the increase of $\rho_f$. When more data are available, more accurate $f_{cc}/f_{co}$-$\rho_f$ and $\varepsilon_{cc}/\varepsilon_{co}$-$\rho_f$ functions can be determined, which will improve the performance of the used analytical model.

## 8. ACKNOWLEDGMENTS

The authors of the present work wish to acknowledge the generous support provide by MBT Bettor Portugal and S&P Clever Reinforcement. The first author would like to thank the financial support by PRODEP action 5.3/N/199.014/01.

## 9. REFERENCES

Barros, J.A.O., Ferreira, D.R.S.M., Partial versus full wrapping confinement systems for concrete columns, accepted to be published in the *International Conference on Concrete Repair, Rehabilitation and Retrofitting*, South Africa, November (2005).

Degussa - Construction Chemicals, in : *Technical and commercial document,* (2003).

Ferreira, D.R.S.M., Barros, J.A.O., Confinamento por cintagem total e parcial de elementos de betão com mantas de fibras de carbono, *Technical Report 04-DEC/E-29,* Dep. Civil Eng., University of Minho, 165 p., (http://www.civil.uminho.pt/composites), November (2004). In Portuguese.

ISO TC 71/SC 6 N, Non-conventional reinforcement of concrete-test methods-part 2: Fiber reinforced polymer (FRP) sheets, *International standard,* (2003).

Lam L., and Teng J.G., Design-oriented stress strain model for FRP-confined concrete, in: *Elsevier Construction and building materials*, 17, 471-489, (2003).

Saadatmanesh H., Ehsani M.R., Strength and ductility of concrete columns externally reinforced with fiber composite straps, *ACI Structural Journal,* 91 (4) 434-447, (1994).

Saadatmanesh H., Ehsani M.R., Seismic strengthening of circular bridge pier models with fiber composite, *ACI Structural Journal,* 93 (6) 639-647, (1996).

Samaan, M., Mirmiran, A., Shahawy, M., Model of concrete confined by fiber composites, *Journal of Structural Engineering*, ASCE, 124(9), 1025-1031,(1998).

Toutanji, H. A., Stress-strain characteristics of concrete columns externally confined with advanced fiber composites sheets, *ACI Material Journal*, 96(3), 397-404, (1999).

Untiveros, C. M. A., Estudio experimental del comportamiento del hormigón confinado sometido a compresión, Tesis doctoral, Barcelona, septiembre, (2002).

Xiao, Y., Wu, H., Compressive behavior of concrete confined by carbon fiber composite jackets, *Journal of Material in Civil Engineering,* ASCE, 125(3), 255-264, (2000).

International Symposium Polymers in Concrete
2 - 4 April 2006
Guimarães, Portugal

# Analysis of the design models suggested on Fib bulletin 14 related to the flexural strengthening of reinforced concrete elements by CFRP systems

J. Alexandre Bogas[2], Augusto Gomes[1]

*DECivil/ICIST, Instituto Superior Técnico,*
*Technical University of Lisbon, Av. Rovisco Pais, 1049-001 Lisbon, Portugal*

## ABSTRACT

The main aim of this paper is to evaluate, argue and criticise the design models and methods concerning the use of CFRP external flexural strengthening of concrete structures proposed in Fib bulletin 14 – Task Group Fib TG9.3 "External bonded reinforcement"(2001).

The three different approaches of flexural strengthening suggested in the above-mentioned document are checked by comparative studies based on different experimental works published by other researchers and analytical applications.

By comparing analytical values with experimental results, we draw important conclusions related to: the evaluation of the suggested approaches in terms of complexity; the adaptability to real case studies; the accuracy of design models proposed in different approaches, and the efficiency and general behaviour of CFRP flexural strengthening reinforcement.

## 1. INTRODUCTION

CFRP systems are relatively recent in the construction market. Therefore, the analysis methods and the design guidelines for these materials are almost inexistent and fairly vague.

The existing models are not consensual and in general either extremely simplified or very theoretical and complex, with no practical application.

The interest in CFRP reinforcement leads to a great development of the research activities in this field. However, the knowledge is still very limited and dispersed. Furthermore, there is only a small number of reinforcement cases and those are just a few years old. Therefore, there is a lack of guidance code that stipulates accuracy design rules of externally bonded CFRP reinforcement for concrete structures.

Due to the lack of normalization, an extensive research program has been conducted to evaluate and criticise the main design models and methods concerning the use of CFRP external flexural strengthening of concrete structures proposed in Fib bulletin 14 (2001).

This paper presents analytical comparative studies based on different experimental works published by other researchers and on the different approaches proposed in Fib bulletin 14 (2001), evaluating the complexity, accuracy, adaptability to real case studies and general behaviour of those recent materials in flexural strengthening reinforcement. Is still suggested a simplified design method for flexural strengthening and new values are proposed for the design effective strains depending on the type of CFRP system used (laminates or sheets).

[1] Professor
[2] Research Assistant (Engº)

## 2. FLEXURAL REINFORCEMENT

### 2.1. Cross section analysis for the ultimate limit state in bending

Fib bulletin 14 proposes, for the ultimate limit state (ULS) section analysis, a simplified safety evaluation approach based on the traditional equivalent rectangle method, used in steel reinforced concrete with a simplified stress distribution at the section. The proposed model is of simple application when the crush failure first occurs at the concrete, but becomes iterative and too complex when the failure by CFRP debonding is premature, which is the most usual situation. In Bogas (2003), there is a comparative study for different steel reinforcement ratios, using the simplified traditional method and the rigorous iterative method proposed in Fib Bulletin 14, for typical situations of premature CFRP debonding. The study concluded that the use of the traditional method instead of the iterative one conduces to non-conservative but approximated results with no meaningful round-off errors. Obviously, in an advanced level of a project, it is recommended to use an "exact method" based on the constitutive laws of materials, easy to implement with the current computer systems. For brief analysis of flexural strengthening the use of simplified expressions is important to draft designs and to evaluate complex models. In these cases the following simplified expression is recommended as a better alternative to the method proposed at Fib bulletin 14 (2001):

$$M_{rd} = A_{seq} \times z_{eq} \times f_{syd} = A_s \times z_s \times f_{syd} + A_f \times z_f \times f_f \quad (2.1)$$

where: $f_f = E_f \varepsilon_f$ and $Z_{eq} \approx 0.95 d_{méd}$ (for usual cases) or $Z_{eq} \approx 0.9 d_{méd}$ (high loaded sections)

As it is concluded in Bogas (2003), for current concrete sections, this expression leads to reasonable results and to strengthening levels close to the ones obtained with the simplified methods proposed in Fib bulletim 14.

### 2.2. Safety evaluation approaches for CFRP flexural strengthening reinforcement proposed in Fib bulletim 14 (2001)

Approach 1 – CFRP strain limitation

This approach consists in restricting the ultimate tensile strain to a conservative value, based up on several experimental results. Therefore, this approach lacks a solid theoretical or analytical basis. Experimental results (see 3.), show that the FRP tensile strain depends on a wide range of factors, such as CFRP and concrete proprieties, internal steel yielding and deformation, relation between bonding area and thickness of CFRP systems, etc. Hence, a global strain limit must be conservative to represent the whole range of applications. Its simplicity and suitability for brief calculations is the most attractive advantage of this method. Table 2.1 shows the strain limit values proposed in different guidance documents

Table 2.1 - Strain limit values

| | **Fib bulletim 14** | **Japanese Standadrd (1998)** | **ACI 440 (2000)** |
|---|---|---|---|
| $\varepsilon_{f,lim}$ ($^{o}/_{oo}$) | 6,5 to 8,5 * | 4,0 to 8,0 | $\varepsilon = f(n;E_f;t_f)$** |

* - For bonding stresses in concrete higher than 1,5 MPa

**- Strain depends on the number of sheets (n), thickness ($t_f$) and stiffness ($E_f$).

In relation to the table above, it is important to note the following:

- ACI 440 (2000) is the only document that stipulates the strain limit values based on the total thickness and stiffness. In fact, the reinforcements with higher stiffness are much suitable to early premature CFRP debonding, and correspond to much lower values of strain limits, Triantafillou (1999);

- None of these documents make the distinction between prefabricated and in situ systems;
- Although the sheets systems are associated with high dispersion of final application conditions, it is demonstrated that, in general, the premature debonding occurs for higher strain values (see 3.). This can be explained by two factors: the stronger relationship between bonded area and thickness of sheet systems; and the bond advantages of the primaries usually applied.

Approach 2 – Calculating of the envelope line of tensile stress

The aim of this approach is to calculate the maximum admissible increase in tensile stress, between two subsequent flexural cracks. Approach 2 is based on more solid concepts such as; bond stress-slip relation at the interface CFRP-concrete, development of tensile stresses along the CFRP system or spacing of flexural cracks.

The calculation of flexural spacing cracks is determinant in this approach, and it is observed, Bogas (2003), that the expression proposed by Niedermeier (2000), for the calculation of spacing cracks is too conservative when compared with other proposed methods. A study comparing the expression proposed by Niedermeier (2000) to the one proposed for the verification of crack width by Fib bulletim 14 (2001), is illustrated in Bogas (2003). Differences of about 60% between the both expressions in the determination of spacing cracks can be observed. These significant differences can be explained by comparing the expressions of bond stresses proposed by Niedermeier, ($\tau_{fm}=0.44f_{ctm}$) and Fib bulletim 14, ($\tau_{fm}=1.25f_{ctm}$). Since the method proposed in Fib bulletim 14 to determine the service limit states (SLS) is relatively well documented (as an adaptation of the method defined in EC2, 1991), and concluding that it gives you a good estimation of the spacing cracks (Bogas 2003), this method is preferable to that proposed by Niedermeier (2001).

Approach 2 potentially provides you with a better estimation for the real behaviour of CFRP flexural strengthening reinforcement, because it is based on analytical calculations. Nevertheless, one should note that, as this method depends on aleatory and uncertain parameters (such as cracking position and spacing crakes) the tendency will be for it to be replaced by more realistic and adequate methods.

Approach 3 – Verification of force transfer between CFRP and concrete

This approach is based on a stress distribution along the CFRP considering homogeneous concrete elements without cracking. By using simplified expressions, the shear flow at the interface CFRP-concrete is calculated and the shear stress is restricted to a design bond shear strength, which is considered equal to the bond shear strength of concrete, $f_{cbd}$.

Approach 3 has the advantage of being easy to implement, because it is less complex than the Approach 2. In Approach 3 the bonding stress is independent of the levels of tension in CFRP, but actually it has been shown that the CFRP systems are more susceptible when the extensions are higher, Rostasy (2001). In comparison with approach 1, this method involves more bonding parameters namely, the area and stiffness of internal steel and CFRP, and the bond shear strength of the concrete.

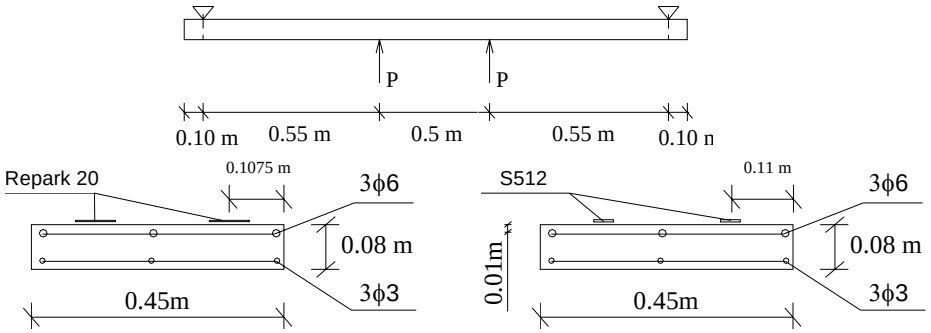
## 3. STUDY OF THE PROPOSED APPROACHES AND THEIR ADEQUABILITY

Comparative studies based on different experimental works published by other researchers have been used to evaluate the complexity, accuracy and adaptability of the proposed approaches in Fib bulletim 14. A wide range of experimental works were evaluated, considering different kinds of loadings, geometries, characteristics of materials, types of reinforcements, etc. The following experimental works have been analysed:

- Experimental tests program of CFRP flexural strengthening reinforcement on reduced slabs models – F.E.U.P.- Juvandes (1999);
- Experimental tests program of CFRP flexural strengthening of reinforced concrete (RC) beams on three models at a real scale – I.S.T. – Resende (2000);
- Flexural strengthening of RC beams with CFRP laminates – Oller (2001);
- Experimental behaviour of RC beams strengthened with CFRP – Ceroni (2001);
- Strengthening of RC beams with CFRP sheets –Bazaa (1996);
- Strengthening of RC beams with composite materials of CFRP – Dias (2000);

Only four of those experimental works are analysed in this paper. The remaining ones are presented in Bogas (2003).

3.1. CFRP flexural strengthening of reinforced concrete slabs – Juvandes (1999)




Serie M ⇒ Sheet systems ("Repark20") – 1 layer 75×0,11 + 1 layer 65×0,11 [mm]
Serie S ⇒ Laminate systems ("S512") – 1 strip 16×1,2 [mm]

Figure 3.1 – Characteristics of slabs Models

Table 3.1 - Characteristics of materials

| **Steel** | **$f_{ym}$ (MPa)** | **$f_{um}$ (MPa)** | **$\varepsilon_{um}$ ($^o/_{oo}$)** | **$E_s$ (GPa)** | **Class** |
|---|---|---|---|---|---|
| $\phi$ 3/$\phi$ 6 | 330,3/635,6 | 464,6/684,9 | 56/18,4 | 225 | Normal(NL)/Ribbed(NR) |

| **Concrete (28days)** | | **$f_{cm}$ (MPa)** | **$f_{ck}$ (MPa)** | **$f_{ctm}$ (MPa)** | **$E_{cm}$ (GPa)** | **Class** |
|---|---|---|---|---|---|---|
| **M** | LC3R e LC4R | 56,3 | 51,3 | 3,8 | 36,8 | C50/60 |
| **L** | LC1S e LC2S | 56,3 | 51,3 | 3,8 | 36,8 | C50/60 |

| **CFRP** | **Tests** | | **Maker** | | |
|---|---|---|---|---|---|
| | **$f_{lu}$ (MPa)** | **$\varepsilon_{lu}$ ($^o/_{oo}$)** | **$f_{lu}$ (MPa)** | **$\varepsilon_{lu}$ ($^o/_{oo}$)** | **Type of CFRP** |
| $E_f$=160GPa/230GPa | 3100/3400 | 19,4/15 | 3100/3400 | >19/15 | S512/sheet Repark 20 |

Table 3.2 - Experimental results

| **Serie** | **Models** | **$\varepsilon_{f,lim}$ ($^o/_{oo}$)** | **$P_{max}$ (kN)** | **$S_{rm}$ (cm)** | **$\sigma_{max}/f_{fu}$ (%)** | **Failure mode** |
|---|---|---|---|---|---|---|
| **M** | **LC3R** | 10,92 | 39,1 | 6,3 | 73,9 | CFRP failure |
| | **LC4R** | 10,30 | 31,3 | 6,4 | 69,7 | CFRP failure |
| **L** | **LC1S** | 10,32 | 34,1 | 6,4 | 53,3 | debonding |
| | **LC2S** | 11,83 | 37,7 | 6,3 | 61,0 | debonding |

Table 3.3 - Analytical design values

| | Approach 1 * | | Approach 2 | | Approach 3 ** |
|---|---|---|---|---|---|
| **Series** | $\varepsilon_{f,lim}$ ($^o/_{oo}$) | $P_{max}$ (kN) | $\varepsilon_{f,lim}$ ($^o/_{oo}$) | $P_{max}$ (kN) | $P_{max}$ (kN) |
| **M** | 6,5 | 26,9 | 4,7 | 22,0 | 70,5 |
| **L** | 6,5 | 25,4 | 2,34 | 12,0 | 15,1 |

* - The considered design strain limit was $\varepsilon_{limit}$ = 0,0065 defined in Fib bulletin 14 (2001)
** - For this approach $P_{max}=2\times P$ is also defined considering the ultimate crush failure of CFRP, and not only the premature CFRP debonding as it is suggested in approach 3.

Approach 1

Tables 3.2 and 3.3, show that the analytical results are conservative. Mean values, obtained from the experimental tests of about $\varepsilon_{m,max}$ = 10,5 $^o/_{oo}$, are much higher than the strain limits proposed in Fib bulletim 14, ($\varepsilon_{f,lim}$.=6,5$^o/_{oo}$ to 8,5$^o/_{oo}$). The relation between $P_{máx}$ (maximum experimental load) and $P_t$ (maximum theoretical load) is $P_{máx}/P_t \cong 1.2$ to 1.45 for series M and $P_{máx}/P_t \cong 1.22$ to 1.46 for series L. The difference between $P_{máx}$ and $P_t$ is lower than the difference between the experimental and theoretical strain limits, due to the strength contribution of internal steel reinforcement.

Approach 2

By analysing and applying the different expressions proposed by Niedermeier (2000) and comparing them to the experimental results, one can conclude the following:

- As can be verified from the practical examples documented in Bogas (2003), this approach is usually very conservative for laminate systems. Analytical results obtained from the proposed expressions are 3 or 4 times lower than the experimental values;
- For sheet systems, usually with lower thickness, the values are less conservative, but still results in values about twice as low as the experimental ones. This can be justified by the fact that the expressions derived by Niedermeier (2000) strongly depend on thickness. For example, if one layer of sheet systems had been used instead of two, the result values would have been more reasonable and approximate, as shown in the practical example illustrated in Bogas (2003);
- In Approach 2, for tensile forces slightly above the internal steel yielding stresses, the premature debonding is quickly achieved. Hence, the Niedermeier expressions, hardly consider the additional increase of CFRP extension after the steel yielding;
- For usual reinforced concrete elements, at real scale, by laminate systems with thickness about 1 mm or more, the Niedermeier expressions lead to maximum strain values about 3$^o/_{oo}$ (Bogas 2003). Values too conservative for a large range of actual reinforced cases;
- As shown in the practical examples documented in Bogas (2003), Approach 2 is not suitable for most of real-life applications of CFRP systems.

Approach 3

By applying the expressions of Approach 3 and comparing them to the experimental results, the following conclusions can be drawn:

- For laminate systems (series L), the obtained analytical results are too conservative, as compared to the observed experimental values. The premature debonding of the CFRP reinforcement strongly depends on its transmission width, which is not exactly the same as the real width of the laminate (spread adhesive at the borders of the laminate). For current widths of laminate systems (10-30 cm), this difference does not constitute a problem. Nevertheless, for lower widths such as that considered in this experimental work (1,6 cm), differences as small as 1 or 2 cm may conduct to as much as twice the

transmission width and load capacity. Correctly adjusting for this effect, the new analytic values are much more accurate and approach 3 suits the experimental results;

- Furthermore, the arbitrated bond shear strength was based in concrete tensile tests, which can be different from the real effective bond shear strength at the experimental tests. This has a great influence in the behaviour of the CFRP reinforcement;
- For sheets (series M), analytical results are higher than the experimental observed values. According to this approach, this means that the premature debonding only occurs for high loading values and the crashing failure of CFRP can happen before that, due to the lack of its strengthening capacity. Experimental results show that the crashing of CFRP occurs first instead of debonding.

3.2. CFRP flexural strengthening of reinforced concrete beams – Resende (2001)

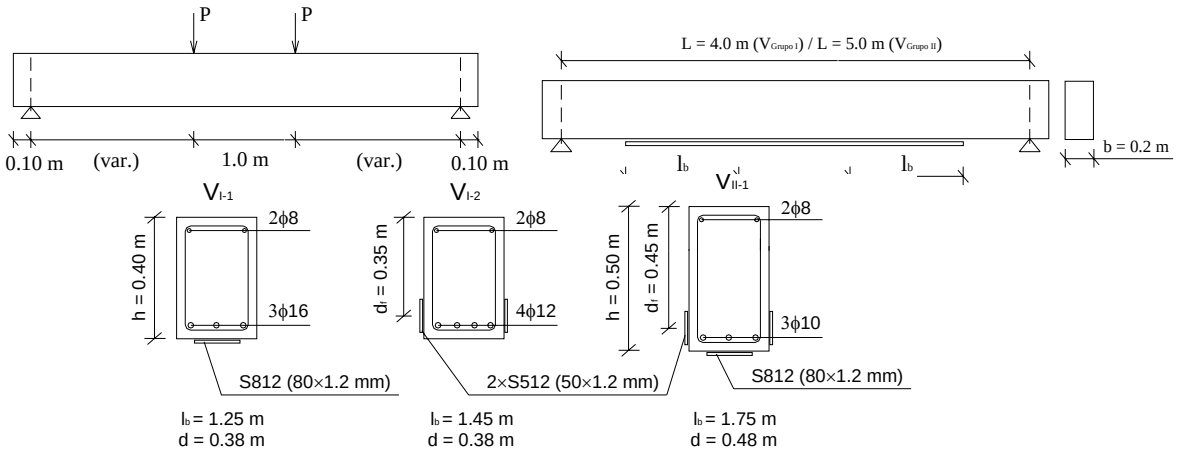



Figure 3.2 – Characteristics of beams Models

Table 3.4 - Characteristics of materials

| **Steel** | **$f_{ym}$ (MPa)** | **$f_{um}$ (MPa)** | **$\varepsilon_{um}$ ($^o/_{oo}$)** | **$E_s$ (GPa)** | **class** |
|---|---|---|---|---|---|
| Steel reinforcement | 475 | 570 | 23,9 | 200 | **A400** |

| **Concrete** | **$f_{cm}$ (MPa)** | **$f_{ck}$ (MPa)** | **$f_{ctm}$ (MPa)** | **$E_c$ (GPa)** | **class** |
|---|---|---|---|---|---|
| age - 28 days | 34,8 | 29,8 | 2,9 | 31 | **B30** |
| age - 108 days | 39,9 | 38,3 | 3,4 | 32,5 | |

| **CFRP** | **Tests** | | **Maker** | | |
|---|---|---|---|---|---|
| **Laminates** | **$f_{lu}$ (MPa)** | **$\varepsilon_{lu}$ ($^o/_{oo}$)** | **$f_{lu}$ (MPa)** | **$\varepsilon_{lu}$ ($^o/_{oo}$)** | **Type of CFRP** |
| $E_f$=160GPa | 3000 | - | 3050 | 17 | **S512/S812** |

Table 3.5 - Experimental results

| **Models** | **$\varepsilon_{f,lim}$ ($^o/_{oo}$)** | **$P_{max}$ (kN)** | **$P_0$ (kN)** | **$S_{rm}$ (m)** | **Crash failure** | **observations** |
|---|---|---|---|---|---|---|
| **$V_{I-1,R}$** | 4,19 | 82,5 | 47,5 | 0,125 | debonding | initial cracking |
| **$V_{I-2,R}$** | 5,24 | 67,5 | 0 | 0,125 | debonding | no initial cracking |
| **$V_{II-1,R}$** | 6.21(b)<br>5.17(L) | 87,2 | 20,2 | 0,125 | debonding | initial cracking |

(b) - Bottom laminate S812; (L) - Lateral laminate S512; ($P_0$) - Load when the beams are strengthening

Table 3.6 - Resume of analytical design values

| | Approach 1 | | Approach 3 |
|---|---|---|---|
| **Models** | $\varepsilon_{f,lim}$ ($^{o}/_{oo}$) | $P_{max}$ (kN) | $P_{max}$ (kN) |
| $V_{I-1,R}$ | 6,5 | 89,3 | 80,8 |
| $V_{I-2,R}$ | 6,5 | 74,73 | 80,57 |
| $V_{II-1,R}$ | 6,5 | 72,6 | 221,5 |

Approach 1

From the values indicated at tables 3.5 and 3.6, it is observed that the experimental results obtained were about $\varepsilon_{m,max} \cong 5^{o}/_{oo}$, which is lower than the strain limits proposed in Fib bulletim 14 (2001). Therefore, as per the present experimental work, the values proposed in Fib bulletim 14 (2001), are not conservative. Analytical strength reinforcement is inadequate and insufficient. The failure mode occurs earlier than assumed in Fib bulletim 14 (2001). Table 3.7 summarises relationship between $P_{max}$ and $P_t$.

Table 3.7 – Relation between theoretical and experimental load

| **Models** | $V_{I-1,R}$ | $V_{I-2,R}$ | $V_{II-1,R}$ |
|---|---|---|---|
| $P_t / P_{max}$ | 1,08 | 1,11 | 0,83 |

The strain limits proposed in normative documents are based on usual experimental results. When the cases are slightly different from the usual tests, as it happens in the present experimental work (real scale models with lateral strengthening), failure mode may occur with unexpected ultimate load. From these experimental results one may conclude that there are some strengthening cases where the values proposed in approach 1 are not conservative.

Approach 3

By applying approach 3 expressions and comparing its results to the experimental ones, the following can be concluded:

- The obtained numerical values are significantly different from the experimental results, except for beam $V_{I-1,R}$, where more accurate results are observed. As a matter of fact, for beam $V_{II-1,R}$, the analytical calculations determine a crushing failure mode of CFRP, but the experimental ones show a premature debonding of the strengthening reinforcement;
- That differences of behaviours and results may be related with the following aspects:
  - Approach 3 was mostly studied for common cases of flexural strengthening of reinforced beams or slabs with externally bonded CFRP systems applied below. On the contrary, in the present experimental work the reinforcements are lateral, which naturally implicates a different distribution of the shear flow at the section. The simplified expression proposed in fib bulletim 14 (2001) has to be changed to account for different types of reinforcements associated to variable shears stresses distribution along the transversal section height of the beam. The results summarised in table 3.6, were obtained assuming the same distribution of shear stress in lateral and bottom reinforcements, according to fib bulletin 14 (2001), but in reality, the bottom reinforcement is the most loaded;
  - The assumed value for the bond shear strength of concrete has great influence in final results. Considering values of about 1,4 kN for shear strength (experimental value obtained from bond tests) instead of the value proposed in Fib bulletim 14 (2001) in the present situation (≅2,6 MPa), the results obtained are more accurate. For example, to the beam $V_{1-2,R}$, the estimated value of the maximum theoretical load ($P_t$), would be of about 63,5 kN instead of 80,57 kN, which is conservative.

Therefore, the proposed method does not always result in conservative values. The results strongly depend on characteristics and disposition of CFRP systems and on the assumed value for the bond shear strength of concrete.

3.3. Flexural strengthening of RC beams with CFRP laminates – Oller (2001)

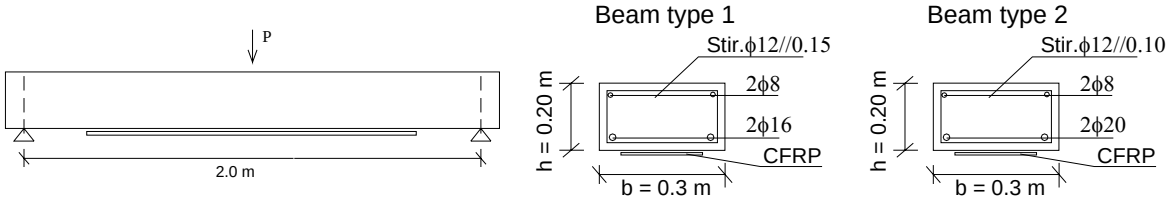



Figure 3.3 –Characteristics of beams Models

Table 3.8 - Characteristics of materials

| **Steel** | **$f_{ym}$ (MPa)** | **$f_{um}$ (MPa)** | **$\varepsilon_{um}$ ($^o/_{oo}$)** | **$E_s$ (GPa)** |
|---|---|---|---|---|
| Steel reinforcement | 550 | - | - | 200 |

| **Concrete** | **$f_{cm}$ (MPa)** | **$f_{ck}$ (MPa)** | **$f_{ctm}$ (MPa)** | **$E_c$ (GPa)** |
|---|---|---|---|---|
| age - 28 days | 35,2 | - | 2,76 | - |

| **CFRP** | **Test** | | **Maker** | |
|---|---|---|---|---|
| **Laminated** | **$f_{lu}$ (MPa)** | **$\varepsilon_{lu}$ ($^o/_{oo}$)** | **$f_{lu}$ (MPa)** | **$\varepsilon_{lu}$ ($^o/_{oo}$)** |
| $E_f$=150Gpa | 1740 | - | 2500 | 16 |

Table 3.9 - Experimental results

| **Models** | | **Strengthening type** | **$\varepsilon_{f,lim}$ ($^o/_{oo}$)** | **$P_{max}$ (kN)** | **$P_{max}/P_{ult}$ (%)** | **Failure mode** |
|---|---|---|---|---|---|---|
| Beam type 1 | **1/D b)** | 2 parallel strips 50X1.4 mm (**) | 4,112 | 100,9 | 35 | Peeling |
| | **1/C a)** | 1 strip 100X1.4 mm | 3,949 | 104 | 26,8 | Peeling |
| | **1/C b)** | 1 strip 100X1.4 mm (*) | 4,181 | 121 | 47,6 | Peeling |
| | **1/B** | 1 strip 100X1.4 mm | 3,646 | 100,5 | 22,4 | Peeling |
| | **1/A** | 1 strip 100X1.4 mm | 4,612 | 109 | 32,9 | Peeling |
| Beam type 2 | **2/D a)** | 1 strip 100X1.4 mm | 3,905 | 128 | 12,6 | Peeling |
| | **2/C** | 2 parallel strips 50X1.4 mm | 5,509 | 118,8 | 25,6 | Peeling |
| | **2/B** | 2 paralel strips 50X1.4 mm (*) | 5,062 | 126 | 34,6 | Peeling |
| | **2/A** | 1 strip 100X1.4 mm | 5,643 | 155 | 35,9 | Peeling |

(*) - additional anchorage by transversal sheets
(**) - Length of CFRP - 1,5m for 1/D a), and 1,8 m for other beams

Results analysis

The values in table 3.9, show that the experimental results obtained were about $\varepsilon_{m,max} \cong 4^o/_{oo}$ to $5^o/_{oo}$, which is lower than the strain limits proposed in Fib bulletim 14 (2001). As per the experimental work of Resende (2000), the estimated values proposed by the normative documents may not be conservative for flexural strengthening of reinforced concrete beams with externally bonded CFRP laminates. The results also depend on the ratio of steel reinforcement, because the steel plastification accelerates the stress concentration on the CFRP systems and the subsequent debonding (for example comparing beam 1/A and 2/A). The result obtained with approach 3 for the maximum analytical load is about $P_{max} \cong 110$ kN, which is a reasonably good estimation considering the experimental data. While, for type 1 beams, the estimation is slightly optimist, for type 2 beams it is conservative. Small

differences in the results must be understood by the uncertainty of the real value of the bond shear strength of concrete ($f_{cmb}$).

3.4. RC beams strengthened with CFRP – Ceroni (2001)

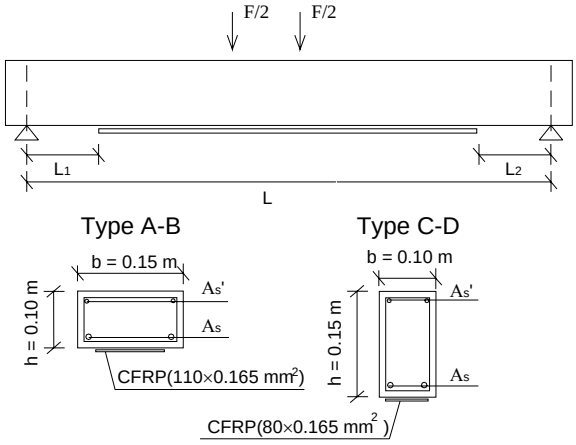



Figure 3.4 – Characteristics of beams Models

Table 3.10 - Geometrical characteristics of beams, [5]

| **Models** | **L (mm)** | **$L_1$ (mm)** | **$L_2$ (mm)** | **$A_s$** | **$A_{s'}$** |
|---|---|---|---|---|---|
| **A2** | 1800 | 150 | 0 | 2ϕ8 | 2ϕ8 |
| **A3** | 1800 | 300 | 200 | 2ϕ8 | 2ϕ8 |
| **D3** | 1400 | 200 | 200 | 2ϕ10 | 2ϕ10 |

Table 3.11 - Characteristics of materials, [5]

| **Steel** | **$f_{ym}$ (MPa)** | **$f_{um}$ (MPa)** | **$\varepsilon_{um}$ ($^o/_{oo}$)** | **$E_s$ (GPa)** |
|---|---|---|---|---|
| ϕ8 | 590 | 690 | - | 200 |
| ϕ10 | 550 | 625 | - | 200 |

| **Concrete** | **$f_{cm}$ (MPa)** | **$f_{ck}$ (MPa)** | **$f_{ctm}$ (MPa)** | **$E_c$ (GPa)** |
|---|---|---|---|---|
| age – 28 days | 29 | - | - | - |

| **CFRP** | **Test** | | **Maker** | |
|---|---|---|---|---|
| **Sheets** | **$f_{lu}$ (MPa)** | **$\varepsilon_{lu}$ ($^o/_{oo}$)** | **$f_{lu}$ (MPa)** | **$\varepsilon_{lu}$ ($^o/_{oo}$)** |
| $E_f$=230GPa | - | - | 3430 | 15 |

Table 3.12 - Experimental results, [5]

| **Models** | **Failure mode** | **$P_{max}$ (kN)** | **$\sigma_f$ (MPa)** | **$\varepsilon_{f,lim}$ ($^o/_{oo}$)** |
|---|---|---|---|---|
| **$A_2$** | Peeling | 18,5 | 2650 | 11,5 |
| **$A_3$** | Peeling | 19,2 | 2138 | 9,30 |
| **$D_3$** | Peeling | 40,1 | 3220 | 14,00 |

Results analysis

The experimental results in table 3.12, indicate a premature failure mode of CFRP, with strain limit values higher than the strain limits proposed in Fib bulletim 14 (2001). This is due to the use of sheets reinforcements instead of laminate systems. With sheet systems, the transmission stresses in the interface between CFRP and concrete, is much lower than the observed in laminate systems, witch implicates a premature delayed failure mode.

Similarly to what had been concluded in other experimental works, the behaviour of the CFRP system also depends on the beam geometry and on the rate of steel reinforcement.

For beam $D_3$, Approach 3 leads to conservative and quite accurate estimation, ($P_{max} \cong 34$ kN). On the contrary, for beams $A_2$ and $A_3$, the estimation is too optimist and too far from the reality, ($P_{max} \cong 39$ kN). This may be due to both the applying of the strengthening at different distances from the endings of the beam ($L1 \neq L2$), and the low steel reinforcement ratios. Therefore, it may be concluded that Approach 3 is not adequate for "A" model beams.

## 4. DISCUSSION OF RESULTS

The aim of this chapter is to synthesize the main observations and relevant aspects, from the study analysis developed on the present work. According to the experimental results obtained it can be shown that:

- The expressions of Niedermeier (approach 2 proposed in Fib bulletim 14 (2001)) leads to extremely conservative results and implicates unattractive solutions, with inappropriate and uneconomic levels of strengthening. Approach 2 leads to strain limit values 3 or 4 times lower than the observed experimental results. In face of this, the viability and suitability of this method may be contested. On top of that, Approach 2 is complex to implement, implicating an high calculation effort, only justified for rigorous analysis. Nevertheless, Approach 2 is based on well scientifically fundamented concepts. Therefore, it may be pertinent to invest in the calibration and development of this approach in order to make it more attractive and accurate in the future;
- The other two approaches also have weaknesses. Some of the expressions and values proposed are not suitable to real-life cases. The proposed models are still simplified and too sensitive to any change in the usual characteristics of the reinforcement system or reinforced material. For instance in Approach 1, the premature debonding does not depend on: the steel reinforcement rate, the width and thickness of the CFRP system, the physical characteristics of the CFRP and its application process. Nevertheless Approach 1 is very easy to apply and therefore, it is quite useful for the technical environment. This Approach depends on the experience and sensibility of the engineer, which may be careful in the selection of strain limits for each kind of reinforced case;
- To conclude, Approach 1 is not suitable for rigorous and advanced analysis, but is a useful method to estimate pre-designed values. It is also, a very helpful method as a complement of a more detailed analysis to verify the range of the results obtained;
- The strain limits suggested in Approach 1 of Fib bulletim 14 (2001), can be too optimistic in flexural reinforced beams with laminated CFRP systems, mainly for thickness of about 1 mm or more. From the analysed tests of Resende (2000) and Oller (2001), it was obtained maximum strain limits of about $4^{o}/_{oo}$ to $5^{o}/_{oo}$, approximate 30 to 45% less than the values suggested in Fib bulletin 14 (2001);
- In table 4.1, it is possible to compare the mean values of strain limits obtained for each test analysed to the values proposed in Fib bulletim 14, (2001);
- Approach 3, is easy to implement and based on more fundamented concepts than Approach 1. Although the analytical results obtained by applying Approach 3 were reasonably satisfactory for some of the studied cases, for the others they were too far from the experimental results;
- In Approach 3 the shear strength of concrete has a very important influence on the failure mode of CFRP. This shear strength strongly depends on the characteristics of the superficial concrete layer where the CFRP system is applied, and its value should be determine by in-situ tests, like pull-off;

- It is very important to distinguish between the different types of analysis adopted in laminate systems and sheet systems. Although the general behaviour of the reinforced elements is similar for both types of systems, the laminates are more susceptible to premature debondings. Laminate systems have a stronger relation between thickness and distribution interface area. Hence, the stress concentration is higher and the peeling occurs faster;
- Due to the simplicity of the proposed approaches (mainly Approach 1 and 3), they cannot account for some important factors like superficial preparation, fibres stretching, adhesive and primary efficiency, status of the reinforced concrete elements, cracking pattern, ending peeling effects, anchorage systems, bonding areas and internal steel ratios, amongst others. Therefore, they are expected to lack accuracy for the less common flexural reinforcement cases (different from the experimental models that were the base for the methods calibration).

Table 4.1 - Summary of the mean values of strain limit, $\varepsilon_{f,lim}$, obtained by the analysed tests

| **Experimental tests** | **Tests type** | **$\varepsilon_{f,lim}$ ($^o/_{oo}$) [tests]** | **$\varepsilon_{f,lim}$ ($^o/_{oo}$) [bulletim14]** |
|---|---|---|---|
| Juvandes (1999) | slabs models<br>sheet and laminate systems | 10,3-11,8 | 6,5-8,5 |
| Resende (2000) | beams<br>laminated systems | 4,2-6,2 | 6,5-8,5 |
| Oller (2001) | beams<br>laminated systems | 3,6-5,6 | 6,5-8,5 |
| Ceroni (2001) | beams<br>sheet systems | 9,3-14 | 6,5-8,5 |
| Bazaa (1996) | beams<br>sheet systems | 6,9 | 6,5-8,5 |
| Dias (2000) | beam models<br>sheet and laminate systems | 6,8-8,1 | 6,5-8,5 |

## 5. CONCLUSIONS

The elaboration of practical examples in Bogas (2003) and the study of several experimental works published by other researchers, allowed for the present evaluation of the approaches defined in Fib bulletim 14.

By applying the expressions proposed in Fib bulletim 14 (2001) to real case studies and by comparing the results to experimental ones, important conclusions, related to the strengthening design of concrete elements reinforced by CFRP systems, could be made.

The implementation of computer programs it is suggested concerning the constitutive laws of materials, when the design procedure must be detailed and rigorous, as it happens in an advanced stage of any engineer project. For brief calculations, quick estimations of reinforcement quantities and as an helpful tool to verify the results of more complex analysis, it is suggested the simplified model proposed in 2.1.

From the analysis of previous experimental tests, it can be concluded that Approaches 1 and 3 are very sensitive to the type of reinforcement applied. The obtained results can be conservative or optimistic depending on the thickness and the bonding area of the reinforcements. In spite of Approach 2 conservative values, the results achieved with this approach are too pessimistic and lead to non economic solutions.

Considering the results of previous studies analysed in chapter 3, it is suggested the following procedure for strengthening design of concrete elements reinforced by CFRP systems:

- For the most common reinforcement cases, the peeling-off using both Approaches 1 and 3 should be verified. Nevertheless, conservative values for strain limits about $\cong 5^{o}/_{oo}$ should be adopted, when laminate systems with more than about 1 mm of thickness or sheet systems with multiple layers are used. For the remaining cases of common reinforcement, the values proposed by Fib bulletim 14 (2001), are satisfactory;
- For uncommon situations of reinforcement, such as high thickness, high Young´s module, lateral reinforcements in beams, other types of CFRP systems, etc., specific additional researches and tests, should be performed.

To conclude, the reported analytical expressions must be constantly improved, to guarantee that their implementation will comprise a wide range of reinforcement situations with more accurate results.

## 6. REFERENCES

ACI 440, "Guide for the design and construction of externally bonded FRP systems for strengthening concrete structures", American concrete institute, 148 pp (2000)

Bogas, J. Alexandre, "Strengthening of reinforced concrete elements with CFRP – design models and safety evaluation" (Portuguese), MSc thesis, IST (2003)

Bazza, M., Missihaun, M. and Labossière, P. "Strengthening of reinforced concrete beams with CFRP sheets", First International Conference on composites in infrastructure, ICCI´96, Tucson, (1996)

Ceroni, F., Prota, A. and Pecce, M., "Experimental Behaviour of RC Beams strengthened with CFRP systems", International Conference composites in construction, CCC2001, Porto; PP.499-504 (2001)

Dias, S.J.E, Juvandes, L.F.P and Figueiras, J.A., Strengthening of reinforced concrete beams with composite materials of CFRP, (Portuguese), Structural concrete 2000, FEUP, Porto, (2000)

Eurocode 2, (EC2) – Design of Concrete Structures, (1991)

Fib bulletin 14, FIB TG 9.3 FRPEBR, "Externally bonded FRP reinforcement for RC structures", Fédération Internacionale du béton (fib), Task Group 9.3 FRP, 130 pp (2001)

Juvandes, L.F.P, "Strengthening and rehabilitation of concrete structures with composite materials of CFRP" (Portuguese), PhD thesis, FEUP (1999)

Neubauer, U., Rostásy, F.S., "Debonding mechanism and model for CFRP-plates as external reinforcement for concrete members", Composites in Construction, 467-472 (2001)

Niedermeier, R. "Envelope line of tensile forces while using externally bonded reinforcement" Doctoral dissertation, TU München, German, (2000)

Oller, E., Salcedo, J., Cobo, D. and Mari, A., "Flexural strengthening of reinforced concrete beams with externally bonded CFRP laminates", International Conference composites in construction, CCC2001, Porto; 473-478 (2001)

Resende, N. "Flexural strengthening of reinforced concrete beams with fiber reinforced plastic plate" (Portuguese), MSc thesis, IST (2000)

S&P,"30×less weight than steel for the same tensile force"; Clever Reinforcement Company, Scherer& Partener bausystem, 30 pp, (1998)

Triantafillou, T.C., "Guidelines for the dimensioning of reinforced concrete elements strengthening with Sika carbodur/Sika wrap", University of Patras, Greece, 19 pp, (1999)

International Symposium Polymers in Concrete
2 - 4 April 2006
Guimarães, Portugal

# Prediction of durability of cold-curing epoxy resins: comparison between natural and artificial weathering

Mariateresa Lettieri

*CNR – IBAM, Campus Universitario, Via Monteroni, 73100 Lecce, Italy*

Mariaenrica Frigione[1], Marianna Stefanelli

*Dept. of Innovation Engineering, University of Lecce, Via Arnesano, 73100 Lecce, Italy*

## ABSTRACT

In recent years, epoxy resins, widely employed in many industrial fields, have been used in several civil engineering applications. Structural repairs are often carried out by either injection of the neat resin or application of fiber-reinforced composites based on epoxy matrix. These materials are also used for restoration works of historic buildings. Despite their wide spread, their durability in the field of built structures is not well documented yet. Since many years of natural exposition would be necessary to evaluate the long-term behavior, artificial aging is usually used to simulate the environment in service conditions and predict the changes in properties of the materials. In these tests, higher environmental stress levels than those achieved in the natural exposure are employed, in order to obtain accelerate aging. Several papers dealing with the artificial weathering are reported in literature; however, they hardly explain how these tests can be correlated to the real long-term natural exposure.

In this report, the first results of a research on the behavior of three cold-curing epoxy resins subjected to aging, either artificial or natural, are presented. The variations of thermal and mechanical properties, as well as color changes, after aging at 70°C and 75% relative humidity and after natural weathering, were compared.

## 1. INTRODUCTION

Epoxy resins are successfully employed in many industrial fields, and, in recent years, they have been also used in civil engineering applications because of their high adhesive strength, toughness, inertness, low shrinkage and resistance to chemicals. They are used as castings, coatings, repairing materials and as structural adhesives or matrices in high-performance composites for the strengthening of structures. The usefulness of epoxy resins injected into cracked and/or crumbling concrete structures for structural consolidation was proved by extensive evidences. Therefore, the application of pressure-injected neat epoxy

[1] Professor

resins was spread to historic buildings in order to rehabilitate those structures and provide them many additional years of service. The epoxy resins can be efficiently used for repairing cracks in stone, mortar, and masonry, since, if formulated to have a proper viscosity, they can penetrate effectively into porous substrates in a way that provides an embedded network into the stone material. In many studies, the epoxy resins are described as the strongest products between different classes of consolidants (Selwitz, 1992). Despite their wide spread, the durability of these materials in the field of built structures is not well documented yet.

Different environmental factors have been identified as affecting the durability of epoxy resins, such as: moisture, temperature cyclical changes, freeze-thaw, alkaline environment, ultraviolet radiations. The artificial weathering is usually used to analyze the effects of such factors on the properties of the materials in order to predict their lifetime. However, many years of natural exposition would be necessary to evaluate the long-term behavior. In particular, in the field of building materials and composites, where lifetimes greater than many decades are expected, it is not possible to plan a real time outdoor exposure to predict the durability of the materials. Therefore, several procedures have been proposed in order to simulate the environment in service conditions and achieve accelerate aging. In these tests, higher environmental stress levels than those achieved in the natural exposure are employed. Some committees work to standardize the methods for accelerated and natural durability testing; as a result, many standard procedures have been published in recent years, firstly by ASTM (American Society for Testing and Materials) and by ISO (International Standards Organization) (Brown, 1991; Jacques, 2000). The most of national standards largely follows the ISO procedures.

In addition, the studies of many research groups have been focused on the prediction of the service lifetime of several materials. Numerous papers reported in literature deal with the effects of the artificial weathering on the epoxy resins, however they do not clearly explain how these aging procedures can be correlated to the real times of the natural exposure. Furthermore, both the aging and the weathering processes have been widely examined for the epoxy resins hardened at high temperatures; on the other hand, few data have been published dealing with the aging of the cold-curing epoxy resins. These latter materials are required for reinforcement works; therefore, they must exhibit an excellent durability in service conditions for many years and their properties should not be strongly affected by the cyclic environmental changes. The physical properties of such materials have already been extensively studied (Ellis, 1993; Mays and Hutchinson, 1992), even those employed in restoration and conservation (Selwitz, 1992; Kotlik et al., 1983; Ginell et al., 1995); however, the knowledge about the durability of these polymeric materials is poor, especially if they are subjected to critical environmental conditions. The lack of data about the durability and the long-term behavior, particularly in aggressive environments, still represents the major drawback to its wider spreading (Karbhari et al., 2003; Zanni-Deffarges and Shanahan, 1995).

For these reasons, a research aimed at investigating the properties of cold-curing epoxy resins subjected to weathering, either artificial or natural, was undertaken. The analyses carried out would relate the behavior of the artificially aged samples of epoxy resins to those naturally weathered. Furthermore, the evaluation of the effectiveness of simple and short-term methodologies of aging in predicting the service life of these materials would be investigated. In this report, the first results of this research work are presented. The thermal and the mechanical properties, as well as the color changes, measured after either natural and artificial aging, are compared.

## 2. EXPERIMENTAL

### 2.1. Materials

The materials under study are commercial two-component adhesives, hardened with amines.

**A1** resin is produced and supplied by Mapei S.p.A. (Italy). This product is provided in two components: Part A is based on diglycidylether of bisphenol-A, Part B is a mixture of polyethylenamine – xylenediamine – nonylphenol used as a curing agent. Samples of this resin were prepared using the recommended ratio, i.e. resin : hardener = 4:1 by weight.

**A2** resin (supplied by Sika Italia S.p.A. (Italy)) is a bisphenolic resin (Part A) hardened with 3-aminomethyl-3,5,5-trimethyl-cycloesilammine (Part B). The recommended ratio resin : hardener = 2:1 by weight was used to prepare the specimens.

**A3** resin (supplied by Sika Italia S.p.A. (Italy)) is again a bisphenolic resin (Part A) hardened with 3-aminomethyl-3,5,5-trimethyl-cycloesilammine (Part B); it contains about 40% of inorganic fillers. The recommended ratio resin : hardener = 4:1 by weight was used to prepare the specimens.

As suggested by the suppliers, the exact amount of each component was weighed with an analytical balance with an accuracy of ± 0.01 g. The hardener (Part B) was poured into the base resin (Part A) and they were gently stirred, avoiding the formation of air bubbles, until the mix was perfectly homogeneous.

In all cases, samples of epoxy resin with standard dimensions (90x10x4 mm) were prepared and cured at a temperature of 23 ± 2°C with a relative humidity (R.H.) of 50 ± 5%. The specimens were stored in a dark area in order to avoid the UV aging.

### 2.2. Treatments

The accelerate aging was carried out in a climatic chamber (Perani – Mod. UC 1000/20). The samples were left at 70± 2°C and 75± 5% R.H. for different time spans, up to 34 days. The accelerate aging conditions followed the procedure C reported in the ASTM D 756-93 standard. This procedure was selected in order to simulate the natural aging conditions by accelerate methods; high temperature and high moisture levels just were take into account, whereas the UV aging was overlooked. Furthermore, a similar practice was reported as leading to thermo-hygrometric conditions comparable and close to those obtained after a two years natural aging in the western Mediterranean basin (Vauthier et al., 1998).

The natural weathering was performed by means of outdoor exposure of the samples, without any protection to the environmental agents. The specimens were exposed in the South Italy and the weathering started in January. Both the A2 and A3 resins were subjected to the natural aging up to 36 months, in a previous stage of the research (Frigione, 2001 (a); Frigione, 2001 (b)); at the present time, the A1 resin is still exposed and the study about the changes in its properties is in progress.

In both artificial and natural aging, to prevent misinterpretation of the results, the exposure of a partly cured system, where the cross-linking is still in progress, was avoided. In fact, the samples were subjected to the different treatments when the slow down of curing reactions was just verified. The glass transition temperature (Tg) was used to monitor the cure and the resins were judged “fully cured” when their Tg leveled off.

## 2.3. Analytical techniques

Thermal and mechanical characteristics and color changes of the untreated resins were determined through the following techniques:

- Differential scanning calorimetry (DSC) was performed, carrying out the thermal dynamic scans between 0°C and 300°C with a heating rate of 10°C/min, under nitrogen atmosphere; a DSC 822 Mettler calorimeter was used and the thermal properties (glass transition temperature, relaxation enthalpy and residual cross-linking) were calculated as the average of 3 measurements, at least;
- Flexural mechanical tests were carried out in three points bending, using a Lloyd LR-MK4 Dynamometer, following the ASTM D 790-92 standard; the experiments were performed at room temperature, with a support span of 60 mm and a crosshead rate of 2 mm/min; flexural mechanical properties (i.e. flexural modulus, maximum flexural strength and strain at break) were calculated as the average of 5 measurements;
- Color measurements were performed with a Minolta Chroma Meter CR300 colorimeter using CIE Standard illuminant C; 10 measurements were performed on each sample and the colorimeter was recalibrated to a white calibration plate at the start of each measuring session; the color changes (ΔE) were calculated through the L*a*b* (CIE 1976) system, using the means values determined on 5 samples.

All tests were repeated immediately after the end of each artificial aging treatment and every three months during the natural exposure.

The color measurements were carried out only on the artificially aged samples, where no UV effect was involved.

## 3. RESULTS AND DISCUSSION

### 3.1. Thermal analyses

In Figure 1, the variations in Tg (ΔTg) measured on samples subjected to accelerate aging are reported as a function of the exposure time.

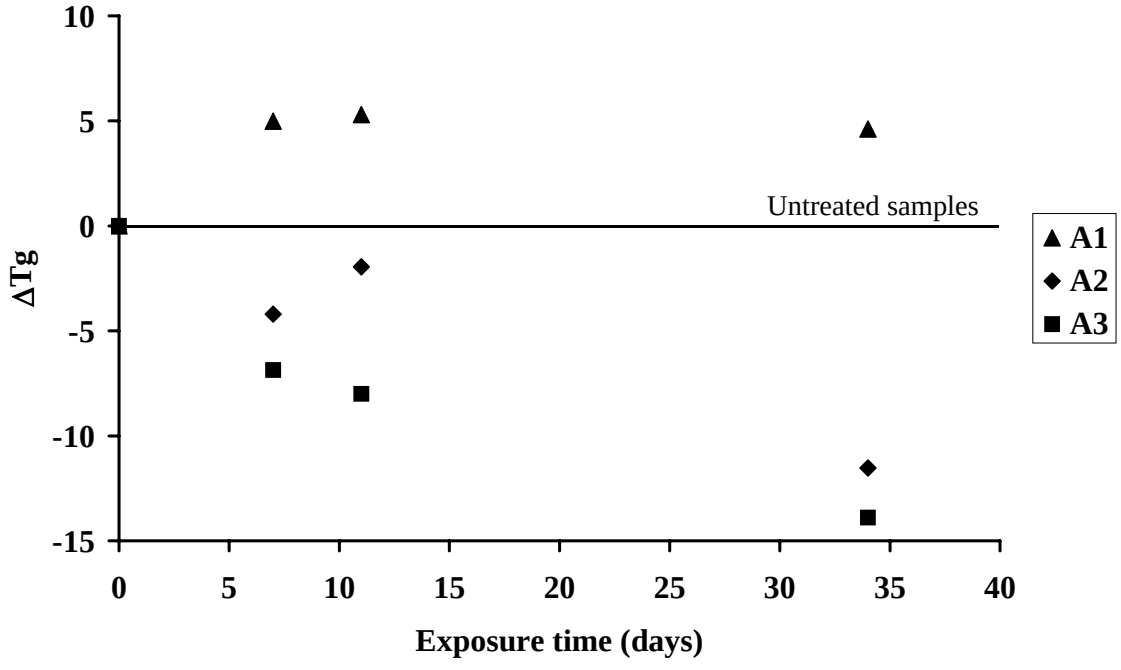



Figure 1. Variations in Tg (ΔTg) of accelerate aged samples versus exposure time.

The Tg of the A1 resin after the treatments is higher than that measured on the untreated samples. The same variations in Tg were detected irrespective of the aging time. On the contrary, a decrease in Tg was detected on samples of both A2 and A3 resin, suggesting a plasticization effect due to the thermo-hygrometric aging. The variations remained almost constant for shorter aging times, then they significantly decreased.

The different behavior can be explained by analyzing the residual heat of reaction ($\Delta H_r$) measured on both the untreated and the treated samples of each resin.

In Table 1, both the residual heat of reaction ($\Delta H_r$) and the relaxation enthalpy ($\Delta H_{rel}$), measured on samples subjected to the thermo-hygrometric treatment, are reported.

As previously stated, the samples were subjected to the treatments after 4.5 months of cure, when their Tg leveled off; however the resins were not fully cross-linked. In fact, an exothermic peak due to the residual reactivity of the system was detected in the DSC thermogram and a residual $\Delta H_r$ was measured on untreated samples cured for 4.5 months. Therefore, when the samples were kept at a temperature higher than the temperature of cure, a post-curing process can occur: as a consequence, the cross-linking reactions start anew, the Tg increases and the exothermic peak related to the residual reactivity decreases.

Table 1. Residual heat of reaction ($\Delta H_r$) and the relaxation enthalpy ($\Delta H_{rel}$) of samples subjected to the thermo-hygrometric treatment.

| Resin | Aging time (days) | $\Delta H_r$ (J/g) | $\Delta H_{rel}$ (J/g) |
|---|---|---|---|
| **A1** | 0 | 2.24 ± 1.90 | 2.81 ± 0.66 |
| | 7 | 0.0 | 0.0 |
| | 11 | 0.0 | 0.0 |
| | 34 | 0.0 | 0.0 |
| **A2** | 0 | 6.14 ± 2.83 | 1.28 ± 0.84 |
| | 7 | 4.37 ± 1.53 | 0.0 |
| | 11 | 3.89 ± 1.94 | 0.0 |
| | 34 | 1.66 ± 0.63 | 0.0 |
| **A3** | 0 | n.d. * | 1.01 ± 0.04 |
| | 7 | 4.49 ± 0.09 | 0.0 |
| | 11 | 1.48 ± 0.04 | 0.0 |
| | 34 | 1.66 ± 0.72 | 0.0 |

* The $\Delta H_r$ for untreated A3 samples cannot be determined.
For each set of measurements the maximum deviation is reported.

In fact, the $\Delta H_r$ was no longer detectable on A1 samples treated for 7 days, indicating that the post-cure process took place. This phenomenon yielded higher Tg values able to counteract the decrease in Tg due to the plasticization effect of water; hence only an increase in Tg was measured on the treated A1 samples. On the other hand, on either A2 and A3 samples the $\Delta H_r$ decreased, but it was still measurable even after 34 days at 70°C and 75% R.H.. In these cases, the increase in Tg due to the post-curing process was less marked, the effect of the plasticization prevailed, therefore, the whole effect of the accelerate aging was the lowering of the Tg.

However, an endothermic peak (centered at about 127°C) was present in the DSC thermograms of the untreated A3 samples. This peak partially overlapped the peak of residual reactivity; therefore, for the A3 resin was impossible to calculate the $\Delta H_r$ on the untreated samples. The disappearance of the endothermic peak by analyzing in the DSC cell the same

samples in a second scan, as well as in analyses performed after the thermo-hygrometric treatments, suggested that the peak was probably related to the evaporation of solvents. Therefore, in order to assess any evaporation process, further investigations by means of Thermo-Gravimetric Analysis (TGA) are in progress.

Before the treatments, since the resins were stored at a temperature lower their Tg for a prolonged period (i.e. 23°C), the physical aging took place. An endothermic peak was detected near the region of the Tg and the related relaxation enthalpy ($\Delta H_{rel}$) was measured on all the untreated samples. During the artificial aging the physical aging was erased since the systems were heated above their Tg; hence the $\Delta H_{rel}$ disappeared.

In Figures 2, 3 and 4 the variations in Tg as a function of aging time are reported for A1, A2 and A3 weathered samples, respectively.

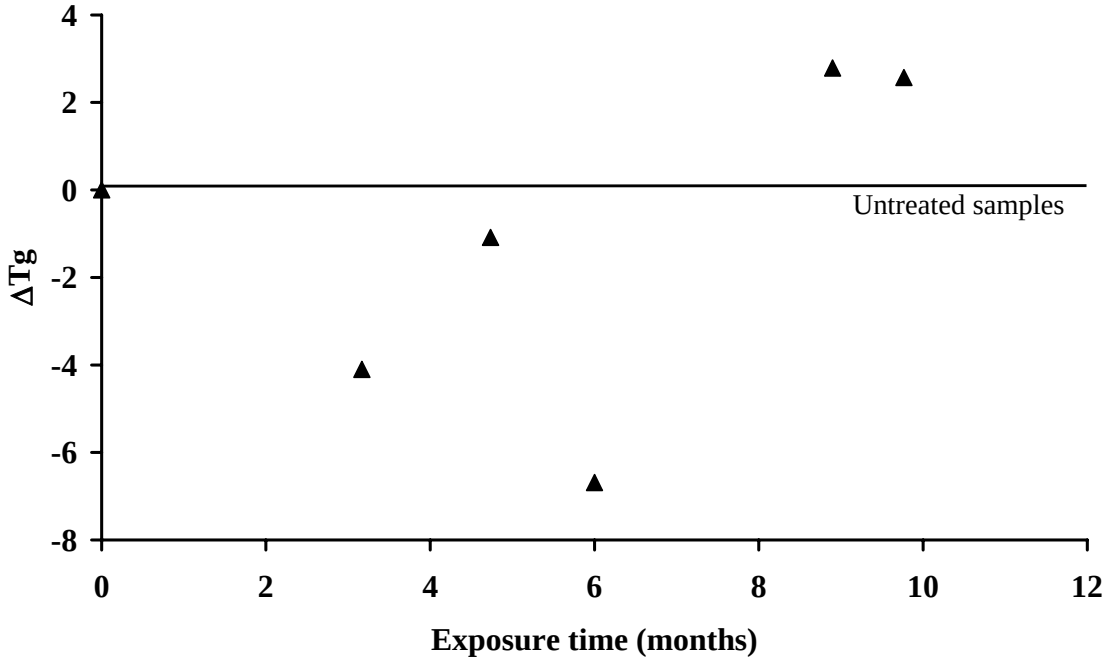



Figure 2. Variations in Tg (ΔTg) versus exposure time, for A1 weathered samples.

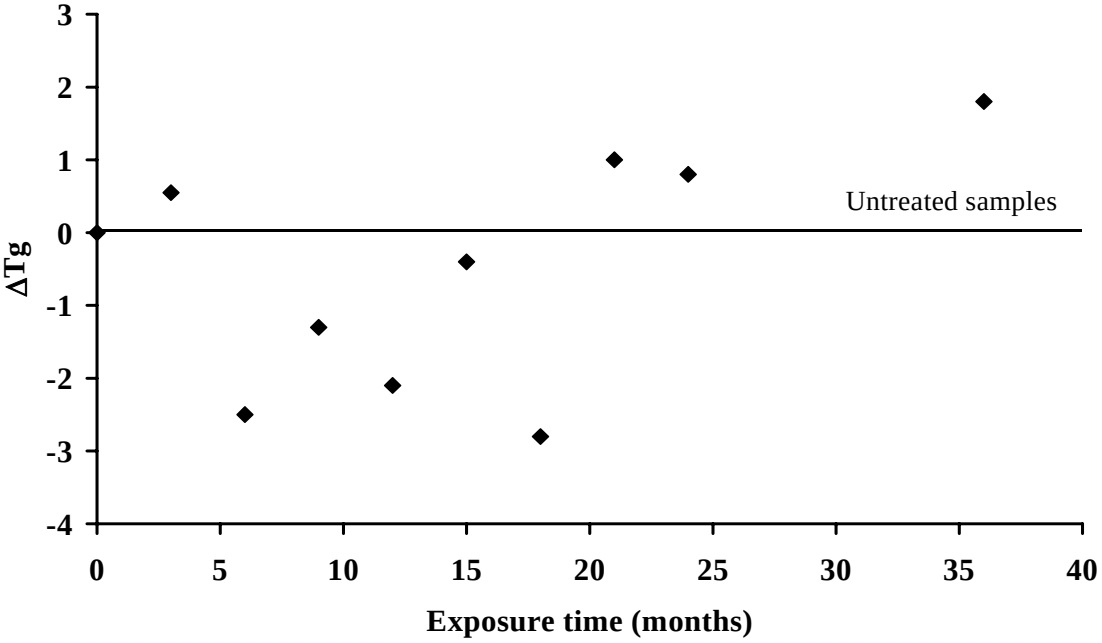



Figure 3. Variations in Tg (ΔTg) versus exposure time, for A2 weathered samples.

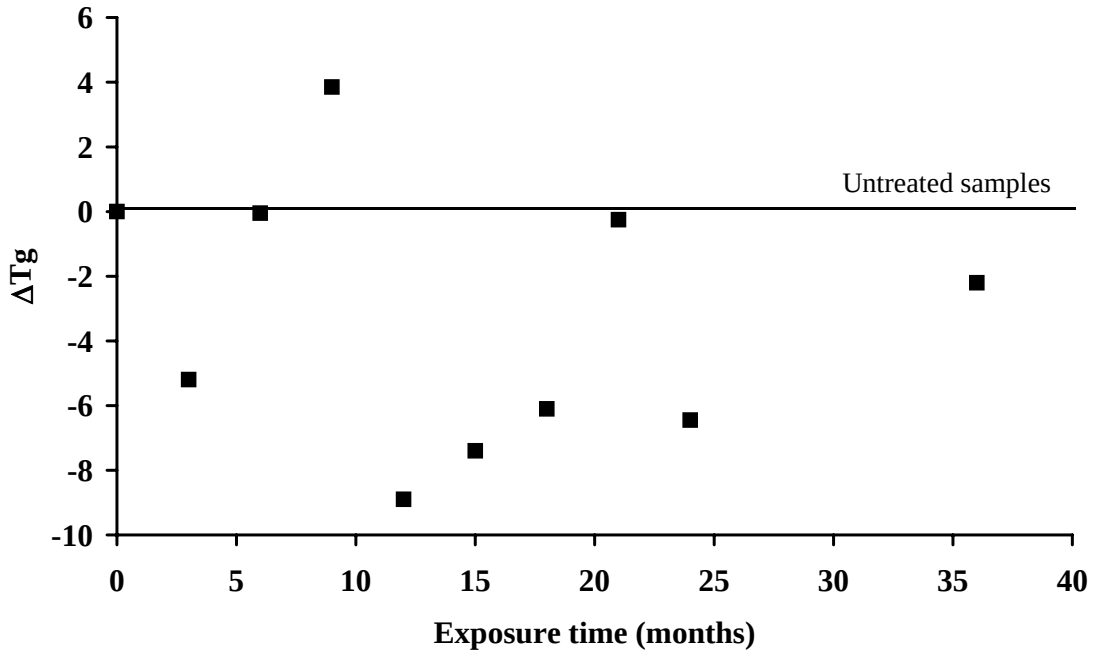



Figure 4. Variations in Tg (ΔTg) versus exposure time, for A3 weathered samples.

A slight decrease in Tg was detected on samples exposed outdoor. This result can be related to the plasticization effect of water absorbed during the weathering. Higher Tg values were measured during the warmest season. This phenomenon seems particularly evident for both A1 and A3 system. Furthermore, in that period no residual heat of reaction was measured on A1 samples subjected to the natural exposure. In fact, the temperatures recorded over the spring seems to be high enough to promote both the post-cure and the evaporation of the sorbed water, leading to an increase in Tg. Moreover, the exposure to higher temperature partially erased the physical aging and a large decrease in $\Delta H_{rel}$ was noticed on all systems investigated. However, the maximum variation in Tg never reached the values measured on the samples subjected to the accelerate aging (see Table 2).

Table 2. Maximum variations in Tg after either accelerate aging or weathering.

| | **A1** | | **A2** | | **A3** | |
|---|---|---|---|---|---|---|
| | *weathering* | *aging* | *weathering* | *aging* | *weathering* | *aging* |
| ΔTg max (°C) | +3<br>-7 | + 4.6 | + 4<br>- 9 | - 11.5 | + 2<br>- 3 | - 13.8 |

The changes in thermal properties of the examined epoxy resins after weathering (i.e. decrease in Tg and erasure of the physical aging) were in part reversible, following the cyclic climatic conditions.

3.2. Mechanical flexural tests

In Table 3, the mechanical properties of the samples subjected to accelerate aging are reported.

The results of the mechanical tests show that the thermo-hygrometric treatments sensibly affected the flexural behavior of the A1 resin. A loss of strength of about 30%, as well as a decrease in flexural modulus (E) and an increase in strain at break ($\varepsilon_b$), were

detected. The same variations in the mechanical properties were measured irrespective the aging time. These data indicate that a plasticization process took place during the treatment at 70°C and 75% R.H.. It was very fast in the first stage of aging, since the variations in mechanical properties were already noticed on samples treated for 7 days. In fact, the high temperature of exposure increases the rate of water absorption into the polymers and, therefore, it could decrease the time necessary to reach the saturation level. Hence, in the A1 resin the absorption process could be almost completed after 7 days of aging. Moreover, the erasure of the physical aging taking place since the resin was aged at a temperature higher its Tg, can contribute to the variations of the mechanical properties. The de-aging process can give rise to both the lowering of the flexural modulus and the maximum strength ($\sigma_y$) and the increase of the strain at the break.

Table 3. Mechanical flexural properties of samples subjected to the thermo-hygrometric treatment.

| Resin | Aging time (days) | E (GPa) | $\sigma_y$ (MPa) | $\varepsilon_b$ (%) |
|---|---|---|---|---|
| **A1** | 0 | 3.09 ± 0.96 | 111.76 ± 25.28 | 8.36 ± 1.55 |
| | 7 | 2.09 ± 0.34 | 75.47 ± 7.16 | 11.24 ± 3.59 |
| | 15 | 2.17 ± 0.14 | 75.92 ± 2.11 | 11.52 ± 2.62 |
| | 34 | 2.14 ± 0.21 | 79.30 ± 1.08 | 11.30 ± 1.90 |
| **A2** | 0 | 1.19 ± 0.20 | 41.59 ± 6.65 | 5.67 ± 1.06 |
| | 7 | 1.07 ± 0.14 | 30.98 ± 2.48 | 8.97 ± 4.16 |
| | 15 | 1.33 ± 0.13 | 39.79 ± 5.23 | 6.84 ± 1.79 |
| | 34 | 1.71 ± 0.04 | 55.29 ± 1.71 | 5.30 ± 1.14 |
| **A3** | 0 | 3.28 ± 0.62 | 50.62 ± 6.77 | 1.84 ± 0.10 |
| | 7 | 1.20 ± 0.69 | 18.40 ± 5.74 | 5.73 ± 0.86 |
| | 15 | 2.57 ± 0.88 | 30.31 ± 3.86 | 1.64 ± 0.40 |
| | 34 | 3.20 ± 0.91 | 41.84 ± 5.57 | 1.48 ± 0.17 |

E = flexural modulus of elasticity; $\sigma_y$ = strength at yield; $\varepsilon_b$ = strain at break.
For each set of measurements the maximum deviation is reported.

Despite the fact that a higher cross-linking degree of the A1 resin was noticed by the thermal analyses after the accelerate aging, the results of the flexural tests indicated a great influence of the plasticization effect on the mechanical properties, while no evidence of the post-cure was detected.

A large decrease in both flexural modulus and strength and a great increase in strain at break were measured on the A3 resin treated for 7 days. This behavior can be due to both the plasticization effect of water and the erasure of the physical aging. However, for longer exposure times, a reverse trend was noticed, i.e. the elastic modulus and the strength increased, the elongation at break decreased with respect to the data calculated at 7 days of exposure. After 34 days of exposure the mechanical properties tended to the initial values. These results would indicate an increase in cross-linking degree of the system in the latter stages of the accelerate aging. Although they are in agreement with the decrease of the residual heat of reaction measured by the thermal analyses, they cannot explain the large decrease in Tg suggesting a strong effect due to the plasticization process.

A similar behavior was detected on the A2 resin, however in this case lower variation were measured in the first stage of the treatment, as well as at longer aging times.

In all cases, the maximum deviation of the experimental results was higher for untreated samples; it became smaller for measurements performed on aged specimens. These results suggested that more homogeneous structures could be obtained as a consequence of the applied thermo-hygrometric treatments.

In Table 4, the mechanical properties of the samples subjected to natural aging are reported.

Table 4. Mechanical flexural properties of samples subjected to weathering.

| Resin | Exposure time (months) | E (GPa) | $\sigma_y$ (MPa) | $\varepsilon_b$ (%) |
|---|---|---|---|---|
| **A1** | 0 | 3.09 ± 0.96 | 111.76 ± 25.28 | 8.36 ± 1.55 |
| | 3 | 2.43 ± 0.15 | 97.53 ± 8.42 | 8.78 ± 1.51 |
| | 6 | 2.24 ± 0.10 | 93.62 ± 2.11 | 10.31 ± 4.08 |
| | 9 | 2.60 ± 0.17 | 103.48 ± 5.15 | 8.39 ± 2.29 |
| **A2** | 0 | 0.83 ± 0.11 | 27.09 ± 4.49 | 13.00 ± 1.70 |
| | 3 | 0.63 ± 0.09 | 22.52 ± 1.19 | 11.30 ± 1.90 |
| | 6 | 0.92 ± 0.16 | 28.84 ± 3.31 | 10.05 ± 2.30 |
| | 9 | 0.90 ± 0.10 | 28.89 ± 4.37 | 9.82 ± 1.18 |
| | 12 | 0.75 ± 0.15 | 27.63 ± 4.54 | 7.86 ± 0.78 |
| | 21 | 0.81 ± 0.01 | 34.89 ± 2.57 | 7.88 ± 0.88 |
| | 36 | 1.32 ± 0.05 | 26.54 ± 3.25 | 2.14 ± 0.51 |
| **A3** | 0 | 1.61 ± 0.23 | 27.49 ± 2.06 | 3.50 ± 0.44 |
| | 3 | 1.58 ± 0.33 | 31.42 ± 3.11 | 1.96 ± 0.22 |
| | 6 | 1.80 ± 0.26 | 33.85 ± 2.49 | 2.50 ± 0.30 |
| | 9 | 1.39 ± 0.40 | 29.84 ± 3.31 | 2.14 ± 0.41 |
| | 12 | 1.57 ± 0.07 | 27.71 ± 2.40 | 1.92 ± 0.39 |
| | 36 | 2.45 ± 0.19 | 31.13 ± 1.55 | 1.36 ± 0.05 |

E = flexural modulus of elasticity; $\sigma_y$ = strength at yield; $\varepsilon_b$ = strain at break.
For each set of measurements the maximum deviation is reported.

The results of the mechanical tests carried out on the weathered A1 samples supported the data obtained by DSC on the same samples. An initial decrease of the flexural modulus and the maximum strength and the decrease of the elongation at break suggested a strong effect of the plasticization process due to water absorption from the atmosphere. The increase of both the modulus and the strength, during the warmest season, indicated the occurrence of a post-curing process. Further analyses, at longer exposure times, are in progress.
As already reported elsewhere (Frigione, 2001 (a); Frigione, 2001 (b)), the flexural tests performed on the weathered A2 and A3 samples led to fluctuating results, close to those measured on the untreated resins. In both cases, a slow, but continuous, decrease in strain at break was measured over the aging time.

It was concluded that the mechanical properties of these resins subjected to natural aging appeared strongly affected by the cyclic environmental conditions. However, the effects of the natural weathering on the mechanical behavior were not well reproduced by the selected aging procedure (i.e. 70°C and 75% R.H.). In fact, the properties of the resins resulted more strongly affected by the thermo-hygrometric treatment and dissimilar results were measured when the effects of the accelerate and the natural aging were compared.

### 3.3. Color measurements

The color changes (ΔE) of the resins subjected to the accelerate aging are reported in Table 5.

The treatment led to higher variations on the A1 resin. The lower ΔE were calculated for the A3 aged specimens, probably due to the presence of fillers in A3 resin. The variation of color were not promoted by UV aging, since the treatment was performed without light sources. The obtained results can be ascribed to processes that are not activated by UV radiations, such as hydrolysis and/or thermo-oxidation. These degradation processes would be incipient and restricted to the superficial layers, hence they did not affect the thermal and mechanical "bulk" properties of the systems.

FTIR spectroscopic analyses are in progress in order to investigate the chemical changes due to either the accelerate aging and the weathering.

Table 5. Color changes (ΔE) of resins subjected to the accelerate aging.

| Aging time (days) | **A1** | **A2** | **A3** |
|---|---|---|---|
| 0 | 0.00 | 0.00 | 0.00 |
| 7 | 9.78 | 6.44 | 3.50 |
| 15 | 16.38 | 6.63 | 6.79 |
| 34 | 34.01 | 23.33 | 8.56 |

## 4. CONCLUSIONS

The accelerate aging at both high temperature and high levels of relative humidity, led to a different thermal and mechanical behavior of the three resins under study. The plasticization effect of water absorbed during the aging treatments, the post-cure and the erasure of the physical aging, due to the high temperature of exposure, are involved in changing the properties of such resins.

A significant decrease in Tg was detected on samples of both A2 and A3 resins, suggesting a plasticization effect due to water absorption during the thermo-hygrometric aging. The post-cure also took place; in fact, the residual heat of reaction decreased after the treatment. However, the increase in Tg due to this process was not marked, the effect of the plasticization prevailed, therefore, the whole effect was the lowering of the Tg. On the contrary, only an increase in Tg was measured on the treated A1 samples. In this case, the post-curing process yielded higher Tg values able to counteract the decrease in Tg due to the plasticization effect of water.

The presence of volatile products embedded into the specimens is hypothesized. In order to assess any evaporation process, further investigations will be performed.

A great influence of the plasticization effect on the mechanical properties was detected for the A1 resin, while no evidence of the post-cure was detected. The results obtained for the A2 and A3 resins indicated a large effect of the plasticization at short aging times and an increase in cross-linking degree of the systems in the latter stages of the accelerate aging. These data are in agreement with the decrease of the residual heat of reaction measured by the thermal analyses, while they cannot explain the continuous decrease in Tg that suggests a strong effect due to the plasticization process. Therefore, further analysis at different aging times are planned in order to investigate the dissimilar influence of the treatments on the thermal and mechanical properties of these resins.

The large color changes in absence of UV sources suggested that incipient degradation processes induced by high temperature, oxygen or water could be occur.

Fluctuating results, close to those measured on the untreated resins, were noticed for both the thermal and mechanical properties of the naturally aged resins. The temperature achieved over the warmest seasons seems to be high enough to promote variations of the properties of these resins. Furthermore, the measured changes are in part reversible and they follow the cyclic climatic conditions.

Finally, the selected aging procedure (i.e. 70°C and 75% R.H.) seems to be extremely severe and it is not able to reproduce the weathering occurred after outdoor exposure. In fact, the effects of the natural aging on both the thermal and the mechanical properties of the analyzed resins resulted less detrimental. Moreover, the variations of such properties did not reach the values measured on the resins subjected to the accelerate aging.

## 5. REFERENCES

ASTM D 756-93, Determination of weight and shape changes of plastics under accelerated service conditions.

ASTM D 790-92, Standard Test Methods for Flexural Properties of Unreinforced and Reinforced Plastics and Electrical Insulating Materials.

Brown R.P., Survey of status of test methods for accelerated durability testing, in *Polymer Testing*, **10**, 3-30 (1991).

Ellis B., *Chemistry and Technology of Epoxy Resins*, Ellis, B. Ed., Blackie Academic & Professional: New York, U.S.A. (1993).

Frigione M., Naddeo C. and Acierno D., Cold-curing epoxy resins: aging and environmental effects. I – Thermal properties, in *Journal of Polymer Engineering*, **21**, 23-51 (2001) (a).

Frigione M., Naddeo C. and Acierno D., Cold-curing epoxy resins: aging and environmental effects. II – Mechanical properties, in *Journal of Polymer Engineering*, **21**, 349-367 (2001) (b).

Ginell W.S., Kotlik P., Selwitz C.M. and Wheeler G.S., Recent developments in the use of epoxy resins for stone consolidation, in *Materials issues in art and archaeology IV*, Vandiver P.B. et alii (ed.), Pittsburgh: Materials Research Society, 823-829 (1995).

Jacques L.F.E., Accelerated and outdoor/natural exposure testing of coatings, in *Prog. Polym. Sci.*, **25**, 1337-1362 (2000).

Karbhari V. M., Chin Hunston D. J. W., Benmokrane B., Juska T., Morgan R., Lesko J. J., Sorathia U., and Reynaud D., Durability Gap Analysis for Fiber-Reinforced Polymer Composites in Civil Infrastructure, in *J. Composites for Construction*, **7(3)**, 238-247 (2003).

Kotlik P., Justa P. and Zelinger J., The application of epoxy resins for the consolidation of porous stone, in Studies in Conservation, 28, pp. 75-79, 1983.

Mays G.C. and Hutchinson A.R., Adhesives in Civil Engineering, Cambridge University Press, 1992.

Selwitz C., Epoxy Resins in stone conservation, *Research in Conservation*, vol. **7**, Getty Conservation Institute, Los Angeles (1992).

Vauthier E., Abry J.C., Bailliez T. and Chatetominois A., Interactions between hygrothermal ageing and fatigue damage in unidirectional glass/epoxy composites, in *Composite science and Technology*, **58**, 687-692 (1998).

Zanni-Deffarges M. P., and Shanahan M.E.R., Diffusion of water into an epoxy adhesive: comparison between bulk behaviour and adhesive joints, in *Int. J. Adhesion & Adhesive*, **15(3)**, 137-142 (1995).

International Symposium Polymers in Concrete
2 - 4 April 2006
Guimarães, Portugal

# Influence of moisture and moderate temperatures on the properties of polymer composite materials for concrete repair

Mariaenrica Frigione[1], Margherita S. Sciolti[2]

*University of Lecce, Department of Innovation Engineering*
*Via per Arnesano, 73100 Lecce, Italy*

## ABSTRACT

The behavior of several commercial composites, based on polymeric thermosetting matrices, reinforced with carbon fibers and employed for the restoration of concrete structures, was analyzed in relation to the most common service conditions. In particular, the durability of these composites under different environmental exposure regimes was investigated. To this aim, a temperature and a level of humidity slightly higher than those commonly encountered in our country, but still achievable, were selected. Tensile mechanical tests were, then, performed on the composite materials before and after the exposition to artificially simulated severe environments, evaluating the effects of the exposition on the properties of the materials. The same exposure parameters were used to simulate the environmental severe conditions on the resins employed as matrices for the composite. For comparison purposes, three different commercial resins, all used as matrices of composites for civil engineering applications, were selected and analyzed. The effect of the exposure on the resins was, therefore, evaluated by measuring their physical (thermal, mechanical) properties before and after any treatment.

## 1. INTRODUCTION

The use of polymeric materials, such as thermosetting resins and their composites, for the repair and/or the strengthening of concrete structures is attaining worldwide an increasing success. Among the thermosets, epoxy and vinylester resins are widely employed in many structural applications, assuring good performance in terms of flexibility, effectiveness of repairing technique and moderate costs. When correctly formulated and cured, epoxy and vinylester resins provide a high level of mechanical properties, excellent resistance to corrosion and to chemicals. Furthermore, the use of FRP (Fiber Reinforced Polymer) composites as reinforcement for concrete structures, to improve the strength and/or the stiffness of structural elements, is becoming very popular. The FRP composites, in fact, exhibit several advantages, such as: low weight, high strength, tailor-ability and prevention to corrosion.

[1] Associate Professor
[2] Ph.D. Student

The long-term durability of the thermosetting resins and of their FRP composites, especially when they are subjected to severe environmental conditions, is still not well known. This issue represents a strong limit for a wider spreading of these materials, since the acceptable lifetime of an effective repair should be in the order of 10-20 years. The performance and the long term behavior of these resins and of their composites depends on the chemical nature of the base materials, on the conditions in which they set and harden and, mainly, on the environmental conditions in which they "operate" (temperature, presence of water, moisture and chemicals, pollution, etc.).

In the present paper, the durability of different commercial composites employed for the restoration of concrete structures, was investigated and discussed. The composites are based on polymeric thermosetting matrices and they are reinforced with carbon fibers. The performance of the composites before and after different environmental treatments was analyzed. A temperature and a level of humidity slightly higher than those commonly encountered in our country, but still achievable, were selected, i.e. 40°C and 90% R.H.. Tensile mechanical tests were performed on the composite materials before and after the exposition to artificially simulated severe environments, evaluating the effects of the treatment on the properties of the materials. In order to measure the effects of the same exposure parameters on the resins employed as matrices for the composites, three different commercial resins were selected and analyzed by measuring their physical (thermal, mechanical) properties before and after the selected treatments.

## 2. MATERIALS

In this study, two commercial epoxy composites, used as reinforcing systems, were analyzed. They are indicated as "CFRP" (Carbon Fiber Reinforced Polymer) and "GFRP" (Glass Fiber Reinforced Polymer) and were supplied (by MAC.spa) in forms of sheets to be impregnated by epoxy systems. The epoxy systems were composed by an epoxy primer, $A_p$, an epoxy putty, $A_t$, an epoxy adhesive, $A_a$; carbon fibers, $A_f$, or glass fiber, $A_g$, were also supplied and both the composites were manufactured through hand-lay up technique, following the procedure indicated by suppliers. The Glass fibers or Carbon fibers sheets were thoroughly soaked in the epoxy adhesive and any excess of the resin was removed by applying a roller; the resulting composite sheet had a uniform thickness of approximately 1 mm and a fiber weight fraction of 25-35%. In any sheet, Glass fibers or Carbon fibers were present only in the lengthwise direction. Epoxy resins specimens were also produced, by pouring the different resins in appropriate moulds. The cure of the composite sheets, the primer, the putty and the adhesive was performed at ambient temperature (≈23°C) for approximately 25-30 days.

## 3. MECHANICAL TESTS

Mechanical tests were performed on unconditioned (as reference) and conditioned samples of both composites and resins, in order to evaluate the effects of any treatment on the mechanical properties of any material. The effect of any environmental agent was evaluated in terms of reductions of the mechanical properties with respect to those measured on unconditioned samples.

The tensile properties of the resins $A_p$, $A_t$, $A_a$, were evaluated following the appropriate code [ASTM D 638M]. At least five specimens (Figure 1) of each epoxy resin were tested using a Lloyd Instruments machine LR5K with displacement control, at a cross-head speed of 5mm/min. Tensile properties (modulus of elasticity and tensile strength) were

calculated, averaging the results. In order to record the strain during the test, two electrical strain gauges were glued on the gauge length of any sample.

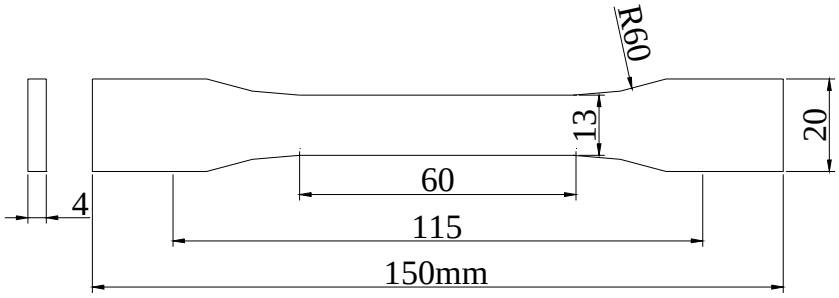



Figure 1 – tensile sample.

The flexural characteristics (flexural modulus, maximum strength and strain at break) of the resins $A_p$ and $A_a$ were measured using the same testing machine through three point bending tests [ASTM D 790]. Samples with rectangular cross section were used in this case (Figure 2). The compliance curve determination was produced by testing the specimens at a cross-head speed of 2 mm/min. The dimensions of the specimens were 80x10x4 mm and the span to thickness ratio was set at 15:1.

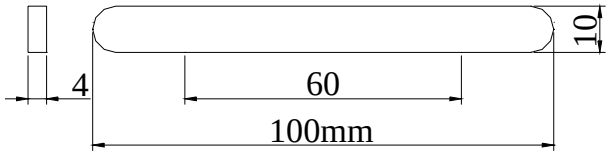



Figure 2 – tensile sample.

For the determination of the “in-plane” tensile properties of reinforced composite (CFRP and GFRP), proper specimens were tested in a Metrocom testing machine under displacement control, at a cross-head speed of 0,2mm/min according to ASTM D3039M. The strain was monitored with strain or displacement transducers, in order to measure the stress-strain response to load of the material; the ultimate tensile strain and tensile modulus of elasticity were calculated. For repeatability purposes, at least five samples of any composite were tested.

## 4. AGING CONDITIONS

The effect of two common environmental agents on the properties of the resins and of the composites was analyzed and reviewed in the present study, i.e. presence of water and treatment in a climatic chamber at 40°C and 90% R.H. (corresponding to warm climate achievable in Mediterranean regions).

Tests of water absorption were performed on the resins $A_p$ and $A_a$ following the proper code [ASTM D 570-81] in order to evaluate the amount of water absorbed at saturation point and the relative saturation time for any resin employed. To this aim, appropriate cured specimens of each resin were immersed in distilled water at a constant temperature of 23°C (±1°C), periodically removed from water and weighed using a digital balance to determine the percent weight change, and, in turn, the water uptake.

Specimens of the resins and the composites ($A_p$, $A_a$, CFRP) were immersed in water, using the same conditions reported on the code for water absorption tests, in order to assess the effect of the presence of water on their properties. After different periods of time, mechanical tests were performed on the immersed specimens: from 16 to 151 days for primer and adhesive resins ($A_p$ and $A_a$), from 16 to 176 days for the composite CFRP. Epoxy resins absorb easily moisture due to the highly polar nature of the cured polymer wherein water is typically hydrogen bonded to hydrophilic groups, mainly hydroxyl and amine groups [Lee and Peppas (1993)]. Depending on the concentration of these groups, the equilibrium water content in epoxy (at saturation point) can be as high as 10% by weight [Carfagna et al. 1982].

The effect of thermo-hygrometric treatments, i.e. 40°C and 90% R.H., performed up to 6 months on the mechanical (tensile) properties of the adhesives and their composites, was analyzed.

The choice of the test temperature was made by selecting a value slightly lower and close to the "Tg" (glass transition temperature) of each resin system ($A_p$, $A_t$, $A_a$). The Tg of each system was previously measured using a Differential Scanning Calorimetry (DSC) and it resulted in all cases ranging between 47° and 55°C. The glass transition temperature, Tg, is defined as the temperature, or the range of temperatures, at which the polymeric resins change from a rigid, glass-like state to an elastomeric-like state, with a consequently dramatic decrease in mechanical properties.

## 5. RESULT AND DISCUSSION

### 5.1.Effects of water

Referring to the effect of the presence of water on the mechanical properties of thermosetting (epoxy) adhesives possessing moderate Tg's, relatively short time of exposure lead to relatively reversible "plasticization", producing a decrease in the stiffness and strength of the adhesive, as well as a reduction of its Tg. On the other hand, after a longer immersion time a new increase in Tg is often observed, due to additional cross-linking taking place during exposure to water. The lowering in Tg upon moisture ingress allows the polymer chains to become mobile; this promotes cross-linking and allows the curing reactions, often not complete at ambient temperature, to tend to completion [De'Neve & Shanahan (1993)]. As a consequence, the tensile strength of these adhesives can increase, followed at very long immersion times by a decrease, maintaining values similar to that of the unaged polymer [Kajorncheappunngam et al. (2002); Gupta (1985)]. The Young's modulus of the aged epoxy results slightly lower than that of the control samples, increasing the reduction in modulus with the immersion time. Additional cross-linking could also imply that the material achieves a higher modulus. The strain at break, finally, tends to increase initially, but, at later times, the material became brittle.

Referring to our results, they are mostly in accordance with the mentioned literature.

The results of flexural tests performed on the primer $A_p$ after immersion in water (Table 1) showed an initial decrease in yield strength (about 50%) after 50-60 days of immersion, corresponding to the saturation time (i.e. 60 days of immersion). Then the strength increased again, to values similar to those relative to un-immersed samples. Similarly, the flexural modulus decreased up to about 70% relative to the value in standard condition. For longer immersion times, on the other hand, the modulus increased again, with a residual reduction by about 15-20%. Finally, the ultimate strain increased up to 50% in correspondence of the saturation time, while at longer immersion times values similar to that of the unaged polymer were measured.

The adhesive $A_a$ (Table 2) showed, on the other hand, a peculiar behavior. It did not reach the saturation conditions, at least after 25 weeks of immersion. The strength increased by about 40% after only 2 weeks of immersion and retained this almost constant value even at longer immersion time. After 22 weeks in water, the increase in strength was by about 10%. The flexural modulus and the ultimate strain, after an initial increase by about 25% at short immersion times, remained roughly constant. The behavior of $A_a$ could be explained by the not yet attained saturation condition.

Table 1 - The results of flexural tests performed on the primer $A_p$ after immersion in water

| Immersion time up to days | average | | | | | |
|---|---|---|---|---|---|---|
| | maximum strength | | flexural modulus | | strain at break | |
| | [MPa] | cov% | [MPa] | cov% | [%] | cov% |
| 0 | 8,0 | 5 | 285 | 11 | 15 | 5 |
| 16 | 4,3 | 7 | 120 | 5 | 11 | 13 |
| 50 | 3,9 | 6 | 82 | 5 | 18 | 5 |
| 63 | 4,7 | 13 | 130 | 10 | 13 | 4 |
| 78 | 7,8 | 3 | 247 | 7 | 12 | 7 |
| 151 | 7,1 | 5 | 220 | 6 | 12 | 6 |

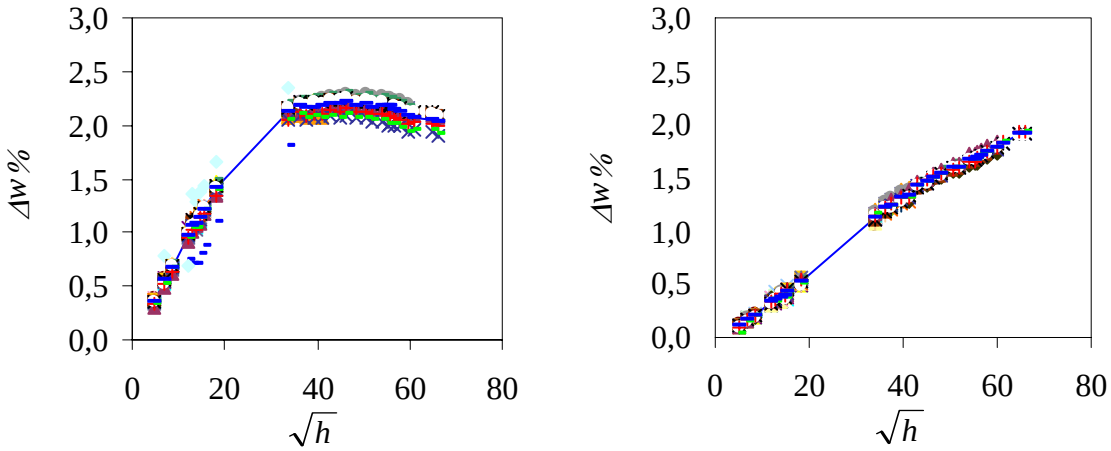
Table 2 - The results of flexural tests performed on the primer $A_a$ after immersion in water

| Immersion time up to days | average | | | | | |
|---|---|---|---|---|---|---|
| | maximum strength | | flexural modulus | | strain at break | |
| | [MPa] | cov% | [MPa] | cov% | (%) | cov% |
| 0 | 76,0 | 5 | 2454 | 6 | 4 | 3 |
| 16 | 109,0 | 11 | 3258 | 16 | 4 | 8 |
| 50 | 97,3 | 6 | 2928 | 8 | 5 | 6 |
| 63 | 93,2 | 8 | 2788 | 12 | 5 | 5 |
| 78 | 103,7 | 7 | 3117 | 9 | 5 | 24 |
| 151 | 85,3 | 16 | 2854 | 6 | 5 | 35 |

The results of tensile tests performed on CFRP composite samples, based on epoxy primer and adhesive, after different time spans in water up to 25 weeks, evidenced an irrelevant influence of this agent on the properties of the composite. Within the experimental errors, in fact, tensile modulus, maximum strength and ultimate strain retained almost the same values after the prolonged immersion in water. The results proved that the mechanical properties of a composite material basically depend on the properties of the fibers, that were not influenced by the presence of water.

Table 3 - The results of tensile tests performed on CFRP composite samples

| Immersion time up to days | average | | | | | |
|---|---|---|---|---|---|---|
| | Modulus of Elasticity | | Tensile strength | | strain at break | |
| | [MPa] | cov% | [MPa] | cov% | (%) | cov% |
| 0 | 229037 | 4 | 3418 | 4 | 1,49 | 2 |
| 16 | 228279 | 5 | 3618 | 6 | 1,59 | 9 |
| 50 | 217230 | 6 | 3427 | 17 | 1,59 | 19 |
| 63 | 225372 | 1 | 3749 | 10 | 1,66 | 11 |
| 78 | 225071 | 4 | 3593 | 8 | 1,60 | 7 |
| 176 | 219963 | 6 | 3425 | 18 | 1,55 | 13 |




a) $A_p$ resin b) $A_a$ resin

Figure 3 - Graphic of water absorption

5.2.Thermo-hygrometric effect

After the conditioning procedure, i.e. 40°C and 90% R.H., the aged specimens were subjected to compression test, tensile tests and bending test to evaluate the compression strength, tensile strength and elastic modulus of the materials. The obtained results are reported in Table 4 and compared to those found for the un-conditioned samples.

Before and after the thermo-hygrometric treatment the samples were weighted. The weight variations as well as the variations in mechanical properties, due to the treatment performed, are shown in Table 5.

The tensile tests on the primer ($A_p$) were not carried out because the conditioned specimens resulted completely damaged after the treatment performed (Figure 4). The results of tensile tests performed on putty ($A_t$) after 6 months at 40°C and 90% R.H. evidenced a considerable influence of this treatment on its properties, especially on the modulus of elasticity. A significant decrease in mechanical properties was registered also for the adhesive ($A_a$), being the tensile strength decreased by about 70%. On the other hand, its modulus of elasticity remained unaltered.

Table 4- Mechanical properties of the reinforcements.

| | | Standard condition | | 40°C and 90% R.H. (6 months) | |
|---|---|---|---|---|---|
| | | average | cov.% | average | cov.% |
| Tensile strength $\sigma[MPa]$ | CFRPS | 3846 | 12 | 3524 | 11 |
| | GFRPS | 1769 | 5 | 1346 | 18 |
| | $A_p$ | 49 | 5 | / | / |
| | $A_t$ | 18 | 4 | 21 | 12 |
| | $A_a$ | 44 | 11 | 12 | 19 |
| Modulus of Elasticity $E[MPa]$ | CFRPS | 234000 | 10 | 239000 | 6 |
| | GFRPS | 81400 | 7 | 91000 | 13 |
| | $A_p$ | 2594 | 16 | / | / |
| | $A_t$ | 5802 | 16 | 10877 | 14 |
| | $A_a$ | 2966 | 10 | 2967 | 15 |

Results of tensile tests performed on the CFRP sheets showed a negligible influence of the treatment performed on both its tensile strength and elastic modulus. Within the experimental errors, in fact, modulus of elasticity and tensile strength retained almost the same values that those calculated in standard condition. The results of mechanical tests performed on GFRP composite samples after the thermo-hygrometric treatment, on the other hand, evidenced a slightly larger influence on the properties of the composite. In this case, the presence of glass fibers, more susceptible to the presence of water, would probably influence in a greater extent the final properties of the composite. The results confirmed that the mechanical properties of a composite material basically depend on the properties of the fibers.

Table 5 - Percentage variations of weight and properties of materials.

| | Weigh Variation (%) | Mechanical properties variation (%) | |
|---|---|---|---|
| Primer | -2 | Tensile strength variation | / |
| | | Elastic modulus variation | / |
| Putty | -3 | Tensile strength variation | -17 |
| | | Elastic modulus variation | -87 |
| Adhesive | -4 | Tensile strength variation | 73 |
| | | Elastic modulus variation | -0,03 |
| CFRP | -6 | Tensile strength variation | 8 |
| | | Elastic modulus variation | -2 |
| GFRP | -4 | Tensile strength variation | 24 |
| | | Elastic modulus variation | -12 |



Figure 4 – Primer specimens after the 6 months treatment at 40°C and 90% R.H..

## 6. CONCLUSIONS

The main conclusions drawn from the present study can be summarized as follows.

The aging conditions have a certain effect on the mechanical properties of the resins, while it has a lower influence on the properties of the composite, in relation to the nature of the composite fibers.

The effect of the presence of water on the mechanical properties of thermosetting resins is noticeable. Even more severe is the effect of the combination of humidity and temperature, since the glass transition temperature of the resins is approached. The selected values of temperature and humidity may be achieved when the materials are externally exposed in the South of Italy.

From these observations, arises the necessity at the design stage to explore the properties of different commercial thermosetting resins and composites and to deeply analyze the environmental conditions where the systems will operate, in order to make an appropriate choice of the adhesive and the composite to use in relation to the specific application and to the service conditions.

## 7. REFERENCES

ASTM D 570-81(Re-approved 1988). Standard Test Method for Water Absorption of Plastics (1988).

ASTM D 638M -93, Standard Test Method of Tensile Proprieties of Plastic (Metric) (1993).

ASTM D 790-92, Standard Test Method of Flexural Proprieties of Unreinforced and Reinforced Plastic and Electrical Insulating Materials (1992).

ASTM D 3039M-93, Standard Test Method for Tensile Properties of Polymer Matrix Composite Materials (1993).

C. Carfagna, A. Apicella, L. Nicolais, Journal of Applied Polymer Science, vol. 27, pp. 105-112, (1982).

B. De'Neve, M.E.R. Shanahan, Polymer, vol. 34, pp. 5099-5105 (1993).

V.B. Gupta, L.T. Drzal, C.Y.-C. Lee, M.J. Rich, Polymer Engineering and Science, vol. 25, pp. 812-823 (1985).

S. Kajorncheappunngam, R.K. Gupta, H.V.S. GangaRao, Journal of Composites for Construction, vol. 6, pp. 61-69 (2002).

C.L. Lee, N.A. Peppas, Progress in Polymer Science, vol. 18, pp. 947–961 (1993).

International Symposium Polymers in Concrete
2 - 4 April 2006
Guimarães, Portugal

# An application of impact-echo and ultrasonic methods for repair efficiency assessment

Andrzej Garbacz[1]

*Department of Building Materials Engineering*
*Warsaw University of Technology*
*00-637 Warsaw, Poland*

## ABSTRACT

Quality control of repair efficiency as well as its monitoring during repaired structure service is one of the important needs. The European Standard EN 1504-10 (2003) and ACI Concrete Repair Manual (2003) give some guidelines for repair efficiency evaluation. According to those documents, the bond strength and quality of bond are the main features of the repair system necessary to be assessed. The pull-off test is commonly used to test the bond strength. However, the non-destructive methods (NDT) are preferred for this purpose, especially in the case of large-area structures. During selection of NDT method, many factors should be taken into account, e.g. type and size of defects at the interface zone, type of repair material (cement or polymer), thickness of overlay, roughness of concrete substrate. A majority of NDT methods mentioned in EN 1504-10 and ACI Concrete Repair Manual for repair efficiency assessment are based on propagation of stress waves. Particularly, ultrasonic methods and impact-echo method are recommended. The aim of this paper is to analyze the usability of impact-echo and ultrasonic methods for assessment of quality of various repair systems. On the basis of the obtained results the capabilities and limitations of these methods are discussed.

## 1. INTRODUCTION

A growing interest in application of non-destructive techniques (NDT) for evaluation of repair efficiency is noted recently. The European Standard EN 1504-10 (2003) and ACI Concrete Repair Manual (2003) give some guidelines for repair efficiency evaluation. According to those documents, the bond strength and quality of bond are the main features of the repair system necessary to be assessed. The pull-off test is commonly used to test bond strength. However, the non-destructive methods (NDT) are preferred for this purpose. A majority of NDT methods mentioned in EN 1504-10 and ACI Concrete Repair Manual for repair efficiency assessment are based on propagation of stress waves. Particularly, ultrasonic methods and impact echo method are recommended.

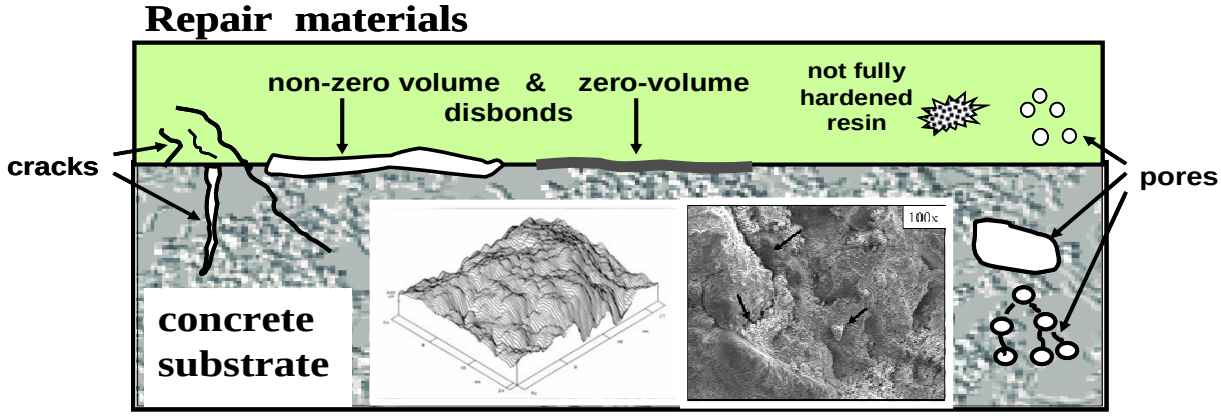
The aim of this paper is to analyse the usability of impact-echo and ultrasonic methods for assessment of quality of various repair systems. The capabilities and limitations of these methods are discussed.

[1] Assistant Professor

## 2. REPAIR SYSTEM AS AN OBJECT OF NDT ASSESSMENT

Two main groups of defects (Fig.1) can occur in a repair system (Adams & Drinkwater 1997):

- adhesion type (at the interface zone: overlay - substrate);
- cohesion type (in overlay or/and concrete substrate).




Rys.1. Sketch of possible defects in repair system and example of surface geometry of concrete substrate after millling

Considering the object of investigation, NDT techniques for quality assessment of the overlays could be divided into two main groups:

- methods for detection of non-zero volume defects (containing air), like: voids, delaminations, honeycombing, etc;
- methods for detection of poor adhesion ("zero-volume" disbonds from point of view of a sensitivity of a given NDT technique).

During selection of NDT method, the following factors should be taken into account (ACI Manual 2003, Popovics et al. 1999):

- type and size of defects at the interface zone;
- type of repair material (cement or polymer);
- thickness of overlay;
- roughness of concrete substrate.

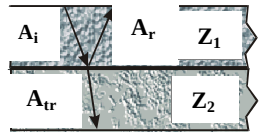
There is the preference to apply the methods requiring the access from only one side of the tested object.

In the case of a multilayer system the propagation of stress waves depends on differences in acoustic impedances (Z = pulse velocity x volume density), of both repair material and concrete substrate (Carino 1997). For two dissimilar materials, part of the energy of the vibration is refracted into the new one, $A_{tr}$, while the other part is reflected back, $A_r$. The wave reflection is characterized by a reflection coefficient, R (Tab 2). Experimental and numerical investigations with I-E method have shown that usually an interface is "visible" if the absolute value of the R coefficient is higher than +0.24 (Sansalone & Carino 1989, Kwaśniewski & Garbacz 2005). Kwaśniewski & Garbacz (2005) showed also that thickness of repair layer is also important. The interface peak disappeared for layer thickness higher than 80 mm (two times thinner than theoretical value of layer thickness) even for high value of R coefficient.

It is often possible to assume that repair material and concrete substrate have similar acoustic impedances (eg. cement or PCC mortars). The detection of flaws at the interface overlay - concrete substrate can be performed with procedures developed for "solid" concrete

structures. For example, Garbacz et al. (2004a) have shown that changes of acoustic impedance for PCC composites are small (<10%) for a wide range of polymer content (0-30%) and close to the typical range for cement concrete and mortars (Lewinska 2001). The effect of interface should be taken into account in the case of overlays with acoustic impedance different than that for concrete substrate. eg. polymer coating, asphalt pavements, etc.

Table 1. R values for common "building interfaces" (acc. to Garbacz & Garboczi 2003)




$$R = \frac{A_r}{A_i} = \frac{Z_2 - Z_1}{Z_2 + Z_1}$$

| Interface | Reflection coeff. R |
|---|---|
| Concrete / air | - 0.99 |
| Concrete / water | - 0.71 |
| Concrete / soil | - 0.63 |
| Granite/concrete | - 0.28 |
| Asphalt / concrete | + 0.29 |
| Concrete / steel | + 0.67 |
| Bitumen/concrete | + 0.80 |
| Polymers/concrete | + 0.39 |

## 3. NDT METHODS APPLICABLE TO QUALITY CONTROL OF REPAIR SYSTEMS

### *3.1. Ultrasonic Echo method*

The ultrasonic echo method was developed for flaw detection and estimation of layer thickness. However it is rarely used for evaluation of concrete structures and repair systems. This method gives lower resolution for concrete compared to metal testing. Impulse duration is long at a frequency of 100 kHz; this leads – in the case of the single transducer in the echo method – to a long "dead zone". In this case, a proper selection of transducer is necessary. Double transducers are difficult to apply due to the small directivity of the ultrasonic beams emitted with low frequencies and the possibility of "cross-talk" between them, as well as the reflection of the wave by the surfaces parallel to the beam axis.

Recently, some works on improving the echo method have been carried out. They are mainly focused on using ultrasonic waves with higher frequency (Popovics et al. 2000). The high frequency pulse echo method has been applied for defects detection for concrete structure strengthened with carbon fiber reinforced polymers (Bastianini et al. 2001). Mapping of defects was done on the base of distribution of an amplitude value of the first echo. Similar results have been obtained by Kundu et. al. (1999) with relatively high frequency (1 MHz) but a special procedure of signal filtering has been used. Multi-transducers system and Synthetic Aperture Focusing Technique (SAFT) seem promising for improvement of flaws and steel reinforcement detection in repair systems (Shevaldykin, 2003; Taffe at al, 2005). Nevertheless, not much field experiences have been gathered with the ultrasonic–echo method for repair systems.

A few papers are related to evaluation of the adhesion strength between repair material and concrete substrate with U-E method. In those studies, the adhesion assessment was based on the assumption that the places with poor adhesion influenced the recorded waveform. The adhesion strength is related to values of selected parameters for reference state - good bonding joint. For example, Tan et al. (1996) have used relative amplitude method for evaluation of cement adhesion in wall tiles. They have assumed that bond quality is measured as the relation between intensity of reflected signal from a free (unbounded) tile and from a tile –

cement interface. If the bond strength decreases, the intensity of reflected signal is higher. They have obtained maximum of the pull-off strength and the minimum of relative signal amplitude for cement adhesive with water to cement ratio, w/c = 0.5.

The evaluation of the adhesion in PC-CC systems using an ultrasonic echo method is more difficult because of the difference between the acoustic impedances. Garbacz & Garboczi (2003) have evaluated the adhesion between polymer coating and concrete substrate using the value of amplitude amplification to 0.8 of maximum amplitude (i.e. 80% of full screen height) - coefficient, W0.8H. Analysis of the W0.8H measurement results showed that there is no relation between the level of amplification and the pull-off bond strength. The value of attenuation W0.8H for a "zero-adhesion" state of polymer coating was located between the points corresponding to different levels of adhesion. The observed differences in the attenuation were explained, at least in 70%, by variation in coating thickness (Fig.2). This justifies that ultrasonic echo method is useful for the evaluation of polymer coating thickness applied on concrete substrate.

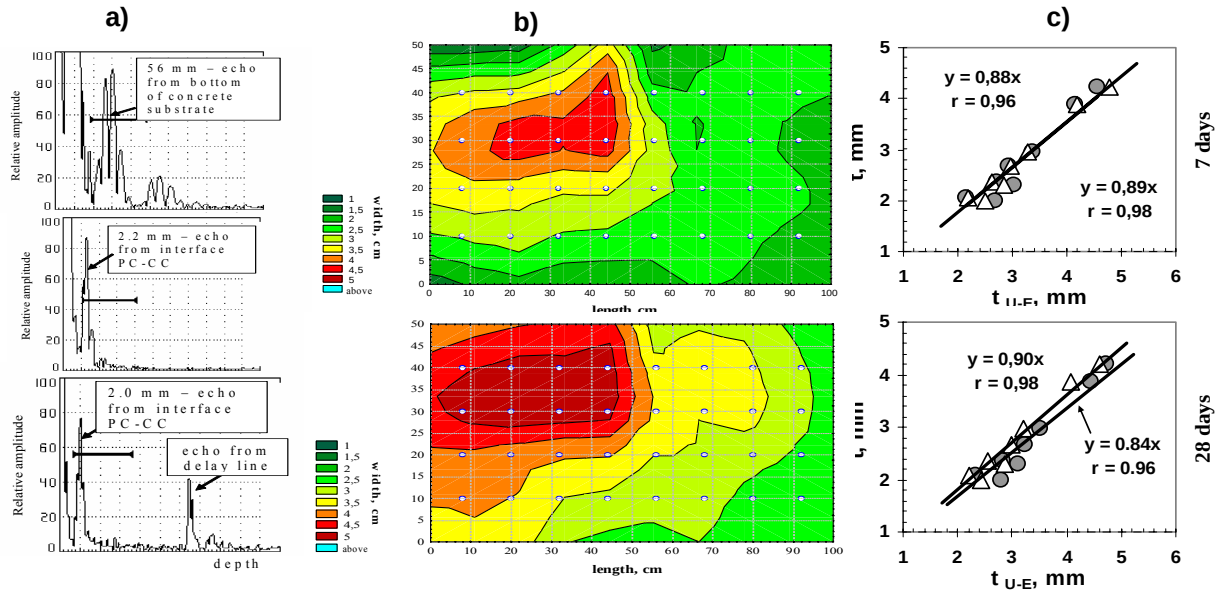



Figure 2. Example of estimation of PC layer thickness with echo method: (a) registered signal (A-scan) after testing the polymer coating of 2 mm thick layered on concrete substrate with commercial transducers: 0.5LN50, S12HB0.8-3, 10V202 (with delay line). The signals recorded for S12HB0.8-3, 10V202 transducers contain echoes from the interface floor - concrete substrate; (b) the PC layer thickness distributions measured with magnifier (up) and estimated with S12HB0.8-3 transducer; (c) relationship between "true" value of floor thickness and estimated with ultrasonic echo method using transducers S12HB0.8-3 (●) and 10V202 (Δ)

### *3.2. Pulse velocity method*

Generally, the pulse velocity method can be performed in two modes:

- direct – transducers located on two opposite surfaces of an object being tested,
- indirect (surface) – both transducers located at the same surfaces of an object being tested.

Direct UPV method is used mainly for the evaluation of compressive strength as well as for assessment of homogeneity of concrete in structures. Indirect pulse velocity is rarely used. This method with variable distance between transducers can be used for estimation of crack depth (e.g. Kaszyński, 2000) and estimation of thickness of external deteriorated layer of concrete (Toeudoru, 2000). This method was used by Jaquerod et al. (1992) for detection of cracks beneath a repair mortar layer. Garbacz et al. (1999) used indirect UP-V for

characterization of the adhesion in the PC-CC system with changes of a mean square value of amplitude – MS(t) in time domain. The investigations were carried out with a commercial concrete tester Unipan-Ultrasonic CT1 with sets of associated transducer pairs. The source pulse frequency of the longitudinal wave was 100 kHz. The distance between transducers was fixed and equal to 80 mm. The amplitude range was constant. The MS value at the given time was calculated from the formula:

$$MS(t) = \left( \sum_{n_o}^{i-n_o} A_i \cdot A_i \right) / (n - n_o) \qquad (1)$$

where: Ai – amplitude of the i-recorded point [V], no – number of the first point with amplitude different from zero.

The investigations were carried out for two boundary conditions:

- maximum adhesion (for a given type of polymer coating; coating prepared according to producer's guideline),
- zero-adhesion (corresponding to delamination); to simulate delamination the polymer coating was prepared on a metallic foil with an anti-adhesion agent, and next put onto a cement concrete substrate.

Additionally, the concrete substrates differed in moisture content, were also prepared with and without primer in order to obtain a continuous range of adhesion. The investigations were carried out for commercial floor systems: epoxy (water-dispersed and solvent), polyurethane and vinyl-ester and containing a quartz filler (maximum grain diameter Dmax < 0.1 mm).

The obtained results indicated that relationships between the pull-off strength and the parameters of ultrasonic wave propagation are valid only for a limited range of pull-off strength (Fig.3). This is a result of the nature of the pull-off test – maximum bond strength corresponds to the tensile strength of the concrete substrate. Figure 4 shows an example of the mapping of adhesion strength obtained with the surface ultrasonic method and analysis of the signal in time domain for epoxy coatings applied on concrete substrate with artificial defects at the interface zone. The adhesion strength distribution was obtained on the basis of statistical fitting procedure of the MS value and the pull-off strength in particular nodes. The obtained results indicate that both the average value of MS and its variation coefficient should be taken into account for the adhesion evaluation with ultrasonic methods. The disadvantage of the above method is the necessity to develop a reference curve for a given type of polymer coating with respect to its composition and thickness (measured on-side with UP-E method) and fixed range of amplitude during ultrasonic testing. The results of adhesion evaluation should be verified with the pull-off test.

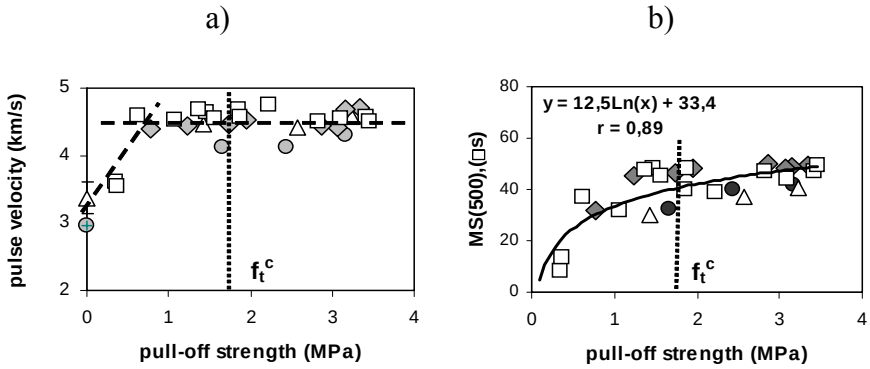



Figure 3: Pulse velocity (a) and MS (500 μs) value (b) vs. the pull-off strength for coatings: water-dispersed epoxy – 2mm (●), solvent epoxy – 2mm (Δ), polyurethane – 1mm (□) and vinyl-ester 4mm (◊); ftc – nominal tensile strength of concrete substrate

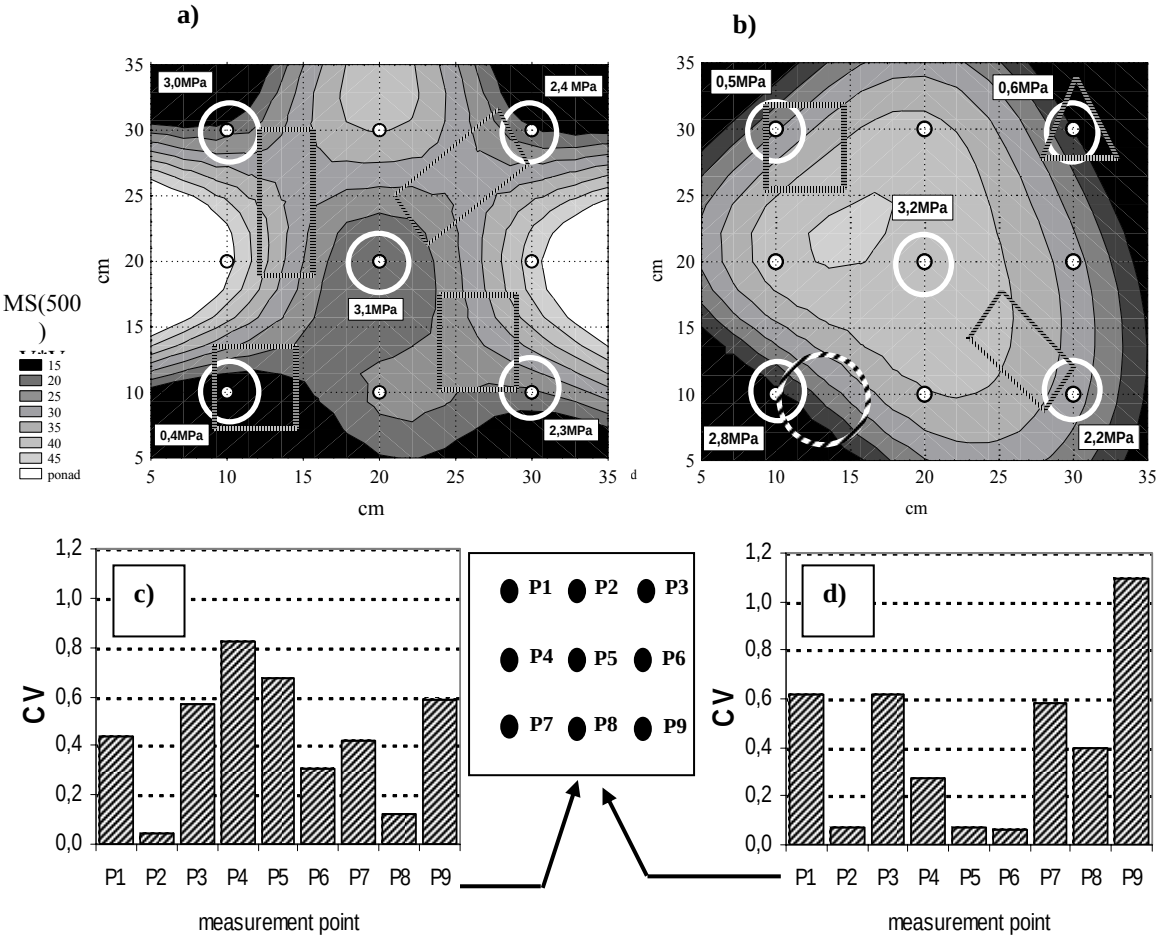



Figure 4. Results of the ultrasonic mapping of the adhesion for (a) water dispersed epoxy and (b) solvent epoxy coatings with nominal thickness of 2mm and artificial defects (dotted line contour); (c,d) corresponding variation coefficient, CV in measurement points P1 – P9. In white rectangles the experi-mental values of the pull-off strength (measured in the solid white line circle); white points stand for the points of ultra-sonic measurements

## 3.3. Impact Echo

Impact-echo method is very often used for quality control of various types of repair, eg. injection of cable ducts, overlays and patches, etc. (eg. Sansalone & Carino 1989, Garbacz & Kazmierczak 2003). The principles of testing with U-E and I-E methods are similar (Fig. 5a). However, stress waves produced in the impact-echo method have lower frequencies (below 30 kHz) – lower sensitivity to natural heterogeneity of concrete. Additional feature of I-E method is an application of frequency analysis besides time-domain analysis (Fig 5b). The selection of the impact source is a critical factor for defect detection in multilayer system with impact–echo. The impact duration determines the frequency content of the stress wave and determines the minimum flaw depth that can be detected. The impact duration depends on the diameter of the impactor (Fig.5c). On the basis of frequency spectrum the depth of the reflecting interface (e.g. flaws) can be determined according to formula:

$$d_d = c_p / 2\, f_d \qquad (2)$$

where: $d_d$ - depth of interface, $c_p$ – P-wave velocity and $f_d$ – frequency of dominant peak in frequency spectrum

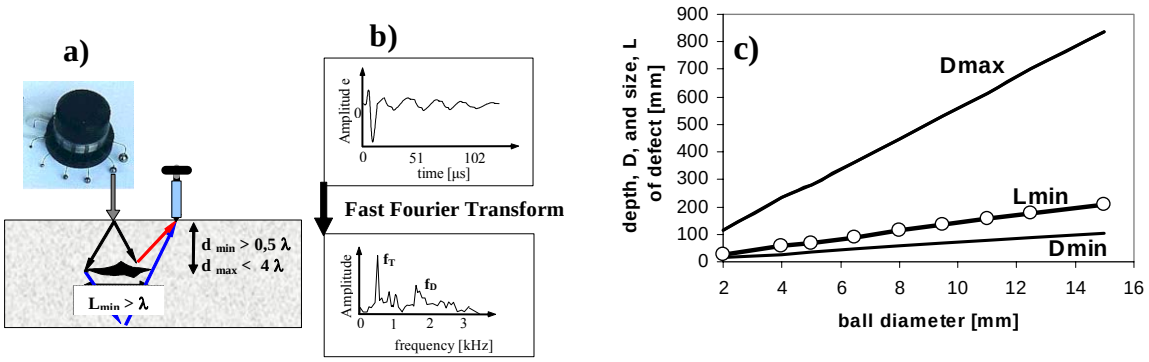



Figure 5. Scheme of impact-echo method (a), examples of waveform and corresponding frequency spectrum (b) and effect of ball size on depth and size of defect possible to detect (c)

If the overlay material has significantly different acoustic impedance (R > 0.24) in comparison to that for concrete substrate the testing procedure should be modified (Sansalone & Carino, 1989). In this case, the defect depth can be estimated from equation:
where:

$$d_d = 0{,}5 \cdot \left[ \frac{C_{pc}}{f_d} + \frac{C_{po} - C_{pc}}{f_o} \right]$$

$C_{pc}$, $C_{po}$ – pulse velocity in concrete substrate and overlay respectively
$f_d$, $f_o$ – frequency peaks for defects and overlay respectively

Above equation, after modification, can be used for estimation of defect depth in a multilayer system (Sansalone & Carino 1989).

Garbacz & Mielańczuk (2004) have used the I-E method for evaluation of the quality of the floor beneath a polymer coating. Although, the polymer coating/concrete interface is characterized by relatively high reflection coefficient, it was possible to detect delamination inside of overlay system. They assumed that the thickness of coating was small and it had no significant influence on the accuracy of defect depth evaluation using Eq. 2 for "solid" structure was used. The P wave velocity for concrete plate (4000m/s) beneath polymer coating was only taken for calculation. The investigations were carried out with Germann DOCter device using 2mm steel ball. All registered frequency spectrums could be divided into three main types (Fig.6):

- type A – multi-peaks frequency spectrum - delamination located close to the surface (Fig 6a);
- type B – integral system; frequency peak corresponds to bottom of concrete slab and no flaws detectable by I-E method (Fig.6b);
- type C - flexural vibration indicates presence of shallow delamination at the interface – depth less than 14 mm (Fig 6c);

On this basis, the mapping of quality of floor system was determined (Fig.6 bottom). The verification of I-E test results by coring and pull-off tests showed good agreement of both non-destructive and destructive tests (Fig. 6 in the middle).

## 4. EFFECT OF PCC/CONCRETE INTERFACE QUALITY ON STRESS WAVE PROPAGATION

Several repair systems (Garbacz et al. 2005): commercial PCC repair mortar – concrete substrate with different surface quality, caused by various surface treatment, and with or without bond coat of PCC type were analyzed. The concrete substrate roughness was

characterized by profilometry methods and surface quality was observed with light scanning electron microscopes.

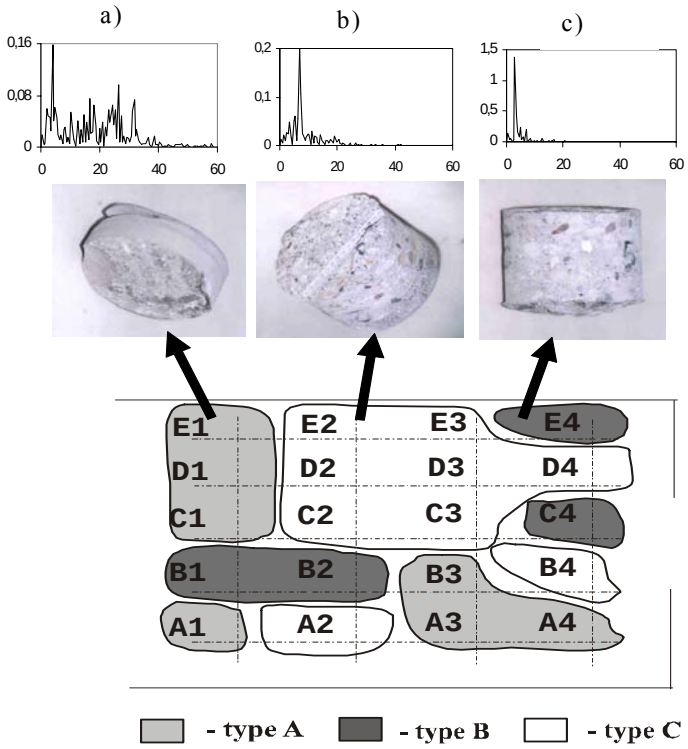



Figure 6. Example of mapping of quality of floor (size 14 x 20 m) with vinyl-ester coating (4mm) and view of sample after coring: a) defect beneath polymer coating at the interface: self-levelling cementitious mortar – concrete substrate; b) integral system ; c) low frequency flexural vibration indicates present of shallow delamination at the interface: polymer coating–concrete substrate (adopted from Garbacz & Mielanczuk, 2004)

The repair systems were tested with I-E method (Garbacz 2004). For each repair system the P wave velocity was calculated and frequency spectrum analyzed for 30 measurements made inside a circle with diameter of 100mm. Three types of frequency spectrum were obtained. The percentage of spectrums useful for analysis, i.e. containing separate peak thickness frequency (type A), was determined. The obtained results indicate that there is no correlation between roughness of concrete surface (beneath repair mortar) and P wave velocity (Fig.7a) and the fraction of useful frequency spectrum (Fig.7b) for both types of repair system. The pull-off strength decreased with the surface roughness increase (Fig.7c) for the system without bond coat. This was a result of presence of small voids at the interface (Garbacz et al. 2005). Simultaneously, for that system type the P wave velocity increased as the roughness increased, while for the system with bond coat such type of relationship was not observed (Fig.7d). In this case the bond coat filled properly irregularities of concrete substrate. The results obtained indicate that for I-E methods the roughness of concrete substrate does not affect significantly the P wave propagation through the repair system if the bond quality is sufficient (no presence of large voids at the interface).

Recently, a new tool for signal analysis – wavelet analysis - is being implemented in NDT assessment, also in the case of concrete structure, e.g. for analysis of acoustic emission or ultrasound signal (Kurtz et al.2003, Grosse & Reinhardt 2003). This method is more flexible for signal analysis in comparison to Fourier analysis. It is a multiresolution time-scale method which enables to extract information like instantaneous frequency, tiny echoes embedded in complex signal or to suppress noise. The question is whether this method could be applied for evaluation of repair efficiency. Figure 8 shows examples of continuous wavelet analysis of the I-E signals previously obtained for the repair systems without bond coat. The obtained diagrams of frequency scale-time were different for different type of wavelet and the tested types of repair systems, but similar for the given type. It is clearly shows that wavelet

selection is very important. The ortogonal or biortogonal wavelets are commonly used for signal analysis because of possibility to perform a discrete wavelet analysis.

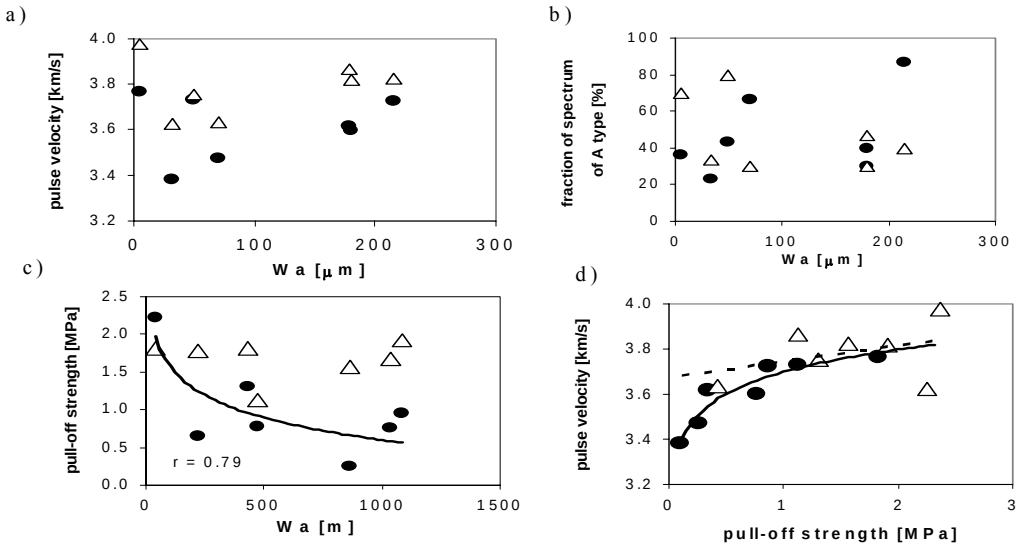



Figure 7. Relationships: mean waviness of profile, Wa vs. pulse velocity (a) and fraction of useful frequency spectrum (b); pull-off strength vs. waviness parameter Wa (c) and pulse velocity vs. pull-off strength; overlays with (Δ) and without (●) the bond coat

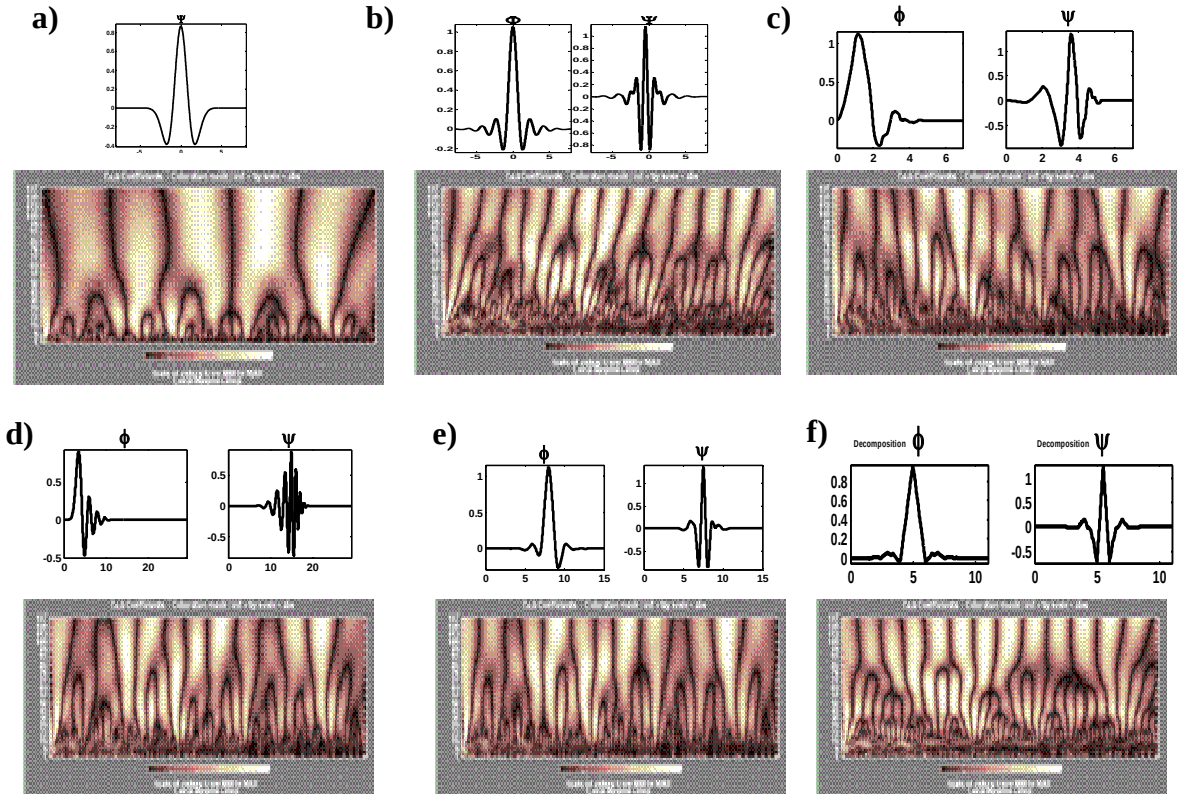



Figure 8. Introductory results of continuous wavelet analysis of I-E signal for different wavelet types for repair system without bond coat for concrete substrate after treatments: (a) mexh, (b) meyr, (c) db4, (d) sym5.5, (e) rbio 5.5, (f) morlet complex

Further steps of analysis need to separate an effect of adhesion strength from effects of surface roughness and presence of flaws at the interface. First results showed that "ordinary" statistical parameters determined for wavelet coefficient distribution as well as reconstructed signal do not correlate with the pull off strength (Fig.9). This mean that more deep analysis of signal is needed for that issue.

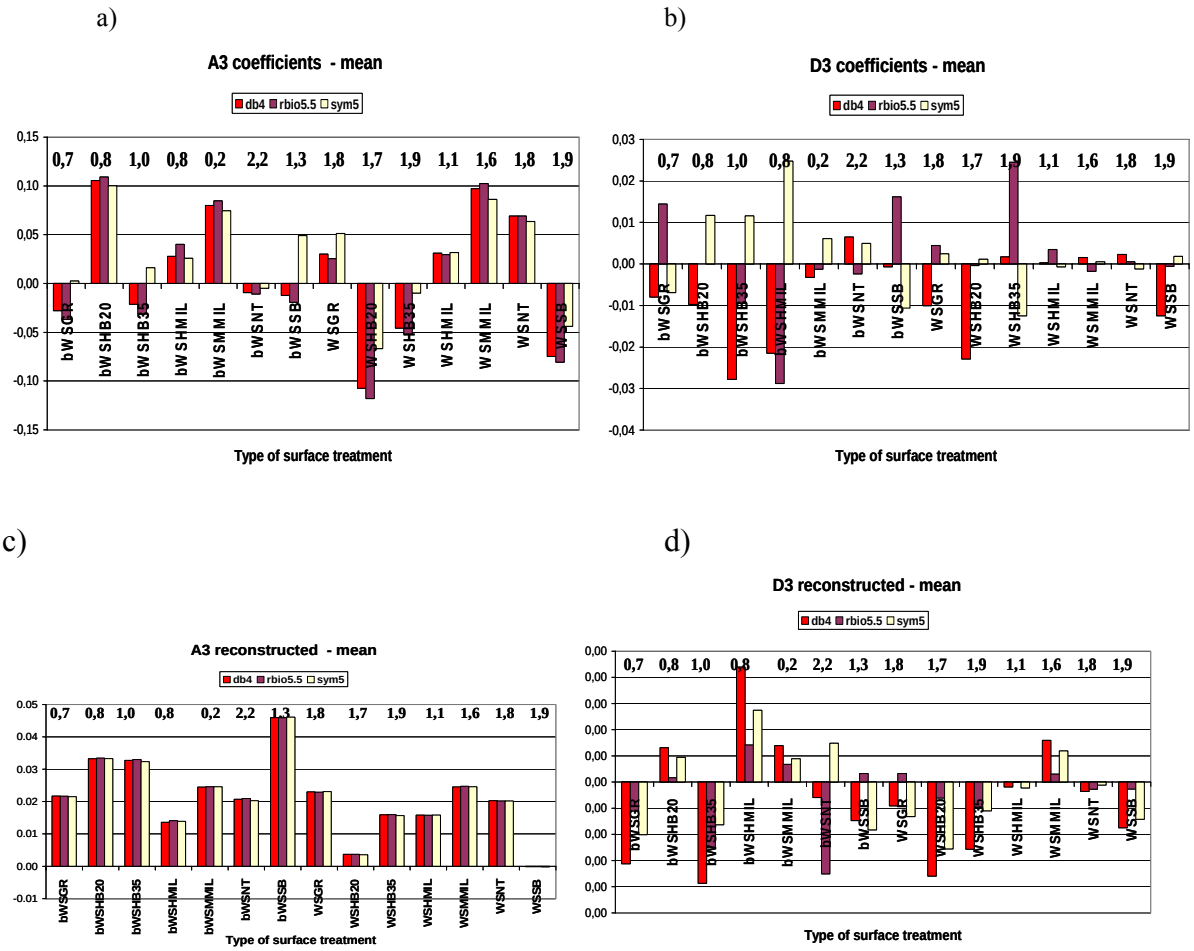



Figure 9. Results of wavelet analysis of impact-echo signals obtained for various model repair systems differing in surface treatment of concrete substrate and presence of bond coat: (a) mean value of wavelet coefficient distribution for signal approximation, (b) mean value of wavelet coefficient distribution for detail at level3, (c) mean value distribution for approximation of reconstructed signal, (d) mean value distribution for detail at level3 of reconstructed signal

## 5. CONCLUSIONS

The presented overview shows usefulness of ultrasonic and impact methods for assessment of various repair systems. These methods have limitations that determine the range of their applications. However, often they can be used as complementary methods. The impact-echo method is useful for detection of larger and deeper located defects, but it is less sensitive on natural heterogeneity of concrete. Smaller defects could be detected with the ultrasonic-echo

method. However, concrete heterogeneity and steel reinforcement make results interpretation more difficult. This implies the necessity for further improvement of NDT techniques applicable to repair system, particularly their accuracy and repeatability. Recent progress in measurement and computer techniques enables improvement of effectiveness of non-destructive assessment of repair efficiency. This can be reached by using advanced methods of signal analysis. Other directions are involved with development of new test equipments (preferably non-contact) and using waves others than longitudinal (e.g. surface wave, plate waves) as well as wave parameters other than wave propagation velocity.

*ACKNOWLEDGMENTS*

The author is grateful to Professor L. Czarnecki, Head of the Building Materials Engineering Division at the Warsaw University of Technology. This work has been done in the framework of project granted by Polish Scientific Research Committee - grant number KBN 4T07E02727.

## 6. REFERENCES

Adams R.D., Drinkwater B.W. 1997. Nondestructive testing of adhesively bonded joints, NDT&E International, 30, 93-98

Austin S., Robins P., Pan, Y. 1995. Tensile bond testing of concrete repairs., Mater. Struct. (28). 249 - 259

Bastianini F., Tommaso A.Di., Pascale G. 2001. Ultrasonic non-destructive assessment of bonding defects in composite structural strengthening, Composite Structures, 53, 463-467

Carino N.J. 1997. Nondestructive Test Methods, Concrete Construction Engineering Handbook, ed.E.G.Nawy, CRC Press, 19.1-19.67

Concrete Repair Manual. 2003. ACI International, Farmington Hills, MI, USA, 2003

Czarnecki L, Emmons P.H. 2002. Repair and protection of concrete structures (in Polish). (Polski Cement ed., Krakow, 2002)

European Standard EN 1504-10:2003. Products and systems for the protection and repair of concrete structures – Definitions - Requirements – Quality control and evaluation of conformity - Part 10: Site application of products and systems and quality control of the works

Garbacz A., Czarnecki L., Clifton J.R. 1999. Non-destructive methods to assess adhesion between polymer composite and portland cement concrete. In Proc. 2nd Int. RILEM Symposium "Adhesion between polymers and concrete"- ISAP'99, Dresden . 467-474

Garbacz A., Garboczi E.J. 2003. Ultrasonic evaluation methods applicable to polymer concrete composites, NIST Report (NISTIR 6975), United States Department of Commerce, National Institute of Standards and Technology, Gaithersburg MD (USA)

Garbacz A., Kaźmierczak P. 2003. Evaluation of quality of mineral floor with impact-echo, Building Materials (in Polish), 9, 46-48

Garbacz A., Mielanczuk P. 2004. Evaluation of quality of polymer industrial floor with impact-echo. In Proc. of XIX Conference "Concrete and Precast Concrete Elements – Jadwisin 2004" (in Polish),

Garbacz A., Łukowski P., Bęcek J. 2004a. Effect of polymer content on ultrasonic wave propagation in polymer-cement composites, accepted for publication. In Proc. of 33th Conference "Nondestructive Test Methods", Lichen, Poland, (in Polish),

Garbacz A., Gorka M., Courard L 2005. On the effect of concrete surface treatment on adhesion in repair systems. Magazine of Concrete Research. 57, 49-60

Grosse Ch.U., Reinhardt H-W. 2003. New developments in quality control of concrete using ultrasound. In Proc. BB 85-CD (ISBN 3-931381-49-8) International Symposium (NDT-CE 2003) Non-Destructive Testing in Civil Engineering, Berlin

Jaquerod C., Chippis Ch., Alou F., Houst Y.F. 1992. Nondestructive testing of repair mortars for concrete, In Proc. of the 3rd Int. Colloquium Materials Science and Restoration, Esslingen (Germany), 872

Kaszyński, J.. 2000. An investigation into the depth of cracks in a reinforced concrete structures using an ultrasonic method. In Proc of 15th World Conference on Non Destructive Testing, Roma, pap.357

Kundu T., Ehsani M., Maslov K.I., Guo, D. 1999. C-scan and L-scan generated images of the concrete/GFRP composite interface, NDT&E International, 32, 61-69

Kurz J.H., Finck F., Grosse Ch.U., Reinhardt H-W. 2003. Automatic analysis of acoustic emission measurements on concrete. In Proc. BB 85-CD (ISBN 3-931381-49-8) International Symposium (NDT-CE 2003) Non-Destructive Testing in Civil Engineering, Berlin

Lewińska-Romicka A. 2001. „Badania nieniszczące. Podstawy Defektoskopii" (Nondestructive techniques. Introduction to flaw detection), Ed. Wydawnictwa Naukowo – Techniczne (in Polish), Warszawa

Popovics J.S., Achenbach J.D., Song W-J..1999. Application of new ultrasound and sound generation methods for testing concrete structures. Mag. of Concrete Research, 51, 35-44

Popovics S., Bilgutay N.M., Karaoguz M., Akgul T. 2000. High-Frequency ultrasound technique for testing concrete. ACI Materials Journal, 97, 58-64

Sansalone M., Carino N.J. 1989. Detecting delamination in concrete slabs with and without overlays using the impact-echo method, ACI Materials Journal 86

Shevaldykin V.G., Samokrutov A.A. Kozlov V.N. 2003. Ultrasonic Low-Frequency Short-Pulse Transducers with Dry Point Contact.Development and Application.. In Proc. of the International Symposium on Nondestructive Testing in Civil Engineering, Berlin

Taffe, A., 2005. Assessment of foundation slabs with US-echo in the re-use process, In: ICCRRR 2005 International Conference on Concrete Repair, Rehabilitation and Retrofitting (Eds. H. Beushausen, F. Dehn and M.G. Alexander), Cape Town, South Africa, 1027-1031

Tan K.S., Chan K.C., Wong B.S., Guan L.W. 1996. Ultrasonic evaluation of cement adhesion in wall tiles, Cement and Concrete Composites, 18, 119-124

# Session 5

International Symposium Polymers in Concrete
2 - 4 April 2006
Guimarães, Portugal

# Modelling the behaviour of the bonding of fibre reinforced concrete at the plate end

Pedro Neto[1]

*Instituto Politécnico de Setúbal, Escola Superior de Tecnologia do Barreiro e ICIST*
*Rua Stinville 14, 2830-114 Barreiro, Portugal*

João Vinagre[2], Jorge Alfaiate[2]

*Universidade Técnica de Lisboa, Instituto Superior Técnico e ICIST*
*Av. Rovisco Pais, 1149-001 Lisboa, Portugal*

## ABSTRACT

In this paper, the finite element method is used to analyse the behaviour of concrete externally strengthened by fibre reinforced polymers (FRP). This model aims to analyse the stress distribution in the FRP-concrete interface at the plate end of a bending beam. The behaviour of the concrete-epoxy-FRP arrangement is modelled with interface elements with initial zero thickness, using a discrete crack approach. A localized damage model is adopted for the interface and a parametric study is performed to approximate the material parameters adopted. The importance of each parameter is assessed. This model is subsequently verified using experimental data collected from the literature. Finally, a proposal is made concerning the adoption of a relation $G_F^{II}/G_F$ for the interface behaviour. Mention is also made to some of the main mathematical models found in the literature, which are compared to the present approach.

## 1. INTRODUCTION

In recent years, the use of composite materials applied to the external strengthening of concrete structures has increased due to their mechanical properties, ease of application and high strength-to-weight ratio. The major problems found with this technique are the local failure modes. Results from experiments reveal that the strength of a glued concrete-FRP (fibre reinforced polymers) bond is determined, in most cases, by the high interfacial stresses. Thus, there is a clear need to study the nature of the bonding as well as developing techniques to permit its design modelling and an accurate quantification of the adherence between the concrete and the reinforcing material.

[1] Assistant
[2] Assistant Professor

The stress distribution on pure shear test models does not precisely match the one obtained in bending reinforcement; in the latter, according to various authors, Malek et al.(1998), Rabinovitch et al. (2000) and Täljsten (1994), in addition to the stresses tangential to the interface, normal stresses are also important. The stress concentrations at the FRP end can be the cause of the collapse of the strengthened concrete beam. This type of local failure generally occurs along a portion of concrete attached to the epoxy-fibre layers, the latter remaining intact. In these cases, the evaluation of the energy dissipated per unit of cracked surface involves both the fracture energy of concrete in mode I and II, denoted by $G_F^{II}$ and $G_F$, respectively. Several experimental and numerical tests have been carried out to study mixed mode fracture. However, the definition of these material parameters is still not well established and the numerical and experimental results reported have often been contradictory. Bazant et al. (1986) and Ozbolt et al. (1998) proposed for $G_F^{II}$ values about 25 times greater than $G_F$. Alfaiate et al. (1998) performed numerical analyses of notched beams subjected to shear and did not detect any significant differences on the value of the failure load when $G_F^{II}/G_F$ varied from 1 to 100. Such result was confirmed by Gálvez et al. (1998), who carried out a similar study. Täljsten (1994) performed a set of experimental tests for determining both values of $G_F$ and $G_F^{II}$. The mode II fracture energy was determined submitting a concrete specimen to both compression and shear. The values determined for $G_F^{II}$ were found to be 10 times greater than the value of $G_F$.

In this paper, special attention is paid to the stress concentration at the FRP end. Subsequent to previous shear-stress studies (Neto et al. (2004)), a numerical model is presented which aims to analyse the stress distribution at the FRP-concrete interface of the composite end of a bending beam. The bond between the FRP and the concrete is modelled using a discrete crack approach based on non-linear fracture mechanics (Hillerborg et al. (1976)). Interface elements with zero initial thickness were considered. The shear and peeling stresses developed at these elements are dependent on the relative displacement between the strengthening material and the concrete surface, according to a local constitutive relationship. The material properties that characterize the interface, namely the shear and peeling stiffness, the cohesion, the tensile strength and the fracture energy in modes I and II, are obtained from a parametric study using experimental data from strengthened reinforced concrete bending beams. From the analysis of the results numerically obtained, it is possible to conclude that mode II fracture plays an important role on these tests and a range of values is proposed for $G_F^{II}$. It is expected that this work may contribute to a better comprehension of the stress transfer mechanisms between the concrete and the strengthening material, particularly with respect to the qualitative and quantitative definition of mixed mode fracture of concrete.

## 2. EXPERIMENTAL TESTING

In this section, the bending tests conducted by Dias et al. (2002) are analyzed. Among the several experimental models tested by Dias et al. (2002), the reinforced concrete beam strengthened with carbon fibre laminates was considered. Figure 1 illustrates the geometry, the internal and external reinforcing schemes and the boundary conditions.

The four point beams had a $0.12\times0.18m^2$ cross section, a total length of 1.95m and a span of 1.80m. The unidirectional carbon fibres were glued, by means of resin epoxy, to reinforced concrete beams with a bond length of 1.74m. One layer of $t_f$=1.4mm thickness were adopted presenting a $b_f$=20mm width.

The MBrace HM laminate FRP system was used. The nominal values for the Young's modulus and the ultimate tensile strain of the CFRP were 200GPa and 1.1%, respectively. The adhesive's Young's modulus was 7GPa. Mean values of 47.7MPa, 4.0MPa and 31.1GPa, for the cylinder compressive strength, tensile strength and Young's modulus of concrete,

respectively, were obtained experimentally. For the steel, mean values of the yielding stress of 555MPa (ϕ6) and 533MPa (ϕ8) were found from the tests.

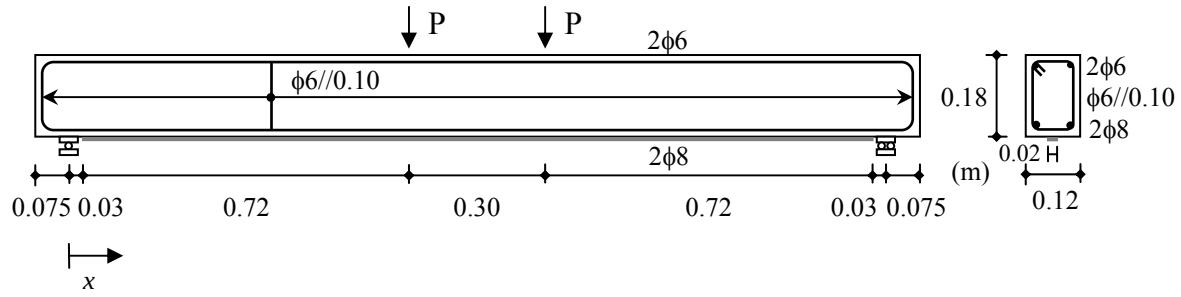



Figure 1 – Geometry, reinforcing schemes and boundary conditions.

## 3. NUMERICAL MODELLING

### 3.1. Constitutive relationships

Taking into account the objective of this study, namely the evaluation of shear and peeling stresses at the plate end, a linear elastic and isotropic constitutive relationship was adopted for the reinforced concrete. Thus, to simulate the loss of stiffness of the reinforced element, two different Young modules were adopted for the concrete as shown in Figure 2: i) the first one simulates the cracked concrete and ii) the second one takes into account the internal reinforcement yielding. The determination of these values was based on the experimental results mentioned above (Dias et al. (2002)). The contribution of the CFRP to the beam stiffness was observed to be negligible.

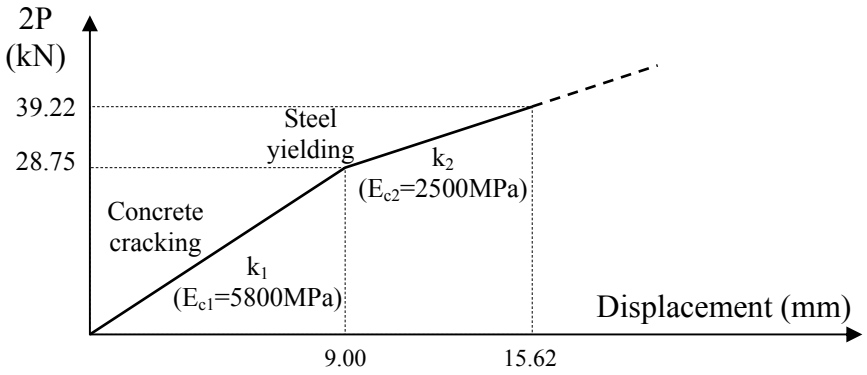



Figure 2 – Structure response and Young's modulus adopted for concrete.

The tensile behaviour of the FRP may be assumed as linear elastic until failure.

The bond between concrete, resin and CFRP was modelled using interface elements of zero initial thickness and a discrete crack approach. A multi-surface plasticity model was adopted (Alfaiate et al. (1998) and Lourenço et al. (1997)); two limit surfaces are considered: a tension cut-off for mode I fracture and a Coulomb friction envelope for mode II failure, as shown in Figure 3. In this figure, the horizontal axis represents the normal stress vector component and the vertical axis represents the tangential stress vector component measured at the interface. The cut-off mode I is defined by the tensile strength of the concrete. This value

is initially considered equal to 4.0MPa, obtained from pull-off tests (Dias et al. (2002)). The Coulomb friction envelope is initially characterized by the cohesion coefficient and by the internal friction angle $\phi$. Both yield functions follow exponential softening flow rules (Figure 4).

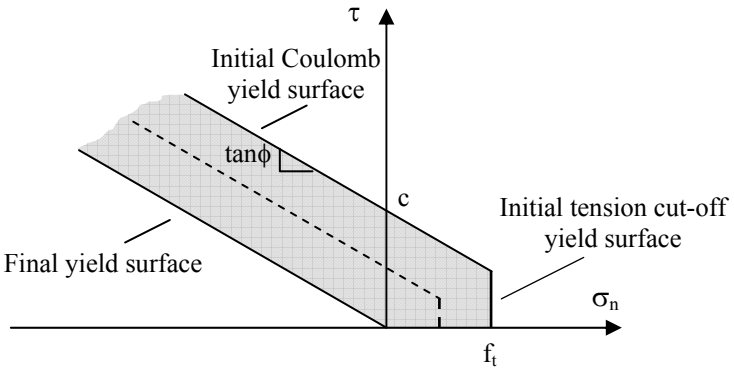



Figure 3 – Yield surfaces adopted for the interface.

The tension mode yield function is given by:

$$f_n = \sigma_n - f_t \exp\left(-\frac{f_t}{G_F^I} w\right), \tag{1}$$

where $\sigma_n$ is the stress vector component measured in the interface. An associated flow rule is considered. The shear mode yield function reads:

$$f_s = |\tau| + \sigma_n \tan\phi - c \cdot \exp\left(-\frac{c}{G_F^{II}} s\right), \tag{2}$$

where $\tau$ is the tangential stress vector component measured in the interface. A non-associated flow rule is adopted with a plastic potential $g_s$ given by:

$$g_s = |\tau| + \sigma_n \tan\psi - c, \tag{3}$$

where $\psi$ is the dilantancy angle. An isotropic softening criterion is adopted, meaning that both yield surfaces shrink the same relative amount in the stress space, and both keep the origin (Figure 3).

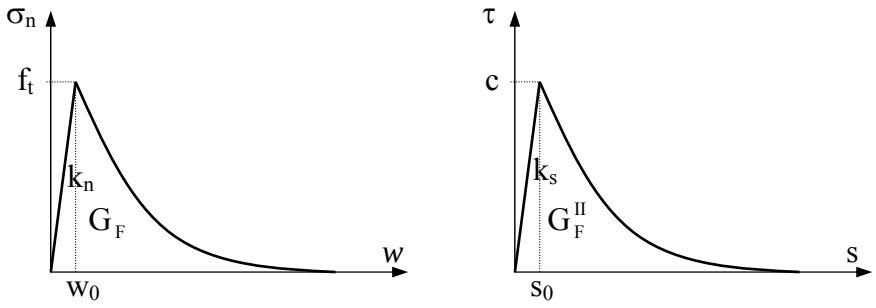



Figure 4 – Normal and tangential constitutive relationships adopted for the interface.

The material parameters characterizing the interface behaviour are: the elastic shear and peeling stiffness, $k_s$ and $k_n$, respectively, the cohesion c, the tensile strength $f_t$, and the fracture energies in mode I and II, $G_F$ and $G_F^{II}$, respectively (area under the curves $\sigma_n$-w and $\tau$-s adopted as shown in Figure 4).

### 3.2. Numerical Implementation

The numerical analysis was performed using the finite element method. The elements used for concrete were 4-node and 5-node isoparametric. For the strengthening material, 4--node isoparametric elements were adopted (instead of the linear 2-node element used in previous analyses (Neto et al. (2004)). These elements allow for taking into account the bending stiffness of the composite. The bond between concrete, resin, and CFRP was modelled by linear interface elements. The specimen response was determined under displacement control, using an incremental and iterative procedure, according to the following algorithm:

1. evaluation of the incremental stiffness matrix of the structure **K**;
2. solving of the system of equations $\mathbf{K}\Delta\mathbf{u}=\Delta\lambda\mathbf{F}$, where $\Delta\mathbf{u}$ is the incremental displacement vector, $\Delta\lambda$ is the load increment size and **F** is the nodal force vector;
3. evaluation of the internal forces $\mathbf{F_i}$. The Newton-Raphson and the arc length methods are used for obtaining convergence towards a solution without unbalanced forces. If equilibrium is not reached within a prescribed tolerance, a new iteration must be performed; otherwise proceed to step 4;
4. update of the total variables, application of another load increment $\Delta\lambda$, and return to step 1.

The symmetric two-dimensional finite element mesh adopted is presented in Figure 5, as well as the obtained structure deformation. In the FRP end, a more refined mesh was considered to capture the high stress gradient which is expected in this region.

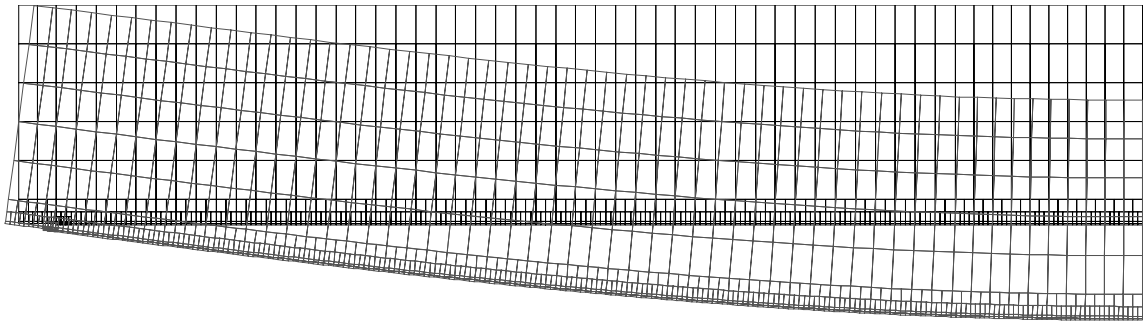


Figure 5 – Finite element mesh adopted and structure deformation.

### 3.3. Numerical analysis

As mentioned above, the constitutive relationship of the interface concrete-CFRP is defined by six parameters: the shear and peeling stiffness, the cohesion, the tensile strength and the fracture energy in mode I and II. In the present analysis only debonding failure was acknowledged. In agreement with Malek et al. (1998), the stiffness of the interface depends on the adhesive properties according to:

$$k_n = E_a / t_a \tag{4}$$

and

$$k_s = E_a / \left(2(1+\upsilon)t_a\right), \tag{5}$$

where υ is the Poisson coefficient, $E_a$ is the Young's modulus for adhesive and $t_a$ is the thickness of the adhesive. According to experimental and fabricant data, the values adopted for the calculation of the interface stiffness were: $E_a$=7000MPa, υ=0.3 and $t_a$=1.75mm, the latter value lying between 1.5mm and 2.0mm. Thus, according to eqs. (4) and (5),we obtain $k_n$=4000MPa/mm and $k_s$=1500MPa/mm.

The value of the cohesion was defined taking into account the dependence, mentioned in several works as seen in Neto (2003), between this value and the mean value of the concrete tensile strength. A cohesion value c=7MPa was adopted. The value of $f_t$ corresponds to the tests results by Dias et al. (2002).

For the mode II fracture energy, a value $G_F^{II}$=1.5N/mm was defined; this value was predicted taking in to account that the concrete used in this study presents higher mechanical characteristics than the one considered in Neto et al. (2004). Assuming a relation $G_F^{II}/G_F$=10 (Täljsten (1994)), we obtain $G_F$=0.15 N/mm.

Next, a numerical study of the behaviour of the beam strengthened with CFRP was performed. The distribution of stresses obtained with the finite element method is represented in Figures 6 to 10. It is possible to notice that shear stress distribution is similar to the one obtained in a pure shear model (Neto et al. (2004)). In the extremity of the CFRP, normal stresses appear. These stresses are tensile stresses along a small length, becoming compressive stress afterwards, almost vanishing along a length of approximately 10mm. This result is confirmed by Rabinovich et al. (2000), who claims that this distance corresponds to 3-4 times the adhesive thickness. High interfacial stresses can be observed in this region (Figures 9 and 10). Along the beam span there are also interfacial stresses (shear stresses), as shown in the Figures 6 to 8, presenting elastic values, caused by the beam deformation.

The maxim value of P was 43.3kN, corresponding to a much larger value than the one experimentally observed. As a consequence, it can be concluded that this local failure mode is not important here. This result seems to be in accordance with the result experimentally observed. The observed behaviour in an experimental model, which only differs from the numerical model in the introduction of exterior fixation mechanisms in the extremity of the laminate, was quite similar to the presented one.

In order to analyse the importance of each material parameter which influences the bond behaviour, a parametric study was performed; the corresponding results are presented in Table 1. From Table 1 it can be concluded that the cohesion is the material parameter which presents a more pronounced influence on the resistance of the connection. Interestingly, in Neto et al. (2004) it was found that the most important parameter influencing the strength of the connection was the fracture energy. In comparison to a pure shear model, the shear stresses are distributed along a bigger length, as shown in Figures 6 to 10, due to the bending deformation. The stresses along the span region are elastic. Within the elastic limit, the cohesion is the parameter which contributes most to the noticed variations of the maximum load (Figure 10b)). The peeling stresses are present in a much reduced length compared to the shear stresses, the fracture energy playing a more important role than $f_t$.

Table 1 – Influence of the material parameters in the value of the beam maximum load.

| $k_n$/4000 | **0.1** | **10.0** | 1.0 | 1.0 | 1.0 | 1.0 | 1.0 | 1.0 | 1.0 | 1.0 | 1.0 | 1.0 |
|---|---|---|---|---|---|---|---|---|---|---|---|---|
| $k_s$/1500 | 1.0 | 1.0 | **0.10** | **10.0** | 1.0 | 1.0 | 1.0 | 1.0 | 1.0 | 1.0 | 1.0 | 1.0 |
| $f_t$/4.0 | 1.0 | 1.0 | 1.0 | 1.0 | **0.3** | **0.5** | **0.3** | 1.0 | 1.0 | 1.0 | 1.0 | 1.0 |
| $c$/7.0 | 1.0 | 1.0 | 1.0 | 1.0 | 1.0 | 1.0 | **0.2** | **1.4** | 1.0 | 1.0 | 1.0 | 1.0 |
| $G_F^I$ /0.15 | 1.0 | 1.0 | 1.0 | 1.0 | 1.0 | 1.0 | 1.0 | 1.0 | **0.1** | **10.0** | 1.0 | 1.0 |
| $G_F^{II}$ /1.50 | 1.0 | 1.0 | 1.0 | 1.0 | 1.0 | 1.0 | 1.0 | 1.0 | 1.0 | 1.0 | **0.5** | **2.0** |
| $P_{max}$/43.3 | **1.0** | **1.0** | **1.0** | **1.0** | **1.0** | **1.1** | **0.4** | **1.2** | **0.6** | **1.1** | **0.9** | **1.1** |

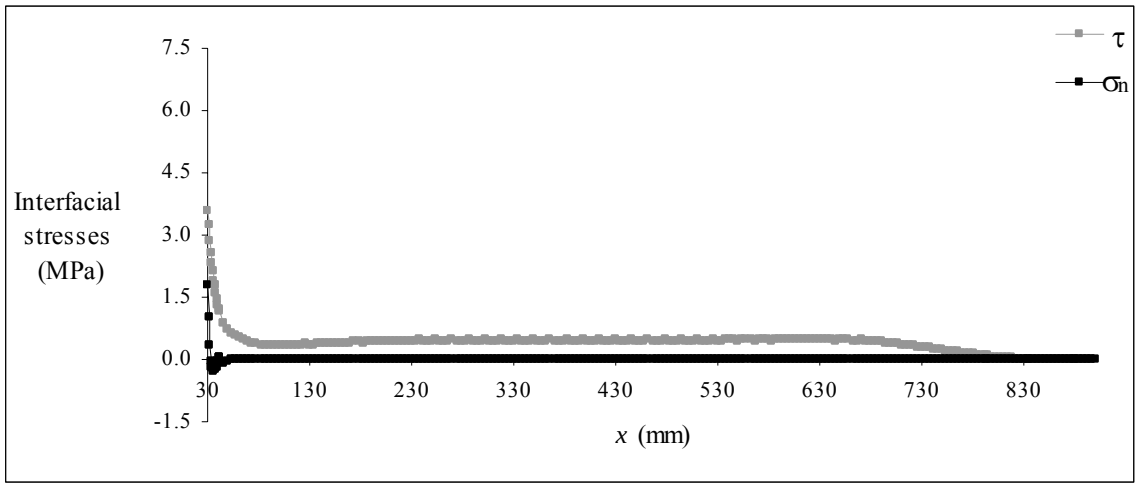



Figure 6 – Interfacial stresses along the beam with $P_{max}$=13.0kN ($t_f$=1.4mm).

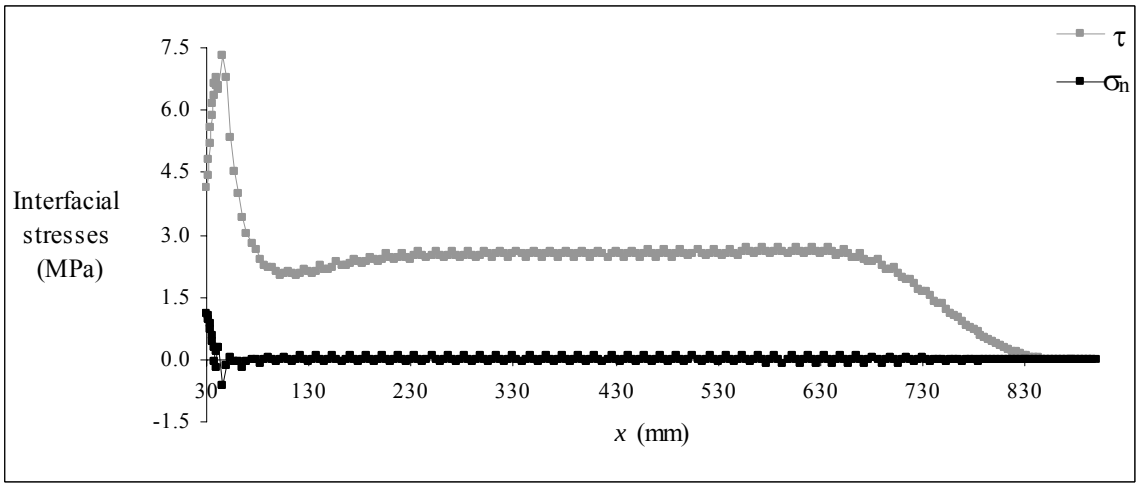



Figure 7 – Interfacial stresses along the beam with $P_{max}$=27.7kN ($t_f$=1.4mm).

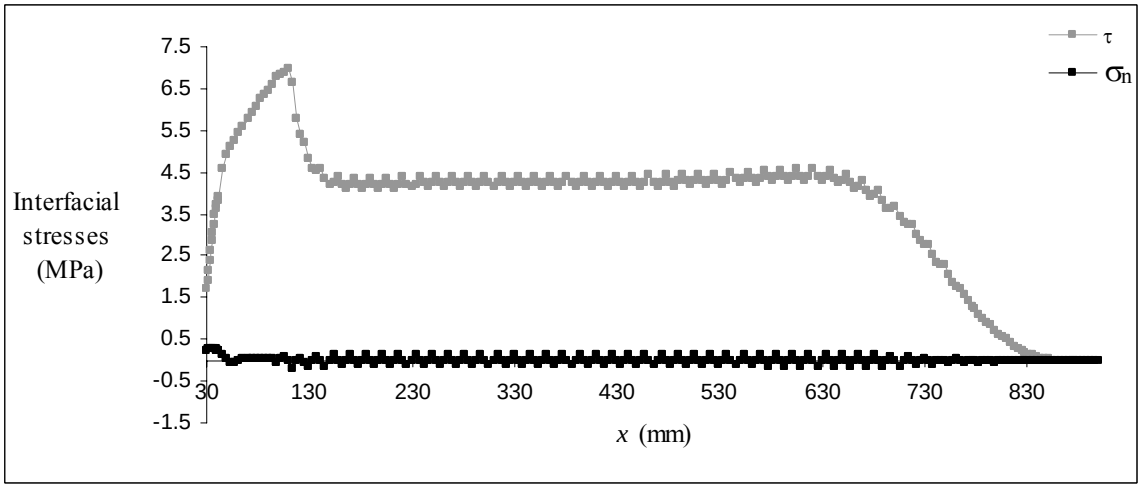



Figure 8 – Interfacial stresses along the beam with $P_{max}$=41.9kN ($t_f$=1.4mm).

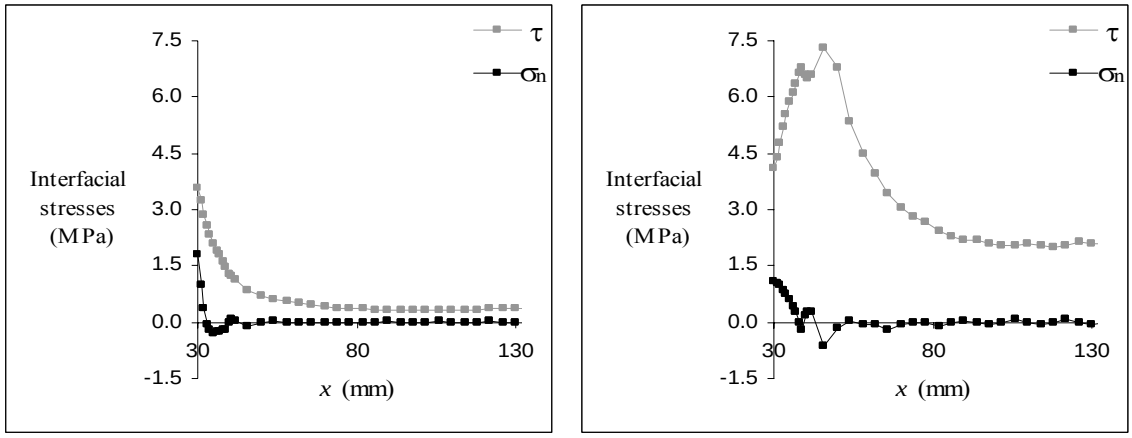



Figure 9 – Detail of the interfacial stresses ($t_f$=1.4mm): (a) $P_{max}$=7.2kN, (b) $P_{max}$=27.7kN.

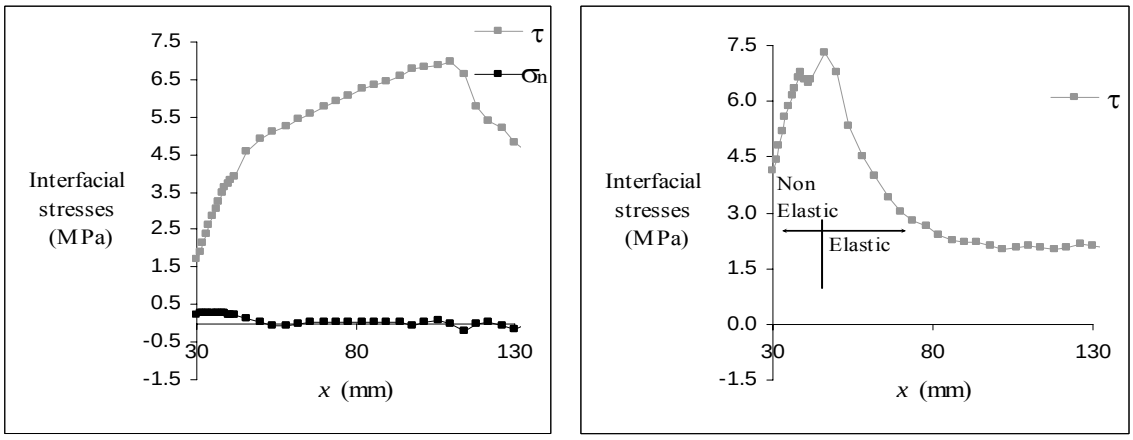



Figure 10 – (a) Detail of the interfacial stresses ($t_f$=1.4mm): $P_{max}$=41.9kN, (b) Distinction between elastic and non elastic phase.

Note that one of the cases corresponded to considerer c=1.5MPa and $f_t$=1.0MPa, since $f_t$>c would be physically unacceptable. In this case the rupture occurred for $P_{max}$=18.4kN, around 40% of the value of the maximum load obtained for the initially defined parameters. This reduction is due to a shrinkage of the surface limit (Figure 3) since $f_t$ and c decreased simultaneously. This value of $P_{max}$ is approximately equal to the experimental value. Thus, the methodology presented by Malek et al. (1998) for the evaluation of the maximum interfacial stresses was applied with c=1.5MPa and $f_t$=1.0MPa. The stress values obtained at *x*=30mm were: $\tau_{max}$=1.5MPa and $\sigma_{n,max}$=0.8MPa. This author considers complete composite action between plate and concrete. The distribution of stresses along the span corresponds to the limit of the elastic phase. The elastic fraction of the load is approximately 16% of the maximum load value, which shows that the resistance of the connection is poorly mobilized.

The small stress concentration found in the laminate end of the beam may be due to the fact that the composite thickness is small enough to mobilize peeling stresses leading to failure.

With the objective of evaluating the importance of the thickness of the reinforcement a similar analysis is next described, considering now $t_f$=6mm. This value of the thickness was chosen based on Malek's et al. (1998) work. The numerical distribution of stresses is shown in Figures 11 to 15. Peeling stresses are present at the plate end, together with shear stress

concentrations (Figures 14 and 15). Along the span, elastic shear stresses at the interface are also present due to the beam deformation. From Figures 11 to 15 can be observed that peeling stresses plays a more important role than the one considering $t_f$ =1.4mm.

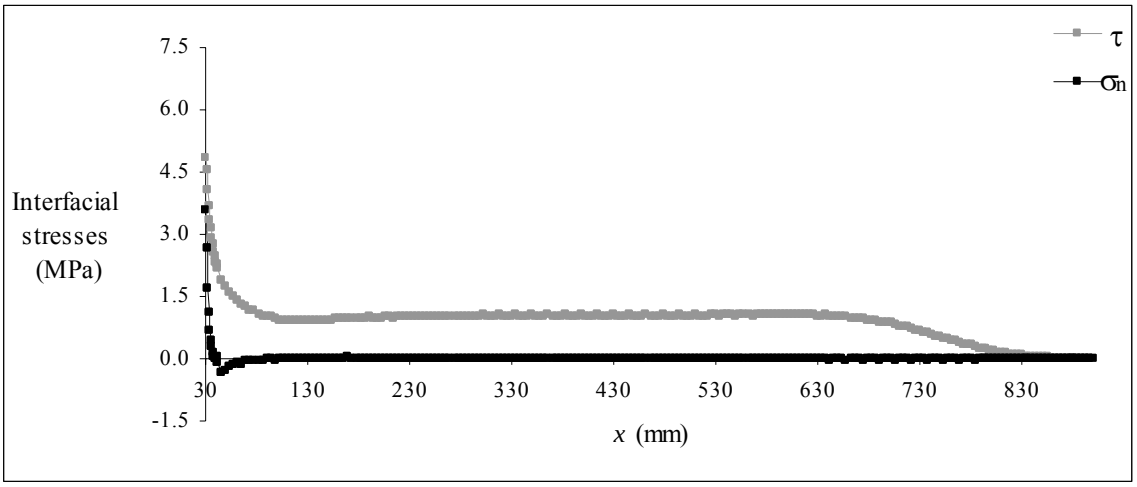



Figure 11 – Interfacial stresses along the beam with $P_{max}$=5.7kN ($t_f$=6.0mm).

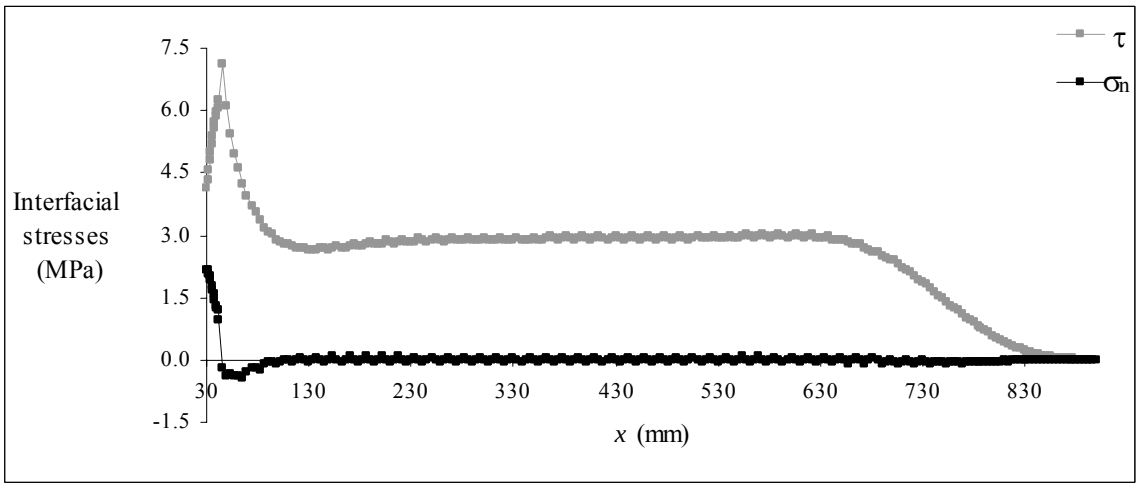



Figure 12 – Interfacial stresses along the beam with $P_{max}$=15.5N ($t_f$=6.0mm).

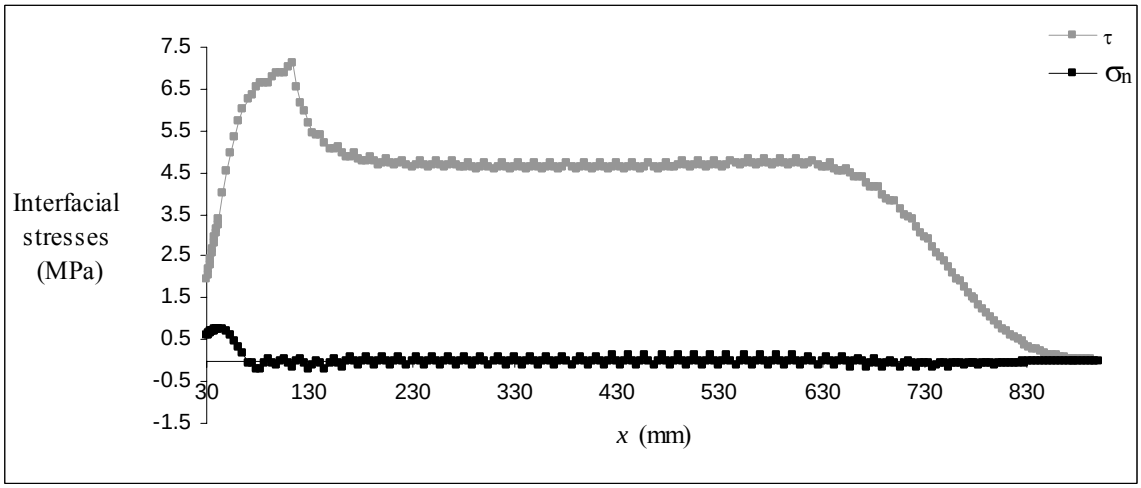



Figure 13 – Interfacial stresses along the beam with $P_{max}$=22.0kN ($t_f$=6.0mm).

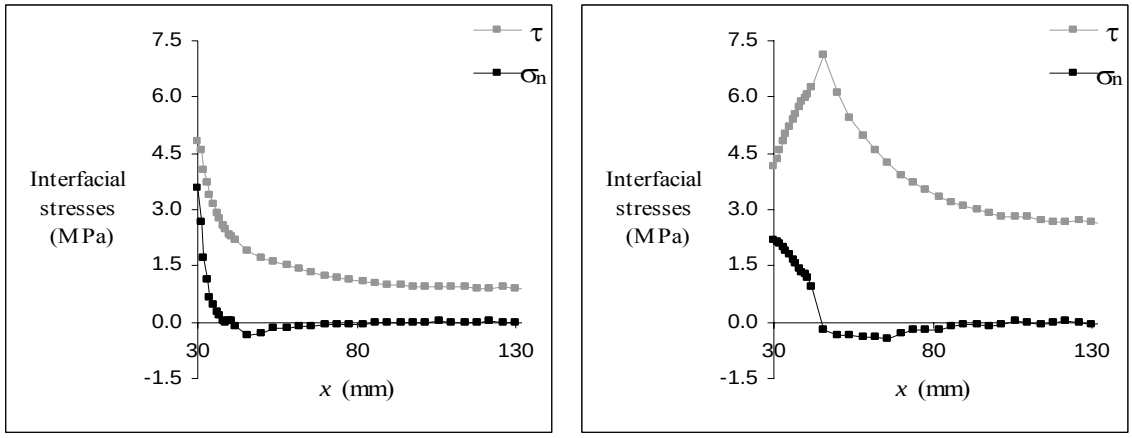



Figure 14 – Detail of the interfacial stresses ($t_f$=6.0mm): (a) $P_{max}$=5.7kN, (b) $P_{max}$=15.5kN.

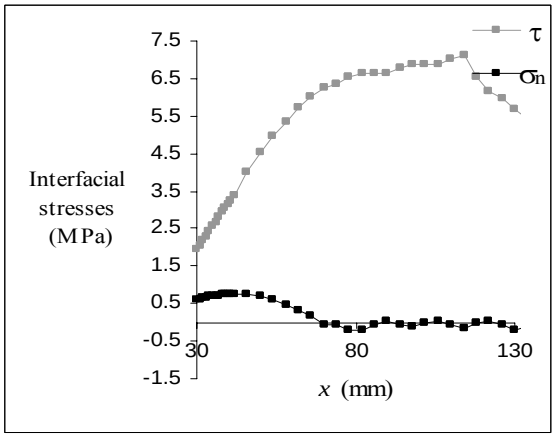



Figure 15 – Detail of the interfacial stresses ($t_f$=6.0mm): $P_{max}$=22.0kN.

The maximum load was now equal to 23.0kN, circa 53% of the previous value (43.3kN). Thus, in spite of the greater reinforcement area, the strength of the beam has decreased due to the increase of the thickness of the laminate, giving rise to higher peeling stresses. In the Figure 16 a detail of the finite element mesh in the FRP end is presented, showing the laminate detachment.

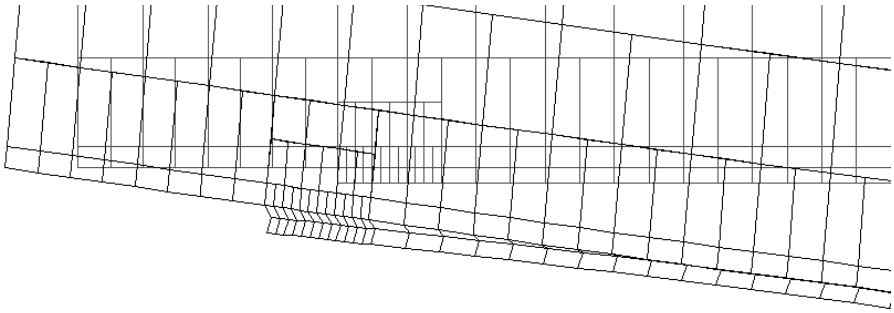


Figure 16 – Detail of the detachment in the CFRP end.

In order to better understand the influence of the reinforcement dimensions, the CFRP width was increased to $b_f$=85.7mm taking $t_f$=1.4mm, thus keeping the same reinforcement area as before ($t_f$=6mm, $b_f$=20mm). The maximum load obtained was now $P_{max}$=62kN, more than 2.5 times the load capacity obtained with $t_f$=6mm. This value was also higher than the

one obtained with $t_f$=1.4mm and $b_f$=20mm. From these results it can be concluded that, whenever possible, it is preferable to increase the width instead of the thickness of the CFRP. Moreover, more layers are more difficult to execute.

From the parametric study performed, the results obtained with $t_f$=6mm and $b_f$=20mm were similar to the ones presented in Table 1. Note that the maximum value P=23kN, although still higher than the experimental maximum value, is closer to this one; nevertheless, the reinforcement areas are distinct.

## 4. CONCLUSIONS

The research focused on the computational modelling, based on non-linear fracture mechanics, of the stress distribution in the FRP-concrete interface at the plate end of a bending beam.

The material properties used in the characterization of the interface behaviour, were: the shear and peeling stiffness, the cohesion, the tensile strength and the fracture energy in modes I and II.

The shear stress distribution was observed to be similar to the one obtained in a pure shear model. In the CFRP end, normal stresses to the interface appear. These stresses are first tensile in a small length, changing into compressive stresses and almost vanishing in a length of approximately 10mm. High interfacial stresses can be observed in this region.

The maximum value of P was much larger than the experimentally observed, which can be concluded that this is a non important local failure mode in this case.

The cohesion is the material parameter which influences most the resistance of the connection. The fracture energy assumes a less important role than the one observed in the pure shear models. In mode I, the fracture energy plays a more important role than $f_t$. From this study a ratio of $G_F^{II}/G_F$ between 10 and15 seems adequate.

The simultaneous variation of $f_t$ and c shows a bigger influence in the variation of the maximum load.

According to the methodology presented by Malek et al. (1998) for the calculation of the maximum interfacial stresses, these occur for the limit elastic value of the load, approximately 16% of the maximum value. As a consequence, it can be concluded that the resistance of the connection is poorly mobilized.

The stress concentration noticed in the laminate end of the beam is found to play a non important role in the global behaviour of he beam; in fact, the composite thickness is less than adequate to mobilize peeling stresses capable leading to failure.

Admitting the possibility of mode II fracture taking place, according to the methodology presented in Neto (2003) based on the rectangular simplified diagram method, the obtained maximum load was 81% of the theoretical value. In accordance with the above mentioned work, the theoretical value of the maximum load is, in general, smaller than the real value. Thus, it is possible to conclude that mode II fracture is important in beams reinforced with FRP, because, in general, the thickness considered is small. Applying this model (Neto (2003)) to the beam without external reinforcement, it is found that the maximum theoretical and experimental loads perfectly match.

The methodologies presents in the FIB report 14 (FIB (2001)) only consider the mode II of fracture, which is adapted to the general cases with FRP reinforcement, taking into account the small thickness adopted.

The maximum load with $t_f$=6mm was around 53% of the value referring to $t_f$ =1.4mm due to the increase of the peeling stresses.

The importance of the stress concentration in the failure of the bending beam was observed for high thickness of the reinforcement, and this is why mechanisms of anchorage are adopted when metal plates are used.

Finally, it was also possible to conclude that, whenever possible, it is preferable to increase the width instead of the thickness of the CFRP. This option also leads to a less amount of material, consequently, less cost. Moreover, more layers are more difficult to execute.

## 5. REFERENCES

Alfaiate, J. and Pires, E.B., Mode I and mixed mode non-prescribed discrete crack propagation in concrete, in: *Proceedings of FRAMCOS-3*, Eds. by H. Mihashi and K. Rokugo, Japan, **2**, 739-748 (1998).

Alfaiate, J., Almeida, J. R., Crack Evolution in Confined Masonry Walls, , in: *Proceedings Computational Mechanics: New Trends and Applications*, Eds. By S.R. Idelshon, E. Oñate and E. Dvorkin, CIMNE, Barcelona, (1998)

Bazant, Z.P. and Pfeiffer, P.A., Shear fracture tests of concrete, *Materials and Structures*, **19**, 111-121 (1986).

Dias, S., Juvandes, L. and Figueiras, J., *Comportamento experimental de vigas de betão armado reforçadas à flexão com sistemas compósitos de CFRP do tipo Mbrace*, relatório técnico, LABEST, Faculdade e Engenharia da Universidade do Porto (2002).

FIB (CEB-FIP), *Technical report on the design and use of externally bonded fibre reinforced polymer reinforcement (FRP EBR) for reinforced concrete structures - externally bonded FRP reinforcement for RC structures*. Fedération International du Béton, Bulletin 14, (2001).

Gálvez, J.C., Cendón, D.A., Planas J., Guinea, G.V. and Elices, M., Fracture of concrete under mixed loading - experimental results and numerical prediction, in: *Proceedings of FRAMCOS-3*, Eds. by H. Mihashi and K. Rokugo, Japan, **2**, 729-738 (1998).

Hillerborg, A., Modeer M. and Petersson P.E., Analysis of crack formation and crack growth in concrete by means of fracture mechanics and finite elements, *Cement and Concrete Research*, **6**, 773-782 (1976).

Lourenço, P.B. and Rots, J.G., A multi-surface interface model for the analysis of masonry structures, *ASCE Journal of Engineering Mechanics,* **123(7)**, 660-668 (1997).

Malek, A. M., Saadatmanesh, H. and Mohammad, R. E., Prediction of failure load of rc beams strengthened with FRP plate due to stress concentration at the plate end, *ACI Structural Journal*, **95(2)**, 142-152 (1998).

Neto, P., Alfaiate, J., Almeida, J.R., Pires, E.B., The influence of mode II fracture on concrete strengthened with CFRP, *Computers & Structures*, **82(17-19),** 1495-1502, (2004).

Neto, P., Estudo numérico da ligação betão-CFRP. MSc. Thesis (in press), Instituto Superior Técnico, Universidade Técnica de Lisboa (2003).

Ozbolt, J., Reinhardt, H.W. and Xu, S., Numerical studies of the double-edge notched mode II geometry, in: *Proceedings of FRAMCOS-3*, Eds. by H. Mihashi and K. Rokugo, **2**, 773-782, Japan, (1998).

Rabinovitch, O. and Frostig, Y., Closed-form high-order analysis of rc beams strengthened with FRP strips, *ASCE Journal of Composites for Construction*, **4(2)**, 65-74 (2000).

Täljsten, B., *Plate bonding – strengthening of existing concrete structures with epoxy bonded plates of steel or fibre reinforced plastics*, Doctoral Thesis, Division of Structural Engineering, Lulea University of Technology (1994).

International Symposium Polymers in Concrete
2 - 4 April 2006
Guimarães, Portugal

# The Study of the Performance of Present Models for the Concrete Reinforced by CFRP Sheets

**Nourivand A.**[1], **Majolan A. S.**[1] , **Chahardeh A. S.**[1]

*Young Researcher Club ,Islamic Azad University of Shabestar, Iran*

ABSTRACT

Nowadays close attention is paid to using CFRP in all parts of the world , and for this , there were a lot of research has been done to design of stress-strain diagram and to devise a mathematical model for predicting reaction of concrete using CFRP . This paper aims to evaluate the present models dealing with concrete reinforced by CFRP. First the exclusive feature of any of the models will be explained and then the maximum stress and strain of the laboratory samples will be compared with the calculated results of the models. The results indicate that the calculations ultimate axial stress and strain in some of the models display a considerable difference with the test results and the results of the few models are closer to the test results.

## 1. INTRODUCTION

Nowadays The benefit and use of CFRP comparing with other consolidators are more attracted. carbon is an element with a density of 2.27 grams per $cm^3$ and in different crystal shapes , with regard to different privileges and benefit of carbon it way be denoted to its high Stress Resistance ,Very low weights ,High performance on fatigue resistance, Resistance toward corrosion, Suitable formability and its resistance to high temperature.
In recent years very extensive studies to define stress-strain diagram and also providing mathematical model have been achieved especially for anticipation of concrete behavior when are strengthened. In this study four models are presented by (Xiao & Wo) (Lam & Teng), (Toutanji),(Mostofinejad) are evaluated . For this work , 100 laboratory results for other researcher are used.

## 2. STUDY OF STRENGTHENED STRUCTURES USING FRP

There are different factors which raised the demand for structure reinforced, among these items, increasing the age of concrete structures, weakness of structures in response to earthquakes and changes of structural forms could be noted .

---

[1] Engineer

One of suitable techniqueto strengthen is using FRP sheets. These sheets due to their high resistance, against corrosion, flexibility speed in operating and application are attracted. Low weight of FRP sheet Is one of The Most important Factors.
One square meter of FRP sheets, including its dried paste is less than 500 grams, but one square meter of a metal sheet with a thickness of 10 millimeter is about 75 kg, which is equal to 150 sheet of FRP. If we use 5 layers of CFRP. Around a pillar of a structure we may have 30% Increase on resistance, and with laying of 10 layers of CFRP sheet we have 60% increase in strength. One of the condition to use FRP sheets to strength structures is to improve the strength of base layer because the lower layer should have adequate resistance so as to be able to provide necessary adhesiveness to FRP sheets. Tensional resistance of base layer should be at least 4 MPa. In this respect appropriate study has been introduced by ACI 503R. the minimum pressure resistance of base layer should not be less than 17MPa. To confined the concrete by FRP sheet is one of the effective method to improve strain diagram and increase of resistance and formability of concrete. This increase of resistance is due to prevention of expansion lateral cracks in concrete. Figure(1) shows the procedure application pressure concrete core reinforced with FRP

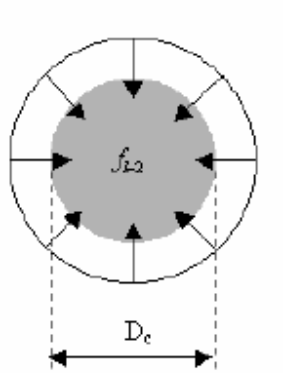



Figure 1 – The procedure application pressure concrete core reinforced with FRP

## 3. COMPARISON OF STRESS-STRAIN DIAGRAM IN STEEL AND FRP

At the beginning the scientist tried to change steel model so as to prepare them to use FRP like models of Fardis&Khalili , Ahmad & et. , saadatmanesh & et. which are based on steel models.
As figures (2) shows. The stress strain diagram which are confined by steel in opposition with figure (3), after reaching to maximum value have deckling slope. Diagram of figure 3 which shows the behavior of concrete by FRP. This diagram has two section, first section relates to linear section and the section is relating to plastic area. The slope of linear section of diagram is similar to the slope of linear section of unconfined concrete. The reason is that the concrete in lesser burden has less lateral expansion, therefore due to confined pressure the FRP will not activated.

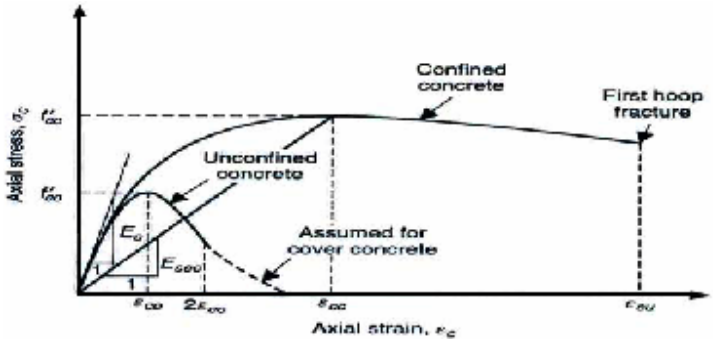



figure 2 – Stress and strain diagram of confined concrete by steel

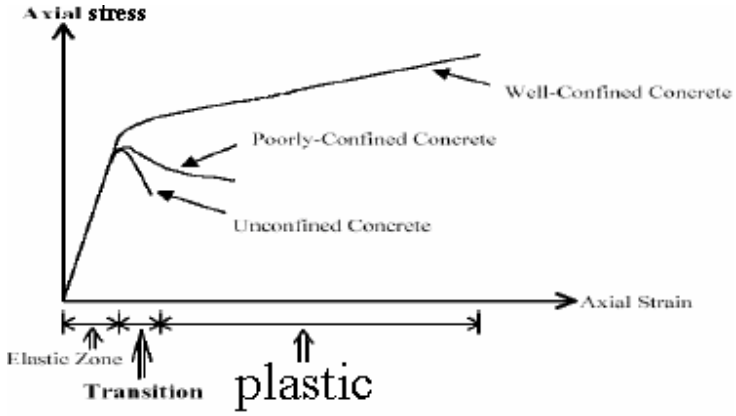



figure 3 – Stress and strain diagram of confined concrete by FRP

## 4. EVALUATION OF THE OTHER RESEARCHER MODELS

According to different researches based on 100 laboratory results from Pessiki ,Watenable, Xiao &Wo, Toutanji , Harmon & Slattery , Shahawy, these results containing different parameter as follows:

- resistance pressure ($f_c$) between 22 - 55 MPa
- diameter of models (d) varies from 51 - 152 mm
- the relation between length and diameter of model (l/d) is about 2 - 4
- type of reinforced polymer is CFRP sheet
- thickness of composite ($t_{FRP}$)varies from 0.18 – 2 mm
- composite hardness($E_{FRP}$) varies from 38.1 – 630 GPa
- maximum strian resistance of the flat model ($f_{FRP}$) is 580-3485 MPa.

### 4.1. EVALUATION OF TOUTANJI MODEL

in 1999 Toutanji made difference on CFRP, GFRP. He acquired increase of maximum stress on confined columns in relation to unconfined column by GFRP which were about 100% and for CFRP about 200% .

the specification or the characteristic of presented model by Toutanji is that the diagram are formed in two different area . in first area the behavior of confined cylinder due to lesser value of expansion in the concrete core has not remarkable difference with unconfined part. In second part FRP will be active completely and the behavior vigorously affects under the confined systems. In this model the value of lateral pressures are defined according to cylindrical strain. As a result the maximum stress will be calculated according to circular or cylindrical rapture strain.
We also for evaluation of model have used the method of lateral rapture strain "$\varepsilon_h$" . In this model maximum axial stress of concrete "$f_{cc}$" will resulted for No (1) equation and maximum strain "$\varepsilon_{cc}$" from No (3) equation.

$$f_{cc} = f_c' + k_1\left(\frac{2E_{frp}t_{frp}\varepsilon_h}{D}\right) \quad (1)$$

$$K_1 = 3.5\left(\frac{2E_{frp}t_{frp}\varepsilon_h}{f_c'D}\right)^{-0.15} \quad (2)$$

$$\varepsilon_{cc} = \varepsilon_o\left[1 + k_2\left(\frac{f_{cc}}{f_c'} - 1\right)\right] \quad (3)$$

$$k_2 = 310.57\varepsilon_h + 1.9 \quad (4)$$

The maximum axial stress acquired by Toutanji Model , comparing with surveyed models in this analysis are more closer to laboratorial results.
Average maximum axial stress acquired by Toutanji model is 8.5% which is an acceptable result. The greater difference in surveyed Toutanji model with laboratory value is about 13% that has a suitable result. In total surveyed results nearly 50% of acquired result from Toutanji model is more than laboratory value , and 50% are less than laboratory values.

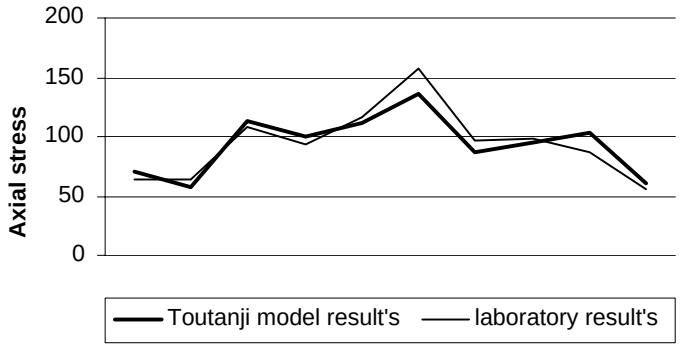



Figure 4 - comparing maximum axial stress of Toutanji model with laboratory result

The acquired value of maximum strain derived from Toutanji model for 100 laboratory examples as an average with laboratory value has a difference of 24% and most of the acquired result from this model show lesser relative value with regard to laboratory results.

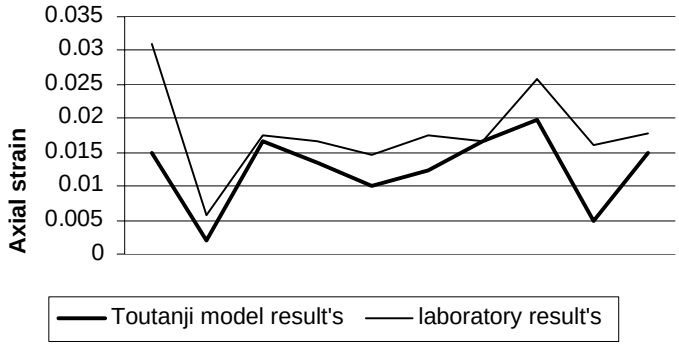



Figure 5 - comparing maximum axial starin of Toutanji model with laboratory result

## 4.2. EVALUATION OF (XIAO & WO) MODEL

In year of 2000 (Xiao & Wo) presented a relation between stress and two linear strain for confined concrete. They showed in their research that confined CFRP in concrete and in cylindrical strain has lesser effect in respect to flat strain. Therefore they recommended that in circular and rapture composite with 50% filament of carbon the proper rapture of strain of example should be attended. Maximum axial stress of this model is from equation No (5) and maximum axial strain will e acquired from equation No (6).

$$f_{cc} = 1.1 f_c' + \left( 4.1 - 0.75 \frac{f_c'^2 D}{2E_{frp} t_{frp}} \right) \times \left( \frac{2E_{frp} t_{frp}\, \varepsilon_h}{D} \right) \tag{5}$$

$$\varepsilon_h = 0.0005 + 7 \left( \frac{f_c' D}{2E_{frp} t_{frp}} \right)^{0.8} \varepsilon_{cc} \tag{6}$$

Evaluation of this model shows that difference of average of maximum axial stress with laboratory value is about 9.78% and the max difference of this model with laboratory result is 24%. Totally all surveyed showed that 70% of the results are more than the value of laboratory results.

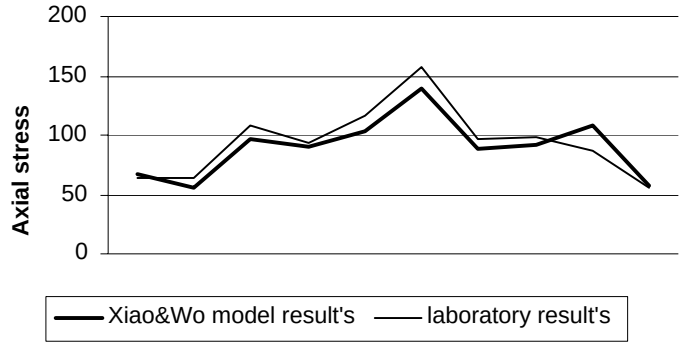



Figure 6 – comparing maximum axial stress of (Xiao&Wo) model with laboratory result

In maximum axial strain survey, the difference of average result with difference of this model to laboratory result is 52.77% as a maximum survey, the total results, nearly 90% of the value acquired from these models are more than the laboratory results.

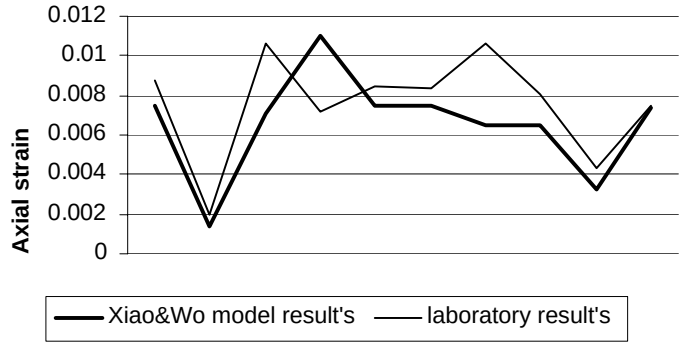



Figure 7 - comparing maximum axial strain of (Xiao&Wo) model with laboratory result

## 4.3. EVALUATION OF (Lam & Teng ) Model

Lam and Teng with other survey and according to 200 Laboratory example, introduced a model in which calculation of confined pressure without paying attention to early rapture of composite which are viscosed to column. Stress and maximum strain in lam & tang model will achieved by formula No (7) and No (8)

$$f_{cc} = f_c' + 2\left(\frac{2F_{frp}t_{frp}}{D}\right) \tag{7}$$

$$\varepsilon_{cc} = 0.002\left(1.75 + 10\left(\frac{2f_{frp}t_{frp}}{Df_c'}\right)\right) \tag{8}$$

Assessment of lam and teng model shows that the average difference of maximum stress pressure of this model in relation to laboratory value is 12% and the most percent of calculated error of this model in relation to laboratory result is 27% maximally the assessed which are surveyed showed that %90 of the results are less than the value of laboratory results.

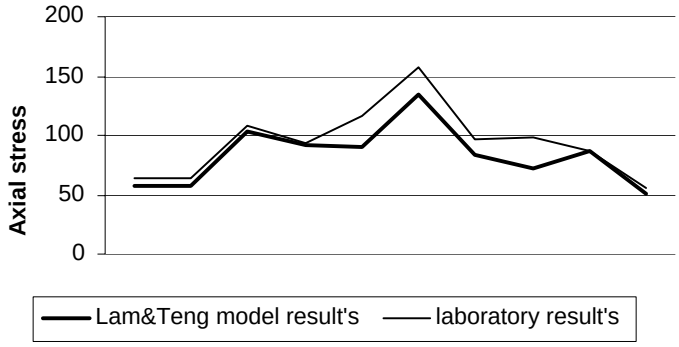



Figure 8 - comparing maximum axial stress of (Lam&Teng) model with laboratory result

In assessment of maximum axial strain also the average maximum difference in relation to laboratory results is 19.73% that has the maximum difference derived from model 72.4% . that shows a great difference . It is interesting to declare that this model with regard to other surveyed model. In this survey calculate more precise survey for maximum average axial strain but some time there is a significant differences. In general all surveyed relation show us that in 70% of cases we can see lesser value in relation to laboratory result and 30% of case more.

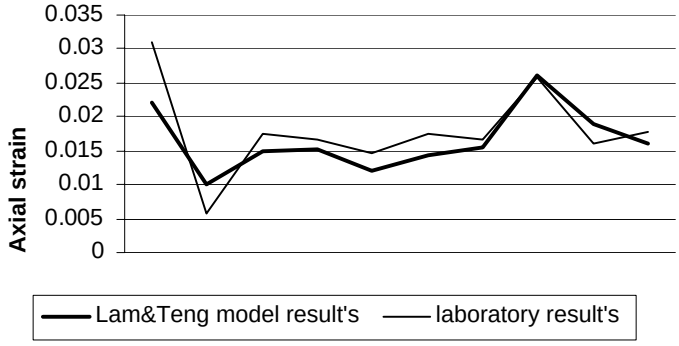



Figure 9 - comparing maximum axial strain of (Lam&Teng) model with laboratory result

## 4.4. EVALUATION OF MOSTOFINEJAD MODEL

In year of 2004 Mostofinejad with evaluation and research and with regard to result of exam presented a model in which the stress and strain of confined concrete by FRP was similar to a two line diagram in which intersection point of linear section of second part of diagram with axial stress is defined as $f_o$ . figure No 10.

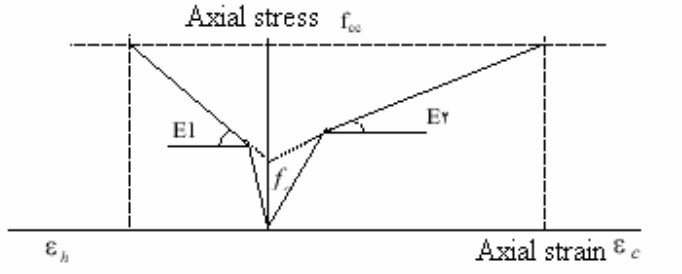



Figure 10 – Confined concrete's stress and strain diagram of Mostofinejad model

in this figure $E_1$,$E_2$ are the second part of linear section of stress and strain diagram , also are in same status with side strain cure and its related diagram in respect to axial strain presented relation by Mostofinejad for maximum axial stress and strain are as follows .

$$f_{cc} = E_1 \times \varepsilon_h + f_o \tag{9}$$

$$f_o = -5.1 + 1.239\, f_c' + 0.0708\left(\varepsilon_{frp} t_{frp} / D f_c'\right) \tag{10}$$

$$E_1 = 4189.7 \ln\left(E_{frp} t_{frp} / D f_c'\right) - 7228.4 \tag{11}$$

$$\frac{\varepsilon_h}{\varepsilon_c} = 7.1925 \frac{f_c^{0.7} D^{0.5}}{\left(E_{frp} t_{frp}\right)^{0.7} \varepsilon_t^{0.04}} + 0.0288 \tag{121}$$

According to research by Mostofinejad model, the average of maximum stress with regard to laboratory value are 14.46% and the maximum difference from this model to laboratory results are 30%. from 60% calculated resulted from this model we can observe lesser value to laboratory result.




Figure 11 - comparing maximum axial stress of Mostofinejad model with laboratory result

In a survey on maximum axial strain the average difference in comparison with to laboratory result is 25.5% as a final conclusion in 90% of cases we reach to a less number in relation to laboratory result.

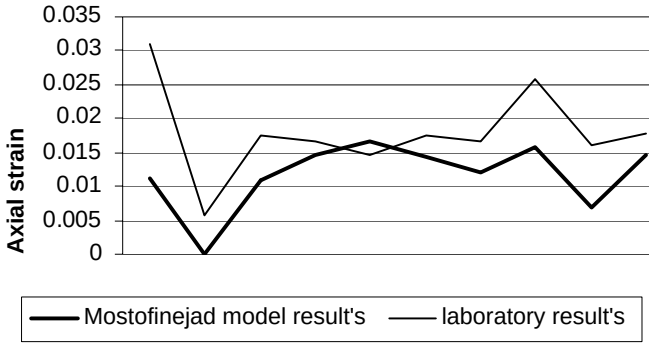



Figure 12 - comparing maximum axial strain of Mostofinejad model with laboratory result

## 5. CONCLUSION

In the four models which were evaluated in this paper , comparing between Average difference calculated model value and labratoary result for maximum axial stress are Toutanji 8.5% ,Xiao&Wo 9.78% , Lam&Tang 11.93% and 15% for Mostofinejad. The most error calculated by models is from Mostofinejad, by an error of 30% . in maximum axial strain, therefore are extensive difference with regards to laboratory results . The most difference belongs to Lam&teng model with a difference of 72.41% .
According to classification and order Lam&teng 19.73% , Xiao&Wo model 23.89% Toutanji model 24.1% and Mostofinejad 25.5 % had difference with laboratory result. as a result in maximum axial stress, Toutanji model and in maximum axial strain the Lam&Teng model in this evaluation had a better result to other models.

## 6. REFERENCES

Demers, M ,Confinement of reinforced concrete Columns with fiber reinforced composite sheets, *Canadian journal of civil engineering* , No. 26, pp. 226-241 , (1999).

Hosseini, A , evaluation of stress and strain FRP confined concrete , *International symposium application of composite FRP in promoting of structures*, Tehran ,Iran, (2004).

Lam, L and Teng, J ,Stress-strain models for FRP-confined concrete , Hong kong polytechnic university , (2002).

Mostofinejad, D ,Presentation of some relation for design concrete model confined in FRP sheets , *International symposium application of composite FRP in promoting of structures*, Tehran ,Iran, (2004).

Pessiki , S ,Axial behavior of reinforced concrete columns confined with FRP jackets , *Journal of composites for construction*, Vol. 5, No., p p.237-245 , (2001).

Shahawy,M ,Test and modeling of carbon-wrapped concrete columns, *Journal of composites*: part B , 31, pp. 471-480, (2000).

Toutanji ,H , Stress-Strain characteristics of concrete columns externally confined with advanced fiber composite sheets , *Aci materials journal* , Vol. 96 ,No. 3,pp .397-404 (1999).

Teng, J ,FRP strengthened RC structures , john wiley & sons, LTD, (2001).

Xiao , Y and Wu , H ,Compressive behavior of concrete by carbon fiber composites jackets, *journal of material in civil engineering*, Vol. 12, pp 139-146, (2000).

International Symposium Polymers in Concrete
2 - 4 April 2006
Guimarães, Portugal

# Development of a ultrasonic system to monitor the mechanical properties of CFRP on concrete

Vincenza A.M. Luprano[1]

*ENEA - CR. Brindisi*
*SS 7 'Appia' km 714 – 72100 Brindisi, Italy*

Flavio Caretto[2]

*ENEA – CR Trisaia*
*SS Jonica 106 km 419,5 – 75026 Rotondella (Matera), Italy*

Angelo Tatì[3]

*ENEA - CR Casaccia*
*Via Anguillarese, 301 – 00060 S. Maria di Galeria – Roma (Italy)*

ABSTRACT

In this work, ultrasonic wave has been used to monitor the mechanical properties of CFRP (Carbon Fibres Reinforced Polymers) applied to concrete during freezing - thawing cycles (-10° ÷ 40° C). Aim of this work is the study of the correlation between the mechanical properties of CFRP measured by means of ultrasonic wave (non destructive method) and that one measured by means of mechanical testing during the change of environmental condition (as temperature and humidity) after cure reaction. For four months two samples of concrete with FRP applied with two different techniques as hand lay up and hand lay up plus vacuum bag were monitored with ultrasonic wave. Furthermore samples of only CFRP, epoxy resin (the same utilized for the matrix of the composite) and primer were monitored by ultrasound probes, thermocouples and LVDT to measure the thickness variation. In order to obtain information on the chemical - physical behaviour of single constituent of the composite were carried out periodically thermal, mechanical and weight analysis during the four months. At the end of the four months a correlation between mechanical properties measured by means of ultrasonic waves and the other characterizations was established.

[1] Researcher
[2] Researcher
[3] Researcher

## 1. INTRODUCTION

Non destructive testing by means of ultrasonic wave is already used to verify in situ the structural integrity of concrete in civil engineering. The characteristics of this technique are the reliability, the transportability, the simplicity and the relatively low costs. In 2004 has been also published by CNR (National Council of Research) an italian guideline for the control of defects at the interface between concrete and FRP (Fiber Reinforced Plastics) composites by means of ultrasonic testing.

FRP composites or advanced composite materials are very attractive to use in civil engineering applications, due to their high strength-to-weight and stiffness-to-weight ratios, corrosion resistance, light weight and potentially high durability. Their application is of most importance in the renewal of constructed facilities infrastructure such as buildings, bridges, pipelines, etc (Nanni, 2003). Recently, their use has increased in the rehabilitation of concrete structures, mainly due to their tailorable performance characteristics, ease of application and low life cycle costs. These characteristics and the success of structural rehabilitation measures have led to the development of new lightweight structural concepts utilizing all FRP systems or new **FRP**/**concrete** composite systems as reported in the overview of the research and development of applications of advanced composites to civil infrastructure of Van Den Einde (2003).

The planning and the application of composite materials in civil engineering does not leave out of consideration about the limits of the " reinforced system in work" (Karbhari, 2000). The state of art of the research on the composite durability under different environmental conditions shows that a lot of work had been done on the behaviour of the single constituent of the composite, but few researches have been done on the reinforced system in service. The European standard (FIB – Federation International du Beton) does not introduce any quantitative request, giving only information about the possible problems, while the USA standard (ACI – American Concrete Insitute) introduces the coefficients of reduction of the resistance of the FRP due to the aging of the composites. The problem of the aging of structural elements reinforced with FRP is qualitatively defined, it is necessary now to find quantitative characterization in situ that can optimize the existing solutions and allow the development of new approaches.

Development of efficient methodologies to determine the presence, location, and severity of hidden damage in critical structural components is an important task in the design and construction of structural health monitoring systems in aging as well as new structures as Mal (2005). In this article, an ultrasonic system to monitor the mechanical properties of CFRP on concrete is presented. The durability and the performance of CFRP-strengthened structures subjected to freezing - thawing cycles (-10° ÷ 40° C) of the CFRP itself, as well as that of the CFRP-to-concrete interface has been studied during the time.

In particular for four months two samples of concrete with FRP applied with two different techniques as hand lay up and hand lay up plus vacuum bag were monitored with ultrasonic wave. Furthermore samples of only FRP, epoxy resin (the same utilized for the matrix of the composite) and primer were monitored by ultrasound probes, thermocouples and LVDT to measure the thickness variation. In order to obtain information on the chemical - physical behaviour of single constituent of the composite were carried out periodically thermal, mechanical and weight analysis during the four months. At the end of the four months a correlation between mechanical properties measured by means of ultrasonic waves and the other characterizations was established.

## 2. EXPERIMENTAL

The materials analyzed for the present research were:

- Concrete (2 tiles of approximately 48x48cm$^2$ and thickness 5cm),
- CFRP (2 layers of carbon fibres monodirectional tissue) in epoxy resin,
- Mapei epoxy Resin (sample of 7x 10cm$^2$ and thickness of 5cm approximately),
- Mapei Primer (sample of 7x10cm$^2$ and thickness of 5cm approximately).

CFRP was applied on concrete in two different preparation processes:

- hand lay up
- hand lay up with successive application of vacuum bag with epoxy resin.

The two tiles of concrete with CFRP applied and the CFRP, epoxy resin and primer samples have been placed in an environmental chamber and submitted to freezing - thawing cycles (-10° ÷ 40°) and humidity of 90% and were monitored by means of longitudinal ultrasonic waves for 4 months. Chemical-physical characterizations on the CFRP, epoxy resin and primer samples were carried out to correlate the material behaviour with the ultrasounds monitoring in environmental chamber, as:

1. DSC (Differential Scanning Calorimeter) measurements - weeklies magazine for the measure of the Tg of epoxy resin, CFRP and primer;
2. Weight measurements - every day in order to verify the water content absorbed in epoxy resin, FRP, primer;
3. Mechanical tensile tests – every months on 5 samples of epoxy resin, FRP and primer.

## 3. ULTRASONIC MONITORING SYSTEM

The propagation of the ultrasonic waves corresponds to a dynamic mechanical deformation imposed to the material. With a piezoelectric transducer (probe) is applied to the material a deformation at the ultrasonic frequency (10 - 20MHz) and by means of the same transducer the velocity of propagation of the elastic waves and the attenuation of the amplitude of the waves can be measured as reported in Frigione (2000).

The ultrasonic monitoring system, home made, is composed from the following instrumentation:

1. Industrial computer PXI of the National Instruments with to the inner Card Switch NI PXI 2565
   Card Data Acquisition 6031 NI
   Controller NI - PXI 8186
   Pentium 4 2,2 GHz with GPIB
2. Ultrasound Instrument (ULTRAN HF401) 1 -20 MHz
3. Oscilloscope Tektronics TDS220,
4. 3 Ultrasound Probes Panametrics (10 MHz) and 2 probes Harisonic (20Mhz).,
5. 2 LVDT,
6. 4 Thermocouples

The system described allows the use of N sensors with only one ultrasonic instrument that drives one sensor for time. In this case one has been used Ultrasound instrument and 5 ultrasound probes (Panametrics (10 MHz) and Harisonic (20Mhz)). The passage from a probe to an other is possible through card PXI Switch, a device to commutation, that is made of 16 microswitch able electrically to support the impulse of excitation of the ultrasonic probe of the order of some hundreds of volts and time of some microsecond. The software, realized

in Labview, allows to program the card, switching singularly in an established interval the several probes with the instrument. The program, after to have set in action the microswitch relative to the probe, acquires ultrasonic signal in Radio Frequency (RF) through the oscilloscope and transfers the digitized signal to the PC through GPIB card. The NI 6031 Data AcQuisition (DAQ) card acquires probe signals of ultrasonic waves, temperatures and movements.
A scheme of the monitoring system is reported in table 1 and visualised in Figs.1 and 2.

Table 1 – Samples monitored by ultrasounds, LVDT, thermocouples

| Sample | Ultrasounds | LVDT | Thermocouple |
|---|---|---|---|
| Epoxy resin | X | X | X |
| Primer | X | | X |
| FRP | X | X | X |
| CFRP (hand lay up) on concrete | X | | |
| CFRP (hand lay up + vacuum bag) on concrete | X | | |

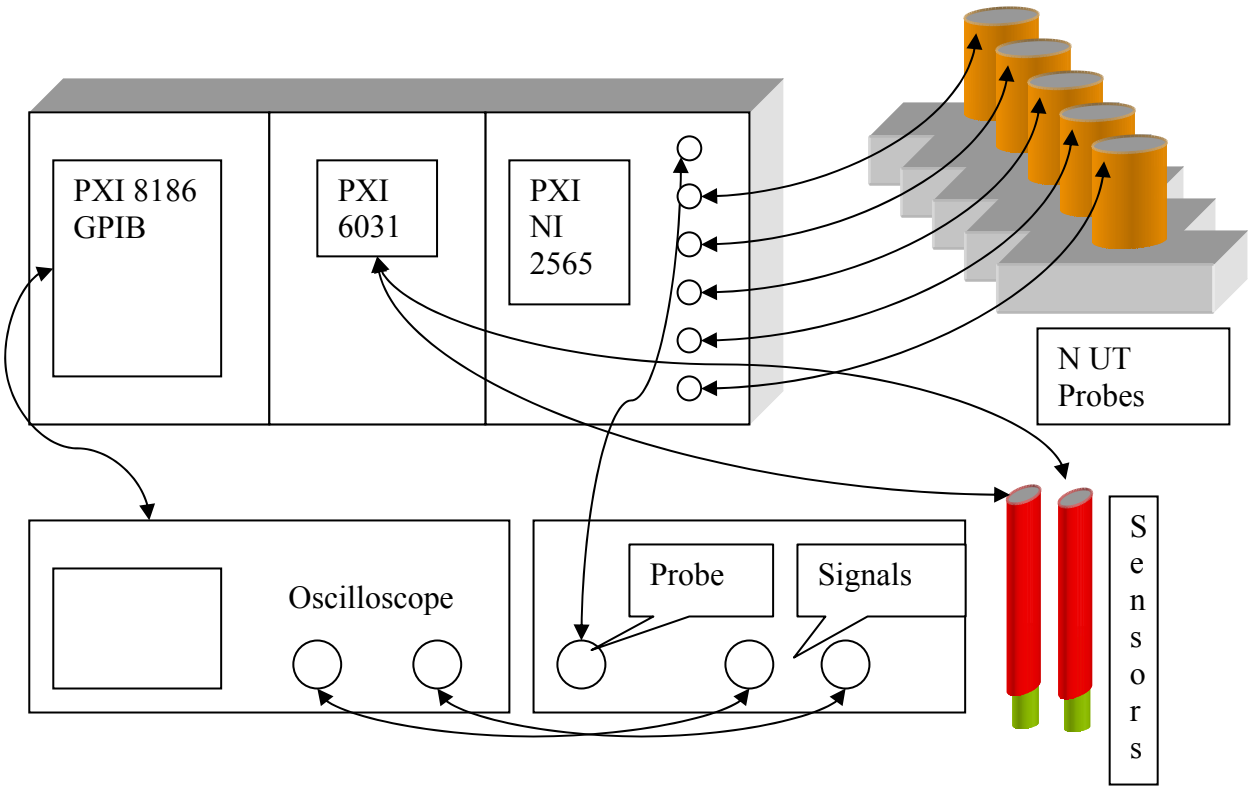



Fig. 1 Scheme of the ultrasonic monitoring system

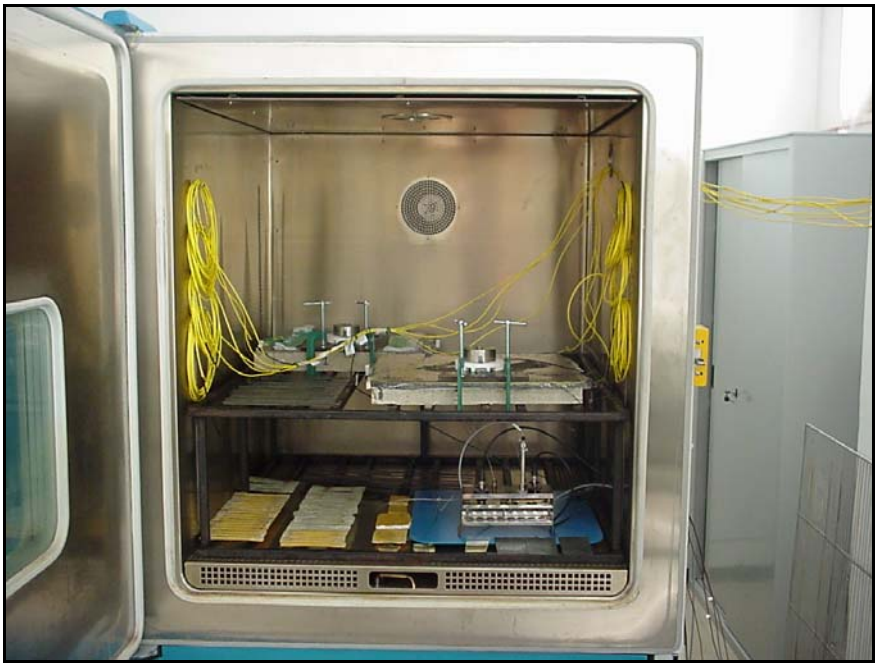


Fig. 2 Environmental chamber with the sensors system mounted on the samples

## 4. RESULTS

The samples indicate in Table 1 have been monitored during the process of aging (freezing- thawing cycles (-10° ÷ 40° C) every 24 hours – 90 % humidity ) by means of a ultrasounds system. The degradation endured from the materials has been characterized from the thermal, gravimetric and mechanical point of view. The scope was to determine a correlation between static and dynamic Young modulus, obtained respectively from the ultrasound velocity measurements, and the mechanical tensile test. In the ultrasound monitoring of the samples in reinforced concrete, particular attention has been placed in finding eventual variations on the interface of adhesion between concrete and reinforces FRP.

### 4.1 Gravimetric characterization

In order to study the water absorption of the primer, epoxy resin and composite FRP, the increase of mass of the samples $\Delta M_{rel}$ it has been represented in function of the square root of the time (eq.1).

$\Delta M_{rel}$ can be defined as:

$$\Delta M_{rel} = \frac{M_t - M_0}{M_0} x100 \qquad (1)$$

where $M_t$ e $M_0$ are the sample mass submitted to an atmosphere with relative humidity of 90%, respective to the time t e t=0.

Two samples for each material has been used, in order to have an index on the repeatability of the measurement.

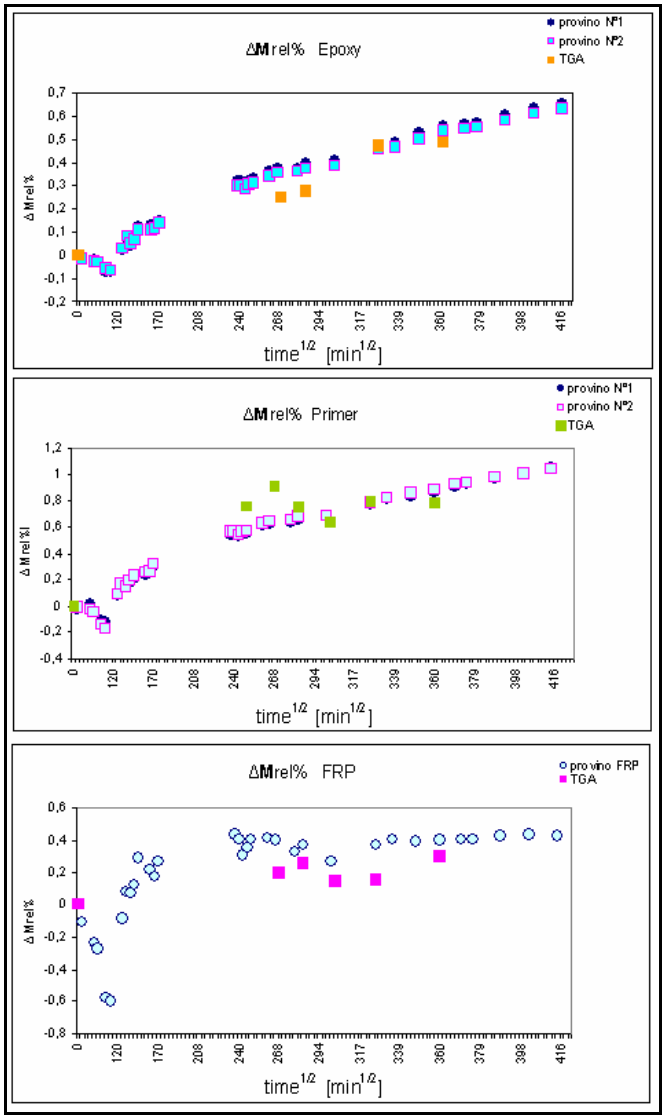



Fig. 3 Increasing of the relative mass of the samples due to the water absorption

In the graphics of fig.3, it can be noticed as at the beginning the weight of the sample decreases, because of the loss of soluble substances presents in the resins, after which it begins to increase, since becomes important the contribution of the absorbed water. The composite FRP soon goes in saturation because the sample thickness is smaller. In Fig. 3 are also reported the values of the TGA analysis, on the water content absorbed from the samples.

## 4.2 Thermal analysis

The temperature has a remarkable effect on the performances of all the polymers. An increase of the temperature of exercise can cause the approaching and the overcoming of the glass transition temperature Tg. The glass transition temperature is the temperature, or the range of temperatures, to which the polymer resin passes from a rigid (glass) state to a rubber state.

Regarding this effect, it was observed as a result of Dynamic Mechanical Analysis (DMA), technique that consists in the contemporary application of a sinusoidal oscillating stress and a

controlled program of temperatures, that, for values near the Tg, there is a decrease of the elastic modulus up to three orders of magnitude.
It is easy to understand such as the value of temperature can implies an alteration and a decay of the mechanical and adhesive property of the material. Moreover, the Tg can be decreased to even lower values in consequence of absorption of water (for exemple, atmospheric moisture) acting as plasticizing (Frigione, 2000). The glass transition temperature Tg for everyone of the materials (epoxy resin, primer and composite FRP) has been measured in the various weeks by means of DSC analysis. In Fig. 4, the Tg values measured for each material during the four months are shown.

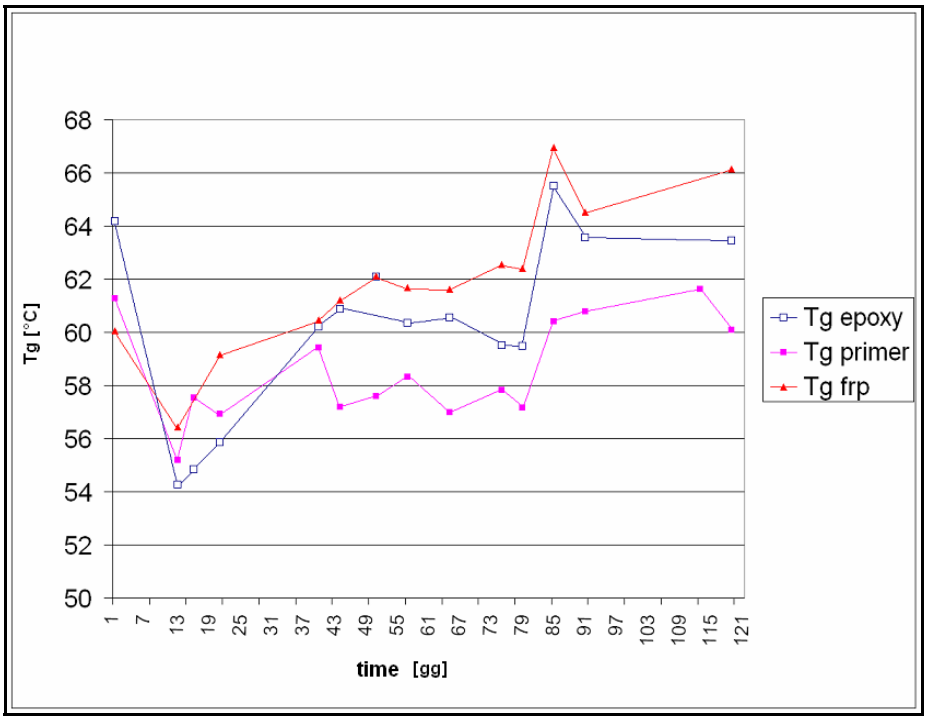



Fig. 4: Tg versus time of epoxy resin, primer and FRP

Analyzing Fig. 4, it can be observed that in the first weeks the Tg decrease due to the water absorption that produces a plasticizing effect. For longer time, an effect of post-polymerization appears, which is due to still present reactive groups in the network of the resin. This last effect produces resin cross-linking and then increases the Tg. The slowness of this reaction is explained thinking that the aging comes with cycles the whose maximum temperature is of 40°C; the resins always remain under the glass transition temperature (than medium it is around to the 60°C) and the macromolecules of the polymer are like frozen, in one state in which insufficient mobility concurs and then there is little possibility to react. We must emphasize as these variations of the Tg are however much light and not indicative of a effective aging of the analyzed material and that in any case the Tg remains over of the maximum temperature with which we have aged the materials.

## 4.3 Mechanical characterization

In order to determine the elastic modulus and the rupture strength of the materials versus the time of aging, have been executed monthly tensile tests on 5 samples carried out from the environmental chamber. In Fig. 5 epoxy and primer mechanical tests results are shown.

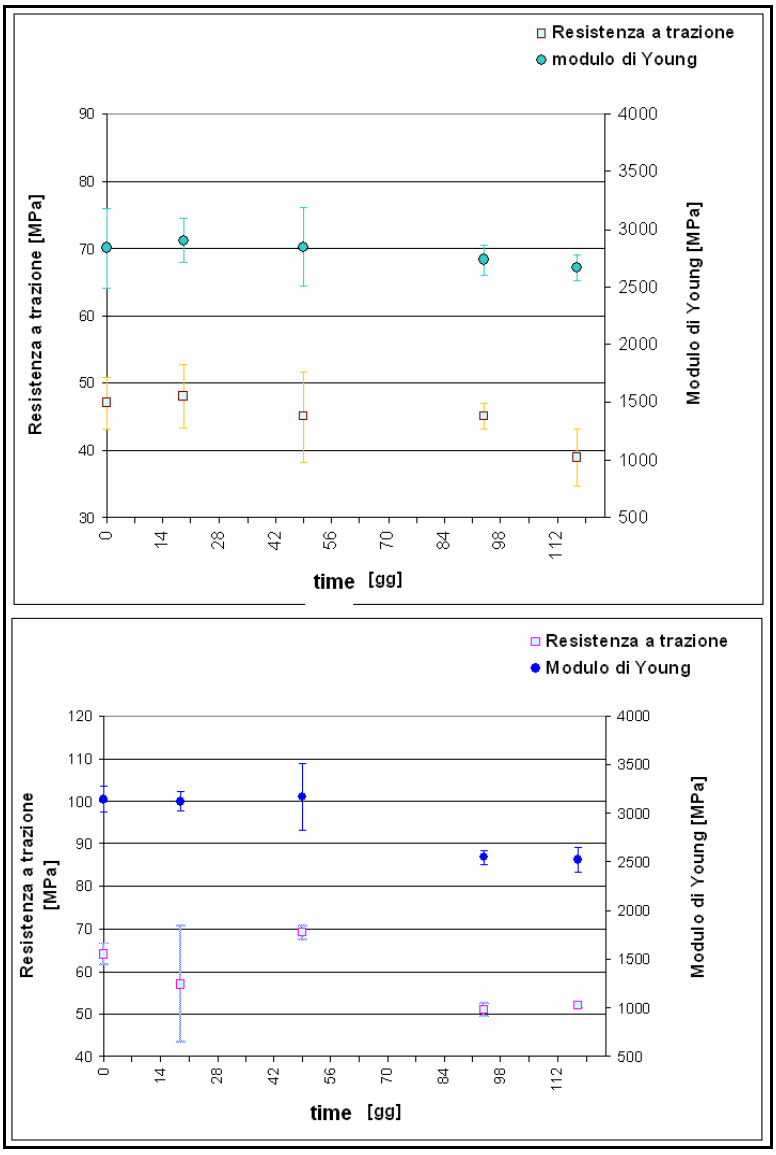



Fig. 5: Young modulus and rupture strength of epoxy resin and primer versus aging time

The CFRP Static Elastic Modulus decreased from 43412 MPa to 36522 MPa in four months for the samples made with hand lay up technology; instead for the CFRP samples made by means of hand lay up plus vacuum bag the Static Elastic Modulus decrease from 43090 MPa to 38790 MPa.

## 4.4 Ultrasonic monitoring measurements

Using the system described in par.3, it has been measured the longitudinal velocity of the ultrasounds and the variations that it endures to varying of the temperature and with passing of the time. It has been done for the samples in epoxy resin, in primer and FRP and for two reinforced tiles. For tiles, in particular, it has been attempted to see if with the aging some variation to the interface of adhesion between composite and concrete appear. For the samples in epoxy resin and FRP, moreover, the thickness d is measured in continuous, in

order to follow the variations that it endures with the temperature and the aging time, and automatically dawned from the software in the calculation of the ultrasound velocity. From fig. 6 and 7, it can be seen as the monitoring system has answered adequately.

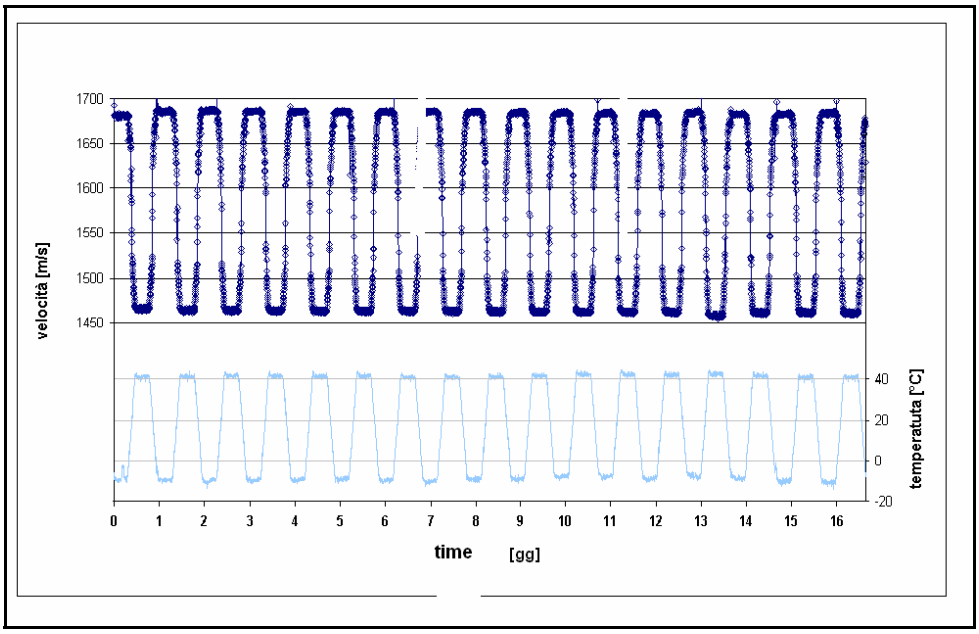



Fig. 6: Longitudinal ultrasonic velocity of epoxy resin (upper curve) and changing in the temperature (lower curve) versus aging time

There is a strict correlation between the chemical structure, physical structure and the molecular mobility of polymers and such parameters as ultrasound velocity, the coefficient of absorption of sound and the components of the complex modulus of elasticity.
The magnitude and the nature of the changes in the dynamic elastic modulus and in the ultrasonic velocity, due to the temperature, are determined both the bond energy of the atoms that form the main chain of the polymer (energy of intramolecolar interaction) and the energy of interaction between the elements of adjacent polymer chains, that is the energy of intermolecular interaction as reported by Perepechko (1975). In fig. 6 are shown the ultrasound measurements carried out on the tile in concrete, covered by means of the technology hand lay up+ vacuum bag.

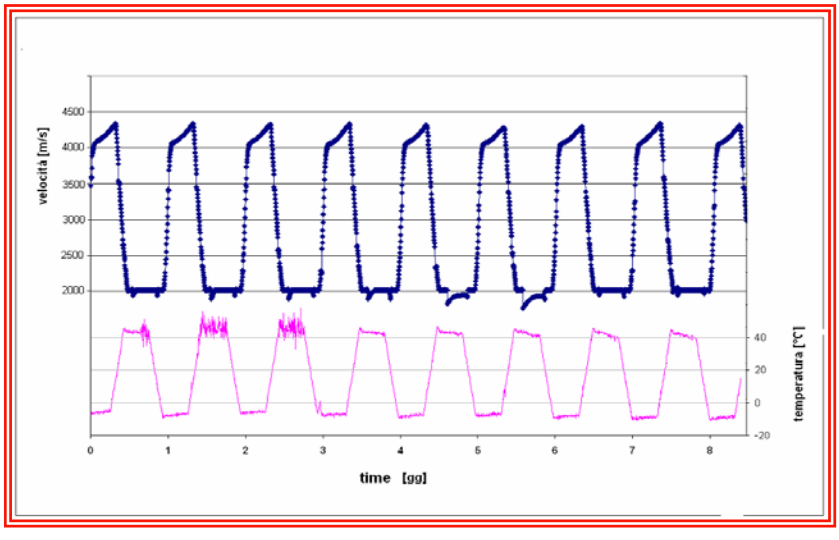


Fig. 7 Longitudinal ultrasonic velocity of tile reinforced with FRP (hand lay up + vacuum bag) (upper curve), changing in the temperature (lower line) versus aging time.

## 5. DISCUSSION

The Dynamic Young modulus of epoxy resin, primer and CFRP can be calculated using measured longitudinal velocity following the eq. 2.

$$v_l = \sqrt{\frac{E'}{\rho} \frac{(1-\mu')}{(1+\mu')(1-2\mu')}} \tag{2}$$

where ν is the longitudinal velocity, E is the dynamic Young Modulus, ρ is the density and μ is the Poisson ratio (in this case μ' =0,315 (value assumed, but acceptable for this kind of material)).
The measured density of the analyzed materials is reported in Table 2.

Tab 2: density of the analyzed materials

| sample | CFRP [kg/m$^3$] | Epoxy resin [kg/m$^3$] | Primer [kg/m$^3$] |
|---|---|---|---|
| ρ | 1298 | 1080 ±0,2 | 1080 ±0,001 |

The values assumed from the longitudinal velocity are those to the temperature at 20°C, the same temperature to which the mechanical tensile tests has been carried out.
Correlation diagrams between the Dynamic Young Modulus (Eultra) measured by means of ultrasonic wave during the monitoring and the Static Elastic Modulus (Emec) measured by means of mechanical tensile test are reported in Fig. 8 and 9 relatively to the epoxy resin and primer. The values of ultrasonic velocity, used to calculate Eultra, were chosen by the monitoring diagram relatively to the same day in which the 5 samples for the mechanical testing were carried out from the environmental chamber. The correlation coefficient value ($R^2$) in the first case is 0,94 and it shows a very good agreement between the non destructive testing and the mechanical testing.

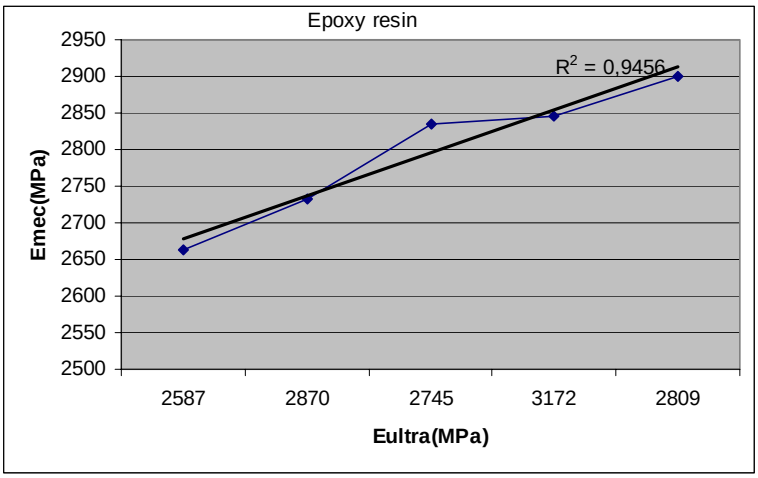



Fig. 8: Correlation diagram between the Dynamic Young Modulus (Eultra) and Static Young Modulus (Emec) of the epoxy resin

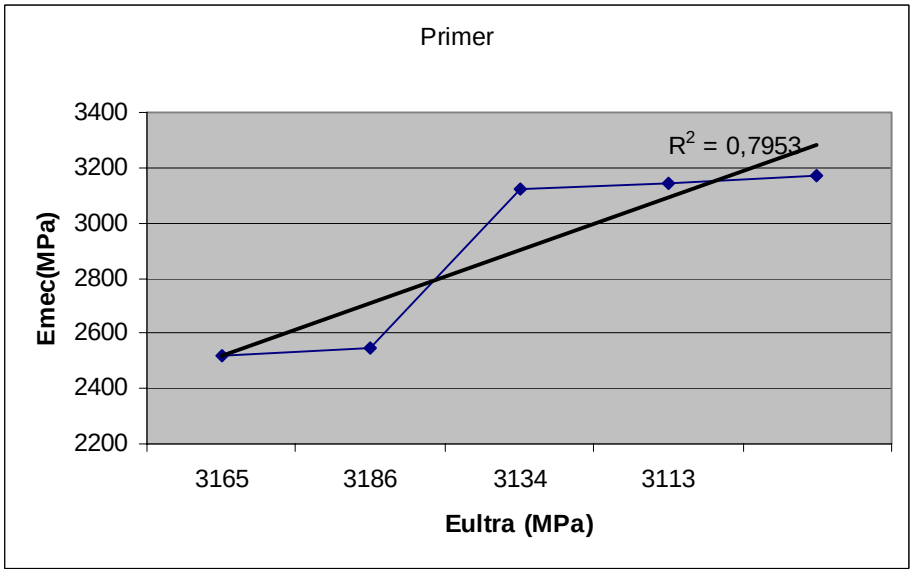



Fig. 9: Correlation diagram between the Dynamic Young Modulus (Eultra) and Static Young Modulus (Emec) of the primer.

The Dynamic Young Modulus of CFRP, monitored by means of ultrasonic wave, gradually decrease as shown in Fig. 10. From the beginning of the freezing-thawing cycles the Dynamic Young Modulus decrease of about 25%. Instead the Static Elastic Modulus decrease of about 16 %. It could be explained by the anisotropic behaviour of the CFRP along the fibres direction and perpendicular to the fibres direction. Any way it can be noted that while the mechanical properties of the epoxy resin decrease of only about 5 % in four months, those of the primer and CFRP decrease of about 20 % and 16% respectively. The Tg of each materials remains for all four months much higher then 40° C. It can be concluded that the decrease of the mechanical properties can be attributed to a decreasing of the adhesion properties between the fibres and the epoxy resin matrix, rather then a reduction of the properties of the epoxy resin.

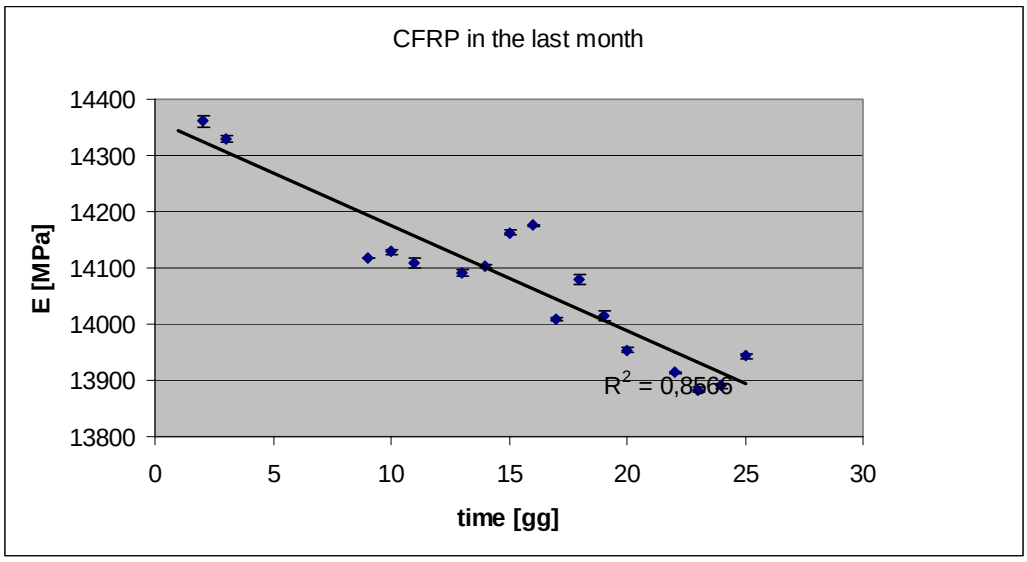



Fig. 10 Dynamic Young Modulus of CFRP measured by means of ultrasonic waves monitored during the last month

## 6. CONCLUSIONS

It was carried out the monitoring of changing in ultrasonic velocity in environmental chamber according to variations of temperature and thickness on samples of epoxy resin, primer, composite (CFRP), arranges tiles of concrete with on FRP applied with two different processes: hand lay up technique and hand lay up plus vacuum bag technique. The realized system has monitored the variations for a period of four months on samples placed in a environmental chamber (cycles of freezing- thawing (-10° ÷ 40° C) every 24 hours – 90 % humidity ). Moreover the physical – chemical variations in the materials as weight, glass transition, mechanical property have been experimentally measured during the cycles. A good correlation between dynamic modules measured by means of ultrasonic wave and static modulus measured by means of mechanical tensile test has been found. This demonstrates that the monitoring system by means of ultrasound can be a useful instrument to use in situ to monitor variation of mechanical property of CFRP applied to civil structures in concrete.

## 7. REFERENCES

CNR - Istruzioni per la progettazione, l'esecuzione ed il controllo di interventi di consolidamento statico mediante l'utilizzo di Compositi Fibrorinforzati Materiali, strutture in c.a. e in c.a.p., strutture murarie – published by CNR - TD 200 (2004)

Frigione M., Naddeo C., Acierno D., Epoxy resins employed in civil engineering applications: effects of exposure to mild temperatures, in: *Materials engineering*, vol. 11, n.1 pp59-80 (2000)

Frigione M., Maffezzoli A., Acierno D., Luprano V.A.M., Montagna G., Non destructive and in situ monitoring of mechanical properties build up in epoxy adhesives for civil applications by propagation of ultrasonic waves in *Polymer Engineering And Science 40* (3): 656-664 MAR (2000)

Karbhari V.M., J.W.Chin, D.Reynaud, Durability Gap Analysis for Fiber-Reinforced Polymer Composites in civil infrastructure, in: *Journal of Composites for Construction*, ASCE, , Vol 7,n.3, p. 241,242 August (2003).

Mal A, Ricci F, Banerjee S, Shih F., A conceptual structural health monitoring system based on vibration and wave propagation, in: S*tructural health monitoring-an international journal* 4 (3): 283-293 SEP (2005)

Nanni Antonio, *Fiber-reinforced-plastic (FRP) reinforcement for concrete structures: properties and applications*, Elsevier, Amsterdam, (1993)

Perepechko I., *Acoustic methods of investigating polymers*, MIR, Mosca, (1975)

Van Den Einde L, Zhao L, Seible F., Use of FRP composites in civil structural applications in: C*onstruction and building materials* 17 (6-7): 389-403 SEP-OCT (2003)

# Development of new casted-in-place water sealant materials

P. Salvador Pereira[1], J. C. Bordado[2]

*Instituto Superior Técnico, Departamento de Engenharia Química,*
*Av. Rovisco Pais 1049-001 Lisboa, Portugal*

Raquel F. Paula[3]

*STAP, S.A., R. Marquês de Fronteira, 8, 3º d^to*
*1070-296 Lisboa, Portugal*

## ABSTRACT

The hydro-triggered water sealing materials are acquiring growing importance in the construction industry. These materials are used in the repair and maintenance of concrete and masonry structures as well as in soil stabilization and increase of resistance. The waterproofing materials are aim at providing permanent protection of concrete or masonry structures against water and moisture. This new generation of *hydro-active* materials relies essentially on liquid quasi-prepolymers with isocyanate functionality (Oertel, 1985), which, in contact with water or gaseous moisture, originates polyurethane elastomeric foams by simultaneous formation of carbon dioxide that acts as expansion agent. Adherent humidity at the time of application is an advantage, once the water reacts with the pre-polymer, increasing the adherence as well as the cohesion energy of the resulting foamed material (Cóias e Silva, 2005). The *hydro-active* sealant materials can be divided in three main groups accordingly to its final application: sealing of construction joints, crack repair of concrete and masonry with water leakages, floor coatings and waterproofing of facades; waterproofing and elimination of water leakages in tunnels, drain galleries, reservoirs, collectors and sewage; soil stabilization and increase of resistance. The macromolecular structure of these materials is tailored to result on a steady durable, neutral, non-toxic and reliable material for applications in constructions in contact with drinking waters.

## 1. INTRODUCTION

Concrete cracks are a recognized and well documented problem. Concrete construction requires construction joints. All of these wanted and non wanted "openings" in concrete structures may cause very serious problems. One of them is water leakage.

Polyurethane elastomeric foams are an effective solution for applications involving crack sealing (waterproofing). Properly formulated polyurethane foams are sufficiently

[1] Researcher
[2] Professor
[3] R&D Project Manager

flexible and resilient to “move” with slight concrete movement without failing in the adhesion interface (Sauders e Frisch, 1983).

During the injection, the polyurethane liquid polymer flows into the crack, mixes with any water present, and quickly expands as it begins to foam. Such foam systems can stop water infiltration very quickly against even flowing water in a concrete crack.

The rapid thickening of polyurethane foams makes possible the removal of the surface seal within one to two hours after beginning injection. It also reduces the chances of liquid polymer flowing back out of the injected crack while still in liquid form. Sometimes the material is leaking out slowly, but it is still capable of further foaming to fill out the crack as well as filling the void beyond the crack.

The consolidation and increase of soil resistance can be achieved by applying the prepolymer into the ground.

Consolidation deep in the ground of building's foundations is achieved by injections of the prepolymer which, in expanding, compact the ground all around them acting as binder. The method is used in all cases in which an increase in the load bearing capacity of the foundation soil is required, either following subsidence or in view of an increase of loading.

A Hydro-active sealing polyurethane prepolymer was developed to solve the above described problems. The properties and the development of the product are described in this paper.

In the first stage it was produced a prepolymer by mixing a calculated excess of Polymeric MDI with poliol. The synthesised prepolymer is then reacted with the accelerator and with the water, forming the final polyurethane water sealing foam.

The accelerator was also developed to assure the required final properties of the foam. Different quantities of the accelerator allow different applications of the prepolymer. Applying therefore different quantities of the accelerator, it is possible to control the kinetics of the reaction, and this is an important factor for the use as sealant in concrete crack repair. If the quantity of the accelerator is low, the product will react slowly, allowing a better impregnation of smaller cracks. If the quantity of accelerator is higher, the reaction will be quicker. This is very important when the product is to be used to seal wide cracks with active water flow.

## 2. PROPERTIES

**Polymeric resin:**
**Chemical basis**: Polyurethane quasi-prepolymer
**Appearance:** brown liquid
**Odour**: mild and slightly sweet
**pH**: neutral
**Boiling point:** thermal degradation occurs before boiling
**Melting point**: < -20 ºC (it can occur partial separation due to MDI crystallization)
**Flash point**: 185 ºC
**Inflamability**: non flammable
**Explosive properties**: non applicable
**Vapour tension**: 0,00665 mm Hg a 25 ºC
**Specific gravity**: 1,087
**NCO content**: 14 ± 2 %
**Water solubility**: non soluble

**Accelerator:**
**Chemical basis**: Amine solution
**Appearance:** transparent
**Odour**: amine
**pH**: > 12
**Boiling point:** 296 ºC
**Melting point**: < 25 ºC
**Flash point**: > 130 ºC
**Inflamability**: non flammable
**Explosive properties**: non applicable
**Vapour tension**: < 1 mbar a 20 ºC
**Specific gravity**: 0,98
**Water solubility**: non soluble

## 3. INJECTION PROCEDURES

Some of the basic steps of the injection procedures are described:
*Surface cleaning* - Cleaning of the surface helps to identify the exact location and the width of the crack to be sealed. Sometimes the concrete surface is hidden under a surface of mineral deposits left from long-term water leakage. Everything that obstructs the crack should be removed. The crack must be clearly seen in order to allow the correct marking of the location of the packers, see Figure 1.
Making of drill injection holes - In order to inject the resin into the crack, it is necessary to install injection packers into holes. Usually, the injection holes are drilled downwards at an adequate angle. The distance of the drilled holes to each other is defined accordingly to the width of the crack.

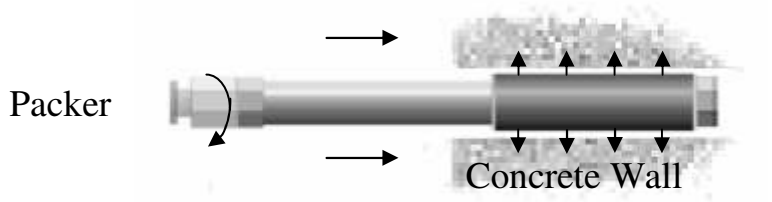



Figure 1 – Application of the packer into the wall

*HQ mixing and injection* - When all preparation work is completed, it is necessary to assure the good working of the injection pump. All equipment that comes in contact with the chemicals must be dry once the hydro active water sealing polyurethane prepolymer (HQ) is water reactive. The hydro active water sealing polyurethane prepolymer and the accelerator are mixed together, using the quantity of accelerator depending on the width of the crack to seal. The Pump is connected to the packer and the injection starts.
*Cleanup* – After finishing the injection, it is very important to cleanup because once the prepolymer expands, it is impossible to dissolve it. Any prepolymer spilled must be cleaned immediately before the product sets. The injection pump, mixers and any other tools that came in contact with the products should be cleaned using special Products.

## 4. TESTS RESULTS

### 4.1. Determination of viscosity using a rotational viscometer

This test was made accordingly to the standard EN ISO 3219:1993. The viscometer used was a HAAKE Viscotester 2 Plus from Thermo Electron Corporation.

The viscosity of the water sealing polyurethane prepolymer was measured 3 times and the final value is the average media.

Viscosity at 21ºC – 4,43 dPa

### 4.2. Determination of non-volatile-matter content

These tests were made accordingly to the standard ISO 3251:2003.

The non-volatile-matter content is given by eq. (1).

$$NV = \frac{(m_2 - m_0)}{(m_1 - m_0)} \times 100 \quad (1)$$

were

$m_0$ is the mass, in grams, of the clean, dry dish

$m_1$ is the mass, in grams, of the dish with the test portion

$m_2$ is the mass, in grams, of the dish with the residue

The non-volatile-matter content (NV) was measured 2 times and the results are expressed in table 1.

Table 1 – Determination of the non-volatile-matter content (NV)

| Meassurements | $m_{0\,(g)}$ | $m_{1\,(g)}$ | $m_{2\,(g)}$ | NV |
|---|---|---|---|---|
| 1 | 2,1599 | 3,1867 | 3,1832 | 99,66 |
| 2 | 2,1766 | 3,1853 | 3,1784 | 99,32 |

Conclusions:

The non-volatile-matter content of the water sealing polyurethane prepolymer, calculated using the method described in the standard ISO 3251:2003, is higher than 99%.

### 4.3. Determination of specific gravity using the Pyknometer method

These tests were made accordingly to the standard NP ISO 2811-1:1999. The Pyknometer used was a Guy-Lussac Pyknometer.

The Pyknometer volume is given by eq. (2).

$$V_t = \frac{m_3 - m_1}{\rho_W - 0{,}0012} \text{ x } 0{,}99985 \quad (2)$$

were

$m_1$ is the mass, in grams, of the clean, dry Pyknometer;

$m_3$ is the mass, in grams, of the Pyknometer full with distilled water at a test temperature $t_T$;

$\rho_w$ is the specific gravity, in grams by milliliter, of pure water at a temperature $t_T$;

The Specific gravity $\rho$ of the hydro active water sealing polyurethane prepolymer HQ is given by eq. (3):

$$\rho = \frac{(m_2 - m_1)}{V_t} \quad (3)$$

were

$m_1$ is the mass, in grams, of the clean, dry Pyknometer;

$m_2$ is the mass, in grams, of the Pyknometer full with the water sealing polyurethane prepolymer at a test temperature $t_T$.

The results obtained for the Pyknometer volume and Specific gravity for the hydro active water sealing polyurethane prepolymer HQ are expressed in Table 2.

Table 2 - Pyknometer volume and Specific gravity for the hydro active water sealing polyurethane prepolymer HQ, at 25 ºC

| Pyknometer Volume | | | |
|---|---|---|---|
| Test | $m_{1\ (g)}$ | $m_{3\ (g)}$ | $V_{t\ (ml)}$ |
| 1 | 31,2078 | 54,6676 | 23,5552 |
| Specific gravity ρ | | | |
| Test | $m_{1\ (g)}$ | $m_{2\ (g)}$ | ρ ($g.ml^{-1}$) |
| 1 | 31,2078 | 56,8205 | 1,08735 |
| 2 | 31,2078 | 56,8214 | 1,08738 |

Conclusions:

The Specific gravity of the water sealing polyurethane prepolymer, calculated using the method described in the standard NP ISO 2811-1:1999, is 1,087 g/ml.

4.4. Determination of Injectability using the sand column test

These tests were made accordingly to the standard EN 1771:2004, with slight modifications.

The system used can be seen in Figure 2.

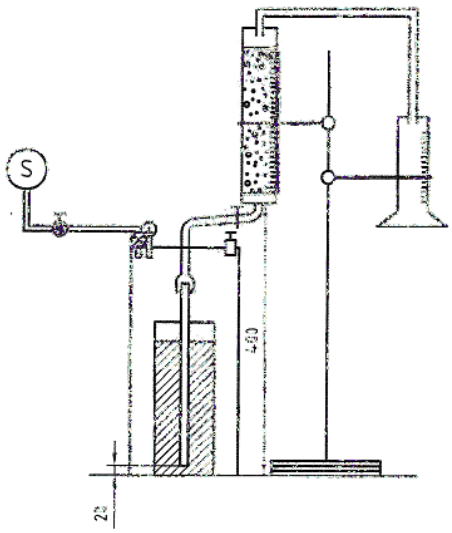



Figure 2 – Injectability system

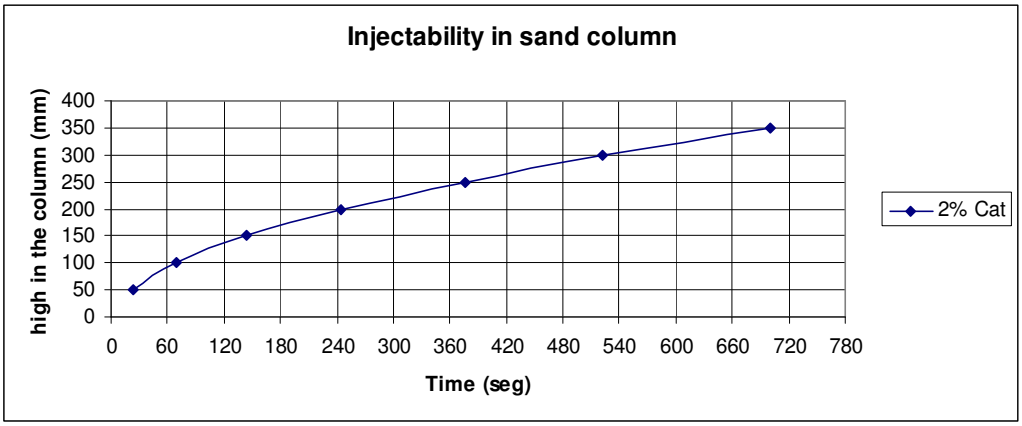



Figure 3 – Injectability of the water sealing polyurethane prepolymer in sand column

According to the standard, the polyurethane prepolymer is easy to inject.

4.5. Expansion Content and Expansion Ratio of the Foam

These tests were made accordingly to the standard EN 14406:2004.

The Expansion Content and Expansion Ratio were measured for different quantities of Accelerator (2, 5 and 10 %/wt).

In Table 3 and Figure 4 (a), (b) and (c) are expressed the final expansion content, the induction time and the growing time of the foam with different % of accelerator.

Table 3 – Influence of different % of accelerator in the final expansion content, inducting time and growing time of the foam.

| Accelerator (%/weight) | Final expansion content | Inducting time (sec) | Growing Time (sec) |
|---|---|---|---|
| 2 | 13,07 | 50 | 720 |
| 5 | 15,91 | 20 | 280 |
| 10 | 18,61 | 5 | 240 |

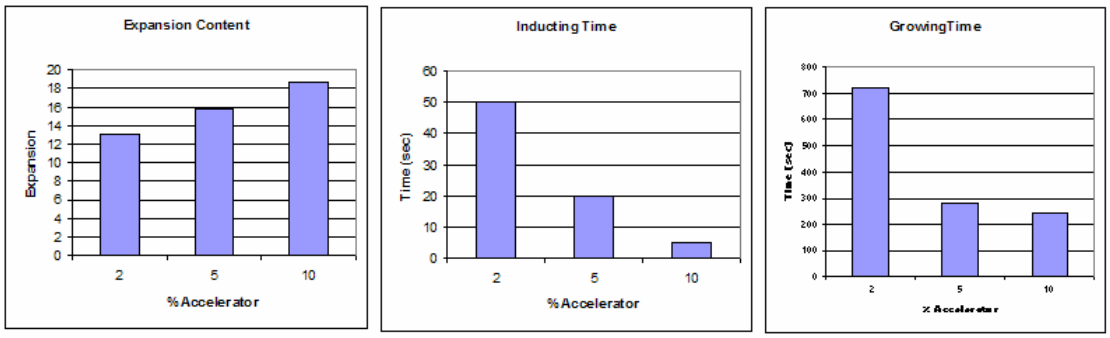



Figure 4 – (a) Expansion Content, (b) Inducting time and (c) Growing time evolution

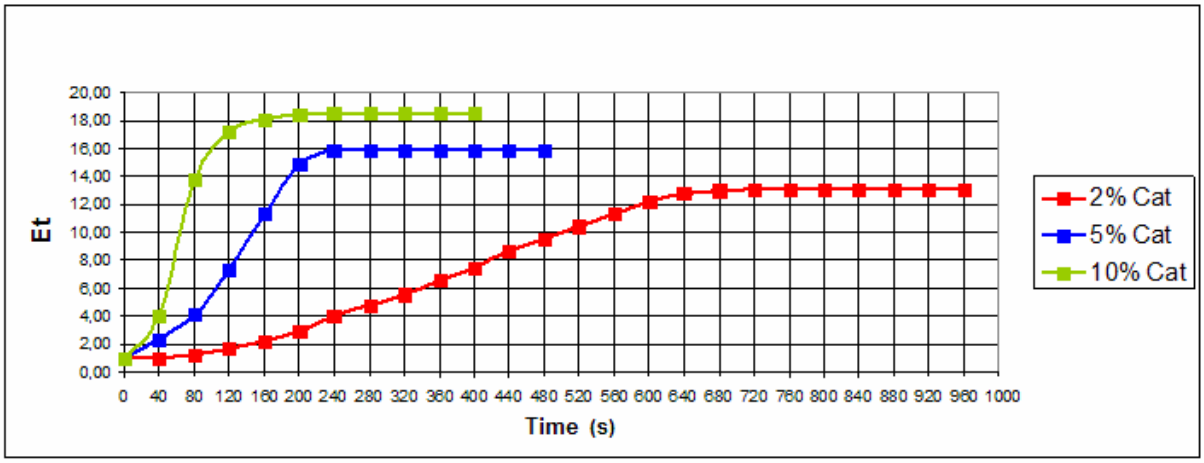



Figure 5 - Expansion Ratio of formed foam with different % of accelerator

In Figure 5 different times of expansion are compared with different quantities of accelerator. This property is very important concerning the application of the product in different crack dimensions. If concrete presents microcracks, it is useful to have a minor quantity of accelerator to assure the complete penetration in the capillary gaps of the structures to be repaired, otherwise the sealing would only be superficial and would not provide the adequate long term protection. If the cracks are larger and, as in many cases, with water flowing, the quantity of accelerator must be higher to assure the sealing of the gaps before flowing out of the product from the concrete.

4.6. Influence of the quantity of accelerator in the physical and kinetic properties of the foam

There were synthesized foam blocs, by reacting the different components in the proportions showed in Table 4:

Table 4 – Proportion for the synthesis of the Blocs

| Accelerator (%/wt) | Accelerator mass (g) | Prepolymer HQ mass (g) | $H_2O$ mass (g) | Stirring speed (RPM) | Time of agitation (s) |
|---|---|---|---|---|---|
| 2 | 4 | 200 | 8 | 400 | 10 |
| 5 | 10 | 200 | 8 | 400 | 10 |
| 10 | 20 | 200 | 8 | 400 | 10 |

After mixing the different components, the mixture was put inside a 10 litter cubic mould inserted in an adiabatic foam mould to prevent thermal losses.

After analysis, the obtained physical properties are showed in Table 5.

Table 5 – Physical properties [ASTM D 2856-94, Hilyard, N.C., *et al*]

| Quantity of Accelerator (%) | Sample Weight (g) | Height (cm) | Sample Apparent Volume ($cm^3$) | Sample Real Volume ($cm^3$) | Apparent Density ($kg/m^3$) | Real Density ($Kg/m^3$) | Open Cell Content (%) | Apparent Foam Volume ($cm^3$) | Teoretical Foam Volume ($cm^3$) |
|---|---|---|---|---|---|---|---|---|---|
| 2 | 2,14 | 5,0 | 79,5 | 2,1 | 26,9 | 1019,0 | 97,4 | 3862,7 | 10943,6 |
| 5 | 1,58 | 5,0 | 79,5 | 1,8 | 19,9 | 877,8 | 97,7 | 5969,4 | 10980,9 |
| 10 | 1,29 | 5,0 | 79,5 | 1,7 | 16,2 | 758,8 | 97,9 | 6468,3 | 11029,5 |

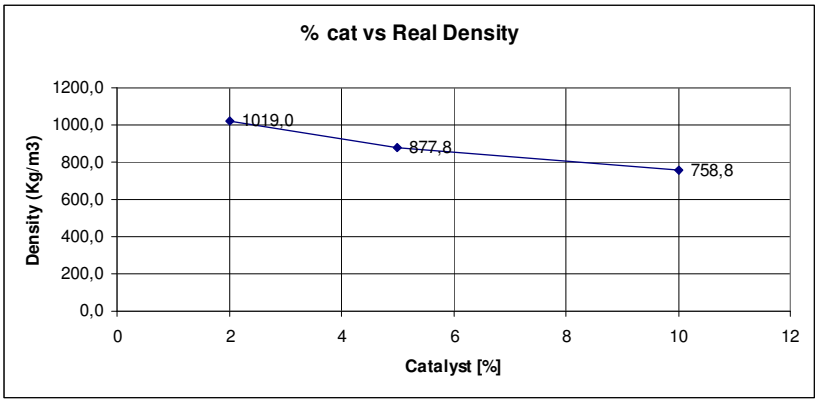



Figure 6 – Real Density foam made with 2, 5 and 10% of accelerator

The open cell content was calculated according to the standard ASTM D 2856, and is given by eq. (4).

$$\text{Open Cell Content} = \frac{(V_{AS} - V_{RS})}{V_{AS}} \tag{4}$$

were

$V_{AS}$ is the apparent volume of the sample and $V_{RS}$ is the real volume of the sample.

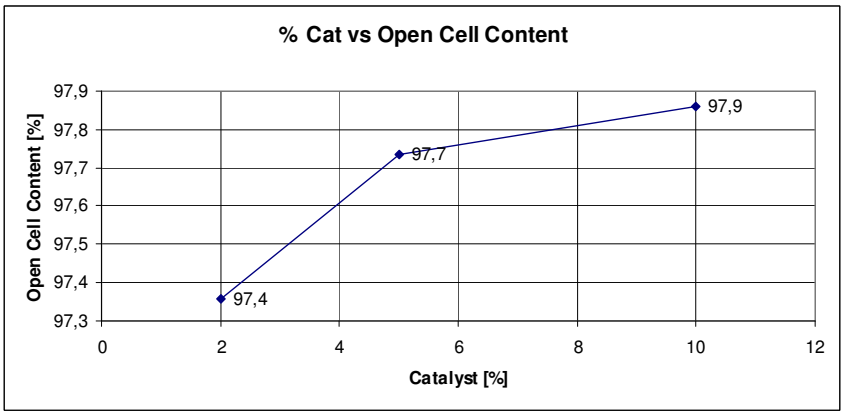



Figure 7 – Open cell content for different % of accelerator

The Kinetic properties of the formation of polyurethane foam were studied. The formation of polyurethane foams is relatively fast (2-4 min), highly exothermic (75 – 160ºC total temperature rise) and involves a large increase in volume (10 – 50×). Consequently, the foaming mixture undergoes changes in macroscopic morphology including bubble nucleation and growth, bubble packaging, cell opening and curing. If the foam is not gelled by the time of cell rupture, it will collapse. If the foam is tightly crosslinked (i.e. has gelled too much), it will shrink. Hilyard, N.C. (1994)

Data on reaction speed is essential for evaluating different polymerizations and comparing accelerators, improving blowing efficiency, and especially for relating the buildup of structure during processing. Therefore, reaction kinetics data combined with an understanding of the structural changes due to crosslinking and phase separation are necessary to optimize the formation of urethane foams.

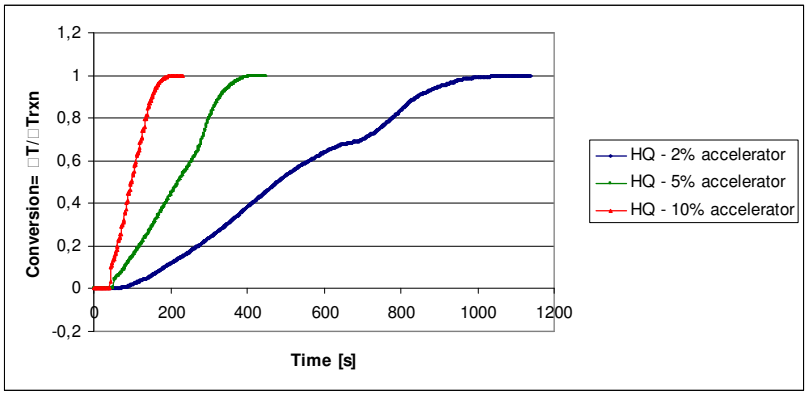



Figure 8 – Different % of accelerator induces different kinetics of the reaction of foam formation.

Fewer % of accelerator means a slower reaction and higher % of accelerator means a much quicker reaction, as shown in Figure 8.

## 5. FIELD TESTS

The HQ was tested in the discharger tunnel of a Dam (Figure 9). The problems presented were concrete, cracks and joints with water leakages.



Figure 9 – Joins to be sealed

In Figure 10 it is possible to observe the crack before and after the application of the water sealing polyurethane prepolymer. Note that after the application, it is possible to observe the formation of the foam.

a) Before b) After



Figure 10 – Aspect of the crack before and after product application

It is important to refer that in Figure 10 a) it seems to have just a big hole to seal but in the Figure 10 b) it is possible to observe that in the same drill injection there were sealed 5 water leak cracks. In the Figure 11 it is possible to observe the sealing of a joint.

a) Before b) After



Figure 11 – Application of the product in a joint.

The product was tested in a floor of a parking law, which is below the freatic level of the near river.

In Figure 12 it is possible to see the drilling of the hole for the injection of the product.



Figure 12 – Hole drilling

In Figure 13 we can observe the aspect of the floor before and after the application of the water sealing polyurethane prepolymer. Note that before the application the floor is all wet and after the application it is possible to observe the dry floor near the packer.

a) Before b) After



Figure 13 – Aspect of the floor a) before and b) after product application

In Figure 14 it is possible to observe the application of the product and the appearance of the foam in the crack.

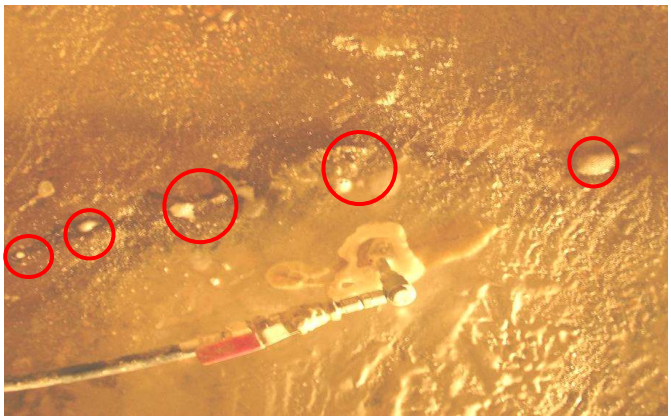


Figure 14 – Application of HQ in a concrete floor crack.

## 6. CONCLUSIONS

The objective of the proposed work was the development of a new hydro active water sealing polyurethane prepolymer to apply in several Civil Engineering applications, mainly in concrete crack waterproofing. The product was successfully developed to meet required final properties. The field tests indicate a very good behaviour in the above mentioned application domain.

## 7. REFERENCES


ASTM D 2856-94, *Standard Test Method for Open Cell Content of Rigid Cellular Plastics by Air Pycnometer*, American Society for Testing and Materials, West Conshohocken, PA, (1998).

Cóias e Silva, V.; Azevedo, R., *STAP – 25 years and 1300 jobs after,* Argumentum, Lisboa, Portugal (2005).

EN 1771:2004, *Standard Method for Products and systems for the protection and repair of concrete; Determination of injectability using the sand column test*, (2004).

EN 14406:2004, *Standard Method for Products and systems for the protection and repair of concrete; Determination of expansion ratio and expansion evolution*(2004).

Hilyard, N.C., Cunningham, A., *Low Density Cellular Plastics – physical basis of behaviour*, 1st Edn., Chapman & Hall, London, United Kingdom (1994).

ISO 3219: 1993, *Standard Method for Plastics – Polymers / Resins in liquid state or as emulsions or dispersions; Determination of viscosity using a rotational viscometer with defined shear rate*, (1993).

ISO 3251:2003, *Standard Method for paints, varnishes and plastics – Determination of non-volatile-matter content*, (2003).

NP ISO 2811-1:1999, *Standard Method for paints and varnishes – determination of Density (specific gravity)*, (1999).

Oertel, G., *Polyurethane Handbook: Chemistry - Raw Materials - Processing - Application - Properties*. Hanser Publishers, Nova Iorque (1985)

Saunders, H.; Frisch, K. C., *Polyurethanes – Chemistry and Technology,* Robert E. Krieger Publishing Company, Malabar, Florida, (1983)

International Symposium Polymers in Concrete
2 - 4 April 2006
Guimarães, Portugal

# Concrete workability and water resistance improvement using polymeric admixtures

Patrício Pires[1], Isabel Azevedo[2]
*Quimidois – Chemical Industry, Portugal*

Ana V. Machado[3]
*University of Minho, Polymer Engineering Department, Guimarães, Portugal*

J. Barroso de Aguiar[3], Rui M. Ferreira[4]
*University of Minho, Civil Engineering Department, Guimarães, Portuigal*

## ABSTRACT

The present work aims to compare the physical and mechanical properties of concrete produced with different incorporation of polymeric admixtures. Two families of admixtures are studied: the superplasticizers and water resisting admixtures. The main results of the experimental program are presented and analysed. The performance of concrete incorporating admixtures is measured using physical and mechanical properties. Properties such as compressive strength, air content, water/cement ratio (W/C), density and, in the case of water resisting admixtures, the capillary absorption were measured.

## 1. INTRODUCTION

An admixture is a substance that can be added to the concrete at up to 5% by cement mass, added during the mixture, to the normal components of mortars and concrete, with the objective of modifying certain properties of these materials, in the fluid state, in the solid state or in the transition between these states. The use of the admixtures is not new, having the Romans used blood, egg white, animal fat and milk as admixtures for concrete to improve workability. Around 1850, gypsum or the calcium chloride was used to obtain a more regular set. These admixtures were added to the cement in the grinding or during the concrete batch. The commercialization of admixtures with the purpose of conferring certain properties to concrete remotes 1910. In that time the admixtures used were essentially for water resistance, accelerating of set, or both simultaneously. Up to the end of the 60's, admixtures were complex industrial by-product mixtures, but, in middle of years 70, with the beginning of the oil crisis, they started to be specific formulations with more defined molecular structures.

Nowadays, the use of admixtures is a necessity and common practice in the manufacture of concrete, but one must be conscious that it does not correct concretes that are badly manufactured.

[1] Graduate Student
[2] Chemical engineer. Technical department
[3] Associate Professor
[4] Assistant Professor

## 2. ADVANCES IN DEVELOPMENT OF ADMIXTURES

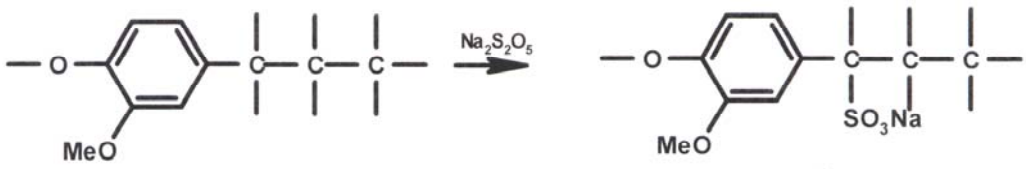
### 2.1 Superplasticizers

Cement is a hydraulic binder, from which concrete is made. Water, which is one component of concrete, reacts chemically with cement; it is a crystallisation reaction. Water is also used to make a fluid material (the fresh concrete) easy to handle and easy to introduce into dies or into foundations for example. Only some of the water is used for the crystallisation, the excess water allows handling the fresh concrete. The higher the amount of excess water, the more fluid the concrete. It is, of course, easier to handle very fluid concrete.

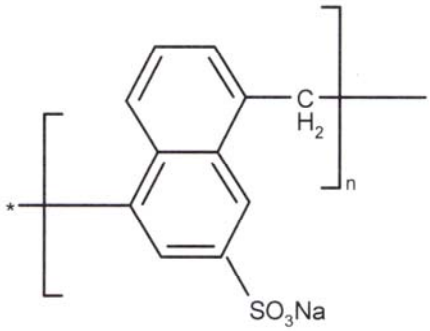
For the complete hydration of the cement needs about 25% of water, that is to say a Water/Cement ratio: W/C = 0.25. The excess water necessary to handle the fresh concrete must be minimised in order to avoid the increase of the porosity. Thus W/C influences dramatically the structure and the mechanical properties of concrete. For this reason, concrete manufacturers use dispersing agents in order to decrease the W/C or to avoid an increase of the W/C when very fluid concrete is needed for special applications.

Dispersing agents, which are called superplasticizers or water reducing agent in the building industry, are polymer based products; they are classified in four families:

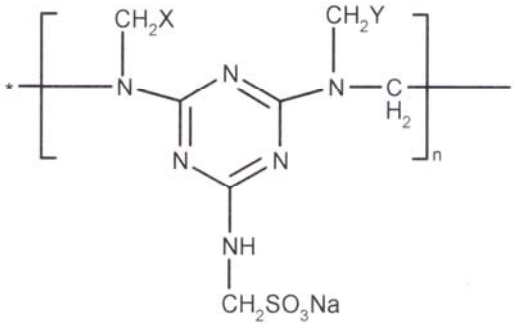
- Modified Lignosulphonate



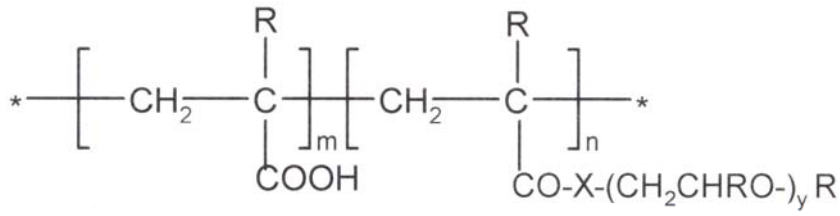

- Sulphonated polymethane naphthalene (SPMN)




- Sulphited formaldehyde melamine (SFM)



- Polycarboxilate (PC)




Other kinds of products based on non-polymeric molecules can also be considered as dispersing agents such as phosphonates or carboxylic acids (gluconic acid, glucoheptonic acid, citric acid…) but they are not used for this application because they increase dramatically the set time of the cement.

Every polymeric admixture can be used either as superplasticizer or as water reducing agent. A superplasticizer decreases the viscosity of the fresh concrete without increasing the W/C while a water reducing agent allows decreasing the W/C while keeping a good fluidity for easy handling of the fresh concrete. A water reducing agent is used in order to improve the mechanical properties of the hardened concrete either after a short time (24 hours) or after a long time (28 days)

Modified Lignosulphonate, SPMN and SFM are the oldest admixtures, they are the cheapest products but they do not allow a large decrease of the W/C ratio and usually a loss of slump occurs rapidly. Indeed, after introduction into the concrete the dispersing effect remains effective about thirty minutes, that is to say beyond this time it is often necessary to add an extra quantity of the dispersing agent to guarantee the right viscosity of the fresh concrete. For these reasons a new kind of dispersing agent based on a modified acrylic polymer has been developed.

Modified acrylic polymers are more expensive than modified lignosulphonates, SPMN and SFM but they are much efficient in terms of dispersing effect and they impart special properties, which are impossible to obtain with other products. Thus, they can be used at a much lower dosage. Furthermore, as a function of their dosage, they can allow the concrete to remain fluid up two hours instead of thirty minutes. They are also better water reducing agents than other admixtures; they are used for the manufacture of high performance concrete, meaning concrete with high mechanical properties, with high density and good chemical resistance.

Plasticizer and superplasticizer admixtures belong to a substance category that reduces the superficial tension of the dissolvent (water). Its molecules are elongated with a hydrophobic part and a hydrophilic part.

The name plasticizer remotes the first admixtures to concrete, of pulvurulent products of a great slimness (such as diatomite, fat whitewash, bentonite and pozzolans), that were added in a very reduced amount, as 2 to 3% of the mass of the cement, thus allowing the reduction of water keeping the workability.

The superplasticizer, in the context of the production of concrete, has the main functions:

- to increase the resistance, reducing the W/C ratio and keeping the workability;
- to increase the workability, keeping the W/C ratio and the resistance;
- to reduce the dosage of cement, keeping the resistance and reducing the W/C ratio;
- to increase the durability, increasing the compactness and reducing the permeability.

Mechanism of water reduction*:* The main function of a superplasticizer is to disperse

the fine particles of the components, namely the cement. When a plasticizing agent is added to the water, it is easily absorbed by the particles surface of the cement due to the favourable electric potential between both, removing the air that conferred a good cohesion between the solid particles.

Because of this mechanism, and because all the cement particles tend to be ionized with load of the same signal, these fine particles start to repel themselves, and the free water is no longer necessary to their mobility. Thus, distance between particles can be reduced and it can now be excused the water that is now in excess, without compromising the adequate rheologic behaviour in fresh state.

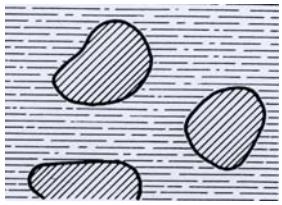


Fig. 1 – Without plasticizer, the amount of necessary water is higher.

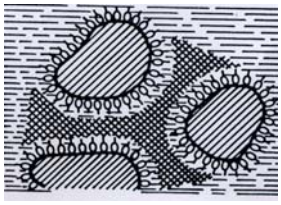


Fig. 2 – When a plasticizer is added there is repulsion between the particles and the water that is set free between them is no longer necessary for their mobility

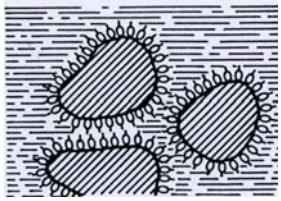


Fig. 3 – The distance between the particles is reduced and the water is expelled.

Still for the fact of cement particles being ionized with load of the same signal, unchains an electric mechanism that gives place to an electric gradient, called as potential zeta (ζ), which produces a dispersion (deflocculation) and stability of particles of the cement, during one determined period of time.




Fig. 4 – Illustration of the action of superplasticizer in the particles.

The polycarboxilates due to the peculiar structure of its molecules of great molecular mass with many radicals, disperses the cement particles not only for the electrostatic repulsion as it happens in (modified lignosulphonates, sulphonated naphthalene polymers, sulphonated melamine polymers) but also due to esteric repulsion.

The polycarboxilates are polymers of linking with chains of oxide ethylene with high resistance to salts and lateral chain molecules. The ethylene oxide chains have a great ability to keep water, forming an absorption voluminous and thick layer on the surface of cement particles. This layer gives rise to a high esteric repulsion.

In figure 5 we can see a very similar representation to the real polycarboxilate molecule that is adsorbed by a cement grain and can compare the same effect produced for a polymer molecule of sulphonated naphthalene polymer b), such as we can observe a polycarboxilate molecule a), because of it structure assures a distance around 100 Å, while the

sulphonated naphthalene polymer only reaches 10 to 20 Å.

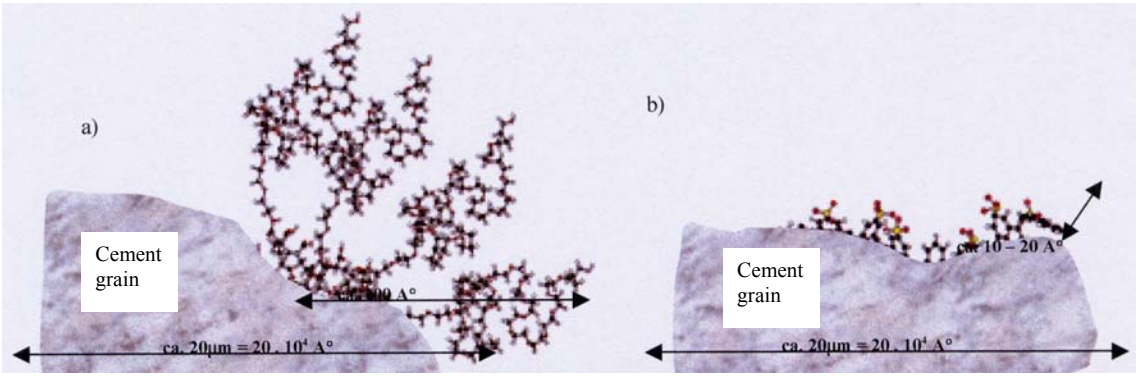



Fig. 5 – Representation of a molecule of superplasticizer being adsorbed by a grain of cement. a) policarboxylate b) sulphonated naphthalene polymer.

## 2.2 Water resisting admixtures

There aren't admixtures that transform the concrete in a complete water resisting material, but they can reduce the permeability of concrete. Water resisting admixtures can be organic or mineral. The organic water resisting admixtures hidrofugate the walls of the capillaries of the cement. The mineral water resisting admixtures precipitates the insoluble salts in the capillaries, closing them.

The molecules of organic products are highly hidrofuge, being adsorbed in the walls of capillaries by the polar edge, hidrophila, the hidrofuge part stays turned to the out side part, generated a hidrofugation of the capillaries, that is only efficacious after the evaporation of the water that is in their interior. Because of this a new wetting of the capillaries is extremely difficult.

We must be conscious that for a bad concrete, with important and heterogeneous voids there is no hidrophobe capable of reduce the water entering by capillarity or pressure even if it is weak.

## 3. EXPERIMENTAL DATA

Experimental data was obtained from the production of concrete without admixtures and concrete produced with admixtures. Table 1 presents the studied admixtures and the doses used. Table 2 presents the technical data of the admixture used.

Tab. 1 – Admixtures used in concrete and their doses.

| | Reference concrete | Superplasticizers | | | | | | | Water resisting | | | | | |
|---|---|---|---|---|---|---|---|---|---|---|---|---|---|---|
| | | MLN | MLN | MLN | SPMN | SPMN | PC | PC | PA | PA | PA | EC | OS | OS |
| % of admixtures (by mass of cement) | - | 0,5 | 1,0 | 2,0 | 1.0 | 2.0 | 0.25 | 0,5 | 0,5 | 1,0 | 2,0 | 1,5 | 1,5 | 3,0 |

Tab. 2 – Technical data of the admixtures

| | MLN (mixture of lignosulphonates and sulphonated naphthalene polymer) | SPMN (sulphonated naphthalene polymer) | PC (policarboxilate) | PA (acrilic ester copolímer ) | EC (mixture of calcium estearate and melamine sulphonated polymer) | OS (sodium oleate) |
|---|---|---|---|---|---|---|
| Colour | Dark brown | Dark brown | Light brown | White | White | White |
| Physical state | Liquid | Liquid | Liquid | solid | solid | solid |
| Density ($g/cm^3$) | 1.16±0.02 | 1.20±0.02 | 1.12±0.02 | 1.06±0.02 | 0.25±0.02 | 0.50±0.02 |
| Dry material content (%) | 31.0±2 | 40.0±2 | 50.0±2 | 47.0±2 | 100 | 100 |
| Chlorides (%) | <0.10 | <0.10 | <0.10 | <0.10 | <0.10 | <0.10 |
| pH | 3.9±0.5 | 6.7±0.5 | 6.4±0.5 | 9.0±0.5 | - | - |

The portland cement used in this work is type I Class 42.5. The cement was supplied by SECIL, Companhia Geral de Cal e Cimentos, S.A. In tables 3 to 5 are presented the chemical compositions and the physical and mechanical properties of the used cement, obtained from supplied technical data sheets.

Tab. 3 – Cement chemical composition

| Composition | Symbol | % |
|---|---|---|
| Silícium oxide | $SiO_2$ | 20.34 |
| Aluminium oxide | $Al_2O_3$ | 4.05 |
| iron oxide | $Fe_2O_3$ | 2.96 |
| Calcium oxide | CÃO | 63.01 |
| Magnesium oxide | MgO | 2.58 |
| Sulphates | $SO_3$ | 2.90 |
| Potassium oxide | $K_2O$ | --- |
| Sodium oxide | $Na_2O$ | --- |
| Chlorides | $Cl^-$ | 0.02 |
| Free lime | --- | 1.31 |
| Not determined | --- | 1.77 |
| Fire loss | --- | 2.40 |
| Insoluble matter | --- | 0.90 |

Tab. 4 – Cement physical properties

| Properties | Value |
|---|---|
| Density ($g/cm^3$) | 3.17 |
| Dry matter - <45µ (%) | 4.4 |
| Blaine specific surface ($cm^2/g$) | 3707 |
| Water in normal paste (%) | 28.8 |
| Initial setting time (min) | 116 |
| Final setting time (min) | 156 |
| Expansibility – Le Châtelier (mm) | 1.0 |

Tab. 5 – Cement mechanical properties

| Strength | MPa |
|---|---|
| Tensile strength (28 days) | 9.4 |
| Compressive strength (2 days) | 30.1 |
| Compressive strength (28 days) | 52.5 |

Two course granitic aggregates from a quarry located in Guimarães were used: a large course aggregate (15/25) with an average specific density of 2.650 g/cm$^3$ and a water absorption of 0.4%; and a course aggregate (5/10) with an average specific density of 2.600 g/cm$^3$ and a water absorption of 1.6%. As a fine aggregate it was used a natural sand (0/4) with an average specific density of 2.461 g/cm$^3$ and a water absorption of 1.5%. The three aggregates mixture comply the grading curve presented in Figure 8.

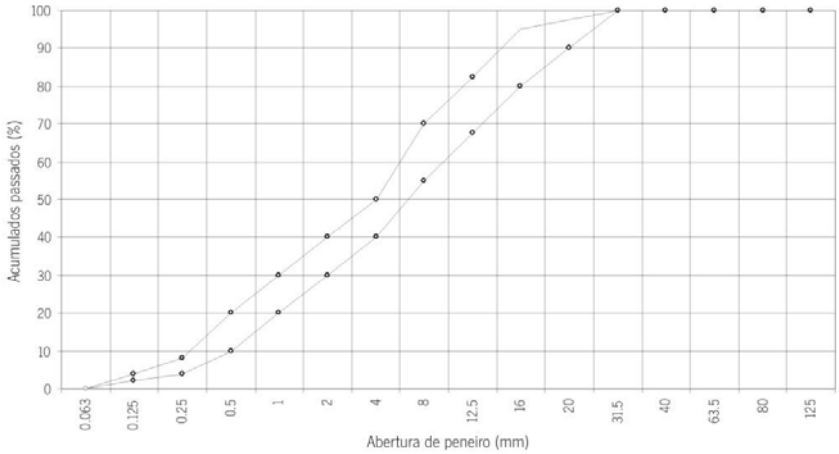



Fig. 8 –Aggregates for the reference concrete and the tested concrete.

The performance of the admixtures is assessed comparing the concrete produced with admixture (tested concrete) with the reference concrete, made without admixture. Both concretes have the same ratio aggregates/cement. The dosage of cement was fixed on 350 ± 5 kg/m$^3$ in the reference concrete. The cement content on tested concrete may vary in function of the concrete volume variations, because of the action of the tested admixture (water reduction or air content). The consistency was determined by the slump test and was fixed in reference concrete and in the tested concretes in 70 ± 10 (mm). Tables 6 to 8 present the compositions of the concretes used and the consistencies obtained.

Tab. 6 – Reference concrete composition (per m$^3$ of concrete)

| Materials | Reference concrete (kg) |
|---|---|
| Cement | 350.0 |
| Water | 234.5 |
| Natural sand | 810.0 |
| Course aggregate (5/10) | 450.0 |
| Course aggregate (15/25) | 540.0 |

Tab. 7 – Compositions of the mixtures for use of superplasticizer admixture

| Material (kg) | REF. | MLN (1.0%) | MLN (2.0%) | SPMN (1.0%) | SPMN (2.0%) | PC (0.25%) | PC (0.5%) |
|---|---|---|---|---|---|---|---|
| CEM I 42.5R | 19.60 | 19.60 | 19.60 | 19.60 | 19.60 | 19.60 | 19.60 |
| Natural sand | 40.00 | 40.00 | 40.00 | 40.00 | 40.00 | 40.00 | 40.00 |
| Course aggregate (5/10) | 22.22 | 22.22 | 22.22 | 22.22 | 22.22 | 22.22 | 22.22 |
| Course aggregate (15/25) | 26.66 | 26.66 | 26.66 | 26.66 | 26.66 | 26.66 | 26.66 |
| Admixture (gr) | - | 196 | 392 | 196 | 392 | 49 | 98 |
| Water | 13.13 | 10.20 | 8.69 | 9.68 | 7.47 | 9.22 | 8.39 |
| Slump (mm) | 70 | 75 | 79 | 65 | 74 | 61 | 71 |

Tab. 8 – Compositions of the mixtures for the use of the water resisting admixture

| Material (kg) | REF | PA (0.5%) | PA (1.0%) | PA (2.0%) | EC (1.5%) | OS (1.5%) | OS (3.0%) |
|---|---|---|---|---|---|---|---|
| CEM I 42.5R | 19.60 | 19.60 | 19.60 | 19.60 | 7.60 | 7.60 | 7.60 |
| Natural sand | 40.00 | 40.00 | 40.00 | 40.00 | 15.68 | 15.68 | 15.68 |
| Course aggregate (5/10) | 22.22 | 22.22 | 22.22 | 22.22 | 8.71 | 8.71 | 8.71 |
| Course aggregate (15/25) | 26.66 | 26.66 | 26.66 | 26.66 | 10.45 | 10.45 | 10.45 |
| Admixture (gr) | 0 | 98 | 196 | 392 | 114 | 114 | 228 |
| Water | 13.13 | 12.53 | 11.64 | 10.12 | 4.68 | 5.15 | 5.01 |
| Slump (mm) | 70 | 80 | 62 | 70 | 65 | 79 | 66 |

After measuring slump, air content and density, the concrete was placed in cubic moulds ($15\times15x15cm^3$) in two consecutive layers, each layer being vibrated accordingly. After moulding, the samples of concrete stayed 24 hours in free air in the laboratory at ambient temperature. Follow, the concrete samples were removed from the moulds and putted in a conservation chamber inside water, at constant temperature of 21 ± 2 ºC, until the test day. Except for the compositions with water resisting admixtures EC and OS that were tested in compressive strength at 28 days with only 4 cubes, in all others the tests were made at 24 hours, 7 days and 28 days.

In the case of water resisting admixtures the test of capillary absorption was made in accordance with the standard EN 480-5. Samples of mortars ($40\times40\times160$ $mm^3$) were prepared in accordance to the standard EN 196-1. The reference mortar was in accordance with the standard EN 480-1, the tested mortars and the reference mortar had the same consistency as described on EN 480-1. Two series of measures of capillary absorption were made, in the reference mortar as in the tested mortar. The first series was made in three samples of each mortar after 7 days of cure. The second series was made after 90 days of curing time. The conservation conditions were 20 ± 2 ºC and 65 ± 5 %. The samples stored during 7 days in

the specified conditions were tested after 1 and 7 days in water contact. The samples stored during 90 days in the specified conditions were tested after 28 days in water contact.

## 4. RESULTS AND DISCUSSION

As the tests were made in accordance with the standard EN 934-2 there are requirements to the superplasticizer and water resistance admixture to comply (Tables 9 and 10).

*Superplasticizers*

Table 9 – Specific requirements for high range water reducing/superplasticizing admixtures (at equal consistence)

| Nº | Property | Reference Concrete | Test method | Requirements |
|---|---|---|---|---|
| 1 | Water reduction | EN 480-1, reference concrete I | Slump EN 12350-2 | In test mix ≥ 12% compared with control mix |
| 2 | Compressive strength | EN 480-1, reference concrete I | prEN 12390-3 | At 1 day: test mix ≥140% of control mix; At 28 days: test mix ≥115% of control mix |
| 3 | Air content in fresh concrete | EN 480-1, reference concrete I | EN 12350-7 | Test mix ≤2% by volume above control mix unless otherwise stated by the manufacturer |

*Water resistance*

Table 10 – Specific requirements for water resistance admixtures (for same workability)

| Nº | Property | Reference Concrete | Test method | Requirements |
|---|---|---|---|---|
| 1 | Capillary absorption | EN 480-1, mortar | EN 480-5 | Tested for 7 days after 7 days curing: test mix ≤50% by mass of control mix. Tested for 28 days after 90 days curing: test mix ≤60% by mass of control mix |
| 2 | Compressive strength | EN 480-1, reference concrete I | prEN 12390-3 | At 28 days: test mix ≥85% of control mix |
| 3 | Air content in fresh concrete | EN 480-1, reference concrete I | EN 12350-7 | Test mix ≤2% by volume above control mix unless otherwise stated by the manufacturer |

## 4.1 Physical properties

The compositions were analysed, in fresh condition, mainly by the incorporation of air and by the density. In the case of water resisting admixtures the capillary absorption was analysed.

### *Superplasticizers*

The air content, W/C ratio and density are presented in figures 9 to 11.

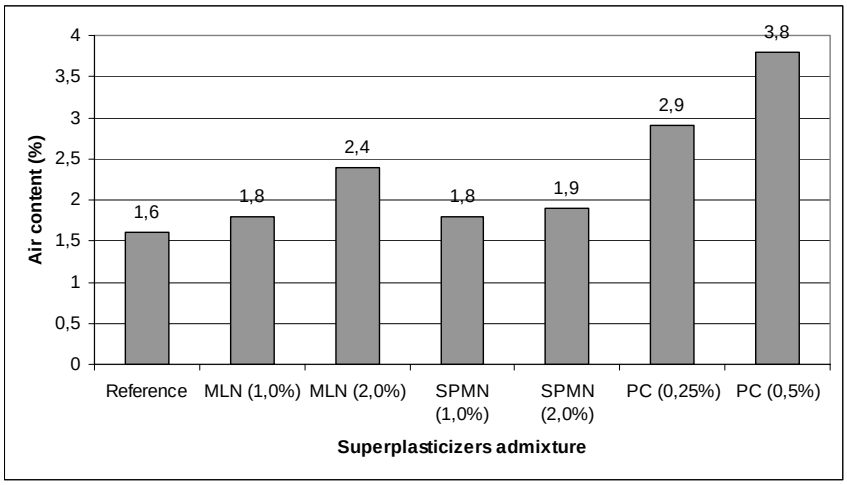



Fig. 9 – Variation of the air content with the type and quantity of superplasticizer.

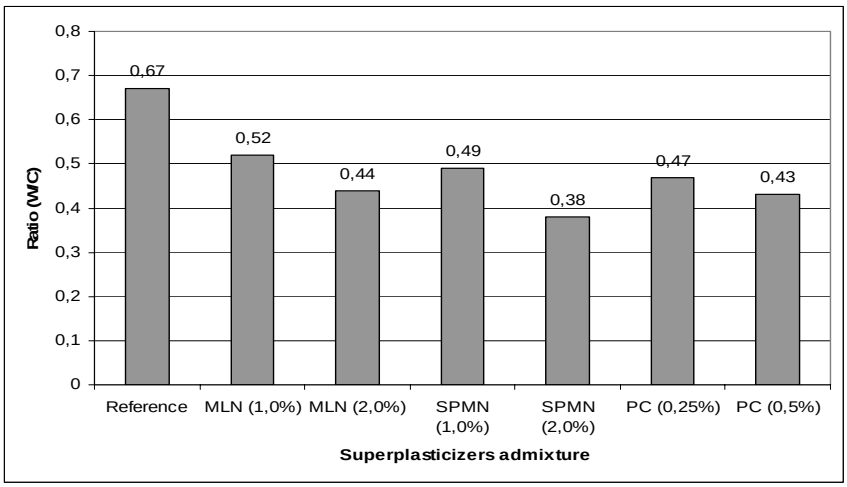



Fig. 10 – Variation of the W/C ratio with the type and quantity of superplasticizer

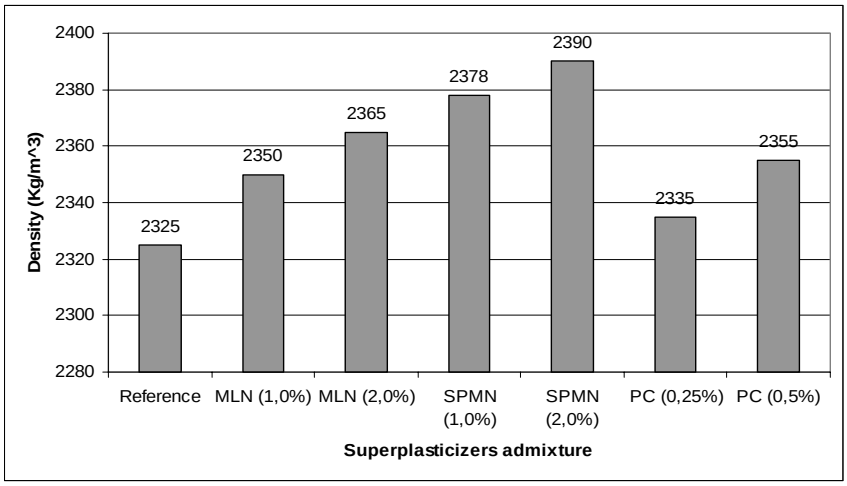



Fig. 11 – Variation of the volumetric mass with the type and quantity of superplasticizer

In the studied compositions, even for small dosages (0.25 and 0.50%) the admixture PC is the one that retains the biggest quantity of air when compared with all other compositions. The compositions with MLN and SPMN are similar in air content. In the case of PC, it will be necessary to add to the formulation an anti-foam, to lower the quantity of air. The compositions with SPMN have the highest densities. This is simple to understand because the admixture SPMN allows a bigger reduction of the W/C ratio, and the quantity of incorporation of air is small. The admixture PC allows a big W/C reduction but the introduction of air in the composition is bigger, not allowing that densities of the compositions with PC to be so height. However the variations on the density of the compositions are not very substantially, because the difference is lower than 3%.

*Water resistance*

The data for air content, W/C ratio and density are presented in figures 12 to 14.

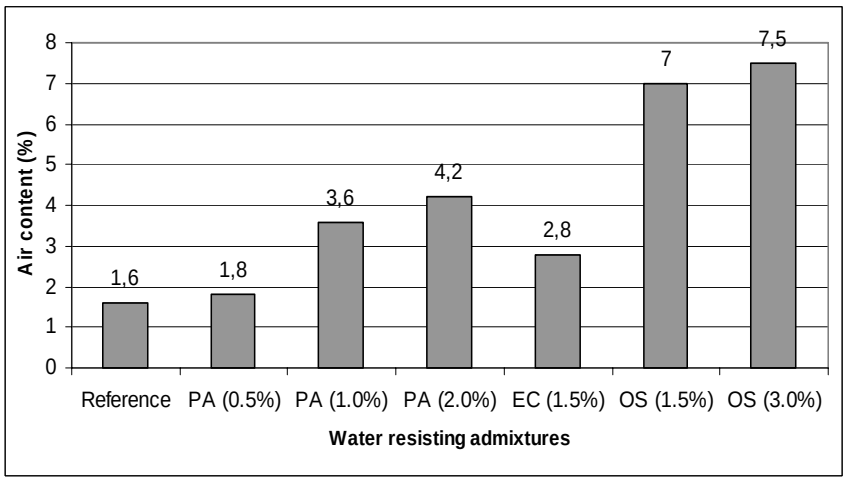



Fig. 12 – Variation of the air content with the type and quantity of water resistance admixture.

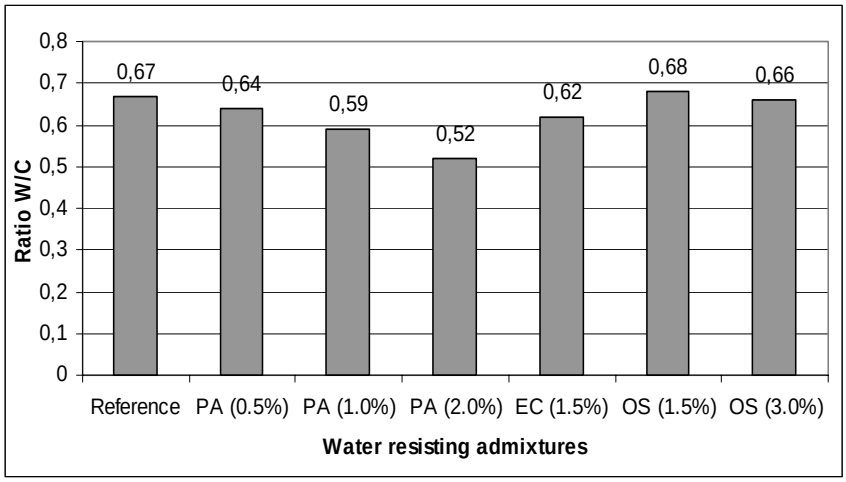



Fig. 13 – Variation of the W/C ratio with the type and quantity of water resistance admixture.

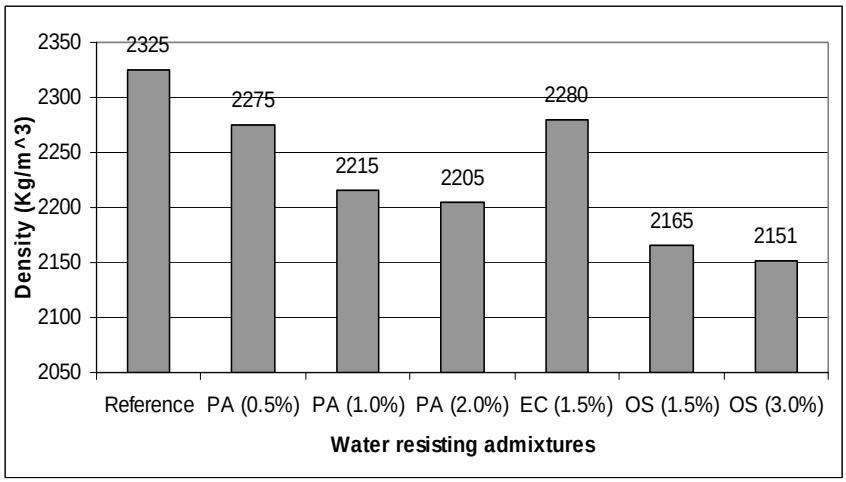



Fig. 14 – Variation of the volumetric mass with the type and quantity of water resistance admixture.

All water resisting admixtures incorporate air in the compositions. The sodium oleate incorporates a very big quantity of air in the compositions, as we can see by the density of the compositions. Because of this the volumetric mass of the compositions is lowered substantially.

There are significant differences in capillary absorption when we use different water resistance admixtures (Table 11 and Figure 15). The PA (acrylic ester copolymer) with 0.5% is not efficacious; there are no significant differences in capillary absorption when compared with reference mortar. In the case of PA (2.0%) there is an important reduction of capillary absorption, but not big enough to comply with EN 934-2. It would be necessary to use a dosage bigger than 2.0% to comply with EN 934-2, but that would not be financially interesting. The water resisting admixtures EC (1.5%) and OS (1.5%) had similar results, exceeding the requirements of EN 934-2 in relation to capillary absorption.

Tab. 11 – Capillary absorption of the studied compositions

| | | Reference mortar | PA (0.5%) | PA (1.0%) | PA (2.0%) | EC (1.5%) | OS (1.5%) | OS (3.0%) |
|---|---|---|---|---|---|---|---|---|
| $C_A$ ($g/mm^2$) 7 days | 24 h | 0.0051 | 0.0051 | 0.0021 | 0.0016 | 0.0009 | 0.0004 | 0.0002 |
| | Reduction of $C_A$ | - | 0% | 58.8% | 68.3% | 82.4% | 92.2% | 96.1% |
| | 7 days | 0.0087 | 0.0086 | 0.0041 | 0.0034 | 0.0019 | 0.0006 | 0.0004 |
| | Reduction of $C_A$ | - | 1.2% | 52.9% | 60.9% | 78.2% | 93.1% | 95.4% |
| $C_A$ ($g/mm^2$) 90 days | 28 days | 0.0154 | 0.0140 | 0.0102 | 0.0069 | 0.0020 | 0.0021 | 0.0017 |
| | Reduction of $C_A$ | - | 9.1% | 33.8% | 55.2% | 87.0% | 86.4% | 89.0% |

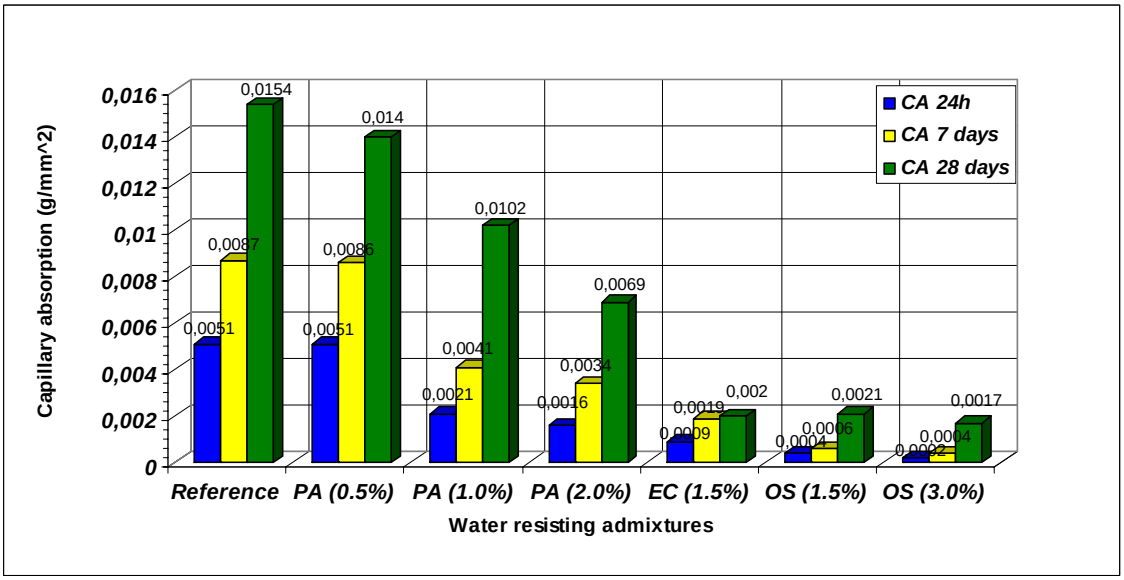



Fig. 15 – Variation of the capillary absorption with the type and quantity of water resistance admixture

Table 12 – Compressive strength and water reduction % in the studied compositions

| | Reference concrete | MLN (1.0%) | MLN (2.0%) | PNS (1.0%) | PNS (2.0%) | PC (0.25%) | PC (0.5%) |
|---|---|---|---|---|---|---|---|
| Compressive strength 24h | 13.7 | 21.4 | 21.8 | 23.2 | 24.2 | 25.2 | 29.1 |
| Variation in Compressive strength at 24 hours | - | +56.2% | +59.1% | +69.3% | +76.6% | +83.9% | +112.4% |
| Compressive strength 7 days | 22.6 | 38.4 | 44.6 | 39.5 | 43.9 | 42.1 | 46.4 |
| Variation in Compressive strength at 7 days | - | +69.9% | +97.3% | +74.8% | +94.3% | +86.3% | +105.3% |
| Compressive strength 28 days | 32.6 | 47.0 | 48.6 | 45.5 | 55.8 | 46.0 | 50.4 |
| Variation in Compressive strength at 28 days | - | +44.2% | +49.1% | +39.6% | +71.2% | +41.1% | +54.6% |
| Water reduction | - | 22.3% | 33.8% | 26.3% | 43.1% | 29.8% | 36.1% |

## 4.2 Mechanical Properties

*Superplasticizers*

The compressive strengths are tested until 28 days, because in a first analysis this is the most important period and with this date it is possible to have an idea about other physic and mechanical properties. The table 12 and figures 16 e 17 show the compressive strength of the studied compositions at 1, 7 and 28 days.

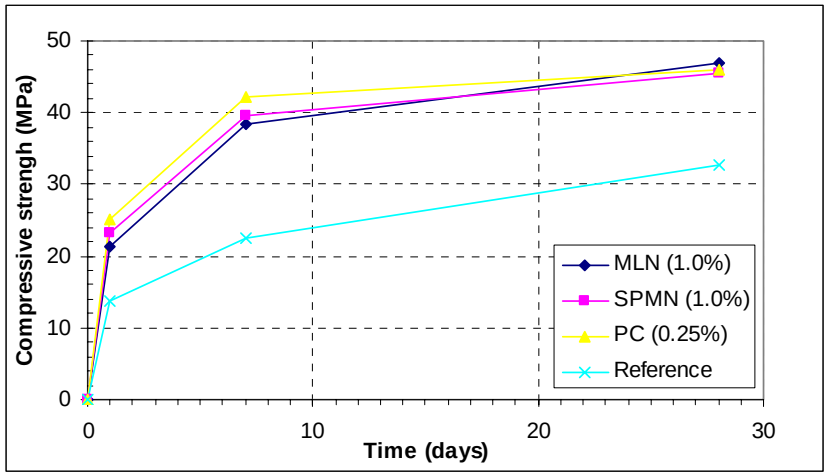



Fig. 16 –Compressive strength at 1, 7 and 28 days.

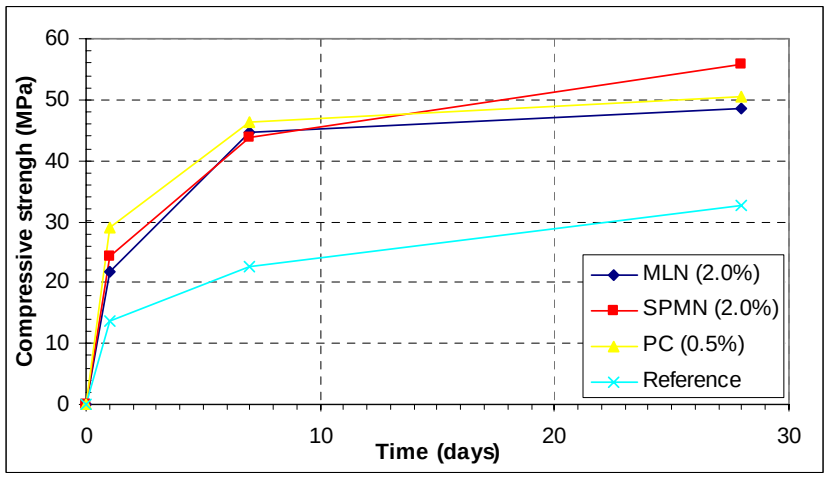



Fig. 17 – Compressive strength at 1, 7 and 28 days.

We can see that with all this admixtures and with those dosages, the mechanical resistances in all ages are increased. In the beginning the increase in mechanical compressive strength is more significant, mainly in composition with PC. In the composition with 2.0% of PNS the best result was achieved at 28 days, allowing a variation of 71.2 % compared with the reference concrete.

We can also see that with PC (policarboxilate, third generation admixture), using a four time lower quantity, we achieve slightly better results in early ages when compared with other admixtures. It is important to point out the excellent result of the composition with 0.5% of PC that allows at 24 hours a raise of 112.4% in compressive strength, compared with reference concrete.

*Water resisting*

The compressive strength was only evaluated at 28 days, in accordance with EN 934-2 (Table 13).

Table 13 – Compressive strength and water reduction % in the studied compositions

| | Reference Concrete | PA (0.5%) | PA (1.0%) | PA (2.0%) | EC (1.5%) | OS (1.5%) | OS (3.0%) |
|---|---|---|---|---|---|---|---|
| Compressive strength 28 days | 32.6 | 30.0 | 30.4 | 30.2 | 29.0 | 18.6 | 16.3 |
| Variation Compressive strength 28 days | - | -8.0% | -6.8% | -7.4% | -11.0% | -42.9% | -50.0% |
| Water reduction | - | 4.5% | 11.7% | 22.4% | 7.5% | - | 1.5% |

In all the compositions there was a decrease in compressive strength. That is not surprising because all the tested admixtures incorporate air in the composition. In the admixture OS the reduction of compressive strength is very pronounced not allowing the accordance with EN 934-2. The compositions with PA and EC complies the standard. Even introducing air in the composition they reduce the water, achieving similar results to the reference concrete.

## 5. CONCLUSIONS

The following conclusions based on experimental data of this study are presented.

With regards to the use of Superplasticizing admixtures:

- The third generation admixture policarboxilate shows a % of air content superior to the others superplasticizers, although all the compositions had a % air content superior to the reference concrete;
- All the tested admixtures, allowed a big reduction of W/C, reaching in the case of SPMN (2.0%) and PC (0.5%) 43.1% and 36.1% respectively;
- The compositions with SPMN had the biggest volumetric mass, although the differences are not very significantly, inferior to 3%;
- Using the tested admixtures there is a significantly rise in compressive strength, comparatively with the reference concrete;
- The compositions with the admixture PC had a more fast development of compressive strength when compared with other admixtures. In the composition with 0.5% of PC, comparing with reference concrete, there is a raise of 112.4% in compressive strength at 24 hours and 105.3% at 7 days;
- The compositions with SPMN (2.0%) have a raise in compressive strength at 28 days of 71.2%;
- In the tested dosages, all the admixtures tried comply the requirements of the standard EN 934-2 for superplasticizing/high range water reduction admixtures (at equal consistence).

With regards to the water resistance admixtures:

- All the water resisting admixtures incorporate a significantly amount of air in the composition specially the OS;
- The PA and PC admixtures allow a small reduction of water;

- All the compositions with water resisting admixtures showed a density reduction, specially the compositions with OS;
- With the tested dosages the PA admixture do not comply the standard EN 934-2, because of the requirement for the capillary absorption;
- In the tested dosages with the OS admixture we can achieve a high reduction on capillary absorption, significantly above the requirements of the standard, but does not complies the compressive strength (values much more under the limit);
- The EC admixture comply the standard EN 934-2 for the water resisting admixtures. Allow a high reduction on capillary absorption, without changing significantly the compressive strength.

## 6. ACKNOWLEDGEMENTS

The authors are indebted to *Quimidois - Indústria Química, Lda* for the supply of admixtures and for all the given support.

## 7. REFERENCES

ACI, Chemical admixtures. American Concrete Institute. ACI compilation 23. 1995, 88 p.

Coutinho, A. Sousa, "Concrete production and properties", LNEC, 1997 (*in portuguese*)

EN 1015-2, Methods of test for mortar for masonry – Part 2: Bulk sampling of mortars and preparation of test mortars (1998).

EN 1015-3, Methods of test for masonry – Part 3: Determination of consistence of fresh mortar (by flow table) (1999).

EN 12350-1, Testing fresh concrete - Part 1: Sampling (2002)

EN 12350-2, Testing fresh concrete - Part 2: Slump test (2002)

EN 12350-6, Testing fresh concrete - Part 6: Density (2002)

EN 12350-7, Testing fresh concrete - Part 7: Air content - Pressure methods (2002).

EN 12390-2, Testing hardened concrete - Part 2: Making and curing specimens for strength tests (2003)

EN 12390-3, Testing hardened concrete - Part 3: Compressive strength of test specimens (2003).

EN 480-1, Admixtures for concrete, mortar and grout - Test methods Part 1. Reference concrete and reference mortar for testing (2000).

EN 480-5, Admixtures for concrete, mortar and grout - Test methods Part – Parte 5: Determination of capillary absorption (1998).

EN 934-2, Admixtures for concrete, mortar and grout - Part 2: Concrete admixtures - Definitions, requirements, conformity, marking and labelling (2003).

Rixom, R., Chemical admixtures for concrete. E & FN Spon, 3rd,1999, 437 p.

Rocha, P. Almeida Rocha, High performance concrete, Master thesis (*in portuguese*), 1999.

International Symposium Polymers in Concrete
2 - 4 April 2006
Guimarães, Portugal

# Strength and Chemical Resistance of Fiber Reinforced Concrete based on Polybutadiene Matrix

Yuriy Borisov, Yuriy Potapov, Dmitriy Panfilov

*University of Architecture and Civil Engineering, Voronezh, Russia*

Oleg Figovsky, Dmitriy Beilin

*Polymate Ltd, Migdal HaEmek, Israel*

**ABSTRACT**

A new type of conglomerate composites – polymer concrete based on polybutadiene belonging among the liquid rubbers containing up to 90% mineral filler by weight has been enveloped and investigated. Concept of this material is based on application of low molecular butadiene hardened by sulfur in presence of special additives. Quartz sand and fly ash are used as fillers and fine grained granites and basalt chipping as coarse aggregate. The resulting material has very high acid and alkali resistance, toughness and adhesion to metal reinforcement, low water absorption and remarkable compression strength (up to 100 MPa).

The fibrous reinforcement of the proposed polymer concrete is particularly attractive for crack resistance increasing at operation in aggressive environment. Influence of various kinds of fiber materials, fiber aspect ratio, reinforcement ratio and particle size of coarse aggregates on compressive, tensile and bending strength is examined. Some physical-mechanical properties of the new continuously reinforced polymer concrete in various corrosion media are investigated.

## 1. INTRODUCTION

For many applications, it is becoming increasingly popular to reinforce the concrete with small, randomly distributed fibers. Their main purpose is to increase the energy absorption capacity and cracking resistance of the material. But also the increase in tensile and flexural strength is often the primary objective. Fiber reinforcements increase concrete's toughness and ductility (the ability to deform plastically without fracturing) by carrying a portion of the load in the case of matrix failure and by arresting crack growth. While steel fibers are probably the most widely used and effective fibers for many applications, other types of fiber are more appropriate for special applications. For example, architectural and decorative concrete products will call for fibers with a minimum of visual impact, so that nylon or polypropylene fibers may be called for.

For fiber reinforcing, the maximum load carrying capacity is controlled by fibers

pulling out of the composite because fibers do not have a deformed surface like steel reinforcing bars. Some fibers are more "slippery" than others when used as reinforcing and exert primary control over a toughness of the concrete product in which they are placed. In freshly mixed concrete, they increase resistance to plastic shrinkage. In hardened concrete they improve strength and toughness depending on fiber type, shape, size and amount.

From this point of view the continuously reinforced new kind of polymeric concrete on the basis of low molecular polybutadiene binder (from here on *RubCon*) with the highest mechanical characteristics and chemical resistance in different aggressive environments has a great potential for engineering practice as it can enhance structural performance, reduce amount of bar reinforcement, provide for a simplified construction technique and lower construction cost.

Properties of a fibrous concrete as composite material depend on properties of its components from which the major are the steel or nonmetallic fibers. Because the Young's modulus of steel fibers is 4-8 times that of concrete it is possible to increase strength of concrete and its crack resistance. According to lab tests, small diameter steel fibers added to concrete mixture reduce its visible shrinkage cracking by more than 80%, increase toughness and atmospheric durability. Different factors such as reinforcement ratio, size and form of fibers and particle size of a coarse aggregate exert a great action on the mechanical properties of a continuously reinforced concrete. The influence of these parameters on strength and deformation characteristics of fibrous polymer concrete is investigated in [1, 2, 3].

Chemical action of corrosive environments changes the structure of polymeric materials and results in irreversible deterioration of compositions. Chemical stability and water absorption of fiber reinforced *RubCon* in acid and alkaline media are studied in the present work. The choice of aggressive environments was based on their prevalence in industrial production and also qualitative and quantitative characteristics of chemical stability of fibrous and plain *RubCon*.

## 2. EXPERIMENTAL RESULTS AND DISCUSSION

### 2.1 Effect of fiber reinforcing ratio and particle size of the coarse aggregates on *RubCon's* strength

Materials used in fiber reinforcing of composite materials include acrylic, asbestos, cotton, glass, nylon, polyester, polyethylene, polypropylene, rayon, rock wool and steel. Acid resistant glass and steel fibers have received a wide application as concrete reinforcement. Behavior of continuously reinforced *RubCon* with arbitrary located steel fibers was examined. Fibers were made from chopped high strength steel tire cord with a brass cover. Our preliminary researches of the fibrous *RubCon* containing fine-grained gravel have shown that fibers with aspect ratio (relative length) L/d=100 are located uniformly, without clots and allow to achieve the high strength and deformation characteristics.

Full two-factorial experiment is carried out. Varied parameters were the reinforcement ratio $\boldsymbol{\mu}$ and particle size of coarse aggregate $\boldsymbol{a}$; response functions were tensile, compressive and bending strength of the polymer concrete samples with size: 4×4×16 cm and 4×4×40 cm. During the experiment the reinforcement ratio and particle size were changed from 0% (without reinforcement) to 3% with step of 1% and from 0 (without crushed stone) to 15 mm with step of 5 mm, correspondingly. Results of the experiments are illustrated on Figures 1-3.

It can be seen that at increase of the particle size of coarse aggregate at constant reinforcement ratio the *RubCon* strength characteristics are decreased. Especially clearly this

tendency is shown for tensile strength. The increase of strength characteristics with growth of reinforcing ratio in all range values was quite expected at beforehand given the particle size of coarse aggregate.

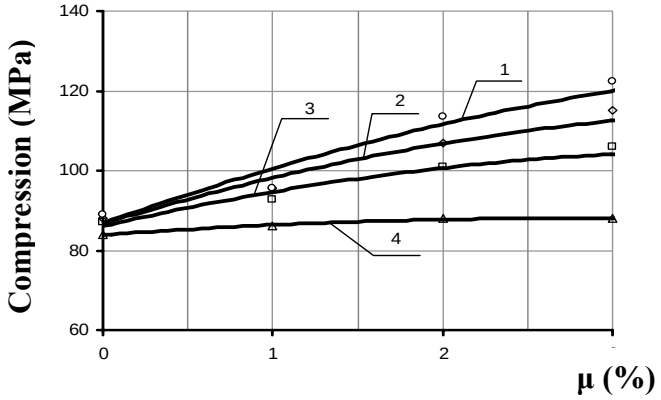



Figure 1: Influence reinforcement ratio and particle size of coarse aggregate on compression strength of fibrous RubCon: 1 - without crushed stone; 2 - with crushed stone up to 5 mm; 3 - with crushed stone up to 10 mm; 4 - with crushed stone up to 15 mm.

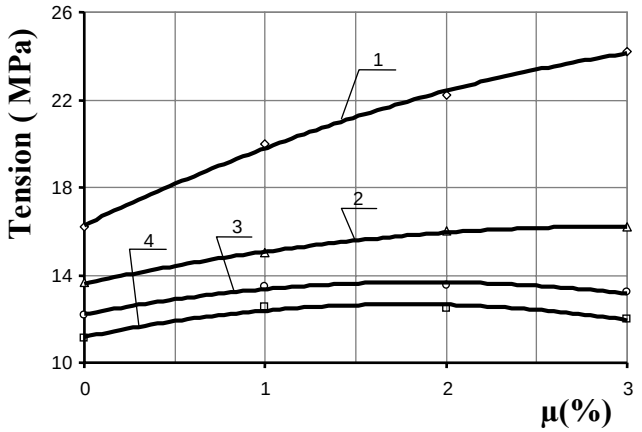



Figure 2: Influence reinforcement ratio and particle size of coarse aggregate on tensile strength of fibrous RubCon: 1 - without crushed stone; 2 - with crushed stone up to 5 mm; 3 - with crushed stone up to 10 mm; 4 - with crushed stone up to 15 mm.

The experiments carried out have made possible to propose the practical method of reinforcing ratio and coarse aggregate quality assignment depending on required strength characteristics of *RubCon*. The compression, tensile and bending strength dependences of aggregate particle size ***a*** and percentage of reinforcement ***μ*** are shown in Figures 4-6.

It should be noted that at ***μ >2%*** the growth of strength is slowed down as a result of fibrous clotting in the process of *RubCon* making. Clotting makes the production process more complicated and causes many defects in *RubCon* structure.

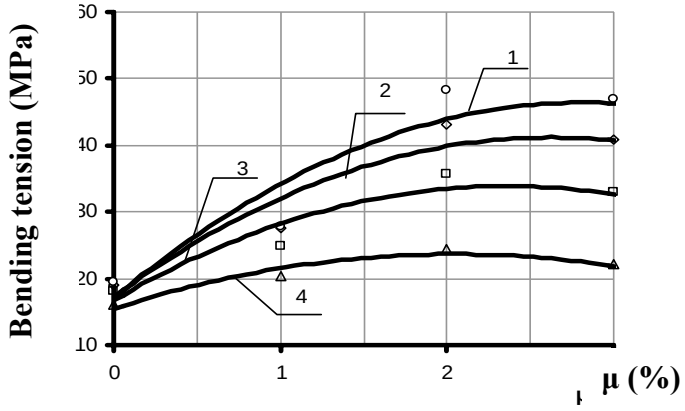



Figure 3: Influence of reinforcement ratio $\mu$ (%) and particle size of coarse aggregate a (mm) on bending strength of fibrous RubCon*:* 1 - without crushed stone; 2 - with crushed stone up to 5 mm; 3 - with crushed stone up to 10 mm; 4 - with crushed stone up to 15 mm.

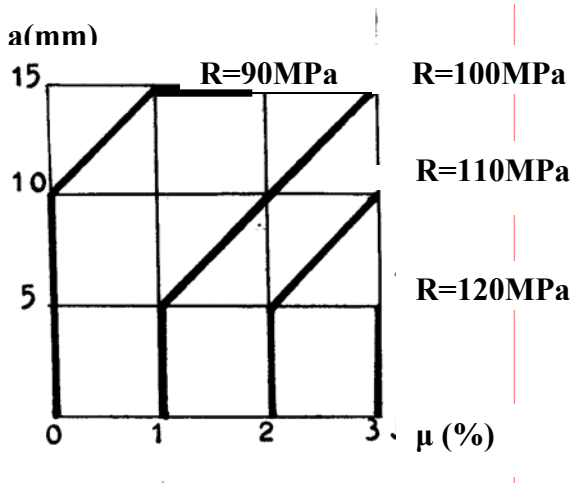



Figure 4: The RubCon compression strength (MPa) dependence on reinforcement ratio $\mu$ (%) and particle size of coarse aggregate $a$ (mm)

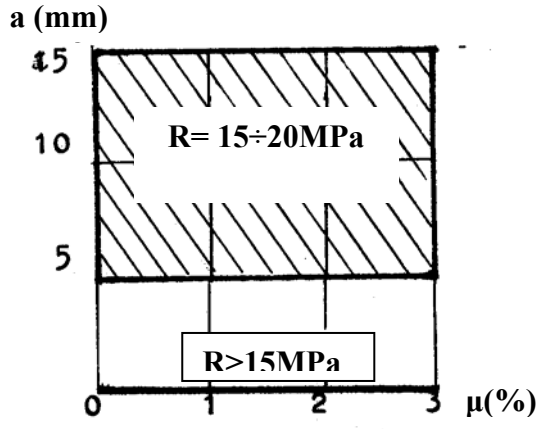



Figure 5: The RubCon tensile strength (MPa) dependence on reinforcement ratio $\mu$ (%) and particle size of coarse aggregate $a$ (mm)

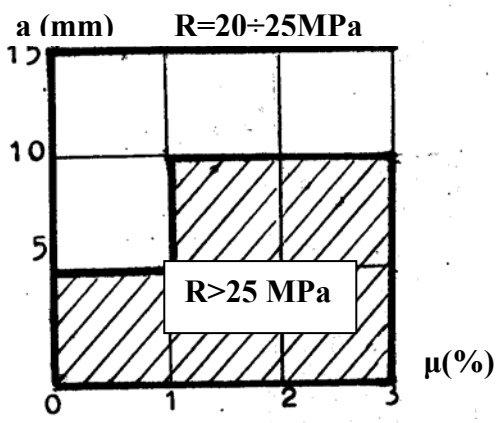



Figure 6: The RubCon bending strength (MPa) dependence on reinforcement ratio (***μ***, %) and particle size of coarse aggregate (***a***, mm).

## 2.2 Strength of continuously reinforced *RubCon* with various kinds of fibers

Investigations to find an effect of kind and sizes of fibers on *RubCon's* strength were carried out. Experiments were performed with samples of 4×4×16 cm. Various materials of fibers were used: steel, polypropylene, rough basalt and glass. The steel fibers with brass cover were manufactured from highly strength metal cord of tires.

Reinforcement ratio for appropriate fibers materials was adopted according to our preliminary researches. So the optimal volume of fiber content is 1.0-1.5% for steel fibers and 1.0-5.0% for glass ones. Control samples without reinforcement were prepared as well.

Figure 7 illustrates the relationship between bending tension of *RubCon* samples and reinforcement ratio and the kind of fibers.

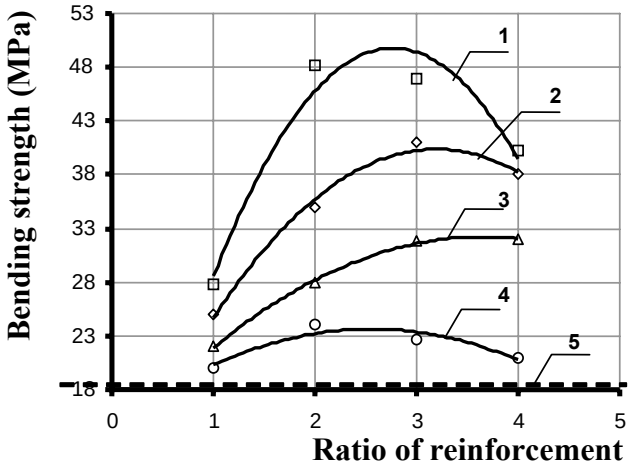



Figure 7: RubCon bending tension dependence of the reinforcement ratio and the kind of fibers: 1- steel fibers; 2- polypropylene fibers; 3- rough basalts fibers; 4- glass fibers; 5- control sample without reinforcement

One can see that bending strength of fibrous reinforcement samples radically differs from strength samples without reinforcement. In this case steel fibers from metal cord provide the highest bending tension. It worth noting, that with increasing reinforcement ratio the bending strength of *RubCon* tends to decrease owing to fibers clotting.

In the course of tests we observed various character of *RubCon* samples destruction depending on a material of reinforcing fibers. The application of rough basalt or glass fibers

results to brittle destruction of samples, which follows break of fibers. In this case the crack formation moment coincides with that of break of fibers. It should be noted, that crack formation of *RubCon* samples reinforced by steel or polypropylene fibers begins much earlier than fracture of fibers.

One of the major areas of *RubCon* application is structures exposed to aggressive environments [1], where crack resistance of the material is important. Our experiments have shown, that steel fibers improve crack resistance and allow to produce a material with high elastic-plastic properties. That is a reason that we have undertaken research of influence of fibers reinforcement ratio and aspect ratio on *RubCon* strength at compression, tension and bending.

Varied parameters were the reinforcement ratio $\boldsymbol{\mu}$ and aspect ratio of the fibers ***L/d***; response functions were tensile, compressive and bending strength. During the experiment the reinforcement ratio and aspect ratio were changed from 1% to 4% with a step of 1% and from 40 to 130 with a step of 30, respectively.

Results of the experiments are illustrated in Figures 8 - 10.

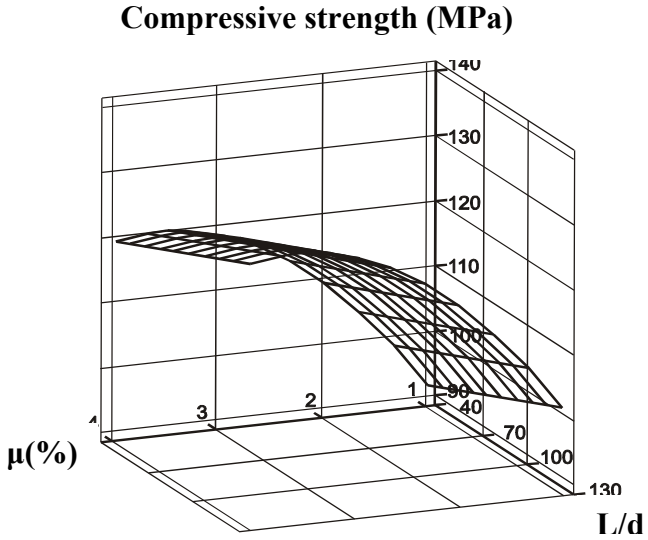



Figure 8: Influence reinforcement ratio μ and aspect ratio L/d of the steel fibers on compression strength of fibrous RubCon

The analysis of the obtained results shows, that with increase in relative length of fibers ***L/d*** strength of *RubCo*n grows and having reached a maximum is reduced. It is especially appreciable in case of bending strength (Figure 10). The explanation of this phenomenon is connected to feature of a plastic matrix and rigid elastic fibers interaction. It should be taken in mind that elasticity modulus of steel fibers is 5-6 times higher than that of *RubCon*. During loading process at relatively large aspect ratio ***L/d*** pull-out of fibers from the polybutadiene binder is observed owing to decrease of adhesion bond between *RubCon* matrix and fibers.

Strength characteristics of steel fiber reinforced *RubCon* depend on the reinforcement ratio $\boldsymbol{\mu}$. Results of experiments show that an optimum of saturation by fiber reinforcement is in the range 2-3%. Fibers' clotting is observed at the greater volume of fibers; it causes decrease of *RubCon* strength and serious structural defects.

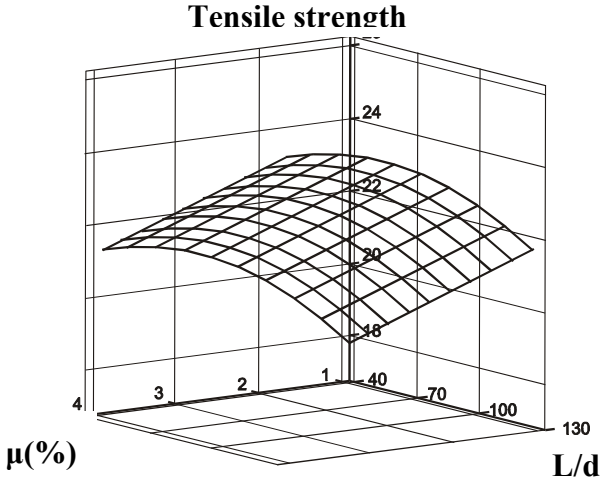



Figure 9: Influence of reinforcement ratio μ and aspect ratio L/d of steel fibers on tensile strength of fibrous RubCon

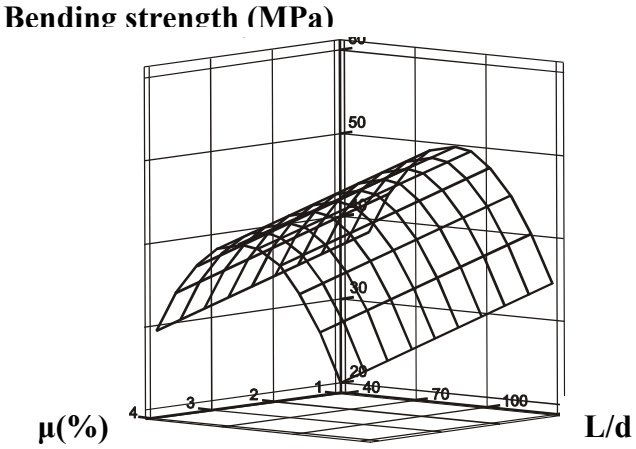



Figure 10: Influence of reinforcement ratio μ and aspect ratio L/d of steel fibers on bending strength of fibrous RubCon

During the experiments we investigated the formation and development of cracks in *RubCon* samples. Crack formation took place at $L/d$=40, 70, 100, 130 and $\mu$=1% and at $L/d$=40 and $\mu$=1, 2, 3%. In that case $N_{crc}/N_u \approx 1$, where $N_{crc}$ – load crack formation, $N_u$ - ultimate load. Crack formation load decreased at high values of $L/d$ and $\mu$ ($N_{crc}/N_u \approx 0.66$).

## 2.3 Chemical resistance of *RubCon*

Durability of *RubCon* depends to as greater extent on its resistance to attack by water and corrosive media. Tests of chemical resistance of *RubCon* samples of 4x4x16 cm size was carried out into water, 70% $H_2SO_4$ solution, 5% $H_3PO_4$ solution, 36% HCl solution and 25% $NH_4$ water solution. Change of weight and compression strength of the samples after exposition in aggressive environments at 10, 30, 60, 90, 180, 270 and 360 day of exposure as compared with control samples was a criterion of *RubCon* chemical resistance.

The results of experiment are shown in Table 1 and Figures 11-13 as the curves of mass absorption and chemical resistance of *RubCo*n samples.

It is apparent that *RubCon* has hydrophobic properties with coefficient of water resistance $\mathbf{K_{xc}}$= 0.995 and water absorption $\mathbf{\Delta m}$ = 0.05%. It is possible to explain such small change of weight by nature of binder (polybutadiene), which practically is not dampened by

water. Compressive strength of *RubCon* is reduced during the first 180 day owing to water penetration into micro pores and micro cracks of the samples. As this takes place the strength of intermolecular interaction is lowered and the stresses in the top of microcracks increase.

Destruction of polymer binding under inorganic acids exposure causes tears of polymer macromolecules. In turn, it results in a lowering of *RubCon* strength and increasing of its deformation.

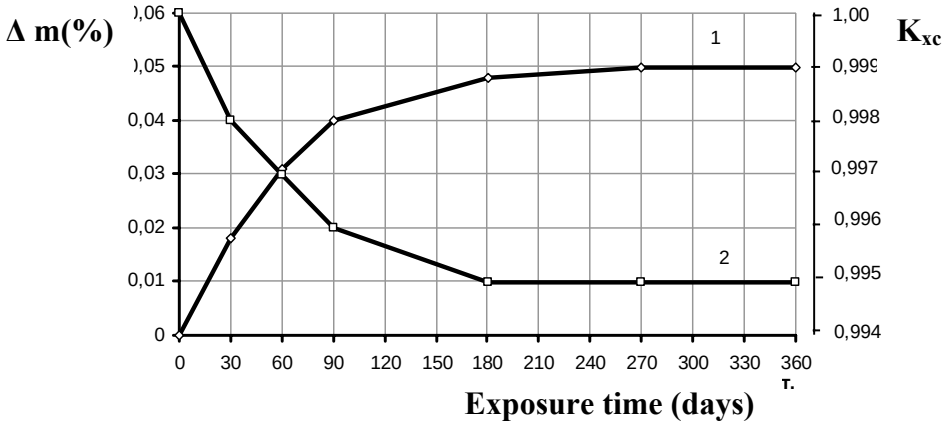



Figure 11: 1 - water absorption of RubCon; $\Delta m = (m_1-m)*100/m$ (m - mass of sample before immersion in water, $m_1$ - mass of sample after immersion in water); 2 - coefficient of water resistance; $K_{xc} = R_1/R_0$ ($R_1$ –compressive strength of sample after immersion in water, $R_0$- compressive strength of control sample

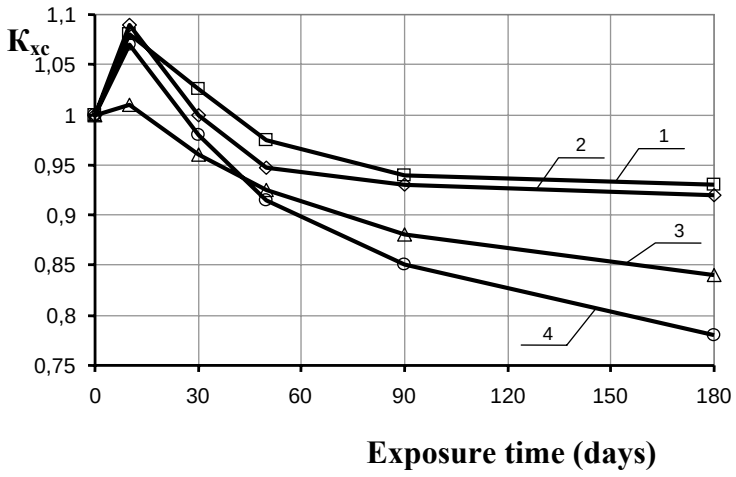



Figure 12**:** Relationship between coefficient of chemical resistance and exposure time in corrosive environments: 1- 70 % solution of $H_2SO_4$, 2 - 5 % solution of $H_3PO_4$, 3- 25 % solution of $NH_4$, 4- 36 %-solution of HCl

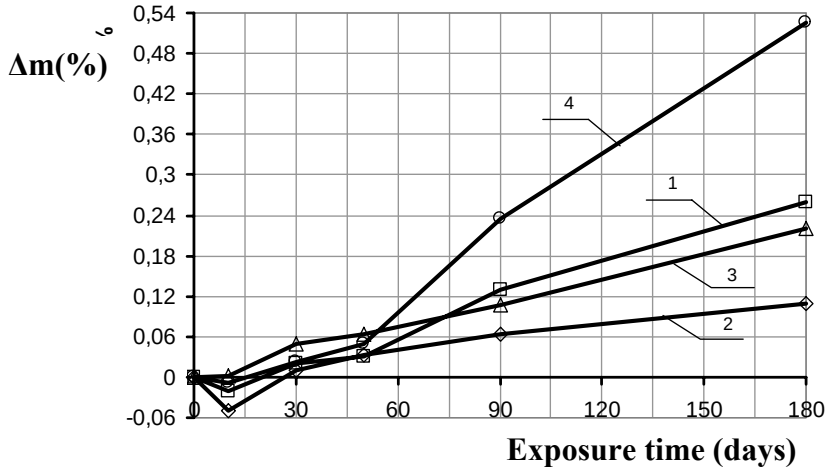



Figure13: Kinetics of RubCon mass absorption: 1- 70 % solution of $H_2SO_4$, 2 - 5 % solution of $H_3PO_4$, 3 - 25 % solution of $NH_4$, 4 - 36 %-solution of HCl

It should be mentioned that during first 10 days exposure in inorganic acid environments compressive strength of *RubCon* samples grows. In a given time strength is increased for 7 % in 36% solution of HCL for 9% in 5% solution of $H_3PO_4$ and for 8% in 70% solution of $H_2SO_4$.

An increase of compressive strength in an initial stage of exposure is directly related to the adsorption by surface micro defects and surface seal. Long time influence of the corrosion environment results in profound changes of *RubCon* structure, destruction of polymeric binding and break of adhesive bonds. All contribute to decrease of *RubCon* strength. Different character of *RubCon* strength decrease in aggressive environments is caused by various speeds of chemical transformations, such as corrosion, oxidation, sulphurizing, chlorination etc.

Table 1: Physical-mechanical properties of *RubCon* at attack of inorganic acids and ammonia solutions

| Corrosive media | Parameter | Time of exposure | | | | | |
|---|---|---|---|---|---|---|---|
| | | 0 | 10 | 30 | 50 | 90 | 180 |
| 36% HCl | Δm, % | 0 | -0.09 | 0.021 | 0.052 | 0.234 | 0.526 |
| | $K_{xc}$ | 1 | 1.07 | 0.98 | 0.915 | 0.85 | 078 |
| 70% $H_2SO_4$ | Δm, % | 0 | -0.02 | 0.023 | 0.031 | 0.13 | 0.26 |
| | $K_{xc}$ | 1 | 1.08 | 1.026 | 0.974 | 0.94 | 0.93 |
| 5% $H_3PO_4$ | Δm, % | 0 | -0.05 | 0.01 | 0.033 | 0.064 | 0.11 |
| | $K_{xc}$ | 1 | 1.09 | 1 | 0.947 | 0.93 | 0.92 |
| 25% water solution $NH_4$ | Δm, % | 0 | 0.002 | 0.05 | 0.063 | 0.107 | 0.22 |
| | $K_{xc}$ | 1 | 1.01 | 0.96 | 0.925 | 0.88 | 0.84 |

## 3. CONCLUSIONS

From the experiment results it may be concluded that:

- The increase of the particle size of coarse aggregate at constant reinforcement ratio results in decrease of *RubCon* compressive, tensile and bending strength.

- The optimal composition of continuously reinforcement *RubCon* from the point of view its strength is: reinforcement ratio **μ** = *2%*; maximal particle size of coarse aggregates **a** = 5 mm.
- At ***μ*** > 2% clotting of fibers is observed, which results in the formation of structural defects. Application of fiber reinforcement made of various materials improves significantly the bending strength of *RubCon*.
- Steel fibers improve crack resistance *RubCon* and allow producing the material with high elastic-plastic properties.
- Optimal parameters of steel fiber reinforcement are: reinforcement ratio ***μ***=2%; relative length of fiber ***L/d***=100.
- Application of steel fibers with the aspect ratio ***L/d*** > 100 is not efficient.
- Continuously reinforced *RubCon* has high compressive, tensile and bending strength.
- *RubCon* is a hydrophobic and chemical resistant material in inorganic acid environments.
- Continuous reinforced *RubCon* can find a wide application in structures exposed to aggressive media and dynamic loading.

REFERENCES

[1] Figovsky,O., Beilin, D., Blank, N. and Potapov, Yu., 'Development of Polymer Concrete with Polybutadiene Matrix '. *J. Cement and Concrete Composites,* **18** (6) (1996) 437-444.

[2] Potapov,Yu., Borisov,Yu., Panfilov, D., Figovsky, O. and Beilin, D., 'Influence of Piratical Size of Coarse Aggregates and Reinforcement Ratio on the Fibrous Polymer Concrete Strength', *J. Scientific Israel - Technological Advantages,* **6** ( 3-4) (2004) 67-70.

[3] Potapov, Yu., Borisov, Yu., Panfilov, D., Figovsky, O. and Beilin, D., 'Strength of Continuously Reinforcement Polymer Concrete with Various Kinds of Fibers', *J. Scientific Israel - Technological Advantages,* **6** (3-4) (2004) 71-74.

International Symposium Polymers in Concrete
2 - 4 April 2006
Guimarães, Portugal

# Effect of the Addition of Synthetic Fibers to Concrete Thin Slabs on Plastic Shrinkage Cracking

Almir Barros S. Santos Neto[1], Fernando Pelisser[1], Daiane dos S. da Silva[2]

*University at the Extreme South of Santa Catarina (UNESC)*
*Av. Universitária, 1105 - Bairro Universitário - C.P. 3167 - CEP: 88806-000 - Criciúma, Brazil*

Henriette Lebre La Rovere[3], Roberto Caldas de Andrade Pinto[3]

*Federal University of Santa Catarina (UFSC)*
*Campus Trindade – Centro Tecnológico P.O. Box 476 PPGEC - CEP: 88040-900*
*Florianópolis, Brazil*

## ABSTRACT

Plastic shrinkage cracks may occur even when standard precautions have been taken, which may impair the durability and serviceability of concrete structures. One way to prevent such cracks is by adding short fibers to the concrete mixture. The aim of this work is to evaluate the effect of the addition of synthetic fibers, such as polypropylene, glass, nylon and PET (Polyethylene Terephtalate) fibers in concrete cracking control. An experimental program was conducted to investigate plastic shrinkage cracking in small thin slabs, by varying the fiber volume fraction (0.05 % and 0.10 %) of fibers in the mixtures. Concluding remarks and a few recommendations are given at the end of the work.

## 1. INTRODUCTION

Concrete is a composite material made of two main phases: a continuous and a discontinuous one. The continuous phase is given by the paste resulting from the cement and water mix, whereas the discontinuous phase is composed of coarse and fine aggregates. This conventional concrete is a brittle material that has little ability to withstand shrinkage effects.

Concrete is subjected to shrinkage in a plastic stage, as well as during hardening. Plastic shrinkage – is defined as the water lost from the concrete paste in the fresh state, before curing takes place and while the solid particles can still move inside the paste. The volume reduction in this case corresponds to the water loss. Drying shrinkage – is defined as the volume reduction in concrete after being cured. In this case shrinkage depends on the size and type of voids in the concrete and also on how the water is connected to the solid particles surfaces of the hardened concrete: if it is free; adsorbed in the internal walls of its structure; in between hydrated silicate layers; or chemically combined. It is generally assumed that the total shrinkage magnitude of the hardened concrete depends directly on the difficulty to remove water, and also on the mechanical properties of concrete.

[1] Assistant Professor at UNESC, Ph.D. Candidate in Civil Engineering - UFSC.
[2] Undergraduate student in Civil Engineering – UNESC.
[3] Associate Professor – UFSC.

Both plastic and drying shrinkage can cause cracking in concrete with the consequent increase on permeability and on the risk of environmental agents penetration onto the exposed surfaces. Thus, the durability and serviceability of concrete structures can be impaired leading to the reduction of the construction lifetime, Bastos [2001] and Soroushian et al. [1995].

The use of short fibers in concrete or mortar mixtures as a way to prevent shrinkage cracking has been continuously increasing in the past few years. One crack control method, widely accepted by researchers, is the use of randomly distributed fibers, particularly fine synthetic fibers with a volume fraction below 0.5 %, Naaman [2005]. Particularly, the addition of short polypropylene fibers with a low volume ratio has been widely employed in USA, Canada, Japan and Europe, mainly in bridge decks and industrial floors, where the composite material has the advantage of no-corrosion as compared to the conventional steel grids or meshes used in concrete slabs, ACI 544 [1997].

The composite material made of concrete and short fibers is named fiber-reinforced concrete (FRC). Different fibers made of steel, glass or polymers, ACI 544 [1997], have been added to concrete in order to improve its performance and durability. Such fibers are found in different shapes and sizes, Mehta and Monteiro [1994].

The use of FRC in structures subjected to dynamic loading, such as pavements, has already been established, Hannant [1994], Bentur and Mindess [1990], Zollo [1997]. More recently other FRC applications in Civil Engineering are arising, like shotcrete in tunnels, precast concrete elements and blocks, concrete pipelines and foundations, etc. The main advantage of the use of FRC is in shrinkage crack control. A low volume ratio of plastic fibers, as for instance 0.10 % of polypropylene fibers is frequently used to reduce plastic shrinkage cracks, Wang et al. [2001], Tanesi [1999], Balaguru and Slattum [1995], Gopalaratnam and Shah [1995].

Code recommendations for design of FRC structures have already been established in a few countries such as the USA and Japan, however Standard Test Procedures for FRC evaluation are still under development. Crack patterns and crack openings as well as the post-cracking capacity of FRC structures are difficult to evaluate. Several methods for measuring the potential crack control of synthetic fibers additions have been proposed in the past few years. However some of these methods adopt distinct assumptions, Tanesi [1999], indicating that a worldwide-accepted method is still missing.

The aim of this work is to evaluate the influence of the addition of polypropylene, glass, nylon and PET (Polyethylene Terephtalate) fibers in concrete cracking control. An experimental program was conducted to investigate plastic shrinkage cracking in small concrete thin slabs, by using two different fiber volume fractions, 0.05 % and 0.10 %, in the mixtures.

A brief review on plastic shrinkage is presented in the next section. Section 3 describes the experimental program, and the results and conclusions are given in the following sections.

## 2. PLASTIC SHRINKAGE

Cracking due to plastic shrinkage of concrete occurs when volume changes are restrained by aggregates, reinforcement, or due to contact with another surface. Shrinkage generates internal stresses in the concrete paste that will cause cracking when the concrete tensile strength is reached. Cracking formation is more pronounced in the first hours, when concrete strength is still very low. Small cracks caused by early loading and environmental effects can initiate formation of deeper cracks and also facilitate crack propagation, Neville [1982].

It has been observed that a very fluid mixture (high water content), while having the potential for greater volumetric shrinkage than a stiffer mixture with lower water content, may in fact show little or no plastic shrinkage cracking. The fluid concrete remained sufficiently mobile to allow for accommodation of volume changes. Similarly, if the development of tensile capacity of concrete is more rapid than the development of shrinkage stresses or strains, little or no cracking may occur, Shaeles and Hover [1988].

Shrinkage, which is the root cause of theses cracks, is induced by loss of water. It is usually assumed that plastic shrinkage cracking develops when the rate of evaporation exceeds the rate at which bleed water is furnished to the surface. When the rate of evaporation from the surface of the concrete is in excess of 1.0 kg/m$^2$/hr there is a high probability of crack formation due to plastic shrinkage, ACI 305.R [1991].

For given evaporative conditions, it is clear that mixtures with higher paste content have a higher tendency to crack. Similarly, it has been demonstrated that formation of plastic shrinkage cracks is influenced significantly by screeding and finishing operations, Kraai [1985].

## 3. EXPERIMENTAL PROGRAM

To evaluate the influence of the addition of polypropylene, glass, nylon and PET fibers to concrete on plastic shrinkage cracking of thin slabs, an experimental program was conducted at the Materials Laboratory in the Civil Engineering Department of the University in the Extreme South of Santa Catarina (UNESC). The program is based on previous studies performed by Kraai [1995], and also by Balaguru [1994].

A total of 25 specimens, measuring 910 mm by 610 mm, as illustrated in Figure 1, were cast for the experimental testing. In order to ensure a geometric surface area-to-volume relation typical of concrete slabs, a thickness of 20 mm was selected for the specimens. Thus, the plates were cast with mortar instead of concrete, to avoid possible restraining of the cement paste caused by the use of coarse aggregates in such thin plates.

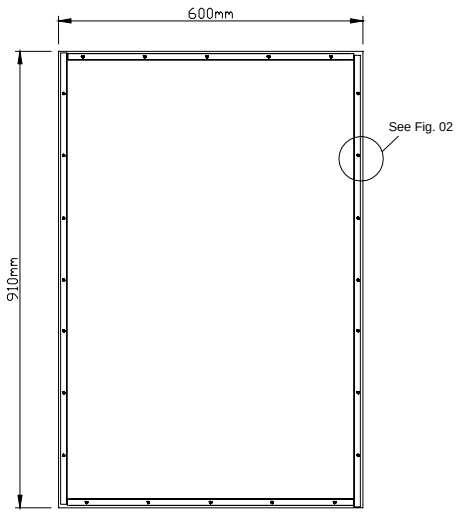



Figure 1 – Concrete plate specimen dimensions.

A modification on the test setup proposed in the previous work by Kraai [1995] is introduced in this work. Instead of restraining the slab edges by means of stiff steel wire meshes, steel brackets of 16 mm flanges were fixed along the entire wooden mold perimeter, as shown in Figure 2. The mold fixture imposes restraining to movement of the cement paste, which is the main cause of cracking in the plates, Grzybowski and Shah [1990].

To avoid water absorption, the bottom and sides of the wooden mold were all covered by a polyethylene film. In this way, the free water movement in the plates can occur only upward without any water absorption by the wooden mold.

Mortar mixtures were prepared according to the mixture proportions presented in Table 1. The fibers were added at three different volume fractions: 1) 0 % (no addition); 2) 0.05 % and 3) 0.10 %. Fiber dimensions, mechanical and physical properties are all given in Table 2. Fine aggregate consisted of natural sand (fineness modulus = 2.97) and a Portland cement type CP-V-ARI-RS (similar to ASTM Type III) was employed. Three specimens (a, b and c) were cast for each fiber volume fraction, of polypropylene, glass and nylon fiber. Two specimens (a, b) were cast for each fiber volume fraction of PET.

Table 1 – Mixture proportions

| | Mixture proportions | | | | | | Flow table (mm) |
|---|---|---|---|---|---|---|---|
| | Fibers | Fibers $V_f$ (%) | Fibers mass (g) | Cement (kg) | Fine aggregate (kg) | W/C ratio | |
| Mix. 1a | 0 | 0 | 0 | 1 | 2.7 | 0.6 | 30.0 |
| Mix. 1b | 0 | 0 | 0 | 1 | 2.7 | 0.6 | 30.0 |
| Mix. 1c | 0 | 0 | 0 | 1 | 2.7 | 0.6 | 30.0 |
| Mix. 2a | Poly. | 0.05 | 8.20 | 1 | 2.7 | 0.6 | 30.0 |
| Mix. 2b | Poly. | 0.05 | 8.20 | 1 | 2.7 | 0.6 | 29.3 |
| Mix. 2c | Poly. | 0.05 | 8.20 | 1 | 2.7 | 0.6 | 29.2 |
| Mix. 3a | Poly. | 0.10 | 16.40 | 1 | 2.7 | 0.6 | 30.0 |
| Mix. 3b | Poly. | 0.10 | 16.40 | 1 | 2.7 | 0.6 | 29.0 |
| Mix. 3c | Poly. | 0.10 | 16.40 | 1 | 2.7 | 0.6 | 29.5 |
| Mix. 4a | glass | 0.05 | 24.20 | 1 | 2.7 | 0.6 | 28.5 |
| Mix. 4b | glass | 0.05 | 24.20 | 1 | 2.7 | 0.6 | 30.0 |
| Mix. 4c | glass | 0.05 | 24.20 | 1 | 2.7 | 0.6 | 29.0 |
| Mix. 5a | glass | 0.10 | 48.40 | 1 | 2.7 | 0.6 | 30.0 |
| Mix. 5b | glass | 0.10 | 48.40 | 1 | 2.7 | 0.6 | 30.0 |
| Mix. 5c | glass | 0.10 | 48.40 | 1 | 2.7 | 0.6 | 30.0 |
| Mix. 6a | Nylon | 0.05 | 10.27 | 1 | 2.7 | 0.6 | 30.0 |
| Mix. 6b | Nylon | 0.05 | 10.27 | 1 | 2.7 | 0.6 | 31.0 |
| Mix. 6c | Nylon | 0.05 | 10.27 | 1 | 2.7 | 0.6 | 30.0 |
| Mix. 7a | Nylon | 0.10 | 20.55 | 1 | 2.7 | 0.6 | 30.0 |
| Mix. 7b | Nylon | 0.10 | 20.55 | 1 | 2.7 | 0.6 | 30.0 |
| Mix. 7c | Nylon | 0.10 | 20.55 | 1 | 2.7 | 0.6 | 30.0 |
| Mix. 8a | PET | 0.05 | 8.20 | 1 | 2.7 | 0.6 | 31.5 |
| Mix. 8b | PET | 0.05 | 8.20 | 1 | 2.7 | 0.6 | 31.5 |
| Mix. 8a | PET | 0.10 | 16.40 | 1 | 2.7 | 0.6 | 33.0 |
| Mix. 8b | PET | 0.10 | 16.40 | 1 | 2.7 | 0.6 | 33.0 |

The mortars were mixed with materials being poured in the following sequence: first the fine aggregate, followed by the water, and finally the cement at the end; in case of fiber addition, the synthetic fibers were poured immediately after the cement. The materials were then mixed for five minutes.

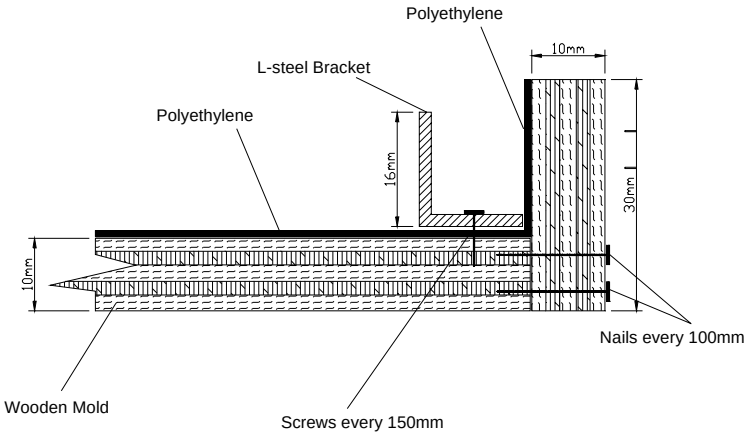



Figure 2 – Detail of wooden mold fixture.

Figure 3 shows the SEM micrograph of the PET fiber.

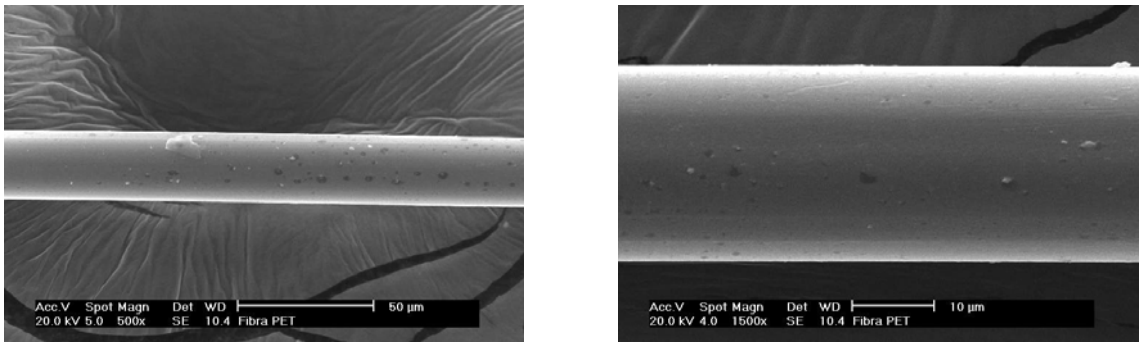



Figure 3 – SEM micrograph of a PET fiber

From Figure 3, it can be observed the smooth texture of the fiber and a circular cross-section shape, with diameter varying from 25 to 30 μm.

Table 2 – Physical and mechanical properties of fibers.

| Properties | Polypropylene | Glass | Nylon | PET |
|---|---|---|---|---|
| Diameter (μm) | 18 | 14 | 18 | 25-30 |
| Length (mm) | 12 | 12 | 13 | 15 |
| Density (g/cm$^3$) | 0.91 | 2.68 | 1.14 | 1.33 |
| Tensile strength (MPa) | 300 | 1700 | 900 | - |
| Elastic Modulus (GPa) | 3 | 72 | 4.76 | - |
| Specific surface area (m$^2$/kg) | 225 | 105 | - | - |
| Melting point ($^o$C) | 160 | - | 260 | 253 |
| Alkaline resistance | high | high | high | - |

After mixing, the mortar consistency was measured in a flow table following the Brazilian Code recommendations, NBR 7215 [1996]. The mortar mixture was then placed into the mold and leveled with a stiff plastic ruler. The plates were leveled manually, keeping the ruler straight and pulling it in the longitudinal direction, without sideways or sawing motion, as shown in Figure 4. A speed of 1 m/min was employed in the leveling or screeding operation.

The plates were exposed to same environmental conditions, i.e., same temperature, air humidity and wind speed, inside an acclimatized room, simulating hot weather concrete placing conditions. Average temperature was kept around 32$^{o}$ C and average relative humidity varied from 37 % to 70 % (see Table 3). According to the ACI Committee normograph, ACI 305.R [1991], rates of evaporation for these environmental conditions are between 0.7 to 1.0 kg/m$^2$/h.



Figure 4 – Leveling operation applied to plate specimens.

In order to increase the evaporation rate on the plates and to simulate worst conditions for casting concrete slabs *in situ*, regarding plastic cracking formation, a wind tunnel was constructed inside the laboratory. Two fans of 580 mm diameter that generates an average wind velocity of 15.5 km/h were employed. To ensure a uniform wind flow over the plates, a tunnel made of wood plies, with a U-shape cross section measuring 650 × 650 × 650 mm, and 800 mm of length, was placed over the fan and the specimen, as shows Figure 5. This was an additional modification to Kraai´s test setup.



Figure 5 – Test setup: plate specimen and fan inside the wind tunnel.

The experiments were conducted for 40 days, with two specimens cast and tested per day. The environmental conditions were measured close to the tunnel exit, at a height of 100 mm from the top of the specimen. Measurements for air temperature, relative humidity and wind speed were taken every hour during the entire testing, which took 9 hours.

The rate of evaporation was also monitored by means of two open containers, of surface dimensions 220 mm × 140 mm, one filled with mortar and another with water, placed next to the specimen, inside the tunnel (see Fig. 5). To measure the water loss, the pans were weighed every hour during the testing, using a scale with a precision of 0.01 g. Mortar

temperature was monitored by thermocouples connected to a datalogger, with measurements taken every 5 minutes.

The fan was turned on right after the completion of leveling of the specimen, which corresponded to approximately 25 min. after the beginning of mixing.

After nine hours of testing, the total cracking length on each specimen surface was measured by using a sewing thread and a precise ruler. The experimental results are presented in the following section.

## 4. EXPERIMENTAL RESULTS

Results from the experimental testing conducted to evaluate plastic shrinkage cracking in concrete thin slabs are summarized in Table 3. The table shows average values from three specimens tested (a, b and c) for each different volume fraction of polypropylene, glass, PET and nylon fibers ($V_f$): 1) 0 % (no addition); 2) 0.05 % and 3) 0.10 %. An ANOVA analysis (analysis of variance) was performed to verify the effect of fiber volume fraction in the mixture on the cracking length of the plates. A level of 95 % of confidence was applied.

It can be noted from Table 3 that air temperature and mixture conditions were kept approximately constant, while the relative humidity showed some variation. A graph – Total length of cracks *versus* Fiber volume fraction – was extracted from Table 3, as shown in Figure 6.

Table 3 – Experimental Results (average values).

| | | Volume Fraction ($V_f$) | | | | | | | | |
|---|---|---|---|---|---|---|---|---|---|---|
| | | Ref. | Polypropylene | | Glass | | PET | | Nylon | |
| | | 0.0 % | 0.05 % | 0.10 % | 0.05 % | 0.10 % | 0.05 % | 0.10 % | 0.05 % | 0.10 % |
| Cracking | Cracking length (cm) | 460.0 | 115.2 | 52.0 | 146.3 | 105.3 | 169.8 | 93.0 | 226.0 | 171.9 |
| | Number of cracks | 35.3 | 18.5 | 9.0 | 17.3 | 12.0 | 11.5 | 5.0 | 13.0 | 10.5 |
| | Cracking average length (cm) | 13.1 | 4.9 | 6.7 | 8.5 | 8.8 | 14.2 | 19.0 | 17.8 | 16.4 |
| Environmental conditions | Wind speed (Km/h) | 14.6 | 13.9 | 13.7 | 16.1 | 15.0 | 15.8 | 15.3 | 14.8 | 15.3 |
| | Air temperature (°C) | 35.5 | 31.1 | 32.4 | 35.4 | 35.7 | 27.7 | 30.0 | 31.6 | 30.0 |
| | Relative humidity (%) | 48.5 | 48.1 | 36.7 | 55.3 | 57.6 | 57.5 | 69.8 | 63.2 | 69.8 |
| Mixture conditions and mass loss | Mortar temperature (°C) | 35.2 | 30.5 | 31.3 | 35.9 | 36.4 | - | - | 31.4 | 23.3 |
| | Mass loss (%) | 6.87 | 6.20 | 6.60 | 5.86 | 12.44 | 6.82 | 3.82 | 5.86 | 3.82 |
| Average rate of evaporation ($kg/m^2/hr$) | | 1.0 | 0.8 | 0.9 | 0.8 | 0.8 | - | - | 0.7 | - |

It can be observed from this figure the strong influence of fiber volume fraction on cracking for all kind of fibers. By increasing the fiber volume fraction from 0.05 to 0.10 %, it was observed (see Table 3) a reduction in crack length of 55 % for polypropylene fibers; 28 % for glass fibers; 45 % for PET fibers and 24 % for nylon fibers.

It can also be noted from Table 3 the influence of the addition of fibers, when comparing the total crack length developed in the mortar with and without fiber addition.

For a volume fraction of 0.05 % it was observed a reduction in crack length of 75 % for polypropylene fibers; 68 % for glass fibers; 63 % for PET fibers and 51 % for nylon fibers; while, for a volume fraction of 0.10 %, the reduction in crack length was 89 % for polypropylene fibers; 77 % for glass fibers; 75 % for PET fibers and 63 % for nylon fibers.

A statistical analysis (ANOVA) of the above results was also performed. A significant effect of volume fraction and type of fibers was obtained at a level of confidence of 95 % (1-p), as shown in Table 4.

Crack initiation was monitored visually, by the naked eye. Cracks began to form about 180 min after starting the fan. Most cracks formed within the first 5 hours of testing.

Table 4 – Statistical analysis: effect of volume fraction and type of fibers in the mixture on cracking length of the plates.

| Variable | Degrees of freedom | Sum of squares effect | Sum of squares error | Statistics F | Statistics p |
|---|---|---|---|---|---|
| Fibers type | 3 | 40971.2 | 13657.1 | 9.5920 | 0.000733 |
| Fiber volume fraction | 1 | 20738.8 | 20738.8 | 14.5657 | 0.001519 |
| Error | 16 | 22780.9 | 1423.8 | - | - |

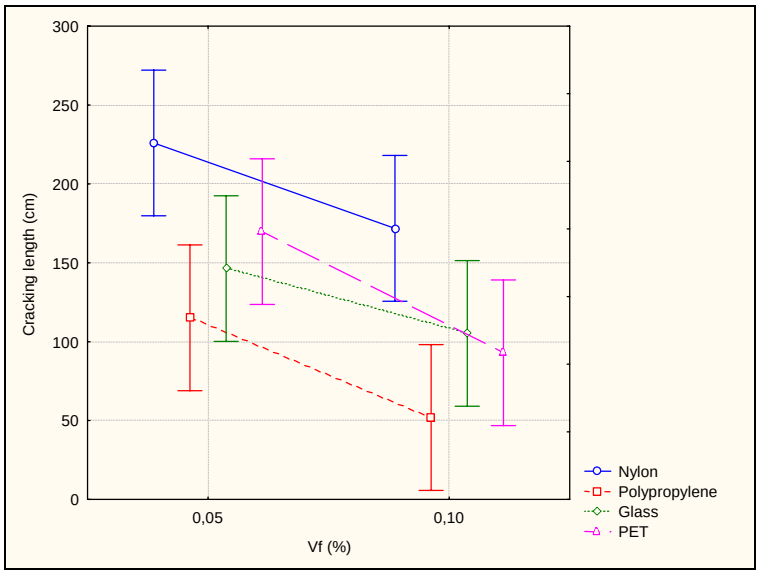



Figure 6 – Effect of fiber volume fraction in mixtures on cracking length of the plates.

Average values of the observed cracking length for each fiber type are presented in Figure 7. Such values were obtained considering both levels of fiber volume ($V_f$=0.05 and 0.10 %). It can be noticed that polypropylene fibers were the most effective addition to reduce cracking. On the other hand, nylon fibers were the least effective addition. In order to investigate the efficiency of each different fiber to reduce plastic shrinkage cracking of concrete, the statistic Duncan Test was performed by taking average results of cracking length obtained using both volume fractions (0.05 % and 0.10 %). Results showed that cracking length of mixtures with nylon fibers differed significantly from mixtures with polypropylene, nylon and PET fibers.

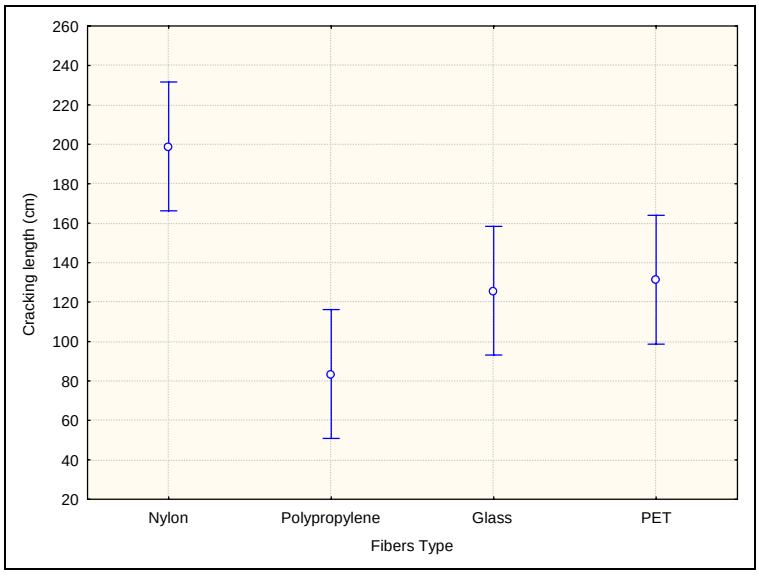
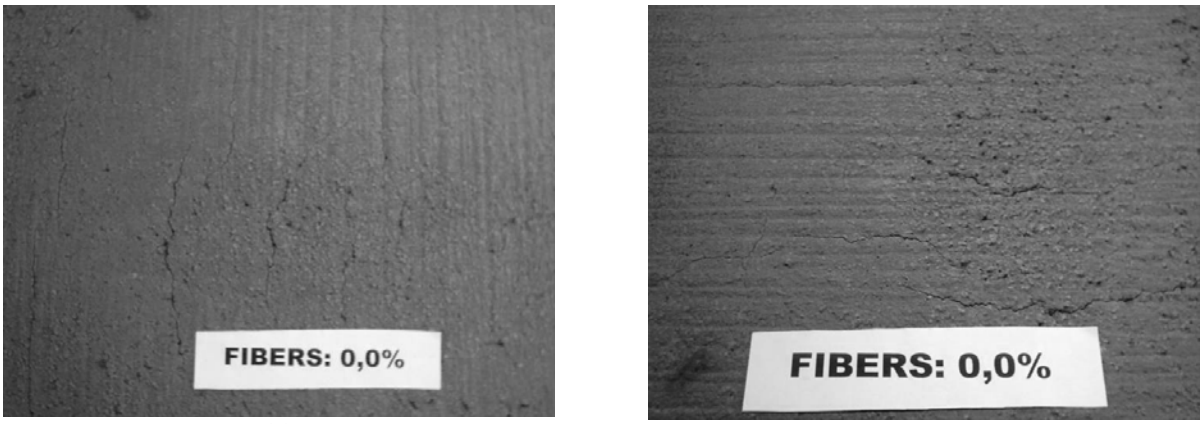



Figure 7 – Effect of different fibers on cracking length of mixtures.

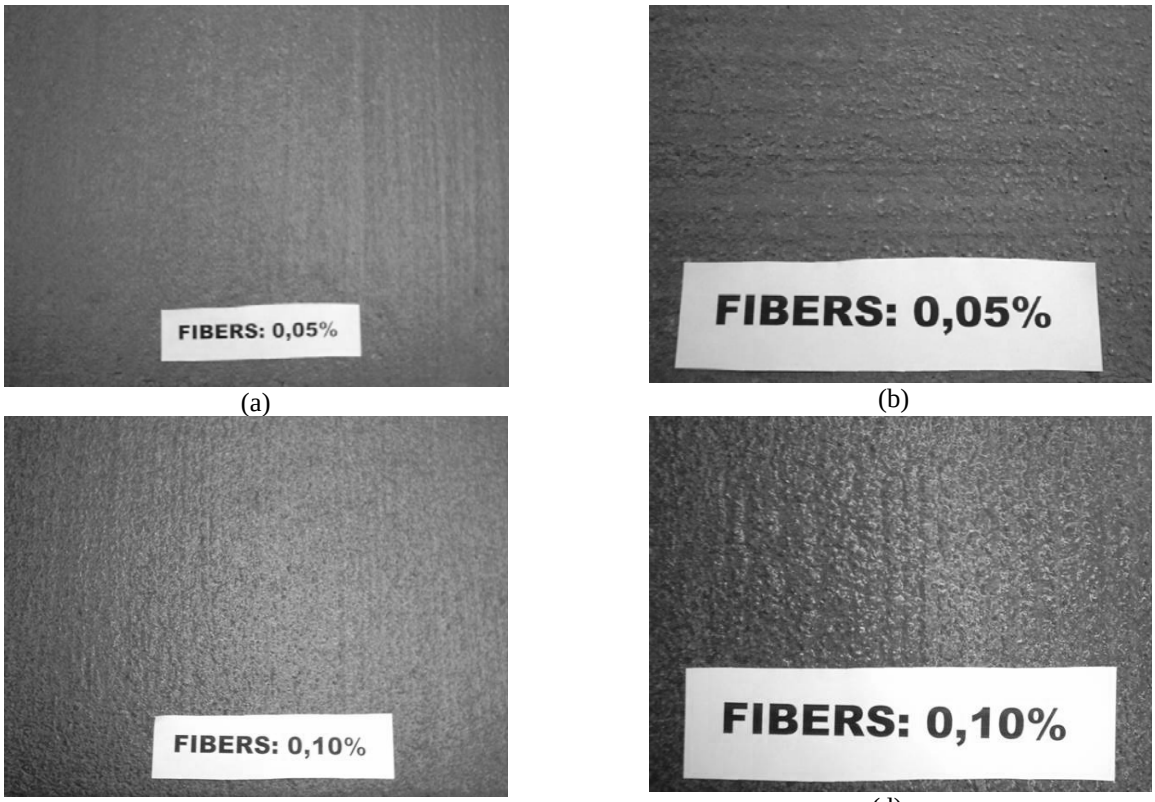
Crack development due to plastic shrinkage can be visualized in the pictures given by Figures 8, 9, 10, 11 and 12 for no fibers and synthetic fiber of polypropylene, nylon, glass and PET, respectively at volume fractions, $V_f$=0.05 % and 0.10 % (except for glass fibers in Figure 11, where pictures for $V_f$= 0.10 % only is shown). A zoom of these pictures is shown too. The pictures show the crack pattern and give an idea of the number of cracks and crack lengths. It can be observed from all figures that most cracks formed parallel to the screeding direction.

Crack openings could also be evaluated qualitatively. From Figures 8 to 12, a hairline crack pattern can be observed, showing that the use of fiber volume fraction of 0.10 % in the concrete (mortar) plates can reduce significantly crack openings. This effect comes from the high tensile strength of the fibers that restrain the mortar against crack opening.




(a) (b)

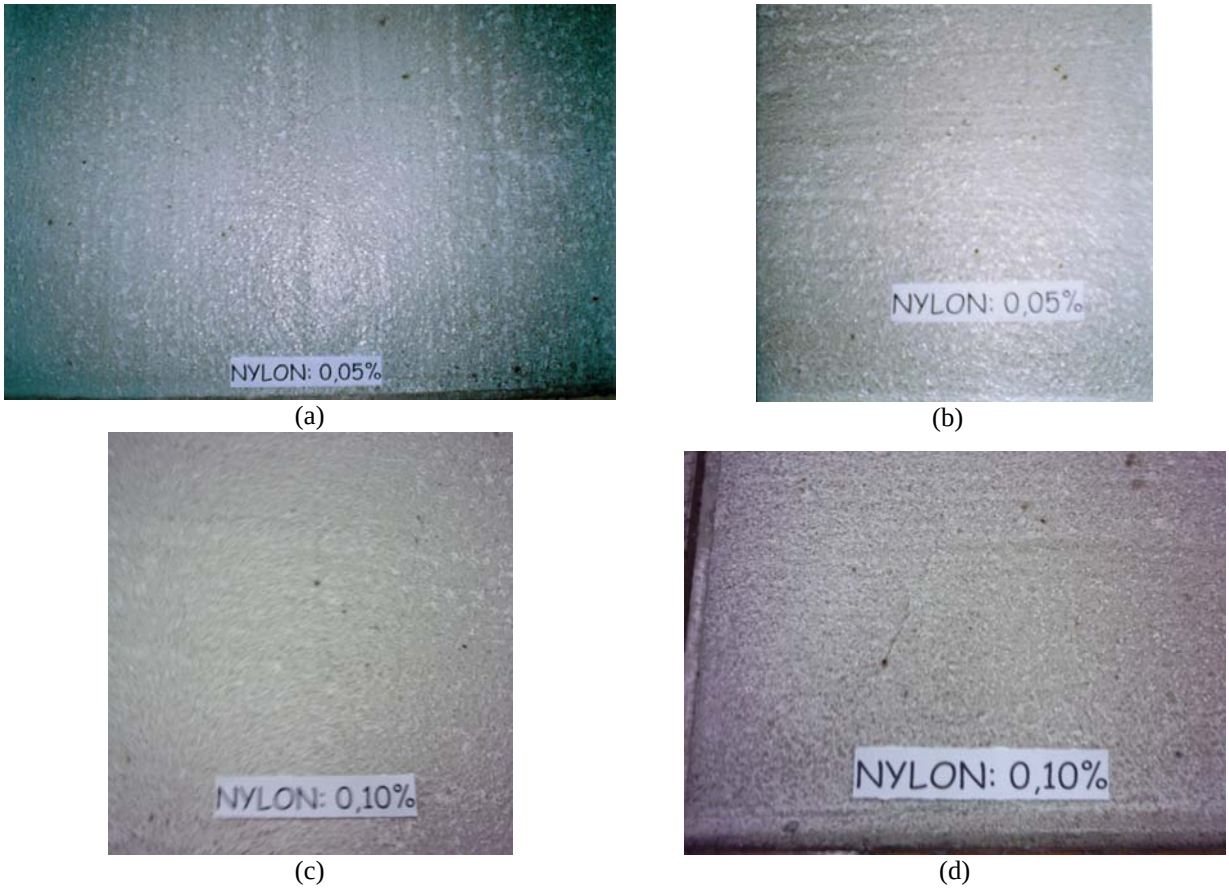
Figure 8 – Crack patterns: no fibers ($V_f$=0.0 %).




(a) (b)

(c) (d)

Figure 9 – Crack patterns: Polypropylene fibers ($V_f$=0.05 % and 0.10 %).




(a) (b)

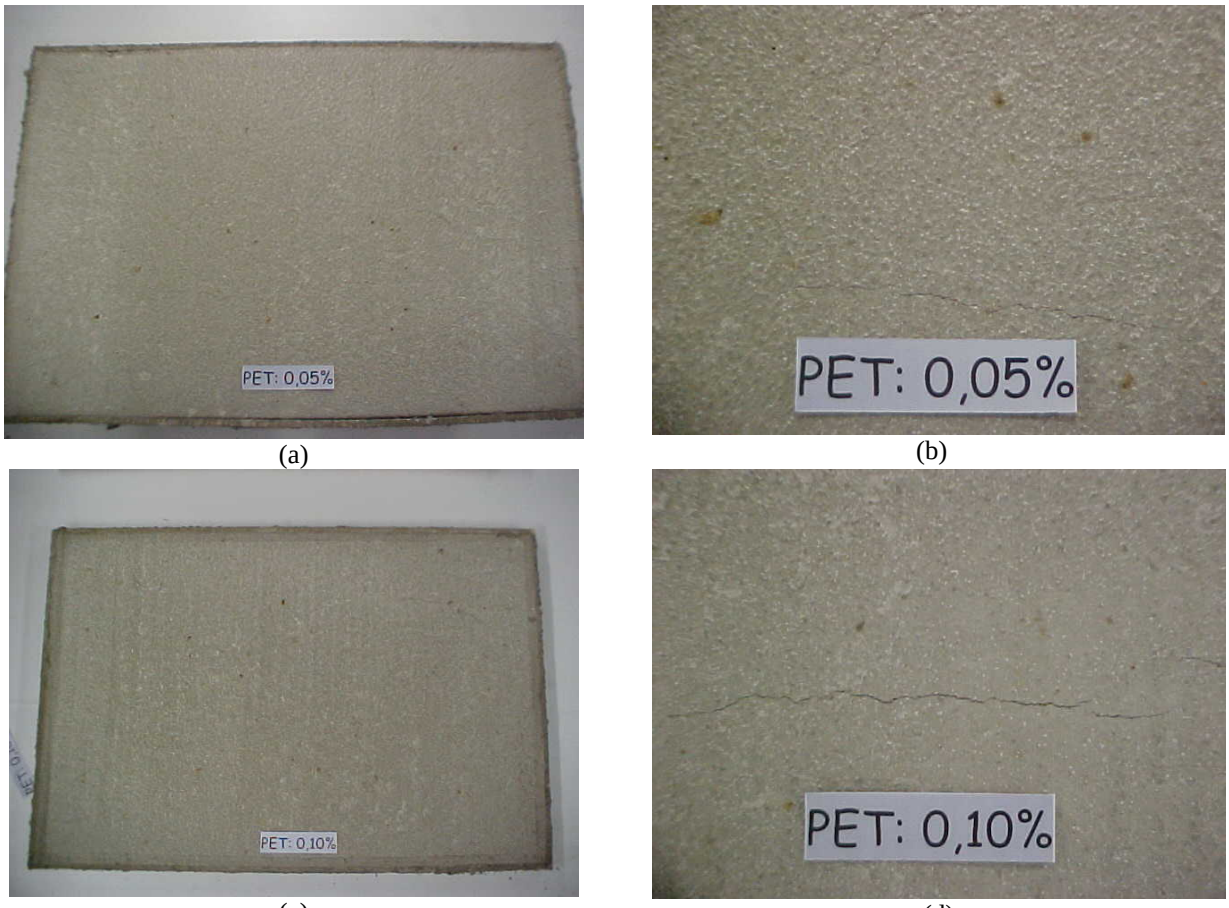
(c) (d)

Figure 10 – Crack patterns: Nylon fibers ($V_f$=0.05 % and 0.10 %).




(a) (b)

Figure 11 – Crack patterns: Glass fibers ($V_f$ = 0.10 %).




(a) (b)

(c) (d)

Figure 12 – Crack patterns: PET fibers ($V_f$=0.05 % and 0.10 %).

## 5. CONCLUSIONS

In this work, an experimental program was conducted to evaluate plastic shrinkage cracking in concrete thin slabs. The experimental results have shown that the addition of short polypropylene fibers to the concrete mixture can restrain considerably crack formation due to plastic shrinkage. The statistical analysis (ANOVA) showed a significant effect of both fiber volume fraction and fiber type on crack length with high levels of confidence

Regarding the crack pattern, most cracks formed parallel to the screeding direction, as also observed by other researchers. Based on visual observations, it can be inferred that fiber

volume fractions of 0.10 % or greater in the concrete plates are necessary to reduce significantly crack openings. These observations are also in agreement with conclusions obtained by other researchers from experimental testing on concrete slabs.

As far as fiber type is concerned, it was observed that nylon fibers were not as effective as polypropelene, glass, and PET fibers to reduce plastic shrinkage cracking.

Acknowledgments

The authors appreciated the financial support given by the Brazilian agency "Fundação de Apoio à Pesquisa Científica e Tecnológica do Estado de Santa Catarina" (FAPESC).

REFERENCES

ACI Committee 305, Hot Weather Concreting. (ACI 305.R-91), American Concrete Institute, Farmington Hills, MI, 20 pp. (1991).

ACI Committee 544, State-of-the-Art Report on Fiber Reinforced Concrete (ACI 544-97), American Concrete Institute, Farmington Hills, MI, 66 pp. (1997).

ASSOCIAÇÃO BRASILEIRA DE NORMAS TÉCNICAS–ABNT, Cimento Portland – Determinação da resistência à compressão, Rio de Janeiro, NBR 7215 (1996).

Balaguru, P., Contribution of Fibers to Crack Reduction of Cement Composites During the Initial and Final Setting Period, *ACI Materials Journal*, Vol. 91, No. 3, pp. 280-288 (1994).

Balaguru, P.; Slattum, K., Test Methods for Durability of Polymeric Fibers in Concrete and UV Light Exposure, ACI-SP 155, Detroit, pp. 115-136 (1995).

Bastos, P., *Retração e Desenvolvimento de Propriedades Mecânicas de Argamassas Mistas de Revestimento*, Doctoral's thesis, University of São Paulo (USP), 172 pp. (2001).

Bentur, A.; Mindess, S., *Fibre Reinforced Cementitious Composites*, London, Ed. Elsever, 448 pp. (1990).

Grzybowski, M.; Shah, S., P., Shrinkage Cracking of Fiber Reinforced Concrete, *ACI Materials Journal*, Vol. 87, No. 2, pp. 138-148 (1990).

Gopalaratnam, V., S.; Shah, G., R., On the Characterization of Flexural Toughness in Fiber Reinforced Concretes, *Cement and Concrete Composites*, Vol. 17, pp. 239-254 (1995).

Hannant, D., J., *Fibre-reinforced cements and concretes. Construction Materials; their nature and behaviour.* 2th Edition, London, pp. 359-403 (1994).

Kraai, P., P., A proposed test to determine the cracking potential due to drying shrinkage of concrete, *Concrete Construction*, Vol. 30, No. 9, pp. 775-778 (1985).

Mehta, P., K.; Monteiro, P., J., M., *Concreto: Estruturas, Propriedades e Materiais*. 1th Edition, São Paulo: Pini, 573 pp. (1994).

Naaman, A., E.; Wongtanakitcharoen, T.; Hauser, G., Influence of Different Fibers on Plastic Shrinkage Cracking of Concrete, *ACI Materials Journal*, Vol. 102, No. 1, pp. 49-58 (2005).

Neville, A., M., *Propriedades do concreto*. Ed. PINI, São Paulo, 738 pp. (1982).

Shaeles, C., A.; Hover, K., C., Influence of Mix Proportions and Construction Operations on Plastic Shrinkage Cracking in Thin Slabs, *ACI Materials Journal*, Vol. 85, No. 6, pp. 495-504 (1988).

Soroushian, P.; Mirza, F.; Alhozaimy, A., Plastic Shrinkage Cracking of Poly-propylene Fiber Reinforced Concrete, *ACI Materials Journal*, Vol. 92, No. 5, pp. 553-560 (1995).

Tanesi, J., *A Influência das Fibras de Polipropileno no Controle da Fissuração por Retração***,** Master's thesis, University of São Paulo (USP), (1999).

Zollo, R., Z., Fiber-reinforced Concrete: an Overview after 30 years of Development, *Cement and Concrete Composites*, Vol. 19, pp. 107-122 (1997).

Wang, K; Shah, S., P.; Phuaksuk, P., Plastic Shrinkage Cracking in Concrete Materials – Inlfuence of Fly Ash and Fibers, *ACI Materials Journal*, Vol. 98, No. 6, pp. 458-464 (2001).

International Symposium Polymers in Concrete
2 - 4 April 2006
Guimarães, Portugal

# Flexural strength of reinforced concrete beams repaired with Polymer-modified cementitious mortars

Nsambu. R[1]

*Universidade Agostinho Neto, Departamento de Engenharia Civil*
*da Faculdade de Engenharia*
*Avenida 21 de Janeiro-Luanda, Angola*

Gomes. A[2]

*Universidade Técnica de Lisboa, Departamento de Engenharia Civil e de*
*Arquitectura do Instituto Superior Técnico*
*Avenida Rovisco Pais*
*1049-001 - Lisboa, Portugal*

## ABSTRACT

This paper presents the results of an extensive experimental program on repair mortars for reinforced concrete beams repaired in flexure. Both pre-dosed polymer cementitious and Ordinary Portland Cement (OPC) based modified with polymers mortars are used. Two types of pre-dosed polymer cementitious mortars of the same manufacturer were investigated: one polymer fiber and synthetic resin modified mortar and other an acrylic polymer modified mortar. The mechanical property of the concrete, steel and mortars were characterized. Free and restrained shrinkage were evaluated. The influence of the surface roughness on the bond strength was studied using the "pull-off" and "slant-shear" tests. The effect of static and cyclic loading was analysed on flexural strength as well as the effect of the two types of the geometrical repair. The beams tested by cyclic loading have shown very ductile index and high ductility ratio. Also monolithic coefficient for all beams was evaluated.

## 1. INTRODUCTION

Deterioration of the Concrete structures may be due to mechanical damage, functional changes, mistakes in the design and during construction phase, incorrect modelling of structural behaviour, accidental loading damage, shock, earthquakes, fires, explosion, among others. Concrete structures may also be destroyed by physico-chemical mechanisms due to chloride ions and carbonation penetration. Others mechanisms such as alkali-aggregate reactions and sulphate attack are responsible by several problems on concrete durability. In

[1] PhD Student
[2] Associate Professor

the last decade, construction materials manufacturers supported by the chemical industry brought important products to face the problems of damaged reinforced concrete structures, leading to the production of several pre-dosed mortars for concrete repair. Among them, cementitious mortars are the most frequent. These new pre-dosed mortars presents a higher performance namely mechanically strength, adherence and durability.

According Emmons (2000), manufacturers tend to use different tests and standards to evaluate the performance of their products. Many standard tests used are modified arbitrarily and some modifications are deficient or provide unrealistic results.

## 2. MATERIALS AND MIX PROPORTIONS

Two commercial thixotropic repair materials A, B were used in this study. According manufacturer, repair materials details are as follows:

- Material A, Sika (2004), is a single component cementitious mortar of Portland cement, graded sand maximum size of 1.19 mm, with selected fine sand, reinforced with polymer fiber, micro silica and synthetic resin. The water/powder ratio is 0.144.
- Material B, Sika (2004), is a two component mortar, with acrylic polymer and Portland cement, graded sand maximum size of 2.38 mm. The polymer/powder ratio is 0.16.

A mortar formulated in laboratory modified with an acrylic polymer addition, designated by M, was used to compare with the pre-dosed repair materials. The M mortar weight composition, according EN 196: Part1 (1996,) is: 1 of Ordinary Portland Cement type CEM I 42.5 R; 1 of fine sand and 2 of coarse sand. For the fine and coarse sand the graded sand maximum size are 0.59 mm and 2.38 mm and the fineness modulus are 1.39, 3.13, respectively. The cement content was 300 kg/m$^3$. The polymer/cement ratio is 0.15 and the water/cement ratio is 0.35. The polymer is composed of 36.6% to 40.4% of solids, has a 8.5 to 10.5 alkalinity and a 1020 kg/m$^3$ density, Master Builders (2003).

One type of a adherence mortar, named by C, Sika (2004), was applied in repair works to improve the bond between the repair mortar and the concrete subtract

Some properties, in particular in fresh stage, of the pre-dosed (A and B), laboratory produced (M) and adherence (C) mortars are shown in table 1 and table 2.

Two types of concrete were used. The C1 concrete was used on the A and VC1 beam models and the C2 concrete was applied on the B1, B2, M1, M2, VC2 and VCC beam models. The average 28 days cube (150 mm) concrete compression strength is 22.8 and 31.6 MPa for the C1 and C2, respectively.

The concretes static modulus of elasticity was obtained by equation 1, REBAP (1984).

$$E_c = 9.5\sqrt[3]{f_c} \quad (1)$$

where $f_c$ is the compressive strength of standard cylinder specimen of 150×300 mm height in MPa and $E_c$ is static modulus in GPa. The static modulus of elasticity at 28 days age for the C1 and C2 concretes are 25.3 and 28.2 GPa, respectively. Factor of 0.83 has been used to estimate the equivalent cylinder strength from the 150 mm cube strength.

Longitudinal steel bars of 8 and 10 mm diameter were used in beams models. The tensile test of the 10 mm bars conducted to a 446MPa average yield strength and a 579 MPa average ultimate strength. For the 8 mm bar, the average yield strength and ultimate strength were 452 and 561 MPa, respectively. The stirrups steel with 6mm diameter has average yield strength of 467 MPa and an average ultimate strength of 501 MPa.

Table 1 - Pre-dosed (A and B) and adherence (C) mortars fresh properties.

| Pre-dosed Mortar | A | B | C |
|---|---|---|---|
| Water/powder or Polymer/powder | 0.144 | 0.16 | 0.23 |
| Consistency by flow* (%) | 54.3 | 76.0 | 128 |
| Alkalinity (pH) | 12.9 | 12.4 | 10.7 |
| Air content (%) | 4.0 | 3.0 | - |
| Density (kN/m$^3$) | 20.3 | 20.9 | 20.0 |
| Particle fine (%) | 41.7 | 39.4 | - |
| Fineness modulus | 1.71 | 1.56 | - |

Table 2 - Modified Mortar (M) - mix design and fresh properties.

| Properties | M | Properties | M |
|---|---|---|---|
| Cement, (kg/m$^3$) | 300 | Emulsion, (kg/m$^3$) | 116.9 |
| Fine sand 0 - 0.59 mm | 76 | Consistency by flow*, (%) | 83.2 |
| Coarse sand 0 - 2.38 mm | 12.4 | Density, (kg/m$^3$) | 1922 |
| Water/cement ratio | 0.35 | Alkalinity **, (pH) | 12.1 |
| Polymer/cement ratio | 0.15 | | |
| Additional water, (kg/m$^3$) | 33.1 | Air content***, (%) | 10.5 |

* measured using flow table test (NP 414), ** using pH meter, ***measured using air-entraining meter type B (ASTM C 231-68).

## 3. EXPERIMENTAL PROGRAM

### 3.1.Mechanical strength tests and curing

For each type of repair materials, three 40×40×160 mm$^3$ specimens were tested to determine the flexural and the compressive strengths in accordance with EN 196: Part1 (1996). These tests were carried out at 3, 7, 14, 28, 90 and 365 days. The specimens were demoulded 24 hours after casting and cured in accordance with product technical information.

The Brazilian test is one of the methods for evaluate the concrete or mortar tensile strength. This test was carried out on three cylindrical specimens of 150 mm diameter and 50 mm thick, tested on their side in diametric compression. Load was applied through a plywood plate (50 mm wide and 25 m thick), according Rocco (1998) interposed between the cylinder and platens of the testing machine. The tensile strength is obtained from the compressive load, P, through the following equation 2, in accordance to EC2 (2004).

$$f_{ct,sp} = \frac{2P}{\pi DL} \quad \text{and} \quad f_{ctm} = 0.9 \times f_{ct,sp} \tag{2}$$

where P is the compressive load in kN, L is the thick of the cylinder, $f_{ct,sp}$, the splitting tensile and, $f_{ctm}$, is the tensile strength in MPa.

Three 40×40×160 mm$^3$ prism specimens of each mortar were tested to determine the static modulus of elasticity at 28 days in accordance to the LNEC E 397 (1975) specification.

The ultimate capacity tensile strain of the mortars was determined according Houghton (1976) and Neville (1982) assumptions.

The mechanical properties gave by the manufacturer's technical information of the material A, B and C mortar at 28 days age are presented in table 3.

The compressive and flexural strength development is show in figures 1 and 2, for the same repair materials. The experimental results of the compressive, flexural and splitting

strength, the elastic modulus and the capacity tensile of strain for the A, B, C and M mortars are presented in table 4. The M mortar compressive strength is 27% greater than the A mortars and is 96% of the B mortar. The adherence mortar C compressive and flexural strengths are 7% and 30% greater than manufacturer values. The splitting tensile strength of repair materials A and B are similar.

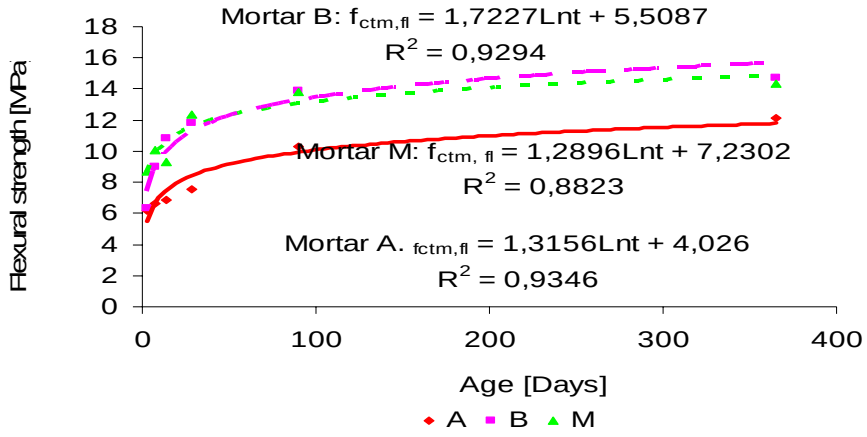



Figure 1 - Flexural strength development.

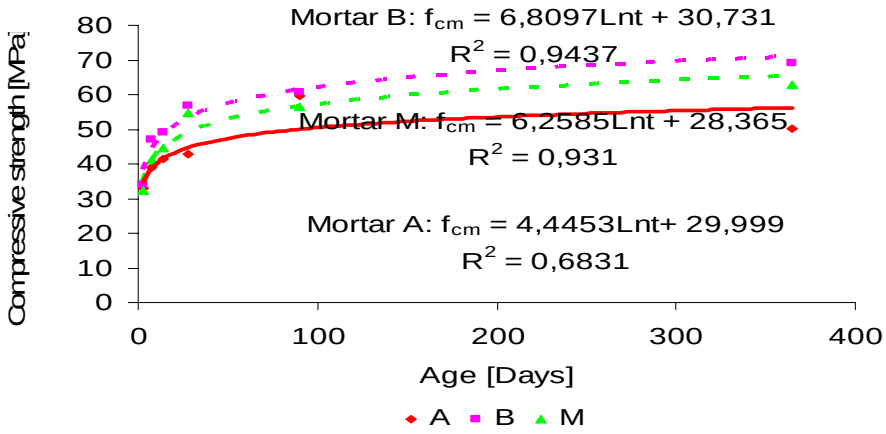



Figure 2 - Development of compressive strength.

Table 3 – Mortars strengths at 28 days age

| Mortars | Compressive Strength (MPa) | Flexural strength (MPa) | Elastic modulus (GPa) |
|---|---|---|---|
| A | 40 to 50 | 8 to 9 | 27.0 |
| B | 50 to 60 | 9 to 12 | 18.0 |
| C | | 10 to 12 | 24.0 |

Table 4 – Mortars strengths at 28 days age.

| Mortars | Compressive strength (MPa) | Flexural strength (MPa) | Splitting tensile (MPa) | Elastic modulus (GPa) | Capacity tensile strain ($10^{-3}$) |
|---|---|---|---|---|---|
| A | 42.9 | 7.55 | 4.13 | 23.9 | 0.155 |
| B | 56.7 | 11.8 | 4.47 | 22.4 | 0.179 |
| M | 54.6 | 12.3 | 3.97 | 23.7 | 0.151 |
| C | 64.3 | 15.6 | - | - | - |

### 3.2.Shrinkage

Awareness of the importance of controlling the drying shrinkage of cementitious and polymer-modified repair materials is increasing, Decter (1997). Figure 3 show the free shrinkage of 40×40×160 $mm^3$ prismatic specimens of the repair mortars (A, B and M) and 100×100×400 $mm^3$ concrete (C1 and C2) specimens. After demoulding, 24 hours behind casting, the mortars were cured in moist conditions at 20ºC temperature and 100% of relative humidity. Figure 3 show that the Pre-dosed mortars present higher shrinkage than M mortar.

Three ages of the moist cure were used: 24, 48 and 72 hours. The ratio between the free shrinkage strain and the capacity tensile strain, at 28 days age for the mortars A, B, M is 3.7, 2.4 and 0.75, respectively. According Emmons (1995), mortars B and M presents low shrinkage compared to pre-dosed mortar A. This work presents only the result at 48 hours moist cure. The conditions of drying are temperature 20 ±2ºC and 60±10% relative humidity.

The authors, Nsambu (2004), recommended the ratio between free shrinkage strains six times less than the ultimate tensile strain at 28 days, as a condition to consider adequate for the repair mortars structural.

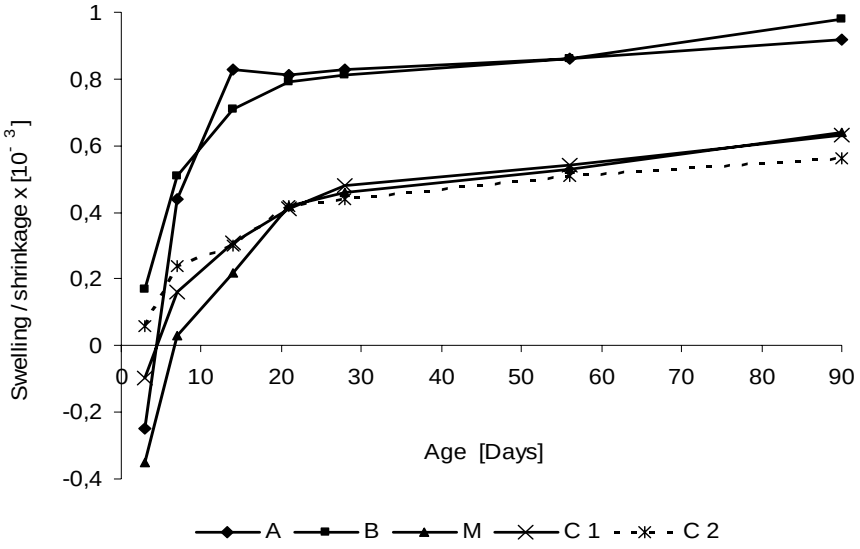



Figure 3 - Drying shrinkage of the pre-dosed A and B mortars, modified mortar, M, formulated in laboratory, and C1 and C2 concretes.

### 3.3.Restrained shrinkage

Restrained shrinkage induces tensile stresses in the repair material and compressive stresses in the substrate. Cracking due to restrained shrinkage is a major problem in repaired concrete elements structures, such as slabs, beams, pavement and walls. Under the effect of restrained shrinkage, tensile stresses are developed and cracks appear when the tensile stresses due to restrained shrinkage are greater than tensile strength of the repair mortar.

Beams B1 and M1 have a negative prismatic shape in tensile zone with 0.15×0.70×0.035 $mm^3$ which was filled with the repair mortar. Beams A, B2 and M2 were repaired in tensile and compressive zones which have 0.15×1.40×0.035 mm in the tensile zone and 0.15×0.70×0.035 in the compressive zone. The A and VCM/C1 was concreted with C1 concrete and the other with C2 concrete. The beams were covered with a waterproof material during seven days. The restrained shrinkage is measured with a mechanical gauge (Demec type) in the longitudinal direction. The measurement length of the gauge is 200 mm. Figure 4 shows the measurement of the restrained shrinkage in a beam.



Figure 4 - Restrained shrinkage measure.

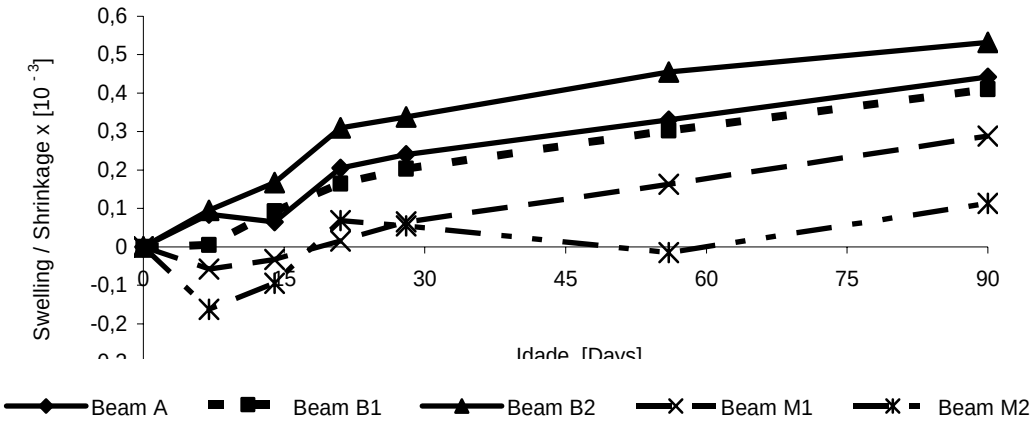



Figure 5 - Beams repaired with repair mortars - Restrained shrinkage development of the A, B1, B2, M1 and M2 Beams.

### 3.4.Bond strength

"Pull-off" and "Slant-shear" are the most widespread tests methods to evaluate the bond strength between a repair material and the substrate. In this work, the "Pull-off" test was conducted through a core drilled on the repair mortar layer to a depth of 35 mm. Test specimens has a dimension of 300×300×100 $mm^3$, according to prEN 1542. Before the repair mortar application the concrete substrate surface was removed using a light jackhammer. "Pull-off" tests were carried out by placing a loading tripod above the core. The load is applying trough a glued steel plate on the surface of the repaired core.

The slant-shear test was also used to evaluate the bond strength of the repair materials. The slant shear specimens are prisms with 100×100×400 $mm^3$ according to prEN 12615. The prisms are made of two parts. The first one is the substrate made with concrete. The second half are made of the repair mortar applied on the concrete substrate. The repair joint run diagonally through the prism at an angle of 30º to the main axis. The surface of the substrate was prepared by the use of a middle rough. Adherence mortar C, was applied on the substrate concrete before the application of the repair mortar on the both specimens type: "Pull-off" and "Slant-shear". A moist cure of 72 hours was used. After that the specimens were conditioned in a room with temperature of 20±2ºC and 60±10% relative humidity. Concrete prisms were made to allow the evaluation of the monolithic which is the ratio between the ultimate compressive loads of the composite prism (concrete and repair mortar) and the monolithic prism (concrete). Figures 6, 7 and 8 present the bond strength results and the monolithic coefficients.

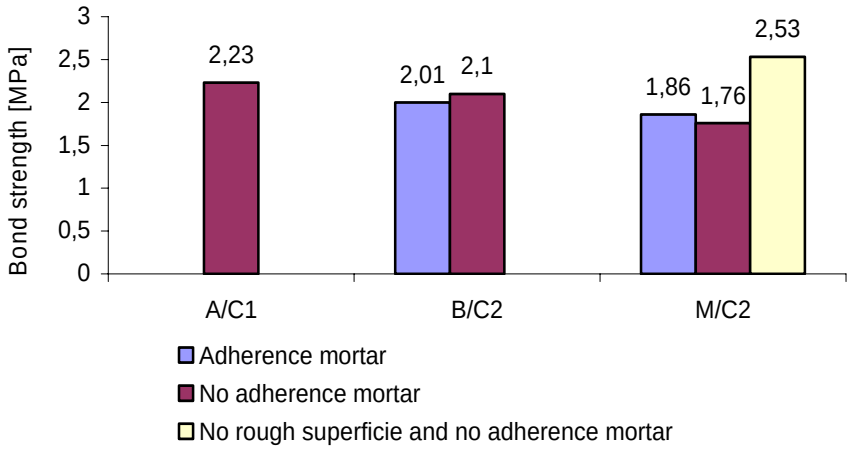



Figure 6 - Pull-off test on the two pre-dosed mortars A and B and mortar M formulated in laboratory at 28 days age.

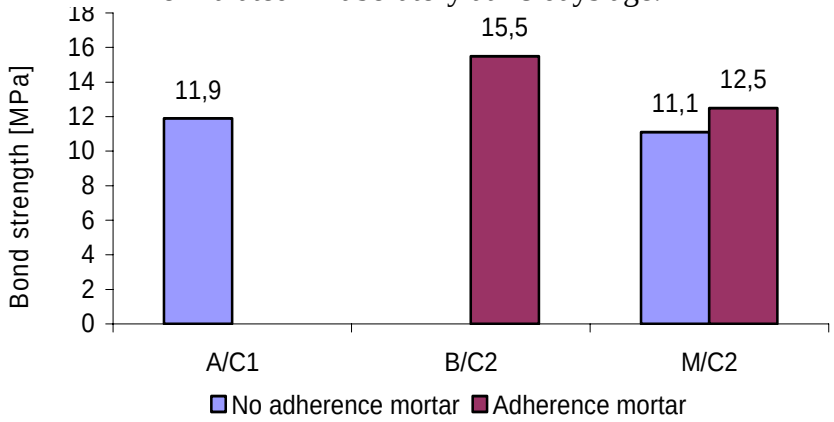



Figure 7 - Slant-shear test on the two pre-dosed mortars A and B and mortar M formulated in laboratory at 28 days age.

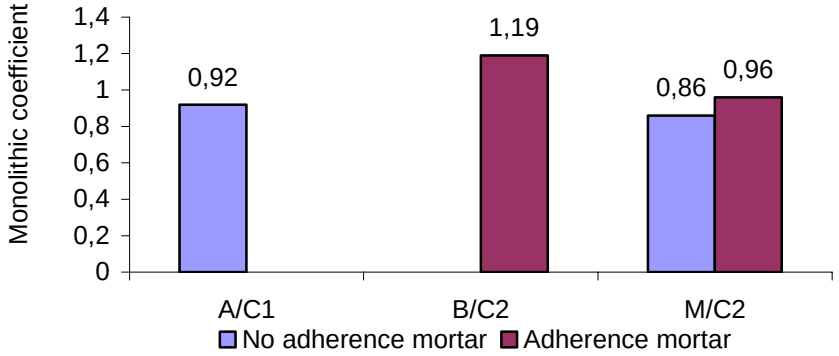



Figure 8 - Monolithic coefficient value on the two pre-dosed mortars A, B and mortar M formulated in laboratory at 28 days age.

3.5.Experimental program of beams test

The experimental program on the study of the behaviour of repaired beams involves a set of 33 beams. In this paper the results of seven beams are presented. Four of then were repaired with a mortar and the others tree are used as reference beams. Figure 9 shows the dimensions and reinforcement details and are shown of the beams. The bottom reinforcements

are two 10 mm steel bars and the top reinforcements are two 8 mm steel bars. The stirrups are 6 mm steel bars spaced at 100 mm in the shear span and at 175 mm in the central span.

Tensile and compressive deteriorated concrete zones were considered in this study. Deteriorated concrete zone was removed and replaced by a repair mortar. Beams B1 and M1 were repaired in tensile zone only, and beams B2 and M2 were repaired in tensile and compressive zone. Beams A, B1, M1 and reference beam VCM models were tested under a monotonic load, while beam B2, M2 and reference beam VCC were tested under cyclically load. All beams were tested under four-point bending after 90 days curing.

Table 6 presents the main results of the tests namely the yielding and ultimate load and deflection. The load values correspond to the total load applied on the beam. Based on the strength of the tested materials a numerical calculation of the yielding and ultimate load gives 33.3 and 43.3 kN, respectively. Figures 10, 11 and 12 show the tested beams experimental results. Beams A, B1, M1 and VCM presented a similar behaviour up to the yielding load.

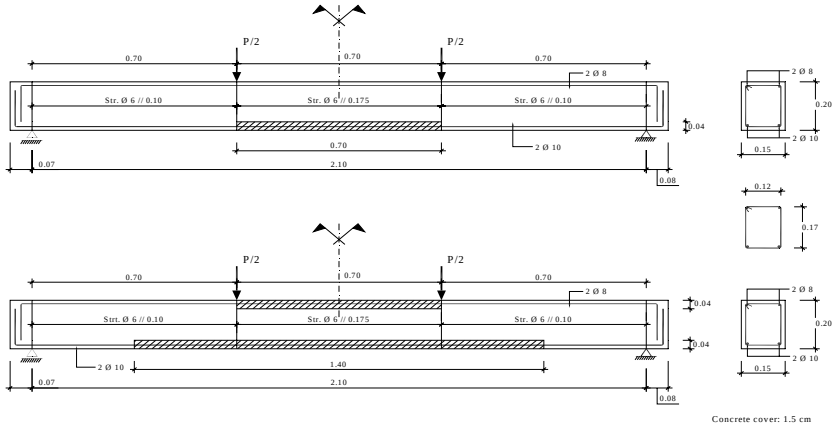



Figure 9 - Dimensions and reinforcement details of the beam models repaired in tensile and in tensile and compressive zone.

On the beam A rupture occurs the failure of the interface bond mortar-concrete, the crushing of the mortar in compressive zone and the tensile rupture of the reinforced bars. The yielding and ultimate failure loads were 33.9 and 35.7 kN, respectively. The tensile reinforcement strain at the yielding, $\varepsilon_{sy}$, and failure, $\varepsilon_u$, were $2.66^0/_{00}$ and $12.6^0/_{00}$, respectively. The observed average crack spacing in the mid-span was 270 mm.

Beams B1 reached failure by concrete crushing. Experimental values of the yielding and ultimate loads were 36.0 and 36.9 kN. The tensile reinforcement strain at the yielding, $\varepsilon_{sy}$, and failure, $\varepsilon_u$, were $\varepsilon_{sy} = 2.76^0/_{00}$ and $\varepsilon_u = 8.95^0/_{00}$, respectively. The average crack spacing in the mid-span was 120 mm.

Beam M1 reached failure by concrete crushing. The yielding and ultimate loads were 34.8 and 36.9 kN. The steel strain in tensile zone at mid-span at yielding and ultimate load were $\varepsilon_{sy} = 2.97^0/_{00}$ and $\varepsilon_u = 16.7\ ^0/_{00}$, respectively. The average crack spacing in the mid-span was 130 mm.

Concrete crushing occurs on the reference beam, VCM, failure. The yielding and ultimate failure loads were 34.9 and 37.2 kN, respectively. This beam presented a large deflection associated to a higher ultimate steel strain ($22.7^0/_{00}$). The yield steel strain was $2.49^0/_{00}$. The average crack spacing in the mid-span was 120 mm.

Figures 11 and 12 present the unloading-reloading cycles results of the beam B1, VCC and M2 models.

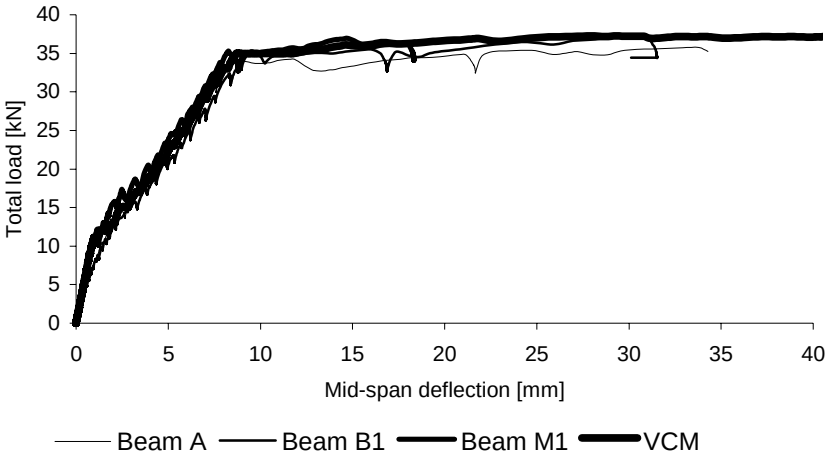



Figure 10 - Load versus mid-span deflection for beam models A, B1, M1 and VCM.

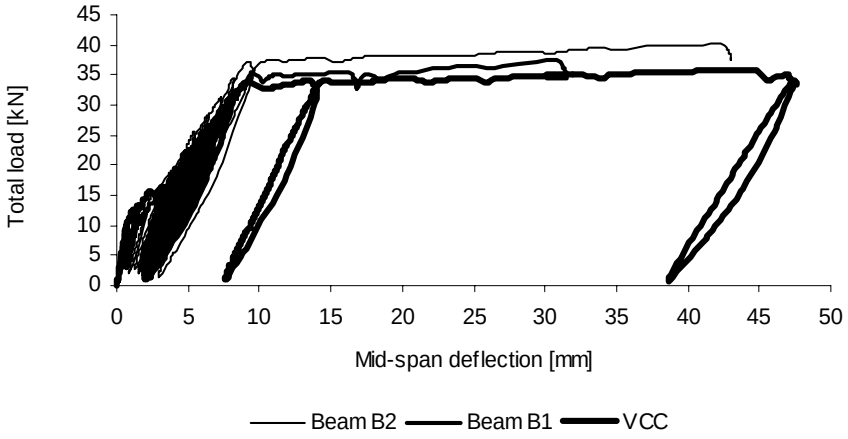



Figure 11 - Load versus mid-span deflection for beam models B1, B2 and VCC.

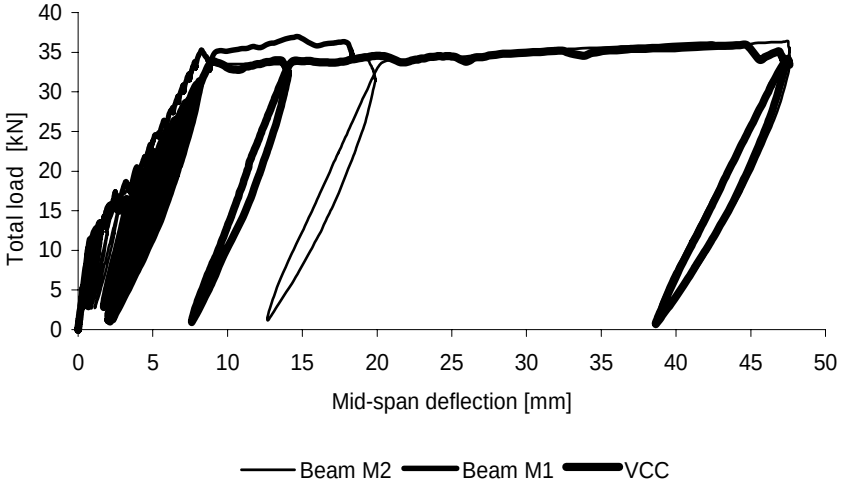



Figure 12 - Load versus mid-span deflection for beam models M1, M2 and VCC.

Figures 11 and 12 show that the behaviour of the Beam B2 (repaired by the pre-dosed mortar B) is different than the Beams M2 (Repaired by a mortar produced in laboratory) and VCC. Beam B2 failed by mortar crushing, loss bond in compressive zone and tensile failure of the reinforced bars. The yielding and ultimate loads observed in B2 test were 37 and 39.1 kN. The yielding and ultimate steel strain are 2.38 $^0/_{00}$ and 19.6$^0/_{00.}$ The average crack spacing is 110 mm.

Beam VCC presents concrete crushing at failure. The yielding and ultimate loads were 33.7 and 35.9 kN, respectively. The yielding and ultimate steel strain of the reinforced bars in the middle-span were 2.69 $^0/_{00}$ and 12.6 $^0/_{00.}$ The average crack spacing is approximately 125 mm.

Beam M2 reaching failure in loss bond repair mortar in the compressive zone. The yielding and ultimate loads were 33.1 and 35.9 kN. The average crack spacing was 120 mm similar to the reference beam VCC. The yielding and ultimate steel strain were 2.84 $^0/_{00}$ and 21.6$^0/_{00}$, respectively. The load-deflection curves shown in figure 10 (monotonic load tests) and figures 11 and 12 (loading and unloading cycles) imply that the concrete repaired could affect the structural ductility of the strengthened beam. Defection ductility and energy ductility were evaluated according Gomes (1992) and Bencardino (2002). The ductility (due to the deflection and energy) indexes are defined by the equations 3 and 4:

$$\text{Deflection ductility } \mu_\delta = \frac{\delta_u}{\delta_y} \tag{3}$$

$$\text{Energy ductility } \mu_E = \frac{E_u}{E_y} \tag{4}$$

where $\delta_u$ and $\delta_y$ are the mid-span deflection at ultimate load and mid-span deflection at tension steel yielding; $E_u$ and $E_y$ are the area under the load-deflection diagram at ultimate load and under the load-deflection diagram up to yielding of tension steel (elastic energy).

Table 6 - Experimental results.

| Beam | Yield Load | | Ultimate Load | | Modes of failure |
|---|---|---|---|---|---|
| | $P_y$ (kN) | $\delta_y$ (mm) | $P_u$ (kN) | $\delta_u$ (mm) | |
| VCM/C2 | 34.9 | 9.34 | 37.2 | 48.3 | Flexural by crushing of concrete |
| VCM/C1 | 34.7 | 9.38 | 35.7 | 29.1 | Flexural by crushing of concrete |
| A/C1 | 33.9 | 8.99 | 35.7 | 34.3 | Flexural by crushing of mortar, adherence in compressive zone and yielding of the bars in tensile zone |
| B1/C2 | 36.0 | 7.8 | 36.9 | 27.3 | Flexural by crushing of concrete and adherence bond in tensile zone |
| M1/C2 | 34.8 | 8.43 | 36.9 | 18.2 | Flexural by crushing of concrete |
| VCC/C2 | 33.7 | 9.31 | 35.9 | 44.8 | Flexural by crushing of concrete |
| B2/C2 | 37.0 | 10.1 | 39.1 | 42.8 | Bond interface, flexural crushing of mortar in compressive zone and reinforced bars |
| M2/C2 | 33.1 | 9.00 | 35.9 | 47.5 | Bond interface and crushing mortar in compressive zone |

Table 6 presents experimental results of the load and deflection at yield and ultimate stage and modes of failure. Table 7 presents the calculated ductility index, the ductility ratios (ratio between the ductility of the repaired beam and the ductility of the reference beam), and the ultimate load monolithic coefficient defined by the ratio between the ultimate load of the repaired beam and the ultimate load of the reference beam.

Referring to table 7, beams B1/C2 and M1/C2 have reduced ductility when compared with reference Beam VCM/C2. Beam M1/C2 show a loss in ductility comparing to Beam B1/C2 because the tensile strength of the mortar B present a favorable effect in the monotonic test. Also in the monotonic test, the Beam A, repaired in tensile and compressive zone, showed a very good ductility when compared with Beams B1/C2, Beam M1/C2 and reference Beam VCM1. This is due to the positive effect of the mortar in compressive zone that develop higher ductility. A similar result was observed for Souza (2000).

Table 7 - Ductility indexes, ductility ratios and monolithic coefficients.

| Beam | Deflection index | | Ductility ratio | | Monolithic coefficient $P_{u,exp}/P_{u,num}$ |
|---|---|---|---|---|---|
| | $\mu_\delta$ | $\mu_E$ | $\mu_\delta$ | $\mu_E$ | |
| VCM/C1 | 3.1 | - | 1.00 | - | 0.86 |
| VCM/C2 | 5.2 | - | 1.00 | - | 0.82 |
| A/C1 | 3.8 | - | 1.23 | - | 0.82 |
| B1/C2 | 3.5 | - | 0.67 | - | 0.85 |
| M1/C2 | 2.2 | - | 0.42 | - | 0.85 |
| VCC/C2 | 4.8 | 8.2 | 1.00 | 1.00 | 0.83 |
| B2/C2 | 4.2 | 6.7 | 0.88 | 0.81 | 0.90 |
| M2/C2 | 5.3 | 8.8 | 1.10 | 1.07 | 0.83 |

## 3.6. Conclusions

This paper presents conclusions based on the experimental investigation on the repair material proprieties for reinforced concrete. Results obtained on free and restrained shrinkage, bond strength and the experimental program of beams tests and comparative analysis with the pre-dosed mortars and the ordinary cement Portland (OPC) mortars formulated in laboratory and modified with a polymer. The main conclusions are following presented.

Pre-dosed mortars A and B present shrinkage when compared with mortar M fabricated in laboratory (fig.3). The restrained shrinkage (fig.4) show the same trend as the free shrinkage result.

Results obtained in the test shows (fig. 6) that bond strengths of the mortars A and B applied on a rough substrate, with and without adherence mortar, reached 112% and 105% of the values presents in the mortar technical information of the manufacturer.

The “Pull-off” tests of specimens without application of adherence mortar and with no rough concrete substrate show that the mortar M is 13% to 20% higher than the values obtained from the A and B pre-dosed mortars.

The “Slant-shear” test results presented very good monolithic coefficients. The failure modes and the ultimate load of the repaired and monolithic (reference) specimens are similar which indicates an excellent bond between the repair material and the concrete substrate.

An improve in the yielding load of the repaired beams with mortar B was observed related to the reference beams and the A, M1, M2, beams.

## 3.7.Acknowledgments

The authors acknowledge financial support from the "Fundation Para Ciência e a Tecnologia of the Portugal Ministry of Science", and the supports of Betecna, Degussa and Sika-Portugal.

## 4. REFERENCES

Baron, J, Ollivier, J. *Les Bétons - Bases et données pour leur formulation*, p 5, Edition Eyrolles, **(3)** (1999).

Bencardino, F, Spadea, G and Swamy. N: *Strength and Ductility of Reinforced Concrete Beams Externally Reinforced with Carbon Fiber Fabric.* ACI Strutural Journal, Vol.92, N.º 2, 163-171, **(20)** (2002).

Decter, M.H and Keely, C: *Durable Concrete Repair-Importance of Compatibility and Low Shrinkage*, Construction and Building Materials, Vol 11.N$^{os}$ 5-6, **(14)** 267-273 (1997).

Emmons, P.H, and Kesner, K.E: *Selecting Durable Repair Materials:* Performance Criteria, Concrete International, Vol. 22, N.º 3, **(1)** (2000).

Emmons, P.H and Vaysburd, A.M, *Classification* bas*ed on drying shrinkage*, Evaluation and Repair of Concrete Structures - Department of Army U.S.Army Corps of Engineers Washington, DC, **(15)** (1995).

EN 196-1*: Methods of testing Cement - Determination of strength*, 4 **(4)** (1996).

EC2: *Design of Concrete structures-Part1-1*: General rules and rules for buildings, **(10)** (2004).

Fichas Técnicas, 6$^{a}$ Edition - Sika, **(2)** (2004).

Houghton Concreto - *Ensaios e Propriedades,* pp 25.8 Ed. Pini Ltda - Brasil São Paulo, **(12)** (1997).

Gomes, A: *Comportamento e Reforço de Elementos de Betão Armado Sujeitos a Acções Cíclicas*, Tese de doutoramento, I.ST, Lisboa, 1992, **(19)** (1992).

LNEC E 397 - *Determinação do modulo de Elasticidade*, Lisboa, **(11)** (1975).

Master Builders Technologies (MBT) - *Construction Chemicals Bettor*, **(5)** (2003).

Neville, A.M: *Properties of Concrete*, Fourth Edition, pp 491, London, Longman, **(13)** (1995).

Norma Portuguesa NP 414: *Consistência do Betão - Ensaio de Espalhamento*, LNEC, Lisboa, **(7)** (1964).

Nsambu, R, Gomes, A: *Shrinkage Characterization of Repair Mortars Elements Concrete*, 2.º Congresso Nacional da Construção, Faculdade de Engenharia da Universidade do Porto, **(16)**, 375-380 (2004).

REBAP: *Regulamento de Estruturas de Betão Armado e Pré-Esforçado* - Imprensa Nacional Casa da Moeda, **(6)** (1986).

Rocco, C, Guinea, G.V, Planas, J and Elices, M: *Size effect and boundary conditions in the Brazilian test: Experimental verification*, Materials and Structures, Vol 32, 210-217, **(9)** **(**1999).

Souza, R, Appleton, J: *Avaliação da Reparação Estrutural em Elementos de Betão Armado*, Encontro Nacional sobre a Conservação e Reabilitação de Estruturas - REPAR 2000, Lisboa, LNEC, 14 a 17 de Junho, **(21)** (2000).

pr EN 1542: Tests methods - *Measurement of bond strength by pull-off*, Brussels, November, **(17)** (2001).

pr EN 12615: Tests methods - *Determination of slant shear strength*, Brussels, December, **(18)** (1998).

International Symposium Polymers in Concrete
2 - 4 April 2006
Guimarães, Portugal

# Impact Resistance of Single-Span Concrete Frames Reinforced by Polypropylene Fibers

Nourivand A , Majolan A. S. , Abbasi S.
*Young Researcher Club ,Islamic Azad University of Shabestar, Iran*

ABSTRACT

The main advantage of the fiber reinforced concrete is the improvement of bending endurance and this property increases the resistance against fatigue and impact. Since of polypropylene fibers are economical in civil engineering projects they were chosen for this research , and the purpose of this research is to show that using of fibers even with a small modulus of elasticity such as polypropylene fibers in producing prefabricated elements will be very effective against impact. In this paper the impact resistance of single-span concrete frames reinforced by polypropylene fibers will be compared with the single-span concrete frames without these polypropylene fibers.

KEY WORDS : Polypropylene fiber , Single-span frame , Impact, Fiber reinforced concrete

## 1. INTRODUCTION

Ordinary concrete has many hair line cracks. Because of the low tensile strength of concrete, theses cracks under imposed stress, develop rapidly and cause the destruction of the concrete. Tensile strength of ordinary concrete with the stress strength of 35 MPa is about only 3.5MPa.The tensile strength of the high compressive strength concrete is also small, for example, the tensile strength of a concrete with compressive strength of 100 MPa is about 6.8 MPa, which is very small. By adding the fiber to concrete, tensile strain at the rupture is also increase. Add the fiber make the concrete more shaping possibility, and help the concrete to endure the tensile cracks, the concrete fatigue, the impact forces, and the shrinkage cracks. Conversely of plain concrete, fiber reinforced concrete do not break immediately after the first cracks. The fibers make the bridge between cracks and until they are not broken or pull out from concrete, prevent the concrete from rupture. Regarding the aspect ratio of fibers, adding them to the concrete result to increase its strength and its toughness. The strength of first crack and the ultimate flexural strength of the fiber reinforced concrete can be calculated with equation 1.

$$\sigma_c = A\,\sigma_m(1- V_f) + BV_f\,(L/D) \qquad (1)$$

$\sigma_c$ & $\sigma_m$ are respectively the synthetic material strength(containing fiber) and concrete matrix strength, **L/D** is fiber aspect ratio, and $\mathbf{V_f}$ is fiber volume. **A** and **B** are also the fixed

numbers which for first crack strength are 0.843 and 2.93, and for the ultimate flexural strength are respectively 0.97 and 3.41.

The aim of this study is that even low modulus fiber like polypropylene plays an important role in increasing concrete strength and toughness. This study shows that by spending 8 US$ per each cubic meter, the toughness and endurance against the impacts up to 60%, and by spending more , concrete resistance against the impacts will be improved up to 300%.

## 2. POLYPROPYLENE FIBER REINFORCED CONCERETE

There are various types of fibers made from synthetic organic materials such as polypropylene or carbon , synthetic inorganic materials such as glass or steel , natural organic materials such as cellulose and natural inorganic material such as asbestos. All types of fibers have their own properties. The some fibers properties are shown in table 1.

Table 1 - The fibers properties

| Type of fiber | Tensile strength ksi | Young modulus $10^3$ ksi | Extensibility % | Density gr/cm$^3$ |
|---|---|---|---|---|
| Polypropylene | 80-110 | 0.5 | ~25 | .91 |
| Steel | 40-400 | 29 | 0.5-35 | 7.8 |
| Polyester | 105-125 | 1.2 | 11-13 | 1.4 |
| Polyethylene | ~100 | 0.02-0.06 | ~10 | 0.95 |
| Asbestos | 80-140 | 12-20 | ~0.6 | 3.2 |
| Glass | 150-550 | 10 | 1.5-3.5 | 2.5 |
| Rock wool | 70-110 | 10-17 | ~0.6 | 2.7 |

The choice of fiber type depend on their diameter, their specific gravity, modulus young, tensile strength and other their properties. The choice of the fiber type is also important in economic point of view. In this project polypropylene fiber is considered, because of its low price it is economically beneficiary in construction projects.

## 3. THE SPECIFICATION OF THE MODELED SYSTEM

To conduct this program , first, a loading jack of concrete frame was built. This jack was constructed according to ACI and to the one is used in American concrete competitions.
It contains a 5 cm diameter and 50cm length cylinder mass with 8.4 kg weight, which goes up and down inside a metal pipe. All impacts we forced on the frames are of 1m distance. Below this jack, there is a square plate with 4 columns in each angle. The modeled concrete frame places on this plate so that the cylinder mass falls exactly in the middle of its span when crashes down.
These impacts repeat alternatively until the complete rupture on the frame. A sample of this frame can be seen in figure 1.

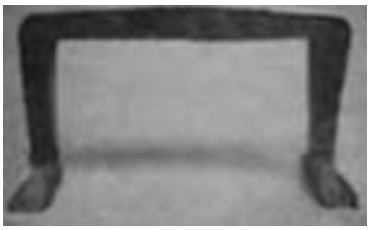


Figure 1 – The modeled single span frame concrete

The used fiber in this project is made by "Polypropylene Bonyad Co." in Iran. The properties of this fiber is as following:

| | |
|---|---|
| Specific gravity | 0.91 gr/cm$^3$ |
| Acid and salt resistance | high |
| Length | 6 mm |
| Water absorption | nil |
| Electrical conductivity | low |
| Thermal conductivity | low |
| Alkali resistance | alkali proof |

The mix design of the used concrete is explained in the table 2 .

Table 2- Mix design concrete

| Cement's Quantity kg/m$^3$ | Microsilica kg/m$^3$ | Aggregate kg/m$^3$ | | Superplasticizer kg/m$^3$ | Water's Quantity lit/m$^3$ | W/(C+S.F) |
|---|---|---|---|---|---|---|
| | | Gravel Max 3/8in | Sand | | | |
| 696 | 104 | 720 | 480 | 8.51 | 184 | 0.23 |

In fiber reinforced concrete, it should be noticed that by increasing the amount of fibers to the concrete, smaller aggregates should be used. ACI Committee 544 recommend 19 mm as the largest size of the aggregates, because using larger aggregates cause the separation of the aggregates from the cement matrix.

The amount of the used fibers in mix design of concrete are respectively 0.5, 2.5, 4.5, 6.5, 8.5 bulk percentage. In this project, we try to use polypropylene fibers as a material to improve the steel reinforced concrete behavior. To do this, first a sample of steel reinforced concrete is tested and then different percentages of fiber are added to this model to improve the concrete mechanical properties.

## 4. THE TEST RESULTS

### 4.1. CONCRETE WITHOUT FIBER SAMPLE

The first test was done on single-span frame of the steel reinforced concrete without fibers. In the first impact, two 45 degree wide cracks are appeared in frame span. The test results show that this frame reach its complete rupture after 5 impacts. Figures 2 and 3 show how is the fracture of this frame.




2 3

Figures 2 and 3 - The frame without fiber after enduring third and fifth impacts

## 4.2. A MODEL WITH 0.5% BULK FIBER IN THE CONCRETE

In the test made for 0.5% bulk polypropylene fiber reinforced concrete, by increasing the number of impacts on the joint area of the beam to the columns, we saw a 45 degree angle crack but 90 degree angle cracks in the middle of the concrete frame span. This frame reaches its complete rupture after enduring 8 impacts. In the other word, by adding only 0.5 % bulk polypropylene fiber to the concrete, the concrete toughness against the impacts up to 60%. Figures 4,5 and 6 show how is the fracture of this frame.





4 5 6

Figures 4,5 and 6-The frame reinforced by 0.5% PP fiber after enduring third ,fifth and eighth impacts

## 4.3. A MODEL WITH 2.5% BULK FIBER IN THE CONCRETE

The third test is done on a 2.5% bulk fiber reinforced concrete sample frame. By repeating the impacts, the cracks start growing from the bottom of middle part of span, and we saw the cracks in the up part of beam joint area to the columns. In this sample, we observe 2 times increase in concrete toughness by adding 2% bulk PP fiber to the concrete. This frame reaches its complete rupture after enduring 16 impacts. Figures 7,8 and 9 show how is the fracture of this frame.





7 8 9

Figures 7,8and 9-The frame reinforced by 2.5%PP fiber after enduring fifth ,eighth and Sixteenth impacts

## 4.4. A MODEL WITH 4.5% BULK FIBER IN THE CONCRETE

In test done to a single span 4.5% bulk polypropylene fiber reinforced concrete sample, we saw the best kind of toughness against impact and fracture. In this frame , by increasing the impacts in all points of the frame, the cracks slowly started to grow and despite the other samples in which the cracks start and grow in a single point, in this frame the cracks grow slowly in beam as well as in column.

The highest impact among the modeled frames in this project is relative to this sample. This frame reaches its complete rupture after enduring 20 impacts. That is, it's 4 times more than the one without fiber , which is a satisfactory result. Figures 10,11, and 12 show how is the fracture of this frame.



10 11 12

Figures 10 ,11 and 12 -The frame reinforced by 4.5% PP fiber after enduring eighth, Sixteenth and Twentieth impacts

## 4.5. A MODEL WITH 6.5% BULK FIBER IN THE CONCRETE

After testing this modeled sample, we observe the descending trend of concrete toughness by increasing the amounts of fibers. So that, this sample which contains 6.5% bulk PP fiber, reaches its complete rupture after enduring 9 impacts.
In this sample, no crack was seen in the tow first impacts, but in next ones, the cracks started to grow slowly. Figures 13,14 and 15 show how the fracture happens in this frame.



13 14 15

Figures 13,14 and 15-The frame reinforced by 6.5% PP fiber after enduring fifth ,eighth and ninth impacts

## 4.6. A MODEL WITH 8.5% BULK FIBER IN THE CONCRETE

In following the descending trend of concrete toughness due to increasing the fiber percentage, this sample reaches its complete rupture after enduring 8 impacts, that’s exactly the same as concrete that contains only 0.5% bulk fiber. Figures 16 .17 and 18 shows how the fracture happens in this frame.



16 17 18

Figures 16,17 and 18-The frame reinforced by 8.5% PP fiber after enduring third , fifth and eighth impacts

## 5. CONCLUSION

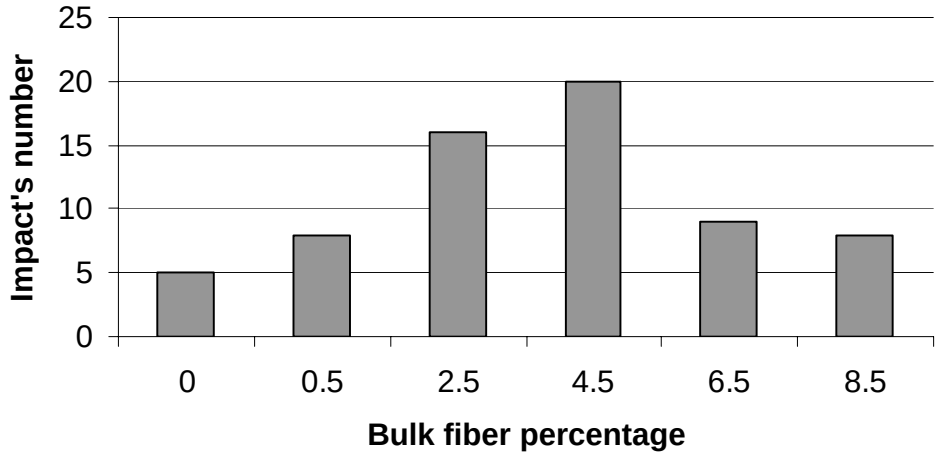



Figure 19 - Comparing impact strength of modeled samples

In this study, to improve the behavior of steel reinforced concrete, polypropylene fiber is used. First, the modeled sample is tested without fiber, which reached its rupture after enduring 5 impacts, and then different percentages of fiber was added to concrete. These percentages are 0.5,2.5,4.5,6.5, and 8.5 bulk percent which result in the increase of the concrete toughness respectively up to 8,16,20,9 and 8 impacts. Finally, among the tested samples, the one which contains 4.5% bulk PP fiber, increased the concrete toughness up to 300%. And which contains 0.5% bulk PP fiber increased the concrete toughness against the impacts, to 60%. That means, with spending 8 US$ per each cubic meter of concrete the tensile strength and toughness of steel reinforced concrete will be increased up to 60%. Consequently, this system is completely economic.

## 6. REFERENCES

[1] Brown. R , Shukla. A "*Fiber reinforcement of concrete structures*" Uritc project No. 536101, University of Rhode Island , September 2002.

[2] Johnston. C ," *in progress in concrete technology"* , ed . V.M .Malhotra, Canmet , Ottawa, 1980, PP.452-504.

[3] Kumar . M , Monteiro. J " *Concrete ( microstructure , properties and materials)*" Translate by Ramezanianpor .A , Amirkabir polytechnic university publications , 2004.

[4] Shokri majolan. A , Abbasi. S " *Optimization of resistance of reinforced single span concrete frames against impact* " , 6th International Conference on Shock & impact loads on structures , Perth, W. Australia , December 2005.

[5] Shoa. Y, Srinivasan. R "Parameters Affecting High Performance Response in Fiber reinfor*ced Concrete*", PP 17-56 in High Performance Fiber-Reinforced Concrete in Infrastructural Repair and Retrofit, edited by Neven Krustolovic-Opara and Ziad Bayasi, ACI, 2000.

[6] Swamy .R , Mangat .P " *Fiber reinforced Concrete* " , ACI Sp-44 , 1974 , PP.1-28.

International Symposium Polymers in Concrete
2 - 4 April 2006
Guimarães, Portugal

# Technical advances within maintenance and repair of concrete structures

H.Azamirad, D.Beheshti zadeh, M.Taghizadeh

*Islamic Azad University of Shabestar, Young Researchers Club, Iran*

## ABSTRACT

In the past the chemical industry developed and offered products and techniques based on the material properties and provided the market in this way with recipies for maintenance and repair of concrete structures. The very complex deterioration mechanisms of concrete and steel in concrete have not sufficiently been taken into account. This situation in the past could be called the trial and error period. The main technical advance in the field in the past 15 years is the fact, that the civil engineering society learned and accepted that maintenance and repair is a real engineering task needing a profound knowledge based design and execution. This starts with the clear understanding of the mechanisms leading to deterioration, followed by strategies, concepts and procedures for maintenance and repair based upon the mechanisms and ends with assessment and monitoring procedures and techniques again based upon the mechanisms. That means that we nowadays solve the problem on a sound technical basis, design the maintenance and repair work and on that basis define the needed material properties for every specific maintenance or repair case. In this way the best technical and economical solution can be found. This change of the situation is documented in the RILEM Recommendation 124 SRC "Strategies for Repair of Concrete Structures Damaged by Steel Corrosion" and in the series of drafts and final versions of CEN-standards on protection and repair of concrete structures.

***Keywords:*** *maintenance, repair of concrete structures, steel corrosion*

## 1. INTRODUCTION

Considerable technical advances have been gained in the area of maintenance and repair of structures within the last two decades. A short contribution like this paper can only highlight some aspects of the recent developments.
Maintenance and repair aspects within this paper are restricted to effects of environmental actions and ageing in service phenomena. Wear and fatigue effects will not be considered.

## 2. IDENTIFICATION OF TECHNICAL ADVANCED

Some years ago the chemical industry developed and offered products and techniques based on the material properties and provided the market in this way with recipies for maintenance

and repair of concrete structures. The very complex deterioration mechanisms of concrete and steel in concrete have-not sufficiently been taken into account. This situation in the past could be called the trial and error period.
The main technical advance in this field in the past 15 years is the feet, that the civil engineering society learned and accepted that maintenance and repair is a real engineering task needing a profound knowledge based design and execution. This starts with the clear understanding of the mechanisms leading to deterioration, followed by strategies, concepts and procedures for maintenance and repair based upon the mechanisms and ends with assessment and monitoring procedures and techniques again based upon the mechanisms. That means that we nowadays solve the problem on a sound technical basis, design the maintenance and repair work and on that basis define the needed material properties for every specific maintenance or repair case. In this way the best technical and economical solution can be found.
This change of the situation is documented in the RILEM Recommendation 124-SRC "Strategies for Repair of Concrete Structures Damaged by Steel Corrosion" (RILEM Technical Recommendation124-SRC 1994) and in the series of drafts and final versions of CEN-standards on protection and repair of concrete structures.

## 3. RELEVANT DEGRADATION PROCESSES-EXAMPLE CORROSION OF STEEL IN CONCRETE

Most of the degradation processes leading to concrete degradation or steel corrosion are fairly well understood nowadays. A presentation of the most important mechanisms on an engineering level as a basis for design for durability has been published by CEB Task Group on Durability (CEB Durability of Concrete Structures 1982, CEB Design Guide for Durable Concrete Structures 1992).
The new approach as indicated in chapter 2 will be demonstrated for one of the most important deterioration processes - corrosion of steel in concrete, being the deterioration mechanism causing by far the greatest problems during the service life of concrete structures - at least with respect to the overall costs to repair damages caused by environmental actions.
It is common knowledge that steel in well composed, placed, compacted and cured concrete is Excellently and durably protected against corrosion by the alkalinity of the pore water, causingpassivation of the steel surface. It is furthermore well known that basically two processes may lead to depassivation of steel in concrete
- Carbonation of concrete
- Chlorides above critical values.
As long as the "depassivation front" has not reached the reinforcement, corrosion protection is ensured. Only after penetration through the concrete cover carbonation or chlorides may initiate corrosion. This situation is normally sketched in a general deterioration scheme first published by Tuutti in 1982 (Tuutti 1982).
Steel corrosion visible with the naked eye is the outward manifestation of the effects of a number of small corrosion cells on the steel surface.
In simplified terms a corrosion cell is essentially a short-circuited battery consisting of a metallically and electrolytic ally connected anode and cathode. Unlike the process in a rechargeable battery, the corrosion process is not, however, reversible.
The corrosion process can be subdivided into two sub-processes.
- At the anode, in the presence of water iron ions pass into solution, separating from the electrons. They are converted into rust products in further reactions.
- At the cathode, electrons, water and oxygen are converted into hydroxyl ions. The cathodic

Process doesn't cause any deterioration of the steel.
These hydroxyl ions transport the negative charge in the electrolyte fluid in the concrete pore system through the electrical field created between the anode and the cathode, towards the direction of the anode. Near the anode, they react with the steel ions in solution. Depending on moisture and aeration conditions, this intermediate product may continue to react, producing the final corrosion products.
Individual processes are in fact much more complicated. The RILEM Report (RILEM Report of Technical Committee 60-CSC 1988) indicates the state of the knowledge in this field
In order for the corrosion process to take place, a number of preconditions for the anodic and cathodicprocess and for the electrolytic process must be satisfied simultaneously:
- As already noted, there must be differences in potential. The preconditions for sufficiently large differences in potential are, however, virtually always met, and in the case of chloride-induced corrosion these may be, after local depassivation, several 100 mV.
- Anodic and cathodic surface zones of the steel must be connected electrically and electrolytically, i.e. a flow of electrons and ions between them must be possible.
- The metallic connection necessary for an electron flow from the anode to the cathode is provided by the reinforcement system in the reinforced concrete. The electrolytic connection is represented by the concrete. This must, however, be sufficiently moist, since otherwise there can be virtually no migration of ions. In dry interior situations, for example, the electrolytic conductivity of the concrete is too low to permit corrosion of the reinforcement, even if the carbonation front reaches the reinforcement, leading to loss of alkaline protection.
- Anodic solution of iron must be possible due to depassivation of the steel surface. The cathodicprocess can, however, take place even in zones with a passive steel surface.
- Sufficient oxygen must be available at the cathode. There must be continuous diffusion of oxygen from the surface of the concrete to the steel surface acting as the cathode. There is therefore practically no risks of corrosion to reinforced steel components which are permanently immersed indeed water.
If all conditions for corrosion are fulfilled simultaneously, the reinforcement will corrode. If only one of the conditions can be eliminated, corrosion can be prevented or brought to a stop. Starting from this knowledge maintenance and monitoring strategies and techniques as well as principles and systems for repair have been developed.

## 4. CONSEQUENCES FOR MAINTENANCE AND MONITORING-EXAMPLE CORROSION OF STEEL IN CONCRETE

### 4.1 Levels of monitoring

As a consequence of the identified degradation process maintenance needs to be oriented towards extending the initiation period to the intended service life. This should be done by regular measurements and observation of the ingress of the depassivation front (chlorides or carbonation) tenable the provision of protective measures before deterioration starts. Protective measures may be suitable surface protection systems or the installation of cathodic prevention systems.
Performance testing and checking the real quality of the finished structure as an important part of the quality assurance and quality control system is the starting point of any monitoring and maintenance procedure.
Jensen & Andersen (Jensen & Andersen 1994) have defined three levels of monitoring of structural performance.

Low Periodic visual general inspections as integrated parts of maintenance management Systems

Medium Periodic visual general inspections in combination with periodic and periodic special inspections using non-destructive and destructive testing techniques all as integrated parts of maintenance management systems

High Systems for monitoring of structural performance implemented already during design and construction, periodic and a periodic special inspections using non-destructive and destructive testing techniques and visual periodic inspections all as integrated parts of maintenance management systems.

4.2 Periodic visual general inspections

This type of monitoring is widely used nowadays. However, it is more trouble-shooting than real monitoring. Most of the environment related deterioration mechanisms show initiation period before deterioration starts.
For the deterioration process "corrosion of reinforcement in concrete" - causing by far most of the damages - the deterioration can be detected by visual inspection only at a rather late stage when cracking and spalling occurs. The cost for repair at this stage of damage is extremely high compared to preventive protection stopping the initiation process (carbonation or chloride ingress in case of reinforcement corrosion) before deterioration starts.

4.3 Special inspections using non-destructive and destructive techniques

Non-destructive testing techniques usually operate from the concrete surface and can detect ongoing deterioration before visual damage occurs (e.g. potential mapping). Therefore repair measures can betake before the structural integrity has been weakened by e.g. cracking and spalling. Additionally destructive testing can be performed (e.g. chloride profiles, moisture content of concrete) to get a better picture of the overall situation. However, all NDT and DT leaves a lot of uncertainty in diagnosis because of uncertainties in the techniques themselves combined with a lack of knowledge of structural performance in the past and a very limited possibility of predicting the future deterioration rates with different levels of maintenance work.

4.4 Continuous monitoring of structural performance with implemented sensors

The highest level of monitoring is the implementation of sensors during the construction process to continuously monitor the performance of the structures. Successfully used monitoring systems of this sort are
- vibrating wire sensors to monitor the time dependent development of stresses
- Optical fiber sensors to monitor deformations and displacements (e.g. Miesseler & Lessing 1989)
- Corrosion cells to monitor the progress of the depassivation front (see below)
- Moisture sensors to monitor the conductivity of concrete and/or the efficiency of protective Measures (Schiessl & Breit 1995).
The evident advantage of these monitoring techniques is that the development of the structural performance with time is continuously monitored and preventive protection or repair measures can betaken at comparatively low costs before real damage occurs and the structural

integrity will be affected. Furthermore a prediction of future performance of the structure is possible at any time and eases the decision on the adequate time of interventions.

### 4.5 Example: Macrocell corrosion sensors

The operation of a macrocell consisting of a piece of black steel (anode) and a noble metal (cathode) is shown in Figure 3. In chloride free and non-carbonated concrete, both electrodes are protected against corrosion due to the alkalinity of the pore solution of the concrete (passive state). The electrical current between both electrodes is negligibly low under such conditions. If, however, critical chloride content is reached, or if the pH-value of the concrete decreases due to carbonation, the steel surface of the anode is no longer protected against corrosion, while the cathode remains passive. The local separation of anodically and catholically acting areas leads to an electron flow between the black steel and the passive cathode if an electrical connection is provided. The flow can easily be measured at the external cable connection using a low resistance amperemeter.The macrocells were embedded with a concrete cover of only 5 mm (0.20 in.) to initiate corrosion by applying a chloride solution on the concrete surface within a short period of time. The results of the macro cell current measurements showed that the critical chloride content reached a depth of 5 mm (0.20 in.) at the specimen with w/c = 0.7 about 80 days after concrete placement. This caused significant increase of the macrocell current while the specimen with a lower w/c and a higher resistance against chloride diffusion remained passive until now about 1,000 macrocell corrosion sensors, measuring the time dependent ingress of thedepassivation front towards the reinforcement have been installed into various structures. The system of the sensors used is sketched in Figure 4. Within one sensor element normally 6 single anodes are positioned between the concrete surface and the reinforcement e.g. at distances of 5 mm from each other. As soon as the depassivation front (e.g. critical chloride content for the given concrete in the given environment or carbonation) has reached an anode a corrosion current can be measured when the anode is coupled to an embedded cathode consisting of a noble metal. With time anodes at increasing depths will be activated thus giving information on the ingress of thedepassivation front .The layout of the sensor systems allows, besides the current readings other measurements improving the information on the overall risk within the monitored structure:

- The measurement of the potential between the anodes or the reinforcement and the noble cathode gives further information on the onset of corrosion.
- The simultaneous measurement of the temperature by means of an incorporated temperature sensor allows a more detailed interpretation of the current readings.
- The anodes can be used as measuring electrodes for AC resistance measurements at different distances from the concrete cover. This type of readings for example can be used to monitor the efficiency of coatings, preventing water ingress into the concrete.

The advantage compared to e.g. taking chloride profiles is that the real corrosion initiating chloride levels are detected directly. By continuously measuring the progress of the depassivation front protective measures can be taken before it reaches the reinforcement.

### 4.6 Installation of macrocell corrosion sensors into the structures of the Great Belt Link

The structures of the Great Belt Link are given here as an example for installing corrosion sensors into huge and important infrastructure projects. All the structures of the Great Belt Link-Tunnel, Western Bridges, and Eastern Bridge - have been instrumented with corrosion sensors. Of course not all single elements need to be instrumented, a representative number of

specific elements (tunnel segments, pier shafts, bridge girders etc.) are sufficient. The basic strategy of high level monitoring is to put results of the continuous monitoring with sensors together with other representative results of NDT- and DT-results at regular inspection intervals and to draw conclusions.
- Tunnel -
Altogether 204 sets of sensors have been installed into the 7.9 km long twin tunnels between Zealand and Sprogö at the eastern end of the Great Belt. Water depths above the tunnel increases to a maximum of about 55 m.84 of the prefabricated segments within 14 tunnel rings have been equipped with sensors. To monitor the corrosion risk for the outer layer (chloride ingress) and the inner layer of reinforcement (chloride accumulation due to evaporation and carbonation) anode ladders have been installed on both sides of the segments. All the cathodes have been positioned on the inner side of the tunnel; as insufficient oxygen supply for the cathodic reaction must be expected at the outer side.

- Western Bridges -
- 6 pier shafts and girders out of 64 have been provided with 30 sets of sensors each (in total 180sets of sensors). The sensors have been positioned in the most critical areas of the structure:
- Construction joints between caissons and pier shafts (in-situ concrete connection under water)
- Tidal and splash zones of the pier shafts
- Construction joints between casting sections of the precast girders
- Salt spray zones of the girders
- Parapets of the girders (deicing salt attack)
- Eastern Bridges -
Altogether 42 anode-ladders have been installed into selected positions of one pylon, one anchor block and one pier shaft. For the determination of the most critical areas the main wind- and water-flowdirectionshave been taken into account. 1/3 of the sensors have been installed into the first casting joints above the mean water level.

## 5. THE ENGINEERING APPROACH TO REPAIR PROJECT

### 5.1 General

The phases of repair projects follow more or less a logical sequence, which is dominated by Engineering aspects, but also includes!) Commercial arguments and personal preferences. The following chapter is related to the new European Standard EN 1504, Part9: "Protection and Repair of Concrete Structures: General Principles for the Use of Products and Systems" and gives background information for the normative rules.

### 5.2 Process of assessment

Assessment may be taken in several stages. The purpose of a preliminary stage is to advise on the immediate safety of the concrete structure, to give an informed opinion on the urgency of Commissioning further surveys, protection or repairs, and to outline what testing should be done to establish the causes and likely extent of the defects.
The purpose of the main assessment is:
- To identify the cause or causes of defects

- To establish the extent of defects
- To establish whether defects can be expected to spread to parts of the structure that is at present unaffected
- To assess the effect of defects on structural safety
- To identify all locations where protection or repair may be needed.

Assessment should include testing or other investigation with the aim of revealing hidden defects and causes of potential defects. Due to the time-dependent deterioration processes previous assessments need to be updated. The process of assessment generally includes:

- Valuation of the original design approach
- Conditions during construction (including climatic conditions)
- The history of the concrete structure
- The conditions of use (e.g. loading)
- The environment, including exposure to contamination
- The present condition of the existing concrete structure, including non-visible and potential defects
- Requirements for the future use of the concrete structure.

The nature and the causes of defects result from a great variety of parameters, as mentioned in Figure8. The causes include:

- Defects due to inadequate construction or materials (such as inadequate structural design, Inadequate mix design, insufficient compaction, insufficient mixing, insufficient cover, Insufficient or defective waterproofing, contamination, poor or reactive aggregates, and Inadequate curing).
- Defects revealed during service (such as foundation movement, impacted movement joints, overloading, impact damage, and expansion forces from fires).
- External environment and agents (such as severe climate, atmospheric pollution, chloride, carbon dioxide, aggressive chemicals, erosion, aggressive groundwater, seismic action and electric stray currents.

As a general rule the initial causes of the defects need to be identified and corrected before a successful repair can be carried out. If correction is not possible, e.g. the use of de-icing salts, the repair must be designed to resist the cause as far as possible.

## 5.3 Repair strategy

The selection of a strategy for repair can never be taken on technical grounds alone. In addition to considering the technical possibilities, it is necessary to consider the economic circumstances which affect the decision. As much information as possible has to be provided to enable an informedjudgement to be reached on the relative costs and benefits of the possible technical options for repair.The design life of the repaired concrete structure is a key consideration in the choice of the repair method. Options range from those which can restore the design life of the concrete structure in comprehensive single operation, to simpler options which may require repeated maintenance activities. Options with a long maintenance-free life are not necessarily preferable to those with a shorter life and the appropriate choice will depend on the circumstances of the individual case. There is normally a wide range of options, such as

- Do nothing for a certain time
- Re-analysis of structural capacity, possibly leading to downgrading of the function of the concrete structure
- Prevention or reduction of further deterioration, without improvement of the concrete structure
- Improvement, strengthening or refurbishment of all or part of the concrete structure

- Reconstruction of part or all of the concrete structure.
- Demolition of all or part of the concrete structure.

Consideration of the options and their consequences will generally include examination of different aspects, for example levels of initial cost, maintenance costs and the possible need to introduce restrictions in the use of the structure. A different level of risk of future deterioration is likely to be associated with each option. The choice of appropriate action needs also an objective analysis and evaluation of the principles and methods which are described in the following.

## 5.4 Principles of repair and protection

The principles are based on the chemical or physical laws which allow prevention orstabilisation of the chemical and physical deterioration processes in the concrete or the electrochemical corrosion processes on the steel surface (EN 1504-9).
Several methods may be used in combination, but of course the possibility of undesirable as well as desirable interactions between them has to be considered. The influence which repair of the concrete may have on the corrosion of reinforcement, for example by entrapping moisture or by raising the ambient temperature, is also part of the consideration to be made.
Examples for undesirable consequences connected with particular methods may be:
- Reducing the moisture content, which may increase the rate of carbonation?
- Surface coating, which may entrap moisture and may destroy adhesion or reduce frost resistance
- Electrochemical methods, which may cause embitterment of susceptible prestressing steel, Alkali aggregate reaction with susceptible aggregates, a decrease in frost resistance due to increased moisture contents, or, if under water, corrosion in adjacent structures or vessels
- limiting oxygen content by surface coating or saturation, which can cause increased corrosion if reinforcement in the protected zone is electrically connected to reinforcement in any unprotected zone. It is self-evident that products and systems should be compatible with each other and with the original concrete structure.

## 5.5 Selection of appropriate products

Only after assessment of the status of the structure, after elaborating the repair strategy and after defining the principles and methods of repair the basis is given to define characteristics and requirements for materials to be used. After these definitions it is up to the design engineer to select commercial products which meet theses requirements. In future, products and systems which have appropriate properties will be described in the EN 1504series or other relevant EN or European Technical Approvals.

## 5.6 Maintenance following the completion of protection or repair

Some parts of the repaired concrete structure may have an expected service life which is short Compared with that of the rest of the concrete structure. Familiar examples are surface coatings, sealant, and weather proofing materials. If the integrity of the protection or repair depends on such parts, it is essential that they be regularly inspected, tested and renewed if necessary. In these cases maintenance should include:
- A precise time schedule for inspections
- The system of inspection which is to be used, how results are to be recorded
- A specification for continuous treatment (if any is required), for example cathodic protection or monitoring equipment

- A statement of precautions to be taken or prohibitions to be enforced, for example maintenance of surface water drainage, maximum pressure for washing or prohibition of the use of de-icing salt.

A maintenance management system should be implemented to ensure that the required maintenance is carried out.

## 6. CONCLUSIONS

Recent developments in maintenance and repair of concrete structures have clearly demonstrated that a profound knowledge of degradation mechanism on a material science level and its transfer to practical application on an engineering level are important driving forces for technical advances in design, execution, maintenance and repair of structures.

## REFERENCES

CEB / Comite Euro-International du Beton 1982. Durability of Concrete Structures: State of The Art Report. Bulletin d'Information, No. 148

CEB / Comite Euro-International du Beton 1992. Durable Concrete Structures: Design Guide. Bulletin d'Information, No. 183

EN 1504-9 Products and Systems for the Protection and Repair of Concrete Structures - Definitions, Requirements, Quality Control and Evaluation - Part 9: General Principles for the Use of Products and Systems

Jensen, J.S. & Andersen, E.Y. 1994. Monitoring of Structural Performance - A Must for the Future. Proceedings of the International Conference "Concrete across Borders", Odense, Denmark, pp. 585-594

Miesseler, H.-J. & Lessing, R. 1989. Monitoring of Load Bearing Structures With Optical Fiber Sensors. IABSE, Lisbon

RILEM (edited by P. Schiessl) 1988. Corrosion of Steel in Concrete. Report of the RILEM Technical Committee 60-CSC

Schiessl, P. & Breit, W. 1995. Monitoring of the Effectiveness of Surface Protection Systems After Repair Measures Using Multi-Ring-Electrodes. International Symposium on Non-Destructive Testing in Civil Engineering (NDT-CE), Berlin, Germany

Tuutti, K. 1982. Corrosion of Steel in Concrete. CBI Forskning Research, No. 4

# Author Index


A
Abbasi, S. 417
Aguado, A. 69
Aguiar, J.B. 225, 367
Akasaki, J.L. 149
Alfaiate, J. 319
Allende, K.A. 119
Aprile, A. 249
Azamirad, H. 425
Azevedo, I. 367
B
Barros, J. 261
Beilin, D. 383
Bettencourt, A. 205
Bogas, J.A. 273
Bordado, J.C. 355
Borisov, Y. 383
Branco, F.G. 131
Butler, M. 173
C
Camões, A. 225
Capuani, D. 249
Caretto, F. 341
Chahardeh, A.S. 331
Courard, L. 99
Czarnecki, L. 13
D
da Silva, D. 393
Darwish, F.A. 119
de Araújo, M. 161
de Freitas, I.M. 119
Dilthey, U. 185
Ducatti, V.A. 193
F
Fangueiro, R. 161
Ferreira, D. 261
Ferreira, R.M. 367
Figovsky, O. 383
Figueiras, J.A. 33
Frigione, M. 285, 297
G
Garbacz, A. 99, 305
Gomes, A. 273, 405
H
Hailu, K. 213
Hempel, R. 173
J
Jalali, S. 161
Juvandes, L.F. 33
K
Knapen, E. 85
L
La Rovere, H.L. 393
Lettieri, M., 285
Lintz, R.C. 193
Lukowski, P. 111
Luprano, V. 341
M
Machado, A.V. 367
Maffezzoli, A. 237
Majolan A.S. 331, 417
Manzi, S. 61
Martins, I.R. 149
Moreira, P.M. 225

N
Neto, A.B. 393
Neto, P. 319
Nourivand, A. 331, 417
Nsambu. R. 405
O
Ohama, Y. 49
Ota, M. 49
P
Panfilov, D. 383
Paula, R.F. 355
Pelisser, F. 393
Pereira, C.G. 161
Pereira, P.S. 355
Pinto, R.C. 393
Piotrowski, T. 99
Pires, P. 367
Potapov, Y. 383
R
Raupach, M 213
Reis, M.L. 131
Rodrigues, P. 205
S
Sadeghi, C.A. 331
Sandrolini, F. 61
Santos, J.M. 193
Schleser, M. 185
Schorn, H. 173
Schwall, D. 99
Sciolti, M.S. 297
Serrano, R. 237
Silva, C.P. 33
Sousa, G. 161
Stefanelli, M. 285
Stifani, C. 237
T
Tadeu, A. 131
Taghizadeh, M. 425
Tarzia, A. 237
Tatematsu, H. 49
Tatì, A. 341
Tomás San-José, J. 69
Trindade, G. 139
V
Van Gemert, D. 1, 85
Vinagre, J. 319
W
Wolff, L. 213
Z
Zadeh, D.B. 425



# CENTRO DE PRODUÇÃO DE BETÃO PRONTO

## ready-mixed concrete central

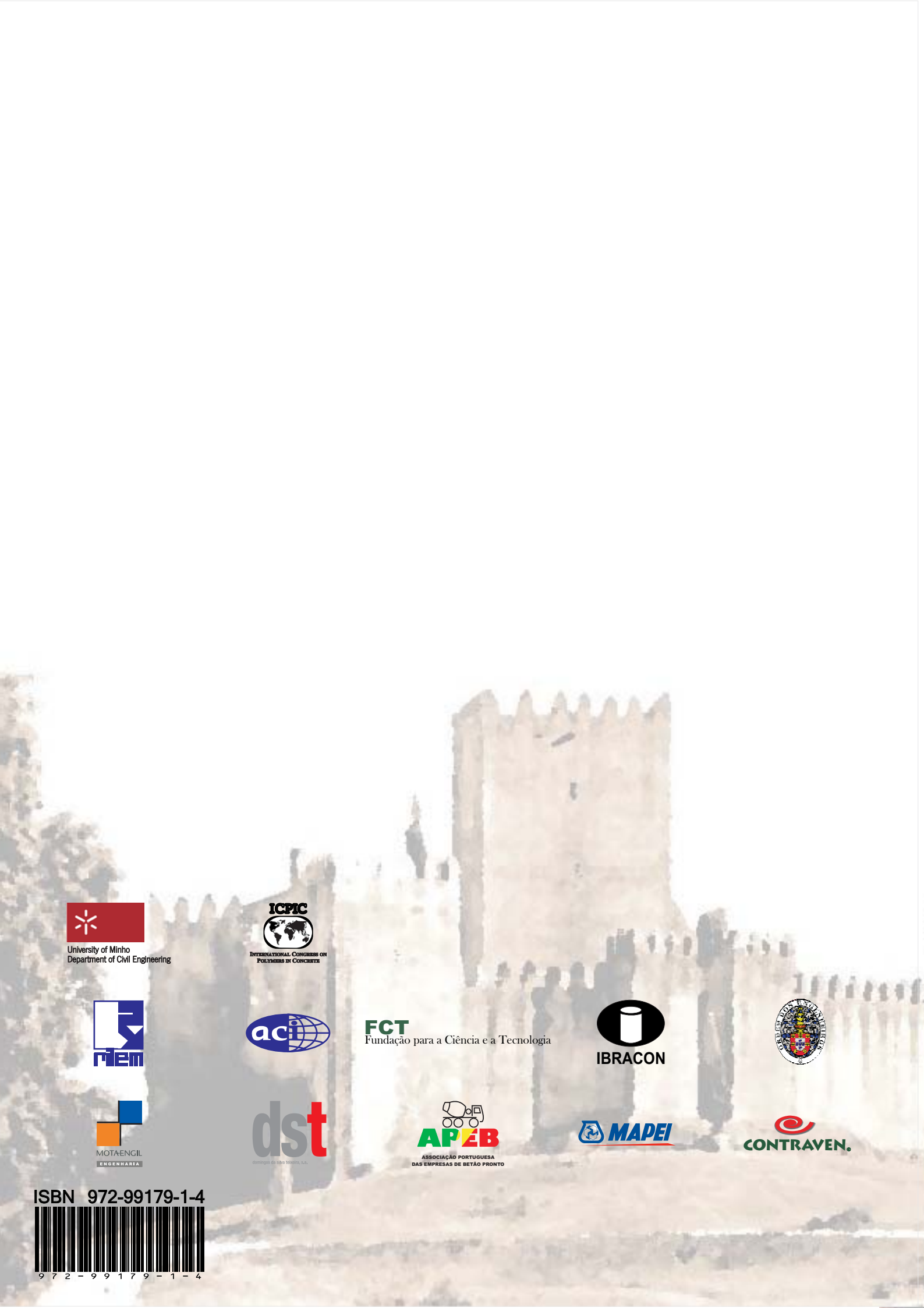
O centro de produção de betão pronto da **dst** estuda e vende todo o tipo de classes de betão. Somos certificados pela norma NP ISO 9001:2000 implementada na concepção, desenvolvimento e produção de betão pronto e sua aplicação, bem como na produção e aplicação de betão betuminoso.

Possuímos três centrais de betão:
em **Braga** - parque industrial de Pitancinhos
em **Guimarães** - urbanização Salgueiral
e em **Vila Nova de Famalicão** - Meães, Esmeriz

**dst**'s ready-mixed concrete central studies and sales all kinds of concrete. We are certified by regulation NP EN ISO 9001:2000. This regulation is carried out in the project, development and production of ready-mixed concrete as well as in the production and applicability of bituminous concrete.

We have three production centres:
in **Braga** - Pitancinhos industrial park
in **Guimarães** - Salgueiral urbanisation
in **Famalicão** - Meães, Esmeriz

**dst**_domingos da silva teixeira, s.a. rua de pitancinhos apartado 208 palmeira 4711-911braga tlf. (+351) 253 307 200/1 fax (+351) 253 307 210 www.dstsgps.com



University of Minho
Department of Civil Engineering

ICPIC
International Congress on Polymers in Concrete

FCT
Fundação para a Ciência e a Tecnologia

IBRACON

MOTA-ENGIL
ENGENHARIA

APEB
Associação Portuguesa das Empresas de Betão Pronto

MAPEI

CONTRAVEN.

ISBN 972-99179-1-4